USGS
science for a changing world

Geology of the National Capital Region— Field Trip Guidebook

Circular 1264

**U.S. Department of the Interior
U.S. Geological Survey**

Geology of the National Capital Region— Field Trip Guidebook

Joint Meeting of Northeast and Southeast Sections
Geological Society of America
Tysons Corner, Virginia
March 24–27, 2004

Edited by Scott Southworth and William Burton
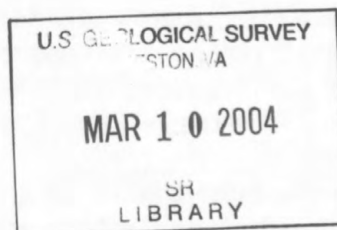
Circular 1264

U.S. Department of the Interior
U.S. Geological Survey

Preface

The 2004 Joint Northeast-Southeast Section Meeting of the Geological Society of America is the fourth such meeting and the third to be held in or near Washington, D.C. This guidebook and the field trips presented herein are intended to provide meeting participants, as well as other interested readers, a means to understand and enjoy the rich geological and historical legacy of the National Capital Region.

The field trips cover all of the major physiographic and geologic provinces of the central Appalachians in the Mid-Atlantic region. Trip 1 outlines the tectonic history of northern Virginia along an east-to-west transect from the Coastal Plain province to the Blue Ridge province, whereas the other field trips each focus on a specific province. From west to east, these excursions investigate the paleoclimate controls on the stratigraphy of the Paleozoic rocks of the Allegheny Plateau and Valley and Ridge province in West Virginia, Pennsylvania, and Maryland (Trip 3); Eocene volcanic rocks that intrude Paleozoic rocks in the westernmost Valley and Ridge province in Virginia and West Virginia (Trip 4); age, petrology, and structure of Mesoproterozoic gneisses and granitoids located in the Blue Ridge province within and near Shenandoah National Park, Virginia (Trip 2); the use of argon data to unravel the complex structural and thermal history of the metamorphic rocks of the eastern Piedmont province in Maryland and Virginia (Trip 5); the use of cosmogenic isotopes to understand the timing of bedrock incision and formation of terraces along the Potomac River in the eastern Piedmont province near Great Falls, Virginia and Maryland (Trip 6); the nature of the boundary between rocks of the Goochland and Chopawamsic terranes in the eastern Piedmont of Virginia (Trip 7); the role of bluffs and fluvial terraces of the Coastal Plain in the Civil War Battle of Fredericksburg, Virginia (Trip 8); and the Tertiary lithology and paleontology of Coastal Plain strata around the Chesapeake Bay of Virginia and Maryland (Trip 9).

Some of the field trips present new geochronological research that uses isotopic techniques to unravel Earth history and processes, including U-Pb dating to determine the timing of metamorphism and igneous activity associated with the Mesoproterozoic Grenville orogeny (Trip 2); argon ($^{40}Ar/^{39}Ar$) analysis to understand the complex Paleozoic history of deformation and metamorphism in the Piedmont (Trip 5); and cosmogenic beryllium-10 data to derive exposure ages of landforms and deposits of the Potomac River valley (Trip 6).

Several trips shed insight on significant or enigmatic geologic features of the region. Trip 3 presents evidence for global paleoclimate controls on the Paleozoic stratigraphy of the Appalachian basin, including evidence for Late Devonian glacial deposits. Trip 4 investigates unusual Eocene igneous rocks in the Eastern United States, and Trip 2 visits several local ductile high-strain zones, offering geologists opportunities to consider the importance of such structures relative to the poorly understood Rockfish Valley fault zone in the Blue Ridge province. In the Piedmont province, Trip 7 focuses on a controversial terrane boundary, whereas Trip 5 crosses several lithologic belts with distinct thermotectonic histories that suggest terrane boundaries. Trip 6 sheds new light on the erosional history of a major river gorge cut into crystalline rocks in the Fall Zone.

Four trips are recommended for Earth science teachers and are cosponsored by the National Association of Geologic Teachers (NAGT). These trips focus on the tectonic history of northern Virginia (Trip 1), terraces of the Potomac River at Great Falls and cosmogenic isotope analysis to date the terraces and the incision history (Trip 6), and Tertiary lithology and paleontology of the Chesapeake Bay region (Trip 9). Trip 8 takes advantage of the rich Civil War history of this region to look at the role that geology played in the strategies and outcome of the Battle of Fredericksburg.

Contents

Conversion Factors

Multiply	By	To obtain
	Length	
inch (in.)	2.54	centimeter (cm)
inch (in.)	25.4	millimeter (mm)
foot (ft)	0.3048	meter (m)
mile (mi)	1.609	kilometer (km)
yard (yd)	0.9144	meter (m)
	Area	
square mile (mi^2)	2.590	square kilometer (km^2)
	Volume	
cubic foot (ft^3)	0.02832	cubic meter (m^3)
cubic mile (mi^3)	4.168	cubic kilometer (km^3)
	Flow rate	
cubic foot per second (ft^3/s)	0.02832	cubic meter per second (m^3/s)
mile per hour (mi/h)	1.609	kilometer per hour (km/h)
	Length	
centimeter (cm)	0.3937	inch (in.)
millimeter (mm)	0.03937	inch (in.)
meter (m)	3.281	foot (ft)
kilometer (km)	0.6214	mile (mi)
meter (m)	1.094	yard (yd)
	Area	
square kilometer (km^2)	0.3861	square mile (mi^2)
	Volume	
cubic meter (m^3)	35.31	cubic foot (ft^3)
cubic kilometer (km^3)	0.2399	cubic mile (mi^3)
	Flow rate	
cubic meter per second (m^3/s)	35.31	cubic foot per second (ft^3/s)
kilometer per hour (km/h)	0.6214	mile per hour (mi/h)

Temperature in degrees Celsius (°C) may be converted to degrees Fahrenheit (°F) as follows:

$$°F = (1.8 \times C) + 32$$

Temperature in degrees Fahrenheit (°F) may be converted to degrees Celsius (°C) as follows:

$$°C = (°F - 32)/1.8$$

1. Regional Tectonic History of Northern Virginia

By Richard Diecchio[1] and Richard Gottfried[2]

Introduction

The objective of this one-day field trip is to examine the field relations that allow us to characterize the major physiographic provinces of northern Virginia and to interpret the tectonic history of this area. We will visit outcrops in the Coastal Plain, Piedmont (including a Mesozoic basin), and Blue Ridge provinces (fig. 1), for the purpose of comparing and contrasting their geology.

We will discuss tectonic events in terms of the Wilson Cycle of ocean-basin opening (rifting) and closing (mountain building), the final product being the mountain belt. The Appalachian Mountains are an excellent example of the repetitive nature of the Wilson Cycle (fig. 2). The tectonic events we will discuss include (oldest to youngest) Middle Proterozoic (Grenville) mountain building, Late Proterozoic (Proto-Atlantic or Iapetus) rifting, Paleozoic Appalachian (Taconic, Acadian, Alleghanian) mountain building, and Mesozoic (Atlantic) rifting.

The dynamic nature of the Earth is a consequence of plate tectonics. These plates are made of rigid continental and oceanic lithosphere. This lithosphere overlies an asthenosphere that is in constant motion. The lithospheric plates experience tensional, compressional, and shearing forces that lead to processes such as rifting, collisional tectonics, and transform faulting. In the process, new ocean floor may be created as well as chains of volcanic islands, areas of earthquake activity, and new mountain ranges. The continents themselves may shift their position as plates move. All of this affects the shape of the land and the distribution of rocks, minerals, fossils, climate, and natural resources. Northern Virginia has experienced several major tectonic episodes that are now recorded in the local rock record and may be visited at many places. The sites to be visited on this trip are selected on the basis of their significance relative to the tectonic history. These sites also illustrate the field relations that allow the recognition of the relative timing of these events.

[1]George Mason University, Fairfax, VA 22030.

[2]Frederick Community College, Frederick, MD 21702.

Geologic History

Over one billion years ago in the Mesoproterozoic, narrow strips of land (microcontinents, volcanic arcs, and suspect terranes) collided with and compressed the eastern edge of the then developing North American continent. The rocks from these events are part of the Grenville province of the Precambrian Canadian Shield of North America. This collision between proto-North America and other continents led to the formation of a supercontinent called Rodinia. The formation of Rodinia also resulted in the formation of a mountain range: the Grenville Mountains, now the Grenville province of the Canadian Shield. This mountain-building event is called the Grenville orogeny. Locally, these rocks are found in the Blue Ridge province and are considered to be the oldest rocks in northern Virginia. They are exposed at the surface only after much weathering and erosion of overlying younger rock. Magmatic processes that accompanied this orogeny produced molten rock that was injected into the crust. These igneous rocks, along with the sediments that were eroded from the eastern margin of the Precambrian shield before this collision, were deformed and metamorphosed. We will see metaigneous rocks of Grenville age below the unconformity at Stop 9.

Following the Grenville orogeny, tensional forces associated with changes in mantle convection and (or) other processes led to a breakup of the Rodinian supercontinent. This latest Precambrian (Neoproterozoic) and Early Cambrian rifting led to the opening of the Proto-Atlantic or Iapetus Ocean that predates the Atlantic Ocean. Basaltic rocks that formed during this rifting (and were subsequently metamorphosed during the Paleozoic) are now part of the Catoctin Formation and will be visited at Stop 8. During rifting, fragments of the Grenville continental crust were broken off and became islands, later to be reunited with North America by subsequent closure of the ocean. The Goochland terrane of the Piedmont province may be one of these Grenville fragments (Spears and others, this volume).

As the Iapetus Ocean continued to widen, the rift margin became passive. Sediment continued to be deposited on the eastern edge of the continent, and a broad clastic shelf developed (Chilhowee Group). As the Grenville Mountains were eroded during the Cambrian, the source of clastics diminished and deposition of limestones predominated into the Early
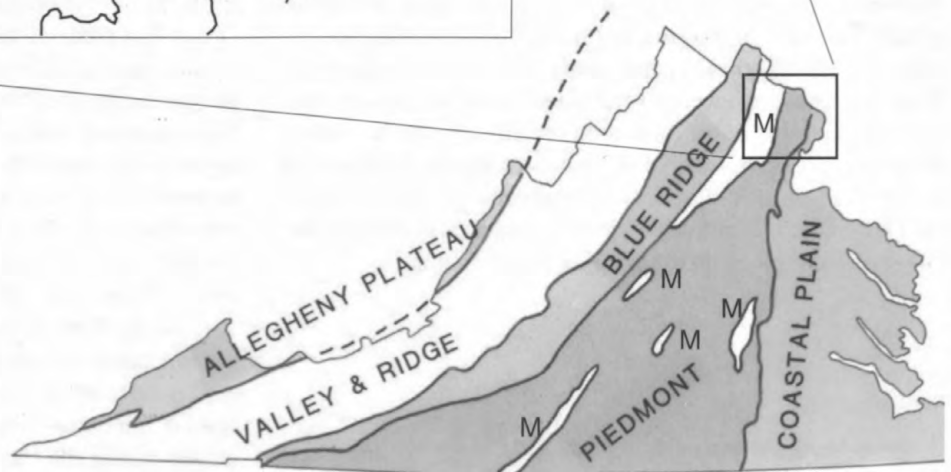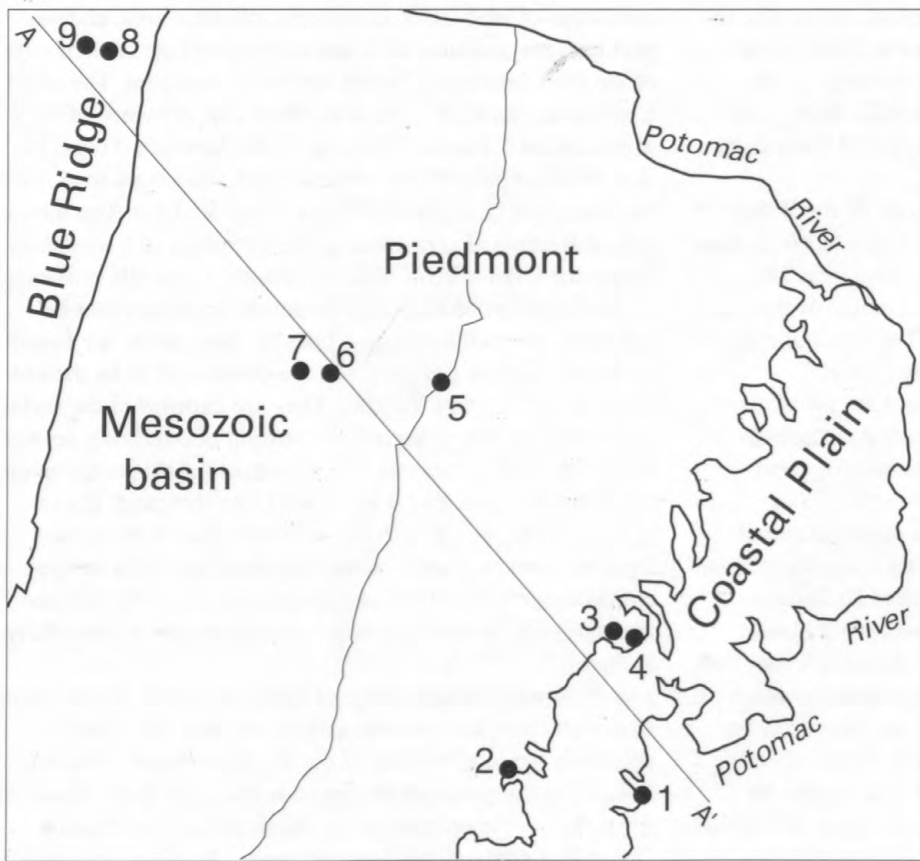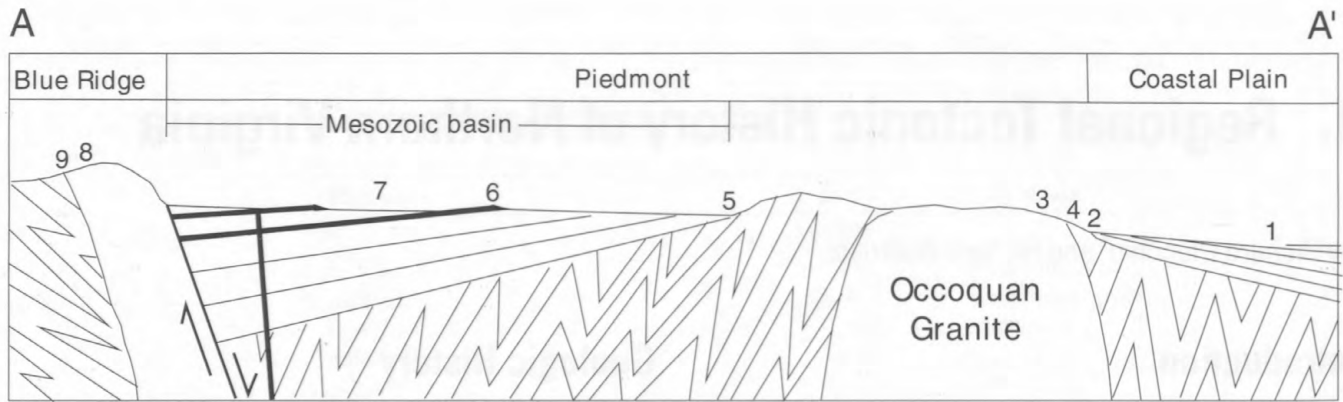
Figure 1. Physiographic provinces of Virginia and in field trip area, and generalized cross section A–A' of field trip. Numbers refer to field trip stops. Heavy lines in Mesozoic basin on cross section are dikes and sills. M, Mesozoic basins.

Ordovician. Locally, these limestones can be seen in the Frederick Valley and the Shenandoah Valley but will not be seen on this trip. Information about this part of the tectonic history of Virginia can be found in Fichter and Diecchio (1993) and in the additional resources listed at the end of this field guide. During the early Paleozoic the east coast of North America was aligned parallel to the equator that passed through the central part of the United States, roughly coincident with the present-day longitude of Kansas.

During the Middle Ordovician, the plate movements reversed, Iapetus began to close, and once again, continental plates began to converge. As Gondwana approached North America, a subduction zone formed and a volcanic arc complex developed off the east coast of North America. Continental fragments like the Goochland terrane (Spears and others, this volume), that had previously detached from North America, were now caught along with the volcanic arc between North America and Gondwana. Over time, the volcanic islands and continental fragments were thrust back onto North America, eventually to become today's Piedmont terrane. The carbonate and clastic rocks that were deposited on the eastern edge of North America during the Cambrian and Ordovician were now caught between the Piedmont and the eastern edge of North America, and subsequently were compressed. This entire compressional episode, like the earlier Grenville orogeny, resulted in thrust faults, folds, felsic intrusions (like the Occoquan Granite of Stop 3), volcanics (like the Chopawamsic Formation of Stop 2), and metamorphism (evident at Stops 2–5). All of this activity was part of a mountain-building episode known as the Taconic orogeny. This was the first phase in the building of the Appalachian Mountains.

We will not visit the Valley and Ridge province on this trip; however we will briefly discuss its geology to complete the story. Further information can be found in Fichter and Diecchio (1993) and in the additional resources listed at the end of this field guide. The results of these events can be seen in sediments deposited west of the Blue Ridge, in the Valley and Ridge province, and in igneous and metamorphic rocks and deformation in the Piedmont. Of note, two additional mountain-building periods, the Acadian orogeny and the Alleghanian orogeny, occurred during the Paleozoic Era. These orogenies are associated with continued collision and the resulting folds, faults, intrusions, and metamorphism as occurred during the earlier Taconic orogeny. While all this mountain-building activity was taking place, sediments were accumulating west of the Blue Ridge, in the Appalachian basin, which developed on the eastern edge of North America in part as a result of loading by thrust sheets and sediment. These sediments were themselves folded and faulted during the orogenies. At the end of the Paleozoic Era, the final result of the full collision of North America and Gondwana was the formation of the Appalachian Mountains on the supercontinent of Pangea.

Pangea existed during most of the Permian and Triassic.

During the Triassic, the plates once again began to pull apart. Rifting began to break up Pangea. One system of rifts opened up along the extent of today's east coast, to become the Atlantic Ocean. This rift system included intracontinental rift basins known as the Mesozoic basins. Here in northern Virginia, one such basin is known as the Culpeper basin (Stops 5–7).

As rifting progressed, erosion of the higher land on either side of the Mesozoic basins produced a variety of sediments that accumulated in fluvial, deltaic, and lacustrine environments (Stops 5–7). The rifting also produced mafic igneous intrusions and volcanism (mafic dikes of Stop 3 and diabase sill of Stop 6) in the basins. Locally the igneous rocks are more resistant to erosion; thus as the sedimentary rocks have been eroded many of these igneous rocks, even intrusions formed at depth, are expressed today as topographic highs.

The Mesozoic basins eventually became inactive as the continental margin became passive. However, the Atlantic continued to open along the Mid-Atlantic Ridge and continues even today. During the Mesozoic, sediments also began to be deposited on the new continental margin, continued to be deposited through the Tertiary, and are still being deposited today. These sediments are now part of the Coastal Plain province and the continental shelf. We will see Coastal Plain deposits at Stops 1 and 2.

Acknowledgments

References Cited

Aleinikoff, J.N., Horton, J.W., Jr., Drake, A.A., Jr., and Fanning, C.M., 2002, Shrimp and conventional U-Pb ages of Ordovician granites and tonalities in the central Appalachian Piedmont; Implications for Paleozoic tectonic events: American Journal of Science, v. 302, p. 50–75.

Drake, A.A., Jr., Froelich, A.J., Weems, R.E., and Lee, K.Y., 1994, Geologic map of the Manassas quadrangle, Fairfax and Prince William Counties, Virginia: U.S. Geological Survey Geologic Quadrangle Map GQ–1732, scale 1:24,000.

Fichter, L.S., 1993, The geologic evolution of Virginia: National Association of Geology Teachers Short Course, Notebook of Illustrations.

Figure 2 (following two pages). Wilson Cycle as it applies to the northern Virginia area (after Fichter, 1993).

The Geological Evolution of Virginia
Divided into Fourteen Stages A–M

A. Proterozoic (1.2 bya) *(Protolith to 1.8)*
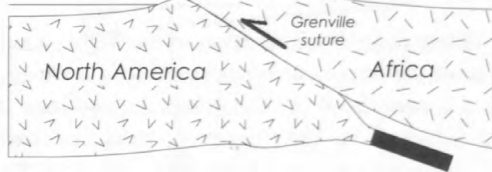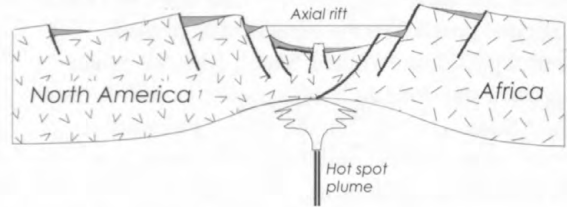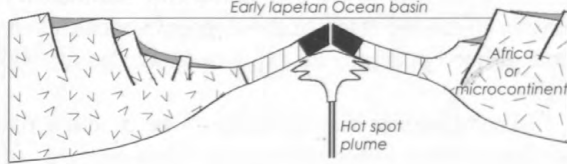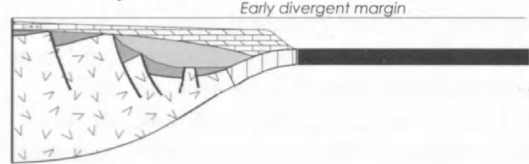
Grenville suture

North America

Africa

B. Late Proterozoic

Axial rift

North America

Africa

Hot spot plume

C. Earliest Cambrian

Early Iapetan Ocean basin

Africa or microcontinent

Hot spot plume

D. Early Cambrian

Early divergent margin

E. Middle Cambrian

Chopawamsic volcanic arc

Unnamed microcontinent

ROB

F. Late Cambrian

Arc-microcontinent collision

Avalon terrane

G. Early Ordovician

Subduction reversal

Arvonia flysch

ROB

Avalon terrane

H. Middle to Late Ordovician

Taconic Mountains

HFRV fault

Taconian foreland basin

Chopawamsic/ Arvonia arcs

Suture zone

Micro-continent

Lower Paleozoic and younger rocks

Avalon terrane
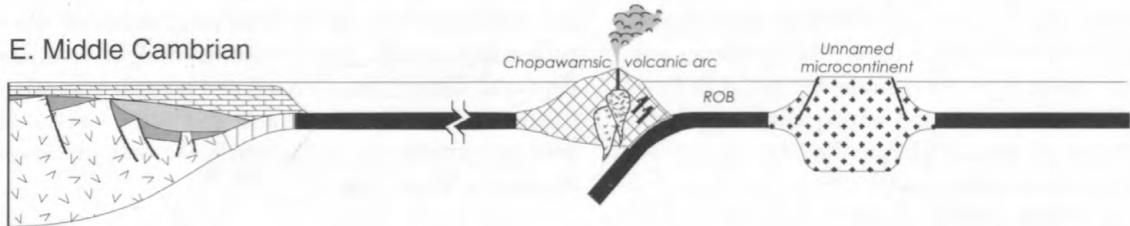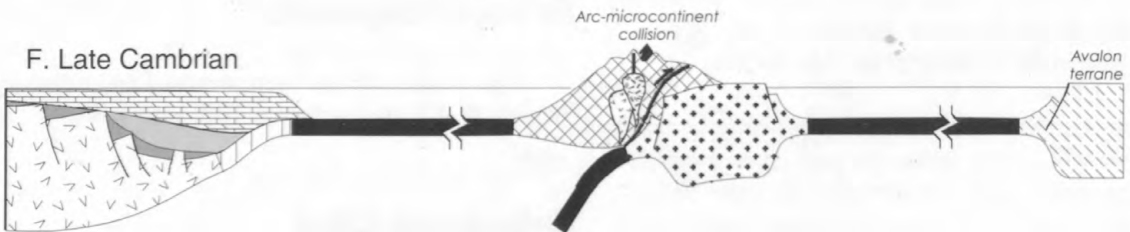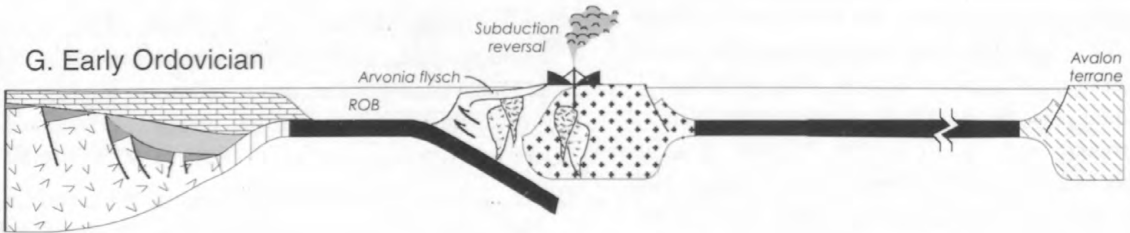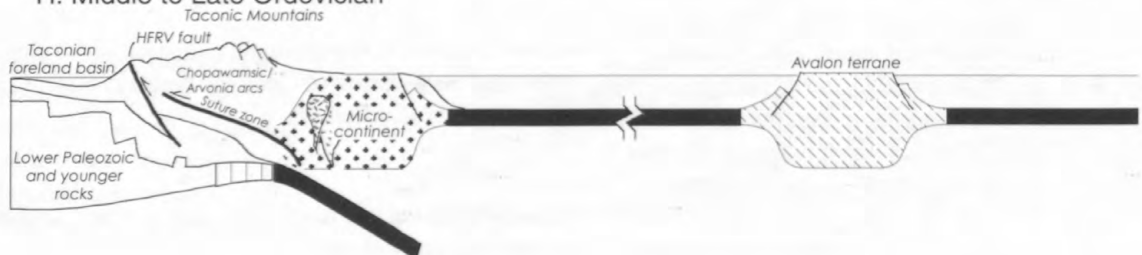
I. Silurian to Early Devonian

Central Appalachian basin

Eroded Taconic Mountains

ROB

Avalon terrane
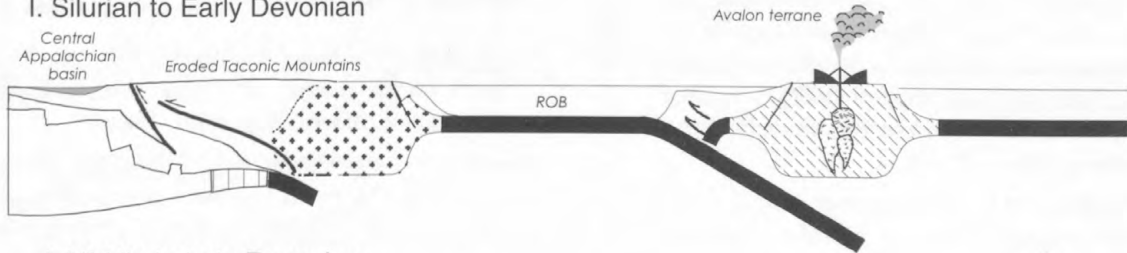
J. Middle to Late Devonian

Catskill foreland basin

Acadian Mountains

Taconic roots

Avalon terrane

Rheic ocean (ROB)

Africa (Gondwana)

J1. Mississippian

Kaskaskia epicontinental sea

Eroded Taconic terranes (Taconic orogeny)

Eroded Avalon terrane (Acadian orogeny)

Taconic roots

Avalon roots

Rheic ocean (ROB)

Africa (Gondwana)

Proto-Atlantic axial rift

K. Late Paleozoic

Alleghanian Mountains

Valley and Ridge

Rift

Detached Taconic terrane

Detached Acadian terrane

North America

Africa

L. Triassic to Early Jurassic

Culpeper basin

Axial rift (Incipient Atlantic)

Taconic

Acadian

Attenuated continental crust

Africa

North America

Hot spot plume
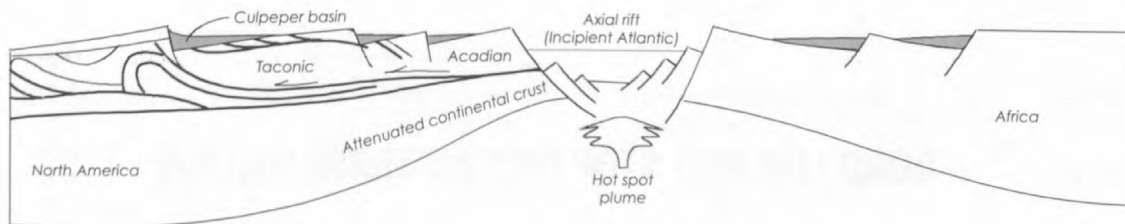
M. Late Cretaceous to early Cenozoic

Coastal Plain

Continental shelf

Atlantic Ocean

Axial rift
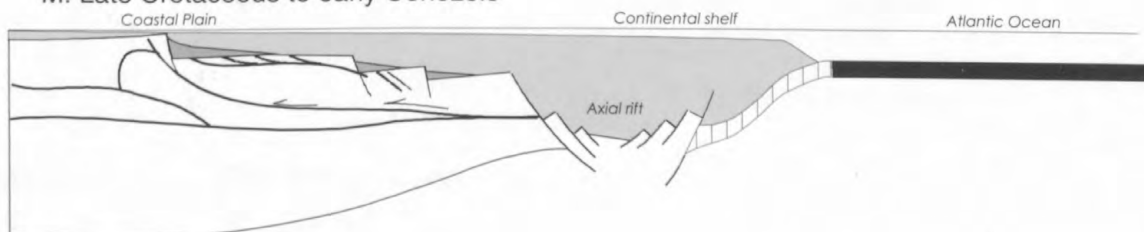
Fichter, L.S., and Diecchio, R.J., 1993, Evidence for the progressive closure of the Proto-Atlantic Ocean in the Valley and Ridge province of northern Virginia and eastern West Virginia: National Association of Geology Teachers, Eastern Section Meeting Field Trip Guidebook, Harrisonburg, Va., p. 27–49.

Kline, S.W., Lyttle, P.T., and Schindler, J.S., 1991, Late Proterozoic sedimentation and tectonics in northern Virginia, in Schultz, Art, and Compton-Gooding, Ellen, eds., Geologic evolution of the Eastern United States, Field Trip Guidebook, NE-SE GSA, 1991: Virginia Museum of Natural History Guidebook 2, p. 263–294.

Lee, K.Y., and Froelich, A.J., 1989, Triassic-Jurassic stratigraphy of the Culpeper and Barboursville basins, Virginia and Maryland: U.S. Geological Survey Professional Paper 1472, 52 p.

Mixon, R.B., Southwick, D.L., and Read, J.C., 1972, Geologic map of the Quantico quadrangle, Prince William and Stafford Counties, Virginia, and Charles County, Maryland: U.S. Geological Survey Geologic Quadrangle Map GQ–1044, scale 1:24,000

Seiders, V.M., and Mixon, R.B., 1981, Geologic map of the Occoquan quadrangle and part of the Fort Belvoir quadrangle, Prince William and Fairfax Counties, Virginia: U.S. Geological Survey Miscellaneous Investigations Series Map I–1175, scale 1:24,000.

Southworth, Scott, Burton, W.C., Schindler, J.S., and Froelich, A.J., 2000, Digital geologic map of Loudoun County: U.S. Geological Survey Open-File Report 99–150, 1 CD-ROM.

Additional Resources

Cecil, K.K., Whisonant R.C., and Sethi, P.S., 2000, Teacher's guide for the geology of Virginia: Charlottesville, Virginia Division of Mineral Resources, 132 p.

Baedke, S.J., and Fichter, L.S., 1999–2000, The geological evolution of Virginia and the mid-Atlantic region: available online at http://csmres.jmu.edu/geollab/vageol/vahist/

Roberts, Chad, and Bailey, C.M., 1997–2003, The geology of Virginia: available online at http://www.wm.edu/geology/virginia/

Sethi, P.S., Whisonant, R.C., and Cecil, K.K., 1999, Geology of Virginia, CD-ROM 1, Introduction and geologic background: Charlottesville, Virginia Division of Mineral Resources, 1 CD-ROM.

Sethi, P.S., Whisonant, R.C., Cecil, K.K., and Newbill, P.L., 2000, Geology of Virginia, CD-ROM 2, Coastal Plain: Charlottesville, Virginia Division of Mineral Resources, 1 CD-ROM.

Sethi, P.S., Whisonant, R.C., Cecil, K.K., and Newbill, P.L., 2000, Geology of Virginia, CD-ROM 3, Piedmont and Blue Ridge: Charlottesville, Virginia Division of Mineral Resources, 2 CD-ROMs.

ROAD LOG AND STOP DESCRIPTIONS FOLLOW

Road Log and Stop Descriptions

Road log begins at entrance station to Leesylvania State Park, Va.

Mileage

Incremental	Cumulative	
0.0	0.0	Entrance station to Leesylvania State Park.
		Proceed straight ahead into park toward Freestone Point.
		Entrance fee may be waived for educational groups if application is filed in advance.
1.7	1.7	Turn right into parking area and park vehicles.
		Proceed on foot to Freestone Point.

Stop 1. Freestone Point, Leesylvania State Park.

Mixon and others (1972) refer to the strata exposed at Freestone Point (and elsewhere on the Quantico quadrangle) as the Potomac Group. Seiders and Mixon (1981) refer to the same strata exposed on the adjacent Occoquan quadrangle (see Stop 2) as the Potomac Formation. For consistency, we will use the more recent terminology and will refer to these strata as the Potomac Formation.

Part of the Lower Cretaceous Potomac Formation is exposed at Leesylvania Park in the bluffs along the shore, beyond the end of the road at Freestone Point, in the northeast end of the park. This is a good exposure of one of the sandstone units in the Coastal Plain. These strata were probably deposited in a beach environment, as indicated by the sorting and the bimodal crossbeds. Note the presence of blue quartz. Blue quartz is common in the Mesoproterozoic Grenville rocks of the Blue Ridge province, indicating the source area of this sediment.

These Cretaceous beach sands occur above present-day sea level. During the Cretaceous, the Earth was probably free of glaciers, climates were warmer, and sea level was higher. In the current global warming controversy, it is significant to note that these conditions existed long before humans could influence the climate system. In the regional historical picture, the sandstone here represents a coastline developed along the eastern shore of North America during the Cretaceous.

Mileage

Incremental	Cumulative	
		Retrace route to leave park.
2.3	4.0	Turn left onto Neabsco Road.
1.5	5.5	Turn right at traffic light onto Jefferson Davis Highway, U.S. 1.
0.2	5.7	Turn left at traffic light onto Neabsco Mills Road.
1.1	6.8	Turn left onto Dale Boulevard.
0.4	7.2	Cross over I-95 and continue straight on Dale Boulevard.
0.6	7.8	Turn right at traffic light onto Gideon Drive.
0.8	8.6	Turn left at traffic light onto Opitz Boulevard.
0.6	9.2	Turn left at traffic light into parking lot for Gar-Field High School.
		Drive to gate in chain link fence directly behind the school.
0.2	9.4	Park at gate and proceed on foot down to Neabsco Creek.
		Prior permission should be obtained to visit this outcrop, especially to arrange for gate to be unlocked.

Stop 2. Neabsco Creek, Gar-Field High School.

This outcrop contains a nonconformity between the gneisses and schists of the Middle Ordovician Chopawamsic Formation (fig. 3) below and the sandstones of the Lower

Figure 3. Fold axis and axial-planar cleavage (parallel to hammer handle) in rocks of the Chopawamsic Formation at Stop 2.

Cretaceous Potomac Formation above (Mixon and others, 1972). The hiatus represents over 300 million years. The surface expression of this nonconformity defines the boundary between the metamorphosed rocks of the Piedmont province to the west and the unconsolidated strata of the Coastal Plain province to the east.

The regional metamorphic event that formed the schist here, along with the other foliated rocks of the Piedmont, can be used to determine the relative ages of other exposures we will see on this trip. This metamorphic event will be the basis for our discussion of the older rocks that predate metamorphism, and the younger rocks that postdate metamorphism.

The northeast strike of the foliation in the schists is consistent with the regional Appalachian trends of metamorphic foliation, as well as the trends of fold axes and thrust faults in the Blue Ridge and Valley and Ridge provinces. In other words, the metamorphism was part of Appalachian mountain building during the Paleozoic.

At this stop the nonconformity and the overlying strata of the Coastal Plain dip gently seaward and comprise the subsurface of the eastern shore. Permeable units, such as these, are aquifers and are usually confined between impermeable clay-rich aquitards. Regional ground-water flow is downdip to the east.

Mileage

Incremental	Cumulative	
		Retrace route to leave school parking lot.
0.2	9.6	Turn left at traffic light onto Opitz Boulevard.
0.9	10.5	Turn right at traffic light onto Minnieville Road.
2.4	12.9	Turn right at traffic light onto Old Bridge Road.

Figure 4. Mafic dike intruding the Occoquan Granite at Stop 3.

1.4	14.3	Turn left at traffic light onto Gordon Boulevard, Va. 123.
0.5	14.8	Cross Occoquan River and continue straight on Va. 123.
0.6	15.4	Turn left into Vulcan Graham Virginia Quarry.
0.4	15.8	Park at quarry office.
		Prior permission is required to visit quarry.

Stop 3. Vulcan Graham Virginia Quarry, Occoquan Granite.

The Occoquan Granite is exposed here and along the fall zone of the Occoquan River. The granite contains a foliation indicated by the orientation of biotite, and therefore the Occoquan is clearly premetamorphic. According to Seiders and Mixon (1981), the Occoquan Granite was emplaced during the Early Cambrian. A recent age determination (Aleinikoff and others, 2002) indicates the Occoquan was emplaced in the Ordovician during the Taconic orogeny. The Occoquan probably underwent metamorphism during a subsequent orogeny.

We will observe one of several mafic dikes that intrude the granite (fig. 4). These dikes are nonfoliated and therefore postdate the metamorphism. Their ages are assumed to be Mesozoic and, if so, provide additional field evidence that basaltic volcanism occurred after emplacement and metamorphism of the granite.

Historically, the Occoquan Granite represents a volcanic arc that existed during the early Paleozoic. The mafic dikes are probably associated with the rifting that occurred during the Mesozoic.

Mileage

Incremental	Cumulative	
		Retrace route to leave the quarry.
0.5	16.3	Turn left onto Va. 123 North.
0.2	16.5	Turn right into Occoquan Regional Park.
1.0	17.5	Turn right into parking lot. Restrooms are available.
		Retrace route to leave park.
0.4	17.9	Park on right, off the pavement, and cross road to outcrop.

Stop 4. Occoquan Regional Park.

Metasedimentary rocks of the Piedmont are well exposed at this stop. We will look at the slates and metasandstones of the Upper Ordovician Quantico Formation, which are the primary rocks exposed in the park. Exposures of the Chopawamsic Formation and Occoquan Granite also are present in the park (Seiders and Mixon, 1981). All of these units are overlain nonconformably by the Lower Cretaceous Potomac Formation. We observed this nonconformity at Gar-Field High School and will not take the time to see it again here.

Mileage

Incremental	Cumulative	
		Continue straight ahead out of park.
0.7	18.6	Turn right onto Va. 123 North.
6.4	25.0	Turn left at traffic light onto Clifton Road.
1.7	26.7	Cross Wolf Run Shoals Road.
		Continue straight on Clifton Road.
3.2	29.9	Turn right onto Main Street in the town of Clifton.
0.3	30.2	Turn left and continue on Clifton Road.
3.5	33.7	Cross Braddock Road.
		Continue straight on Clifton Road.
0.6	34.3	Turn left onto Regal Crest Drive. Park on right.

Stop 5. Clifton Road, Centreville.

This locality is on the eastern edge of the Culpeper basin, a Mesozoic continental rift basin. Here is the nonconformable relation between the late Precambrian or Early Cambrian Piney Branch Complex and the Late Triassic Reston Member of the Manassas Sandstone (Drake and others, 1994).

> Proceed on foot back to Clifton Road and turn right.
> Walk to intersection of Moore Drive and observe small outcrop of the Piney Branch Complex on northeast corner of intersection.

The Piney Branch Complex clearly is pre-metamorphic, with a northeast-trending foliation.

> Walk north on Clifton Road to a small outcrop on the east side of the road across from Regal Crest Drive.

The Reston Member here is a conglomerate (polymict diamictite, see figure 5). Various types of pebbles occur here and most contain a metamorphic foliation. The pebbles are contained in a nonfoliated hematitic mud matrix. The overall rock itself is therefore non-metamorphic or post-metamorphic. However, the foliated pebbles are clearly derived from an older, pre-metamorphic source. The contact between the Piney Branch Complex

Figure 5. Pebbles and cobbles of metamorphic rock in basal conglomeratic facies of the Reston Member of the Manassas Sandstone at Stop 5.

and the Manassas Sandstone is a nonconformity that is not exposed here and represents over 300 m.y. missing.

The historical significance of this stop is to illustrate the relative ages of the older pre-metamorphic Piedmont rocks and the younger post-metamorphic strata of the Culpeper basin.

Mileage

Incremental	Cumulative	
		Return to vehicles, turn around, and continue north on Clifton Road.
0.2	34.5	Turn left at traffic light onto Lee Highway, U.S. 29 South.
4.8	39.3	Turn left into Luck Stone Quarry.
		Stay to the right and park vehicles.
		Prior permission is required to visit quarry.

Stop 6. Luck Stone Quarry, Centreville.

The quarry is in a Lower Jurassic diabase sill (Drake and others, 1994) that was intruded into the sedimentary rocks of the Culpeper basin. The strata have a gentle westward dip due to the downdropping along the western border fault between the Culpeper basin and the Blue Ridge (fig. 2). Basalts are known to occur in the western part of the

Figure 6. West-dipping Mesozoic strata cut by east-dipping normal fault (arrows) at Stop 6. Strata on east (right) side of fault are overlain by diabase sill and have dropped down relative to the west (left) side. Photograph faces north.

basin; hence there was also extrusive volcanic activity. Because the igneous rocks of this area are more resistant to erosion than the sedimentary rocks, the intrusive and volcanic rocks form topographic highs within the basin. Elsewhere in the basin, contact-metamorphosed sedimentary rocks, such as hornfels, also form topographic highs.

Proceed through the tunnel under U.S. 29 to the north end of the quarry.

An east-dipping normal fault separates the Mesozoic strata from the diabase (fig. 6). The diabase does not have any metamorphic texture. It is therefore post-metamorphic and represents mafic plutonism-volcanism associated with extensional tectonics after Appalachian mountain building. The historical significance of this stop is Mesozoic continental rifting that accompanied the initial opening of the Atlantic Ocean.

Mileage

Incremental	Cumulative	
		Drive out of quarry and turn left onto U.S. 29 South.
0.7	40.0	Turn right into parking lot for Manassas Battlefield. Park vehicles. Walk west to the Stone Bridge.

Stop 7. Stone Bridge over Bull Run.

Upper Triassic red clastic sediments of the Balls Bluff Siltstone (Lee and Froelich, 1989; Southworth and others, 2000) are exposed here along Bull Run. These strata also display the regional westward dip seen at Stop 6. Note that this is a finer grained facies than the red conglomerates of Stop 5 even though both had a common source. The conglomerates near both the east and west margins of the basin are closer to the source. The much finer sediments (now rocks) in the center of the basin were transported a greater distance from the source.

Mileage

Incremental   **Cumulative**

		Exit parking area and turn right onto U.S. 29 South.
1.5	41.5	Turn right at traffic light onto Sudley Road, Va. 234 North.
7.5	49.0	Turn right at traffic light onto James Madison Highway, U.S. 15 North.

Route 15 runs along the western side of the Culpeper basin. The western border fault lies to the west of U.S. 15, and just west of the fault is the Blue Ridge, which is visible on the horizon to the left. As we drive north, U.S. 15 gets closer to the western edge of the basin.

6.7	55.7	Cross U.S. 50, continue straight on U.S. 15 North.
4.1	59.8	Cross Goose Creek, continue straight on U.S. 15 North.
0.5	60.3	Turn left onto Lime Kiln Road, Va. 733.

Within a few hundred feet is the western border fault of the Culpeper basin.

3.7	64.0	Pass outcrop of metabasalt (greenstone) of the Catoctin Formation on right. Drive ahead 0.1 mile and carefully park vehicles on right across from house. Walk back to the outcrop.

Stop 8. Goose Creek near Steptoe Hill.

The Neoproterozoic Catoctin Formation is a foliated greenstone and greenschist interbedded with metasedimentary rocks. The Catoctin greenstone is metabasalt as indicated elsewhere by vesicles and amygdules, porphyritic texture, flow-top breccias, and pillows (Kline and others, 1991). The Catoctin is commonly referred to as greenstone (a field term) because of the abundance of green-colored chlorite and epidote.

The Catoctin Formation represents an episode of continental rifting. Its pre-metamorphic age (Southworth and others, 2000) indicates that it was emplaced before Appalachian mountain building in the Paleozoic, and certainly before the opening of the Atlantic Ocean in the Mesozoic. The Catoctin rifting occurred during the Neoproterozoic (latest Precambrian) and is good evidence of the opening of the Proto-Atlantic Ocean or Iapetus.

Mileage

Incremental   **Cumulative**

		Continue west on Lime Kiln Road.
1.7	65.7	Turn left into Groveton Farm.
		This stop is on private land, and permission is required.

Stop 9. Goose Creek at Groveton Farm.

Here is the nonconformity between the gneiss (metagranite) of the Mesoproterozoic Marshall Metagranite and the arkosic metaconglomerate of the Neoproterozoic Fauquier Formation, as described by Kline and others (1991) and Southworth and others (2000). The Fauquier Formation is overlain by the Catoctin Formation.

Compare the relations here with the nonconformities observed earlier today at Gar-Field High School (Stop 2) and on Union Mill Road in Centreville (Stop 5). Similar to the earlier stops, this nonconformity represents younger sediments overlying older metamorphic rocks. However, one major difference exists here: the younger sediments (Fauquier Formation) are foliated (like the overlying Catoctin Formation) and therefore are pre-metamorphic. The older basement gneisses here are more severely metamorphosed than the overlying metasediments. This indicates that the older basement rocks had undergone metamorphism before deposition of the overlying sediments. Subsequently, these sediments and the underlying metamorphic basement rocks were metamorphosed. Two episodes of metamorphism are therefore evident, the older of which predates the metamorphism of the Appalachian events. This older metamorphism is associated with the Mesoproterozoic Grenville orogeny, which represents mountain building prior to the opening of the Proto-Atlantic Ocean.

Return to Leesylvania State Park.

2. Mesoproterozoic Geology of the Blue Ridge Province in North-Central Virginia: Petrologic and Structural Perspectives on Grenvillian Orogenesis and Paleozoic Tectonic Processes

By Richard P. Tollo,[1] Christopher M. Bailey,[2] Elizabeth A. Borduas,[1] and John N. Aleinikoff[3]

Introduction

This field trip examines the geology of Grenvillian basement rocks located within the core of the Blue Ridge anticlinorium in north-central Virginia over a distance of 64 kilometers (km) (40 miles (mi)), from near Front Royal at the northern end of Shenandoah National Park southward to the vicinity of Madison. This guide presents results of detailed field mapping, structural analysis, petrologic and geochemical studies, and isotopic investigations of Mesoproterozoic rocks directed toward developing an understanding of the geologic processes involved in Grenvillian and Paleozoic orogenesis in the central Appalachians. Stops included in this field guide illustrate the lithologic and structural complexity of rocks constituting local Blue Ridge basement, and demonstrate the type of integrated, multidisciplinary studies that are necessary to decipher the protracted Mesoproterozoic through Paleozoic geologic history of the region.

The field trip traverses the crest of the Blue Ridge along Skyline Drive and the adjacent foothills located east of the mountains. This largely rural area is characterized by locally steep topography and land-use patterns that are dominated by agriculture and recreation. In late June 1995, a series of tropical storms affected parts of the central Virginia Piedmont and adjacent Appalachian Mountains. These storms produced abundant rainfall, ranging from 75 to 175 millimeters (mm) (3–6.9 inches (in)) throughout the region, which increased the moisture content of the relatively thin soils and shallow rock debris that cover the mountains (Wieczorek and others, 2000). On June 27, following this extended interval of rainfall, an exceptionally intense, localized period of precipitation, resulting from the interaction of tropical moisture and a cold front that stalled over the region, produced up to 770 mm (30.3 in) of rain in the vicinity of Graves Mills (near Stops 18 and 19) in northwestern Madison County. During this storm, more than 1,000 shallow rock, debris, and soil slides mobilized into debris flows that were concentrated in northwestern Madison County (Morgan and others, 1999). The debris flows removed large volumes of timber, soil, and rock debris, resulting in locally widened channels in which relatively unweathered bedrock commonly was exposed. Stops 18 and 19 are located within such channels, and are typical of the locally very large and unusually fresh exposures produced by the event. Materials transported by debris flows were typically deposited at constrictions in the valley pathways or on top of prehistoric fans located at the base of many of the valleys that provided passageways for the flows. Water emanating from the debris flows typically entered streams and rivers located in the valley floors bordering the mountains, greatly increasing flow volume and resulting in flooding and scoured channels. The enormous exposures at Stops 17 and 20 were enlarged and swept clean by scouring during this flooding event. Analysis of this and other events suggests that such high-magnitude, low-frequency events are a significant means of delivering coarse-grained regolith from mountainous hollows and channels to the lowland floodplains (Eaton and others, 2003). Such events may happen in the Appalachian mountains of Virginia and West Virginia with a recurrence interval of 10 to 15 years (Eaton and others, 2003).

Geology of the Blue Ridge Anticlinorium

The Blue Ridge province is one of a series of thrust-bounded inliers that expose Laurentian basement within the Appalachians (Rankin and others, 1989a). The province consists of two massifs: the Shenandoah, located mostly in Virginia, and the French Broad, which extends from western North Carolina to southwestern Virginia (fig. 1). The Shenandoah massif, where the field trip area is located, constitutes part of an allochthonous, northwest-vergent, thrust-bounded sheet that, in central and

[1]Department of Earth and Environmental Sciences, The George Washington University, Washington, DC 20052.

[2]Department of Geology, College of William and Mary, Williamsburg, VA 23187.

[3]U.S. Geological Survey, Denver, CO 80225.
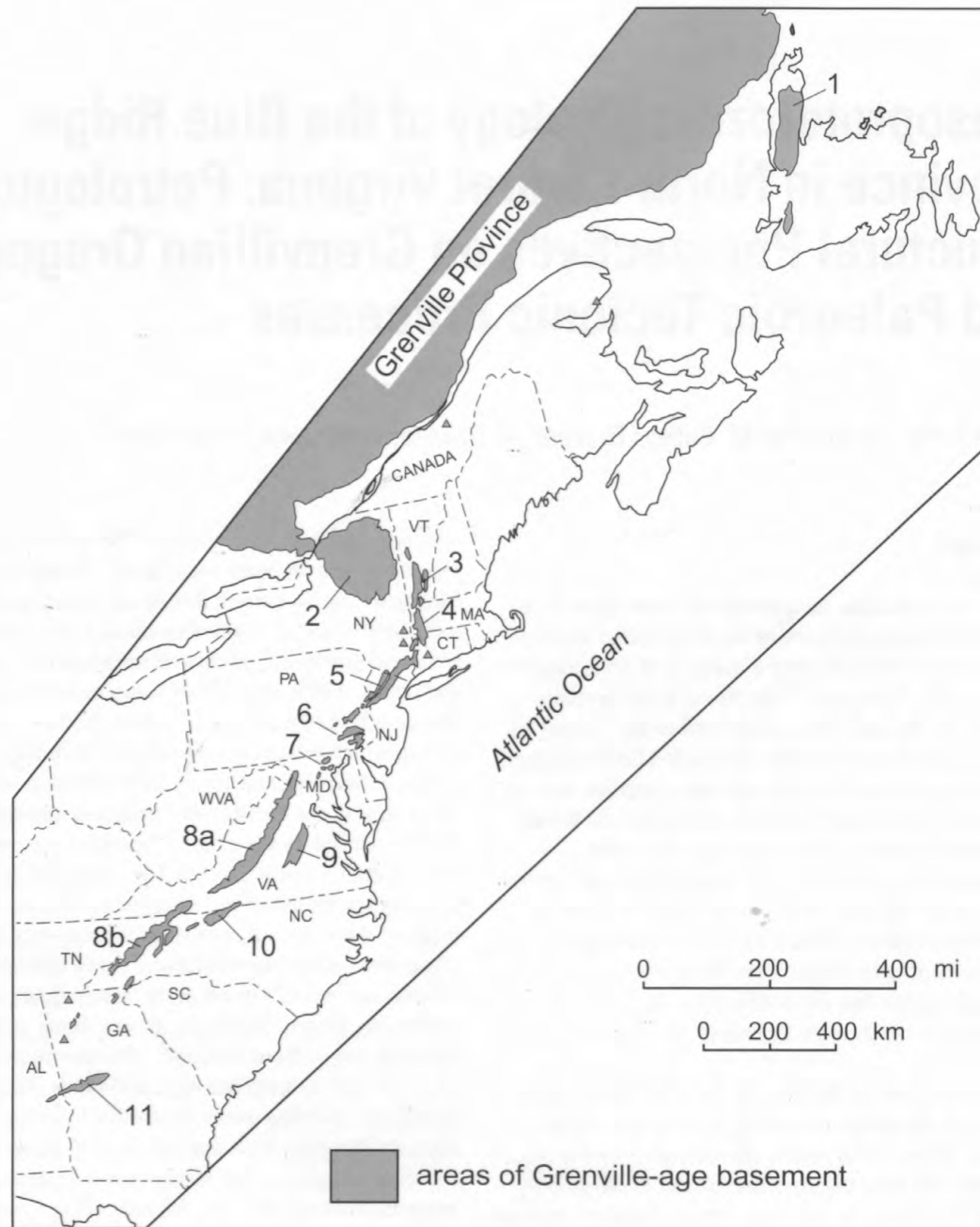
Figure 1. Map showing locations of major occurrences of Grenville-age basement in eastern North America. Labelled areas include: 1, Long Range massif; 2, Adirondack massif; 3, Green Mountains massif; 4, Berkshire massif; 5, Hudson Highlands–New Jersey Highlands–Reading prong; 6, Honey Brook upland; 7, Baltimore Gneiss antiforms; 8, Blue Ridge province, including Shenandoah (8a) and French Broad (8b) massifs; 9, Goochland terrane; 10, Sauratown Mountains anticlinorium; and 11, Pine Mountain belt. Map modified after Rankin and others (1989a).

northern Virginia, defines a northeast-trending anticlinorium that is overturned toward the northwest with Mesoproterozoic basement rocks constituting most of the core and a Neoproterozoic to lower Paleozoic cover sequence defining the limbs (Virginia Division of Mineral Resources, 1993) (fig. 2).

The igneous and high-grade metamorphic rocks of the basement preserve evidence of tectonic events associated with Grenvillian orogenesis at 1.2 to 1.0 Ga. These events resulted

from a series of dominantly convergent tectonic events marking accretion of Laurentia and eventual assembly of the supercontinent Rodinia (Dalziel and others, 2000). Locally within the Blue Ridge massifs, as throughout much of the Grenville province of North America, Grenvillian orogenesis involved polyphase metamorphism, high-temperature deformation, and both synorogenic and postorogenic magmatism. In the Blue Ridge, these processes resulted in formation of a Mesoproterozoic terrane

composed of a wide range of plutonic rocks of largely granitic composition that contain screens and inliers of preexisting country rocks.

Eastern Laurentia and the Grenvillian orogen experienced two episodes of crustal extension during the Neoproterozoic (Badger and Sinha, 1988; Aleinikoff and others, 1995). Magmatic rocks formed during the first episode include granitoids and associated volcanic deposits of the 730- to 700-Ma Robertson River batholith (Tollo and Aleinikoff, 1996) and other smaller plutons that occur throughout the Blue Ridge province of Virginia and North Carolina. Collectively, these plutons were emplaced across the region during crustal extension at 760 to 680 Ma (Fetter and Goldberg, 1995; Su and others, 1994; Bailey and Tollo, 1998; Tollo and others, 2004). This earlier episode of encratonic rifting resulted in development of local-scale rift basins in which terrestrial and marine sedimentary deposits of the Fauquier, Lynchburg, and Mechum River, and Swift Run Formations were deposited (Wehr, 1988; Tollo and Hutson, 1996; Bailey and Peters, 1998). However, this episode of rifting did not lead to development of an ocean.

A second episode of Neoproterozoic extension at about 570 Ma produced extensive basaltic and relatively minor rhyolitic (only in the northern part of the anticlinorium) volcanism, ultimately resulting in creation of the pre-Atlantic Iapetus Ocean (Aleinikoff and others, 1995). The basaltic rocks produced during this latter episode constitute the Catoctin Formation, which includes a locally thick series of basaltic (now greenstone) lava flows and thin interlayered sedimentary deposits (Badger, 1989, 1999). Both the Catoctin basalts and sedimentary strata of the underlying and discontinuous Swift Run Formation were produced in a dynamic tectonic environment characterized by locally steep topography and local interaction between lava flows and stream systems, producing a series of complexly interlayered deposits that are well exposed on the western limb of the Blue Ridge anticlinorium (Simpson and Eriksson, 1989; Badger, 1999). Sedimentary deposits of the Lynchburg and Fauquier Formations, which underlie the Catoctin Formation on the east limb of the Blue Ridge anticlinorium, preserve a regional transition from braided-alluvial facies in the west to deeper-water facies in the east that is interpreted to result from a late Neoproterozoic hinge zone developed in response to extension-related crustal thinning (Wehr, 1988). The Catoctin Formation is overlain by rocks of the late Neoproterozoic to Early Cambrian Chilhowee Group and younger Paleozoic strata that were deposited on the rifted Laurentian margin during Iapetan onlap and represent local development of a tectonically passive margin (Simpson and Eriksson, 1989).

Blue Ridge basement rocks include igneous and metamorphic rocks containing orthopyroxene-bearing mineral assemblages (Rankin and others, 1989b; Bailey and others, 2003) that, in the latter, indicate that ambient metamorphic conditions reached granulite facies during Mesoproterozoic orogenesis (Spear, 1993). Many of these basement rocks and most of the overlying cover sequence display mineralogic evidence of

metamorphism at upper greenschist-facies conditions that occurred as a result of Paleozoic orogenesis (Kunk and Burton, 1999). Paleozoic metamorphism is responsible for development of greenstone and chlorite-rich phyllite throughout the Catoctin Formation and some of the related cover rocks, and for production of retrograde minerals in the basement rocks such as biotite, chlorite, and uralitic amphibole.

Mesoproterozoic Basement Rocks
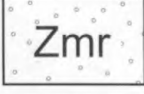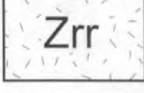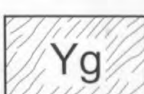
Introduction

Basement rocks of the Virginia Blue Ridge include a diverse assemblage of granitoids and gneissic lithologies that were emplaced in thickened crust and locally metamorphosed at high-grade conditions at about 1.2 to 1.0 Ga (Aleinikoff and others, 2000; Tollo and others, in press a). The oldest rocks, which include a compositionally variable group of gneisses and deformed granitoids, typically display widespread evidence of penetrative ductile deformation. These rocks occur both as regional map units and as smaller inliers that form screens and probable roof pendants within younger intrusive bodies (fig. 3). The younger, more areally extensive group is composed mostly of compositionally diverse granitoids that are variably deformed. Granitoids throughout the area vary widely in mineralogic composition, ranging from quartz monzonite to leucocratic alkali feldspar granite (fig. 4; table 1). Both age groups include orthopyroxene-bearing charnockitic types (table 2). Most rocks exhibit geochemical characteristics that indicate derivation from crustal sources and show compositional similarities to granitic rocks produced in within-plate tectonic settings (Tollo and others, in press a).

Blue Ridge basement rocks were historically divided into two regional suites based largely on mineralogy and inferred metamorphic grade. Bloomer and Werner (1955) grouped a wide spectrum of orthopyroxene-bearing rocks into the Pedlar Formation, distinguishing these mostly high-grade rocks from lower grade, biotite±amphibole-bearing varieties designated as the Lovingston Formation by Jonas (1928). Bartholomew and others (1981) extended this classification through definition of the areally extensive Pedlar and Lovingston massifs, wherein the former occurs west of the north-south-trending Rockfish Valley fault zone (and its along-strike extensions) and the latter occurs east of this structural feature. According to this model, rocks of the lower-grade Lovingston massif were juxtaposed against the Pedlar massif as a result of movement along the Rockfish Valley fault zone (Bartholomew and others, 1981; Sinha and Bartholomew, 1984). In proposing an alternative explanation for this lithologic juxtaposition, Evans (1991) suggested that the biotite-bearing assemblages of the Lovingston terrane were produced through fluid-enhanced retrograde metamorphic recrystallization of original orthopyroxene-bearing rocks. However, results from recent studies sug-
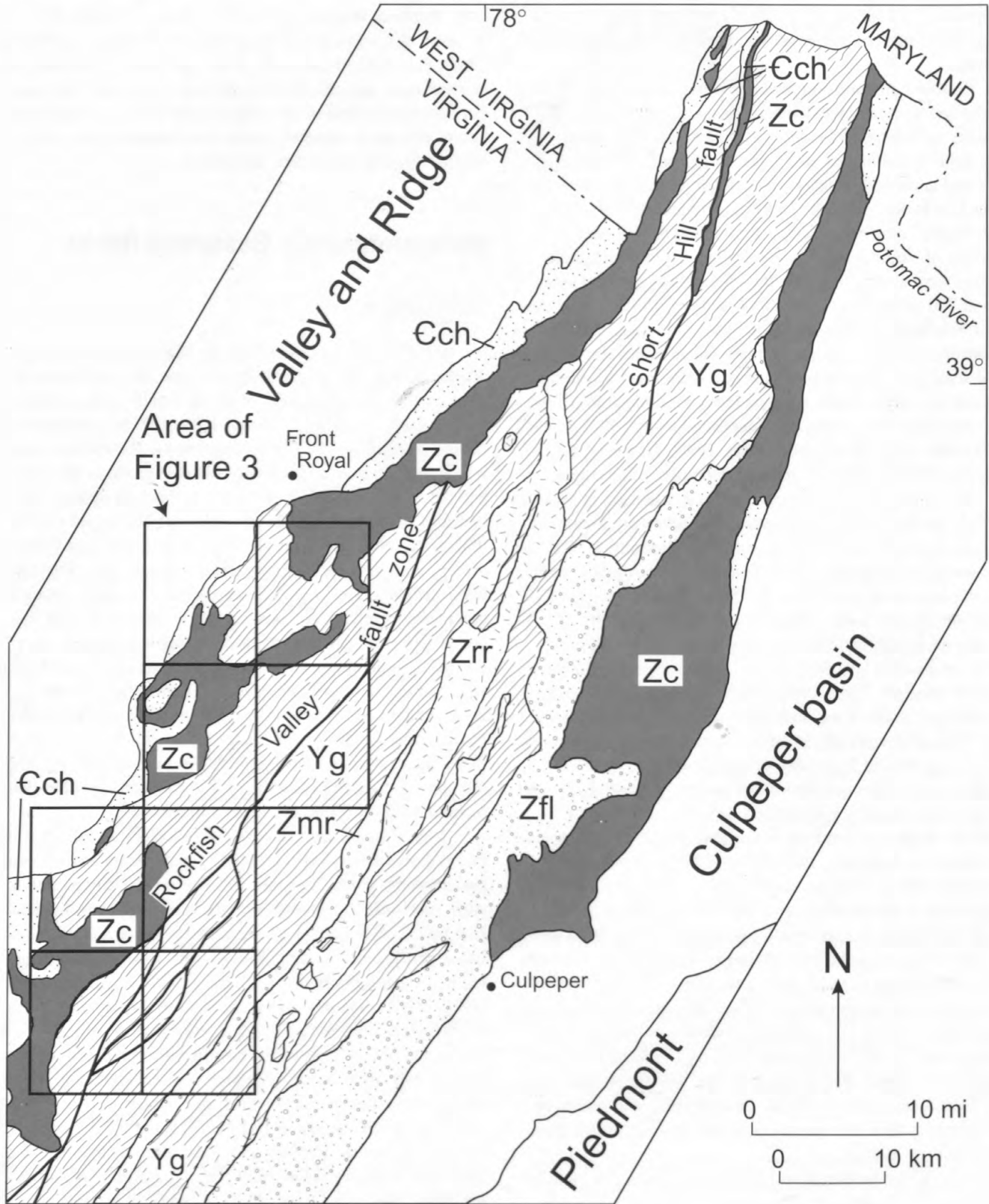
EXPLANATION

Era/Period		Formation
Early Cambrian	€ch	Chilhowee Group
Neoproterozoic	Zc	Catoctin Formation
	Zfl	Lynchburg/Fauquier Formation
	Zmr	Mechum River Formation
	Zrr	Robertson River batholith
Mesoproterozoic	Yg	Blue Ridge Basement Complex (undifferentiated)

Figure 2 (this page and opposite page). Generalized geologic map of the northern Blue Ridge anticlinorium in Virginia. Outlined area corresponds to 7.5-minute quadrangles illustrated in figure 3. Map modified after Virginia Division of Mineral Resources (1993).

gest that neither model adequately accounts for the observed regional distribution of rocks. For example, recent detailed mapping and related structural studies indicate that the areal distribution of lithologies is more heterogeneous than indicated by the reconnaissance mapping that formed the basis of the earlier studies (Bailey and others, 2003; Tollo and others, in press b). Recent field-based studies also indicate that other ductile fault zones may have played a more significant role in the tectonic evolution of the north-central and northern Blue Ridge, thus diminishing the structural significance of the Rockfish Valley fault zone, especially in the north-central Blue Ridge (Bailey, 2003). Additionally, recent advances regarding the petrology of charnockitic rocks indicate that formation of orthorhombic pyroxene in the igneous systems that constitute the protoliths of most of the Blue Ridge Mesoproterozoic rocks is controlled by numerous characteristics of the original melt, such as aH_2O, pCO_2, $Fe/(Fe+Mg)$, and depth of crystallization, and is thus not necessarily a reflection of ambient metamorphic grade (Frost and others, 2000).

U-Pb Geochronology

Zircons were extracted from seven samples of

Mesoproterozoic basement rocks from the field area for U-Pb geochronology. In all samples, zircon generally is medium to dark brown, subhedral to euhedral, stubby to elongate prisms. Zircons in all samples contain multiple age components, a characteristic illustrated by igneous zircons in rocks from other studies of Grenvillian basement in the Blue Ridge and elsewhere (McLelland and others, 2001; Aleinikoff and others, 2000; Carrigan and others, 2003; Hamilton and others, in press). As a result, we decided to analyze the zircons using the high-spatial-resolution capabilities of spot analysis by the sensitive high-resolution ion microprobe (SHRIMP).

Areas on zircons about 25 microns in diameter by 1 micron in depth were dated using SHRIMP. Prior to isotopic analysis, all zircons were photographed in transmitted and reflected light, and imaged in cathodoluminescence (CL) on a scanning electron microscope. Analysis locations were chosen on the basis of crystal homogeneity (lack of cracks, inclusions, and other imperfections as shown by transmitted light photographs) and apparent age homogeneity (cores and overgrowths can usually be distinguished using CL). In all samples except SNP-02-197 (garnetiferous syenogranite, Ygg), igneous cores are distinct and obvious. Observed under CL illumination, cores typically contain concentric, euhedral, oscillatory, compositional zoning, consistent with crystalliza-

N

0 _____ 5 miles

0 _____ 5 km

Quadrangle Key
B: Bentonville
CG: Chester Gap
TG: Thornton Gap
W: Washington
ORM: Old Rag Mountain
BM: Big Meadows
F: Fletcher
M: Madison
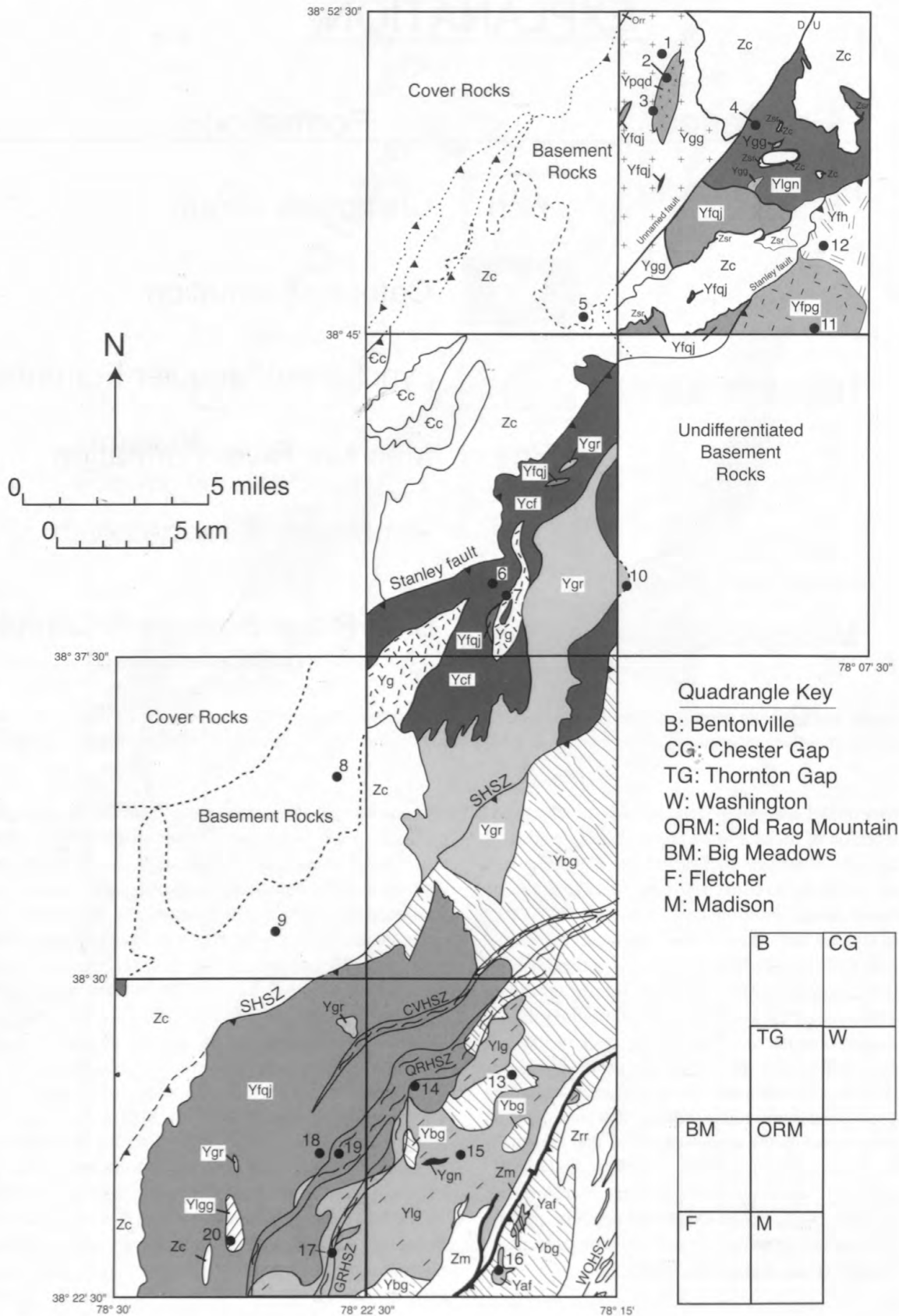
EXPLANATION TO FIGURE 3 AND SUMMARY OF LITHOLOGIC UNITS

Neoproterozoic to Lower Paleozoic Cover Rocks

Orr   Rockdale Run Formation

Cc   Chilhowee Group

Zc   Catoctin Formation

Zsr   Swift Run Formation

Neoproterozoic Extension-Related Rocks (730-700 Ma)

Zm   Mechum River Formation

Zrr   Robertson River batholith

Mesoproterozoic Basement

Lithologic Units Dated by U-Pb Isotopic Analysis	Lithologic Units With Ages Constrained by Field Relations	Lithologic Units With Unconstrained Ages
Yfqj low-silica charnockite		
Ygr Old Rag magmatic suite ≈ Yaf alkali feldspar granite		
Ygg garnetiferous syenogranite		
Ylgg leucogranite gneiss		
Yfpg foliated pyroxene granite	Ybg biotite granitoid gneiss	
		Ypqd pyroxene quartz diorite
	Yfh Flint Hill Gneiss	
Ycf high-silica charnockite		
Ylg leucogranite and foliated megacrystic leucocratic granite	Yg garnetiferous granite gneiss	Ylgn layered gneiss
	Ygn garnetiferous gneiss	

regional faults

high-strain zone

• 10   Field trip stop
(numbers keyed to text)

SHSZ: Sperryville high-strain zone
CVHSZ: Champlain Valley high-strain zone
QRHSZ: Quaker Run high-strain zone
GRHSZ: Garth Run high-strain zone
WOHSZ: White Oak high-strain zone

Figure 3 (this page and opposite page). Geologic map of basement rocks in the field trip area. Numbered locations refer to field trip stops described in the text. Geology is shown only where mapped in detail. Geology of the Madison 7.5-minute quadrangle is adapted from Bailey and others (2003).
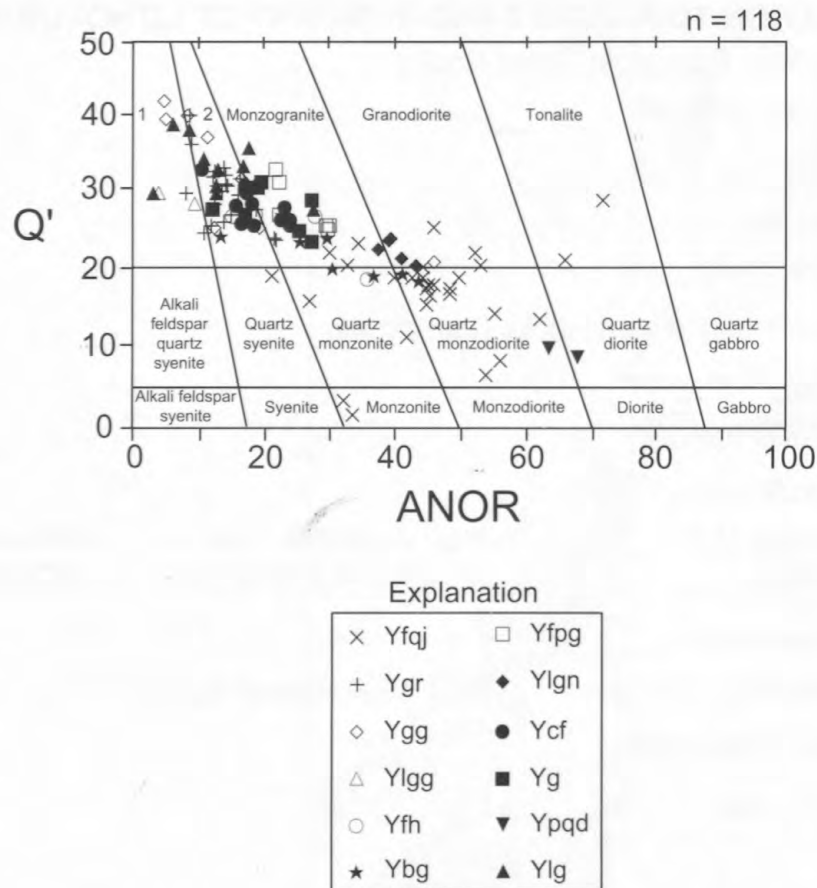
Figure 4. Plot of normative [anorthite/(orthoclase+anorthite)] × 100 versus normative [quartz/(quartz+orthoclase+albite+anorthite)] × 100 (ANOR versus Q′, after Streckeisen and Le Maitre, 1979). Normative compositions calculated with $Fe^{2+}/Fe_{total}=0.9$. Numbered field labels include (1) alkali feldspar granite, and (2) syenogranite. Abbreviations for lithologic units include: Yfqj, low-silica charnockite (*farsundite and quartz jotunite*); Ygr, Old Rag magmatic suite (after Hackley, 1999); Ygg, garnetiferous alkali feldspar granite and syenogranite; Ylgg, leucogranite gneiss; Yfh, Flint Hill Gneiss; Ybg, biotite granitoid gneiss; Yfpg, foliated pyroxene granite; Ylgn, layered granodiorite gneiss; Ycf, high-silica charnockite (*charnockite and farsundite*); Yg, garnetiferous granite gneiss; Ypqd, pyroxene quartz diorite; Ylg, leucocratic granitoid and megacrystic granite gneiss.

tion in a magma (Hanchar and Miller, 1993; Hanchar and Rudnick, 1995). Most cores typically have Th/U of about 0.3 to 0.6. Metamorphic overgrowths usually are unzoned and have distinctive, very low Th/U of 0.01 to 0.1. Rare xenocrystic cores can be distinguished by locally rounded morphology and truncated oscillatory zoning.

Igneous crystallization ages of the seven dated samples range from 1,183±11 Ma to 1,050±8 Ma (table 3). All samples contain younger overgrowths with ages of about 1,040 to 1,020 Ma; a few overgrowths that apparently formed during a younger, post-Grenville event(s) have ages of about 1,000 to 980 Ma. Compared to most zircons of igneous origin, zircons in the garnetiferous syenogranite (Ygg) have very unusual CL zoning patterns. Although crosscutting relations are observed, it is impossible to determine which zone formed during igneous crystallization because the typical igneous concentric zoning patterns are lacking. Four age groups were resolved for this sample (table 3). On the basis of field relations, we conclude that the age group at 1,064±7 Ma is the most likely

time of crystallization of the garnetiferous syenogranite. Two older dates (1,135±6 Ma and 1,099±9 Ma) are interpreted as ages of inherited material; a younger age of 1,028±14 Ma probably represents the time of regional metamorphism, as indicated by overgrowth ages in other samples.

The age range of basement rocks in the study area is similar to ages of Grenville rocks elsewhere in the central and southern Appalachians. For example, in the northern Blue Ridge, Aleinikoff and others (2000) dated a series of gneisses and granitoids at about 1,150 to 1,050 Ma and noted three pulses of magmatic activity occurring at about 1,150 to 1,140 Ma, 1,110 Ma, and 1,075 to 1,050 Ma. In the southern Appalachians, Carrigan and others (2003) documented a regional pulse of granitic magmatism that occurred at ~1,165 to 1,150 Ma and presented evidence for nearly ubiquitous metamorphism at ~1,030 Ma. In the Adirondacks, McLelland and others (1996) recognized a similar geochronologic sequence for tectonomagmatic activity associated with Grenvillian orogenesis but including an older period, identify-

Table 1. Nomenclature for lithologic units within the field trip area.

Lithologic Unit	Descriptive Field Nomenclature[*]	General Petrologic Nomenclature[†]	Charnockitic Nomenclature[‡]
Yfqj	low-silica charnockite (5)	monzogranite to quartz monzodiorite	farsundite to quartz jotunite
Yaf	*alkali feldspar granite[§] (4)*		
Ygr	*Old Rag magmatic suite (3)*	*alkali feldspar granite to syenogranite*	*alkali feldspar charnockite to charnockite*
Ygg	*garnetiferous alkali feldspar granite and syenogranite (1)*	*alkali feldspar granite to syenogranite*	
Ylgg	*leucogranite gneiss (5)*	*alkali feldspar granite*	
Ybg	biotite granitoid gneiss (3)	monzogranite to quartz monzonite and quartz monzodiorite	
Yfh	Flint Hill Gneiss (1)	syenogranite to monzogranite	
Yfpg	foliated pyroxene granite (1)	monzogranite	farsundite
Ylgn	layered granodiorite gneiss (1)	granodiorite	opdalite
Ypqd	pyroxene quartz diorite (1)	quartz diorite	orthopyroxene quartz diorite
Ycf	high-silica charnockite (2)	syenogranite to monzogranite	charnockite to farsundite
Yg	garnetiferous granite gneiss (2)	syenogranite to monzogranite	charnockite to farsundite
Ygn	garnetiferous gneiss (4)		
Ylg	*leucocratic granitoid and foliated megacrystic leucocratic granite (4)*	*alkali feldspar granite to syenogranite*	

[*] Number following nomenclature refers to the 7.5-minute quadrangle containing the reference locality within the area of new mapping: (1) Chester Gap, (2) Thornton Gap, (3) Old Rag Mountain, (4) Madison, and (5) Fletcher.
[†] Nomenclature determined using molar normative compositions calculated on basis of $Fe^{2+}/Fe_{(total)} = 0.9$ plotted on Q' vs ANOR plot of Streckeisen and Le Maitre (1979).
[‡] Nomenclature following recommendations of Le Maitre and others (1989).
[§] Leucocratic rocks are indicated by italics.

Table 2. Field and petrologic characterisitics for lithologic units within the field trip area.

Lithologic Unit	Rock Type(s)*	Primary Minerals[†]	Accessory Minerals[†]	Megascopic Field Characteristics[†]
low-silica charnockite Yfqj	monzogranite to quartz monzodiorite (*farsundite to quartz jotunite*)	Mipt (Mc), Pl, Qtz, Opx, Amph, Cpx,	Ap, Ilm, Mag, Zrn, Ep, Act	medium- to very coarse-grained, massive to weakly foliated, lenticular magnetite-rich xenoliths, Af megacrysts
alkali feldspar granite Yaf	alkali feldspar granite	Af, Pl, Qtz, Bt	Ttn, Fe-Ti Oxides	coarse-grained, porphyritic, massive
Old Rag magmatic suite Ygr	alkali feldspar granite to syenogranite	Pt (Mc), Pl, Qtz, Opx, Grt, Bt	Ap, Ilm, Mag, Zrn, Ep, Act	medium- to very coarse-grained, massive to weakly foliated
garnetiferous syenogranite Ygg	alkali feldspar granite to syenogranite	Or, Pl, Qtz, Grt, Bt, Opx	Ap, Ilm, Zrn	medium- to very coarse-grained, weakly to locally strongly foliated, medium-grained Af dikes, rare pegmatite dikes
leucogranite gneiss Ylgg	alkali feldspar granite	Mept (Mc), Pl, gray Qtz, Bt	Ilm, Mag, Zrn, Ep, Ms	coarse- to very coarse-grained, strongly foliated, Mept megacrysts
biotite granitoid gneiss Ybg	monzogranite to quartz monzonite and quartz monzodiorite	Mc, Pl, Qtz, Bt	Ap, Ilm, Ttn, Zrn, Ep, Chl	medium- to coarse-grained, strongly foliated
Flint Hill Gneiss Yfh	syenogranite to monzogranite	Mc, Pl, Qtz, Bt, Chl	Ap, Leux, Ilm, Zrn	medium- to very coarse-grained, strongly foliated
foliated pyroxene granite Yfpg	monzogranite (*farsundite*)	Mc, Pl, Qtz, Opx, Amph, Bt	Ap, Ilm, Zrn	medium- to coarse-grained, strongly foliated, pegmatitic dikes, Grt leucogranite dikes
layered granodiorite gneiss Ylgn	granodiorite (*opdalite*)	Mc, Or, Pl, Qtz, Amph, Opx	Ap, Ilm, Zrn	medium- to coarse-grained, strongly foliated, gneissic layers locally folded, massive leucogranite sheets, boudins
pyroxene quartz diorite Ypqd	quartz diorite (*orthopyroxene quartz diorite*)	Or, Pl, Qtz, Opx, Bt	Ap, Mag, Zrn	medium-grained, moderately to strongly foliated, gneissic layering
high-silica charnockite Ycf	syenogranite to monzogranite (*charnockite to farsundite*)	Mipt, Pl, Qtz, Opx, Amph, Cpx	Ap, Ilm, Mag, Zrn, Ep, Act	coarse- to very coarse-grained, moderately to strongly foliated, locally prominent gneissic layering, Af megacrysts
garnetiferous granite gneiss Yg	syenogranite to monzogranite	Mipt, Pl, Qtz, Opx, Grt, Bt, Cpx	Ap, Ilm, Mag, Zrn, Chl	medium- to coarse-grained, strongly foliated, prominent gneissic layering
garnetiferous gneiss Ygn	granodiorite (*opdalite*)?	Af, Pl, Qtz, Gt, Opx	Ttn, Fe-Ti Oxides	fine- to coarse-grained, layered
(1) foliated megacrystic leucocratic granite (2) leucogranite Ylg	alkali feldspar granite to syenogranite	1) Mept (Mc & Or), Pl, Qtz, intergrown Bt & Chl 2) Mc, Pl, Qtz, minor secondary Bt	Zrn, Ep, Ttn	(1): coarse-grained, strongly foliated (2): medium-grained, massive to weakly foliated Unit also includes coarse-grained leucogranite pegmatite

* Rock types determined using molar normative compositions calculated on basis of $Fe^{2+}/Fe_{(total)} = 0.9$ plotted on Q' vs ANOR diagram of Streckeisen and Le Maitre (1979). Charnockitic nomenclature included in parentheses following recommendations of Le Maitre and others (1989).

[†]Abbreviations: Af, alkali feldspar; Leux, leucoxene; Mipt, microperthite; Mept, mesoperthite; Pt, perthite. Other abbreviations after Kretz (1983): Act, actinolite; Aln, allanite; Amph, amphibole; Ap, apatite; Bt, biotite; Cal, calcite; Chl, chlorite; Cpx, clinopyroxene; Ep, epidote; Fl, fluorite; Grt, garnet; Ilm, ilmenite; Mag, magnetite; Mc, microcline; Or, orthoclase; Opx, orthopyroxene; Pl, plagioclase; Qtz, quartz; Ttn, titanite; Zrn, zircon.

Table 3. SHRIMP U-Pb isotopic ages of basement rocks in the field trip area.

Lithologic Unit	Sample Number	Igneous Crystallization Age (Ma) [± 2 sigma]	Metamorphic Ages (Ma) [± 2 sigma]	Inheritance Ages (Ma) [± 2 sigma]
low-silica charnockite (Yfqj)	SNP-99-93	1050 ± 8	1018 ± 14	
Old Rag magmatic suite (coarse-grained leucogranite) (Ygr)	OR-97-35	1060 ± 5	1019 ± 15	
			979 ± 11	
		*1059 ± 8**	*1027 ± 9*	
garnetiferous syenogranite (Ygg)	SNP-02-197	1064 ± 7	1028 ± 14	1135 ± 6
				1099 ± 9
leucogranite gneiss (Ylgg)	SNP-99-90	1078 ± 9	1028 ± 10	
			997 ± 19	
foliated pyroxene granite (Yfpg)	SNP-02-177	1117 ± 14	1043 ± 12	1175 ± 14
high-silica charnockite (Ycf)	SNP-96-10	1159 ± 14	1052 ± 14	
foliated megacrystic leucocratic granite (Ylg)	SNP-02-189	1183 ± 11	1110 ± 38	
			1043 ± 16	

* monazite ages indicated by italics; all other ages obtained from zircon.

ing episodes at 1,350 to 1,190 Ma, about 1,090 Ma, and 1,090 to 1,030 Ma. The Adirondack ages overlap episodes of major magmatic and metamorphic events recognized in the Grenville province of Canada (Gower and Krogh, 2002) and suggest that the two areas share some aspects of orogenic activity. However, extrapolation of these tectonic events to the Blue Ridge is tempered by the allochthonous nature of the Blue Ridge and the possibility that the terrane was separated from the Adirondack-New England region by a major tectonic boundary during Grenvillian orogenesis (Bartholomew and Lewis, 1988).

Lithologies and age relations

Textures, compositional characteristics, and field relations suggest that nearly all basement rocks within the study area were originally igneous in origin. Nomenclature was determined using normative compositions and standard procedures recommended by the International Union of Geological Sciences (IUGS) because the locally very coarse grain size and strongly preferred orientation of fabrics in some rocks hindered direct application of standard modal-based proce-

dures. General petrologic nomenclature using parameters calculated from normative data are presented in table 1, with IUGS-recommended names for orthopyroxene-bearing varieties included where appropriate. The basement rocks collectively display a wide range of normative compositions; however, in most cases, individual lithologic units are characterized by relatively restricted compositional variation (fig. 4; table 4). Syenogranite to monzogranite compositions are most common, especially for the older rocks that predate local Grenvillian deformation. The low-silica charnockite (Yfqj), which includes numerous chemically consanguineous dikes of both similar and less-evolved composition, is characterized by the greatest internal variation, ranging from orthopyroxene-bearing monzogranite (*farsundite[1]*) to quartz monzodiorite (*quartz jotunite*). Older rocks that predate regional Grenvillian deformation are dominated by orthopyroxene-bearing, charnockitic granitoids, whereas rocks that postdate

---

[1]Nomenclature suggested for orthopyroxene-bearing rocks of probable igneous origin by Le Maitre and others (1989). Such terms are italicized wherever used throughout the text. Where charnockite is used to refer to orthopyroxene-bearing granitoids in general, it is not italicized.

Table 4. Geochemical data for basement rocks from the field trip area.

Stop	1	--	2	3	3	4
Map Unit	Ygg	Ygg	Ypqd	Ygg	Ypqd	Ylgn
Sample	SNP-03-197	SNP-01-164	SNP-01-175	SNP-01-174	SNP-01-155	SNP-01-150
SiO_2	64.10	68.94	55.29	72.51	63.51	66.49
TiO_2	0.23	0.51	1.71	0.45	1.20	0.79
Al_2O_3	18.44	16.13	16.49	14.63	15.18	15.83
Fe_2O_3*	6.59	3.02	9.33	1.92	9.19	5.08
MnO	0.26	0.03	0.14	0.03	0.13	0.07
MgO	0.28	0.42	4.78	0.40	4.54	1.04
CaO	2.92	1.30	6.54	1.17	1.93	3.43
Na_2O	4.13	2.59	3.00	2.14	1.85	2.95
K_2O	2.71	6.50	2.00	6.18	2.66	4.43
P_2O_5	0.11	0.16	0.52	0.14	0.05	0.20
Total	99.77	99.60	99.80	99.55	100.23	100.31
Rb	65.9	173.3	57.9	155.7	111.4	193.9
Ba	786	1524	1030	1198	726	896
Sr	511	327	993	308	194	213
Pb	39	44	11	49	17	26
$Th^\dagger$	38.20	21.68	0.59	50.9	5.9	3.6
U	1	0.8	0.63	1.9	1.1	n.d
Zr	331	305	188	286	259	388
Hf	10.38	10.98	6.55	9.30	7.88	11.37
Nb	7.8	7.9	6.7	4.4	12.1	12.5
Ta	0.42	0.47	0.70	0.60	1.10	1.28
Ni	1	3	32	3	35	5
Zn	41	54	130	23	192	87
Cr	20	24	144	30	139	34
Ga	27	24	25	17	22	23
V	1	17	161	11	168	45
La	103.2	100.6	39.2	120.2	35.0	45.7
Ce	323.4	203.1	79.4	264.1	70.0	108.7
Nd	121.4	79	47	102	32	54.5
Sm	16.83	9.55	8.43	17.12	6.56	10.85
Eu	2.02	2.48	2.66	2.00	1.91	2.01
Tb	1.65	0.71	1.04	1.37	1.51	1.77
Yb	5.21	1.1	1.80	2.0	5.7	4.6
Lu	0.79	0.16	0.28	0.25	0.92	0.65
Y	38.8	12.4	21.8	24.3	53.4	52.7
Sc	5.04	4.38	20.24	4.04	24.29	14.02
Ga/Al	2.77	2.81	2.86	2.20	2.74	2.75
A/CNK	1.23	1.18	0.87	1.19	1.61	1.00
FeOt/(FeOt+MgO)	0.95	0.87	0.64	0.81	0.65	0.81

* total iron expressed as Fe_2O_3.　　　　　　　　　　　　　　　　　　　　　　　　n.d.: not detected

　† elements measured by instrumental neutron activation (INA) analysis noted in italics; all other elements measured by X-ray fluorescence.

Table 4. Geochemical data for basement rocks from the field trip area.—Continued

Stop	4	5	5	6	7	--
Map Unit	dike	Ycf	Ycf	Ycf	Yg	Yfqj
Sample	SNP-01-149	SNP-01-142	SNP-01-143	SNP-96-10	SNP-96-1	SNP-96-17
SiO_2	50.03	74.58	70.09	69.78	68.37	63.75
TiO_2	2.72	0.30	0.46	0.74	0.64	1.29
Al_2O_3	14.03	12.84	14.22	13.64	14.93	15.22
Fe_2O_3*	10.10	2.57	4.09	4.23	4.22	5.97
MnO	0.15	0.02	0.04	0.07	0.06	0.09
MgO	6.61	0.25	0.40	0.66	0.70	1.23
CaO	7.12	1.00	1.93	2.29	2.45	3.51
Na_2O	2.58	1.94	2.33	2.38	3.19	3.17
K_2O	4.71	6.90	6.50	5.63	4.94	5.30
P_2O_5	1.61	0.04	0.15	0.19	0.18	0.47
Total	99.65	100.45	100.23	99.60	99.66	99.99
Rb	276	238.7	212.6	199.3	170.3	181.2
Ba	2388	563	870	668	986	1650
Sr	611	85	107	128	175	579
Pb	39	49	39	28	30	38
$Th^†$	7.2	40.0	10.93	2.3	12.0	2.2
U	2.0	3.5	1	0.7	n.d.	1.4
Zr	644	444	474	260	330	501
Hf	17.1	14.7	15.84	11.2	10.7	15.1
Nb	13.4	11.5	19.0	9.3	9.6	14.6
Ta	2.10	0.46	1.10	0.85	0.64	1.49
Ni	123	3	3	3	7	3
Zn	154	66	90	63	81	120
Cr	267	21	19	28	34	22
Ga	22	19	24	21	21	25
V	142	5	10	25	36	44
La	109.7	258.4	94.8	52.8	58.0	102.0
Ce	226.4	477.0	224.5	94.3	105.0	185.0
Nd	112	165	102	47	47	91
Sm	17.22	23.50	17.91	10.30	10.00	19.10
Eu	3.7	1.81	2.70	2.09	1.82	3.31
Tb	1.97	1.41	2.26	1.50	1.25	2.30
Yb	3.60	2.6	5.6	3.4	2.2	5.3
Lu	0.49	0.35	0.73	0.42	0.23	0.60
Y	42.3	31.4	72.6	38.2	26.2	63.5
Sc	20.88	2.44	8.75	8.90	9.08	11.30
Ga/Al	2.96	2.79	3.19	2.91	2.66	3.10
A/CNK	0.63	1.03	0.99	0.96	0.99	0.88
FeOt/(FeOt+MgO)	0.58	0.90	0.90	0.85	0.84	0.81

* total iron expressed as Fe_2O_3.   n.d.: not detected

   † elements measured by instrumental neutron activation (INA) analysis noted in italics; all other elements measured by X-ray fluorescence.

Table 4. Geochemical data for basement rocks from the field trip area.—Continued

Stop	--	--	11	12	13	14
Map Unit	Yor	Ygr-d	Yfpg	Yfh	Ybg	Yfqj
Sample	OR-97-35	OR-97-51	SNP-02-177	SNP-01-146	SNP-02-186	SNP-02-180
SiO_2	72.18	72.85	67.36	69.69	62.41	53.24
TiO_2	0.28	0.43	0.78	0.58	1.44	2.69
Al_2O_3	14.44	14.36	14.73	15.21	13.87	15.69
Fe_2O_3*	2.76	1.61	5.34	3.80	9.13	11.96
MnO	0.06	0.03	0.08	0.05	0.15	0.18
MgO	0.34	0.44	0.95	0.68	0.81	2.14
CaO	1.15	1.38	2.72	1.87	3.97	6.51
Na_2O	2.85	2.50	2.73	2.34	2.80	3.11
K_2O	6.04	5.69	4.83	6.13	4.43	2.72
P_2O_5	0.10	0.23	0.22	0.15	0.69	1.31
Total	100.19	99.53	99.74	100.49	99.70	99.55
Rb	305.1	240.6	186.2	166.7	109.1	52.8
Ba	425	746	863	951	2112	1926
Sr	80	151	161	170	314	633
Pb	65	53	28	28	28	19
$Th^{\dagger}$	75.1	53.8	15.00	3.19	1.40	1.4
U	9.5	4.2	1.5	n.d.	0.83	0.5
Zr	230	392	336	239	1354	988
Hf	9.0	12.1	13.07	9.26	43	22.90
Nb	10.9	12.6	10.4	8.6	25.2	35.5
Ta	0.72	0.68	1.1	0.50	1.4	1.57
Ni	2	2	8	5	1	2
Zn	70	48	77	64	249	241
Cr	25	18	39	27	11	21
Ga	25	24	22	20	25	30
V	8	10	49	33	39	95
La	112.0	170.9	69.5	46.2	83.6	117.8
Ce	202.0	339	129.2	100.4	170	250.2
Nd	81	130	61	42.9	106	127
Sm	20.80	23.70	10.82	7.06	18.87	28.61
Eu	0.91	1.49	1.72	1.83	5.0	4.51
Tb	3.61	1.45	0	0.85	1.9	3.24
Yb	10.2	1.5	3.9	1.9	4.6	5.40
Lu	1.10	0.22	0.57	0.27	0.73	0.8
Y	62.6	32.4	40.1	20.5	58.6	84.1
Sc	6.27	2.72	12.57	10.84	20.0	20.82
Ga/Al	3.27	3.16	2.82	2.48	3.41	3.61
A/CNK	1.09	1.12	1.00	1.10	0.83	0.79
FeOt/(FeOt+MgO)	0.88	0.77	0.84	0.83	0.91	0.83

* total iron expressed as Fe_2O_3.   n.d.: not detected

$\dagger$ elements measured by instrumental neutron activation (INA) analysis noted in italics; all other elements measured by X-ray fluorescence.

Table 4. Geochemical data for basement rocks from the field trip area.—Continued

Stop	15	20	20	20
Map Unit	Ylg2	Ylgg	Yfqj	Yfqj
Sample	SNP-03-199	SNP-99-90	SNP-99-91	SNP-99-92
SiO_2	75.67	74.26	62.57	58.59
TiO_2	0.14	0.20	1.58	1.78
Al_2O_3	12.65	13.93	13.87	15.44
Fe_2O_3*	0.85	1.94	9.45	10.79
MnO	0.02	0.02	0.12	0.17
MgO	0.01	0.22	0.85	2.99
CaO	0.61	0.79	3.26	2.16
Na_2O	3.02	3.15	2.35	3.40
K_2O	6.73	6.16	4.82	3.26
P_2O_5	0.02	0.04	0.60	0.85
Total	99.71	100.71	99.47	99.45
Rb	237.1	161.5	144.0	89.6
Ba	126	1009	2132	978
Sr	60	157	351	92
Pb	46	28	31	8
$Th^\dagger$	34.64	33.4	1.75	3.1
U	13	1.2	1.1	0.2
Zr	75	169	1676	1157
Hf	4.53	6.8	45.0	34.7
Nb	3.9	6.7	24.2	32.7
Ta	0.16	0.72	1.45	2.2
Ni	1	4	2	1
Zn	20	18	286	420
Cr	19	30	13	13
Ga	17	22	28	22
V	1	5	42	50
La	81.7	94	91.1	123.7
Ce	144.4	190	193	273
Nd	58.7	64	105	142
Sm	11.25	8.35	22.4	20.8
Eu	0.52	1.65	4.95	5.01
Tb	0.96	0.62	1.54	1.53
Yb	1.22	1.38	6.4	6.8
Lu	0.15	0.2	1.10	1.0
Y	10.6	8.1	69.7	83.1
Sc	3.19	3.75	18.71	20.35
Ga/Al	2.54	2.98	3.81	2.69
A/CNK	0.95	1.05	0.92	1.18
FeOt/(FeOt+MgO)	0.98	0.89	0.91	0.76

* total iron expressed as Fe_2O_3.

$\dagger$ elements measured by instrumental neutron activation (INA) analysis noted in italics; all other elements measured by X-ray fluorescence.

Table 5. Geochemical data for mafic dike rocks from the field trip area.

Stop	1	5	5	--	--	18	18	18	18
Sample	SNP-01-159	SNP-01-144	SNP-01-145	SNPD-99-1	SNPD-99-3	SNPD-99-7	SNPD-99-8	SNPD-99-9	SNPD-99-6
SiO_2	51.64	50.98	47.48	51.14	49.43	53.67	51.80	53.59	49.68
TiO_2	2.92	2.75	1.90	2.98	2.82	1.26	1.23	1.07	2.66
Al_2O_3	13.03	13.05	16.41	12.97	12.92	15.07	15.06	15.14	13.05
Fe_2O_3*	15.32	15.26	12.12	15.75	16.22	11.49	12.43	10.70	15.66
MnO	0.22	0.21	0.18	0.23	0.23	0.15	0.17	0.15	0.22
MgO	4.18	4.65	7.58	4.52	4.69	6.74	6.91	7.48	5.72
CaO	8.66	7.19	8.62	9.02	9.88	7.87	7.76	7.84	9.93
Na_2O	2.77	4.32	4.00	2.77	2.16	3.14	3.23	3.01	2.02
K_2O	0.97	0.81	0.66	0.97	1.06	0.72	0.77	0.64	0.81
P_2O_5	0.49	0.43	0.47	0.44	0.37	0.16	0.15	0.13	0.30
Total	100.22	99.66	99.43	100.79	99.79	100.27	99.50	99.75	100.04
Rb	20.4	40.6	40.1	32.2	25.3	18.3	20	16.5	18.8
Ba	353	338	201	373	326	197	249	246	313
Sr	340	168	279	282	263	369	299	358	227
Pb	5	5	12	3	2	4	5	4	2
Th[†]				1.74	1.86	0.64	1.00	0.89	1.34
U	n.d	n.d	n.d	0.4	0.4	0.2	0.0	0.2	0.4
Zr	267	297	151	270	229	78	100	106	197
Hf				7.1	6.5	2.2	3.0	3.1	5.4
Nb	17.0	19.9	18.7	20.1	22	4.6	5.4	6.5	17.1
Ta				1.17	1.44	0.29	0.38	0.43	1.14
Ni	9	25	122	26	36	130	108	104	48
Zn	160	170	129	158	136	97	115	114	140
Cr	20	52	276	54	107	385	278	249	124
Ga	23	21	19	22	21	19	20	20	20
V	316	321	125	329	303	115	132	130	291
La	25	22	14	26	21	10	13	10	17
Ce				54.2	49.5	17.7	23.9	24.3	40.0
Nd				30	30	10	14	14	21
Sm				7.12	6.92	2.76	3.45	3.74	6.37
Eu				2.41	2.40	1.06	1.23	1.35	1.98
Tb				1.52	1.40	0.49	0.58	0.70	1.24
Yb				3.7	3.2	1.0	1.4	1.3	3.0
Lu				0.48	0.47	0.15	0.22	0.18	0.40
Y	38.5	39.4	19.0	41.5	36.7	12.2	16.5	16.2	34
Sc				31.45	33.44	16.91	18.79	18.20	34.95

* total iron expressed as Fe_2O_3.   n.d.: not detected

[†] elements measured by instrumental neutron activation (INA) analysis noted in italics; all other elements measured by X-ray fluorescence.

deformation include both leucocratic granitoids ranging from alkali feldspar granite to syenogranite and low-silica charnockite that is likely unrelated to the contemporaneous leucocratic rocks. Results from U-Pb isotopic analysis of zircons indicate that mineralogically similar leucocratic granitoids were emplaced during each of the three magmatic intervals presently identified within the Blue Ridge study area. The ~1,180-Ma leucocratic granitoid and megacrystic leucocratic granite gneiss (Ylg), which also includes abundant leucogranite pegmatite, constitutes an intrusive complex characterized by multiple generations of igneous activity and represents the oldest dated rock in the region. Pervasively deformed screens and xenoliths of leucogranite gneiss (Ylgg) of ~1,080-Ma age occur within low-silica charnockite and represent the youngest intrusive unit presently recognized to predate regional Grenvillian deformation. Following deformation, magmatic activity continued to produce leucocratic granitoids represented by the garnetiferous syenogranite (Ygg), Old Rag magmatic suite (Ygr), and two small bodies of coarse-grained alkali feldspar granite (Yaf) exposed in the Madison quadrangle (fig. 3) which may be correlative with the larger Old Rag magmatic suite.

Geologic mapping and related studies throughout five contiguous 7.5-minute quadrangles in the north-central Blue Ridge (fig. 3) indicate that Mesoproterozic basement rocks define three groups based on age and field characteristics: (1) foliated rocks of about 1,180- to 1,160-Ma age, (2) foliated rocks of 1,115- to 1,080-Ma age, and (3) largely nonfoliated rocks of ≤1,060-Ma age. Each group is characterized by the following features.

Foliated rocks of 1,180- to 1,160-Ma age: This group comprises a compositionally diverse assemblage of lithologies, including leucocratic granitoids and granitoid gneisses, layered gneiss, and foliated charnockite. All rocks display evidence of pervasive, typically ductile deformation that is interpreted as Grenvillian in origin. Within the mapped quadrangles, this group includes the following lithologic units: (1) leucocratic granitoid and megacrystic leucocratic granite gneiss (Ylg); (2) high-silica charnockite (Ycf, *charnockite and farsundite*); (3) garnetiferous granite gneiss (Yg); and (4) garnetiferous gneiss (Ygn). Charnockitic layered granodiorite gneiss (Ylgn) may also belong to this group.

Foliated rocks of 1,115- to 1,080-Ma age: Rocks within this group also predate the major deformational event believed to be responsible for developing pervasive, high-temperature fabrics in many of the basement units. Two dated lithologic units are placed within this group: (1) foliated pyroxene granite (*farsundite*, Yfpg) and (2) leucogranite gneiss (Ylgg). Similar to the older high-silica charnockite (Ycf), the foliated pyroxene granite (Yfpg) contains abundant orthopyroxene of likely magmatic origin and is likewise also charnockitic.

Nonfoliated rocks of ≤1,060-Ma age: Nonfoliated lithologic units are interpreted as postorogenic with respect to the main period of Grenvillian deformation in the Blue Ridge. All rocks in this group within the field trip area are broadly

granitic and include the following: (1) garnetiferous syenogranite (Ygg); (2) the Old Rag magmatic suite (Hackley, 1999), which includes pyroxene-bearing leucogranites of varying grain size and mineralogical composition (Ygr); (3) alkali feldspar granite (Yaf); and (4) low-silica charnockite (Yfqj, *farsundite and quartz jotunite*). The compositionally similar granitic units (including Ygg, Ygr, and Yaf) are distinctive leucocratic rocks with high potassium feldspar to plagioclase ratios and likely constitute a regional suite.

In summary, results from recent field, petrologic, and geochronological studies indicate that basement rocks of the northern Blue Ridge preserve evidence of tectonomagmatic events that spanned over 160 m.y. of Grenvillian orogenesis (Aleinikoff and others, 2000; Tollo and others, in press a). Presently, ages derived from high-precision U-Pb isotopic analyses of zircons indicate that an early interval of magmatic activity occurred at about 1,180 to 1,140 Ma and involved granitoids (now gneisses and deformed megacrystic leucogranites) of considerable compositional diversity. This episode was followed at about 1,110 Ma by a second period of magmatism presently defined by two compositionally dissimilar plutons within the northern Blue Ridge. Following another hiatus, plutonism resumed at about 1,080 Ma and was rapidly followed by a significant period of deformation that occurred within the interval 1,080 to 1,060 Ma. Most of the ductile fabrics developed in many of the older plutonic rocks were likely formed during this episode. Following deformation, plutonism continued to about 1,050 Ma, producing granitoids of considerable compositional diversity, including charnockite of A-type affinity. Isotopic evidence further indicates that thermal disturbances occurred throughout the region at 1,020 to 980 Ma. This temporal framework is similar to the sequence of Grenvillian events documented in the Adirondacks and Canadian Grenville province (McLelland and others, 1996; Rivers, 1997), suggesting the possibility of tectonic correlations between the Blue Ridge and these Laurentian terranes.

Geochemical characteristics

Geochemical data indicate that basement rocks within the field trip area are characterized by diverse chemical compositions and a range in silica content of nearly 30 weight percent (figs. 5A–F). Most lithologic units are felsic, containing ≥65 weight percent SiO_2, a compositional characteristic that is reflected in the abundance of granitoids throughout the field area (figs. 3, 4). Mafic to intermediate rock types are represented only by the low-silica charnockite (Yfqj) and foliated pyroxene quartz diorite (Ypqd), which form a large pluton and small inlier, respectively (fig. 3). Although variation for the region as a whole is extensive, most individual lithologic units are characterized by relatively modest chemical diversity, suggesting that significant differentiation did not occur at or near the emplacement level of most individual
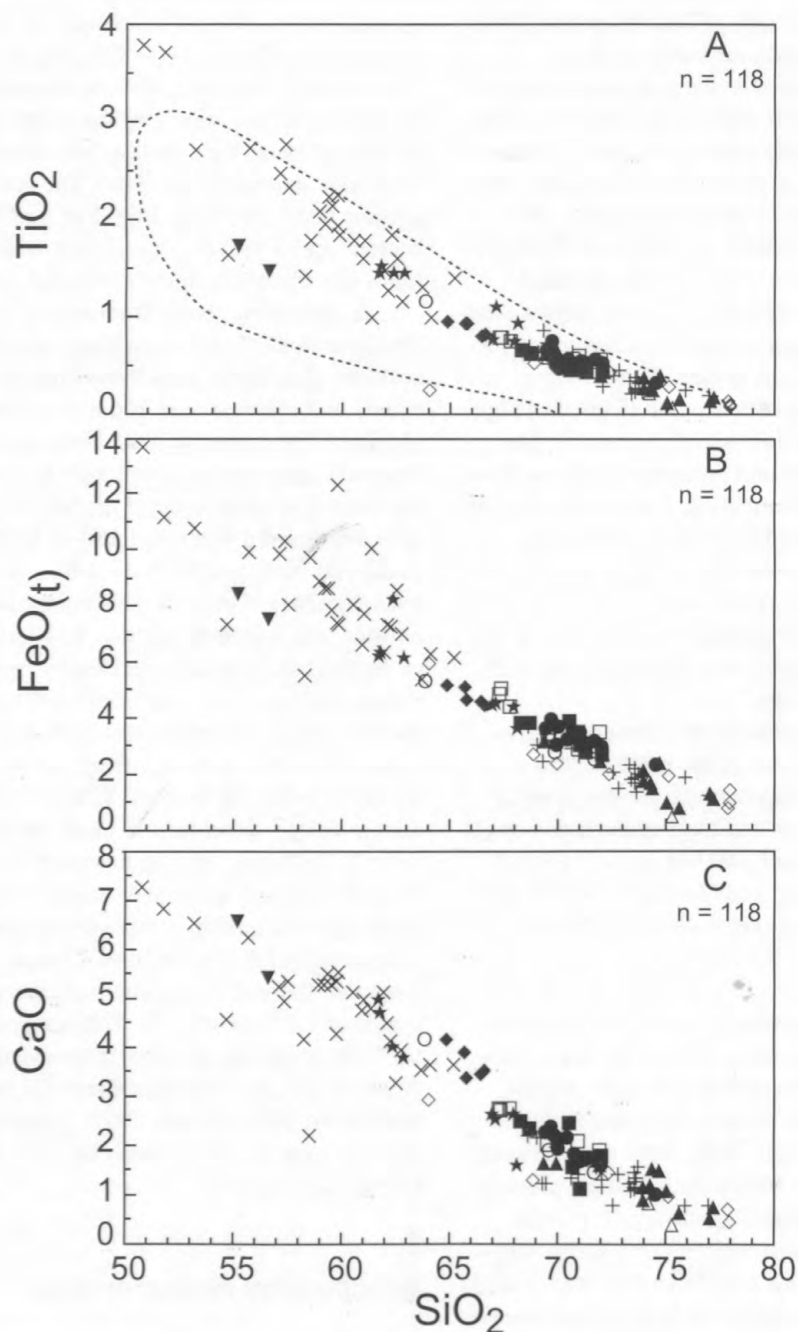
Figure 5. Plots of SiO_2 versus (A) TiO_2, (B) FeO_t (total iron expressed as FeO), (C) CaO, (D) aluminum saturation index (A/CNK=molar $Al_2O_3/(CaO+Na_2O+K_2O)$), (E) Na_2O+K_2O, and (F) FeO_t/MgO for basement rocks from the field trip area. Dashed line in A encloses field of igneous charnockites from Kilpatrick and Ellis (1992). Dashed line separating alkaline and subalkaline fields in E is from Irvine and Baragar (1971). Dashed line separating tholeiitic and calc-alkaline fields in F is from Miyashiro (1974). All data are expressed in weight percent. Symbols are the same as in figure 4.

plutons. In contrast to most lithologic units, the low-silica charnockite (Yfqj) and biotite granitoid gneiss (Ybg) exhibit trends in compositional and normative variation that are both considerable and petrologically distinctive. The internally differentiated low-silica charnockite, which includes abundant compositionally related dikes and fractionated pegmatite (Tollo and others, in press a), ranges in silica content from 50

to 65 weight percent, defining about half of the variation documented to date in the study area (fig. 5). Chemical variations in the biotite granitoid gneiss are bimodal, with compositions clustering at about 62 and 67 weight percent SiO_2 (fig. 5). This compositional diversity corresponds to normative compositions ranging from syenogranite to quartz monzonite (fig. 4), and is likely a reflection of compositional layering that
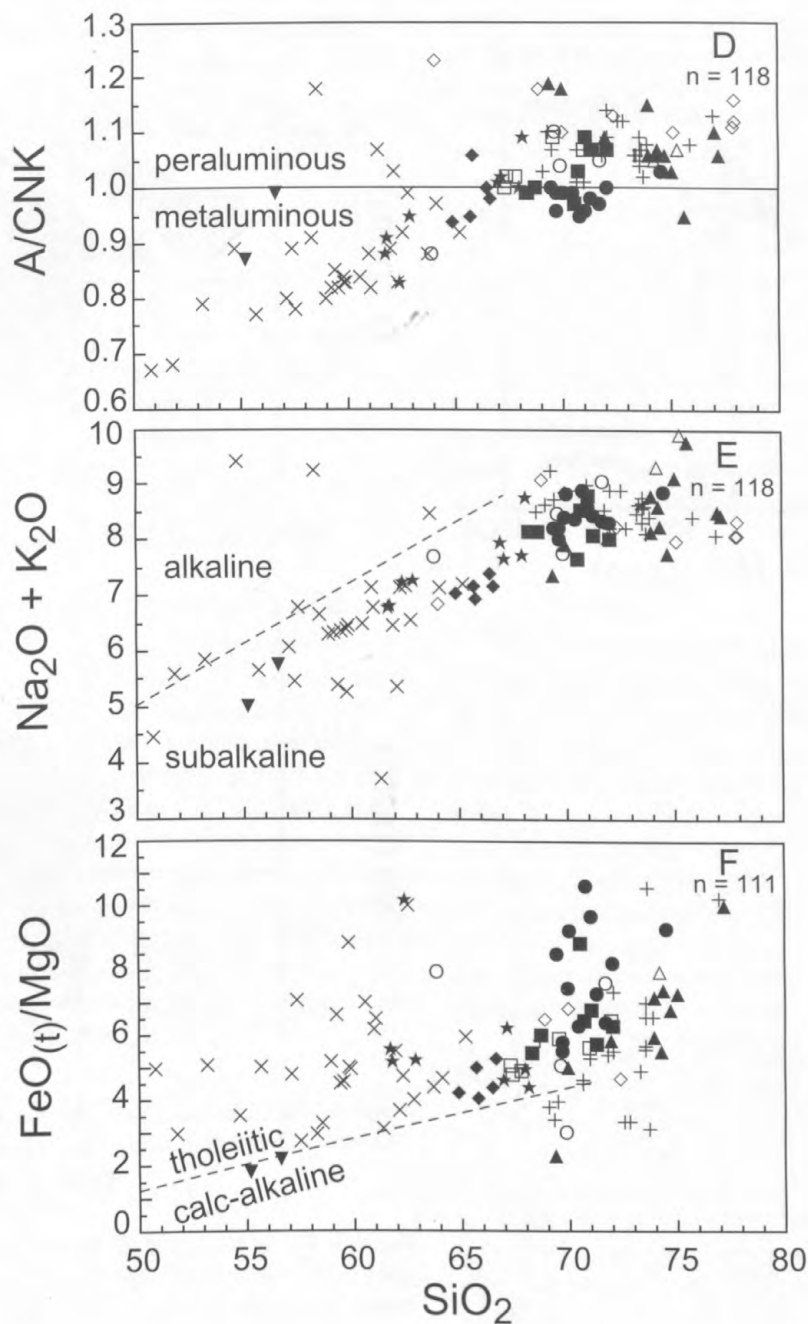
Figure 5. Continued

characterizes this lithologic unit in the field (Bailey and others, 2003; Hackley, 1999).

Most lithologic units are transitional metaluminous to peraluminous in composition, consistent with the typical pyroxene±amphibole mineral assemblages (fig. 5D); however, all leucogranitic rocks are characteristically peraluminous, as reflected in their locally biotite- and garnet-bearing compositions. Collectively, basement rocks within the field trip area are subalkaline and tholeiitic (figs. 5E and F, respectively), and thus share many compositional features with granitoids and charnockites of the classic anorthosite-mangerite-

charnockite-granite (AMCG) suites documented in the Adirondacks and other Precambrian massifs that include abundant intrusive rocks (McLelland and Whitney, 1990; Frost and Frost, 1997). Trace-element concentrations of most of the Blue Ridge granitoids plot in a region of the source-sensitive Nb+Y versus Rb diagram of Pearce and others (1984) (fig. 6) that is characteristic of granitoids emplaced in broadly defined post-orogenic geologic settings. Such compositional characteristics suggest that magmas were derived from mixed sources that included both crustal and arc-related components (Sylvester, 1989; Förster and others, 1997). As noted by previous studies
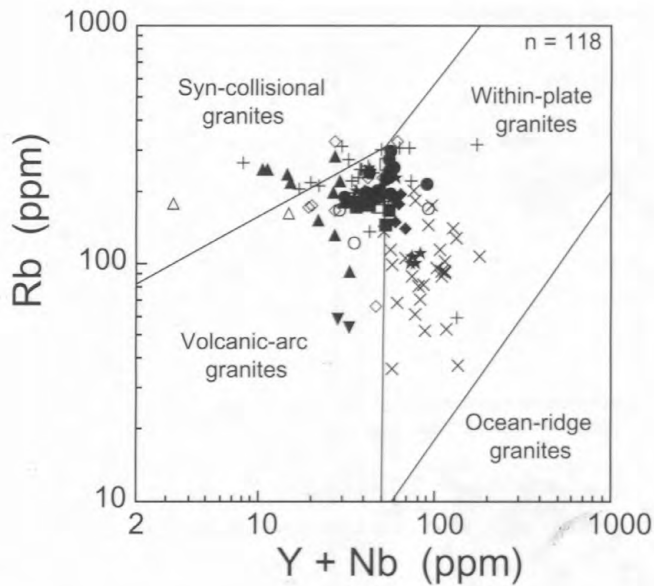
Figure 6. Plot of Y+Nb versus Rb for basement rocks from the field trip area. Symbols are the same as in figure 4. Diagram modified after Pearce and others (1984).

(Pearce and others, 1984; Sylvester, 1989; Maniar and Piccoli, 1989; Eby, 1990, 1992; Förster and others, 1997), granites associated with postorogenic processes and (or) within-plate tectonic environments include both anorogenic and postorogenic types. Such suites typically include A-type granitoids characterized by broad compositional variation that reflects derivation from sources of mixed origin (Sylvester, 1989; Eby, 1990, 1992; Förster and others, 1997). Geochemical data indicate that the low-silica charnockite (Yfqj) displays considerable similarity to A-type granitoids, whereas most other rocks within the study area exhibit compositional features that are transitional between I- and A-types (fig. 7) (Tollo and others, in press a). The contemporaneous low-silica charnockite and leucogranitoids (Ygr, Ygg, and Yaf) display compositional characteristics, such as comparable FeO/MgO (fig. 5F) and similar Eu/Eu* (not shown), which suggest that these contrasting rock types are unlikely to define a continuous liquid line of descent. The occurrence of A-type and relatively evolved I-type granitoids that are closely related in both space and time is not unusual in orogenic belts worldwide, as illustrated by examples from Australia (Landenberger and Collins, 1996).
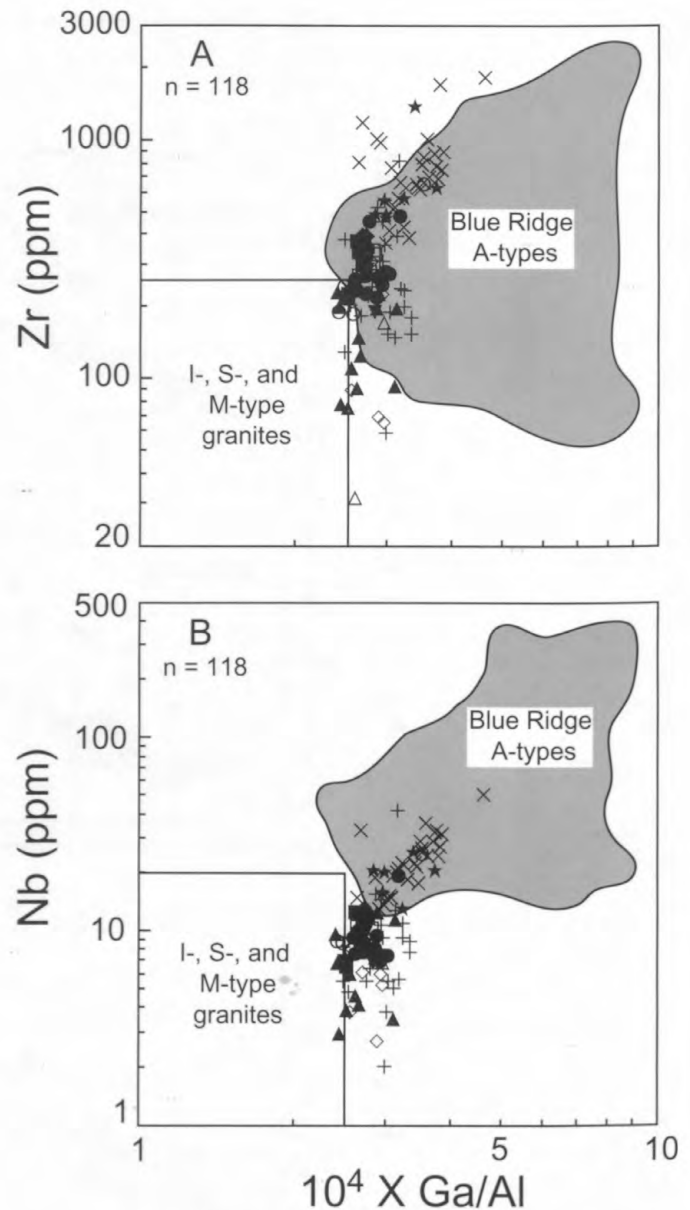
Figure 7. Plot of (A) Zr and (B) Nb versus $10^4 \times$ Ga/Al for basement rocks from the field trip area, compared to Neoproterozoic A-type granitoids from the central Appalachians (shaded field, 150 analyses from Tollo and Aleinikoff, 1996; Tollo and others, in press a). Diagrams modified after Whalen and others (1987). Symbols are the same as in figure 4.

The Blue Ridge rocks thus appear to have been derived through melting of mixed sources present in the evolving Grenvillian orogenic belt. Compositionally transitional intermediate and felsic rocks, including peraluminous leucogranites, were emplaced episodically over a 100-m.y. time span that largely predated local orogenesis at 1,080 to 1,060 Ma. Peraluminous leucogranitoids and low-silica charnockite,
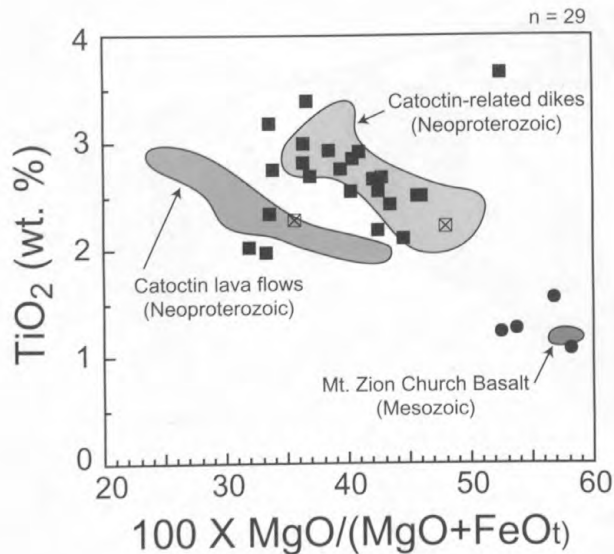
Figure 8. Plot of $100(MgO/MgO+FeO_t)$ versus TiO_2 for mafic (metabasalt, metadiabase, and diabase) dikes of inferred late Neoproterozoic (25 samples, filled squares) and Early Jurassic (4 samples, filled circles) age that intrude basement rocks within the field trip area. Data for samples of two greenstone dikes (squares with diagonal crosses) that intrude basement are also plotted. Data from Hackley (1999), Wilson and Tollo (2001), and Tollo and others (in press b). Compositional fields for (a) relatively unaltered lava flows from the Neoproterozoic Catoctin Formation (10 samples; Badger, 1989), (b) mafic dikes associated with and assumed to be contemporaneous with the Catoctin Formation (20 samples; Badger, 1989), and (c) Early Jurassic Mount Zion Church Basalt from the nearby Culpeper basin (18 samples; Tollo and others, 1988) are plotted for comparison.

which geochemical data suggest were derived from separate sources, postdated orogenesis and marked the termination of local magmatic activity.

Structural Relations

Mesoproterozoic

The older Mesoproterozoic units (>1,060 Ma) commonly display foliations and compositional layers that developed under high-grade metamorphic conditions during Grenvillian orogenesis. Foliation is defined by aligned feldspars and quartz aggregates, and individual grains have a very weak grain-shape preferred orientation with straight grain boundaries. Microstructures and certain mineral assemblages that define this foliation, such as orthopyroxene+garnet, are consistent with high-temperature (>600°C) upper amphibolite- to granulite-facies conditions (Passchier and Trouw, 1996). Regionally, this foliation generally strikes approximately east-west and dips steeply to both the north and south. Folded foli-

ation is only rarely observed, but at some outcrops it is axial planar to folds developed in competent layers such as coarse-grained leucogranitic dikes. The kinematics of this high-grade deformation are unclear; however, based on foliation and fold orientations, the Blue Ridge basement experienced significant ~north-south (in present-day geometry) shortening during this event. The high-temperature fabric is best preserved in units with crystallization ages of >1,080 Ma (Yg, Ygn, Ylg, and Yfpg) and generally absent in units ~1,060 Ma. Grenvillian fabrics are cut and overprinted by a lower temperature foliation defined by greenschist-facies metamorphic minerals and microstructures of probable Paleozoic age. Such low-grade fabrics are present in numerous mafic dikes of late Neoproterozoic age that locally intrude basement but are absent in mafic dikes of probable Mesozoic age. Such dikes are also compositionally distinguishable on the basis of TiO_2 content (fig. 8).

Paleozoic

The identification and interpretation of structural elements of Paleozoic age has evolved greatly during the past three decades, leading to recent recognition of the important role of high-strain zones in the structural development of the Blue Ridge. Indeed, recent discoveries regarding Paleozoic structures have called into question some longstanding ideas regarding the structural genesis of the terrane and have served as the basis for new developmental models of the Blue Ridge. Nevertheless, because of the complex, multi-stage structural evolution of the Blue Ridge, precise determination of timing relations characterizing such structural features remains in its infancy.

A younger fabric of probable Paleozoic age, defined by aligned phyllosilicates, elongate quartz, and fractured feldspars, is common in many Mesoproterozoic units. The foliation generally strikes to the northeast and dips moderately toward the southeast, and is commonly associated with a downdip mineral lineation. The microstructures and minerals that define this fabric are indicative of deformation that occurred at greenschist-facies conditions. In the northern Virginia Blue Ridge, Burton and others (1992) obtained late Paleozoic (~300 Ma) $^{40}Ar/^{39}Ar$ cooling ages on similar fabrics, whereas Furcron (1969) reported early Paleozoic (~450 Ma) K-Ar ages for metamorphic minerals in the Mechum River Formation in central Virginia.

Mitra (1977, 1979) was among the first to demonstrate the kinematic and mechanical significance of high-strain zones (ductile deformation zones) in the northern Virginia Blue Ridge. In central Virginia, Bartholomew and others (1981) named the Rockfish Valley fault zone and suggested that it forms a major tectonic boundary that separates Mesoproterozoic basement massifs (Pedlar and Lovingston) of distinctly different character. Bartholomew and others (1981) and Bartholomew and Lewis (1984) extended the Rockfish Valley fault zone northward from central Virginia to northern Virginia and linked it southward with the Fries fault
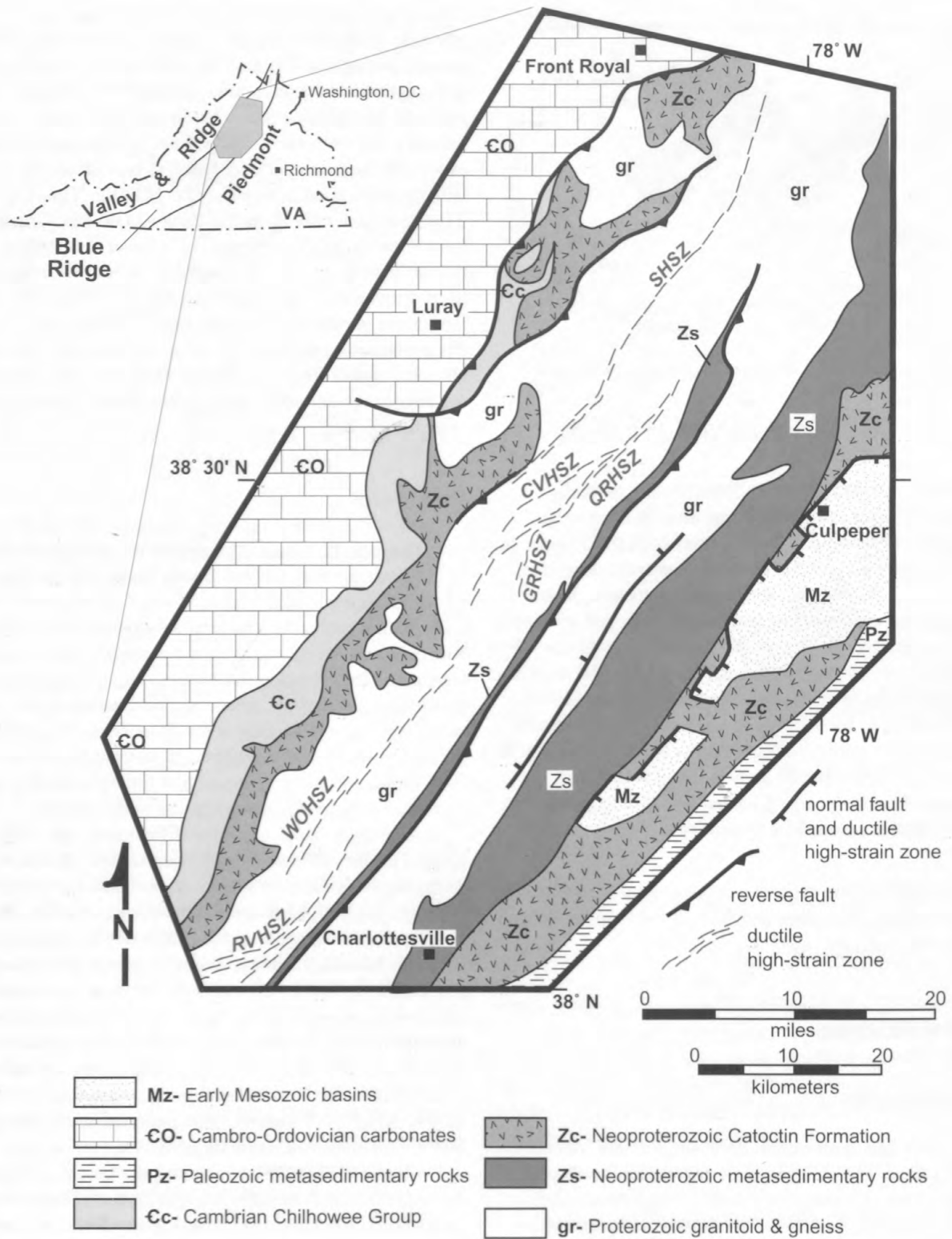
Figure 9. Generalized geologic map of the north-central Virginia Blue Ridge illustrating the location of major Paleozoic high-strain zones, including (from south to north) RVHSZ, Rockfish Valley high-strain zone; WOHSZ, White Oak high-strain zone; GRHSZ, Garth Run high-strain zone; QRHSZ, Quaker Run high-strain zone; CVHSZ, Champlain Valley high-strain zone; and SHSZ, Sperryville high-strain zone. Geology based, in part, on Virginia Division of Mineral Resources (1993); high-strain zones based on 1:24,000- and 1:100,000-scale mapping by authors.
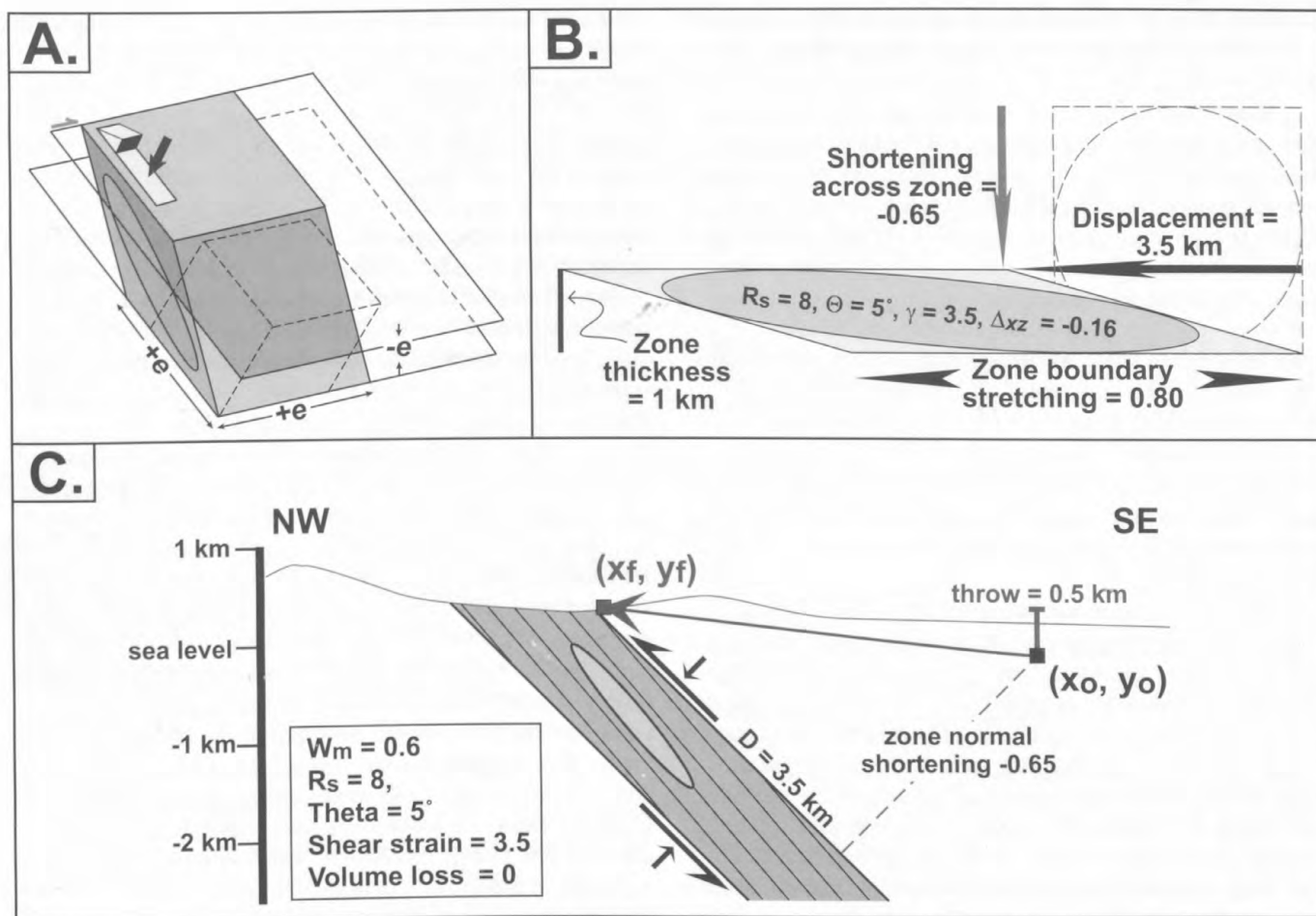
Figure 10. A, Idealized finite deformation for Blue Ridge high-strain zones characterized by a weak triclinic symmetry, general shear, and flattening strain (elongation in two directions, shortening in one). Ellipse represents XZ section of the three-dimensional finite strain ellipsoid. B, Kinematic model for deformation in the Quaker Run high-strain zone. The box and circle represent basement in undeformed state that is transformed into parallelogram and ellipse during homogeneous deformation. The model assumes a monoclinic deformation symmetry, general shear (W_m=0.6), flattening strain (K=0.6), and no volume loss (delta=0). The zone is ~1 km (0.6 mi) thick, the mean XZ strain ratio (R_{xz}) is 8:1 (based on strain estimates from quartz grain shapes), shear strain (gamma) is 3.5, and the orientation between the foliation and high-strain zone boundary (theta) is 5°. There is a sectional area loss (delta$_{xz}$ =-0.16) because of flattening strain with no volume change. Displacement across the zone is 3.5 km (2.2 mi) and is accompanied by 80 percent stretching parallel to the zone boundary and 65 percent shortening across the zone. C, Displacement, shortening, and tectonic throw across the Quaker Run high-strain zone viewed in cross section, based on deformation parameters illustrated in figure 10B. Rock exposed at (X_f,Y_f) originated at (X_o,Y_o) prior to deformation.

zone in the southern Virginia Blue Ridge. The temporal, kinematic, and tectonic significance of the Rockfish Valley zone has been discussed by a number of workers (Bartholomew and others, 1981; Conley, 1989; Simpson and Kalaghan, 1989; Bailey and Simpson, 1993; Burton and Southworth, in press). Different workers have variously interpreted the Rockfish Valley fault zone to be a reverse, normal, and strike-slip structure.

Recent mapping in the central and northern Virginia Blue Ridge (at both 1:24,000 and 1:100,000 scale) indicates that basement rocks are cut by a series of anastomosing high-strain fault zones (fig. 9) rather than by a single fault zone

(for example, the Rockfish Valley fault zone). Individual high-strain zones form northeast-southwest-striking belts of mylonitic rock, 0.5 to 3 km (0.3–1.9 mi) thick, that dip moderately to the southeast. Mineral elongation lineations plunge directly downdip to obliquely downdip. Deformation is heterogeneous and associated penetrative fabrics diminish away from the high-strain zones. From north to south, these zones include the Sperryville, Champlain Valley, Quaker Run, White Oak, and Rockfish Valley zones (fig. 9). Collectively, these zones display an en-echelon map pattern. Individual zones extend 30 to 100 km (19–60 mi) and pinch out along strike. Mylonitic rocks are characterized by microstructures

consistent with deformation occurring at greenschist-facies (~350–400°C) conditions with abundant fluids (Bailey and others, 1994).

Blue Ridge high-strain zones are characterized by both monoclinic and triclinic deformation symmetries (fig. 10) (Bailey and others, in press; Bailey, 2003). Triclinic symmetries are revealed by the geometry of fabric elements with respect to high-strain zone boundaries and fabric asymmetries on planes both parallel and normal to elongation lineations. Elongation lineations plunge to the southeast and kinematic indicators on XZ sections record a northwest-directed (reverse) sense of shear. Mylonitic rocks with a triclinic symmetry also record a component of strike-parallel sinistral shear. Strain ratios, measured with quartz grain shapes and boudinaged feldspars, range from 4 to 20 in XZ sections. Three-dimensional strains are moderately to strongly oblate (K=0.8–0.0). Vorticity analysis indicates that these high-strain zones experienced bulk general shear deformation (W_m=0.6–0.9).

The total displacement across individual high-strain zones, estimated by integrating shear strains over zone thickness, range from 1 to 4 km (0.6–2.5 mi) (fig. 10). Total displacement estimates are in accord with field relations demonstrating that, at many locations, the same basement unit occurs in both the footwall and hanging wall of the high-strain zone. These modest offsets are incompatible with tectonic models that suggest Blue Ridge high-strain zones separate distinctly different Grenvillian massifs. The kinematic significance of Blue Ridge high-strain zones indicates that (1) these zones accommodated significant crustal shortening, (2) displacement on these zones is on the order of a few kilometers, and (3) widespread flattening strains require significant strike-parallel (orogen-parallel) material movement (fig. 10).

The absolute age of movement on Blue Ridge high-strain zones is not precisely known. Field relations from the central Virginia Blue Ridge indicate that mylonitic high-strain zones are cut by brittle thrusts of Alleghanian (~320–280 Ma) age (Bailey and Simpson, 1993). Polvi (2003) reported an $^{40}Ar/^{39}Ar$ plateau age of 355±3 Ma for muscovite from a greenschist-facies contractional high-strain zone in Nelson County, located approximately 100 km (60 mi) southwest of the field trip area. This cooling age is incompatible with an Alleghanian age for ductile deformation, but could reflect cooling from either a Taconian (Ordovician) or Devonian event possibly synchronous with the Acadian orogeny in New England.

Summary and Regional Implications

The new mapping and supporting investigations of basement in the study area illustrate the lithologic complexity and protracted geologic evolution of rocks associated with Mesoproterozoic orogenesis. The structural studies indicate the importance of multiple high-strain zones in accommodating the effects of Paleozoic deformation within the Blue Ridge core, and suggest that the role of the Rockfish Valley

fault zone was not as significant as previously suggested. This finding necessitates a re-evaluation of models for Paleozoic structural development of the Blue Ridge that involve the Rockfish Valley fault zone as the dominant internal tectonic element responsible for the present distribution of major rock types in the anticlinorium. The lithologic variation documented in Blue Ridge basement rocks by these studies refines previous models of the province that were based largely on reconnaissance-scale mapping by demonstrating the complex juxtaposition of rocks of different composition, age, and tectonic significance. The dominance of granitic rocks in the study area is similar to the compositional characteristics documented elsewhere in the Appalachian massifs (for example, Rankin and others, 1989b; Carrigan and others, 2003). However, the lack of rocks generally associated with orogeny is noteworthy and contrasts with the presence of lithologies of calc-alkaline affinity in the Adirondacks (McLelland and others, 1996) and New Jersey Highlands (Volkert, in press). Results from geochronologic studies completed to date indicate that the northern Blue Ridge also differs from the well-documented Adirondacks in lacking rocks of >1,200-Ma age. Correspondingly, there is at present no evidence of Elzevirian orogenic processes in the Blue Ridge of Virginia, suggesting either that the province did not undergo this earlier pulse of Grenvillian orogenic activity that is otherwise well documented in the Adirondacks and some parts of the southeastern Canadian Grenville province (Rivers, 1997; Wasteneys and others, 1999; Gower and Krogh, 2002), or that the lithologic signature of this event was destroyed by subsequent Mesoproterozoic orogenesis. Nevertheless, trace-element geochemical characteristics of many of the Mesoproterozic granitic rocks of the northern Virginia Blue Ridge indicate the presence of components of calc-alkaline affinity in the magmatic sources, suggesting that pre-existing Laurentian crust contains evidence of pre-1,200-Ma tectonic processes (Tollo and others, in press a). The geochronology of basement rocks from the northern Blue Ridge indicates that the province shares many temporal characteristics with other Appalachian massifs (Aleinikoff and others, 1990; Carrigan and others, 2003; Hatcher and others, in press) and supports definition of the Appalachian outliers as outposts of Laurentian crust affected by Grenvillian orogenic processes (Rankin and others, 1989b). Nevertheless, the petrologic and compositional heterogeneity and substantial range in emplacement ages that characterize Blue Ridge basement rocks suggest that detailed correlation of events and processes recorded within individual massifs will depend on continued scientific advances.

References Cited

Aleinikoff, J.N., Burton, W.C., Lyttle, P.T., Nelson, A.E., and Southworth, C.S., 2000, U-Pb geochronology of zircon and monazite from Mesoproterozoic granitic gneisses of the northern Blue Ridge, Virginia and Maryland, USA:

Precambrian Research, v. 99, p. 113–146.

Aleinikoff, J.N., Ratcliffe, N.M., Burton, W.C., and Karabinos, P.A., 1990, U-Pb ages of Middle Proterozoic igneous and metamorphic events, Green Mountains, Vermont [abs.]: Geological Society of America Abstracts with Programs, v. 22, no. 2, p. 1.

Aleinikoff, J.N., Zartman, R.E., Walter, M., Rankin, D.W., Lyttle, P.T., and Burton, W.C., 1995, U-Pb ages of metarhyolites of the Catoctin and Mount Rogers Formations, central and southern Appalachians; Evidence for two pulses of Iapetan rifting: American Journal of Science, v. 295, p. 428–454.

Allen, R.M., 1963, Geology and mineral resources of Greene and Madison Counties, Virginia: Virginia Division of Mineral Resources Bulletin 78, 102 p.

Andersen, D.J., Lindsley, D.H., and Davidson, P.M., 1993, QUILF; A Pascal program to assess equilibria among Fe-Mg-Mn-Ti oxides, pyroxenes, olivine, and quartz: Computers and Geosciences, v. 19, no. 9, p. 1333–1350.

Badger, R.L., 1989, Geochemistry and petrogenesis of the Catoctin volcanic province, central Appalachians: Blacksburg, Virginia Polytechnic Institute, Ph.D thesis, 337 p.

Badger, R.L., 1999, Geology along Skyline Drive: Helena, Mont., Falcon Publishing, Inc., 100 p.

Badger, R.L., and Sinha, A.K., 1988, Age and Sr isotopic signature of the Catoctin volcanic province; Implications for subcrustal mantle evolution: Geology, v. 16, p. 692–695.

Bailey, C.M., 2003, Kinematic significance of monoclinic and triclinic high-strain zones in the Virginia Blue Ridge province [abs.]: Geological Society of America Abstracts with Programs, v. 35, no. 1, p. 21.

Bailey, C.M., and Peters, S.E., 1998, Glaciogenic sedimentation in the Late Neoproterozoic Mechum River Formation, Virginia: Geology, v. 26, p. 623–626.

Bailey, C.M., and Simpson, C., 1993, Extensional and contractional deformation in the Blue Ridge province, Virginia: Geological Society of America Bulletin, v. 105, p. 411–422.

Bailey, C.M., and Tollo, R.P., 1998, Late Neoproterozoic extension-related magma emplacement in the central Appalachians; An example from the Polly Wright Cove pluton: Journal of Geology, v. 106, p. 347–359.

Bailey, C.M., Berquist, P.J., Mager, S.M., Knight, B.D., Shotwell, N.L., and Gilmer, A.K., 2003, Bedrock geology of the Madison quadrangle, Virginia: Virginia Division of Mineral Resources Publication 157.

Bailey, C.M., Mager, S.M., Gilmer, A.G., and Marquis, M.N., in press, Monoclinic and triclinic high-strain zones; Examples from the Blue Ridge province, central Appalachians: Journal of Structural Geology.

Bailey, C.M., Simpson, C., and De Paor, D.G., 1994, Volume loss and tectonic flattening strain in granitic mylonites from the Blue Ridge province, central Appalachians: Journal of Structural Geology, v. 16, p. 1403–1416.

Bartholomew, M.J., and Lewis, S.E., 1984, Evolution of Grenville massifs in the Blue Ridge geologic province, southern and central Appalachians, in Bartholomew, M.J., Force, E.R., Sinha, A.K., and Herz, N., eds., The Grenville event in the Appalachians and related topics: Geological Society of America Special Paper 194, p. 229–254.

Bartholomew, M.J., and Lewis, S.E., 1988, Peregrination of Middle Proterozoic massifs and terranes within the Appalachian orogen, eastern U.S.A.: Trabajos de Geología, Universidad de Oviedo, v. 17, p. 155–165.

Bartholomew, M.J., Gathright, T.M., II, and Henika, W.S., 1981, A tectonic model for the Blue Ridge in central Virginia: American Journal of Science, v. 281, p. 1164–1183.

Berquist, P.J., and Bailey, C.M., 2000, Displacement across Paleozoic high-strain zones in the Blue Ridge province, Madison County, Virginia; The Pedlar and Lovingston massifs reconsidered [abs.]: Geological Society of America Abstracts with Programs, v. 32, no. 2, p. 4.

Bloomer, R.O., and Werner, H.J., 1955, Geology of the Blue Ridge in central Virginia: Geological Society of America Bulletin, v. 66, p. 579-606.

Burton, W.C., and Southworth, Scott, in press, Tectonic evolution of the northern Blue Ridge massif, Virginia and Maryland, in Tollo, R.P., Corriveau, L., McLelland, J., and Bartholomew, M.J., eds., Proterozoic tectonic evolution of the Grenville orogen in North America: Geological Society of America Memoir 197.

Burton, W.C., Froelich, A.J., Pomeroy, J.S., and Lee, K.Y., 1995, Geology of the Waterford quadrangle, Virginia and Maryland, and the Virginia part of the Point of Rocks quadrangle: U.S. Geological Survey Bulletin 2095, 30 p., scale 1:24,000.

Burton, W.C., Kunk, M.J., and Lyttle, P.T., 1992, Age constraints on the timing of regional cleavage formation in the Blue Ridge anticlinorium, northernmost Virginia [abs.]: Geological Society of America Abstracts with Programs, v. 24, no. 2, p. 5.

Carrigan, C.W., Miller, C.F., Fullagar, P.D., Bream, B.R., Hatcher, R.D., Jr., and Coath, C.D., 2003, Ion microprobe age and geochemistry of southern Appalachian basement, with implications for Proterozoic and Paleozoic reconstructions: Precambrian Research, v. 120, p. 1–36.

Clarke, J.W., 1984, The core of the Blue Ridge anticlinorium in northern Virginia, in Bartholomew, M.J., Force, E.R., Sinha, A.K., and Herz, N., eds., The Grenville event in the Appalachians and related topics: Geological Society of America Special Paper 194, p. 155–160.

Conley, J.F., 1989, Stratigraphy and structure across the Blue Ridge and Inner Piedmont in central Virginia: International Geological Congress Field trip guidebook T207, American Geophysical Union, 23 p.

Dalziel, I.W.D., Mosher, S., and Gahagan, L.M., 2000, Laurentia-Kalahari collision and the assembly of Rodinia: Journal of Geology, v. 108, p. 499–513.

Deer, W.A., Howie, R.A., and Zussman, J., 1992, An introduction to the rock-forming minerals: Essex, Addison Wesley Longman Limited, 696 p.

Duchesne, J.C., and Wilmart, E., 1997, Igneous charnockites and related rocks from the Bjerkreim-Sokndal layered intrusion (southwest Norway); A jotunite (hypersthene monzodiorite)-derived A-type granitoid suite: Journal of Petrology, v. 38, p. 337–369.

Eaton, L.S., Morgan, B.A., Kochel, R.C., and Howard, A.D., 2003, Role of debris flows in long term landscape denudation in the central Appalachians of Virginia: Geology, v. 31, no. 4, p. 339–342.

Eby, G.N., 1990, The A-type granitoids; A review of their occurrence and chemical characteristics and speculations on their petrogenesis: Lithos, v. 26, p. 115–134.

Eby, G.N., 1992, Chemical subdivision of the A-type granitoids; Petrogenetic and tectonic implications: Geology, v. 20, p. 641–644.

Evans, N.H., 1991, Latest Precambrian to Ordovician metamorphism in the Virginia Blue Ridge; Origin of the contrasting Lovingston and Pedlar basement massifs: American Journal of Science, v. 291, p. 425–452.

Fenneman, N.M., 1938, Physiography of eastern United States: New York, McGraw-Hill, 714 p.

Fetter, A.H., and Goldberg, S.A., 1995, Age and geochemical characteristics of bimodal magmatism in the Neoproterozoic Grandfather Mountain rift basin: Journal of Geology, v. 103, p. 313–326.

Förster, H.-J., Tischendorf, G., and Trumbull, R.B., 1997, An evaluation of the Rb vs. (Y+Nb) discrimination diagram to infer tectonic setting of silicic igneous rocks: Lithos, v. 40, p. 261–293.

Froelich, A.J., and Gottfried, D., 1988, An overview of early Mesozoic intrusive rocks in the Culpeper basin, Virginia and Maryland, in Froelich, A.J., and Robinson, G.R., Jr., eds., Studies of early Mesozoic basins of eastern North America: U.S. Geological Survey Bulletin 1776, p. 151–165.

Frost, C.D., and Frost, B.R., 1997, Reduced rapakivi-type granites; The tholeiitic connection: Geology, v. 25, p. 647–650.

Frost, B.R., Frost, C.D., Hulsebosch, T.P., and Swapp, S.M., 2000, Origin of the charnockites of the Louis Lake batholith, Wind River Range, Wyoming: Journal of Petrology, v. 41, p. 1759–1776.

Furcron, A.S., 1969, Late Precambrian and Early Paleozoic erosional and depositional sequences of northern and central Virginia: Georgia Geological Survey Bulletin, v. 101, p. 339–354.

Gathright, T.M., II, 1976, Geology of the Shenandoah National Park in Virginia: Virginia Division of Mineral Resources Bulletin 86, 93 p.

Gower, C.F., and Krogh, T.E., 2002, A U-Pb geochronological review of the Proterozoic history of the eastern Grenville province: Canadian Journal of Earth Sciences v. 39, p. 795–829.

Hackley, P.H., 1999, Petrology, geochemistry, and field relations of the Old Rag Granite and associated charnockitic rocks, Old Rag Mountain 7.5-minute quadrangle, Madison and Rappahannock Counties, Virginia: Washington, D.C., The George Washington University, M.S. thesis, 244 p.

Hackley, P.H., and Tollo, R.P., in press, Geology of basement rocks in a portion of the Old Rag Mountain quadrangle, Virginia: Virginia Division of Mineral Resources Publication 170, Part C, scale 1:24,000.

Hamilton, M., McLelland, J., and Selleck, B., in press, SHRIMP U-Pb zircon geochronology of the anorthosite-mangerite-charnockite-granite (AMCG) suite, Adirondack Mountains, New York; Ages of emplacement and metamorphism, in Tollo, R.P., Corriveau, L., McLelland, J., and Bartholomew, M.J., eds., Proterozoic tectonic evolution of the Grenville orogen in North America: Geological Society of America Memoir 197.

Hanchar, J.M., and Miller, C.F., 1993, Zircon zonation patterns as revealed by cathodoluminescence and backscattered electron images; Implications for the interpretation of complex crustal histories: Chemical Geology, v. 110, no. 1–3, p. 1013.

Hanchar, J.M., and Rudnick, R.L., 1995, Revealing hidden structures; The application of cathodoluminescence and back-scattered electron images to dating zircons from lower crustal xenoliths: Lithos, v. 36, no. 3–4, p. 289–303.

Hatcher, R.D., Jr., Bream, B.R., Miller, C.F., Eckert, J.O., Jr., Fullagar, P.D., and Carrigan, C.W., in press, Paleozoic structure of internal basement massifs, southern Appalachian Blue Ridge, incorporating new geochronologic, Nd and Sr isotopic, and geochemical data, in Tollo, R.P., Corriveau, L., McLelland, J., and Bartholomew, M.J., eds., Proterozoic tectonic evolution of the Grenville orogen in North America: Geological Society of America Memoir 197.

Hughes, S.S., Lewis, S.E., Bartholomew, M.J., Sinha, A.K., and Herz, N., in press, Geology and geochemistry of granitic and charnockitic rocks in the central Lovingston massif of the Grenvillian Blue Ridge terrane, U.S.A., in Tollo, R.P., Corriveau, L., McLelland, J., and Bartholomew, M.J., eds., Proterozoic tectonic evolution of the Grenville orogen in North America: Geological Society of America

Memoir 197.

Irvine, T.N., and Baragar, W.R.A., 1971, A guide to the chemical classification of the common volcanic rocks: Canadian Journal of Earth Sciences, v. 8, p. 523–548.

Jonas, A.I., ed., 1928, Geologic map of Virginia: Charlottesville, Virginia Division of Mineral Resources, scale 1:500,000.

Kilpatrick, J.A., and Ellis, D.J., 1992, C-type magmas; Igneous charnockites and their extrusive equivalents, *in* Brown, P.E., and Chappell, B.W., eds., The Second Hutton Symposium on the origin of granites and related rocks: Geological Society of America Special Paper 272, p. 155–164.

Kretz, R., 1983, Symbols for rock-forming minerals: American Mineralogist, v. 68, p. 277–279.

Kunk, M.J., and Burton, W.C., 1999, ^{40}Ar/^{39}Ar age-spectrum data for amphibole, muscovite, biotite, and K-feldspar samples from metamorphic rocks in the Blue Ridge anticlinorium, northern Virginia: U.S. Geological Survey Open-File Report OF–99–0552, 110 p.

Landenberger, B., and Collins, W.J., 1996, Derivation of A-type granites from a dehydrated charnockitic lower crust; Evidence from the Chaelundi Complex, eastern Australia: Journal of Petrology, v. 37, p. 145–170.

Leake, B.E., Woolley, A.R., Arps, C.E.S., Birch, W.D., Gilbert, M.C., Grice, J.D., Hawthorne, F.C., Kato, A., Kisch, H.J., Krivovichev, V.G., Linthout, K., Laird, J., Mandarino, J.A., Maresch, W.V., Nickel, E.H., Rock, N.M.S., Schumacher, J.C., Smith, D.C., Stephenson, N.C.N., Ungaretti, L., Whittaker, E.J.W., and Youzhi, G., 1997, Nomenclature of amphiboles; Report of the Subcommittee on Amphiboles of the International Mineralogical Association, Commission on New Minerals and Mineral Names: American Mineralogist, v. 82, p. 1019–1037.

Le Maitre, R.W., Bateman, P., Dudek, A., Keller, J., Lameyre, J., Le Bas, M.J., Sabine, P.A., Schmid, R., Sørensen, H., Streckeisen, A., Woolley, A.R., and Zanettin, B., 1989, A classification of igneous rocks and glossary of terms; Recommendations of the International Union of Geological Sciences Subcommission on the Systematics of Igneous Rocks: Oxford, United Kingdom, Blackwell Scientific Publications, 193 p.

Lindsley, D.H., 1983, Pyroxene thermometry: American Mineralogist, v. 68, p. 477–493.

Malm, O.A., and Ormaasen, D.E., 1978, Mangerite-charnockite intrusives in the Lofoten-Vesterålen area, north Norway; Petrography, chemistry, and petrology: Norges Geologiske Undersokelse, v. 338, p. 38–114.

Maniar, P.D., and Piccoli, P.M., 1989, Tectonic discrimination of granitoids: Geological Society of America Bulletin, v. 101, p. 635–643.

McLelland, J., and Whitney, P., 1990, Anorogenic, bimodal emplacement of anorthositic, charnockitic, and related rocks in the Adirondack Mountains, New York, *in* Stein, H.J., and Hannah, J.L., eds., Ore-bearing granite systems; Petrogenesis and mineralizing processes: Geological Society of America Special Paper 246, p. 301–315.

McLelland, J., Daly, J.S., and McLelland, J.M., 1996, The Grenville orogenic cycle (ca. 1350–1000 Ma); An Adirondack perspective: Tectonophysics, v. 256, p. 1–28.

McLelland, J., Hamilton, M., Selleck, B., McLelland, J.M., Walker, D., and Orrell, S., 2001, Zircon U-Pb geochronology of the Ottawan orogeny, Adirondack Highlands, New York; Regional and tectonic implications: Precambrian Research, v. 109, p. 39–72.

Mitra, G., 1977, The mechanical processes of deformation of granitic basement and the role of ductile deformation zones in the deformation of Blue Ridge basement in northern Virginia: Baltimore, Md., Johns Hopkins University, unpublished Ph.D. dissertation, 219 p.

Mitra, G., 1979, Ductile deformation zones in Blue Ridge basement and estimation of finite strains: Geological Society of America Bulletin, v. 90, p. 935–951.

Mitra, G., and Lukert, M.T., 1982, Geology of the Catoctin-Blue Ridge anticlinorium in northern Virginia, *in* Lyttle, P.T., Central Appalachian geology, Field trip guidebook for the joint meeting of the Northeastern and Southeastern Sections of the Geological Society of America, Washington, D.C., 1982: Falls Church, Va., American Geological Institute, p. 83–108.

Miyashiro, A., 1974, Volcanic rock series in island arcs and active continental margins: American Journal of Science, v. 274, p. 321–355.

Morgan, B.A., Wieczorek, G.F., and Campbell, R.H., 1999, Map of rainfall, debris flows, and flood effects of the June 27, 1995, storm in Madison County, Virginia: U.S. Geological Survey Geologic Investigations Series Map I–2623–A, scale 1:24,000.

Morimoto, N., 1988, Nomenclature of pyroxenes: Mineralogical Magazine, v. 52, p. 535–550.

Passchier, C.W., and Trouw, R.A.J., 1996, Microtectonics: New York, Springer Verlag, 283 p.

Pearce, J.A., Harris, N.B.W., and Tindle, A.G., 1984, Trace element discrimination diagrams for the tectonic interpretation of granitic rocks: Journal of Petrology, v. 25, p. 956–983.

Polvi, L.E., 2003, Structural and geochronological analysis of the Lawhorne Mill high-strain zone, central Virginia Blue Ridge province: Williamsburg, Va., College of William and Mary, unpublished B.S. thesis, 51 p.

Rankin, D.W., Drake, A.A., Jr., and Ratcliffe, N.M., 1989a, Geologic map of the U.S. Appalachians showing the

Laurentian margin and Taconic orogen, *in* Hatcher, R.D., Jr., Thomas, W.A., and Viele, G.W., eds., The Appalachian-Ouachita orogen in the United States, v. F–2 *of* The geology of North America: Boulder, Colo., Geological Society of America, plate 2.

Rankin, D.W., Drake, A.A., Jr., Glover, L., III, Goldsmith, R., Hall, L.M., Murray, D.P., Ratcliffe, N.M., Read, J.F., Secor, D.T., Jr., and Stanley, R.S., 1989b, Pre-orogenic terranes, *in* Hatcher, R.D., Jr., Thomas, W.A., and Viele, G.W., eds., The Appalachian-Ouachita orogen in the United States, v. F–2 *of* The geology of North America: Boulder, Colo., Geological Society of America, p. 7–100.

Rivers, T., 1997, Lithotectonic elements of the Grenville province; Review and tectonic implications: Precambrian Research, v. 86, p. 117–154.

Sheraton, J.W., Black, L.P., and Tindle, A.G., 1992, Petrogenesis of plutonic rocks in a Proterozoic granulite-facies terrane—The Bunger Hills, East Antarctica: Chemical Geology, v. 97, p. 163–198.

Simpson, C., and De Paor, D.G., 1993, Strain and kinematic analysis in general shear zones: Journal of Structural Geology, v. 15, p. 1–20.

Simpson, C., and Kalaghan, T., 1989, Late Precambrian crustal extension preserved in Fries fault zone mylonites, southern Appalachians: Geology, v. 17, p. 148–151.

Simpson, E.L., and Eriksson, K.A., 1989, Sedimentology of the Unicoi Formation in southern and central Virginia; Evidence for Late Proterozoic to Early Cambrian rift-to-drift passive margin transition: Geological Society of America Bulletin, v. 101, p. 42–54.

Sinha, A.K., and Bartholomew, M.J., 1984, Evolution of the Grenville terrane in the central Virginia Appalachians, *in* Bartholomew, M.J., Force, E.R., Sinha, A.K., and Herz, N., eds., The Grenville event in the Appalachians and related topics: Geological Society of America Special Paper 194, p. 175–186.

Southworth, Scott, 1994, Geologic map of the Bluemont quadrangle, Loudoun and Clarke Counties, Virginia: U.S. Geological Survey Geologic Quadrangle Map GQ–1739, scale 1:24,000.

Southworth, Scott, 1995, Geologic map of the Purcellville quadrangle, Loudoun County, Virginia: U.S. Geological Survey Geologic Quadrangle Map GQ–1755, scale 1:24,000.

Southworth, Scott, and Brezinski, D.K., 1996, Geology of the Harpers Ferry quadrangle, Virginia, Maryland, and West Virginia: U.S. Geological Survey Bulletin 2123, 33 p., scale 1:24,000.

Spear, F.S., 1993, Metamorphic phase equilibria and pressure-temperature-time paths: Mineralogical Society of America Monograph 1, 799 p.

Streckeisen, A.J., and Le Maitre, R.W., 1979, A chemical approximation to the modal QAPF classification of the igneous rocks: Neues Jahrbuch für Mineralogie, Abhandlungen, v. 136, p. 169–206.

Su, Q., Goldberg, S.A., and Fullagar, P.D., 1994, Precise U-Pb zircon ages of Neoproterozoic plutons in the southern Appalachian Blue Ridge and their implications for the initial rifting of Laurentia: Precambrian Research, v. 68, p. 81–95.

Sylvester, P.J., 1989, Post-collisional alkaline granites: Journal of Geology, v. 97, p. 261–280.

Tollo, R.P., and Aleinikoff, J.N., 1996, Petrology and U-Pb geochronology of the Robertson River igneous suite, Blue Ridge province, Virginia; Evidence for multistage magmatism associated with an early episode of Laurentian rifting: American Journal of Science, v. 296, p. 1045–1090.

Tollo, R.P., and Hutson, F.E., 1996, 700 Ma age for the Mechum River Formation, Blue Ridge province, Virginia; A unique time constraint on pre-Iapetan rifting of Laurentia: Geology, v. 24, p. 59–62.

Tollo, R.P., Aleinikoff, J.N., Bartholomew, M.J., and Rankin, D.W., 2004, Neoproterozoic A-type granitoids of the central and southern Appalachians; Intraplate magmatism associated with episodic rifting of the Rodinian supercontinent: Precambrian Research, v. 128, p. 3–38.

Tollo, R.P., Aleinikoff, J.N., Borduas, E.A., and Hackley, P.C., in press a, Petrologic and geochronologic evolution of the Grenville orogen, northern Blue Ridge province, Virginia, *in* Tollo, R.P., Corriveau, L., McLelland, J., and Bartholomew, M.J., eds., Proterozoic tectonic evolution of the Grenville orogen in North America: Geological Society of America Memoir 197.

Tollo, R.P., Borduas, E.A., and Hackley, P.C., in press b, Geology of basement rocks in the Thornton Gap, Old Rag Mountain, and Fletcher quadrangles, Virginia: Virginia Division of Mineral Resources Publication 170.

Tollo, R.P., Gottfried, D., and Froelich, A.J., 1988, Field guide to the igneous rocks of the southern Culpeper basin, Virginia, *in* Froelich, A.J., and Robinson, G.R., Jr., eds., Studies of early Mesozoic basins of eastern North America: U.S. Geological Survey Bulletin 1776, p. 391–403.

Virginia Division of Mineral Resources, 1993, Geologic map of Virginia: [Richmond], Virginia Division of Mineral Resources, scale 1:500,000.

Volkert, R.A., in press, Mesoproterozoic rocks of the New Jersey Highlands, north-central Appalachians; Petrogenesis and tectonic history, *in* Tollo, R.P., Corriveau, L., McLelland, J., and Bartholomew, M.J., eds., Proterozoic tectonic evolution of the Grenville orogen in North America: Geological Society of America Memoir 197.

Wadman, H.M., Owens, B.E., and Bailey, C.M., 1998, Petrological analysis of the White Oak Dam exposure, Blue Ridge province, Virginia [abs.]: Geological Society of

America Abstracts with Programs, v. 30, no. 4, p. 64.

Wasteneys, H., McLelland, J., and Lumbers, S., 1999, Precise zircon geochronology in the Adirondack Lowlands and implications for revising plate-tectonic models of the Central Metasedimentary Belt and Adirondack Mountains, Grenville province, Ontario and New York: Canadian Journal of Earth Sciences, v. 36, p. 967–984.

Wehr, F.L., II, 1988, Transition from alluvial to deep-water sedimentation in the lower Lynchburg (Upper Proterozoic), Virginia, *in* Bartholomew, M.J., Hyndman, D.W., Mogk, D.W., and Mason, R., eds., Characterization and comparison of ancient and Mesozoic continental margins; Proceedings of the 8th International Conference on Basement Tectonics: Dordrecht, The Netherlands, Kluwer Academic Publishers, p. 407–423.

Whalen, J.B., Currie, K.L., and Chappell, B.W., 1987, A-type granites; Geochemical characteristics, discrimination and petrogenesis: Contributions to Mineralogy and Petrology, v. 95, p. 407–419.

Wieczorek, G.F., Morgan, B.A., and Campbell, R.H., 2000, Debris-flow hazards in the Blue Ridge of central Virginia: Environmental and Engineering Geoscience, v. VI, no. 1, p. 3–23.

Wilson, E.W., and Tollo, R.P., 2001, Geochemical distinction and tectonic significance of Mesozoic and Late Neoproterozoic dikes, Blue Ridge province, Virginia [abs.]: Geological Society of America Abstracts with Programs, v. 33, no. 2, p. 70.

ROAD LOG AND STOP DESCRIPTIONS FOLLOW

Road Log and Stop Descriptions

The field trip begins at the McDonald's restaurant on U.S. 522/U.S. 340 directly south of Exit 6 off I-66 in Front Royal, Va.

NOTE: Throughout the road log, numbers in the left-hand column indicate cumulative mileage for the entire field trip; numbers in the right-hand column indicate cumulative mileage within each stop-to-stop segment of the trip.

Mileage

Trip Cumulative	Stop-to-Stop Cumulative	
	0.0	Proceed south on U.S. 522/U.S. 340.
0.5	0.5	Cross the North Fork of the Shenandoah River.
		Relatively undeveloped flood plain is visible on both sides of the highway.
0.8	0.8	Proceed straight at intersection with Va. 55 toward Front Royal.
1.0	1.0	Cross the South Fork of the Shenandoah River.
		Residential development bordering the flood plain is visible on the left.
		Remain in left lane.
1.6	1.6	Turn left at traffic light to remain on U.S. 522/U.S. 340/Va. 55.
		Remain in right lane.
2.2	2.2	Proceed straight through traffic light to remain on U.S. 340 S/ Va. 55 E.
		Proceed straight through Front Royal on U.S. 340 S (Royal Avenue).
3.0	3.0	Pass United Methodist Church.
		The church is constructed largely of limestone of the type commonly obtained from carbonate valleys of the central Appalachians.
3.5	3.5	Proceed straight through traffic light to remain on U.S. 340 S.
		Merge into left lane.
4.0	4.0	Pass entrance to Shenandoah National Park on the left.
4.2	4.2	Turn left onto Va. 649 S (Browntown Road).
8.2	8.2	*Roadcut on left side exposes very fresh, medium- to coarse-grained, garnet+biotite leucogranite that contains locally abundant, disseminated graphite.*
8.4	8.4	Stop 1.
		Turn right onto Gooney Falls Lane.
		Follow Trip Leaders
		PRIVATE PROPERTY

Stop 1. Garnetiferous alkali feldspar granite to syenogranite (Ygg).

This outcrop is part of a series of exposures along Gooney Run located near the northern end of the garnetiferous alkali feldspar granite to syenogranite (Ygg) pluton, which extends south to the vicinity of Gravel Springs Gap Road where it is cut, but not truncated, by a northeast-southwest-striking fault (fig. 3). This lithologic unit is typically garnet-bearing, leucocratic, and characterized by alkali feldspar-to-plagioclase ratios >1. The rock at this outcrop is syenitic, and may represent a feldspar cumulate. The syenitic composition is in contrast to that of other exposures in the area which are generally granitic, especially in the southern part of the pluton. The foliation visible in this outcrop (strike 355°, dip 65° E.) is likely to have developed during regional Paleozoic orogenesis due to the absence of high-temperature textural and mineralogical characteristics. This lithologic unit is inferred to intrude the orthopyroxene+amphibole quartz diorite (Ypqd), on the basis of field relations observed at Boyd's Mill (Stop 3). The granitoid is intruded by north-south-striking metadiabase dikes at this outcrop, one of which is about 20 m (66 ft) wide. The chemical

composition of a sample collected from the largest dike is presented in table 5 (sample SNP-01-159), and the significance of these data is discussed in the text devoted to Stop 6). Such dikes are very common throughout the Blue Ridge, but are especially abundant in the northern Blue Ridge (Burton and others, 1995).

Throughout the field trip area, the Ygg unit includes white, medium- to very coarse-grained, inequigranular, weakly to strongly foliated syenogranite and white, medium-grained, equigranular, weakly foliated alkali feldspar granite to syenogranite composed of 35 to 40 percent orthoclase, 15 to 25 percent plagioclase, and 20 to 25 percent quartz with 2 to 10 percent garnet, 2 to 5 percent biotite, and 2 to 5 percent pseudomorphs after orthopyroxene. Accessory minerals include apatite, zircon, and ilmenite. Locally strong foliation within medium- to very coarse-grained syenogranite is defined by alignment of tabular feldspar megacrysts and elongate, polygranular garnet in garnet+biotite-rich domains. Weak foliation in the medium-grained, equigranular alkali feldspar granite to syenogranite is defined by alignment of polygranular garnet-rich domains. Meter- to decimeter-scale dikes of medium-grained, equigranular alkali feldspar granite to syenogranite locally intrude medium- to very coarse-grained syenogranite. Rare pegmatitic dikes, typically <10 cm (4 in) in width, locally intrude all lithologic phases of this unit. This lithologic unit is mineralogically and geochemically similar to medium- to very coarse-grained, inequigranular, massive to weakly foliated granite and medium-grained, equigranular to inequigranular, massive to weakly foliated leucocratic granite (Ygr) that occurs in the Old Rag Mountain 7.5-minute quadrangle (Hackley and Tollo, in press) and adjacent areas (fig. 3). However, these units can be distinguished in the field on the basis of quartz color: quartz is typically gray to white in garnet-bearing alkali feldspar granite to syenogranite (Ygg); whereas coarse-grained Old Rag Granite (Yor of Hackley and Tollo, in press) and associated medium-grained leucogranite (Ygr of Hackley and Tollo, in press) typically contains blue quartz.

Rocks within this lithologic unit typically have silica contents in excess of 69 weight percent and are mildly to moderately peraluminous (fig. 5). These leucocratic granitoids have high concentrations of Na_2O+K_2O, a compositional feature that is reflected in the characteristic modal abundance of alkali feldspar relative to plagioclase (fig. 4). K_2O/Na_2O molar ratios are characteristically high and similar to those of other leucocratic rocks in the field trip area. The high-silica, alkali-rich compositions are a distinctive geochemical characteristic of the post-tectonic leucocratic granitoids in the field trip area (fig. 5E). The low-silica concentration characterizing the granitoid at this exposure (table 4, sample SNP-03-197) is compositionally atypical of the Ygg unit in the field trip area and appears to be representative of a relatively minor lithologic variant. For this reason, the composition of a more chemically typical sample of the pluton collected 0.67 km (0.42 mi) northwest of the field trip stop along Gooney Run is also included in table 4 (sample SNP-01-164).

Ygg is part of a group of leucocratic granitoids that were emplaced following the main episode of local Grenvillian orogenesis that occurred at 1,080 to 1,060 Ma (Tollo and others, in press a). In addition to Ygg, these postorogenic rocks in the field trip area include the typically garnet- and (or) biotite-bearing leucocratic granitoids of the Old Rag magmatic suite (Ygr) (Hackley, 1999), which is associated with the pluton at Old Rag Mountain (fig. 3), and alkali feldspar granite (Yaf) that occurs as two small bodies near Madison (Bailey and others, 2003) (fig. 3). Southworth (1994, 1995) and Southworth and Brezinski (1996) mapped possibly correlative, nonfoliated to weakly foliated, leucocratic rocks in the northern Blue Ridge of northernmost Virginia and Maryland as garnet monzogranite (unit Ygt on the geologic map of Virginia (Virginia Division of Mineral Resources, 1993)).

Detailed SHRIMP analysis indicates that zircons from this locality are compositionally and isotopically complex. SHRIMP data suggest that crystallization occurred at 1,064±7 Ma (table 3, sample SNP-02-197). This age is similar to isotopic data obtained by conventional isotope-dilution thermal ionization mass spectrometry (ID-TIMS) techniques obtained by Aleinikoff and others (2000) for possibly related garnetiferous metagranite (Ygt) and white leucocratic metagranite (Yg) from the northern Blue Ridge dated at 1,077±4 Ma and 1,060±2 Ma, respectively.

Mileage

Trip Cumulative	Stop-to-Stop Cumulative	
	0.0	Proceed to intersection of Gooney Falls Lane and Va. 649.
8.7	0.3	Turn right (south) onto Va. 649.
		Buck Mountain, visible on the right, is underlain by typically coarse-grained leucocratic granitoid of the Ygg lithologic unit.
9.1	0.7	*Prominent roadcut on the left exposes relatively fresh foliated pyroxene+biotite quartz diorite (Ypqd).*
9.8	1.4	Stop 2.
		Outcrop on left (east) side of Va. 649.

Stop 2. Pyroxene+biotite quartz diorite (Ypqd).

This fresh outcrop of pyroxene+biotite quartz diorite (Ypqd) is typical of roadcuts along Va. 649. The unit is mapped as a small, elongate body that is intruded by and enclosed within garnetiferous alkali feldspar granite to syenogranite (Ygg). The body is interpreted to form an inlier within the larger leucocratic Ygg pluton. Gneissic layering defined by alternating feldspar- and pyroxene+biotite-rich domains is characteristic of this unit, and is best seen on weathered surfaces. Isoclinal folds developed locally within the compositional layering exhibit considerable thickening of the layers in the hinge zones, and are interpreted to have formed under ductile conditions during Grenvillian orogenesis.

Samples of this lithologic unit are typically dark-gray, medium-grained, equigranular, moderately to strongly foliated quartz diorite to quartz monzodiorite (fig. 4) composed of 20 to 25 percent orthoclase, 60 to 65 percent plagioclase, and 12 to 15 percent quartz with 5 to 7 percent orthopyroxene and 2 to 4 percent biotite. Accessory minerals include apatite, zircon, and Fe-Ti oxide. Alignment of biotite and orthopyroxene grains typically defines foliation that is parallel to centimeter-scale gneissic layering.

The Ypqd lithologic unit is one of the most chemically distinctive lithologic units documented within the field trip area. Two samples have similar low-silica compositions (fig. 5), with SiO_2 contents ranging from 55 to 57 weight percent. These compositions rank among the most chemically primitive observed within the field trip area. Although major-element abundances are similar to the most silica-poor variants of the low-silica charnockite (Yfqj), trace-element concentrations differ significantly, indicating likely separate petrologic lineages. Lower concentrations of high-field-strength elements in the Ypqd samples suggest an origin involving sources with a significant volcanic-arc component, in contrast to the more typical crustal-type sources from which the low-silica charnockite was likely derived. Compositionally, the Ypqd unit corresponds closely to typical I-type granites, whereas the low-silica charnockite (Yfqj), with high Nb+Y concentrations and elevated $10^4 \times Ga/Al$ and FeO_t/MgO ratios, exhibits close chemical affinity to A-type granitoids (fig. 7).

Field relations observed at Boyd's Mill (Stop 3) indicate that the Ypqd unit is older than, and likely intruded by, the surrounding Ygg leucogranitoids, suggesting that the former is older than 1,062 Ma. The available field and petrologic data are insufficient to suggest correlation between the Ypqd lithologic unit and older, similarly charnockitic units of known age that occur to the south.

Mileage

Trip Cumulative	Stop-to-Stop Cumulative	
	0.0	Proceed south on Va. 649.
10.2	0.4	Stop 3.
		Intersection of Va. 622 and Va. 649 at Boyd's Mill.

Outcrop on left side of Va. 649.

Park on right side beyond intersection.

Stop 3. Garnetiferous alkali feldspar granite to syenogranite (Ygg) intruding pyroxene+biotite quartz diorite (Ypqd).

Field relations observed at this roadcut indicate intrusion of the Ygg leucocratic granitoid into medium-grained, equigranular, charnockitic rocks of the Ypqd inlier. Coarse-grained, garnet+biotite-bearing leucocratic granite is interlayered on a scale ranging from decimeters to meters with medium- to dark-gray, medium- to coarse-grained, foliated pyroxene-bearing gneissic granitoid that locally contains garnet. Geologically, this roadcut is located along the mapped north-south-trending contact separating leucocratic granitoid rocks of the Ygg pluton from the western border of the Ypqd inlier (fig. 3), and thus the exposure is interpreted as part of the contact zone formed by intrusion of leucogranitoid into the melanocratic gneissic rocks. The leucocratic granitoid in this roadcut is composed of abundant perthitic orthoclase+plagioclase+quartz+garnet+biotite+Fe-Ti oxide+chlorite. Plagioclase is typically altered to sericite; primary garnet is partly replaced by chlorite+minor titanite. Garnet in the melanocratic granitoid occurs in proximity to leucocratic granite and is interpreted as metamorphic in origin.

Geochemical data for a sample of leucocratic granitoid from this roadcut (table 4, sample SNP-01-174) indicate a high-silica, peraluminous composition with high K_2O/Na_2O molar ratio, corresponding closely to the average composition of rocks constituting the Ygg pluton. The composition of a representative sample of the melanocratic granitoid (table 4, sample SNP-01-155) bears close chemical similarity to rocks collected elsewhere from the inlier except for distinctly higher silica contents, lower concentrations of CaO, K_2O, and Na_2O, and correspondingly high values of aluminum saturation index (molar $Al_2O_3/(Na_2O+K_2O+CaO)$. Such differences in composition are interpreted to reflect chemical exchange that occurred as a result of metamorphic reactions induced by intrusion of the leucogranite.

Mileage

Trip Cumulative	Stop-to-Stop Cumulative	
	0.0	Turn around and proceed north on Va. 649.
15.9	5.7	Turn right (northeast) onto U.S. 340.
16.1	5.9	Turn right into the entrance to Shenandoah National Park and Skyline Drive South.
16.7	6.5	Pass through entrance station to Shenandoah National Park.
18.9	8.7	Shenandoah Valley Overlook. *The view from the overlook on the right includes the abandoned former Avtek factory located along the Shenandoah River in Front Royal. This factory and the surrounding environmentally sensitive area constitute a designated Superfund site slated for remediation.*
20.8	10.6	Dickey Ridge Visitor Center.
21.9	11.7	Signal Knob Overlook. *On a day with high visibility, the view from this overlook provides a rich perspective on the geology of the central Appalachians. The double-topped linear ridges in the middle distance define Massanutten Mountain, a complex syncline whose topographic expression is defined by resistant Silurian sandstone. Most of the floor of the surrounding Shenandoah Valley is underlain by the Ordovician Martinsburg Formation and Cambrian and Ordovician carbonate rocks exposed in the footwall block beneath the Blue Ridge thrust that runs*

along the base of the foothills in the foreground. North Mountain, which forms the long linear ridge on the horizon, is capped by Devonian sandstone and is a typical landform of the Appalachian Valley and Ridge province.

The roadcut on the east side of Skyline Drive exposes two lava flows of the Neoproterozoic Catoctin Formation separated by a 1- to 1.5-m (3.3–4.9 ft)-thick stratum of terrestrial sedimentary deposits. Jasper veins developed in the metasedimentary layer are typical of the contact zone beneath and between lava flows in this area.

23.1   12.9   Gooney Run Overlook.

View to the west overlooks areas of the Chester Gap 7.5-minute quadrangle visited in Stops 1–3. Buck Mountain, underlain by leucocratic granitoids of the Ygg pluton, is located directly west of the overlook. Stop 1 is located at the northern end of the mountain; Stops 2 and 3 are located along the road extending along its eastern flank.

25.6   15.4   Stop 4.

Outcrop on left (east) side of Skyline Drive.

Stop 4. Orthopyroxene+amphibole layered granodiorite gneiss (Ylgn).

The large roadcut at Lands Run Gap on Skyline Drive exhibits characteristics typical of the orthopyroxene+amphibole layered granodiorite gneiss (Ylgn) and is designated as the lithologic type locality for this unit (Tollo and others, in press b). This stop is located about 0.5 km (0.3 mi) east of an unnamed fault that juxtaposes basement units and greenstone against basement (fig. 3). The Ylgn lithologic unit underlies a large area in the central part of the Chester Gap quadrangle where it is both overlain by and in fault contact with greenstones of the Catoctin Formation. Compton Peak, visible to the south, represents an isolated erosional remnant of the cover sequence that preserves a succession of rocks of the Swift Run and Catoctin Formations nonconformably overlying basement (Gathright, 1976) (fig. 3).

The Ylgn lithologic unit consists of dark-gray, medium- to coarse-grained, inequigranular, strongly foliated granodioritic (*opdalite*) gneiss composed of 35 to 40 percent alkali feldspar (microcline or orthoclase), 30 to 40 percent plagioclase, and 20 percent quartz with 3 to 5 percent amphibole and 3 to 5 percent orthopyroxene. Accessory minerals include apatite, zircon, and ilmenite. Characteristic gneissosity is defined by alternating centimeter-scale quartz+feldspar-rich (light) and pyroxene+amphibole-rich (dark) layers that form intrafolial folds within a foliation plane defined by discontinuous polygranular domains of amphibole and orthopyroxene. Interlayered and crosscutting, decimeter-scale sheets of light-gray to white, medium- to coarse-grained, inequigranular, massive leucogranite composed mostly of white feldspar and gray quartz are characteristic, and likely represent dikes of younger granitoid that may be related to the circa-1,060-Ma postorogenic type that includes the Old Rag magmatic suite and other similar rocks. The development of gneissosity, leucogranitoid boudins, and isoclinal intrafolial folds are interpreted to reflect deformation of probable Grenvillian age.

Geochemical data indicate that the Ylgn lithologic unit is mildly metaluminous and intermediate in composition with SiO_2 contents of 64 to 67 weight percent (fig. 5D). The overall chemical correspondence of this unit to typical granodioritic compositions is interpreted as evidence for an igneous protolith. Ylgn is the least chemically evolved of the orthopyroxene-bearing granitic units characterized by silica contents >60 weight percent in the field area. Like the other charnockites, Ylgn exhibits compositional features that are transitional between I- and A-type granitoids (fig. 7) and was likely derived from sources of mixed composition, including both volcanic-arc and crustal components (fig. 6).

The characteristic gneissic fabric of this lithologic unit indicates that Ylgn is part of the older group of deformed rocks in the area. This group includes a compositionally diverse array of charnockitic and non-charnockitic granitoids that display mineralogic and

textual evidence of deformation that occurred at high-grade conditions. Dated rocks within this group, which include the Ycf (1,147±16 Ma) and Ylg (1,183±11 Ma) lithologic units, represent the oldest recognized lithologies in the field area. Two tabular bodies of dark-colored, foliated to massive, fine-grained, biotite-rich granitoid, both <1.3 m (4.3 ft) in width, occur at a slight angle to foliation and gneissosity in a nearby roadcut, and are interpreted to be dikes cutting the Ylgn lithologic unit. Mineralogic and geochemical similarity of these dike rocks (table 4, sample SNP-01-149) to the pyroxene quartz diorite (Ypqd) lithologic unit (table 4, sample SNP-01-175) suggest that Ypqd is younger than Ylgn.

Mileage

Trip Cumulative	Stop-to-Stop Cumulative	
	0.0	Proceed south on Skyline Drive.
26.9	1.3	Indian Run Overlook.
		Rocks exposed in the long roadcut display one of the finest examples of columnar jointing in metabasalt of the Catoctin Formation within Shenandoah National Park. Such columns, which are common throughout the Catoctin Formation on the west limb of the Blue Ridge anticlinorium, are evidence of the subaerial eruptive origin of the lava flows.
28.5	2.9	Jenkins Gap Overlook.
33.7	8.1	Gravel Springs Gap.
35.1	9.5	Mount Marshall Overlook.
36.1	10.5	Stop 5.
		Little Devil Stairs Overlook. Outcrop on west side of road.

Stop 5. Orthopyroxene+amphibole syeno- and monzogranite (Ycf).

The large roadcut at Little Devil Stairs Overlook is located about 200 ft (61 m) north of the unconformable contact separating basement from the overlying Catoctin Formation, exposed in the hillslope to the south (Gathright, 1976). This stop is located about 1.1 km (0.7 mi) west of a fault that intersects the Stanley fault near Keyser Mountain to the southeast (Gathright, 1976). Despite their appearance in the roadcut, basement rocks at this locality are intensely weathered and preserve only partial evidence of the primary ferromagnesian mineral assemblage. Throughout the exposure, fine-grained charnockite forms meter-scale dikes cutting coarser grained charnockite. The rocks exhibit weak to moderately developed, steeply dipping foliation striking 075° to 090°. The predominantly east-west strike of the foliation is unusual in an area that is otherwise dominated by northeast-southwest fabrics associated with Paleozoic orogenesis (Mitra and Lukert, 1982), and is likely to have been developed during the Grenvillian orogeny. Both the fine- and coarse-grained varieties of charnockite are composed of alkali feldspar microperthite (dominantly microcline in the coarse-grained variety, mostly orthoclase in the fine-grained variety), plagioclase and quartz, with rare amphibole and abundant pseudomorphs that likely formed after orthopyroxene. This primary mineral assemblage is also characteristic of the foliated pyroxene granite (Yfpg) (table 2, fig. 3).

Chemical compositions of samples of both fine- and coarse-grained charnockite collected from this outcrop (table 4, samples SNP-01-142 and SNP-01-143, respectively) display geochemical similarities to samples of both the high-silica charnockite (Ycf) and foliated pyroxene granite (Yfpg) (table 4, samples SNP-96-10 and SNP-02-177, respectively). The Ycf unit and the foliated pyroxene granite (Yfpg), which have crystallization ages that differ by 45 m.y., are both foliated, amphibole+orthopyroxene-bearing, siliceous charnockites, and thus the mineral assemblage and chemical composition of the rocks at this roadcut do not represent sufficient evidence on which to establish lithodemic correlation. However, the more homogeneous (albeit foliated) fabric and more disseminated nature of the

orthopyroxene in Ycf are features that are similar to the rocks at this exposure, contrasting with the characteristically very coarse and clustered nature of orthopyroxene in Yfpg. Thus, on the basis of this fabric, the rocks at Little Devil Stairs Overlook are considered part of the Ycf lithologic unit, pending detailed mapping of basement lithologies in the Bentonville 7.5-minute quadrangle.

The charnockite is cut by five large metabasalt (greenstone) dikes of meter-scale thickness at the northern end of the exposure. Numerous fine- to medium-grained mafic dikes intrude basement rocks throughout the field trip area and across the Shenandoah massif. Such dikes exhibit diverse textures, metamorphic grade, and mineralogic compositions ranging from basalt to diabase to greenstone. Although largely undated by modern isotopic techniques, most mafic dikes have been mapped as either Mesozoic or Neoproterozoic in age on the basis of crosscutting relations, mineralogic composition, and the presence or absence of metamorphic fabrics (for example, Burton and others, 1995; Southworth, 1995; Southworth and Brezinski, 1996; Bailey and others, 2003). In general, dikes of late Neoproterozoic age contain mineralogic evidence of recrystallization at greenschist-facies metamorphic conditions, including development of assemblages containing actinolite+biotite+serpentine, which are commonly absent in Mesozoic dikes (Wilson and Tollo, 2001). Many Neoproterozoic dikes display tectonic cleavage as a result of deformation and retrograde metamorphic recrystallization; such cleavage is absent in Mesozoic dikes. Samples of the dikes cutting basement at this stop contain abundant chlorite+epidote±serpentine, and are typical of the most abundant type documented by studies within the Blue Ridge which generally have weakly quartz-normative, tholeiitic compositions. Nevertheless, dikes throughout the area show major- and trace-element characteristics that are largely bimodal and may be indicative of two ages of emplacement. As illustrated in figure 8, the bimodal major-element compositions of Blue Ridge dikes correspond closely to either the Mesozoic Mt. Zion Church Basalt in the nearby Culpeper basin or relatively unaltered lava flows and associated dikes of likely Neoproterozoic age (Badger, 1989). Chemical analyses of two of the dikes at this locality (table 5, samples SNP-01-144 and SNP-01-145) indicate high TiO_2 contents and low values of $100(MgO/(MgO+FeO_t))$ (fig. 8), suggesting close compositional affinity to dikes and lava flows associated with the Catoctin Formation (Badger, 1989). Such dikes may have served as conduits for magma moving toward the surface during eruption, an interpretation that is consistent with the physical proximity of these dikes to the overlying Catoctin greenstones. The usefulness of the chemical discriminants plotted in figure 8 is underscored by the similarity in compositions of two samples of thoroughly retrograded greenstone (squares with diagonal crosses) to those of less retrograded metabasalt and metadiabase (filled squares), indicating that, in many cases, Paleozoic greenschist-facies metamorphism did not result in mass transfer of chemical components. Dikes formed during Mesozoic rifting are apparently much less abundant in the Blue Ridge, and can be distinguished chemically from dikes of inferred Neoproterozoic age on the basis of lower TiO_2 contents and higher $100(MgO/(MgO+FeO_t))$ ratios (Wilson and Tollo, 2001) (fig. 8). Mesozoic dikes also contain higher SiO_2 contents, are relatively enriched in compatible elements such as Ni and Cr, and show lower concentrations of high-field-strength elements, including Zr, Nb, and Y (Wilson and Tollo, 2001). In figure 8, only 4 dikes (from the total population of 29 dikes sampled as part of this study) correspond closely in composition to the tholeiitic Mount Zion Church Basalt, which is the oldest and most primitive basalt type in the nearby early Mesozoic Culpeper basin (fig. 2). This composition also corresponds to the most common type of diabase sheets that intruded sedimentary strata within the basin, and is the only Mesozoic diabase magma type that is comparable to any of the dikes in the Blue Ridge (Froelich and Gottfried, 1988).

Mileage

Trip Cumulative	Stop-to-Stop Cumulative	
	0.0	Proceed south on Skyline Drive.
40.0	3.9	Pass Elkwallow Store.
47.3	11.2	Pass intersection with U.S. 211 at Thornton Gap.
47.4	11.3	Pass Panorama on right of Skyline Drive.
48.0	11.9	North portal of Mary's Rock Tunnel.

A large, northeast-striking mafic dike displaying prominent columnar jointing cuts high-silica charnockite (Ycf) on the west side of the tunnel portal. The fine-grained diabase contains microphenocrysts of clinopyroxene+pigeonite+plagioclase and shows relatively little evidence of retrograde metamorphism. Nevertheless, the chemical composition of the dike (table 5, sample SNPD-99-1) indicates high-TiO₂ content and trace-element characteristics that are typical of dikes of Neoproterozoic age (Wilson and Tollo, 2001). The overall lack of development of retrograde mineral assemblage and tectonic cleavage in the dike is a likely consequence of its occurrence within the rigid, relatively anhydrous charnockite pluton.

Trip Cumulative	Stop-to-Stop Cumulative	
48.2	12.1	South portal of Mary's Rock Tunnel. Stop 6. Parking on left (east) side of Skyline Drive.

Stop 6. Orthopyroxene+amphibole syeno- and monzogranite (Ycf).

The view toward the east from the tunnel parking lot provides an informative perspective on the physiographic Piedmont province of the central Appalachians and geological framework of the Blue Ridge anticlinorium. The Blue Ridge foothills located in the foreground directly to the east are underlain mostly by Mesoproterozoic basement rocks, including some lithologic units that also occur along Skyline Drive. These foothills give way eastward to the typical low topography of the core of the Blue Ridge anticlinorium, most of which is included in the Piedmont physiographic province (Fenneman, 1938). The core of the anticlinorium is underlain primarily by Mesoproterozoic basement rocks and, locally, by igneous and metasedimentary rocks formed during Neoproterozoic rifting. The two symmetric hills in the middle distance (Little Battle Mountain and Battle Mountain, north and south peaks, respectively) are underlain by the Battle Mountain volcanic complex that includes both volcanic and subvolcanic felsic rocks associated with the extension-related, 730- to 702-Ma Robertson River batholith (Tollo and Aleinikoff, 1996; Tollo and Hutson, 1996). The elongate batholith continues both north and south of these hills, ultimately stretching nearly 110 km (70 mi) across the anticlinorium from the west limb in the north to the east limb in the south (fig. 2); however, the intrusion only locally underlies steep topography. The flat-topped ridge of the Bull Run Mountains occupies the horizon and is underlain by resistant quartzite of the upper Neoproterozic to Lower Cambrian Weverton Formation, which is stratigraphically underlain by the Catoctin Formation for much of the length of the ridge. These rocks constitute part of the Blue Ridge cover-rock sequence, thus locally defining the eastern limb of the Blue Ridge anticlinorium.

This stop is located in the central part of a pluton consisting of moderately to strongly foliated, coarse- to very coarse-grained, orthopyroxene±amphibole-bearing syeno- and monzogranite (*charnockite* and *farsundite*, Ycf). This lithologic unit occurs across most of the Thornton Gap quadrangle (fig. 3) and is a member of the oldest group of plutonic rocks in the region. In this area, the Ycf pluton includes map-scale inliers of coarse-grained, orthopyroxene+garnet granite gneiss (*farsundite* gneiss, Yg), which constitute probable screens of older rocks. Mapping also indicates that Ycf is intruded by elongate bodies of

massive to weakly foliated granite of the Old Rag magmatic suite (Ygr) and massive to weakly foliated, low-silica charnockite (Yfqj) (fig. 3). Collectively, charnockitic rocks of the Ycf, Yg, and much younger Yfqj lithologic units constitute part of the classic orthopy-roxene-bearing Pedlar Formation that was mapped throughout much of this part of the Blue Ridge (Gathright, 1976) before the advent of modern analytical methods made geochemical and age-based differentiation of mineralogically similar units possible.

The rocks near the tunnel expose strongly foliated, coarse- to very coarse-grained, orthopyroxene±amphibole, inequigranular to megacrystic syeno- and monzogranite (*charnockite* and *farsundite*) that is typical of the Ycf pluton. The rock is composed of 22 to 57 percent alkali feldspar microperthite (chiefly microcline), 10 to 37 percent plagio-clase, and 11 to 49 percent quartz with <1 to 14 percent orthopyroxene, 0 to 11 percent amphibole, and rare clinopyroxene. Accessory minerals include apatite, ilmenite, mag-netite, zircon, epidote, and actinolite. Locally prominent gneissic layering is defined by interlayered quartz+feldspar- and ferromagnesian mineral-rich domains ranging from less than 1 cm (0.4 in) to greater than 13 cm (5 in) and is especially visible on weathered sur-faces. Foliation is defined locally by planar alignment of ferromagnesian minerals and is parallel to gneissic layering. Subhedral to euhedral, monocrystalline alkali feldspar megacrysts range up to 13 cm (5 in) in length and are best observed on weathered surfaces. The strongly developed fabric is characteristic of the older group of plutonic rocks in the field trip area.

Electron microprobe analyses indicate that pyroxenes in the Ycf lithologic unit display strong Quad (Ca-Fe-Mg) compositional features, according to the criteria of Morimoto (1988). Pyroxene compositions show very little variation both within individual grains and between grains in single thin sections. Clinopyroxenes in the Ycf charnockite are relatively Fe-rich (average $Wo_{43}En_{22}Fs_{35}$); however, application of the charge-balance criteria of Lindsley (1983) indicate that ferric iron contents are negligible. Orthopyroxenes in Ycf are very Ca-poor and Fe-rich (average $Wo_2En_{27}Fs_{71}$). Visible exsolution is rare in either pyrox-ene type. Compositions of coexisting pyroxenes in Ycf indicate equilibration temperatures of less than 500°C, as calculated by the QUILF program of Andersen and others (1993) for pressures consistent with observed granulite-facies mineral assemblages. Because such temperatures fall hundreds of degrees below likely crystallization temperatures for igneous charnockites (Kilpatrick and Ellis, 1992), and because the pyroxenes exhibit evidence of thorough compositional homogenization, the rocks are inferred to have undergone an extended interval of subsolidus re-equilibration at temperatures that remained elevated but below peak granulite-facies conditions.

Amphiboles are typically brown and closely associated with orthopyroxene, locally separated by a narrow optical transition zone. Compositions of the amphiboles correspond to hornblende (*sensu lato*) according to the criteria of Deer and others (1992) and to the calcic group of Leake and others (1997). Data from electron microprobe traverses of indi-vidual grains indicate little evidence of compositional zoning, and repeated analyses of multiple grains within single samples indicate restricted compositional variation. Amphiboles in Ycf (and Yfqj) display compositional similarities to amphiboles observed in charnockites from the calc-alkaline Louis Lake batholith in the Wind River Range of Wyoming, which were interpreted by Frost and others (2000) to represent primary phases that crystallized from igneous melts. Amphiboles of likely igneous origin occur in charnockitic rocks of tholeiitic affinity from many other locations (Malm and Ormaasen, 1978; Duchesne and Wilmart, 1997; Sheraton and others, 1992), suggesting that the occur-rence of igneous amphiboles in charnockitic rocks is not uncommon. For this reason, and because of their association with pyroxene that displays textural features consistent with original igneous crystallization, the Blue Ridge charnockitic amphiboles are also interpret-ed as primary magmatic minerals.

Chemical analyses indicate that Ycf rocks show only restricted compositional varia-tion throughout the field trip area. The granitoids are mildly metaluminous, with SiO_2 con-tents in the range of 68 to 72 weight percent (table 4; fig. 5). The high-silica Ycf pluton is one of several siliceous rocks of charnockitic affinity in the northern part of the study area.

Others include the garnetiferous granite gneiss (Yg), foliated pyroxene granite (Yfpg) (both units shown on fig. 3) and a small, typically medium-grained, equigranular charnockitic pluton documented by recent mapping in the Big Meadows quadrangle (not shown in fig. 3). However, of these four orthopyroxene-bearing units, only the charnockite from Big Meadows and the distinctive Ycf unit are characterized on fresh surfaces by the dark-greenish-gray appearance that is typical of charnockites worldwide. Trace-element analyses of Ycf rocks suggest derivation from mixed sources of possible volcanic-arc and crustal affinity (fig. 6) and indicate that the pluton displays chemical characteristics that are transitional between I- and A-type granitoids (fig. 7).

U-Pb isotopic analyses obtained using SHRIMP techniques indicate that zircons in the Ycf lithologic unit are compositionally complex. Two populations are present, based on crystal morphology: (1) euhedral, elongate prisms displaying dipyramidal terminations and (2) smaller, nearly equant grains (Tollo and others, in press a). Examination of the prismatic zircons in cathodoluminescence (CL) indicates the presence of cores characterized by concentric oscillatory zoning surrounded by narrow unzoned rims. Multiple analyses indicate a weighted average $^{206}Pb/^{238}U$ age of 1,159±14 Ma for the zoned cores, which is interpreted as the time of igneous crystallization. Analyses of the equant grains and overgrowths on the prismatic grains indicate a composite age of 1,052±14 Ma, which likely corresponds to a period of regional thermal activity. Results from ID-TIMS dating by Aleinikoff and others (2000) indicate that meta-igneous rocks of similar age, possibly including a charnockite, occur in the Blue Ridge north of the field trip area.

Mileage

Trip Cumulative	Stop-to-Stop Cumulative	
	0.0	Proceed south on Skyline Drive.
48.7	0.5	Stop 7.
		Buck Hollow Overlook.
		Parking on left (east) side of Skyline Drive.

Stop 7. Orthopyroxene+garnet granite gneiss (Yg) and orthopyroxene+amphibole syeno- and monzogranite (Ycf).

The roadcut opposite the overlook exposes one of the freshest examples of orthopyroxene+garnet granite gneiss in Shenandoah National Park. Field relations indicate that this exposure is part of a large screen of garnetiferous gneiss mapped as lithologic unit Yg that is enclosed within high-silica charnockite (Ycf) (fig. 3), suggesting that the latter pluton intruded and enveloped the former (Tollo and others, in press a,b). Direct crosscutting relations have not been observed in outcrop, however. This field relation and the ubiquitous, strongly developed fabric of the granitic gneiss, which is characteristic of rocks that predate the main episode of Grenvillian orogenesis in the area, suggest that Yg predates the high-silica charnockite (Ycf) and therefore is older than 1,159 Ma. The curved contacts of the screen and adjacent rocks of the Old Rag magmatic suite suggest the presence of map-scale folds developed in the basement rocks (fig. 3). The locally parallel alignment of gneissic layering defined by primary minerals and the trend of the folded contacts further suggest that such deformation may be Grenvillian in age.

Rocks at this locality include light-gray to gray, medium- to coarse-grained, inequigranular, strongly foliated syeno- to monzogranite gneiss (*farsundite* gneiss) composed of 28 to 49 percent alkali feldspar microperthite (chiefly microcline), 14 to 30 percent plagioclase, and 28 to 35 percent quartz with 4 to 6 percent orthopyroxene, <1 to 7 percent garnet, <1 to 3 percent biotite, and rare clinopyroxene. Accessory minerals include apatite, ilmenite, magnetite, zircon, and chlorite. Typically prominent gneissic layering is defined by interlayered quartz+feldspar- and ferromagnesian mineral-rich domains ranging

from less than 1 cm (0.4 in) to greater than 70 cm (28 in) in thickness. Foliation is defined locally by planar alignment of ferromagnesian minerals and is parallel to gneissic layering. A locally well-developed mineral lineation is defined by elongate domains of garnet and biotite located within the foliation plane.

Clinopyroxene in the garnetiferous granite gneiss (Yg) is generally too altered for meaningful chemical analysis. However, orthopyroxene ($Wo_1En_{28}Fs_{71}$) is similar in composition to orthopyroxene in the high-silica charnockite (Ycf), but consistently indicates slightly lower temperatures of equilibration. Like orthopyroxene, garnet exhibits very little compositional variation both within individual grains and among multiple grains. Garnet in Yg is Fe-rich (Grs: 9.3, Alm: 79.5, Prp: 11.2), reflecting the elevated FeO_t/MgO whole-rock ratio (fig. 5F).

Samples of the Yg lithologic unit are borderline metaluminous to moderately peraluminous with SiO_2 contents of 70 to 75 weight percent (fig. 5D). The Yg rocks display overall compositional features that are similar to other siliceous charnockites in the region, including relatively low TiO_2, FeO_t, and CaO contents (table 4). Compositionally, Yg differs from the Ycf unit that encloses it in having generally higher SiO_2 contents, higher FeO_t/MgO ratios, and distinctly peraluminous bulk compositions (table 4; fig. 5D, F). These geochemical characteristics and normative compositions of granitic affinity suggest that Yg is meta-igneous in origin.

Map relations and the characteristic deformed fabric of the garnetiferous granite gneiss suggest that the lithologic unit is one of the oldest rocks in the area. Like the leucogranite gneiss (Ylgg) lithologic unit that occurs in the Fletcher 7.5-minute quadrangle (fig. 3), Yg rocks occur only as inliers that are isolated within igneous plutons of likely younger age. These field relations suggest that the present erosion surface in the Blue Ridge coincides with a paleodepth interval at which Grenvillian plutons were successively emplaced. This zone of emplacement is dominated by plutons and is characterized by an apparent paucity of preexisting country rocks. Whether the missing country rock was removed by subsequent erosion of higher levels or remains as roof pendants concealed at depth is not presently known.

Large outcrops and roadcuts of medium-grained, gray-green, orthopyroxene+amphibole syeno- and monzogranite (Ycf) occur nearby, adjacent to Skyline Drive about 200 ft (61 m) north of the Buck Hollow Overlook exposure. The contact separating Ycf from the Yg inlier is not exposed, but likely is located in the east-trending stream valley that crosses Skyline Drive south of Skinner Ridge. The atypical finer grain size of the Ycf rocks in this area is interpreted to result from contact-related cooling against the Yg screen during magmatic emplacement.

Mileage

Trip Cumulative	Stop-to-Stop Cumulative	
	0.0	Proceed south along Skyline Drive.
49.3	0.6	Meadow Springs Overlook and Parking Area.
		Exposures of low-silica charnockite (Yfqj) along the west side of Skyline Drive opposite the overlook are part of a small dike that intruded along the contact separating high-silica orthopyroxene+ amphibole syeno- and monzogranite (charnockite+farsundite, Ycf) from garnetiferous granite gneiss (farsundite gneiss, Yg) (fig. 3). Sample SNP-96-17 (table 4) was collected from the roadcut and is mineralogically and geochemically typical of the Yfqj pluton, but generally finer grained.
52.3	3.6	Jewel Hollow Overlook.
		The view to the west includes the Massanutten Mountain synclinorium in the middle distance and North Mountain on the horizon. Outcrops at the overlook expose high-silica charnockite of the Ycf lithologic unit.

53.5	4.8	*A large northeast-striking mafic dike cuts garnetiferous granite gneiss (Yg) in the roadcut on the west side of Skyline Drive. The chemical composition of the dike (table 5, sample SNPD-99-3) is typical of Catoctin-related mafic rocks in the area. This geochemical affinity and close spatial association with extrusive metabasalt of the Catoctin Formation occurring to the south suggest that the dike is part of the feeder complex that provided magma to the rift-related basalt flows.*
54.4	5.7	*Stony Man Mountain, a well-known landmark in Shenandoah National Park, is visible directly to the south. The mountain is underlain by metavolcanic and metasedimentary rocks of the Catoctin Formation (Gathright, 1976) that define five major eruptive flow units and at least two layers of intercalated metasedimentary rocks and volcanic breccia, all of which dip gently toward the southeast (Badger, 1999). The view to the west includes a broad expanse of the eastern Shenandoah Valley. The South Fork of the Shenandoah River is visible east of Massanutten Mountain, where it has a low-gradient path characterized by numerous meanders.*
55.1	6.4	*Skyline Drive ascends uphill through roadcuts of Catoctin Formation greenstone.*
57.5	8.8	*Entrance to Skyland on the right, highest point on Skyline Drive at 3,680 ft (1,122 m). Like the eastern part of Skyland, most of the higher elevations in the Park are underlain by greenstones of the Catoctin Formation. Examples include Hawksbill Mountain at 4,050 ft (1,234 m), Stony Man Mountain at 4,011 ft (1,223 m), and Hazeltop Mountain at 3,812 ft (1,162 m).*
59.0	10.3	Stop 8. Timber Hollow Overlook.

Stop 8. Unakite developed in nonfoliated low-silica amphibole-bearing charnockite (Yfqj).

This overlook provides views to the west of the eastern Shenandoah Valley and Massanutten Mountain in the middle distance. On a clear day, talus slopes composed of variably sized blocks of white Silurian quartz arenite of the Massanutten Formation can be observed on the flanks of the ridges. Such talus deposits are a characteristic feature of the hillslopes, which are typically capped by resistant quartz-rich sandstone. New Market Gap, where U.S. 211 crosses Massanutten Mountain, can also be observed west of Luray. The north-striking Stanley fault, part of the thrust that transported Blue Ridge basement rocks northwestward over lower Paleozoic sedimentary strata during late Paleozoic Alleghanian orogenesis, is located about 4.0 km (2.5 mi) west of the overlook in the valley below.

Timber Hollow Overlook is underlain by low-silica charnockite that is correlated mineralogically and geochemically with a larger pluton composed of amphibole-bearing *far-sundite* and *quartz jotunite* (Yfqj) mapped to the south (fig. 3). Gathright (1976) mapped stratified rocks of the Catoctin Formation (dominantly greenstones) and underlying Swift Run Formation (dominantly phyllites) as unconformably overlying charnockite in this area, with a contact located about 1,000 ft (305 m) to the east of the overlook. As a result of the low dip of this contact, charnockite outcrops located below the overlook display abundant mineralogic evidence of contact metamorphism related to thermal effects caused by extrusion of overlying lava flows. The normally dark-greenish-gray charnockite is typically bleached light gray due to retrograde recrystallization of abundant primary plagioclase and lesser alkali feldspar. Ferromagnesian minerals are completely pseudomorphed by hydrous, low-temperature assemblages. Parts of the charnockite located adjacent to major joints are locally converted to unakite, in which plagioclase is mostly replaced by green epidote-group minerals, alkali feldspar is replaced largely by a pink hematite-bearing assemblage, and small amounts of originally blue quartz remain relatively unaltered. The localization of

well-developed unakite adjacent to fractures is a likely consequence of hydrothermal fluid migration induced by heat from the overlying lavas during Neoproterozoic extension. The effects of thermal metamorphism decrease rapidly downhill away from the contact. Unakite is a visually distinctive, but rare, rock type that is typically developed in Blue Ridge basement rocks through retrograde recrystallization associated with (1) extrusion of the overlying Catoctin Formation, (2) enhanced fluid flow associated with fault zones, or (3) local effects of regional Paleozoic metamorphism (Tollo and others, in press b; Wadman and others, 1998).

Mileage

Trip Cumulative	Stop-to-Stop Cumulative	
	0.0	Proceed south along Skyline Drive.
63.5	4.5	Stop 9.
		Fisher's Gap.
		Proceed to Dark Hollow Falls.

Stop 9. Erosional window exposing coarse-grained, inequigranular, amphibole-bearing charnockite (Yfqj).

Fisher's Gap and the surrounding area are located within the thrust sheet that carried basement and overlying rocks northwest over Paleozoic strata during Alleghanian orogenesis. Drainage from the nearby Big Meadows area flows northeast along Hogcamp Branch, which is partly responsible for developing an erosional window through cover rocks north of the falls (Gathright, 1976). Dark Hollow Falls is located within stratified rocks of the Catoctin Formation, which locally include massive and phyllitic greenstone, amygdaloidal greenstone, and metaconglomerate containing cobble-sized clasts of basement rocks (Badger, 1999). The Catoctin Formation nonconformably overlies basement rocks throughout the area, but has been removed by erosion in the vicinity of Hogcamp Branch, leading to exposure of the underlying basement rocks. The contact separating greenstone from charnockite is located in the stream valley below the intersection of the access road and Hogcamp Branch (Gathright, 1976). Charnockite is well exposed in ledges located within and adjacent to the stream, from an elevation of about 2,600 ft (790 m) down to near the intersection of Hogcamp Branch and the small stream that descends from Rose River Falls. The basement rocks are composed of massive to weakly foliated, coarse-grained, inequigranular, amphibole-bearing charnockite that is correlated with the large Yfqj pluton located about 3.2 km (2 mi) to the southeast (fig. 3). This low-silica charnockite is distinguished in the field by typically massive to weakly foliated fabric, relatively low quartz content, abundance of pyroxene, and local presence of magnetite. This widespread lithologic unit underlies a significant part of the Big Meadows 7.5-minute quadrangle (geology not shown in fig. 3), as well as most of the Fletcher 7.5-minute quadrangle (fig. 3).

Mileage

Trip Cumulative	Stop-to-Stop Cumulative	
	0.0	Proceed north along Skyline Drive.
68.0	4.5	Timber Hollow Overlook.
78.3	14.8	Buck Hollow Overlook.
78.8	15.3	Mary's Rock Tunnel.
79.8	16.3	Turn right off Skyline Drive toward U.S. 211.
79.9	16.4	Turn left onto U.S. 211 and proceed east.
80.6	17.1	*Earth flows are continually developed in loose soils underlying*

		the steep slope adjacent to the road on the left.
81.3	17.8	*A small quarry in greenstone of the Catoctin Formation is located on the left.*
81.7	18.2	*Outcrops located along the road expose garnetiferous granite gneiss (Yg) near the northern end of a large screen within foliated amphibole-bearing high-silica charnockite (Ycf) of 1,159-Ma age.*
85.4	21.9	Stop 10. Outcrop on left side of U.S. 211.

Stop 10. Old Rag magmatic suite (Ygr).

This outcrop is located near the eastern border of a map-scale dike of garnet-bearing leucogranite that cuts foliated amphibole-bearing high-silica charnockite (Ycf). The large dike is part of the Old Rag magmatic suite and is composed of both medium- and coarse-grained leucogranites that, in this area, cannot be mapped separately at a scale of 1:24,000. The lithologically similar, large pluton that underlies Old Rag Mountain and vicinity is the most likely source of this magma but may be separated from the dike by the Sperryville high-strain zone (SHSZ, fig. 3) originally mapped by Gathright (1976).

Rocks of the Old Rag magmatic suite include massive to moderately foliated, fine- to coarse-grained, inequigranular granite and leucogranite that locally contains biotite+orthopyroxene+garnet (Hackley, 1999). This composite unit was mapped as Old Rag Granite by previous workers (Allen, 1963; Gathright, 1976). In this study, Old Rag Granite is defined only in the vicinity of Old Rag Mountain, where it forms a triangular-shaped plutonic body composed of homogeneous, massive to weakly foliated, coarse- to very coarse-grained, inequigranular, garnet+orthopyroxene granite and leucogranite. Using mineralogic, geochemical, and field criteria, Hackley (1999) demonstrated that the fine- to locally coarse-grained, inequigranular granite and leucogranite that is the dominant litholo-gy of the map-scale dike (and other smaller bodies) and the coarse- to very coarse-grained granite at Old Rag Mountain are petrologically consanguineous, and considered both litho-logic varieties to constitute the Old Rag magmatic suite. All granitoids within the suite are composed of variable amounts of alkali feldspar+plagioclase+quartz (typically blue). Orthopyroxene, biotite, and garnet occur nonsystematically as primary ferromagnesian phases. The rocks are typically massive to weakly foliated; alignment of ductilely deformed quartz locally defines a crude lineation.

Rocks of the Old Rag magmatic suite are characterized by high SiO_2 contents (table 4) and peraluminous compositions (fig. 5D). The suite includes some of the most chemically evolved rocks in the area; however, similar FeO_t/MgO ratios suggest that the Old Rag rocks are not petrologic derivatives of the penecontemporaneous low-silica Yfqj charnock-ite (fig. 5F). Two representative chemical analyses of rocks of the suite are included in table 4: OR-97-35, coarse-grained garnetiferous leucogranite; and OR-97-51, fine-grained biotite leucogranite. Both samples were collected from Old Rag Mountain; zircons from OR-97-35 were analyzed isotopically for U-Pb geochronology, as described below. These leucogranites display trace-element features that suggest derivation from sources of mixed composition and are typical of post-tectonic granitoids (Förster and others, 1997) (fig. 6). As such, rocks of the Old Rag magmatic suite display geochemical characteristcs that are transitional between I- and A-type granitoids (fig. 7).

Mineralogically and geochemically similar, massive to weakly foliated, leucocratic granitoids constitute a significant lithologic component of Blue Ridge Mesoproterozoic basement, including the Old Rag magmatic suite, garnetiferous alkali feldspar and syenogranite (Ygg), and alkali feldspar granite (Yaf). Gathright (1976) was among the first to recognize that the nonfoliated to weakly foliated fabric and crosscutting field relations of the Old Rag granitoids indicated a relatively late emplacement age among basement rocks. Results from high-precision SHRIMP analyses of zircons from a sample of coarse-grained Old Rag Granite collected from Old Rag Mountain demonstrate a complex geochronologi-cal history for this unit. CL imaging indicates that nearly all of the zircons have oscillatory

zoned cores and dark overgrowths. Thirteen analyses of the oscillatory zoned portions of zircons from the Old Rag Granite yield a weighted average of the $^{207}Pb/^{206}Pb$ ages of 1,060±5 Ma, which we interpret as the time of emplacement of the Old Rag Granite and, by extension, the Old Rag magmatic suite. Ages of overgrowths indicate two episodes of post-magmatic crystallization occurring at 1,019±15 Ma and 979±11 Ma, which we interpret as indicating times of thermal disturbance. Monazite from the Old Rag Granite was also dated by SHRIMP methods. Five analyses yield an age of 1,059±8 Ma, identical within uncertainty to the emplacement age interpreted from zircon. Six other monazite analyses yield an age of 1,027±9 Ma and one grain is 953±30 Ma, both within uncertainty of the zircon overgrowth ages of 1,019±15 and 979±11 Ma, respectively. Thus, these data appear to indicate that a significant episode of post-tectonic igneous activity occurred at about 1,060 Ma, following a period of deformation that must have begun after 1,080 Ma (Tollo and others, in press a). This magmatism was, in turn, followed by one or two periods of regional thermal disturbance.

Mileage

Trip Cumulative	Stop-to-Stop Cumulative	
	0.0	Proceed east on U.S. 211.
91.5	6.1	Turn left onto U.S. Bus. 211 and proceed north toward Washington, Va.
92.7	7.3	Continue straight on Main Street at intersection with Va. 622.
		Va. 622 branches left from Va. 628; continue straight on Va. 628.
95.2	9.8	Stop 11.
		Turn right onto Horseshoe Hollow Lane.
		Follow Trip Leaders
		PRIVATE PROPERTY

Stop 11. Foliated pyroxene granite (Yfpg).

Foliated pyroxene granite (Yfpg) defines a circular pluton that appears to cut Flint Hill Gneiss in the southeastern part of the Chester Gap 7.5-minute quadrangle (fig. 3). The northwest border of the body is truncated by the Stanley fault, which juxtaposes Yfpg charnockite against greenstone of the Catoctin Formation. This meta-igneous intrusive body is part of a subset of charnockitic rocks characterized by high to moderately high silica contents, but its emplacement age is different from any other charnockites presently dated within the field trip area. The ages of silica-rich charnockitic rocks already dated and field characteristics of a recently discovered high-silica charnockite in the Big Meadows 7.5-minute quadrangle suggest that silica-rich charnockitic magmas were emplaced during each of the three main episodes of magmatic activity in the northern Blue Ridge.

The Yfpg pluton is composed of light-gray, medium- to coarse-grained, inequigranular, strongly foliated monzogranite (*farsundite*) composed of 30 to 40 percent microcline, 30 to 40 percent plagioclase, and 15 to 20 percent quartz with 5 to 7 percent orthopyroxene, 0 to 2 percent amphibole, 0 to 5 percent biotite, and rare garnet. Accessory minerals include apatite, zircon, and ilmenite. Foliation is defined by discontinuous, centimeter-scale domains composed of ferromagnesian minerals. Dikes composed of coarse-grained, nonfoliated alkali feldspar+blue quartz, that range up to 1 m (3.3 ft) in width, and coarse-grained, nonfoliated garnet-bearing leucogranite, that range up to 1.5 m (4.9 ft) in width, locally intrude monzogranite and are typically oriented parallel to foliation. The strong foliation defined by discontinuous clusters of minerals sets this lithologic unit apart from all other charnockites in the area. Overall grain size is greatly reduced, and mineralogic segregation becomes less pronounced where the pluton is affected by deformation along the Stanley fault.

Rocks analyzed from the Yfpg pluton exhibit a range in SiO_2 content of 67 to 72 weight percent and are weakly peraluminous to borderline metaluminous (fig. 5D). The

composition of a sample collected from this outcrop for U-Pb geochronologic analysis is included in table 4 (sample SNP-02-177). The Yfpg rocks are geochemically similar to other, older high-silica charnockites, including the garnetiferous gneiss (Yg) and amphi-bole-bearing *charnockite* and *farsundite* (Ycf) (fig. 5). Trace-element data indicate that, like these rocks, Yfpg was probably derived from sources of mixed composition.

Zircons analyzed from a sample collected from this outcrop are isotopically complex and provide considerable insight into the regional geologic history. Analyses of zircon cores provide a weighted average age of 1,178±14 Ma, which we interpret as indicative of inheritance. Analyses of zoned mantles indicate a likely crystallization age of 1,115±13 Ma, which is interpreted as the time of pluton emplacement. Analyses of rim overgrowths indicate ages of 1,050±13 Ma and ~1,010 Ma. The 1,115-Ma emplacement age indicates that the Yfpg pluton intruded nearly contemporaneously with the 1,111-Ma Marshall Metagranite, a lithologically complex noncharnockitic granitoid that occurs in the Blue Ridge approximately 32 km (20 mi) to the northeast, and which was dated by Aleinikoff and others (2000) using ID-TIMS techniques. The local significance of this magmatic episode is not yet understood; however, McLelland and others (1996) suggested that mag-matism of similar age in the Adirondacks resulted from far-field effects of activity associat-ed with development of the Midcontinent Rift. The 1,178-Ma inherited age of the Yfpg pluton corresponds closely to the age of megacrystic leucocratic granite gneiss (Ylg) that occurs in the southern part of the field trip area and suggests that crust produced during the earlier magmatic episode was partly recycled during subsequent magma genesis. Finally, the overgrowth ages of 1,050 and 1,010 Ma are each considered to preserve evidence of thermal disturbance. The former age corresponds to the timing of the final magmatic episode in the Blue Ridge, during which rocks such as the Old Rag magmatic suite (Ygr) and low-silica charnockite (Yfqj) were emplaced, and the 1,010-Ma date falls within the range of a possible heating event for which evidence is preserved as overgrowths on zir-cons from other basement rocks in the Blue Ridge (table 3) (Tollo and others, in press a).

Mileage

Trip Cumulative	Stop-to-Stop Cumulative	
	0.0	Proceed north on Va. 628.
96.6	1.4	Turn left to continue on Va. 628 at intersection with Va. 606.
97.4	2.2	Turn right onto Va. 628 at (poorly marked) four-way intersection.
99.3	4.1	Turn left onto Va. 630, which becomes unpaved.
101.2	6.0	Stop 12.
		Outcrop on left side of Va. 630 before bridge.

Stop 12. Flint Hill Gneiss (Yfh).

The Flint Hill Gneiss constitutes a distinct lithologic unit that underlies a large, elon-gate area of the Blue Ridge basement core east of the Sperryville high-strain zone in north-ern Virginia (Virginia Division of Mineral Resources, 1993). The rock is characterized by a strongly developed gneissic fabric and abundance of typically blue quartz. The unit has not been dated by modern isotopic techniques, but the strongly deformed fabric suggests that it is likely part of the oldest group of basement rocks in the region.

The Yfh lithologic unit includes dark-gray, medium- to coarse-grained, inequigranular, strongly foliated syeno- to monzogranitic gneiss composed of 35 percent microcline, 20 percent plagioclase, and 20 percent quartz with 2 percent biotite and 5 percent chlorite. Accessory and secondary minerals include apatite, leucoxene, zircon, and ilmenite. Gneissic layering is defined by alternating quartz+feldspar-rich and biotite+chlorite-rich domains that are typically 1 to 10 cm (0.4–4 in) in thickness. Foliation is defined by planar alignment of biotite and is parallel to gneissic layering. Granular quartz ranges from dark gray to blue; locally abundant quartz veins are typically blue. The characteristic composi-

tional banding in the gneiss is commonly contorted and kinked (Clarke, 1984), preserving visible evidence of the high degree of deformation that has affected this unit. Veins composed primarily of blue quartz and dikes composed of fine- to medium-grained leucocratic granite are common within the Flint Hill Gneiss. Clarke (1984) reported that the widespread blue quartz veins are generally conformable to gneissic layering, whereas dikes typically crosscut banding.

The Flint Hill Gneiss is characterized by SiO_2 contents that are generally in the range of 69 to 72 weight percent (table 4; fig. 5). Limited sampling of Flint Hill rocks suggests that a lower silica variant with SiO_2 contents about 64 weight percent is present in nearby quadrangles. The rocks are generally mildly peraluminous, consistent with the ubiquitous presence of biotite. Normative compositions and trace-element characteristics and occurrence of this lithologic unit within a terrane that is otherwise dominated by rocks of intrusive magmatic origin suggest that the Flint Hill Gneiss is meta-igneous in origin. Results from previous geochronologic investigations involving U-Pb isotopic analysis of zircons from the Flint Hill Gneiss are considered unreliable due to the isotopic complexities that have been documented in zircons from other Grenvillian rocks in the area (Aleinikoff and others, 2000; Tollo and others, in press a).

Mileage

Trip Cumulative	Stop-to-Stop Cumulative	
	0.0	Turn around and proceed east on Va. 630.
103.1	1.9	Turn left to continue on Va. 630.
103.9	2.7	Turn right onto U.S. 522 and proceed south through the town of Flint Hill.
108.7	7.5	Turn right onto U.S. 522/U.S. 211 and proceed west.
116.7	15.5	Turn left onto U.S. 522/Va. 231 in Sperryville and proceed south. Cross bridge over the Thornton River.
116.8	15.6	Turn left to remain on U.S. 522 and proceed southeast.
117.4	16.2	Turn right onto Va. 231 and proceed south.
126.6	25.4	*Old Rag Mountain is visible to the west (right). The mountain, formerly called "Old Raggedy," is characterized by steep rocky slopes and is a popular local recreational destination. The mountain is underlain by typically coarse-grained, locally garnet-bearing leucogranite of the Old Rag magmatic suite, defining a fault-bounded pluton.*
132.5	31.3	Turn right onto Va. 670 and proceed west. *View toward the west (straight ahead) of Double Top Mountain, which is underlain primarily by amphibole-bearing low-silica charnockite (Yfqj).*
133.3	32.1	Stop 13. Follow Trip Leaders. PRIVATE PROPERTY

Stop 13. Biotite granitoid gneiss (Ybg) containing xenoliths of medium-grained foliated leucocratic granitoid (Ylg).

Medium- to coarse-grained biotite granitoid gneiss and layered granitoid gneiss, mapped together within a single lithologic unit (Ybg), underlie a large area east of the Quaker Run fault zone in the northern part of the Madison 7.5-minute quadrangle (fig. 3). This mineralogically distinctive unit, and other similarly biotite-rich rocks mapped east of the Rockfish Valley fault zone in areas of the Blue Ridge province located to the south (Hughes and others, in press), contrast sharply with the more typical granites, leucogranites, and charnockitic rocks that underlie much of the area. Pegmatites associated with the Old Rag Granite pluton appear to cut biotite granitoid gneiss along the southeastern margin of the body southeast of Old Rag Mountain (Hackley, 1999), indicating that the peraluminous leucogranitoids of the Old Rag magmatic suite are likely younger than the Ybg rocks. Dikes of probable Ybg affinity intrude leucogranite gneiss (Ylg) at Stop 15 and elsewhere

Figure 11. Photograph of xenolith of medium- to coarse-grained foliated leucocratic granitoid (Ylg) within foliated medium-grained biotite granitoid gneiss (Ybg) at Stop 13. Hammer handle, oriented parallel to foliation in the gneiss, is 82 cm (32 in) long.

in the Madison area, indicating that Ybg is younger than the Ylg lithologic complex.

The Ybg unit includes gray to grayish-black, medium- to coarse-grained, massive to foliated, biotite granitoid containing a dominant mineral assemblage of alkali feldspar+plagioclase+quartz+biotite. The unit also contains medium- to coarse-grained, layered granitic gneiss with 1- to 3-cm (0.4–1.2-in)-thick felsic domains composed of plagioclase+alkali feldspar+quartz separated by weakly developed layers of biotite+epidote+quartz (Bailey and others, 2003). Biotite typically constitutes 15 to 25 percent of the rock. This outcrop exposes protomylonitic biotite granitoid gneiss containing porphyroclasts of white feldspar and elongate quartz lenses. Abundant biotite+epidote bands define a foliation that strikes 020° and dips steeply to the east. The mineralogic assemblage defining this foliation is indicative of formation at greenschist-facies conditions and suggests that the fabric was developed during Paleozoic orogenesis.

Geochemical data indicate that the Ybg lithologic unit is characterized by a bimodal range in silica contents, with compositions corresponding to SiO_2 values of 61 to 63 and 67 to 68 weight percent (fig. 5). The rocks are metaluminous to mildly peraluminous (fig. 5D), and display trace-element characteristics such as high concentrations of high-field-strength elements and modestly high Ga/Al ratios that suggest affinity to A-type granites (figs. 6, 7). These compositional characteristics and the overall tholeiitic and subalkaline nature of the rocks suggest that Ybg rocks were likely igneous in origin.

Xenoliths of foliated medium- to coarse-grained leucocratic granitoid, interpreted to be derived from the Ylg lithologic unit, occur within the foliated biotite granitoid gneiss at this locality (fig. 11). Foliation defined by alignment of feldspar megacrysts and discontinuous compositional banding involving recrystallized quartz within the xenoliths is oriented at an angle to foliation in the surrounding biotite granitoid gneiss. This relation, and the likely higher-temperature ductile origin of foliation within the xenoliths, suggests that the fabric in the leucogranite formed during Grenvillian orogenesis. This field relation is consistent with the presence of dikes of Ybg affinity that cut Ylg rocks elsewhere in the vicini-

ty, and thus provides a maximum age constraint of 1,183±11 Ma (age of emplacement for part of the Ylg lithologic complex) for emplacement of protolith magmas for the Ybg rocks.

Mileage

Trip Cumulative	Stop-to-Stop Cumulative	
	0.0	Continue west on Va. 670 through Criglersville.
134.1	0.8	*Outcrops within and adjacent to the riverbed on the left expose contact relations between the Ylg and Ybg lithologic units (Bailey and others, 2003).*
134.3	1.0	Turn left onto Va. 649 (Double Top Road.)
136.8	3.5	Becomes dirt road.
137.3	4.0	Stop 14. Pull over to the right at hairpin turn.

Stop 14. Low-silica charnockite (Yfqj) and mylonite in the Quaker Run high-strain zone.

Amphibole-bearing low-silica charnockite (Yfqj) ranging from monzogranite (*farsundite*) to quartz monzodiorite (*quartz jotunite*) in normative composition (fig. 4) is widespread throughout the field trip area, constituting a large pluton located east of the crest of the Blue Ridge. Similar rocks also occur as dikes and small plutons in areas located to the north. The characteristic nonfoliated to weakly foliated fabric of this rock unit indicates that it is part of the youngest group of Grenvillian plutonic rocks in this part of the Blue Ridge.

The outcrop at the sharp bend in the road is an outstanding example of a fresh, massive, coarse-grained charnockite. This lithologic unit is composed of dark-gray to dark-gray-green, medium- to very coarse-grained, equigranular to inequigranular, massive to weakly foliated monzogranite, granodiorite, and quartz monzodiorite (*farsundite, opdalite,* and *quartz jotunite*) composed of 9 to 30 percent alkali feldspar microperthite (chiefly microcline), 30 to 49 percent plagioclase, and 14 to 26 percent quartz with 10 to 17 percent orthopyroxene, 0 to 7 percent amphibole, and rare clinopyroxene. Accessory minerals include apatite, ilmenite, magnetite, zircon, epidote, and actinolite. Rare, typically weakly developed foliation is defined locally by planar alignment of ferromagnesian minerals. Lenticular, magnetite-rich enclaves, which range in length to 0.5 m (20 in), occur locally and are aligned parallel to foliation. Subhedral to euhedral, monocrystalline alkali feldspar megacrysts range up to 10 cm (4 in) in length and are best observed on weathered surfaces. The rock typically weathers to form a distinct orange rind and similarly colored, clay-rich soils that are useful in mapping. This outcrop is located within the Quaker Run high-strain zone (fig. 3) (Bailey and others, 2003), as indicated by fabric observed in other exposures along the road where undeformed charnockite grades into mylonite with multigranular feldspar porphyroclasts and elongate quartz ribbons. The occurrence of undeformed rock within highly strained rocks illustrates the heterogeneous nature of strain within the Quaker Run high-strain zone. The northwestern boundary of the high-strain zone is clearly defined by massive charnockite; however, the southeastern boundary is more difficult to define due to the abundance of phyllosilicates and the foliated nature of the biotite granitoid gneiss (Ybg).

The compositionally diverse Yfqj lithologic unit is characterized by relatively low silica contents (51 to 65 weight percent SiO_2) that distinguish the unit from most of the other, typically high-silica Grenvillian rocks in the area (fig. 5). The rocks are generally metaluminous and exhibit subalkaline tholeiitic characteristics (fig. 5D–F). The Yfqj rocks are also distinguished compositionally by relatively high Ga/Al ratios and concentrations of high-field-strength elements, including Y, Nb, and Zr (figs. 6, 7). These features, especially the high concentrations of both Zr and Nb, distinguish this unit from nearly all other rocks studied in the area, and suggest geochemical affinity to A-type granitoids (Eby, 1990;

Whalen and others, 1987) and within-plate granitoids (Pearce and others, 1984). These features suggest that Yfqj magmas were derived from dominantly crustal sources (Landenberger and Collins, 1996), in contrast to the typically mixed heritage that characterizes most other units in the region (Tollo and others, in press a).

Yfqj charnockite is locally cut by dikes of coarse-grained leucogranite that are likely related to the 1,060±5-Ma Old Rag Granite (Tollo and others, in press a,b). The characteristic unfoliated to weakly foliated fabric of both units indicates that the rocks were emplaced after the major episode of deformation that affected the 1,078±9-Ma leucogranite gneiss (Ylgg) unit. Analysis of a sample of the Yfqj pluton collected from the Fletcher 7.5-minute quadrangle indicates that the euhedral to subhedral prismatic zircons contain (1) cores distinguished by oscillatory zoning that likely reflects compositional variation resulting from igneous crystallization and (2) unzoned rims that typically contain higher U concentrations than the cores (Tollo and others, in press a). Tollo and others (in press a) reported results from 18 analyses of cores that yielded a weighted average of the $^{207}Pb/^{206}Pb$ ages of 1,050±8 Ma, which they interpreted as the time of igneous crystallization of the charnockite. Five analyses of the overgrowths indicated a subsequent episode of thermal flux related to metamorphism at 1,018±14 Ma. The 1,060±5-Ma emplacement age of the Old Rag Granite overlaps the emplacement age of the charnockite and, considering the crosscutting field relations documented in the area, suggests that the magmatic protoliths of these rocks intruded over possibly extended, penecontemporaneous intervals.

Mileage

Trip Cumulative	Stop-to-Stop Cumulative	
	0.0	Turn around and proceed downhill along Va. 649.
140.1	2.8	Turn right onto Va. 670 and proceed southeast.
141.4	4.1	*Outcrops in river are biotite granitoid gneiss (Ybg).*
142.0	4.7	Turn right onto Va. 231 and proceed southeast.
142.5	5.2	Intersection with Va. 609. Bridge across the Robinson River.
142.7	5.4	*Outcrop to the south exposes the eastern contact of the Mechum River Formation and Ylg lithologic unit.*
143.0	5.7	Turn right onto Va. 651 (Aylor Road).
		Outcrops in the field to the left expose biotite granitoid gneiss (Ybg) near the intrusive contact with alkali feldspar syenite of the Neoproterozoic Robertson River batholith (Bailey and others, 2003).
145.9	8.6	Bear right to remain on Va. 651.
146.5	9.2	Stop 15.
		Follow Trip Leaders
		PRIVATE PROPERTY

Stop 15. Ylg basement complex exposed in debris-flow scar.

The dominant rock types in this exposure constitute a composite felsic pluton composed of multiple lithologies including (from oldest to youngest): (1) foliated, coarse-grained to megacrystic leucocratic granite (Ylg1), (2) medium-grained, equigranular, weakly to moderately foliated leucogranite (Ylg2), and (3) coarse-grained to very coarse-grained, inequigranular, nonfoliated to weakly foliated leucogranite pegmatite (Ylg3). Because of similarities in mineral assemblage and geochemical composition, these distinctive rocks are collectively mapped as the Ylg lithologic unit in the southern part of the field trip area (Bailey and others, 2003; Tollo and others, in press b).

Although dominantly leucogranitoids, constituent lithologic units of the Ylg plutonic complex exhibit minor differences in mineral assemblage. The strongly foliated, megacrystic leucocratic granite is composed of alkali feldspar mesoperthite (both microcline and orthoclase), plagioclase, quartz, and intergrown biotite+chlorite, whereas the medium-

Figure 12. Photograph of folded medium-grained leucocratic granite dike within coarse-grained to megacrystic leucocratic granitoid at Stop 15. Pen (top center), oriented parallel to foliation in the megacrystic granitoid and parallel to the trace of the axial plane in the folded dike, is 14 cm (5.5 in) long. Development of small lens of pegmatite within the dike on the left limb of the fold suggests that pegmatite was derived through differentiation of the medium-grained granitoid magma.

grained, equigranular, weakly to moderately foliated leucogranite is composed of alkali feldspar (chiefly microcline), plagioclase, and quartz with minor secondary biotite; and the nonfoliated to weakly foliated leucogranite pegmatite is composed of alkali feldspar (microcline), minor plagioclase, and quartz. These mineralogic differences, especially the progressive decrease in biotite content, reflect a weak trend toward more evolved chemical compositions.

This large exposure illustrates crosscutting relations among several Blue Ridge basement units. Field relations indicate that the foliated coarse-grained to megacrystic leucocratic granite is the oldest rock at this outcrop. Dikes exposed in some of the steep ledges indicate that the megacrystic granite was intruded by medium-grained leucogranite that was subsequently folded with axial planes that are nearly parallel to foliation in the coarse-grained megacrystic granitoid (fig. 12). Very coarse-grained leucogranite pegmatite occurs as locally boudinaged dikes cutting both the coarse-grained leucocratic granitoid (Ylg1) and medium-grained equigranular leucogranite (Ylg2). Local development of leucogranitic pegmatite within medium-grained leucogranite (fig. 12) further suggests that the pegmatite was derived through differentiation of medium-grained leucogranite magma. A 30- to 50-cm (12–20-in)-wide dike of fine- to medium-grained biotite granodiorite intrudes all of the leucocratic granitoid units in ledges located near the base of the exposure. This dike, which contains a mineral assemblage that is similar to biotite granitoid gneiss (Ybg), clearly post-dates the deformation recorded in the leucocratic rocks, and suggests that Ybg is younger than Ylg, a relation that is consistent with field relations observed at Stop 14.

At the base of the outcrop a ~15-cm (6-in)-thick dike of coarse-grained pegmatite cuts medium-grained leucogranite and is deformed into a series of tight folds with rounded hinges (fig. 13). The medium-grained leucogranite displays weak foliation that strikes ~070°, dips steeply to the northwest, and is axial planar to the folds in the leucogranite dike. Line-length restoration of the dike indicates ~70 percent shortening in a north-north-
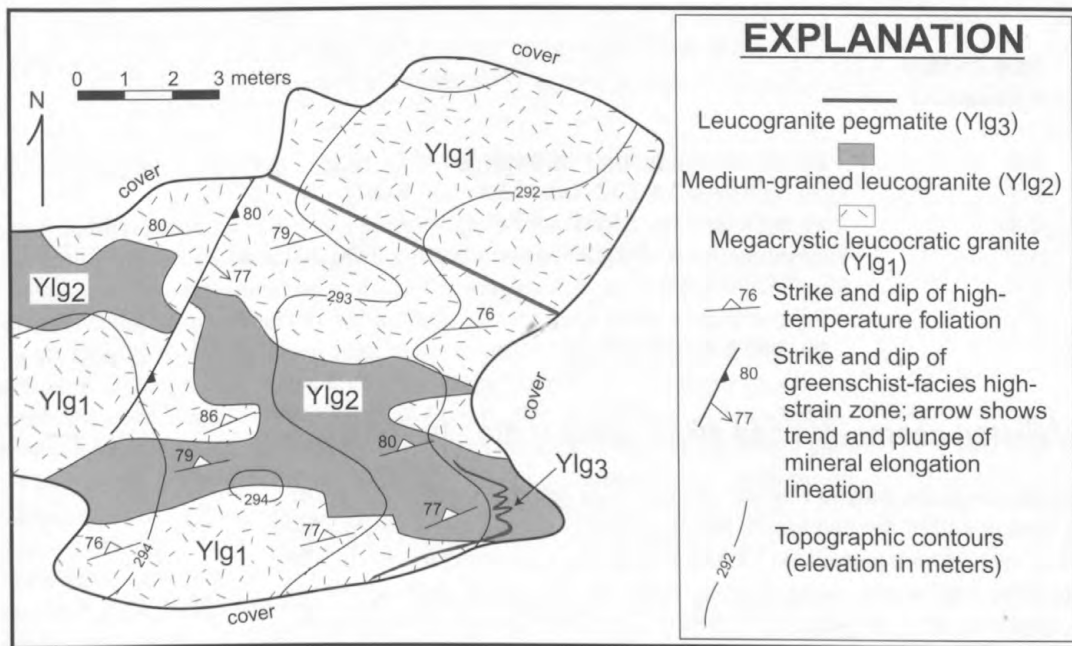
Figure 13. Detailed geologic map of outcrop exposed at the base of debris-flow scar at Stop 15.

west–south-southeast direction, but the fabric in the enclosing leucogranite is barely visible. We interpret the medium-grained leucogranite to have statically recrystallized at high temperatures after deformation, and thus it does not faithfully record the total strain history. The high-temperature deformation recorded in the pegmatite is interpreted to be Mesoproterozoic in age and is commonly overprinted by a foliation defined by aligned micas. Crosscutting relations observed throughout the exposure are interpreted to indicate multiple episodes of magmatic injection occurring throughout an extended interval of time.

Basement units are cut by a northeast-striking, ~5-m (16-ft)-wide dike of porphyritic hornblende metagabbro. The metagabbro is composed of hornblende, extensively altered plagioclase, epidote, and chlorite. The dike is part of a suite of mafic to ultramafic igneous rocks that intrude Blue Ridge basement and Neoproterozoic metasedimentary units and which are interpreted to be associated with an early, pre-Catoctin pulse of Neoproterozoic rifting (Bailey and others, 2003).

A set of discrete high-strain zones cuts all basement units in this exposure. These zones range from a few centimeters in thickness to millimeter-scale. Where discernible, mineral elongation lineations plunge obliquely downdip. The apparent offset, as illustrated on the subhorizontal outcrop surface, is dextral. However, there clearly was out-of-section movement as well. The mineralogy and microstructures in the high-strain zones are consistent with formation at greenschist-facies conditions and are interpreted to result from Paleozoic contraction.

U-Pb isotopic analysis of zircons from foliated megacrystic granitoid collected from this exposure indicate igneous crystallization at 1,183±11 Ma, followed by metamorphic recrystallization at 1,043±16 Ma and ~1,110 Ma (table 3, sample SNP-02-189). These data indicate that Ylg is currently the oldest lithologic unit recognized in the area. Chemical analyses of samples collected from both the medium-grained and megacrystic leucocratic granitoids indicate that the rocks are characterized by SiO_2 contents of 69 to 77 weight percent, with most compositions in the range of 74 to 76 weight percent (table 4, fig. 5). Such chemically evolved compositions are similar to those of the much younger, ~1,060-Ma leucocratic granitoids of the Old Rag magmatic suite (Ygr) and garnetiferous alkali feldspar granite (Ygg), and thus suggest that production of leucogranite magmas was cyclic. Compositions of Ylg samples differ from the younger leucocratic rocks in having lower concentrations of Y+Nb (fig. 6), a characteristic that suggests derivation from different sources.

Mileage

Trip Cumulative	Stop-to-Stop Cumulative	
	0.0	Turn around and return east along Va. 651.
147.0	0.5	Turn right onto Va. 652 (Gaar Mountain Road).
149.3	2.8	Turn right onto Va. 656 (Ruth Road).
149.7	3.2	First intersection (Ruth Road and Courtney Hollow Lane).
150.0	3.5	Stop 16.
		Follow Trip Leaders
		PRIVATE PROPERTY

Stop 16. Nonfoliated coarse-grained alkali feldspar granite (Yaf).

Nonfoliated, coarse-grained alkali feldspar granite (Yaf) defines two small (< 1 km^2; 0.4 mi^2) plutons located within foliated biotite granitoid gneiss (Ybg) east of the Mechum River Formation in the southern part of the Madison 7.5-minute quadrangle (fig. 3). This lithologic unit includes gray-white, coarse-grained, equigranular to porphyritic alkali feldspar granite composed of 1- to 5-cm (0.5–2.0-in) white alkali feldspar+blue-gray quartz with minor plagioclase, biotite, titanite, and Fe-Ti oxide minerals (Bailey and others, 2003).

Anastomosing high-strain zones (up to 30 cm (12 in) thick) composed of well-foliated, mica-rich mylonite and ultramylonite locally cut the coarse-grained leucogranite. Detailed kinematic, fabric, and chemical analysis of the largest high-strain zone suggests bulk isochemical (isovolumetric?) behavior, modest flattening strains, and a general shear deformation with monoclinic symmetry (Bailey and others, in press).

The nonfoliated fabric and abundant alkali feldspar+quartz mineral assemblage of the Yaf unit indicates that these bodies are likely correlative with the group of postorogenic leucocratic granitoids documented to the north that includes the Old Rag magmatic suite (Ygr) and garnetiferous syenogranite (Ygg), which have emplacement ages of 1,060±5 Ma and 1,064±7 Ma, respectively (table 3). Consistent with this correlation, alkali feldspar granite dikes of Yaf affinity that range in width from 0.1 to 3 m (0.3–10 ft) cut both the leucocratic granitoid complex (Ylg) and the biotite granitoid gneiss (Ybg) (Bailey and others, 2003).

Mileage

Trip Cumulative	Stop-to-Stop Cumulative	
	0.0	Turn around and proceed east on Va. 656.
		Continue straight at intersection with Va. 652.
154.0	4.0	Turn right onto Main Street.
154.1	4.1	Intersection with Va. 634 (Washington Street); continue straight.
155.1	5.1	Merge onto U.S. 29 (Seminole Trail) and proceed south.
157.0	7.0	Turn right onto Va. 230 (Wolftown-Hood Road) and proceed west.
160.6	10.6	Turn right onto Va. 622 (Graves Mill Road).
162.1	12.1	Turn left onto Va. 665 (Garth Run Road).
162.9	12.9	Turn right to remain on Va. 665.
		Kirtley Mountain, visible to the west, was the site of numerous debris flows in the 1995 storm that affected this area. The large exposures of bedrock in the denuded channels visible from the highway are composed dominantly of amphibole-bearing low-silica charnockite (Yfqj) (Tollo and others, in press b).

164.3   14.3   Stop 17.
                             Pull over south of the bridge over Garth Run.
                             Proceed to exposures in stream valley.

Stop 17. Mylonitic rocks of the Garth Run high-strain zone.

The Garth Run high-strain zone is well exposed in a 200-m (650-ft)-long outcrop scoured out along the channel of Garth Run during the June 1995 storm. This exposure has proven to be seminal to our understanding of ductile deformation in the Blue Ridge. The high-strain zone strikes north-northwest to north-northeast and joins the 1- to 2-km (0.6–1.2-mi)-wide Quaker Run high-strain zone to the north and tips out to the south (Berquist and Bailey, 2000). Although the high-strain-zone boundary is not exposed, outcrop data indicate the zone is approximately 125 m (410 ft) thick). The zone is bounded to the west by medium- to coarse-grained, equigranular to porphyritic charnockite (Yfqj), and to the east by rocks of the leucogranite complex (Ylg). Medium-grained layered granitic gneiss is the dominant rock type east of the Garth Run high-strain zone. The gneiss is intruded by a series of fine- to coarse-grained leucogranite dikes ranging from 0.3 to 5 m (1–16 ft) in thickness.

Rocks exposed in the Garth Run high-strain zone are dominantly porphyroclast-bearing protomylonites and mylonites. Finely-layered mylonitic leucogneiss, leucogranite, and well-foliated fine-grained metabasalt occur as tabular to lenticular bodies that are 0.2 to 2 m (0.6–6.5 ft) thick throughout the high-strain zone. These tabular bodies are both subparallel and slightly discordant to the foliation. Foliation, defined by mica-rich surfaces, elongate quartz grains, and fractured feldspars, strikes 345° to 010° and dips 30 to 50° to the east. A mineral elongation lineation plunges downdip or obliquely to the east-northeast; however, mineral elongation lineations are not present everywhere.

Sheath folds occur in the finely-layered mylonitic leucogneiss and sheath axes plunge moderately to the east, parallel to the mineral elongation lineation. Coarse-grained leucogranitic bodies display pinch-and-swell structures, and are commonly isolated as lozenge-shaped boudins surrounded by porphyroclastic mylonites. Leucogranitic boudins record elongation both parallel and normal to the east-northeast-plunging elongation lineation, indicating bulk extension in both the Y and X directions. Leucogranites have a weak foliation and are cut by numerous transgranular fractures. Slightly discordant, tabular, boudinaged leucogranitic dikes are locally folded. At a few locations, the mylonitic foliation is kinked into narrow bands that are 2 to 5 cm (0.8–2.0 in) wide.

Asymmetric structures such as sigma and delta porphyroclasts, shear bands, and asymmetric boudins are common in the Garth Run high-strain zone. Asymmetric structures, both parallel (reverse sense of shear) and perpendicular (sinistral sense of shear) to the mineral elongation lineation, are consistent with triclinic deformation symmetry. Sectional strains estimated from discrete quartz lenses and ribbons range from 3:1 to 23:1. Three-dimensional strains record apparent flattening. The kinematic vorticity number was estimated using the porphyroclast hyperbolic distribution method of Simpson and De Paor (1993) on ultramylonite thin sections and joint faces with well-exposed porphyroclasts. W_n-values range from 0.6 to 0.4, indicating general shear deformation. Shear strain is conservatively estimated at 4 and integrates to a total displacement of ~500 m (1,640 ft) across the Garth Run high-strain zone. Discrete brittle faults with displacements of 0.2 to 2 m (8–79 in) cut the mylonitic fabrics.

Folded leucogranite boudins may offer a clue about the progressive deformation history of the Garth Run high-strain zone. These structures formed when competent leucogranite dikes were first elongated and then shortened. During progressive steady-state deformation, material rotated from the field of shortening into the field of extension, a progression that did not fold boudins. Folded boudins are generally interpreted to develop by polyphase deformation, such that material elongated during the first deformation is shortened by a second deformation having a different orientation. However, a change in the incremental vorticity will cause some material that was originally deformed in the field of extension to

move into the field of shortening. There are no crosscutting ductile fabrics in the Garth Run high-strain zone. Bailey and others (in press) proposed a model in which the dominant mechanism of deformation changed from simple shear to pure shear over time.

Mileage

Trip Cumulative	Stop-to-Stop Cumulative	
	0.0	Turn around and proceed south on Va. 665.
165.7	1.4	Turn left to remain on Va. 665.
166.4	2.1	Turn left onto Va. 622 (Graves Mill Road) and proceed north.
167.4	3.1	*View of debris-slide scars to the east on German Mountain.*
170.2	5.9	Graves Mill.
		Continue straight onto Va. 615 (Bluff Mountain Road).
171.4	7.1	Stops 18 and 19.
		Pull into parking area on right side of Va. 615.

Stop 18. Kinsey Run, west branch: low-silica amphibole-bearing charnockite (Yfqj) and associated pegmatite; mylonite, and protomylonite.

Stops 18 and 19 are located about 2 km (1.2 mi) uphill from the road and can be reached by hiking along a logging trail to the upper reaches of Kinsey Run. The stops include the denuded channels caused by mass-wasting processes resulting from the intense rainfall that affected the area in June 1995. The stops are located on two branches of Kinsey Run that were significantly widened by the debris flows. Stop 19 can be reached from the logging trail by hiking eastward from the west branch over the drainage divide to the east branch.

Both stops are located within medium- to very coarse-grained, equigranular to inequigranular, massive to weakly foliated, amphibole-bearing low-silica charnockite (Yfqj) that defines a large pluton in the southern part of the field trip area (fig. 3). The generally nonfoliated fabric of the charnockite indicates postorogenic emplacement and is consistent with the 1,050±8-Ma age determined by U-Pb isotopic analysis (Tollo and others, in press a; table 3). Microstructural characteristics also indicate emplacement within a post-deformation environment. Quartz grains (2–7 mm), which compose 15 to 25 modal percent of the rock, are bleb-like and display no grain-shape preferred orientation, attesting to the relatively undeformed nature of the charnockite. Orthopyroxene exhibits partial alteration to a mixture of fine-grained uralitic amphibole+secondary biotite that is localized along grain boundaries and most likely indicative of Paleozoic retrograde metamorphism.

The Yfqj charnockite in the main area of exposure contains several decimeter- to meter-size pods of coarse-grained amphibole+magnetite-bearing pegmatite that generally grades into the surrounding medium- to coarse-grained charnockite. The mineral assemblage within these pegmatite pods is similar to the surrounding charnockite. Moreover, amphiboles in these pegmatites are characterized by edenitic (nomenclature after Leake and others, 1997) compositions that are similar to amphiboles within the surrounding charnockite, indicating that the pegmatites are most likely derived from the charnockitic magmas through local fluid saturation and differentiation.

Three subvertical mafic dikes, striking ~350°, are exposed intruding the charnockite (fig. 14). Contacts are well exposed and display both chilled margins and fragments of country rocks that indicate emplacement under brittle conditions. The dikes are composed of clinopyroxene+plagioclase±pigeonite, with minor amounts of magnetite, chlorite, actinolite, biotite, and quartz. The presence of pigeonite is especially characteristic of dikes of Mesozoic age (Wilson and Tollo, 2001), and is consistent with the whole-rock chemical compositions that indicate high SiO_2 and relatively low TiO_2 contents (table 5, samples SNP-99-7, -8, and -9) compared to metabasalt of the Neoproterozoic Catoctin Formation.
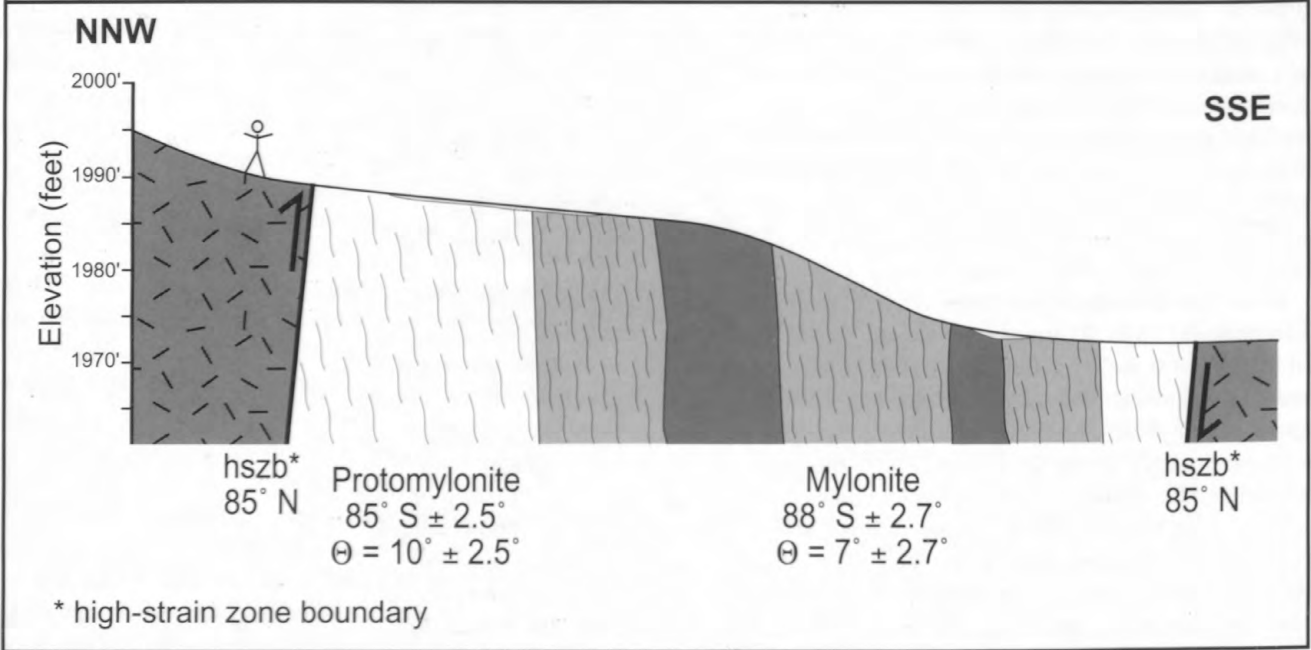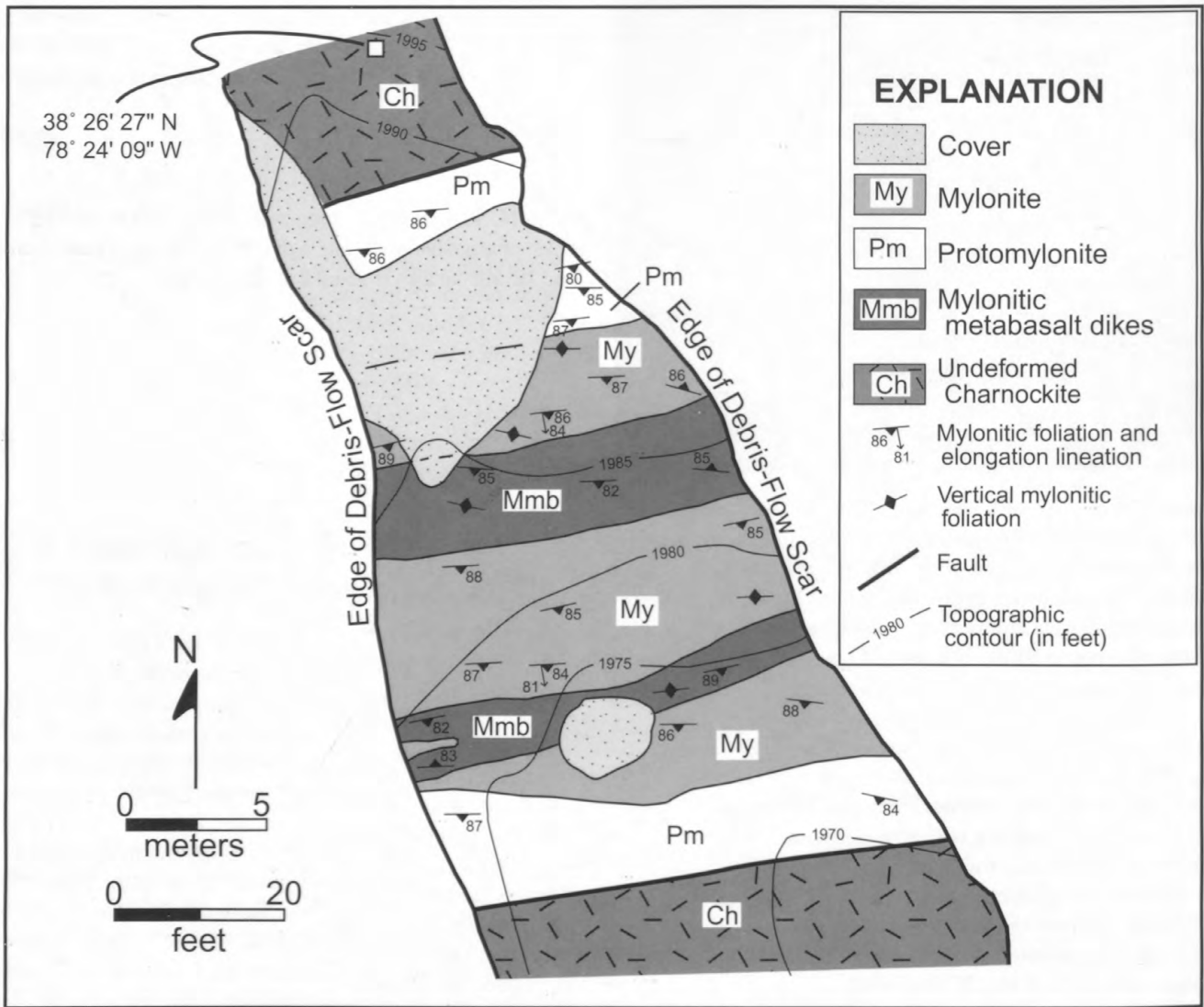
Figure 14. Photograph of three mafic dikes (darker colored rocks) of probable Mesozoic age cutting low-silica charnockite at Stop 18. Middle dike is about 2 m (80 in) wide.

These dikes are part of a widespread suite of Jurassic (~200 Ma) igneous bodies that intruded Blue Ridge, Piedmont, and Valley and Ridge country rocks during early Mesozoic rifting. In contrast, an east-west-striking greenstone dike that occurs in outcrops located below the main bedrock exposure contains highly altered orthopyroxene phenocrysts and abundant retrograde chlorite+epidote+actinolite. The low SiO_2 and high TiO_2 content of this dike (sample SNP-99-6 in table 5) is similar to the composition of Catoctin greenstones and suggests a Neoproterozoic age.

An approximately 30-m (98-ft)-wide high-strain zone is exposed in the channel above the diabase dikes. This zone strikes ~080° and dips steeply to the northwest (fig. 15). The zone is bounded by charnockite that passes into protomylonite and mylonite within the high-strain zone. Two deformed metabasalt dikes occur within the zone and strike subparallel to the zone boundary (fig. 15). Foliation internal to the high-strain zone dips steeply to both the northwest and southeast, and a downdip mineral elongation lineation occurs at a few locations. Asymmetric kinematic indicators generally display a reverse sense of shear on foliation normal and lineation parallel sections. Protomylonite and mylonite developed within the charnockite are composed of 30 to 50 percent quartz, 10 to 25 percent fine-grained muscovite, 10 to 20 percent alkali feldspar, 10 to 15 percent epidote, and 10 percent biotite. Feldspars are extensively fractured with quartz-filled cracks and muscovite mantles along grain boundaries. Quartz grains form monocrystalline lenses and ribbons with a moderate to strong crystallographic preferred orientation. The general lack of recrystallized quartz and the abundance of brittle microstructures in feldspar are consistent with greenschist-facies deformation conditions (T ~300–400°C). Undeformed charnockite, protomylonite, and mylonite are composed of approximately 61 percent SiO_2 and have nearly identical concentrations of other major elements. Although significant mineralogical changes occurred between the undeformed charnockite and mylonitic rocks, volume loss appears to be minimal (Bailey and others, in press).

Strain was estimated from monocrystalline quartz lenses and ribbons using standard R_f/f techniques: 16 to 40 grains were measured per sample, and strain in *XZ* sections averaged 3.8 (3.6–4.0, n=2) for the protomylonites and 5.8 (5.5–6.2, n=3) for the mylonites. Three-dimensional strains for all samples plot in the field of apparent flattening on a Flinn diagram, and mylonitic samples consistently have lower K-values than protomylonites (K=0.6 versus 0.8). In the *YZ* section (which approximates the outcrop surface), both metabasalt and epidotized leucocharnockite dikes exhibit pinch-and-swell structure or form boudins, consistent with true flattening strains and elongation parallel to *Y*. The kinematic vorticity number was estimated using the R_s/Q method. In both the protomylonite and mylonite, W_m=0.65. Integrating shear strains across the Kinsey Run high-strain zone yields a total displacement of 60±10 m (197±33 ft). These results indicate that the Kinsey Run high-strain zone experienced a weak triclinic flow characterized by flattening strains that developed under general shear conditions (Bailey and others, in press).

38° 26' 27" N
78° 24' 09" W

Edge of Debris-Flow Scar

Edge of Debris-Flow Scar

N

0   5
meters

0   20
feet

EXPLANATION

Cover

My   Mylonite

Pm   Protomylonite

Mmb   Mylonitic metabasalt dikes

Ch   Undeformed Charnockite

Mylonitic foliation and elongation lineation

Vertical mylonitic foliation

Fault

1980   Topographic contour (in feet)

NNW

SSE

2000'

Elevation (feet)

1990'

1980'

1970'

hszb*
85° N

Protomylonite
85° S ± 2.5°
Θ = 10° ± 2.5°

Mylonite
88° S ± 2.7°
Θ = 7° ± 2.7°

hszb*
85° N

* high-strain zone boundary

Stop 19. Kinsey Run, east branch: Quaker Run high-strain zone.

This debris-flow scar, which exposes the base of the Quaker Run high-strain zone, is one of the largest created by the rainstorm in June 1995 (Morgan and others, 1999). Medium- to coarse-grained, massive to weakly foliated, low-silica charnockite (Yfqj) passes uphill into protomylonite and mylonite. The contact between undeformed charnockite and mylonitic rocks strikes to the northeast and dips moderately to the southeast. The angle between the foliation and high-strain-zone boundary is <10°. Mylonitic rocks are characterized by a southeast-plunging, downdip elongation lineation. Kinematic indicators, especially visible at this outcrop because of the vertical exposure, are plentiful and record top-to-the-northwest sense of shear. There are, however, numerous back-rotated porphyroclasts (mostly feldspar megacrysts), suggesting that this zone experienced general rather than simple shear. Leucopegmatite dikes are commonly oriented subparallel to foliation and exhibit pinch-and-swell structures along their margins. These competent dikes are cut by fibrous quartz-filled extension fractures. A 2- to 4-m (6.5–13.1-ft)-wide zone of fine-grained chlorite-bearing mylonite may be derived from a Neoproterozoic metabasalt dike.

The Quaker Run high-strain zone was defined by Berquist and Bailey (2000) for exposures a few kilometers to the north. At this latitude, the Quaker Run high-strain zone is the thickest (0.5–1.5 km; 0.3–0.9 mi) Paleozoic mylonite zone in the north-central Blue Ridge and can be traced for over 30 km (19 mi) parallel to the regional trend. Strain throughout the zone is very heterogeneous. On the basis of estimates of shear strain using values determined from other Blue Ridge mylonite zones, Berquist and Bailey (2000) estimated a total displacement of 1.5±0.5 km (4,900±1,650 ft) across the Quaker Run high-strain zone.

Mileage

Trip Cumulative	Stop-to-Stop Cumulative	
	0.0	Turn around and proceed east and south on Va. 615.
172.6	1.2	Intersection with Va. 622; continue south on Va. 622.
176.5	5.1	Bridge across the Rapidan River.
177.9	6.5	Turn right onto Va. 230 (Wolftown-Hood Road) and proceed west.
179.2	7.8	Bridge across the Rapidan River.
181.5	10.1	Bridge across the Conway River.
181.9	10.5	Turn right onto Va. 667 (Middle River Road) and proceed northwest.
185.2	13.8	*View on the right of home built in flood plain.*
185.6	14.2	Kinderhook.
		View on the right of the dredged riverbed and rocks piled on the embankment. Dredging was undertaken after the June 1995 flooding in order to deepen and widen the debris-choked channels.
187.5	16.1	Va. 667 becomes unpaved; continue north.
187.9	16.5	*Large outcrops in Conway River are leucogranite gneiss (Ylgg).*
188.4	17.0	Stop 20.
		Follow Trip Leaders
		PRIVATE PROPERTY

Stop 20. Leucogranite gneiss (Ylgg) xenoliths enclosed within nonfoliated low-silica charnockite (Yfqj).

Outcrops exposed at the base of the hill within the scoured channel of the Conway

Figure 15 (opposite page). Detailed geologic map showing ~30-m (100-ft)-wide high-strain zone exposed in debris-flow scar at Stop 18. Cross section shows structural relations approximately perpendicular to strike of units.

Figure 16. Photograph of strongly foliated leucogranite gneiss (Ylgg) xenolith within nonfoliated low-silica charnockite (Yfqj) at Stop 20. Hammer handle, oriented parallel to foliation in the leucogranite gneiss, is 82 cm (32 in) long.

River provide critical field relations and age information bearing on the timing of local Grenvillian deformation. The hill located on the east side of the river is underlain by light-greenish-gray, strongly foliated leucogranite gneiss (Ylgg) that defines an isolated screen within low-silica charnockite (fig. 3) (Tollo and others, in press a,b). The coarse- to very coarse-grained, inequigranular, strongly foliated leucogranite gneiss is composed of 80 percent alkali feldspar mesoperthite (chiefly microcline), <1 percent plagioclase, and 20 percent gray quartz with <1 percent biotite. Accessory minerals include ilmenite, magnetite, zircon, epidote, and muscovite. Locally prominent gneissic layering is defined by interlayered quartz+feldspar-rich and quartz-rich domains ranging from less than 3 cm (1.2 in) to greater than 13 cm (5 in). Foliation is locally defined by planar alignment of tabular mesoperthite megacrysts. Subhedral to euhedral, monocrystalline mesoperthite megacrysts range up to 10 cm (4 in) in length. Chemical analyses of the leucogranite gneiss collected from this riverside exposure indicate very high SiO_2 contents (74–75 weight percent) (table 4); however, low Y+Nb concentrations in one sample suggest that chemical alteration resulting from interaction between the xenoliths and surrounding charnockitic magma likely occurred. Although extensively altered in the outcrop, the nonfoliated charnockite contains the same mineral assemblage that is typical of the Yfqj lithologic unit. Two samples of charnockite collected from this exposure (samples SNP-99-91 and SNP-99-92 in table 4) generally plot with other data points from the Yfqj lithologic unit but are characterized by significantly different SiO_2 contents (table 4) that suggest that local chemical exchange occurred between the charnockite magma and leucogranite gneiss xenoliths.

The outcrops along the river channel display a crosscutting relation that is similar to the map pattern: xenoliths of strongly foliated leucogranite gneiss are enclosed within dark-gray-green, nonfoliated to weakly foliated, amphibole-bearing charnockite (Yfqj) that locally truncates the foliation of the leucogranite gneiss at the contacts of individual xenoliths (fig. 16). This relation is confirmed by U-Pb SHRIMP isotopic analyses of zircons. Subhedral, typically prismatic zircons in the leucogranite gneiss have broad cores charac-

terized by concentric, oscillatory zoning surrounded by distinct, unzoned rims. Thirteen analyses of cores yield a weighted average of the $^{207}Pb/^{206}Pb$ ages of 1,078±9 Ma, which is interpreted as the crystallization age of the igneous protolith (table 3) (Tollo and others, in press a). Analyses of a limited number of overgrowths suggest two periods of metamorphism at 1,028±10 Ma and 997±19 Ma (table 3). The occurrence of these foliated leucogranite gneiss xenoliths within the 1,050±8-Ma charnockite indicates that local deformation took place within the interval 1,078 to 1,050 Ma. The age of this Blue Ridge deformation partly overlaps the period of tectonomagmatic activity associated with Ottawan orogenesis in the Adirondacks that was constrained to the interval 1,090 to 1,035 Ma by McLelland and others (2001). As a result, ductile fabrics and gneissosity developed in the leucogranite gneiss and older units are interpreted to result from a possibly correlative period of orogenesis in the Blue Ridge.

End of Field Trip.

3. The Paleozoic Record of Changes in Global Climate and Sea Level: Central Appalachian Basin

By C. Blaine Cecil,[1] David K. Brezinski,[2] and Frank DuLong[1]

With stop contributions by Bascombe Blake,[3] Cortland Eble,[4] Nick Fedorko,[3] William Grady,[3] John Repetski,[1] Viktoras Skema,[5] and Robert Stamm[1]

Introduction to the Field Trip

By C. Blaine Cecil

This field trip provides an update of an earlier trip that was conducted in conjunction with the 1998 Annual Meeting of The Geological Society of America (Cecil and others, 1998). The present trip emphasizes global climate change and eustatic sea-level change (allocyclic processes of Beerbower, 1964) (in a global paleogeographic context) as the predominant controls on Paleozoic sedimentation and stratigraphy in the Appalachian foreland basin. The trip stops illustrate long- to short-term paleoclimate change (table 1) as the predominant control on sediment supply, both chemical and siliciclastic (fig. 1A, B). Interpretations of climate variations are based on paleoclimate indicators such as paleosols, physical and chemical sedimentation, sedimentary geochemistry and mineralogy, and paleontology.

Selected stops in Paleozoic strata provide evidence for sedimentary response to paleo-tropical rainfall regimes that ranged in duration from long term to short term (table 1) and in rainfall amounts that ranged from arid to perhumid (table 2, fig. 1F). Eustatic processes also are discussed at each stop, and the role of tectonics may be mentioned briefly where appropriate. These later two allocyclic processes are generally accepted as the predominant control on sediment supply in contrast to climate, which is often not considered. For example, tectonic uplift is commonly considered as the predominant control on rapid influxes of siliciclastic material into depocenters, whereas siliciclastic sediment starvation is usu-

ally attributed to trapping of sediment in estuaries in response to sea-level rise. More specifically, basal sandstone units of the Cambrian, Silurian, Mississippian, and Pennsylvanian in the Appalachian basin are generally attributed to influx induced by tectonic uplift, whereas laterally extensive shale deposits, such as the Ordovician Martinsburg Formation and Devonian black shale units, are inferred to result from sediment trapping or autocyclic deposition of prodelta muds. Although tectonics clearly plays a role in uplift and subsidence, and eustasy also governs the amount of accommodation space, variation in climate, particularly long- to short-term variation in rainfall in tropical conditions, is of greater importance as a control on sediment supply and sedimentation (for example, Ziegler and others, 1987; Cecil, 1990 and references therein; Cecil and others 1993; Cecil and others, 2003a). The trip stops illustrate why climate change is a far more important first-order control on stratigraphy than is generally recognized.

Classification of Tropical Rainfall

Many definitions of tropical climatic regimes are based on annual rainfall; few, however, attempt to incorporate seasonality of rainfall (for example, Thornthwaite, 1948). It is becoming increasingly apparent, however, that it is the seasonality of annual rainfall that governs weathering, pedogenesis, variations in soil moisture, vegetative cover, and erosion and sediment yield for a given catchment basin (for example, Ziegler and others, 1987; Cecil, 1990, 2003; and Cecil and others, 2003a and references therein), not the total amount of annual rainfall. In order to assign degrees of seasonality, climate regimes, as used herein, are based on the number of wet months in a year. A wet month is defined as a month in which precipitation exceeds evapotranspiration (table 2, fig. 1F) (Cecil, 2003).

By the limits set forth in table 2 and figure 1F, both arid and perhumid conditions are nonseasonal. All other rainfall conditions have some degree of seasonality. Maximum sea-
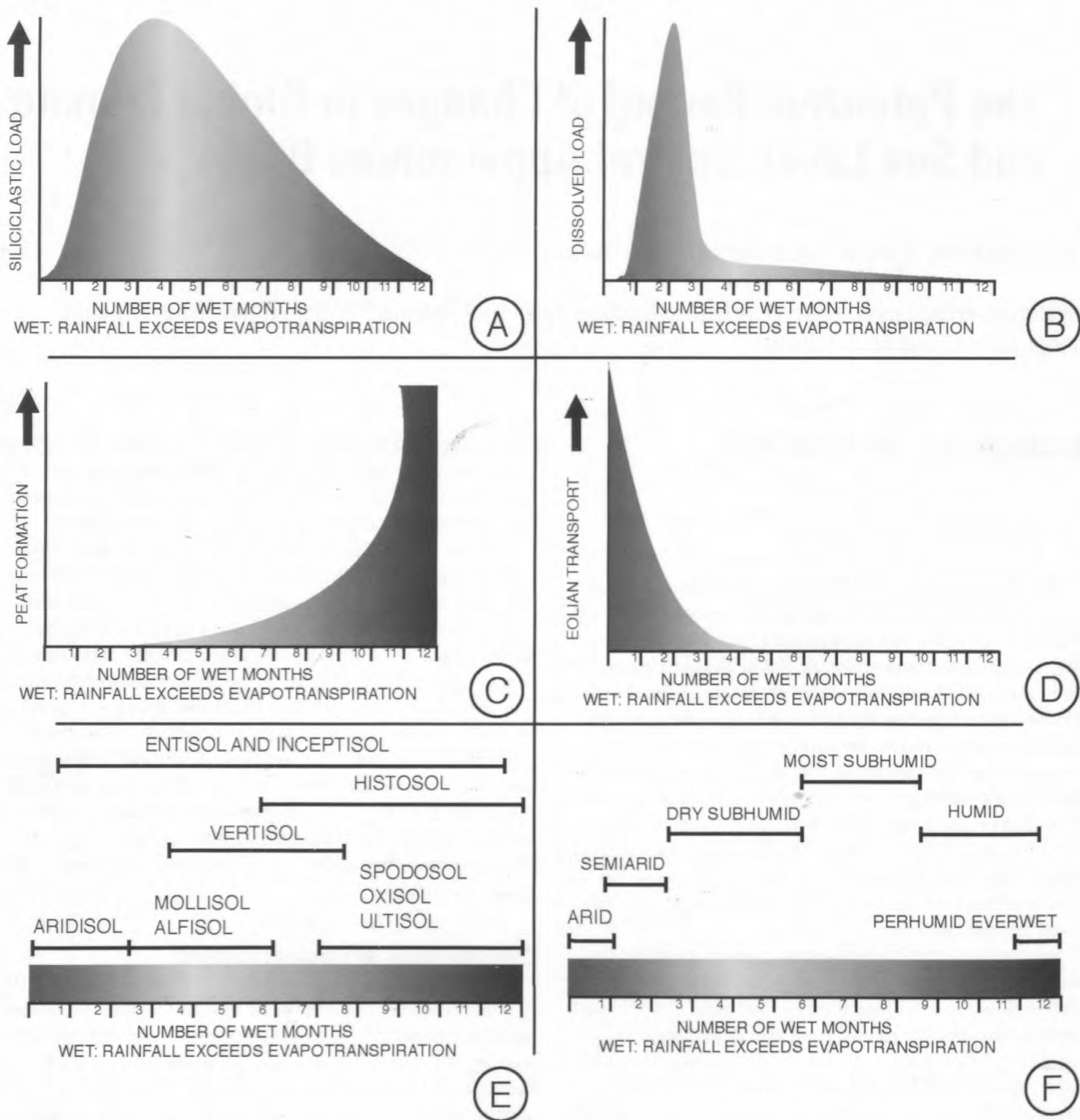
Figure 1. A, Potential for fluvial siliciclastic load as function of climate; B, Potential for fluvial dissolved load as a function of climate; C, Potential for peat formation as a function of climate; D, Potential for eolian transport as a function of climate; E, Formation of U.S. Department of Agriculture soil orders as a function of climate; and F, Climate classification based on the number of wet months per year. From Cecil and Dulong (2003).

sonality and maximum fluvial siliciclastic sediment supply occur under dry subhumid conditions when there are approximately three to five consecutive wet months (fig. 1A). Maximum dissolved inorganic supply occurs under semiarid to dry subhumid conditions (fig. 1B). The most ideal conditions for the formation and preservation of peat, as a precursor to coal, occur under humid and perhumid conditions (fig. 1C) when

both dissolved and siliciclastic sediment supply approach zero (Cecil and others, 1993). The conditions for eolian transport in sand seas are illustrated in figure 1D.

Climate is also a major control on weathering and soil formation (pedogenesis); conversely, paleosols can be used to reconstruct paleoclimate and paleo water-tables. Climate may be the primary control on pedogenesis in epicontinental

Table 1. Tropical and subtropical climate change classification (modified from Cecil, 1990, 2003).

Relative duration	Cause	Time (years)
Long term	Continental drift; orogenesis; Ice house/ greenhouse	10^6–10^8 10^5–10^7
Intermediate term	100- and 400-ka cycles of orbital eccentricity; glacial/interglacial	10^5
Short term	Cycles in orbital obliquity and precession	10^4
Very short term (Millennial)	Uncertain	10^3
Instantaneous	Weather	10^{-2} (weeks, days, or hours)

Table 2. Tropical climate regimes and degree of seasonality based on the number of consecutive wet months per year (modified from Thornthwaite, 1948, and Cecil, 2003).

Average number of wet months	Climate regime	Degree of seasonality
0	Arid	Nonseasonal
1–2	Semiarid	Minimal
3–5	Dry subhumid	Maximum
6–8	Moist subhumid	Medial
9–11	Humid	Minimal
12	Perhumid	Nonseasonal

basins where other parameters, such as parent material and relief, are relatively constant. On the basis of structure, chemistry, and mineralogy, paleosols can be classified at the level of soil orders using the U.S. Department of Agriculture classification (Soil Survey Staff, 1975). Once classified, paleosols can be used to interpret paleoclimate (fig. 1E), including the amount and seasonality of rainfall as is illustrated at a number of stops on the trip.

Mechanisms of Climate Change

Continental Drift

A major component in long-term global climate variation, as expressed in Appalachian basin sedimentation, was the movement of the continents through paleolatitudes. The region of what is now the central Appalachian basin moved northward from about lat 40° S. in the latest Precambrian and Early Cambrian to lat 30° S. ± 5° during the Early Ordovician where it remained well into the Mississippian (Scotese, 1998). Northward movement continued from about lat 30° S. in the Early Mississippian to about lat 3° N. by the beginning of the Permian (figs. 2–9). From the perspective of zonal atmospheric circulation, the field trip study area moved from the dry subhumid belt of the southern hemisphere (prevailing easterlies) in the Early Cambrian into the high pressure belt of aridity by Late Cambrian where it remained well into the Mississippian. Late Precambrian and Early Cambrian sediments are dominated by siliciclastics, whereas Middle Cambrian through Early Devonian strata contain abundant limestone, dolomite, and evaporites. These strata are totally consistent with paleogeographic interpretations (for example, Scotese, 1998). By the Late Devonian the region began to move northward toward the humid low-pressure equatorial region. Movement continued through the equatorial region during the Pennsylvanian.

Orbital Climate Forcing

There are clear and distinct effects of orbital parameters (obliquity, eccentricity, and precession) on intermediate- to short-term climate change. Orbital climate forcing is an important control on variation in sediment supply because orbital parameters have a marked effect on the seasonality of incoming solar radiation (insolation), which results in variations in the seasonality of rainfall. As a result, orbital climate forcing plays a major role in sedimentation and stratigraphy. The lithostratigraphic signal induced by intermediate- to short-term climate change may be somewhat suppressed during periods of long-term aridity or humidity, but is not obliterated as is illustrated at stops in Ordovician, Silurian, and Pennsylvanian strata.

Tectonics

As pointed out above, continental drift may explain some of the long-term climate changes in the Appalachian basin, but it does not explain all such changes. Some long-term climate changes may be better explained by the alteration of atmospheric zonal circulation as a result of mountain building. Such effects are well known, as illustrated by the development of the Asian monsoon in response to the formation of the Himalayan Mountains and the Tibetan Plateau, when the Indian subcontinent collided with Asia. Similar tectonic controls on late Paleozoic paleoclimate have been suggested for the development of a humid climate in the Early Pennsylvanian by the formation of an equatorial high plateau, which pinned the intertropical convergence zone to the plateau causing a permanent low-pressure cell and high rain-
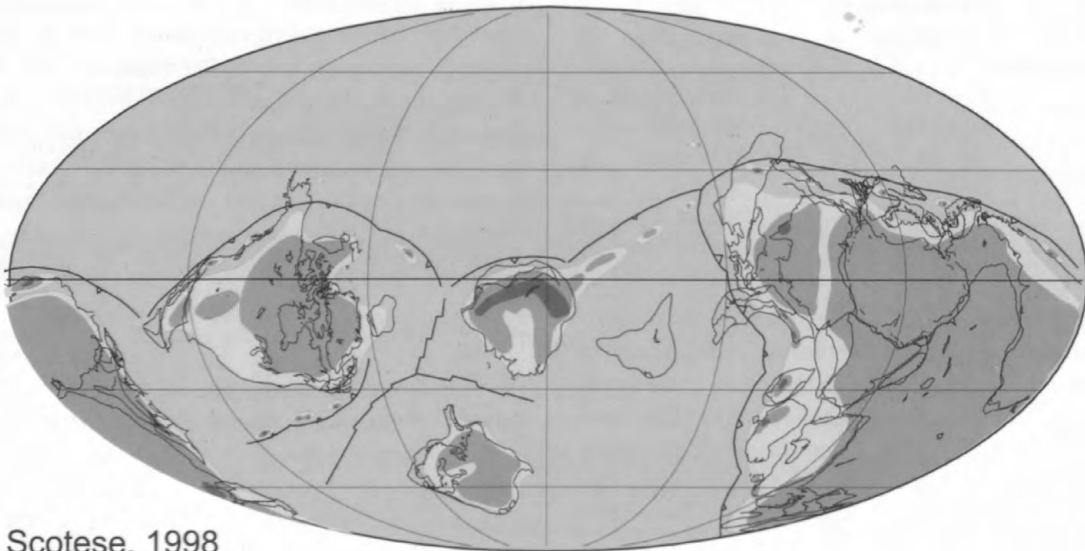
Early Cambrian 547 Ma
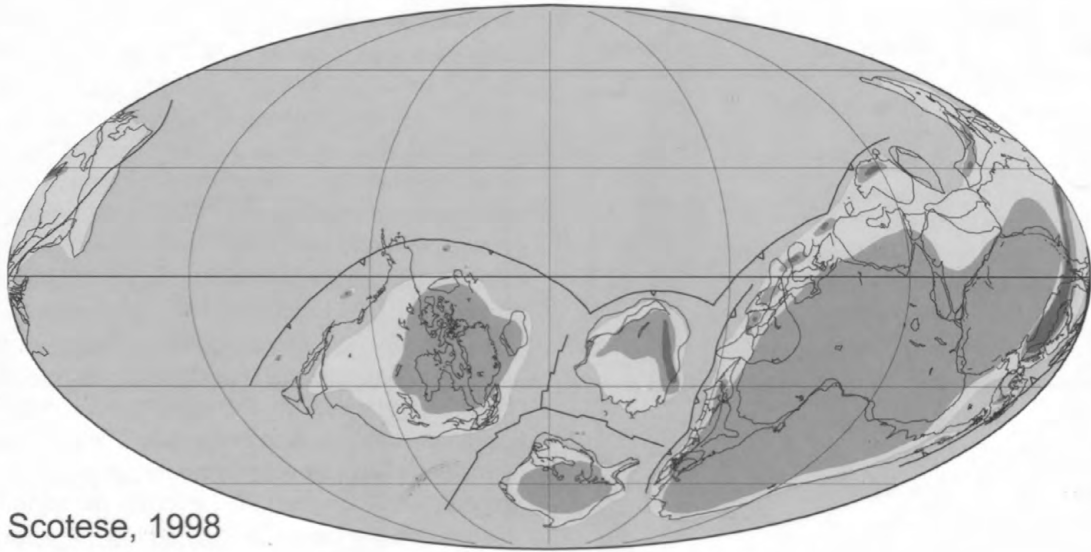
Scotese, 1998

Figure 2. Paleogeographic reconstruction showing how the continents might have appeared during the Early Cambrian (547 Ma).
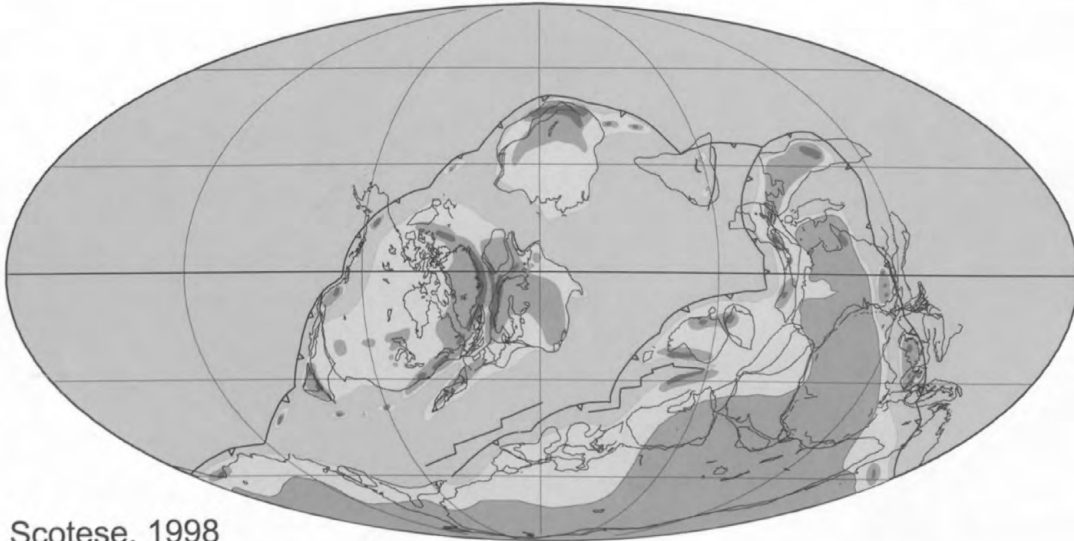
Early Ordovician 497 Ma

Scotese, 1998

Figure 3. Paleogeographic reconstruction showing how the continents might have appeared during the Early Ordovician (497 Ma).
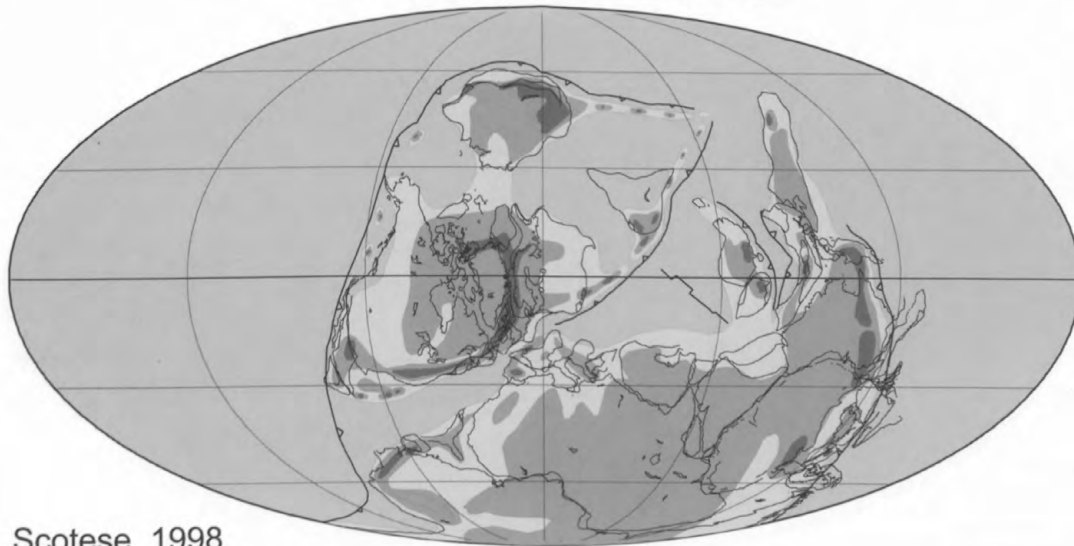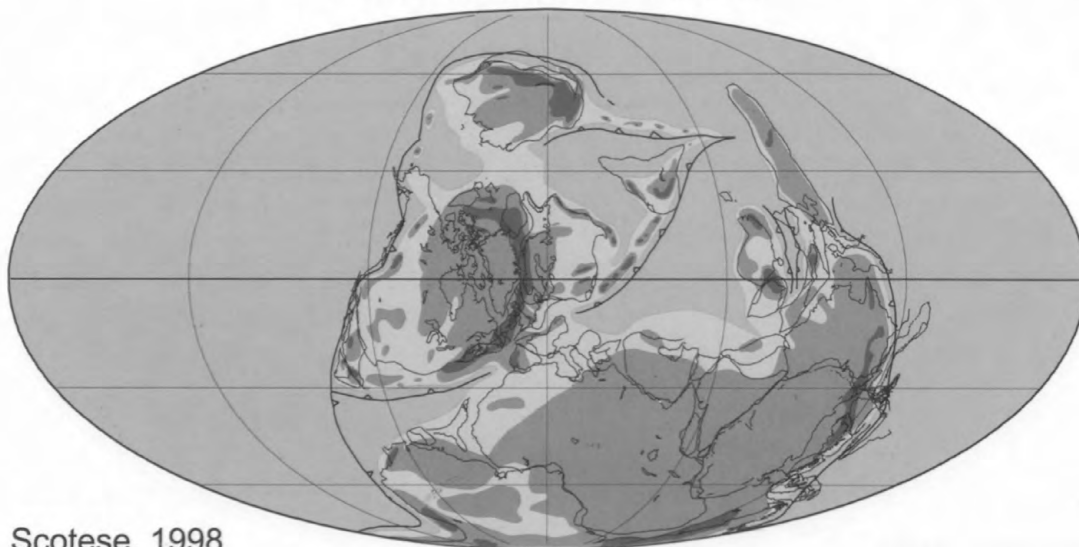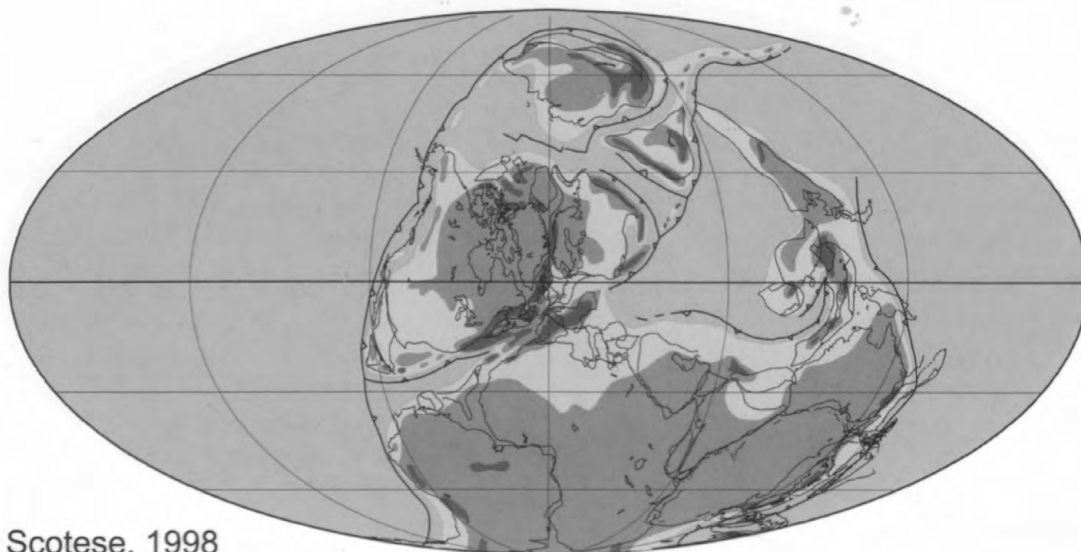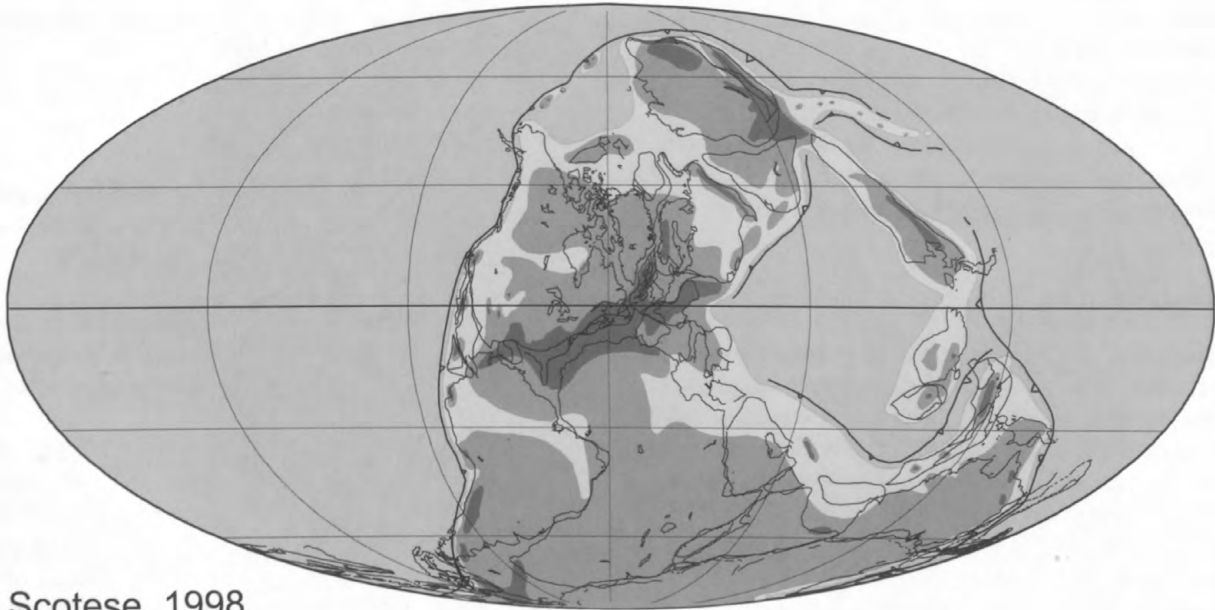
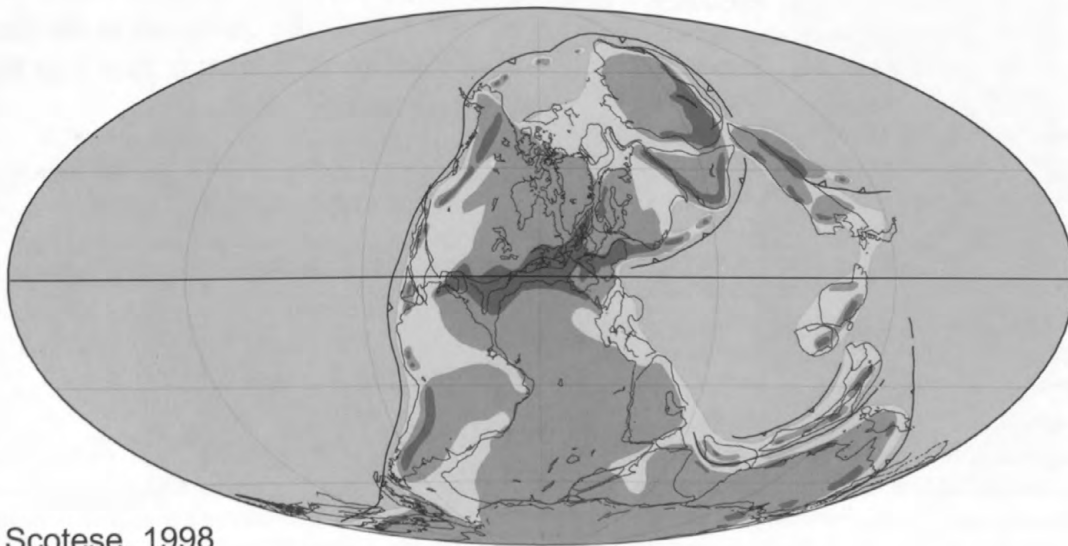## Middle Silurian 425 Ma

Scotese, 1998

Figure 4. Paleogeographic reconstruction showing how the continents might have appeared during the Middle Silurian (425 Ma).

Middle Devonian 377 Ma

Scotese, 1998

Figure 5. Paleogeographic reconstruction showing how the continents might have appeared during the Middle Devonian (377 Ma).

Late Devonian 363 Ma

Scotese, 1998

Figure 6. Paleogeographic reconstruction showing how the continents might have appeared during the Late Devonian (363 Ma).

Early Carboniferous 342 Ma

Scotese, 1998

Figure 7. Paleogeographic reconstruction showing how the continents might have appeared during the Early Carboniferous (342 Ma).

Late Carboniferous 306 Ma

Scotese, 1998

Figure 8. Paleogeographic reconstruction showing how the continents might have appeared during the Late Carboniferous (306 Ma).

Early Permian 277 Ma

Scotese, 1998

Figure 9. Paleogeographic reconstruction showing how the continents might have appeared during the Early Permian (277 Ma).

fall (Rowley and others, 1985). Such a permanent low-pressure cell could have been modulated by orbital forcing parameters and southern hemisphere glacial conditions (Cecil, 1990; Cecil and others, 2003b). The Taconic and Acadian orogenies also may have affected long-term climate change from regional orographic to global scales, although such effects have not been documented nor are they well understood. Although difficult to quantify, paleo-ocean circulation is yet another control on long-term climate change.

Unknown Mechanisms

Perhaps the most enigmatic, yet most important of all climate change processes are those that control long-term ice house and greenhouse conditions and the shorter term glacial-interglacial cycles. The geologic record is replete with evidence indicating that such extreme changes in paleoclimate have been occurring throughout geologic time (fig. 10) (Frakes and others, 1992). These climatic changes are sometimes accompanied by major biotic events, such as the Cambrian explosion of marine organisms following the "snowball earth" condition at the end of the Precambrian or the mass extinction that was coeval with a relatively short ice house world during the Devonian-Mississippian transition. Some of the enigmas and uncertainties associated with both near-time and deep-time ice-related global climate change are as follows:

1. Weather patterns, atmospheric composition data, and numerical models have led many researchers to conclude that the perceived present-day global warming is induced by greenhouse gases of anthropogenic origin. It is evident, however, that global climate commenced warming (although in "fits and spurts") following the last glacial maximum (18 ka), long before anthropogenic effects were significant.

2. The mechanisms that have controlled climate oscillations since the last glacial maximum are very poorly understood, and there is an equally poor understanding of the factors that control glacial-interglacial cycles and the longer term "ice house" to "greenhouse" transitions.

3. Among the multiple hypotheses regarding ice-related climate-forcing mechanisms (for example, orbital forcing, atmospheric composition (greenhouse gases), ocean circulation, bolide impacts, volcanism, solar variation, and so on), none document clear and unequivocal triggers of abrupt climate change, even when "feedbacks" are considered.

Even though the factors that trigger changes in ice volume remain unknown, there is a clear empirical correlation between ice volumes during the Paleozoic and paleoclimates (rainfall) in the Appalachian basin (fig. 10). The sense of paleoclimate change (increasing or decreasing rainfall) in the

Appalachian basin that was coincident with changes in ice volume also is related to paleolatitudes. As is pointed out on the trip, paleoclimate change is best explained by estimates of both paleolatitudes and ice volume.

Summary

This trip investigates evidence for Paleozoic global climate change in the Appalachian basin. The objectives of individual trip stops are as follows:

1. Present stops in a global paleogeographic context.
2. Provide interpretations that relate stratigraphy and sedimentation to short-term and long-term global climate changes (table 1).
3. Interpret the seasonality of annual rainfall (fig. 1A, table 2) as the predominant control on sediment supply.
4. Empirically correlate changes in paleoclimate and sea level to changes in ice volume. Figure 10 depicts long-term climate change for the Paleozoic of the central Appalachian basin along with long-term changes in ice volume.

Field Trip Stops

Stop 1. Upper Conemaugh and lower Monogahela Group strata on the north side of the Morgantown Mall complex on Interstate 79 at Exit 152, Morgantown, W. Va.

Lat 39°37.82' N., long 80°00.03' W., Morgantown North, W. Va., 7.5-minute quadrangle.

Leaders: Nick Fedorko, Bill Grady, Cortland Eble, and Blaine Cecil

Introduction

The strata at Stop 1 gently dip to the northwest. Earlier cuts made for the construction of the Morgantown Mall and upper commercial area exposed approximately 18 m (meters) (59 ft (feet)) of upper Conemaugh Group strata and 32 m (105 ft) of lower Monongahela Group strata (fig. 11). Prior to removal by later construction, the section included five coal beds (some multi-benched) and an abundance of nonmarine, lacustrine limestone beds. The lowermost coal bed is the Little Pittsburgh coal of the Casselman Formation in the upper part of the Conemaugh Group. Several benches of the Little Pittsburgh coal bed interbedded with shales, mudstones, and lacustrine carbonates are exposed at the updip eastern end
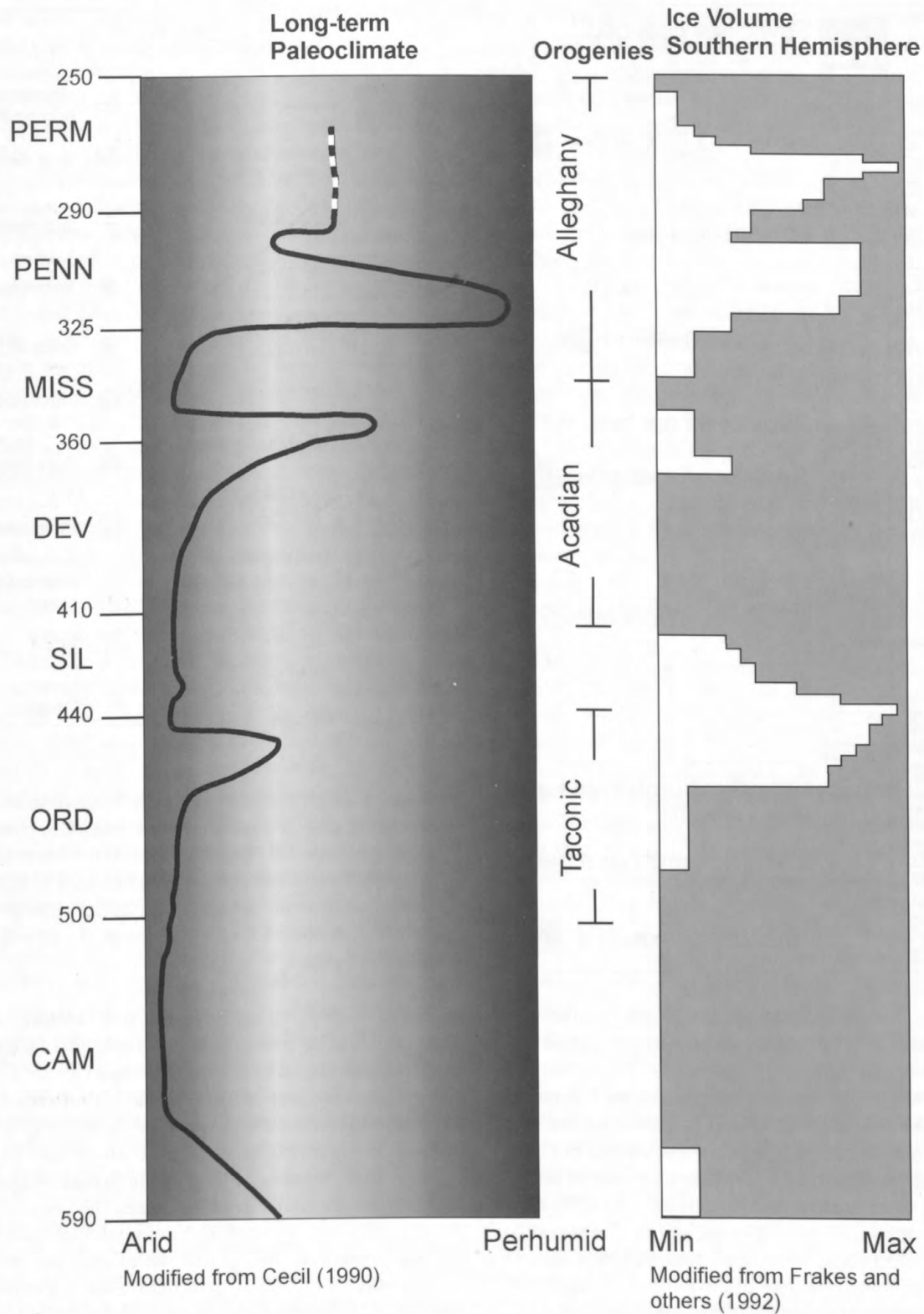
Figure 10. Paleozoic paleoclimate curve, central Appalachian basin. Series names are abbreviated as follows: CAM, Cambrian; ORD, Ordovician; SIL, Silurian; DEV, Devonian; MISS, Mississippian; PENN, Pennsylvanian; PERM, Permian.
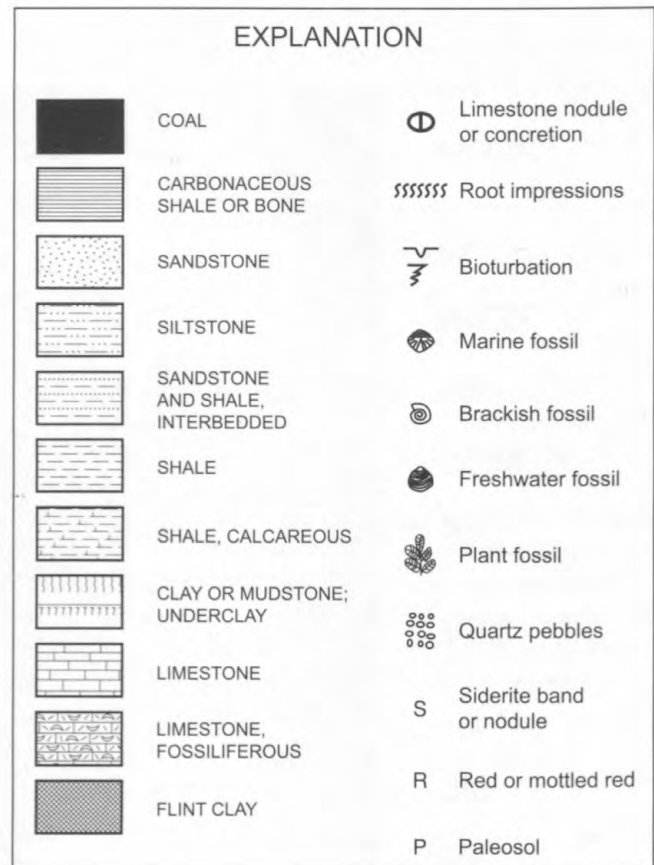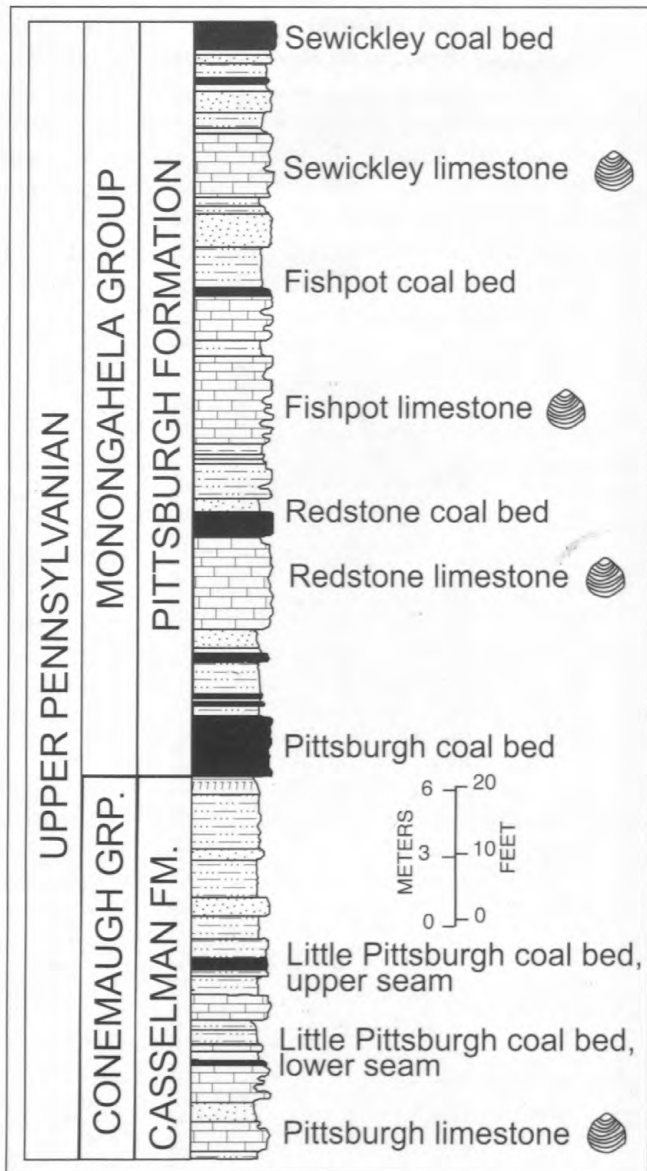
Figure 11. Stratigraphic section, Upper Pennsylvanian Monongahela and Conemaugh Groups. Sewickley coal bed; Sewickley limestone of Platt and Platt (1877); Fishpot coal bed; Fishpot limestone of Stevenson (1876); Redstone coal bed; Redstone limestone of Platt and Platt (1877); Pittsburgh coal bed; Little Pittsburgh coal bed, upper and lower seams; and Pittsburgh limestone are shown.

of the outcrop. The Little Pittsburgh coal bed is of minor economic importance but is persistent enough to serve as an important regional stratigraphic marker.

The Pittsburgh coal bed, the basal unit of the Pittsburgh Formation of the Monongahela Group, is exposed at the western end of the outcrop. Important to our discussions of climatic impact on the rock record is the development of the soil profile beneath the Pittsburgh coal bed. Here, where the coal facies are well developed, the subjacent soil profile is poorly developed, thin, and contains some carbonate in the form of small lenses. The massive nature of the mineral paleosol and the absence of subaerial exposure features indicate that the paleosol was permanently waterlogged or nearly so. A correlation of paleosol profiles along a 60-mi (mile) (97 km (kilometer)) transect from this stop southward elucidated the effects of paleotopography and paleoclimate on the genesis of mineral paleosols and coal. Southward, the paleosol becomes thicker and better developed, and it contains features that are

indicative of subaerial exposure and well-drained conditions of pedogenesis. In contrast, the overlying coal facies thin and are poorly developed or absent. The characteristics of the mineral paleosols and the inverse relation between coal bed and mineral paleosol thickness suggests that Stop 1 was topographically lower relative to areas 60 mi (97 km) to the south.

The main benches of the Pittsburgh coal bed exposed in the Morgantown Mall have a combined thickness of 2.6 m (8.5 ft), and they are generally low in ash yield and moderate in sulfur content. Including roof shales and rider coal beds, the Pittsburgh is 5.2 m (17.1 ft) thick. At this location the coal consists of six benches, two more than are present 6 mi (10 km) to the northeast where the coal was extensively studied in a surface mine at the Greer estate. The basal bench (lower 0.3 m; 1 ft) is present across most of the areal extent of the Pittsburgh coal. It is high in sulfur and has a moderate ash yield. Tree fern spores dominate the palynoflora, but there are distinct calamite and cordaite contributions. The palynoflora

of the lower bench is interpreted as the pioneering plant community of the Pittsburgh swamp. The ash yield and sulfur content indicate that these plants grew in a planar swamp with a significant influx of surface and ground water. Peat oxidation was minor, and the preservation of plant debris was moderate. Above the basal bench, up to the parting at the 1.2- to 1.4-m (3.9- to 5.0-ft) level, the coal is low ash, has moderate sulfur content, and petrographically shows two trends in swamp development. These trends of increased peat preservation, as shown by increased >50-micron (μ) vitrinite components, are reflected in the sulfur content and palynofloral succession, but not in ash yield. The first trend, terminated by a fusain parting, displays an upward increase in vitrinite content, especially the >50-μ component, an increase in calamite and arboreous lycopsid spores, and increased sulfur content. The bone coal parting at 4 ft (1.2 m) above the base of the bed terminates a second similar trend. Increased vitrinite and >50-μ vitrinite, arboreous lycopsid and calamite spores suggest a slight increase in surface water depth as peat accumulation proceeded. The increased sulfur content probably represents increased introduction of sulfur into the swamp by surface or ground water as water depth increased. The termination of these trends by fire followed by sediment deposition demonstrates a rapid and significant change in the water table. The fusain parting changes laterally into a bone coal parting and is present sporadically throughout the areal extent of the Pittsburgh coal. The extremely widespread 4-ft (1.2-m) parting (Cross, 1952) occurs at approximately the same stratigraphic level throughout the lateral extent of the Pittsburgh coal bed. The vast lateral extent of the parting suggests a regional rise in paleo-water levels and drowning of the peat swamp flora. Such a rise in water levels may have been driven by a protracted period of increased rainfall in response to changes in orbital parameters.

The Redstone limestone (*sensu* Platt and Platt, 1877), a well-developed nonmarine, regionally extensive, lacustrine carbonate occurs above the Pittsburgh coal bed at this stop. In most other localities, however, the Redstone limestone is separated from the coal by shale and (or) sandstone. The Redstone limestone generally occurs as a monolithic micrite, the result of deposition in an areally extensive lake that underwent periodic drying and subaerial exposure, as evidenced by pedogenic brecciation and the formation of subaerial crusts. Lacustrine limestones such as this one first occur in the Middle Pennsylvanian Allegheny Formation but are most abundant in the Monongahela Group in the region encompassing northern West Virginia, southwest Pennsylvanian, and eastern Ohio. These carbonates are exclusively micrites, occurring in complexes interbedded with argillaceous limestones, calcareous mudstones, and calcareous and noncalcareous shales.

The Fishpot coal bed of the Pittsburgh Formation (Monongahela Group), which has now been removed from this site by construction, was only 2.5 cm (centimeters) (1 in (in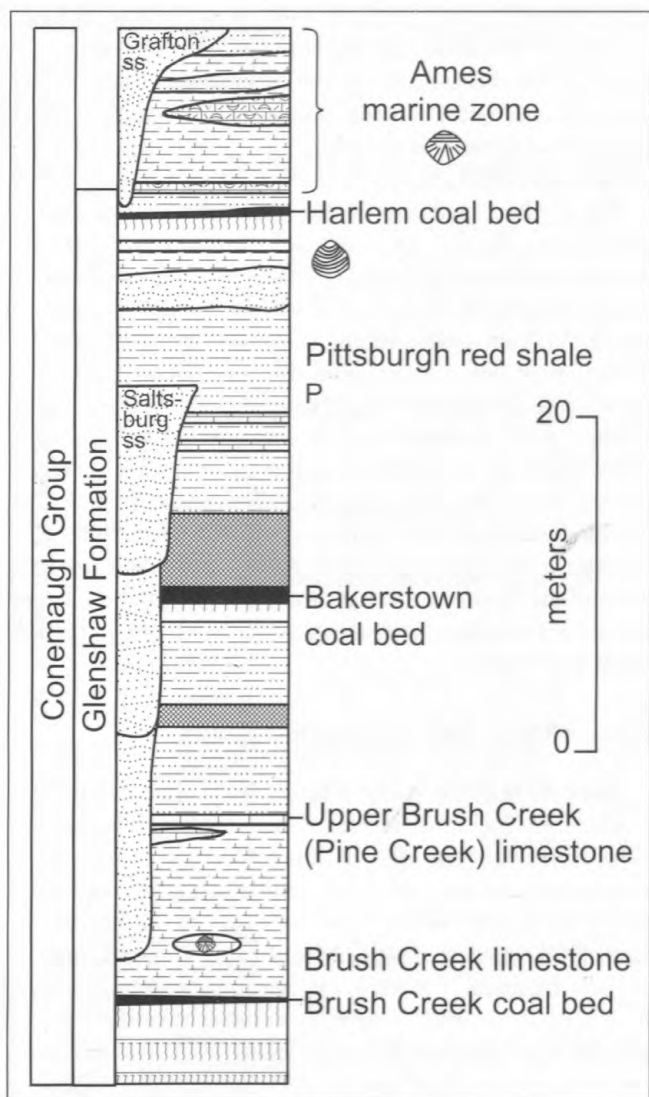ch)) thick in this section and, with few exceptions, rarely exceeds 0.6 m (2 ft) in thickness. However, thin coal or carbonaceous shale can be found at this stratigraphic position at widely separated points throughout the Dunkard basin. Persistent occurrences of beds, such as the Fishpot coal bed, are indicative of the allocyclic processes that controlled sedimentation and stratigraphy.

The thickest sandstone in this section occurs in a clastic interval above the Fishpot coal bed. It is tabular, varying in thickness from 0.9 to 2.3 m (3.0–7.5 ft). Another clastic interval occurs above the Sewickley limestone (*sensu* Platt and Platt, 1877). Thin sandstone and shale beds are interbedded with the Sewickley coal bed here. The association of the Sewickley coal bed with fine- to coarse-grained clastic strata is characteristic basinwide. Lower coal benches or "splits" of the Sewickley are sometimes miscorrelated with the underlying Fishpot coal bed. The main mineable bench of the Sewickley coal bed is not well exposed at this location. Weathered coal (blossom), 1.2 m (3.9 ft) thick, can be seen at the top of the section at the extreme western end of the cut. This bed also has been mined extensively underground in the Morgantown area.

Paleoclimate and Sea-Level History

Deposition of the strata at Stop 1 was coincident with the onset of a long-term humid interval that began in the latest Pennsylvanian (fig. 10) (Cecil, 1990). At approximately the same time, global ice house conditions began in the latest Pennsylvanian and culminated in the Permian (Frakes and others, 1992). Although deposition of latest Pennsylvanian and Early Permian(?) strata in the Appalachian basin occurred during long-term humid conditions coincident with ice in high latitudes, short-term to intermediate-term climate cyclicity was the predominant control on the stratigraphy of sedimentary cycles, such as those illustrated at Stop 1 (Cecil, 1990). For example, the paleosol underlying the Pittsburgh coal bed (underclay) at Stop 1 is typical of a soil that was permanently waterlogged or nearly so (hydromorphic soil). The paleosol transect noted above delineates a regional toposequence of paleosols that are indicative of humid paleoclimate. The transect demonstrates that the paleosol at Stop 1 formed in a waterlogged topographic low, while coeval soils to the south were forming under better drained conditions in upland areas. The toposequence of mineral paleosols that unconformably underlies the Pittsburgh coal bed is typical of modern tropical soils that are acidic and highly leached, and that have high base-exchange capacity and high soil moisture. These types of soils predominantly form under humid climate conditions (see table 2) where soil pore waters are exceedingly low in dissolved solids in response to soil leaching induced by high rainfall with little seasonality. An increase in rainfall triggered the onset of permanent swamp conditions and peat formation subsequent to mineral paleosol formation.

Allocyclic factors in addition to climate doubtless contributed to the vast areal distribution of the Pittsburgh coal

Figure 12. Stratigraphic section, Upper Pennsylvanian Conemaugh Group. Grafton sandstone of White (1903); Ames marine zone, Harlem coal bed; Pittsburgh red shale of White (1903); Saltsburg sandstone of Stevenson (1876); Bakerstown coal bed; Brush Creek marine zone; and Brush Creek coal bed are shown. See figure 11 for explanation of lithology symbols.

and sulfur content, as well as the degree of degradation of the peat plant debris, were greater to the west of the Morgantown area, perhaps because of more frequent and extensive incursions of fresh surface and ground water into the peat swamp. To the east, in western Maryland, the Pittsburgh coal bed is thicker, lower in ash yield and sulfur content than in the Morgantown area, and appears to have been, except for the basal high-ash and high-sulfur bench, more influenced by rainfall. Sixty miles (~100 km) to the south, in south-central West Virginia, the Pittsburgh coal bed is thin, or completely absent, as a result of paleotopographic controls on the development of the swamp and contemporaneous paleosols.

The ash yield and ash composition of the coal suggests that the peat was moderately acidic and that dissolved solids and clastic influx were mostly nil. These conditions are consistent with modern peat swamp precursors of commercial-grade coal. Such modern swamps tend to be acidic, low in dissolved solids, low in nutrients (oligotrophic), and essentially devoid of any clastic influx.

Following deposition of peat and overlying clastics, the occurrence of the Redstone limestone strongly suggests a significant change in sedimentary geochemistry. Subaerial exposure features within the Redstone limestone are indicative of repeated and persistent climate drying. In sharp contrast to the low dissolved solids and acidic water chemistry associated with the formation of the mineral paleosol and peat, chemical conditions for limestone deposition require alkaline waters that were saturated with dissolved solids.

Any relation between sea-level fluctuation and latest Pennsylvanian sedimentation in the Appalachian basin remains equivocal. Sediments of marine origin have not been documented in the Monongahela Group, even though cyclic sedimentation (analogous to the Virgilian cyclothems in the Midcontinent) occurs throughout the group. These cycles are interpreted herein as fourth-order sequences with sequence boundaries defined by the unconformities at the base of the coal beds. The periodic rise and fall of water levels in the Dunkard basin, therefore, may have been controlled by cyclic variations in both the amount and seasonality of rainfall that were associated with the well-known glacial eustatic cycles in the Midcontinent.

Stop 2. Paleosols in the Pittsburgh red shale, Conemaugh Group on Interstate 79 at Exit 146.
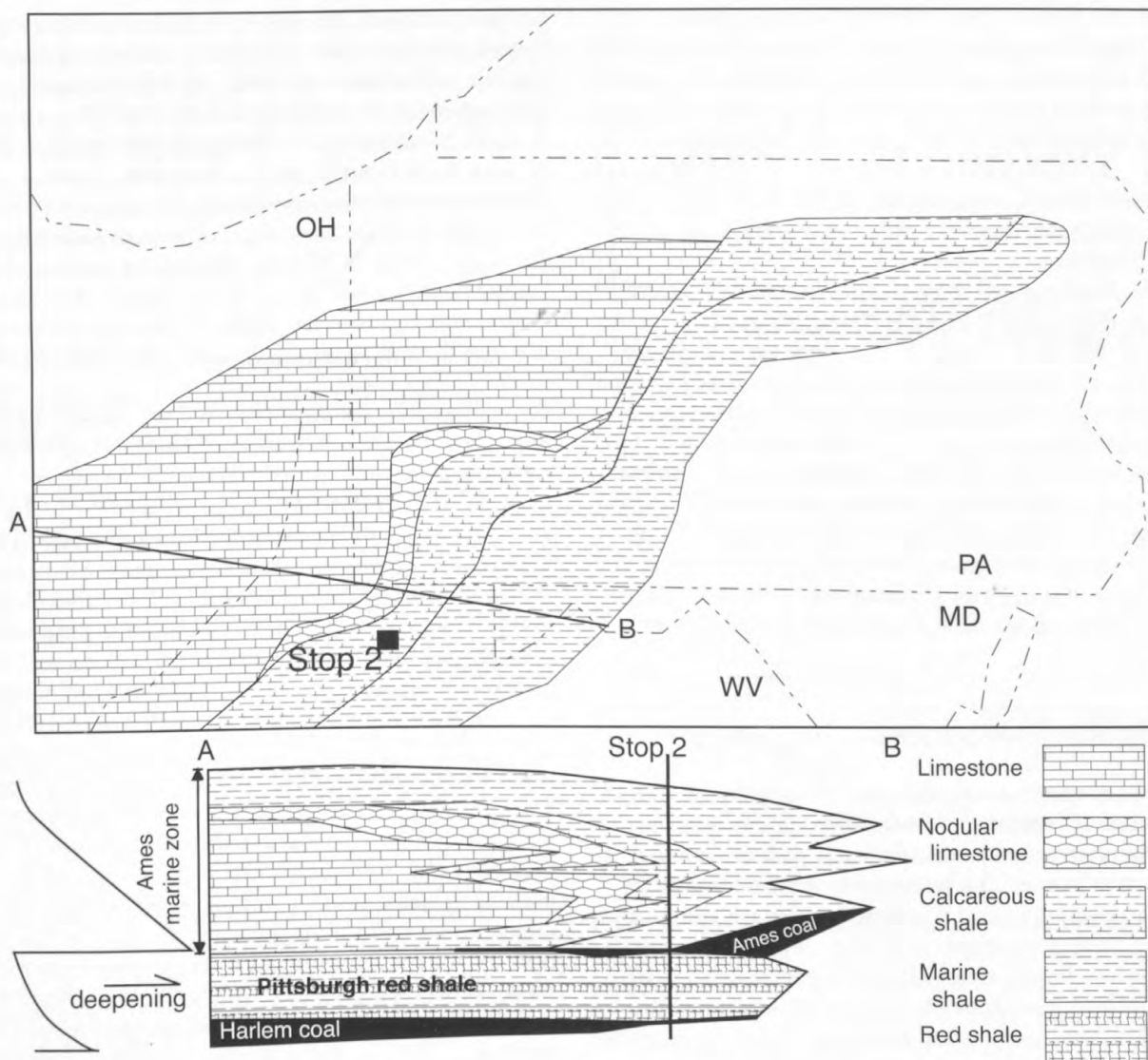
Lat 39°32'25" N., long 79°59'23" W., Morgantown South, W. Va., 7.5-minute quadrangle.

Leaders: Nick Fedorko, Blaine Cecil, and Rob Stamm

Introduction

Upper Pennsylvanian strata assigned to the Conemaugh Group are exposed in a roadcut along I-79 adjacent to the

bed. However, the thickness and quality of the coal appear to be strongly climate controlled. Following mineral paleosol formation, the paleoclimate became wet enough to flood vast flat-lying areas and initiate swamp development. Water levels within the swamp were maintained primarily by rainfall along with an influx of surface water from around the margins of the swamp. During the initial stages of peat formation, annual rainfall, augmented with surface water flow, was sufficient to allow the development of a large planar swamp. During the later stages of peat development, the influential effects of rainwater versus surface-ground water on peat composition, which, in turn, influenced ash yield, sulfur content, and maceral composition, varied with location and time. Ash yield

Figure 13. Lithofacies distribution of the Ames marine zone in the central Appalachian basin. Cross sectional interpretation (bottom) of fifth-order deepening episodes with corresponding lithotopes (modified from Brezinski, 1983).

Goshen Road exit (Exit 146) in Monongalia County, West Virginia. The cut exposes approximately 34 m (~110 ft) at, and just above road level, including the following units, in descending order: the Grafton sandstone, Ames marine zone, Harlem coal bed, and Pittsburgh red shale, all of the Glenshaw Formation. This stratigraphy is depicted in the upper half of figure 12.

Lithostratigraphy

The Grafton sandstone (*sensu* White, 1903), exposed at the top of the section, consists of interbedded siltstone and sandstone, and elsewhere is overlain by the Casselman Formation. Underlying the Grafton is the Ames marine zone

of the Glenshaw Formation. It represents the last known major marine transgression and inundation in the central Appalachian basin. As such, the Ames serves as an important unit for lithostratigraphic correlation across the basin. The Ames is an impure, shaley, fossiliferous limestone to calcareous shale in the area immediately surrounding the area of Stop 2, but grades westward into a greenish-gray, highly fosssiliferous limestone in eastern Ohio (Brezinski, 1983) (fig. 13).

The coal bed directly beneath the Ames marine zone is termed the Harlem coal bed by the West Virginia Geological Survey (fig. 13). In Ohio, there are two coal beds beneath the Ames marine zone; the coal bed immediately underlying the Ames marine zone is the Ames coal and the second is the Harlem coal. This guidebook will continue to follow the terminology of the West Virginia Geological Survey. The

Harlem coal bed is a thin (generally less than 0.6 m (2.0 ft) thick), laterally persistent unit that occasionally attains mineable thickness. Compositionally, the Harlem coal bed generally contains high percentages of vitrinite group macerals, and low to moderate amounts of liptinite and inertinite group macerals. Ash yields and sulfur content commonly are moderate to high. Other Conemaugh Group coal beds of regional extent include the Mahoning, Bakerstown, Elk Lick, and Little Clarksburg.

The Pittsburgh red shale (*sensu* White, 1903) directly underlies the Harlem coal bed at this stop (fig. 12). Here the Pittsburgh red shale consists of alternating beds of impure limestone and variegated red-green claystone that often contain calcium carbonate nodules. This unit contains features indicative of repeated and (or) prolonged subaerial exposure and pedogenesis. These features include calcareous nodules and mukkarra structures (crosscutting slickensides) of pedogenic origin. In addition, midway between the base of the exposure and the Harlem coal bed there is a lateral break in soil structure that includes a channel-form structure indicating that the Pittsburgh red shale may be composed of two or more paleosols.

Depositional Environments

The abundant calcium carbonate in the paleosol section is indicative of repetitive prolonged dry seasons. A nonmarine limestone often occurs as discontinuous pods at the top of the Pittsburgh red shale. This limestone is of mixed lacustrine and pedogenic origin, and it occurs in topographic lows on the gilgai surface (paleosol relief) of the Pittsburgh red shale. Rainy periods lasting months to a few years resulted in lacustrine carbonate deposition. During drier climatic periods, these lakes dried up, resulting in pedogenesis of the lacustrine carbonates. The lateral persistence of the Pittsburgh red shale throughout the Dunkard basin indicates that pedogenesis occurred during a lowstand in sea level and that the climatic conditions were basinal in extent.

Unlike the underlying Pottsville Group and Allegheny Formation strata, the Conemaugh Group contains abundant calcareous red shales and mudstones. Regionally, these calcareous red sediments first appear in the section 30 to 60 m (100–200 ft) below the Ames marine zone and are present to varying degrees in the upper two thirds of the Conemaugh Group throughout its area of occurrence. The calcium carbonate content of Conemaugh Group strata is high as compared to Middle Pennsylvanian strata (Cecil and others, 1985). Calcium carbonate occurs as admixtures in marine intervals, as nonmarine lacustrine beds (for example, Clarksburg limestone of White (1891)), and as pedogenic nodules, discontinuous lenses, and admixture within mudstones and shales.

Although of regional extent, Conemaugh Group coal beds tend to be fewer, thinner, and more impure than those in the underlying Allegheny Formation or overlying Monongahela Group. For example, the Little Clarksburg coal

bed rarely exceeds 0.6 m (2 ft) in thickness in this region. It is thicker and mineable in the Potomac Basin of eastern West Virginia and western Maryland, but is of poor quality, locally known there as the "Dirty Nine-foot." The Elk Lick coal bed, exposed just above the first bench on I-68 (milepost 4.0) between Stops 2 and 3, also has been mined in the Potomac Basin in western Maryland and also in central West Virginia and is known as the Barton coal in western Maryland. The Elk Lick is 0.9 m (3 ft) thick along I-68 at milepost 4.0, but has not been commercially exploited locally. As a group, Conemaugh coal beds are higher in ash yield and sulfur content than the underlying Allegheny Formation coal beds, and comparable in sulfur content with the overlying Monongahela Group coal beds, but higher in ash yield. The Elk Lick coal bed exposed in the I-68 roadcut is 3 ft (0.9 m) thick and represents peat that accumulated during the long-term Conemaugh drier interval (see fig. 10) than the stratigraphically lower Upper Freeport or Mahoning coal beds. The Elk Lick coal was formed after the demise of the peat-swamp arboreous lycopsids at the Westphalian-Stephanian boundary. The Elk Lick coal bed is high in ash yield and high in sulfur and contains significantly greater inertinite, and less well-preserved (>50-μ) vitrinite than the Upper Freeport or coal beds lower in the Pennsylvanian. At the top of the I-68 section the Little Clarksburg coal is exposed, and the stratigraphically lower Harlem and West Milford coals are exposed in nearby outcrops. These coal beds are similar in ash yield, sulfur content, petrographic composition, and floral character to the Elk Lick and typify Conemaugh coal beds that apparently accumulated in planar swamps with significant surface and ground-water influx of minerals and dissolved solids in moderate pH waters. Sulfur emplacement, especially as pyrite, was extensive and coincided with severe degradation of the peat and loss of >50-μ vitrinite components, probably by anaerobic microbes. These attributes suggest a seasonal paleoclimate with insufficient annual rainfall to maintain a highly acidic ombrogenous swamp.

Paleoclimate and Sea-Level History

The strata at Stop 2 were deposited during a long-term dry interval that began in the middle Late Pennsylvanian and ended in the late Late Pennsylvanian (fig. 10) (Cecil, 1990). This long-term drier interval is coincident with the Late Pennsylvanian global greenhouse condition noted by Frakes and others (1992). In contrast to the humid climatic conditions of pedogenesis at Stop 1, the paleosols at Stop 2 are indicative of a paleoclimate that was dry subhumid to semiarid. A short- to intermediate-term increase in humidity (moist subhumid climate) must have been associated with peat formation (Harlem coal) during maximum lowstand (maximum ice) as suggested by Cecil and others (2003b). This stop illustrates both the long-term dry conditions associated with long-term greenhouse conditions and the short-term climate cycles associated with glacial-interglacial conditions.

The compound nature of the paleosols at this stop suggests at least two periods of deposition followed by exposure and pedogenesis. This interpretation is supported by a reconnaissance study (by R.G. Stamm) that identified conodonts within the paleosols. If further work unequivocally demonstrates the presence of conodonts within the paleosols, then some of the Missourian marine transgression deposits in the Appalachian basin were nearly obliterated by pedogenesis during subsequent glacioeustatic lowstands.

Stop 3. Late Middle Pennsylvanian Lower Freeport coal bed(?) and associated strata on Interstate 68 at milepost 11.4

Lat 39°42.5' N., long 78°17.6' W., Lake Lynn, Pa.-W. Va., 7.5-minute quadrangle.

Leaders: Blaine Cecil, Nick Fedorko, Frank Dulong, and Cortland Eble

Introduction

An accurate stratigraphic correlation of the coal beds at this stop remains equivocal. However, the palynoflora in these coal beds suggest that they are the Lower and Upper Freeport coal beds of the Allegheny Formation. The section at Stop 3, therefore, includes the stratigraphic interval from the Lower Freeport limestone up to the Upper Freeport coal bed of the Middle Pennsylvanian Allegheny Formation (Wilmarth, 1938) (fig. 14). The primary emphasis at this stop is the stratigraphic interval from the base of the Lower Freeport limestone to the top of the Lower Freeport coal bed.

Lithostratigraphy

The Lower Freeport coal bed(?) of Platt and Platt (1877) crops out just above road level at Stop 3. The overlying stratigraphic succession (in ascending order) includes the Upper Freeport sandstone and shale (Butler sandstone of White, 1878), Upper Freeport limestone (absent at this locality) of Platt and Platt (1877), Upper Freeport fire clay (underclay of the Upper Freeport coal bed) of Stevenson (1878), and Upper Freeport coal bed of Platt and Platt (1877). At Stop 3, the clastic interval above the Lower Freeport coal bed is predominantly sandstone. The Upper Freeport fire clay (paleosol) and coal are exposed at the top of the roadcut on the south side of I-68.

Lower Freeport Coal

The Lower Freeport coal at Stop 3 consists of three splits over a 4.3-m (14.1-ft) interval. The main (lower) split is 0.9 m (3 ft) thick, is vitrinite-rich, especially the >50-μ vitri-
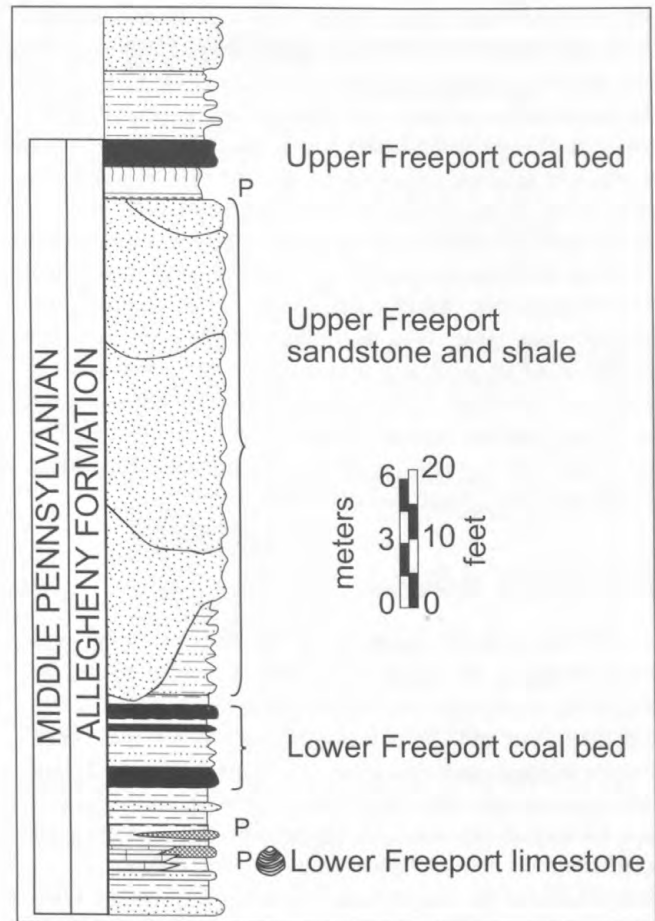
Figure 14. Stratigraphic section, Middle Pennsylvanian Allegheny Formation. Upper Freeport coal bed; Upper Freeport sandstone and shale (Butler sandstone of White, 1878); Lower Freeport coal bed; and Lower Freeport limestone of Platt and Platt (1877) are shown. See figure 11 for explanation of lithology symbols.

nite types, and is low in ash yield and sulfur. Palynologic results show a tree fern spore-dominant swamp palynoflora throughout, but with a moderate arboreal lycopsid spore contribution. At this location, development of the Lower Freeport swamp was not at its best (mineable) quality, but the lower and middle benches of this split probably represent paleoenvironments of the thicker coal to the north. Initial peat accumulation was in a planar swamp (Cecil and others, 1985) with minor emplacement of minerals and sulfur. Tree ferns dominate the flora and the pre-vitrinite plant debris was preserved moderately well, with little oxidation of the peat. With further peat accumulation (middle bench) the planar swamp may have become slightly elevated. Mineral and sulfur emplacement was low. Tree fern spores dominate the palynoflora, but increased arboreal lycopsid spore abundance may indicate a standing water cover.

The paleoclimate at the time of Lower Freeport peat accumulation probably was transitional between the perhumid Early and early Middle Pennsylvanian climate and the drier

and more seasonal climate of the early Late Pennsylvanian. The paleoclimate was obviously wet enough to allow for the widespread development of the Lower Freeport coal, and for the accumulation of some low ash and sulfur, pre-vitrinite-rich peat. However, while the annual rainfall may have been insufficient to allow for extensive domed peat formation (in other words, to the extent inferred for many Lower and Middle Pennsylvanian swamps), it certainly was adequate to allow for the development of an extensive peat swamp that, in some areas, may have attained some elevation above the regional water table. With the buildup of the peat, oxidation became more frequent in a seasonal paleoclimate where insufficient seasonal rainfall did not allow for extensive doming during peat accumulation. Oxidation of the peat surface and an increase in inertinite abundance preceded the ultimate drowning of the Lower Freeport coal.

Stratigraphy at Stop 3

The top of the Upper Freeport coal bed (top of the road-cut) is defined as the top of the Allegheny Formation and the base of the overlying Conemaugh Group (Stevenson, 1873). Both the Lower and Upper Freeport coal bed horizons occur throughout the Appalachian basin in Pennsylvania, Maryland, West Virginia, and Ohio. Where they are sufficiently thick, these laterally extensive coal beds have been mined from the eastern outcrop belt in western Maryland and eastern Pennsylvania to the western outcrop belt in east-central Ohio, a distance of over 150 mi (250 km). Nonmarine strata, including underclay, sandstone, siltstone, shale, flint clay, and the Lower Freeport limestone underlie the Lower Freeport coal bed.

Above the top of the Lower Freeport coal bed at Stop 3 is the Upper Freeport sandstone and shale (Butler sandstone of White, 1878) and overlying underclay (paleosol) and Upper Freeport coal bed. The Upper Freeport coal bed is of particular significance in that it is the stratigraphically highest coal bed that contains abundant *Lycospora* sp., the dispersed spore of some of the giant lycopsid trees (for example, *Lepidophloios* and *Lepidodendron*) that dominated many Lower and Middle Pennsylvanian coal beds throughout Euramerica.

Paleoclimate and Sea-Level History

The interval from the base of the Lower Freeport limestone to the top of the Lower Freeport coal bed is interpreted to be the result of a complex set of conditions that occurred in response to a cyclic paleo water-table, sediment flux, pedogenesis, and paleoclimate (Cecil and others, 1985). The limestone is nonmarine and was probably deposited in large, shallow lakes, as indicated by multiple subaerial exposure features that include subaerial crusts, pedogenic brecciation, and residual pedogenic clay. Intermittent deposition and subaerial exposure of the limestone is indicative of a fluctuating lake level and water table. The frequency of water level fluctua-

tion is unknown but may have been controlled by short-term or very short term variations in paleoclimate (table 1). Lake waters must have been alkaline, pH 7.8 or greater (Krumbein and Garrels, 1952), during deposition of the limestone. The alkalinity and high concentrations of dissolved solids in lake waters during deposition of the limestone was, in part, the result of a relatively dry paleoclimate that concentrated dissolved solids through evaporation (Cecil and others, 1985; Cecil, 1990). The Lower Freeport limestone was then buried by a thin (~1–2 m; 3–7 ft), but widespread, influx of siliciclastics. Subsequently, both were subjected to an extended period of subaerial exposure, weathering, and pedogenesis (Cecil and others, 1985). The weathering and resultant residual clay deposits imply a drop in the water table during the onset of increasing pluvial conditions. Further increases in rainfall led to increased vegetative cover, rainfall dilution of runoff, and leaching of residual soils, all of which reduced erosion and the influx of siliciclastic sediment and dissolved solids. Extensive leaching of the landscape, during the pluvial part of intermediate-term climate cycles, restricted the buffering capacity of surface water systems by reducing the concentration of dissolved solids. A rising water table with low buffering capacity led to acidic water (pH <6) from decaying vegetal matter. These conditions of a high water table and low pH are necessary for the formation of thick, laterally extensive, high-quality peat (Cecil and others, 1985).

On a regional scale, a complex of kaolin-enriched paleosols occurs in a facies mosaic at the base of all upper Middle Pennsylvanian coal beds, including the Lower and Upper Freeport. These paleosols appear to be the result of a fluctuating water table and weathering during humid parts of climatic cycles. The most intensely developed paleosols formed on well-drained paleotopographic highs. The kaolin-enriched deposits have been mined locally and used in the manufacture of refractory brick. The unconformity at the top of the paleosols and the base of the coal is interpreted as a fourth-order sequence boundary.

Interruption of peat formation, as illustrated by the three benches of coal and interbedded partings at Stop 3, are sometimes interpreted as crevasse splays or other autocyclic depositional events (for example, Ferm and Horne, 1979). Alternatively, these interruptions are interpreted herein as the result of allocyclic controls that caused a change in water table and an influx of siliciclastic sediment. The latter interpretation is supported by the regional extent of many partings, which suggests a drowning of the peat-forming environment by a prolonged elevation of the water table, and concomitant siliciclastic deposition in a lacustrine environment (Cecil and others, 1985).

Peat formation in both the Lower and Upper Freeport paleoswamp environments was terminated by an allocyclically controlled rising water table that finally outpaced peat formation (Cecil and others, 1985). The lacustrine environment of the drowned paleoswamp became the site of an autocyclic facies mosaic of siliciclastic deposition. The shales may represent deposition in a lacustrine environment, whereas the

sandstones are the result of a prograding fluvial system (Cecil and others, 1985). Channel incision appears to have been in response to progradation of a fluvial system. In the climate model of cyclic stratigraphy (Cecil, 1990), the shale and sandstone are the result of an increase in siliciclastic influx in response to a return to drier and more seasonal conditions (dry subhumid climate, table 2). This increased siliciclastic influx was coeval with the development of lacustrine systems where a rising water table was controlled by a eustatic rise in sea level. Maximum drying occurred at the time of limestone deposition. The underclay (P) and Upper Freeport coal bed overlying the Upper Freeport sandstone and shale at Stop 3 is coincident with sea-level fall and a return to humid conditions and reduced siliciclastic influx, and the correct climatic and chemical conditions necessary for pedogenesis followed by the onset of peat formation.

The Middle to Upper Pennsylvanian floral transition occurs in Upper Pennsylvanian Conemaugh Group strata approximately 100 ft (~30 m) above the Upper Freeport coal bed (at the level of the Brush Creek marine zone), when all but one of the major arboreous lycopsid genera, several tree fern, and one sphenopsid spore genera become extinct (Kosanke and Cecil, 1996). This transition is time-equivalent with the Westphalian-Stephanian boundary in western Europe and is believed to represent the culmination of a major but gradual climatic shift from a basically perhumid climate in the Early through middle Middle Pennsylvanian, to one that was subhumid, and more seasonal, in the Late Pennsylvanian (Cecil and others, 1985; Cecil, 1990). Both the floral transition and the coeval onset of deposition of calcareous red beds in the Appalachian basin were coincident with the onset of Late Pennsylvanian greenhouse conditions at the end of the ice house world that began in the Late Mississippian (fig. 10).

Stop 4. The Lower Kittanning coal bed and fourth-order sequence ("cyclothem") on Interstate 68 at milepost 15.9.

Lat 39°39′21″ N., long 79°45′47″ W., Lake Lynn, W. Va., 7.5-minute quadrangle.

Leaders: Frank Dulong and Blaine Cecil

Introduction

The upper Middle Pennsylvanian Lower Kittanning coal bed has been correlated with the Block No. 6 coal bed in southern West Virginia (Kosanke, 1984), the Princess No. 6 coal bed in eastern Kentucky, the Colchester No. 2 coal beds of the Eastern Interior basin, and the Croweburg coal bed of the Western Interior basin (Kosanke, 1973; Peppers, 1970; Ravn, 1986; Cecil and others, 2003b; Eble, 2003). These correlations are indicative of a period of extremely widespread peat formation across eastern North America from the
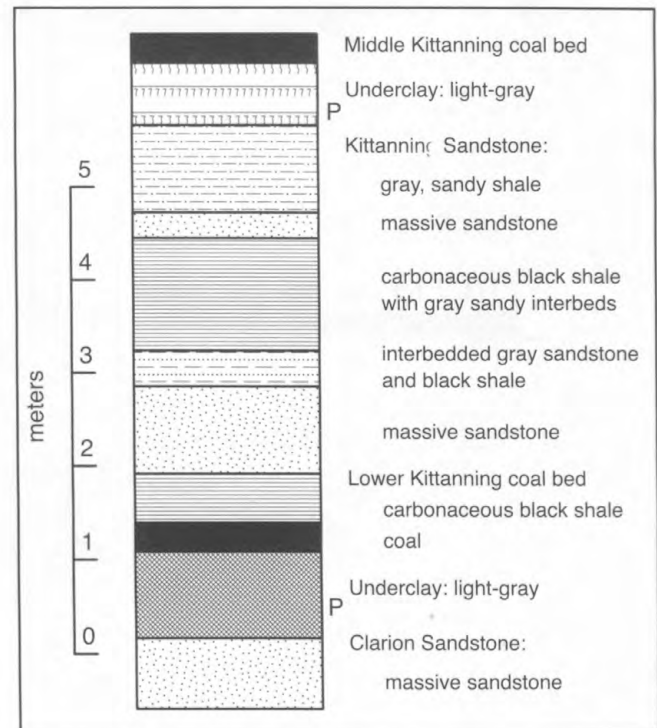

Figure 15. Stratigraphic section, Middle Pennsylvanian Allegheny Formation. Middle and Lower Kittanning intervals are shown. See figure 11 for explanation of lithology symbols.

Appalachian basin through the Western Interior basin during a lowstand in sea level. Although thin in the Chestnut Ridge area, the Lower and Upper Kittanning coal beds attain mineable thickness and represent a significant coal reserve in northern West Virginia, eastern Ohio, and western Pennsylvania. The Lower Kittanning at Stop 4 is a thin coal bed that unconformably overlies a paleosol that is composed of flint clay and pedogenically altered sandstone. It is the interval from the base of the Lower Kittanning underclay up to the base of the Middle Kittanning coal bed that has been the focus of interbasinal correlations across the United States (Cecil and others, 2003b).

Lithostratigraphy

The interval considered at Stop 4 commences in ascending order with the flint clay (underclay) at the base, Lower Kittanning coal bed, overlying siliciclastic unit (Kittanning Sandstone) capped by another underclay, and finally the Middle Kittanning coal bed horizon. This generalized lithostratigraphy (fig. 15) can be traced throughout the central Appalachian basin. On the basis of biostratigraphy (Stamm and Wardlaw, 2003; Eble, 2003), lithostratigraphy, and sequence stratigraphy (Cecil and others, 2003b), time-equivalent strata have been traced across the North American continent. The underclay horizons in the Appalachian basin, including the flint clay here, are intensely weathered paleo-

Middle Pennsylvanian (Desmoinesian) 306 Ma

A
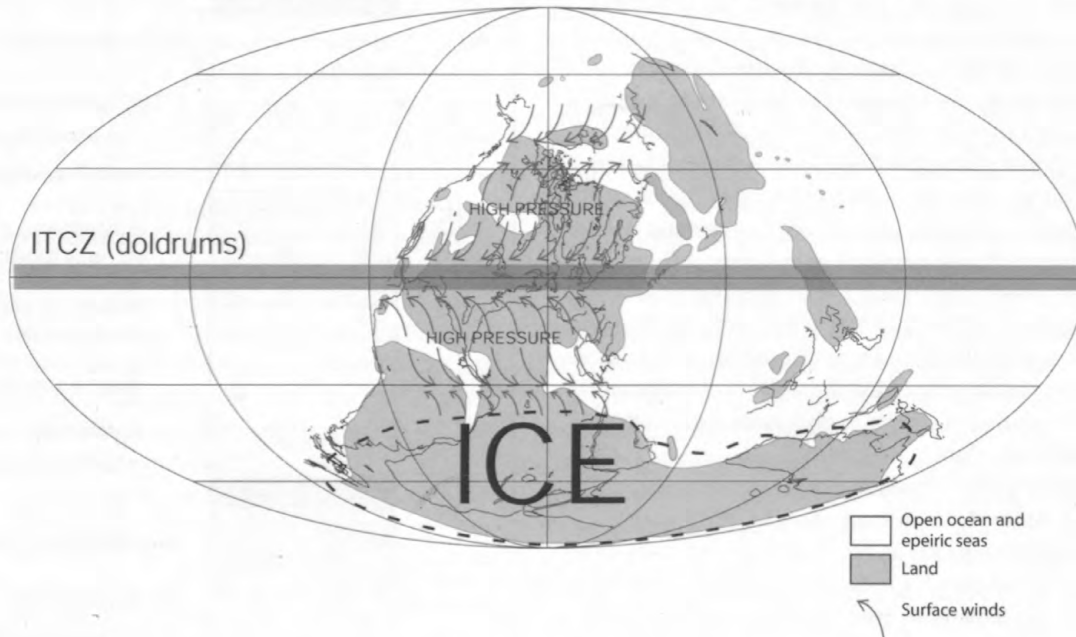
## Middle Pennsylvanian (Desmoinesian) 306 Ma
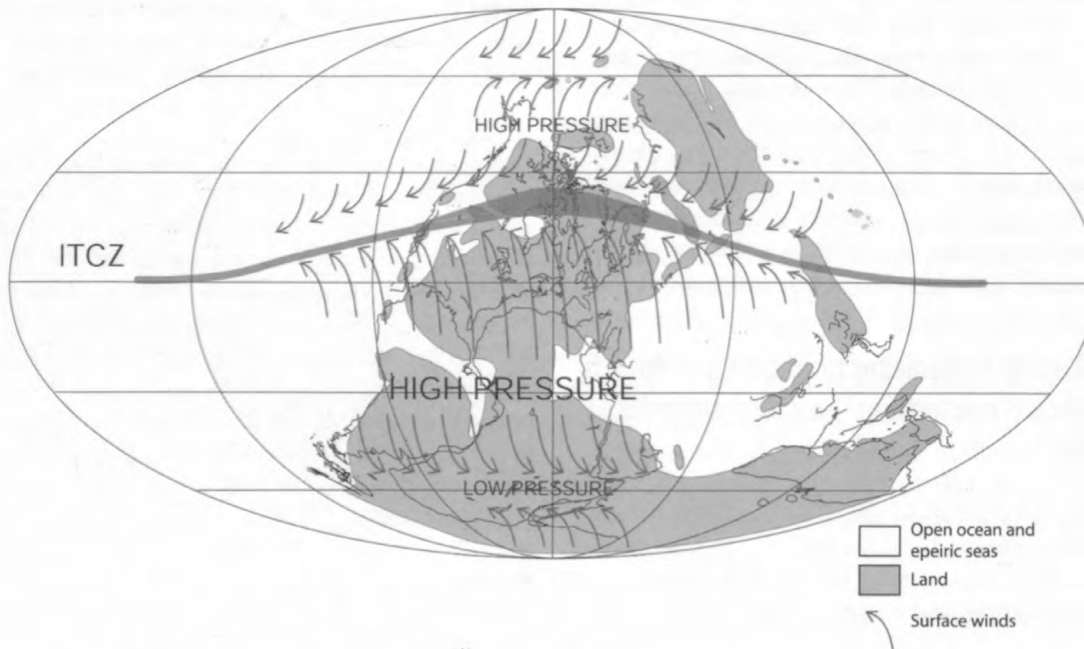
B

sols. As noted above, the coal beds have been correlated among basins across the Eastern United States. Cecil and others (2003b) have shown that the underclay deposits are even more continuous than the overlying coal beds, and coeval exposure surfaces have been traced across the continent into Arrow Canyon in southeastern Nevada. The siliciclastic unit overlying the coal varies from a marine black shale and limestone in Ohio, northern West Virginia, and western Pennsylvania to coarse-grained sand in easternmost outcrops along the Allegheny Front and in southern West Virginia.

Another laterally extensive underclay paleosol and the overlying Middle Kittanning coal bed cap the sequence.

Depositional Environments

The underclay (paleosol) horizons have characteristics of intensely weathered, well-drained mineral soils that had high soil moisture regimes. These features include gleying, angular peds, high-alumina clay content, mukkarra structures, and

Middle Pennsylvanian (Desmoinesian) 306 Ma
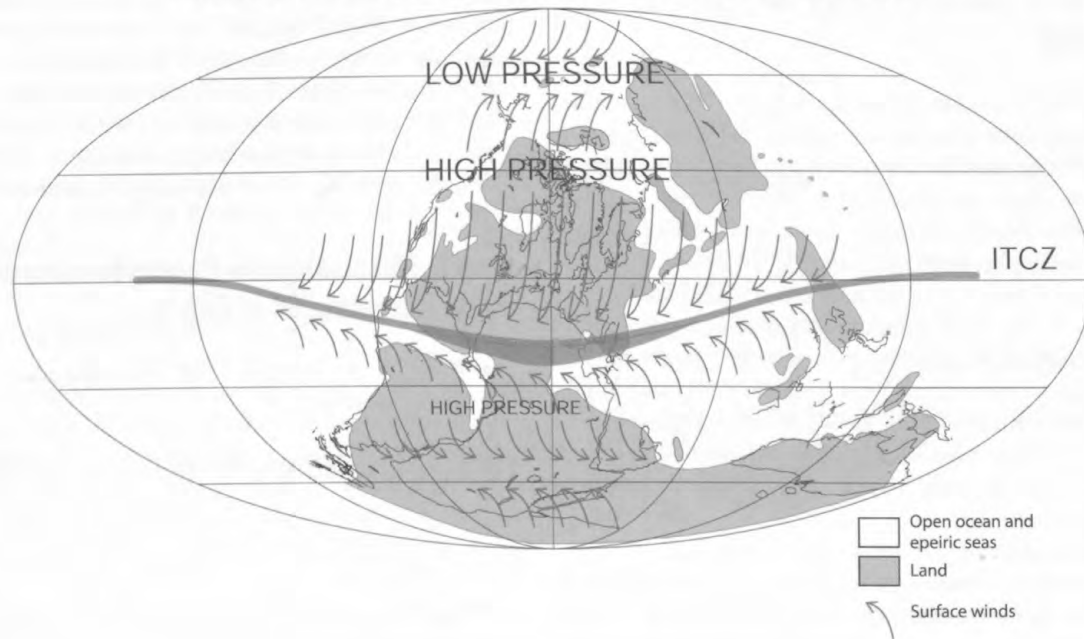
C

Figure 16 (this page and facing page). A, Conceptual model of Middle Pennsylvanian surface winds over Pangea during glacial intervals. Continental ice in the southern hemisphere limited the southern excursion of the intertropical convergence zone (ITCZ) during the southern hemisphere summer. Confinement of the ITCZ to equatorial regions created a low-pressure rainy belt (doldrums) that spanned approximately 10° of latitude. Schematic interpretation of continental ice is adapted from Caputo and Crowell (1985), Veevers and Powell (1987), Scotese (1998), and Frakes and others (1992). Paleogeography is modified from Scotese (1998). From Cecil and others (2003b). B, Conceptual model of Middle Pennsylvanian surface winds over Pangea during interglacial intervals. Interpreted northern excursion of the ITCZ during the northern hemisphere (Boreal) summer. Paleogeography is modified from Scotese (1998). C, Conceptual model of Middle Pennsylvanian surface winds over Pangea during interglacial intervals. Interpreted southern excursion of the ITCZ during the southern hemisphere (Austral) summer. The cross-equatorial movement of the ITCZ during interglacials resulted in significant increases in both dryness and seasonality of rainfall in low latitudes. Paleogeography is modified from Scotese (1998).

distinct soil horizonation. The interbasinal extent of these Middle Pennsylvanian paleosols and coeval exposure surfaces across the United States is indicative of a major eustatic drawdown of sea level and continental-scale exposure (Cecil and others, 2003b). In contrast, the overlying coal beds are the result of a rising water table and the onset of peat formation when the water table perpetually remained above the surface of the underlying mineral paleosol.

Paleoclimate

The paleosols, including coal beds, developed in environments where fluvial sediment supply (both dissolved and siliciclastic) was low (Cecil and others, 1985, 2003b). Such environments require perhumid or humid climates where soils are intensely leached and vegetation inhibits soil erosion as in equatorial Indonesia (Cecil and others, 1993, 2003a). The onset of peat formation has been attributed to a rise in the water table as a result of increased rainfall when the intertrop-

ical convergence zone (ITCZ) was stabilized within equatorial latitudes by maximum southern hemisphere ice (Cecil and others, 2003b). As the climate switched to interglacial conditions, sea-level rise and marine flooding outpaced peat formation and the vast peat swamps were flooded with marine, brackish, or nonmarine waters (Cecil and others, 1985, 2003b). Flooding resulted in black shale deposition over much of the craton (from the Appalachian basin westward through the Paradox basin). In the Appalachian basin, black shale deposition was followed by an input of sand from the east and southeast as the climate became progressively drier and rainfall more seasonal in response to increases in the amplitude of the annual swings of the ITCZ between hemispheres (fig. 16A, B). Deposition of clastic materials was terminated by a eustatic fall and the return of a humid climate, subaerial exposure, and pedogenesis. The interbasinal extent of paleosols including coal beds provides clear and unequivocal evidence that global climatic processes controlled sedimentation and stratigraphy.

Rolling "Stops" Through the Pottsville Group, West Flank of Chestnut Ridge Anticline on Interstate 68.

Strata of the Pottsville Group equivalent to Stop 8 are traversed (from top to base) as the trip ascends the west flank of the Chestnut Ridge anticline from Stop 4 to Stop 5. The uppermost Pottsville sandstone exposed is the Homewood(?) Sandstone (*sensu* White, 1878), the top of which (milepost 11.7) marks the boundary between the Pottsville Group and the overlying Allegheny Formation in the northern Appalachian basin. The top of the Pottsville is approximately time-equivalent with the Kanawha Formation-Charleston Sandstone (Allegheny Formation) contact in southern West Virginia. Pottsville Group strata on Chestnut Ridge contain units that are indicative of marine flooding of the Mississippian-Pennsylvanian (mid-Carboniferous) unconformity, unlike Stop 8 where the unconformity is erosional.

After passing by the Homewood Sandstone(?), the Upper and Lower Connoquenessing sandstones (*sensu* White, 1878) crop out along the highway (mileposts 11.7–14). Strata of the Pottsville Group in northern West Virginia typically consist of massive pebbly sandstones and sandy conglomerates intercalated with shale, siltstone, and thin, discontinuous coal beds. Pottsville Group sandstones, like the ones shown along I-68 on the west flank of Chestnut Ridge, generally occur as multistoried units up to 30 m (98 ft) thick, averaging 9 to 12 m (30–39 ft). Presley (1979) suggested that this group of strata was deposited by bed load, braided fluvial systems onto an alluvial plain. Meckel (1967) and Donaldson and Schumaker (1981) suggested that Pottsville sediments in the Chestnut Ridge area were derived from orogenic highlands located to the east and southeast. However, the quartzose nature of the sandstones and conglomerates is suggestive of a provenance area that had an intensely weathered and mature regolith, rather than immature sediments that would be derived from orogenic highlands.

A palynological analysis of a thin, discontinuous coal bed, informally designated herein as Pottsville coal j (mileposts 13.4–13.8), in a shale lens in the Upper Connoquenessing sandstone indicates that it is age equivalent with the early Middle Pennsylvanian (Atokan) Fire Clay-Chilton coal interval of the Kanawha Formation in southern West Virginia (Eble, 1994).

As the trip approaches the axis of the Chestnut Ridge anticline, an unnamed marine zone occurs in a siderite bed (milepost 14) beneath the Lower Connoquenessing sandstone, which is at the top of the cut. This marine unit contains a fauna that compositionally is similar to the Dingess Shale Member of the Kanawha Formation (early middle of the Middle Pennsylvanian) in southern West Virginia (T.W. Henry, oral commun., 1990). The Dingess Shale Member crops out and is found in core from southern West Virginia northward into central West Virginia but was not previously known to onlap into the Morgantown, W. Va., area. A

miospore analysis of the thin (0.3 m; 1.0 ft), discontinuous coal bed, informally designated herein as Pottsville coal 2, that occurs directly beneath the Lower Connoquenessing sandstone but above the marine siderite zone at this location has shown the palynoflora to correlate with the Cedar Grove No. 2 Gas coal interval in southern West Virginia (Eble, 1994). This biostratigraphic age assignment is consistent with the invertebrate data from the marine siderite bed.

Stop 5. Mississippian-Pennsylvanian unconformity on Interstate 68 at Exit 15.

Lat 39°39′29″ N., long 79°47′00″ W., Lake Lynn, W. Va., 7.5-minute quadrangle.

Leaders: Blaine Cecil, Mitch Blake, and Rob Stamm

Introduction

Stop 5 is at the Mississippian-Pennsylvanian (mid-Carboniferous) unconformity (White, 1891), on the axis of Chestnut Ridge anticline (fig. 17). The unconformity is exposed along the eastbound lanes of I-68 (formerly U.S. 48) just east of the exit for Coopers Rock State Forest (milepost 14.7). This unconformity is global in extent (Saunders and Ramsbottom, 1986), and it is exposed at interbasinal scales across the North American craton.

Lithostratigraphy

The red beds, which crop out at the west end of the eastbound exit, are assigned to the Upper Mississippian Mauch Chunk Group (Namurian A) (see Stop 8 for explanation of Mauch Chunk terminology). Three Pottsville coal beds are present at or near Stop 5. All three are thin (<0.3 m; 1 ft) and contain low to moderate ash yields and high sulfur contents. The stratigraphically lowest coal bed occurs approximately 4 m (13 ft) above the level of the interstate highway drainage ditch. This coal bed, like most coal beds assigned to the Pottsville Group in the northern West Virginia area, is laterally discontinuous and irregular in occurrence (Presley, 1979). This coal bed was palynologically analyzed and yielded a miospore assemblage that correlates with the lower part of the Middle Pennsylvanian Kanawha Formation (unnamed coal bed below the Matewan coal) (Eble, 1994). This assemblage indicates that the stratigraphically youngest Pennsylvanian strata at this location are early, but not earliest, Middle Pennsylvanian (Westphalian B) in age. Lower Pennsylvanian strata, assignable to the Pocahontas and New River Formations are absent here. As compared to thicknesses of equivalent Mississippian and Pennsylvanian strata in southern West Virginia and southeastern Virginia, over 1,500 m (5,000 ft) of Upper Mississippian (Chesterian), Lower (Morrowan)

and lowest Middle (early Atokan) Pennsylvanian strata are missing at Stop 5. Here, the Mississippian-Pennsylvanian systemic boundary occurs within the 4-m (13-ft) interval between the lower Middle Pennsylvanian unnamed coal bed and the Mississippian Mauch Chunk Group red beds. Petrographically, these coal beds contain high percentages of vitrinite and low to moderate amounts of inertinite. Despite their thinness, these coal beds display petrographic characteristics similar to age-equivalent Kanawha coal beds in southern West Virginia.

Depositional Environments

The interval exposed at Stop 5 appears to contain at least two mineral paleosols and a paleo-Histosol represented by the coal bed at the top of the paleosol sequence. The stratigraphy of the mineral paleosols is quite complex at this locality, but they appear to represent at least two periods of deposition, each followed by subaerial exposure, weathering, and pedogenesis. The top of the lowermost paleosol occurs about 2.1 m (6.9 ft) below the base of the overlying coal bed. The lower paleosol overlies and appears to grade downward into green and red strata of the Upper Mississippian Mauch Chunk Group; thus, deposition probably occurred during the Mississippian, whereas subaerial exposure and pedogenesis appears to have been during the Early Pennsylvanian. The well-developed lower paleosol may be classified as a paleo-Ultisol whereas the poorly developed upper paleosol may be more properly classified as a paleo-Inceptisol or Entisol (U.S. Department of Agriculture classification system (Soil Survey Staff, 1975; Retallack, 1989; Buol and others, 1989)). The intensely burrowed and pyritic sandstone (Betsie Shale Member equivalent) overlying the coal bed is suggestive of marine onlap and rising sea level.

On the basis of an analysis of the "mid-Carboniferous eustatic event" (Saunders and Ramsbottom, 1986), up to 4.5 m.y. may be represented in the 4-m (13-ft) interval exposed at Stop 5. The interbasinal complexity of the stratigraphy at the Mississippian-Pennsylvanian systemic boundary appears, therefore, to be the source of a great deal of confusion as to the "age" of the unconformity.

Paleoclimate

On an interbasinal scale, high-alumina refractory clay deposits, such as the Mercer clay in Pennsylvania, the Olive Hill clay in eastern Kentucky, and the Cheltenham clay on the flanks of the Ozark dome in Missouri, also occur at the Mississippian-Pennsylvanian systemic boundary. The high-alumina deposits in the eastern half of the continent are interpreted as paleo-Ultisols. In addition, residual chert (chat) occurs at the boundary in southern Missouri, northern Arkansas, and parts of Kansas. Farther west in Colorado, a thick sequence of residual cherty limestone breccia (Molas
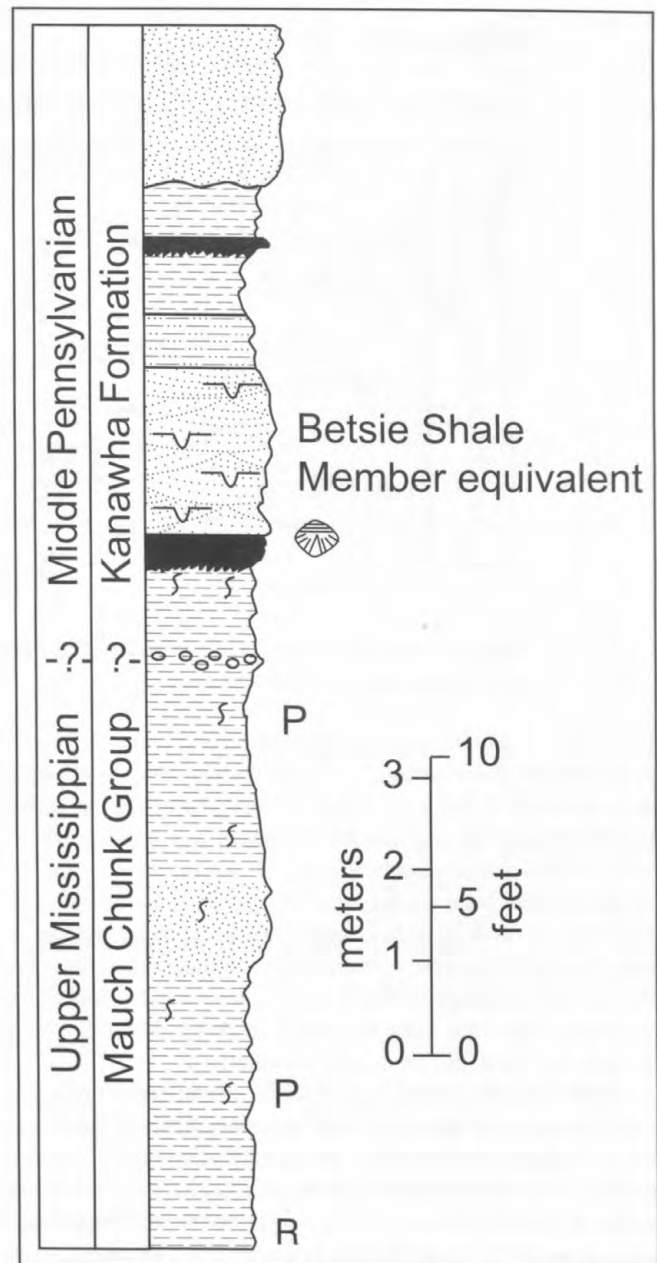
Figure 17. Stratigraphic section of the Mississippian-Pennsylvanian unconformity along Interstate 68 at Exit 15. See figure 11 for explanation of lithology symbols.

Formation) occurs at the top of the Leadville Limestone and is associated with the mid-Carboniferous unconformity. The Molas Formation is unconformably overlain by an arenaceous marine limestone of early Middle Pennsylvanian age (late Atokan) (R.G. Stamm, unpub. data). The lithologies of all residual deposits at the systemic boundary appear to be the result of intense long-term weathering and pedogenesis under high annual rainfall, which was fairly evenly distributed throughout the year (humid to perhumid). Weathering may have commenced as early as 330 Ma during the Late

western Md.   southwestern Pa.
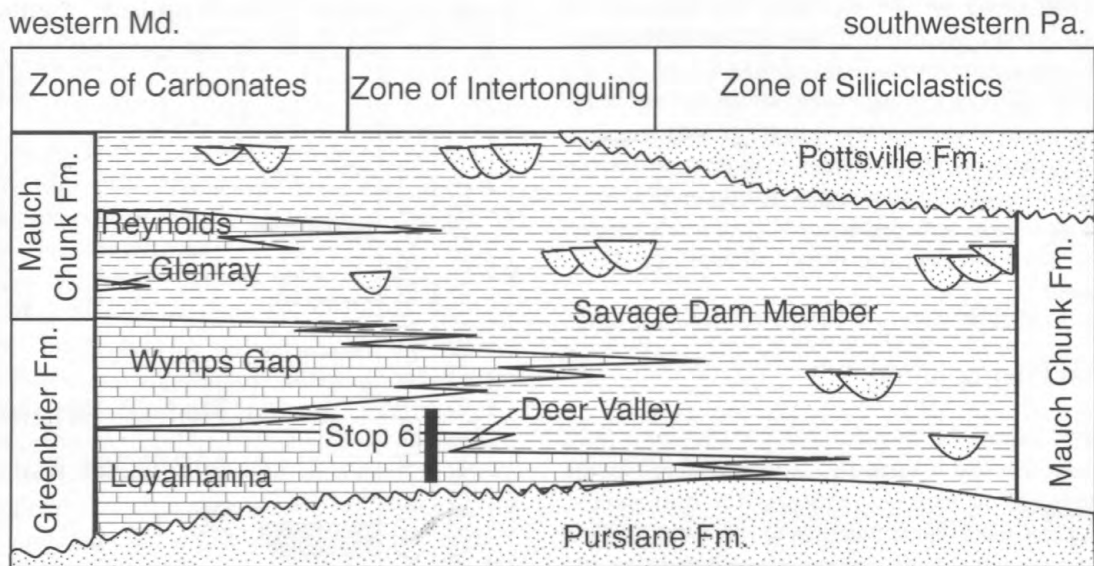
Figure 18. Regional stratigraphic relations of the Mauch Chunk and Greenbrier Formations. See figure 11 for explanation of lithology symbols.

Mississippian at the onset of the global eustatic event (Saunders and Ramsbottom, 1986). Exposure may have persisted for up to 4.5 m.y. in much of North America, including the aforementioned areas, as the continent was moving northward into the paleo-equatorial zone. However, weathering appears to have been particularly protracted and intense across the North American continent from the Appalachian basin through Colorado. Compared to the paleosol at Stop 5, other coeval exposure surfaces across the continent appear to have been somewhat more elevated and better drained, which accounts for the depth of intense weathering.

Paleosol development at the mid-Carboniferous unconformity progressed during the 4.5-m.y. period of subaerial exposure (latest Mississippian into the Middle Pennsylvanian). Sea-level fall became significant in the Late Mississippian, continued through the Early Pennsylvanian, before beginning to rise again in the early Middle Pennsylvanian (Atokan), evidenced at this stop by marine strata in the lower part of the Pottsville Group. The deep weathering (in response to a long-term humid climate), therefore, was primarily an Early Pennsylvanian event. This long-term Early Pennsylvanian humid period in the Appalachian basin was coincident with long-term ice house conditions that began in the Late Mississippian, culminated in the Early Pennsylvanian, and ended in the early Late Pennsylvanian as discussed at Stops 2 and 3. Available climate and sea-level data indicate that the mid-Carboniferous eustatic event was glacial in origin resulting from long-term ice house conditions.

Stop 6. Loyalhanna Limestone Member of the Mauch Chunk Formation at the Keystone quarry, Springs, Pa.

Lat 39°44.65′ N, long 79° 12.28′ W, Grantsville, Md.-Pa., 7.5-minute quadrangle.

Leader: Rob Stamm

Introduction

The Late Mississippian Loyalhanna Limestone Member of the Mauch Chunk Formation is examined at this stop. Also exposed are the Deer Valley and Savage Dam Members of the Mauch Chunk (Greenbrier Formation in West Virginia and Maryland) (fig. 18). The Loyalhanna's origin, with its large crossbed sets, has long been debated.

Lithostratigraphy

The Loyalhanna Limestone Member of the Mauch Chunk or Greenbrier, as it is called in Maryland, is equivalent to the Loyalhanna Formation of Pennsylvania (fig. 18). This is a widespread unit that extends at least as far north as Scranton, Pa. The Loyalhanna at this location is a 15-m (49-
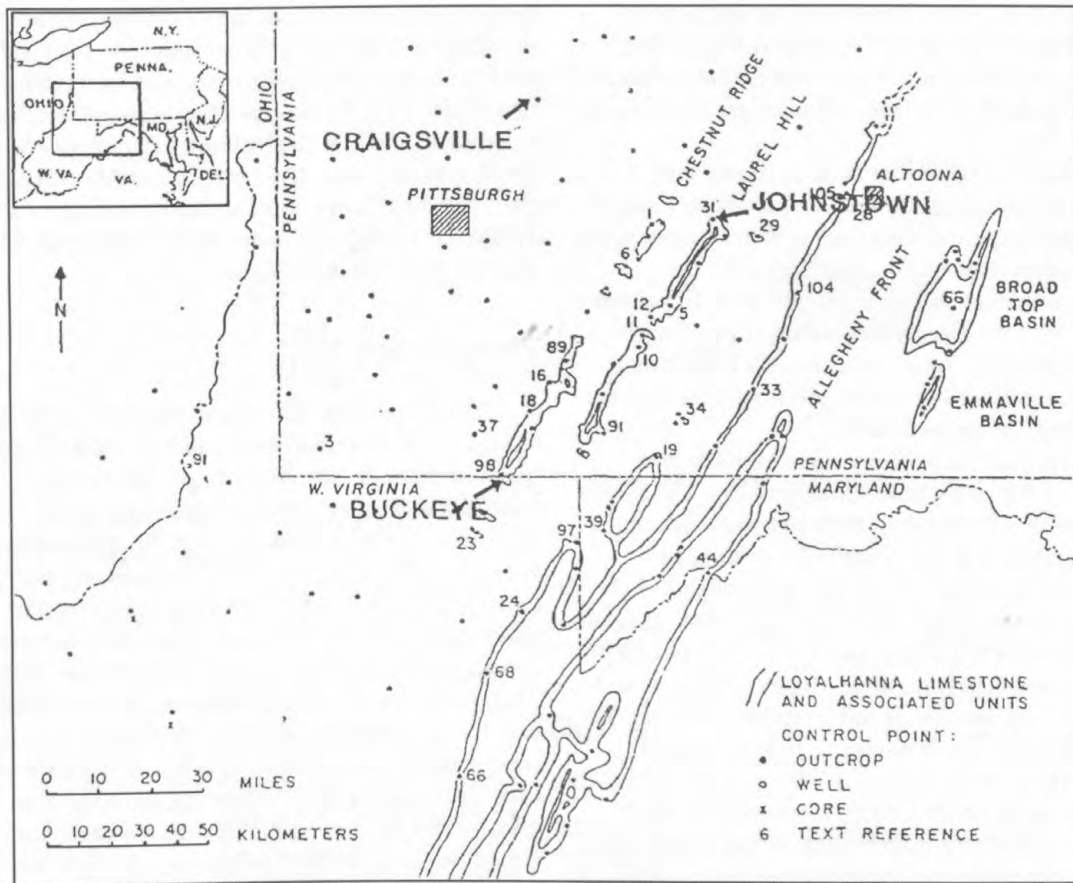
Figure 19. Map of Loyalhanna Limestone and associated units, showing outcrop, well, and core occurrences. Numbers refer to localities defined by Adams (1970).

ft)-thick, festoon crossbedded, arenaceous grainstone to calcareous sandstone. The Loyalhanna in this area and adjacent Maryland has a reddish tint caused by a small admixture of red clays that appear to be syndepositional. The quartz sand is medium to fine grained, and the carbonate grains consist of ooids, coated grains, intraclasts, and fossil fragments. The fossil fragments consist of brachiopod, bryozoan, crinoids, and endothyrid foraminifers. In addition R.G. Stamm (unpub. data) has recovered wind-abraded conodonts of probable Late Devonian age from the festoon crossbeds. Although the fossils have been typically comminuted to sand-size grains in this high-energy environment, at some nearby localities complete articulated brachiopods and straparollid gastropods have been recovered from this unit. Adams (1970) partially documented the regional extent of the Loyalhanna Member (fig. 19). Adams (1970) suggested that much, if not most, of the quartz sand has its origin from a northern Pocono source. This is indicated by the increase in terrigenous sand content in the Loyalhanna in that direction. In contrast, crossbeds are directed mainly to the east and northeast (Adams, 1970; Hoque, 1975) suggesting a provenance area to the west if the Loyalhanna is eolian in origin.

The large-scale crossbeds are accentuated on weathered joint faces along the entrance into the main working face of the Keystone quarry. This typical weathering character is caused by the more arenaceous layers, which are less soluble than the carbonate-rich layers. Thus, the more arenaceous layers stand out in relief on weathered surfaces.

At many locations on the worked face one can usually observe thin (<1.0 ft; 0.3 m), tan siltstone lenses. These lenses pinch out laterally, are convex downward, and are truncated on the upper surface. Brezinski (1989b) interpreted these lenses as representing remnants of shallowing episodes or slack water deposits preserved in swales between submarine dunes, that later were scoured and largely removed by subsequent dune migration.

Overlying the Loyalhanna is the Deer Valley Limestone Member (Flint, 1965) of the Mauch Chunk (Greenbrier) Formation, a white limestone 3 m (10 ft) thick. The Deer Valley is separated from the subjacent Loyalhanna by a 6-in (15-cm) red siltstone (not shown at the scale of figure 18). The Deer Valley differs from the underlying Loyalhanna in that the former is wavy bedded, rather than crossbedded, and lacks the quartz sand that characterizes the Loyalhanna.

Furthermore, the Deer Valley Limestone contains a more abundant, although low diversity, brachiopod fauna. The Deer Valley is composed of a peloidal lime packstone-grainstone carbonate sand. Many of the carbonate grains are ooids and intraclasts.

The Deer Valley depositional basin is largely confined to northern West Virginia and Maryland. It extends only slightly into Pennsylvania and feathers out only a short distance to the north of this location (Brezinski, 1989c), whereas the Loyalhanna extends much farther north and west. In southern Garrett County, Md., the Deer Valley Member interfingers with dark-gray limestone contained within the Loyalhanna Member of the Greenbrier Formation, attesting to at least partial contemporaneity of the two units.

Overlying the Deer Valley Limestone Member is an interval ranging in thickness from 15 to 70 m (49–230 ft) of red and green clastics. Brezinski (1989b) named this unit the Savage Dam Member of the Greenbrier Formation. In Pennsylvania this interval is considered the basal part of the Mauch Chunk Formation, although it can only be recognized where it separates the Deer Valley and (or) Loyalhanna from the overlying Wymps Gap Limestone Member. White cross-bedded sandstone, calcareous red and green siltstone and silty shale, and thin, fossiliferous limestone intervals, especially near the top of the member, characterize the Savage Dam Member. These marine lithologies are interbedded with red-brown siltstone, shale, and mudstone that are commonly mud-cracked and contain pedogenic surfaces. The alternation of marine and nonmarine lithologies led Brezinski (1989c) to contend that these strata were deposited during a number of short-lived sea-level cycles. As many as six marine-nonmarine cycles can be recognized within the Savage Dam Member (Brezinski, 1989c).

Depositional Environments

The depositional origin of the Loyalhanna has been debated for some time. Although the large-scale crossbedded foresets are suggestive of an eolian depositional setting, the abundant ooids, intraclasts, fossils, and fossil fragments, intertonguing with marine carbonates, basin geometry, and interpreted shallowing-up facies in presumed nearshore facies indicate a shallow marine origin for the unit. In contrast, Ahlbrandt (1995) presented compelling evidence indicating that the Loyalhanna is eolian.

The Deer Valley represents a submarine sand shoal environment that submerged a small area of southern Somerset County, Pa., and Garrett County, Md. It represents a distinct

depositional episode from the Loyalhanna as indicated by the red siltstone that invariably separates the Deer Valley from the Loyalhanna. The cyclic marine and nonmarine lithologies that characterize the Savage Dam Member were deposited in a peritidal setting, with shallow marine sandstone and shale forming during short-lived marine transgressions, and tidal flat, rooted mudstone forming during periods of shallowing. Brezinski (1989c) interpreted these shallowing episodes as representing fifth-order cycles.

Paleoclimate

The Loyalhanna Limestone Member can be traced from as far as northeastern Pennsylvania to south-central West Virginia (figs. 19, 20). According to Ahlbrandt (1995), the Loyalhanna is an eolianite, as evidenced by sand sheets, sand flow toes, inverse graded bedding, dissipation structures, and wind ripples. The presence of eolian abraded conodonts of Late Devonian to Early Mississippian age support an eolian interpretation (pl. 1). In contrast, the many occurrences of complete, articulated, and identifiable benthic macrofauna argue for normal marine conditions. This would be in keeping with most earlier interpretations that have suggested a high-energy marine environment of deposition. However, such widespread high-energy conditions are difficult to explain. If the Loyalhanna is an eolianite, then the basin-scale distribution of this sand sea attests to aridity during a lowstand of sea level during the Late Mississippian when eastern North America was approximately 15° south of the paleoequator (fig. 7). These arid conditions contrast sharply with the humid to subhumid conditions of the Late Devonian and Early Mississippian (Stop 11) and the long-term perhumid climate of the Early and early Middle Pennsylvanian (see fig. 10).

A long-term period of aridity to semi-aridity, developed in the Mississippian during the late Kinderhookian, was most severe during the Osagean (evidenced by evaporites from Nova Scotia through the midcontinent of the United States), and continued through the Meramecian before beginning to diminish in the late Chesterian. This long-term period of aridity was coincident with general long-term Mississippian greenhouse conditions (Frakes and others, 1992). Deposition of the Loyalhanna, however, appears to be related to short- to intermediate-term (fourth-order) climate forcing mechanisms. Following deposition of the Loyalhanna and Deer Valley Members, fluvial influxes of siliciclastic sediments in the latest Mississippian foretell the onset of increases in rainfall, sea-level fall, and global climate change associated with the development of ice house conditions.
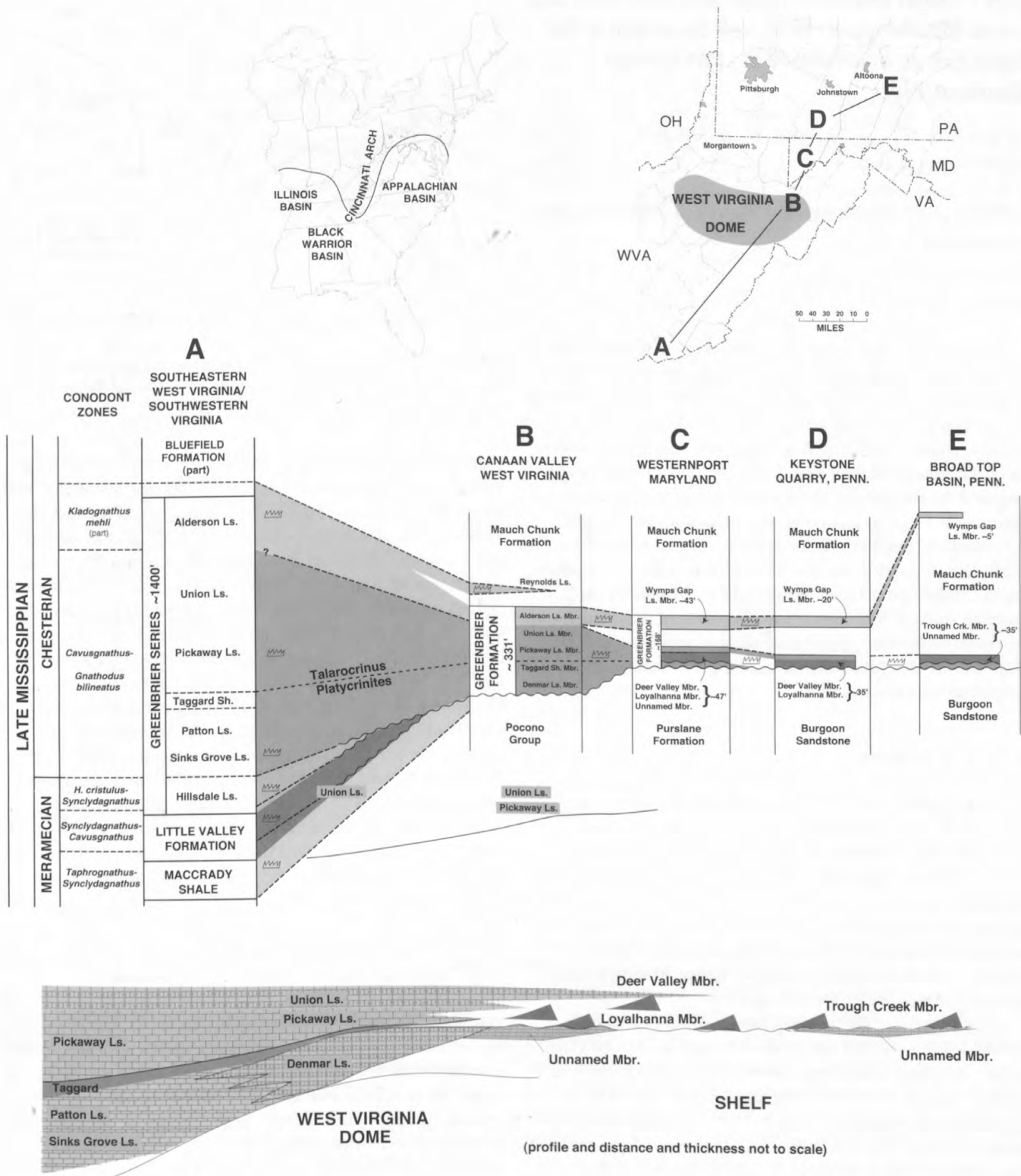
Figure 20. Conodont biostratigraphy and correlations of Greenbrier age strata from southeastern West Virginia/southwestern Virginia to south-central Pennsylvania.

Stop 7. Upper Devonian Hampshire Formation and Lower Mississippian Rockwell Formation at the Finzel Exit on Interstate 68 at Little Savage Mountain, Md.

Lat 39°40.95' N., long 78°58.44' W., Frostburg, Md., 7.5-minute quadrangle.

Leaders: Dave Brezinski, Rob Stamm, Vik Skema, and Blaine Cecil

Introduction

The stratigraphic sequence exposed in the highway cut through Little Savage Mountain comprises the upper Hampshire and lower Rockwell Formations (Upper Devonian-Lower Mississippian). The Rockwell succession here is part of a regional, paralic lithosome that records the ultimate foundering of the Catskill delta during latest Devonian (Famennian) time, and the subsequent evolution of an Early Mississippian (Tournaisian) coastal plain that was alternately submergent and emergent (Beuthin, 1986a–c; Bjerstedt and Kammer, 1988). Our discussion focuses on sedimentologic and stratigraphic evidence for Late Devonian-Early Mississippian shoreline shifts in this area, the implications of these shifts for placement of the Devonian-Mississippian boundary, and the relation of the Rockwell marine zones to Famennian-Tournaisian eustatic events.

Lithostratigraphy

Data for the Finzel outcrop presented herein are compiled mostly from measured sections of the Hampshire-Rockwell sequence made by Dennison and Jolley (1979), Beuthin (1986a), Bjerstedt (1986a), and Brezinski (1989a). Regionally, the Hampshire-Rockwell contact is placed at the horizon where the predominantly red strata of the Hampshire pass upward into predominantly green and gray strata of the lower Rockwell. At Finzel, the color change is abrupt, making the formational contact easy to pick.

The uppermost Hampshire consists of thin- to thickly interbedded, grayish-red mudstone, siltstone, shale, and fine-grained sandstone with sharp, convex-down bases as well as a few thin beds of green sandstone and siltstone. Many of the red beds have abundant root impressions, and pedogenic slickensides appear to be weakly developed in some of the mudstones. These strata were deposited on the Catskill deltaic-alluvial plain, mostly by aggradational overbank processes.

The Rockwell is 67 m (220 ft) thick here, but it ranges from 0 to 120+ m (0–400+ ft) in the Maryland-Pennsylvania-West Virginia tristate area (fig. 21). The basal 21 m (69 ft) of the Rockwell at Finzel constitutes a marine zone that records the final transgression over the Catskill coastal plain in this
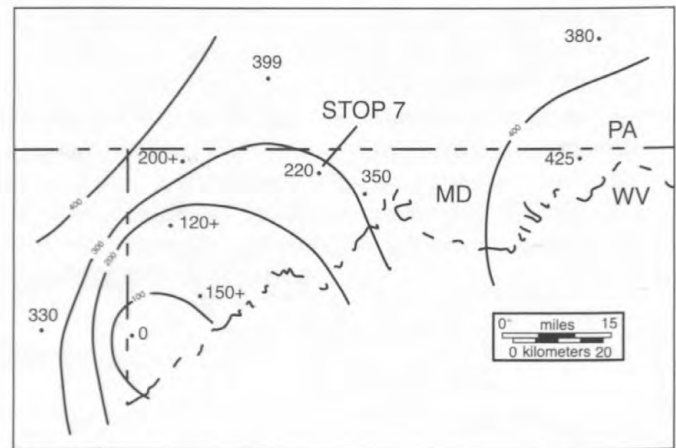
Figure 21. Isopach map of the Rockwell Formation in the Maryland-Pennsylvania-West Virginia tristate area. From Brezinski (1989a). Contour interval is 100 ft.

part of Maryland (fig. 22). Dennison and others (1986) informally termed this marine zone the "Finzel marine tongue" and correlated it with the marine Oswayo Formation of western Pennsylvania and the black Cleveland Shale of Ohio. Bjerstedt and Kammer (1988) and Brezinski (1989a,b) also have equated this marine zone with the Oswayo Formation of northwestern Pennsylvania. The Finzel tongue (Oswayo) also correlates with the "upper sandy zone" of the Venango Formation that crops out in the Conemaugh Gorge through Laurel Mountain, Pa. The "Venango upper sandy zone" in the Conemaugh Gorge was reported and described by Harper and Laughrey (1989) and Laughrey and others (1989). Although various names have been used for the basal Rockwell marine zone, this body of strata is a lithologically distinctive and mappable lithostratigraphic unit throughout western Maryland and Somerset County, Pa. (Beuthin, 1986a). At some locations in western Maryland, the basal beds of the Oswayo transgression are intercalated with red alluvial-plain strata of the Hampshire (fig. 23). Along the Allegheny Front, the Oswayo marine zone grades into coeval Hampshire red strata, so that at Sideling Hill (Stop 11) no Oswayo facies is evident.

The Oswayo marine zone at Finzel is a coarsening-upward (shoaling) sequence of intensely burrowed, green and gray shale, siltstone, and sandstone. The lower 9 m (30 ft) of the sequence consists mostly of gray to black silty shale interstratified with thin to medium beds of gray, fine-grained sandstone. Wave-ripples and ball-and-pillow structures are common in the sandstones. Fossils from throughout the basal 30 ft (9 m) of the marine zone include a *Planolites*-dominated assemblage of bedding-plane traces, and a low diversity shelly fauna of *Lingula, Camarotoechia*, and unspecified bivalves. Several distinctive, thick beds of *Scolithus*-burrowed, fine-grained, greenish-gray sandstone are interbedded with gray and green shale in the upper 12 m (40 ft) of the marine zone. Marine fossils are unknown from the upper part of the marine zone. Brezinski (1989b) inferred a shallow
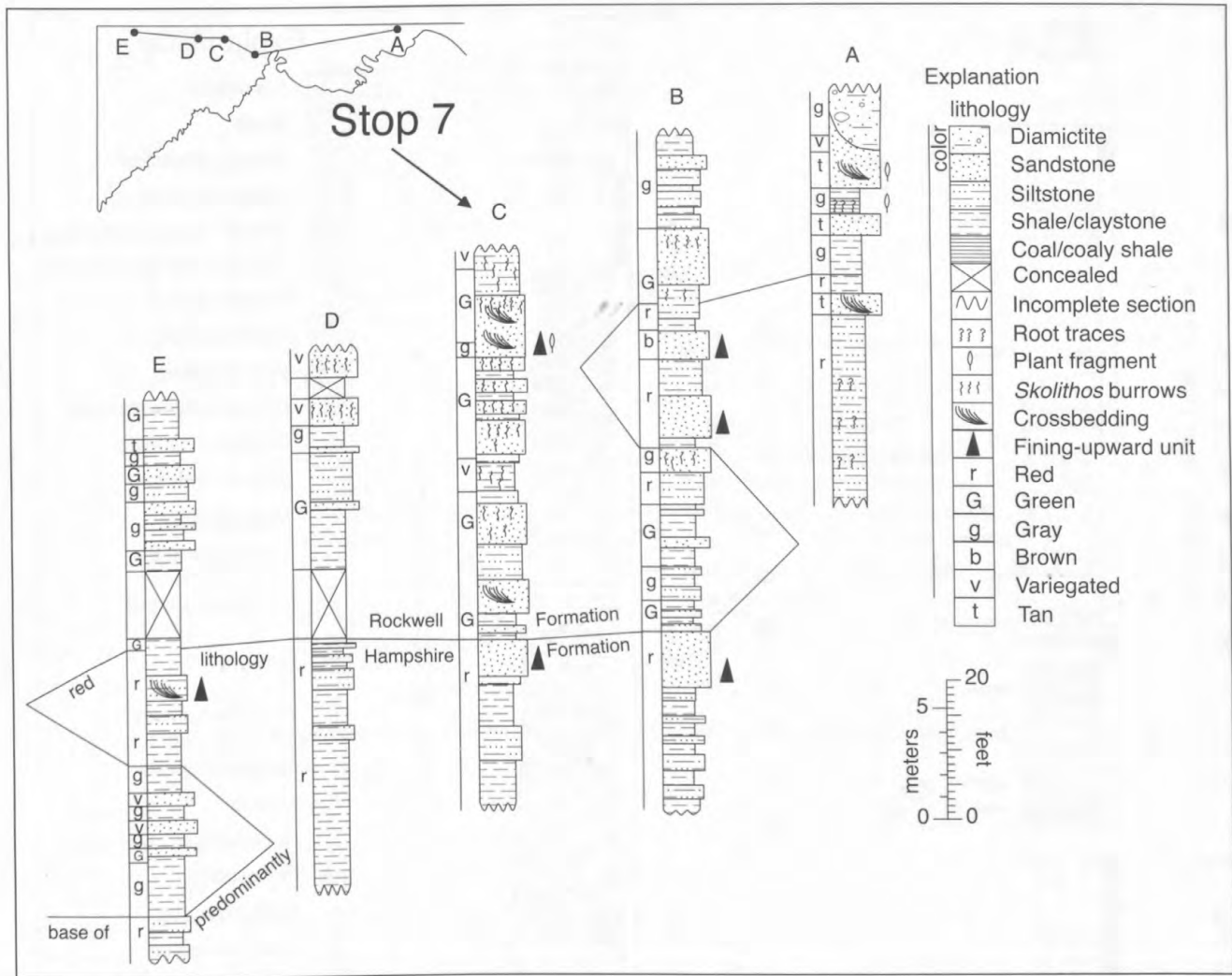
Figure 22. Intertonguing relation between the Devonian Hampshire and Rockwell Formations in western Maryland. From Brezinski (1989a).

shelf environment for the deposition of this marine zone at Finzel. Beuthin (1986a,b) and Bjerstedt and Kammer (1988) favored a restricted bay environment and interpreted the *Skolithos*-burrowed sandstones as the sand-bar complex of a prograding tidal or bayhead delta.

A 115-ft (35-m)-thick interval of lenticular, greenish-gray sandstone and reddish-brown and greenish-gray siltstone and shale overlie the Oswayo marine zone at Finzel. The sandstones exhibit erosional bases, shale-pebble basal conglomerates, crossbedding, and fining-upward texture. These beds probably were deposited on a prograding alluvial plain concomitantly with Oswayo regression (Brezinski, 1989b). Just west of Finzel, the middle nonmarine zone of the Rockwell Formation is punctuated by a thin marine unit that Dennison and others (1986) equated with the Bedford Shale of eastern Ohio. The "Cussewago equivalent" (lower Murrysville sandstone), exposed in the Conemaugh River

gorge through Laurel Mountain (Harper and Laughrey, 1989; Laughrey and others, 1989), is probably equivalent to the middle nonmarine zone of the Rockwell Formation at Finzel.

A second Rockwell marine unit overlies the nonmarine Rockwell facies at Finzel. Although it is not well exposed, this upper marine zone is represented by a tan, fine-grained, medium-bedded, bioturbated sandstone. This sandstone is lithologically recognizable at other Rockwell exposures in western Maryland and adjacent Pennsylvania. This marine sandstone is correlative with the Riddlesburg Member of the Rockwell Formation in the Broad Top synclinorium of Pennsylvania (Bjerstedt and Kammer, 1988; Brezinski, 1989a,b), and exposures from the Conemaugh River gorge through Laurel Mountain (Harper and Laughrey, 1989; Laughrey and others, 1989). Throughout most of western Maryland, littoral sandstones rather than black, silty lagoonal shales, as in the Broad Top region of Pennsylvania, represent the Riddlesburg trans-
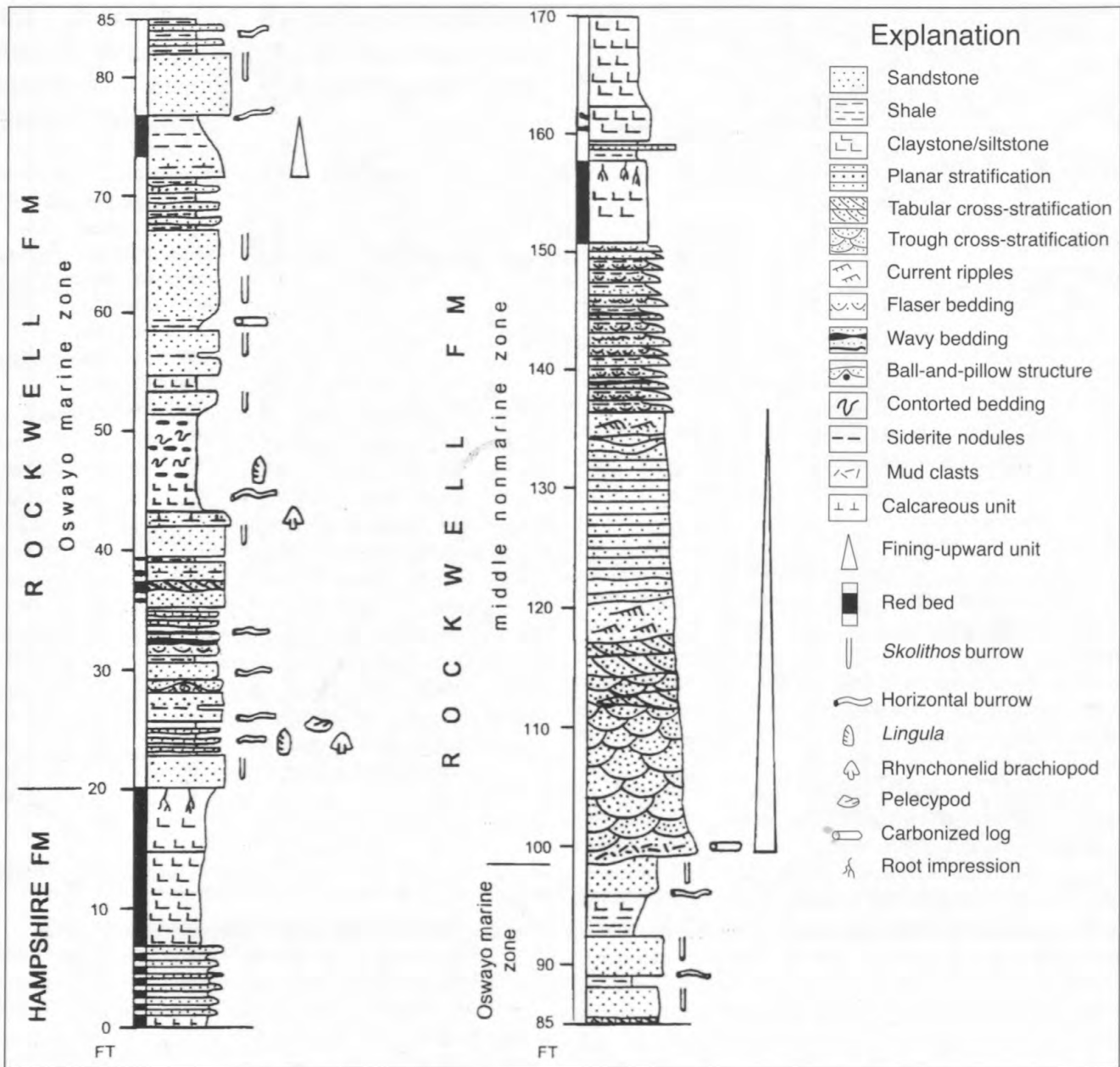
Figure 23. Measured section of upper Hampshire Formation and lower Rockwell Formation along Interstate 68 at Finzel Road interchange, Garrett County, Maryland. Section is based on exposure along eastbound entry ramp.

gression. However, a black-shale facies of the Riddlesburg marine zone has been reported about 24 mi (39 km) southeast of Finzel at Altamont, Md. (Beuthin, 1986a).

The Riddlesburg sandstone facies is exposed on the north side of I-68 at Finzel. The remaining Rockwell and overlying Purslane Formation are not exposed at this stop.

Devonian-Mississippian Contact

As concerns the Devonian-Mississippian boundary in the central Appalachians, Harper and Laughrey (1989) stated that

"the exact placement of this boundary is still up for grabs and should provide some interesting discussion during this field conference." Their words are no less true for the present field trip.

Using brachiopod species considered to be index fossils, Kammer and Bjerstedt (1986) and Carter and Kammer (1990) correlated the Oswayo Member of the Price Formation of northern West Virginia with the Oswayo Formation of northwestern Pennsylvania. Those workers assigned a late Late Devonian age to the Oswayo of northern West Virginia (except for the uppermost portion) on the basis of fossil content. A Mississippian age for the Riddlesburg Member of the Rockwell Formation is generally supported by biostratigraphically significant fossils
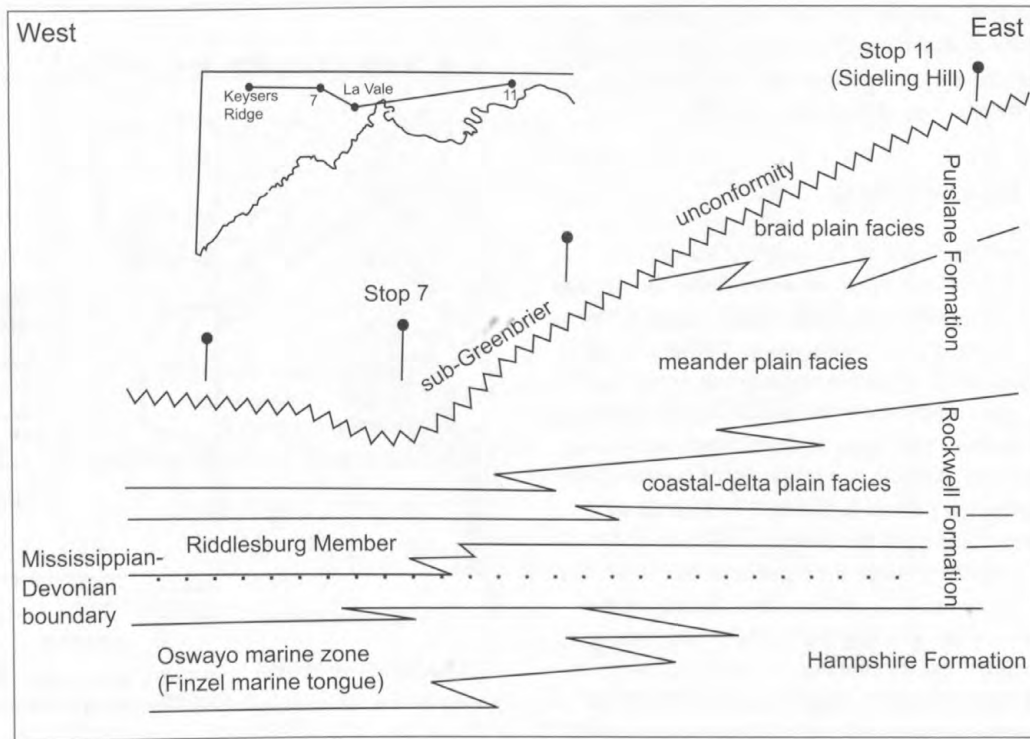
Figure 24. Environments of deposition within the Rockwell Formation of western Maryland. From Brezinski (1989b).

(Kammer and Bjerstedt, 1986). Furthermore, several recent studies (Dennison and others, 1986; Beuthin, 1986c; Bjerstedt, 1986b; Kammer and Bjerstedt, 1986; Bjerstedt and Kammer, 1988) have interpreted the Riddlesburg marine zone as an eastern facies equivalent of the Sunbury Shale of Ohio, which conventionally is assigned to the Lower Mississippian (Pepper and others, 1954; De Witt, 1970; Eames, 1974). On the basis of the aforementioned age determinations, the Devonian-Mississippian contact in western Maryland apparently falls within the interval comprising the uppermost Oswayo beds and the middle nonmarine zone of the Rockwell Formation (fig. 23).

Bjerstedt (1986b) and Bjerstedt and Kammer (1988) placed the base of the Mississippian System in West Virginia and Maryland at what they interpreted to be a regional unconformity that is equivalent to the interval of the Berea Sandstone of Ohio and subsurface deposits in West Virginia. This unconformity occurs at the base of the Riddlesburg Member of the Rockwell Formation at Sideling Hill, Town Hill, and La Vale, Md. At those locations the lower Riddlesburg consists of interbedded diamictite and crossbedded, light-gray sandstone. Lower Riddlesburg beds were deposited in shallow marine or shoreline settings that were quite likely highly erosive in nature. As a result, one would expect unconformable contacts

at the base of such units. Where these marine beds are absent, physical evidence of a "Berea-age" unconformity beneath the Riddlesburg is lacking. At Keysers Ridge, the Riddlesburg Member grades into the underlying strata, indicating apparent conformity. Consequently, deposition during the Devonian-Mississippian transition probably was continuous throughout much of western Maryland, and Berea equivalents are likely present, even through they may be represented by a more terrestrial facies than the type Berea in Ohio. Harper and Laughrey (1989) and Laughrey and others (1989) have reported a Berea equivalent (upper Murrysville sandstone) from the section exposed in the Conemaugh River gorge through Laurel Mountain. At Finzel, the top of the Oswayo marine zone (Finzel marine tongue) approximates the Devonian-Mississippian contact, although the contact probably occurs slightly higher in the overlying nonmarine interval (fig. 24). At Sideling Hill (Stop 11), the Devonian-Mississippian boundary is relatively closer to the Hampshire-Rockwell Formation contact because a diamictite and the overlying Riddlesburg Member occur near the base of the Rockwell.

The intertonguing nature of the Hampshire-Rockwell Formation contact, the eastward pinchout of the Oswayo marine zone, and apparent upsection migration of the contact

from west to east (fig. 24) indicate that the Hampshire-Rockwell transition is diachronous; therefore, this lithostratigraphic boundary cannot be equated with the Devonian-Mississippian systemic boundary across the region.

Depositional Environments

Figures 25 and 26 illustrate the relative sea-level changes in western Maryland and vicinity during the deposition of the Rockwell. Shaly beds of the basal Oswayo marine zone (Finzel marine tongue of Dennison and others, 1986) record the culmination of a late Famennian sea-level rise. The *Skolithos*-burrowed sandstones of the upper Finzel tongue and the crossbedded channel sandstones of the overlying nonmarine Rockwell interval indicate progradation of coarse clastics and shoreline regression during highstand. In Maryland, the sea-level drop associated with the Berea Sandstone of Ohio and West Virginia locally caused emergence above base level, sedimentary bypassing, and fluvial incision. Shortly thereafter, sea level rose again, causing the Riddlesburg transgression (fig. 25). Because the Riddlesburg extends farther east than the Oswayo marine zone, a larger rise in sea level is inferred for the former. Rockwell nonmarine beds overlying the Riddlesburg probably represent post-Riddlesburg highstand. Using microspore zonation of strata enclosing the Devonian-Mississippian boundary, Streel (1986) demonstrated the presence of two interregional transgressions on the Devonian Old Red Continent (Euramerica). The earlier of these two events was initiated during the late Famennian and is represented in Pennsylvania and Maryland by the Oswayo marine zone. The later transgression occurred during the early Tournaisian and corresponds to the Sunbury Shale of Ohio. Interregional correlations therefore strongly indicate that the Oswayo sea-level rise was eustatic. If, as inferred by Dennison and others (1986), Beuthin (1986c), and Bjerstedt and Kammer (1988), the Riddlesburg marine zone is an eastern facies equivalent of the Sunbury Shale (or a portion of it), then it also was probably eustatically controlled. Streel (1986) further suggested that the interregional late Famennian transgression was a glacioeustatic event. Caputo and Crowell (1985) and Veevers and Powell (1987) documented evidence for a mid-Famennian glacial episode in Brazil and adjacent (then) northwest Africa. Late Famennian waning of the Gondwana ice sheet perhaps was the major control on the Oswayo transgression. A glacioeustatic mechanism for the early Tournaisian (Sunbury) sea-level rise remains somewhat speculative because Early Mississippian glaciation on Gondwanaland is unresolved (Caputo and Crowell, 1985).

Paleoclimate

The paleoclimate in the Appalachian basin region during the Devonian-Mississippian transition is presented in the paleoclimate section for Stop 11.
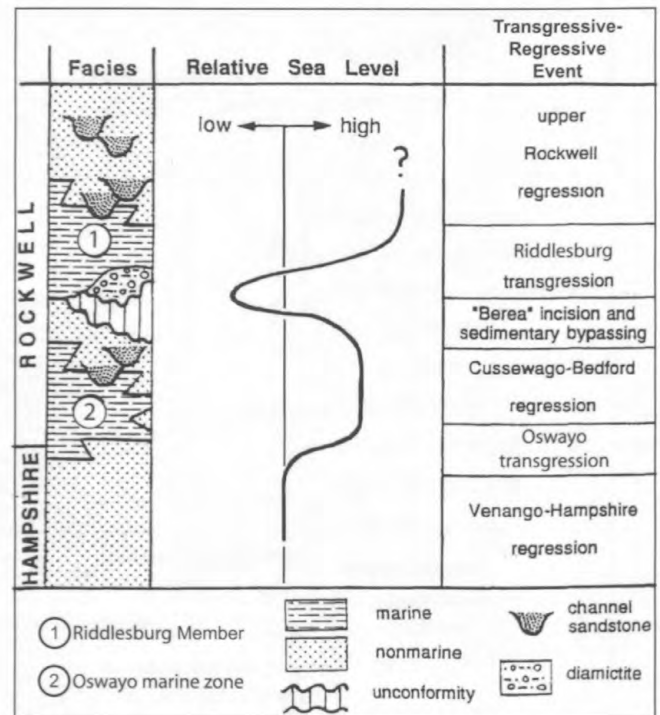
Figure 25. Relative sea-level curve for the Upper Devonian-Lower Mississippian (upper Famennian-lower Tournaisian) Rockwell Formation of western Maryland (based on Beuthin (1986a) with minor modifications). Curve does not indicate absolute magnitude, nor absolute duration of any sea-level event. Devonian-Mississippian transition probably occurred during the time-interval encompassing Cussewago-Bedford regression or "Berea" incision and sedimentary bypassing.

Stop 8. Upper Mississippian and Middle Pennsylvanian strata at the mid-Carboniferous unconformity on Interstate 68 at Big Savage Mountain, Frostburg, Md.

Lat 39°40.36' N., long 78°57.77' W., Frostburg, Md., 7.5-minute quadrangle.

Leaders: Blaine Cecil, Cortland Eble, and Rob Stamm

Introduction

The Upper Mississippian Mauch Chunk Formation and Middle Pennsylvanian Pottsville and Allegheny Formations are exposed in the I-68 roadcut at the top of Big Savage Mountain. The Mauch Chunk exposure is 56 m (184 ft) thick and the Pottsville and Allegheny exposures are 31 m (102 ft) and 27 m (88 ft) thick, respectively (fig. 27). The Mississippian-Pennsylvanian contact is unconformable. The laterally extensive units exposed at this locality, and their correlatives, occur throughout the central Appalachian basin.
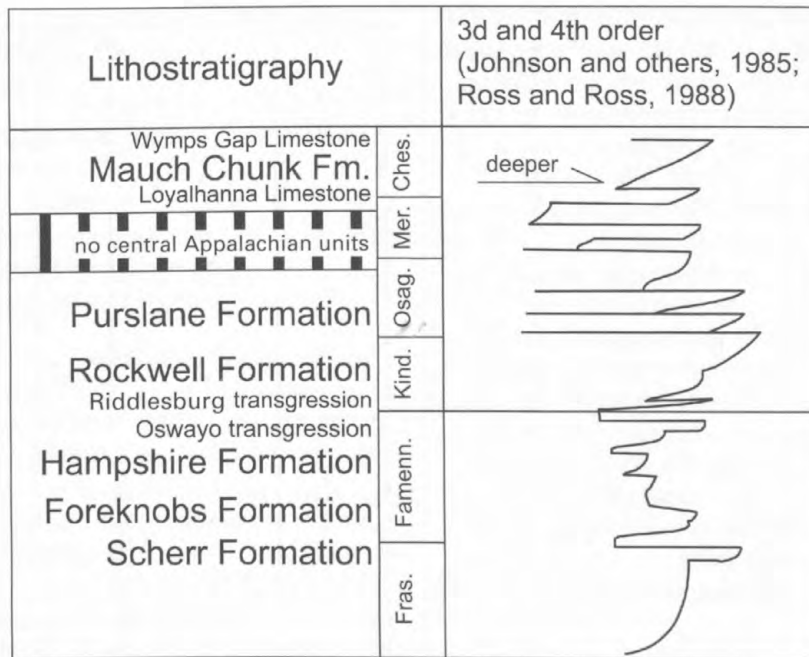
Figure 26. Third- and fourth-order global sea-level events of the Late Devonian and Early Mississippian (modified from Johnson and others (1985) and Ross and Ross (1988)), and corresponding lithologic units of the central Appalachians. Fras., Frasnian; Famenn., Famennian; Kind., Kinderhookian; Osag., Osagean; Mer., Meramecian; Ches., Chesterian.

Lithostratigraphy

The Mauch Chunk Formation in Maryland, approximately 170 m (560 ft) thick, extends from the top of the Wymps Gap (Alderson) Limestone Member of the Greenbrier Formation to the base of the Pottsville Formation (Brezinski, 1989b). The Mauch Chunk, as defined in adjacent Pennsylvania, extends from the base of the Loyalhanna Member (Stop 6) or any subjacent red beds to the base of the Pottsville. In southern West Virginia, the Mauch Chunk has group status and extends from the top of the Greenbrier Formation to the base of the Lower Pennsylvanian Pocohontas Formation. The Mauch Chunk Group in southern West Virginia includes the Bluefield, Hinton, and Bluestone Formations in ascending order. Collectively, these formations are over 2,500 m (8,200 ft) thick.

The Loyalhanna through Wymps Gap interval is a facies of the upper Greenbrier Limestone sequence to the south and west and the upper part of the Maxville Limestone of Ohio. The Mauch Chunk Formation correlates, in part, with the marginal marine Mauch Chunk Group of southern West Virginia and western Virginia and with the Bangor Limestone and Pennington Formation of Georgia, eastern Tennessee, and eastern Kentucky.

The unconformable Mississippian-Pennsylvanian boundary in western Maryland (White, 1891) is associated with the global mid-Carboniferous unconformity as discussed by Saunders and Ramsbottom (1986). At Stop 8, the Atokan-age base of the Pottsville Formation disconformably overlies the Chesterian-age Mauch Chunk Formation. This disconformity

is the result of a major eustatic sea-level drop in the Early Pennsylvanian (early Morrowan). Section from the late Chesterian to late Atokan is missing here within the disconformity because of erosion and (or) nondeposition. At this stop the disconformity is at a thin claystone (fig. 27). It is often difficult to separate the Mauch Chunk and Pottsville Formations in western Pennsylvania, Maryland, and northern West Virginia because it is often difficult to distinguish nonred Mauch Chunk sandstones from those of the Pottsville Formation. The last occurrence of red coloration is not a consistently reliable criterion to separate the two units (Edmunds and Eggleston, 1993).

The Pottsville Formation usually contains a large proportion of sandstone with lesser amounts of shale and mudstone as exposed in the rolling stop between Stops 4 and 5. Here at Stop 8, the Pottsville is primarily sandstone. The olive-gray coloration of the lower part of the sandstone is atypical, as the Pottsville is usually medium gray to light gray.

The thickness of the Pottsville in this area ranges from 18 m (59 ft) near the Maryland-Pennsylvania border 11 km (7 mi) to the northeast to 100 m (328 ft) near Kitzmiller, 35 km (22 mi) to the southwest (Waagé, 1950). Here, the Pottsville is relatively thin (32 m; 105 ft). If the Pottsville here at Stop 8 is equivalent to the upper part of the Kanawha Formation of southern West Virginia, it is late Atokan and early Desmoinesian in age.

Correlations of the Allegheny Formation coal beds and, therefore, the Pottsville-Allegheny boundary are those of Waagé (1950). His coal bed correlations were derived from
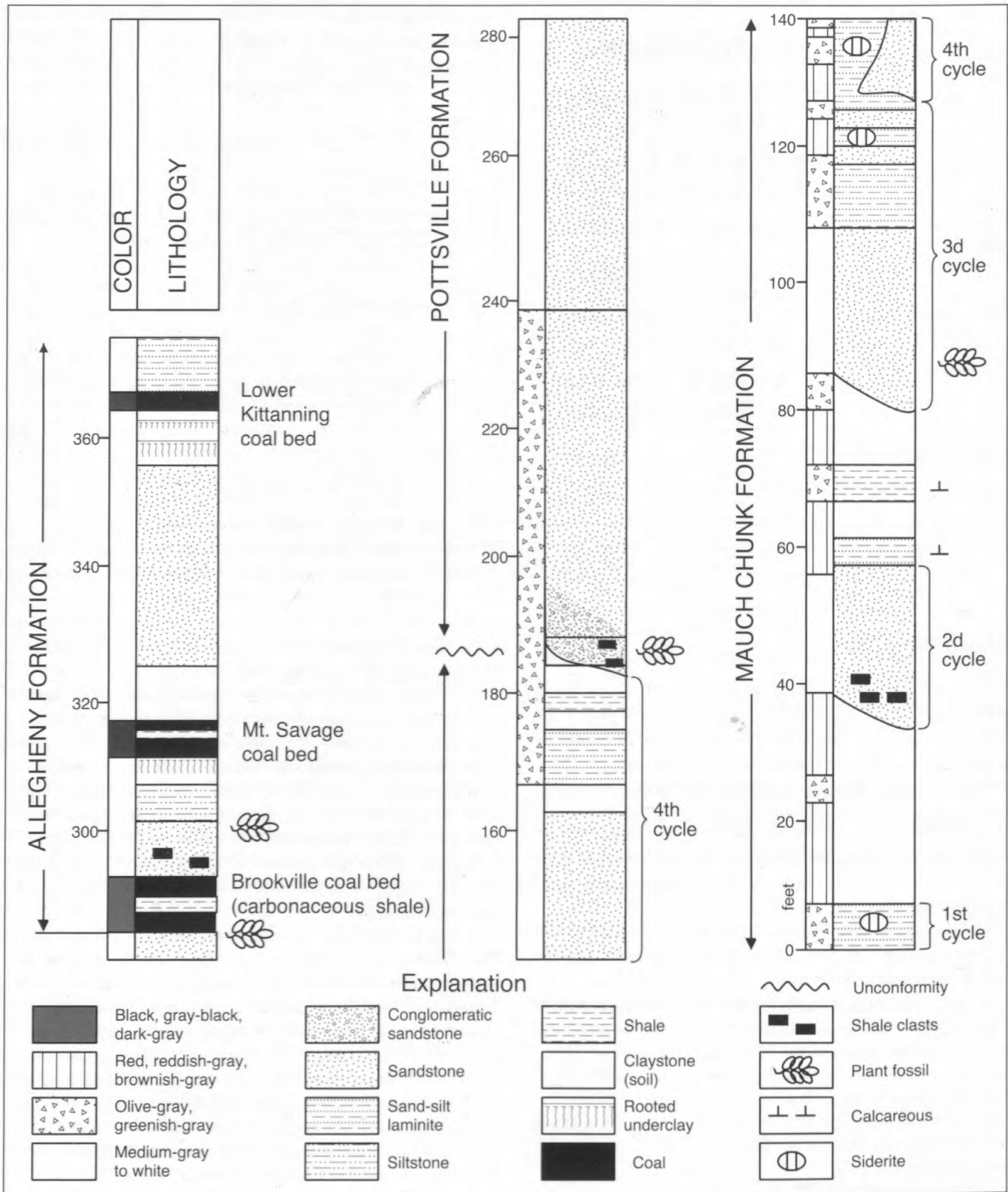
Figure 27. Interstate 68 roadcut at Big Savage Mountain, Md. Mauch Chunk Formation (west end of outcrop) through Pennsylvanian Allegheny Formation (east end of outcrop). Modified from Edmunds and Eggleston (1993).

many logs of long drill holes taken from the Conemaugh Formation to the Mauch Chunk Formation.

Pennsylvanian and Mississippian Depositional Environments

According to Edmunds and Eggleston (1993), the Mauch Chunk Formation exposed at Stop 8 was deposited in an upper-delta-plain setting. If so, then deposition was controlled by autocyclic processes.

Edmunds and Eggleston (1993) described the Mauch Chunk Formation in this area as a sequence of litharenite and sublitharenite sandstones (McBride, 1963) intercalated with mudstone and shale. Illite, mixed-layer clay, kaolinite, calcite, and siderite are common. Metamorphic and igneous rock fragments, and both potash feldspars and plagioclase are common. Grains appear to be angular, poorly sorted, and generally immature. Edmunds and Eggleston (1993) recognized four fining-upward cycles, which they interpreted as fluvial (fig. 27). Only the top of their lowest cycle is exposed. Their second cycle consists of a medium-gray, fine-grained sandstone with a scoured base and a basal lag gravel of shale clasts and caliche nodules. The second cycle culminates with reddish- and greenish-gray silty shale and hackly siltstone and claystone. Their third fluvial cycle grades upward from a medium-gray, fine-grained sandstone with an incised base containing a zone of preserved plant fragments into reddish- and greenish-gray sand-silt laminate and hackly silty shale and claystone. Their fourth fluvial cycle is medium-light-gray to pinkish-gray, fine-grained sandstone with a scoured base. The lower part of the sandstone also grades laterally into upper part of the hackly shale and siltstone of the underlying cycle. They interpret this sequence as a distributary building across and into the terminal fine-grained clastics of the previous cycle. The sandstone passes upward into medium-gray and olive-gray interbedded hackly shale and fine-grained sandstone. The upper part of the fourth cycle is truncated by the sub-Pottsville erosion surface.

The Mauch Chunk at Stop 8 also contains calcic paleosols of unknown lateral extent. These paleosols are indicative of a drop in the paleo water-table, which generally is the result of a drop in base level or a decrease in rainfall, both of which are allocyclic processes.

Edmunds and Eggleston (1993) interpret the Pottsville Formation here as a high-energy fluvial-alluvial deposit. They suggested that the olive color of the lower of the Pottsville sandstone reflects the high content of clay altered from rock fragments. This olive color, however, is the result of modern weathering of syngenetic or early diagenetic pyrite, probably the opaque minerals noted in Edmunds and Eggleston (1993). The pyrite is the result of reducing conditions and relatively high sulfate concentrations at the time of deposition. The source of the sulfate for the pyrite was from either marine waters or high dissolved solids in fluvial systems. We suggest that the sulfate was derived from marine water in what may

have been an estuarine setting. In contrast to the Mauch Chunk, the Pottsville Formation here consists of coarse-grained quartz arenite and sublitharenite. Clay minerals are generally less abundant than in the Mauch Chunk; feldspar and calcite are generally absent.

Edmunds and Eggleston (1993) attributed deposition of the clastics and coal beds within the Allegheny Formation to autocyclic delta plain depositional processes. It seems clear, however, that allocyclic processes were the primary controls on sedimentation and stratigraphy (Cecil and others, 2003b). Basin and interbasin scale paleosols (underclays and coal beds) clearly document lowstands of sea level and major fluctuations of the water table. The apparent lack of marine or brackish fossils and the general coarseness of the clastics noted by Edmunds and Eggleston (1993) is part of a facies mosaic within highstand deposits. Eastern or proximal facies along the eastern outcrop belt are of probable deltaic origin whereas distal facies in western Pennsylvania, West Virginia, and Ohio contain marine or brackish water deposits.

Paleoclimate

On the basis of the occurrence of calcic paleosols, calcic nodules as channel lags in paleostream channels, and the textural and mineralogical maturity of the sandstones, the paleoclimate of the Late Mississippian must have been semiarid to dry subhumid. Unaltered feldspar, illite, and mixed layered clays in Mauch Chunk sandstones are a good indication of limited chemical weathering in the source area and a relatively dry paleoclimate. Syngenetic and early diagenetic calcite is a further indication of a high dissolved solids content in fluvial systems. In contrast, Pottsville sandstones contain mostly quartz that is texturally immature. The absence of feldspar, mixed layered clays, and illite, and the texturally immature quartz are indicative of chemical weathering in a humid climatic regime. The absence of syngenetic and early diagenetic calcite in Pottsville sandstones is indicative of fluvial systems that were low in dissolved solids, which is consistent with a leached source area regolith that was deeply weathered under a humid tropical climate. This stop illustrates the production of quartz arenites through humid tropical weathering, in contrast to Stops 9 and 12 where the quartz arenites appear to be the product of mechanical weathering under an arid or semi-arid tropical climate. This stop further indicates the change in rainfall patterns from the relatively dry conditions of the Late Mississippian to the humid conditions of the Early and Middle Pennsylvanian.

Although the Mississippian unconformity is erosional at Stop 8, residual weathering deposits commonly are developed on Mississippian and older strata (see Stop 5 discussion). In the Appalachian basin, these deposits consist of high-alumina clays, such as the Mercer clay in Pennsylvania and the Olive Hill clay in Kentucky. On the margins of the Ozark dome, residual deposits include the Cheltenham clay and unnamed chert residuum in the tristate district of Kansas, Missouri, and

Oklahoma. These residual deposits resulted from humid tropi-
cal weathering on topographic highs mainly during the Early
and earliest Middle Pennsylvanian. They were subsequently
buried by onlap of Middle Pennsylvanian strata in response to
eustatic sea-level rise as the long-term ice house world of the
mid-Carboniferous waned.

Stop 9. Upper Ordovician Juniata Formation and Lower Silurian Tuscarora Sandstone at Wills Creek Water Gap, Cumberland, Md.

Lat 39°39.75′ N., long 78°46.81′ W., Cumberland, Md.,
7.5-minute quadrangle.

Leaders: Dave Brezinski, John Repetski, and Blaine
Cecil

Introduction

The Upper Ordovician Juniata and Lower Silurian
Tuscarora Formations are exposed in the Wills Creek Water
Gap, Wills Mountain anticline, Cumberland, Md. The accom-
modation space and sediment supply for the underlying
Middle Ordovician Martinsburg Formation, the Upper
Ordovician Juniata Formation, and the basal Silurian
Tuscarora Sandstone are generally thought to be the result of
the Taconic orogeny when an island arc or microcontinent
collided with eastern Laurentia (Drake and others, 1989).
According to the tectonic model, clastics for these units were
supplied from mountains created by the Taconic orogeny.

The Lower Silurian Tuscarora Sandstone is a major ridge
former in the Appalachian Valley and Ridge physiographic
province and, here, the Tuscarora is exposed on the west limb
of the Wills Mountain anticline. The Tuscarora and equivalent
sandstone strata extend from central New York (Medina
Group) through Pennsylvania, Ohio ("Clinton sandstone"),
Maryland, West Virginia, Virginia, and Kentucky to the
Valley and Ridge in northeast Tennessee (Clinch Sandstone).

Lithostratigraphy

The Upper Ordovician Juniata Formation, which is
approximately 600 ft (183 m) thick at this locality
(Dennison, 1982), consists primarily of red lithic wacke
interbedded with dark-red mudstone. In Pennsylvania, the
Juniata is subdivided into three members on the basis of dif-
ferences in the relative proportions of sandstone and mud-
stone (summarized in Cotter, 1993). In the lowest member,
laterally extensive sheet-like sandstones dominate over the
mudstones and the sandstones. The middle member contains
more mudstone beds than sandstone beds. The upper member
contains more sandstone beds than mudstone beds (Cotter,
1993 and references therein). In central Pennsylvania, up to

1,200 ft (366 m) of nonmarine gray and red sandstone and
conglomerate of the Bald Eagle Formation intervenes strati-
graphically between the Martinsburg Formation (or the equiv-
alent Reedsville Formation) and the Juniata Formation
(Thompson, 1999). The Bald Eagle Formation thins rapidly in
south-central Pennsylvania and is very thin and only locally
present in Maryland. The lower contact is generally placed at
the first occurrence of red beds at the top of the underlying
marine Martinsburg Formation (Cotter, 1993). Where the
Bald Eagle Formation is present, it is placed at the first per-
sistent occurrence of red beds. The upper contact is placed
where quartz arenite defines the base of the overlying
Tuscarora Sandstone (Cotter, 1983).

In contrast to the underlying Juniata, the Tuscarora pri-
marily is a quartz arenite. In New York, strata equivalent to
the Tuscarora are referred to as the Medina Group, and in
eastern Pennsylvania equivalent strata are referred to as the
Shawangunk Conglomerate (Thompson and Sevon, 1982).

Depositional Environments

Depositional environment interpretations of the Juniata
and Tuscarora Formations presented herein are based primari-
ly on the summaries by Cotter (1983, 1993) and references
therein. According to Cotter (1993), the Juniata Formation
was deposited in a lower alluvial plain setting, and the lower
and upper sandstone members were deposited by braided
streams. The medial member, however, may have been the
result of a glacioeustatic-induced transgression toward the
southeast with deposition occurring in a paralic, coastal, or
lower delta plain setting (Dennison, 1976). Allocyclic
changes in sea level, therefore, may have been the dominant
control on accommodation space and the depositional envi-
ronments of the three members of the Juniata.

Many of the mudstones in the Juniata are paleosols
(Retallack, 1993). According to Retallack (1993), calcic pale-
osols formed on stream terraces and along alluvial fan
streams. According to these interpretations, the Juniata pale-
osols are autocyclic in origin and not the result of allocyclic
fluctuations in sea level.

The origin of the Lower Silurian Tuscarora Sandstone
remains enigmatic. Cotter (1983) summarized earlier work and
presented his own comprehensive sedimentological analyses
of the Tuscarora in Pennsylvania. He suggested that the
Tuscarora was the result of an Early Silurian transgressive
event and renewed tectonic elevation of the Taconic terrane.
He divided the Tuscarora into five regional and stratigraphic
lithofacies. "Lithofacies one," his eastern cross-laminated
lithofacies, was attributed to braided stream deposition.
"Lithofacies two," his western cross-laminated lithofaces, was
deposited in a marine-shelf sand wave and shoreface-connect-
ed sand ridge environment. Cotter noted that sand grains in
"lithofacies two" were well rounded. "Lithofacies three," his
basal horizontal laminated facies, was deposited in foreshore
and shoreface environments; quartz grains in this lithofacies

also are well rounded. "Lithofacies four," basal pink transitional lithofacies, was deposited in paralic conditions. Texturally mature grains also were noted in this lithofacies in contrast to the lithic arenites of the underlying Juniata. "Lithofacies five," the uppermost part of the Tuscarora, is the red Cacapon Sandstone Member in West Virginia and Maryland (Castanea Member in Pennsylvania), which he suggested was deposited in a low-energy coastal flat complex that prograded over the underlying quartz arenite facies during regression. The Cacapon Sandstone Member is intensely burrowed locally, and it is composed primarily of rounded quartz sand grains in a hematitic matrix (C.B. Cecil, unpub. data).

Paleoclimates of the Late Ordovician and Early Silurian

On the basis of carbonate occurrence and other paleosol features in the Juniata Formation, Retallack (1993) suggested that the climate of the Late Ordovician was semiarid and that annual rainfall, although limited, was seasonal. This interpretation is consistent with the presence of braided stream deposits in the upper and lower members. However, Late Ordovician sea-level oscillations, controlled by advance and retreat of ice sheets in what is now North Africa (Dennison, 1976), must have been accompanied by global climate change. Given a paleolatitude of approximately 30° south for the Appalachian basin in Late Ordovician time, the amount and seasonality of annual rainfall was the predominant form of climate change. Such changes in rainfall patterns could account for the variation in sediment supply within and among members of the Juniata. The braided stream sheet sands of the upper and lower members of the Juniata may represent increased sediment supply whenever the climate shifted from semiarid toward dry subhumid conditions. In an alluvial plain setting, the return from dry subhumid to semiarid conditions would favor a reduction in sediment supply, deposition of finer grained material, and a lowering of the water table resulting in conditions necessary for soil development.

The change in lithology from the immature red wacke sand of the Juniata to the mature quartz arenite of the Tuscarora and equivalent strata remains problematic. Most interpretations attribute the textural and mineralogical maturity of the Tuscarora to marine depositional processes (for example, Cotter, 1983). However, an eolian mechanism for winnowing and rounding of grains is far more likely because, unlike gravel and cobbles, sand is far more susceptible to rounding under eolian conditions than in aqueous environments (for example, Kuenen, 1960). It appears, therefore, that the Tuscarora was derived from a mature eolian regolith that consisted primarily of quartz.

Dennison and Head (1975) and Brett and others (1995) recognized an unconformity at the contact between Upper Ordovician and Lower Silurian strata that extends from Ontario southward through the central Appalachian basin. This regional unconformity (Cherokee unconformity of Dennison

and Head, 1975) separates the immature lithic sand and mudstone of the Upper Ordovician from quartz arenite of the Lower Silurian. It is highly probable that a mature eolian regolith developed on the exposed surface as a result of eolian mechanical weathering and winnowing, given the long-term semiarid to arid conditions of the latest Ordovician and earliest Silurian. Although there appears to be some fluvial deposition along the eastern outcrop belt, most workers believe that the Tuscarora was deposited under marine conditions during transgression (for example, Cotter, 1983). Reworking of texturally and mineralogically mature eolian materials by marine transgressive processes appears to account for the lithology and the widespread distribution of the Tuscarora and equivalent strata over the Cherokee unconformity.

Stop 10. Silurian strata of the Wills Creek and Tonoloway Formations on Interstate 68.

Lat 39°41.48' N., long 78°39.37' W., Evitts Creek, Md., 7.5-minute quadrangle.

Leaders: Dave Brezinski, John Repetski, and Blaine Cecil

Introduction

The Late Silurian tidal flat facies of the Wills Creek and Tonoloway Formations is exposed along the south side of I-68 at this stop. The section exposed at this stop includes (from bottom to top) the upper Rose Hill Formation, Keefer Sandstone, McKenzie Formation, including the Rochester Shale Member at the base, followed by the Wills Creek Formation and, finally, the Tonoloway Formation. The Bloomsburg Formation is not exposed. We will concentrate on the upper part of the section, which is Late Silurian in age (fig. 28).

Lithostratigraphy

The upper part of the section begins along the ramp of eastbound I-68 within the basal strata of the Tonoloway Formation. Although the Tonoloway is more than 120 m (390 ft) thick, only about 3 m (10 ft) of this unit is exposed at this location. The Tonoloway consists of thinly bedded to thinly laminated shaly limestone. The formation characteristically weathers into tan, platy and shaly chips. The only fauna known from this part of the Tonoloway are leperditiid ostracodes, eurypterids, and a low diversity conodont association. Some of the platy limestone chips exhibit casts of gypsum and halite crystals. Westward (downsection), the strata become increasingly shaly. With this increase in siliciclastics the laminated Tonoloway passes into the underlying Wills Creek Formation. The Wills Creek is characterized by thin- to medium-bedded, gray-green to tan weathering, calcareous shale and laminated silty dolomite. The formation contains
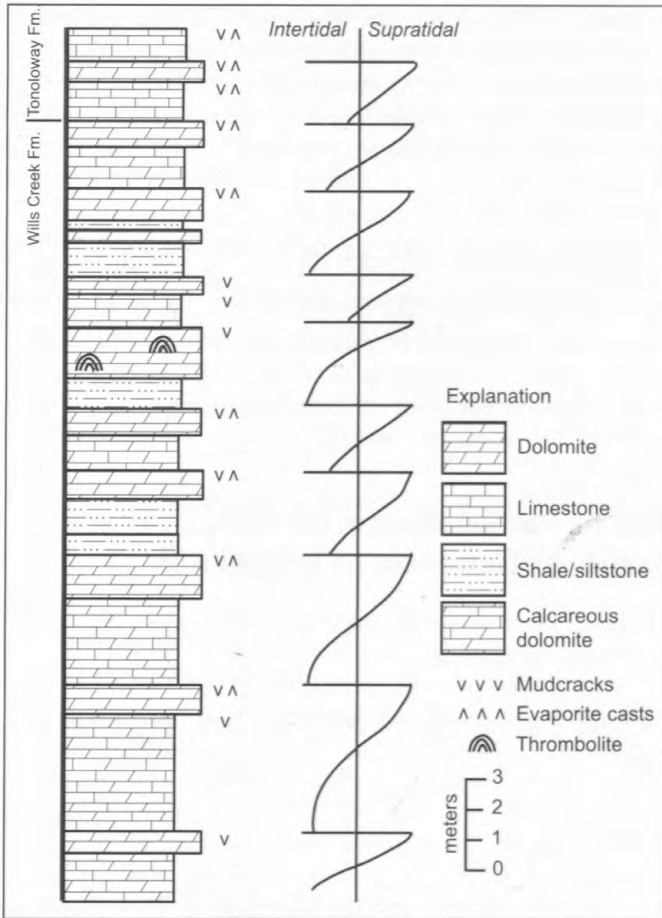
Figure 28. Stratigraphic section exposed at Stop 10 of the upper Wills Creek and basal Tonoloway Formations and their interpreted depositional environments.

horizons of desiccation cracks and domal stromatolites. Halite and gypsum casts also are common in some intervals near the top of the formation. The Wills Creek Formation is approximately 150 m (490 ft) thick in this area (Swartz, 1923). It is correlative with the salt beds of the Salina Formation that occur in the subsurface to the west in Pennsylvania and West Virginia, and to the north in New York (Allings and Briggs, 1961; Smosna and Patchen, 1978).

Along Md. 144, the Wills Creek strata seen on the north side of I-68 also are exposed. Here the alternating shale-dolomite couplets that characterize the Wills Creek Formation can be observed (fig. 29).

Depositional Environments

During the Late Silurian much of the Appalachian basin became a restricted salt basin. The greatest thickness of salts (halite and anhydrite) was formed in an elongate basin stretching from northern West Virginia through western Pennsylvania into western New York (Allings and Briggs, 1961; Smosna and Patchen, 1978) (fig. 30). Along the eastern margin of this salt basin, extensive supratidal mud flats and

sabkhas formed. It was on these mud flats that the peritidal lithologies of the Wills Creek and Tonoloway Formations were deposited. The regional extent of these peritidal units documents basin-scale tidal sedimentation. The shaly component of these formations appears to have been the result of either of the following: (1) the distal facies of a Silurian clastic wedge that formed to the east and resulted in the deposition of the Bloomsburg Formation or (2) the result of eolian (dust) deposition as suggested by Grabau (1932, p. 569) for equivalent strata in New York. The great thickness of mud flat lithologies records a large number of small-scale (fifth-order?) shallowing cycles (fig. 29). Rarely are any subtidal lithologies preserved within these cycles, indicating that most of the deposition occurred within the intertidal and supratidal setting. Indeed, the preponderance of evaporite casts in some horizons attest to the supratidal salt flat (sabkha) environment of deposition.

The shaly evaporite flats persisted through most of the Late Silurian with the deposition of the Tonoloway Formation. During the latest Silurian, the Appalachian basin was once again submerged with normal marine waters as a deepening seaway resulted in the deposition of the Keyser Formation as seen at Stop 12.

Late Silurian Paleoclimate

There is abundant evidence for long-term aridity in the Late Silurian in the Appalachian basin. It was during this time that extensive salt deposition was occurring in deeper parts of the basin and in the Michigan basin. The common evaporite casts are indicative of an arid climate as well as a supratidal, salt flat (sabkha) environment of deposition. The formations seen at this stop are regional in extent and record mixed tidal and eolian processes on the flat floor of a continental basin under arid climatic conditions. The general conditions of Late Silurian sea-level lowstand and coeval aridity suggest significant amounts of ice in high latitudes. If so, glacial-interglacial fluctuations would account for the intermediate-term sea-level fluctuations that are recorded at this stop.

Stop 11. Upper Devonian and Lower Mississippian strata on Interstate 68 at Sideling Hill, Md.

Lat 39°38.9′ N., long 79°50.0′ W., Bellegrove, Md., 7.5-minute quadrangle.

Leaders: Blaine Cecil, Dave Brezinski, Vik Skema, and Rob Stamm

Introduction

As the trip progresses eastward, Upper Devonian and Lower Mississippian strata are exposed in a syncline at

Figure 29. Shale-dolomite couplets and corresponding interpreted fifth-order sea-level events in the upper Wills Creek Formation along Md. 144 at Rocky Gap State Park, Md.

Sideling Hill, Md. At this stop we will examine the transition from the red alluvial plain deposition at the end of the Devonian to the coal-bearing strata of the Early Mississippian. Evidence for Late Devonian-Early Mississippian glacial conditions in the Appalachian basin is emphasized at this stop.

Lithostratigraphy

The roadcut through Sideling Hill exposes the Lower Mississippian Rockwell and Purslane Formations (fig. 31). The Rockwell Formation, the lower of the two units, extends from the lowest strata exposed up to the base of the first thick (>10 m; 32 ft) sandstone unit. The Purslane Formation, which is composed mainly of sandstone, is resistant to erosion and forms the prominent ridge of Sideling Hill.

The Rockwell Formation consists of interbedded thin sandstone, siltstone, and coaly marine shale. This exposure of the Rockwell Formation contains a polymictic diamictite near the base. This basal diamictite is a sandy, mud-supported, unsorted mass, containing clasts ranging in size from pebbles through boulders. Some of the clasts are composed of granite, chert, and graywacke. At some locations large masses, meters in diameter, of the underlying Hampshire Formation are incorporated in the diamictite lithology. The provenance of most clasts, however, is unknown. Overlying the diamictite is a 10-m (33-ft)-thick interval of herringbone crossbedded, medium- to coarse-grained sandstone. Upsection from the

herringbone crossbedded sandstone is a 30-m (98 ft)-thick interval of interbedded thin coal beds and sandstone and siltstone that contains marine fossils along some horizons. This interval has been correlated with the Riddlesburg Shale of central Pennsylvania, an Early Mississippian marine transgression equivalent to the Sunbury Shale of Ohio (Bjerstedt, 1986a; Bjerstedt and Kammer, 1988; Brezinski, 1989a). Some of the brachiopods contained within this interval include lingulid brachiopods; the articulate brachiopods, *Rugosochonetes*, *Macropotamorhyncus*, and *Schuchertella*; as well as indeterminate bivalves (Brezinski, 1989b).

Overlying the Riddlesburg Shale Member, in the upper part of the Rockwell Formation, is a 50-m (164-ft)-thick interval of interbedded channel-phase sandstones, 3 to 10 m (10-33 ft) thick, and reddish-brown and medium-gray, root-mottled siltstone and mudstone.

The first thick sandstone encountered upward marks the base of the overlying Purslane Formation. This basal sandstone of the predominantly sandy Purslane Formation is 25 m (82 ft) thick, is medium grained, exhibits epsilon crossbedding, and contains basal lag gravels. The basal unit is overlain by a thin interval (7 m; 23 ft) of root-mottled, reddish mudstone and then another (15 m; 49 ft) thick, crossbedded sandstone unit. Overlying this second sandstone unit is an interval of interbedded coaly shale and thin coal. A 30-m (98-ft)-thick third sandstone unit caps the ridge. This uppermost unit is much coarser grained than either of the lower units and contains many crossbedded conglomeratic intervals (Brezinski, 1989b).
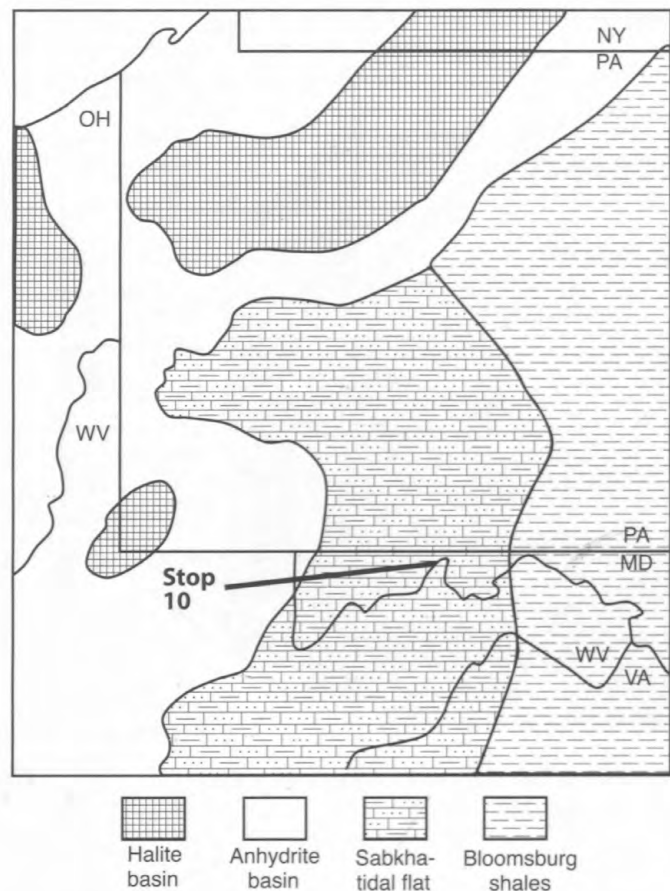
Figure 30. Regional-scale environments of deposition for the Middle to lower Upper Silurian.

Depositional Environments

The Lower Mississippian sequence at Sideling Hill was interpreted by Brezinski (1989a) as a prograding clastic wedge that progressively replaced marine deposits with coastal plain (marsh), meandering fluvial, and braided fluvial deposits (fig. 31). The basal polymictic diamictite is, however, an enigmatic stratigraphic interval (ESI). The unsorted character, strike-localized extent, and presence of "slump-blocks" of the underlying Hampshire Formation lithologies led Sevon (1969) and Bjerstedt and Kammer (1988) to interpret these deposits as subaqueous mud and debris flows that occupied an older sediment dispersal system. The consistent stratigraphic relation between the diamictite and overlying herringbone crossbedded sandstone further led Bjerstedt and Kammer to propose that the sandstone deposits represented tidal inlet-fill sequences created by tidal processes during drowning of the preexisting channels during the Riddlesburg transgression. Suter (1991) similarly proposed that the polymictic diamictite is the result of an estuarine debris flow. However, as discussed below, Cecil and others (2002) have suggested that the diamictite and overlying laminated strata are related to glacial conditions in the Appalachian basin during the Devonian-Mississippian transition.

The strata overlying the diamictite and herringbone crossbedded sandstone (tidal?) become increasingly darker in color and consist of interbedded coaly shale and siltstone. These coaly strata grade upsection into marine strata. The restricted brachiopod-bivalve fauna present in these shales indicates deposition in an estuarine or restricted lagoonal setting (Brezinski, 1989a). The return upsection to coaly shale indicates progradation of the tidal marsh environments back over previously deposited lagoonal deposits. The upper Rockwell's characteristic interbedded thin channel sandstone and finer grained overbank deposits that are pervasively root-mottled, indicate that the upper Rockwell was deposited in an alluvial-coastal plain environment.

The thick, channel-phase sandstones with epsilon cross-bedding and thin overbank deposits of the lower Purslane Formation indicate a channel-dominated, meandering fluvial environment. The coarser conglomeratic deposits in the upper part of the formation may indicate that gradients increased and environments changed from a meandering fluvial to braided fluvial facies near the end of Purslane deposition (Brezinski, 1989a-c) (fig. 31). The recent recognition of the pervasive occurrences of moderately well-developed paleosols throughout the section at this locality may require reinterpretation of certain aspects of the Lower Mississippian depositional systems.

Late Devonian and Early Mississippian Paleoclimate

The Late Devonian and Early Mississippian strata exposed at Stop 11 are indicative of paleoclimates that ranged from dry subhumid to moist subhumid to humid in sharp contrast to the aridity of the Early Devonian and subsequent Mississippian arid climatic conditions (fig. 10). Upper Devonian paleo-Vertisols and Histosols (coal beds), the influx of siliciclastic material, and a paucity of calcareous materials, are all indicative of relatively wet climatic conditions. Mineral paleosols include weakly to moderately developed non-calcic paleo-Vertisols. Such Vertisols are the result of a soil moisture regime and chemistry in which concentrations of exchangeable cations are low, which precludes precipitation of pedogenic carbonate. Non-calcic Vertisols primarily form under a moist subhumid climate. The soil structures, including mukkarra structures, are clear and unequivocal evidence, however, for a climate with a distinct dry season (Retallack, 1989).

The Early Mississippian sandstone exposed at the top of the cut is exceedingly widespread and extends from New York and Pennsylvania (Pocono Sandstone) to at least as far south as Kentucky (Borden Formation) and Tennessee (Price Formation). This clastic wedge, with its sporadic coal beds, represents a period during which massive amounts of sand were transported into the basin. Rainfall conditions ranged from dry subhumid to moist subhumid, and rainfall was somewhat seasonal (fig. 1A). The transition from meandering
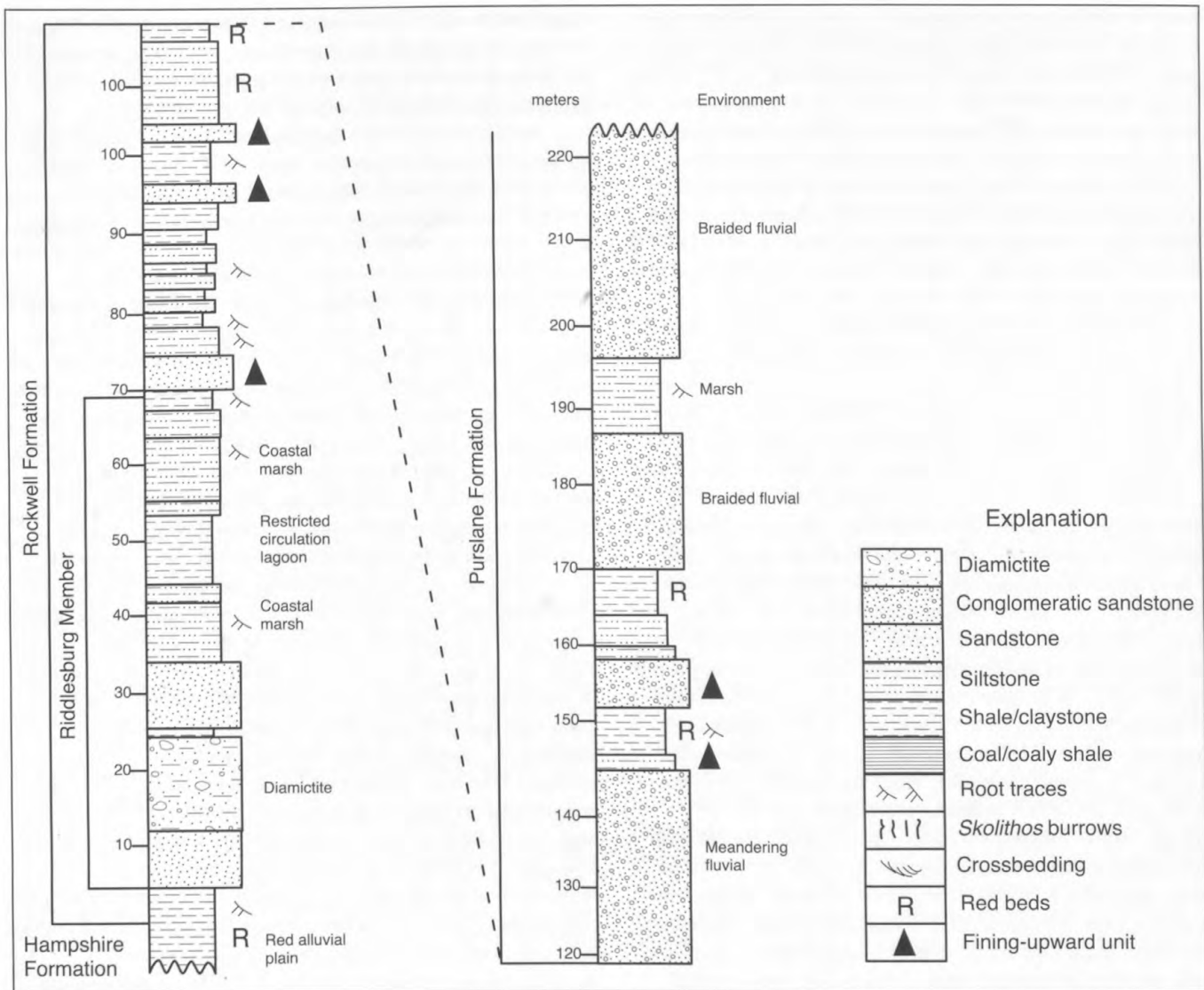
Figure 31. Stratigraphic section exposed at Stop 11 and interpreted depositional environments. Modified from Brezinski (1989a).

fluvial deposition in the lower Purslane to braided fluvial deposition in the upper Purslane can be attributed to increasingly seasonal rainfall and a progression from a humid or moist subhumid climate to dry subhumid conditions and finally arid conditions during deposition of the overlying Maccrady and Greenbrier Formations (Cecil, 1990). This interpretation is consistent with coal occurrences in the Pocono and equivalent units and evaporites, Aridisols, and carbonates in overlying Mississippian strata (Cecil, 1990). It is highly unlikely that the changes from Devonian aridity to the humid conditions of the Late Devonian and Early Mississippian, followed by a return to aridity in the Mississippian (Osagean), were the result of either long-term climate change caused by continental drift through paleolatitudes or tectonic processes.

Evidence for Late Devonian and Early Carboniferous Global Cooling and a Humid Climate in the Appalachian Basin

There is compelling evidence for Late Devonian glaciation in the Amazon Basin and in northern Africa (Libya and Algeria) (Caputo and Crowell, 1985; Veevers and Powell, 1987). In addition, Frakes and others (1992) suggested that the Late Devonian-Early Mississippian was a time of global cooling (ice house conditions). Even though evidence for Late Devonian glacial conditions in the Appalachian basin has been recognized for many years, this evidence has consistently been discounted (Sevon, 1969, p. 7; Berg, 1999, p. 133). However, compelling evidence for Late Devonian glaciation in the Appalachian basin is evident in the Spechty Kopf Formation and overlying strata in Pennsylvania, and the correlative units

(lower Rockwell) in Maryland and northern West Virginia. This is the enigmatic stratigraphic interval (ESI) referred to above in the section that discusses depositional environments. The ESI is known to occur in a 40-km (25 mi)-wide belt extending 400 km (249 mi) from northeastern Pennsylvania, across western Maryland, into north-central West Virginia. This belt is about 45 km (28 mi) wide in the northeast as measured between Jim Thorpe and Wilkes Barre, Pa., in the region of the anthracite coal fields. Southward in Maryland, it narrows to approximately 25 km (16 mi), but this may be very misleading and strictly a result of erosion and of a lack of exposure to the east. The original eastern extent of the ESI is unknown because of erosional removal of the section. The western border of the ESI belt is a well-defined curvilinear edge. There are many exposures of the horizon to the west of the belt and none contain the diamictite or related lithologies. For example, Stop 7 at the Finzel exit of I-68 is 10 km (6 mi) west of the La Vale ESI exposure, but none of the same lithologies are contained at the horizon. The same is true at a number of locations in Pennsylvania where the western edge of the ESI terminates abruptly. The ESI thickness in northeastern Pennsylvania varies locally from 0 to 185 m (0–607 ft) (Berg, 1999). The following features suggest a glacial to periglacial control on the origin of the ESI (in ascending stratigraphic order): (1) a basal, nonbedded polymictic diamictite containing matrix-supported clasts (of known and unknown origin) up to 2 m (7 ft) in diameter (tillite), (2) bedded siltstone and sandstone containing matrix-supported polymictic clasts, up to 2 m (7 ft) in diameter (dropstones), and (3) laminites (flaser-bedded sandstone, as discussed above) with clasts (glacial varves and dropstones, respectively). Striated facets, which we interpret to be glacial in origin, are present on some clasts. The tillite, dropstones, varves, and faceted-striated clasts in the ESI are indicative of deposition at or near the terminus of either a continental ice sheet that was centered in Gondwanaland (South America) or glaciers that debouched from undocumented highlands to the southeast. The regular nature of the curvilinear western edge of the belt is most consistent with the ice sheet hypothesis. In either case, the study region was situated in the vicinity of lat ~30° S. during the Devonian-Carboniferous transition (Scotese, 1998), which is approximately coeval with the onset of Late Devonian conditions of global cooling (Frakes and others, 1992).

The ESI unconformably overlies the Upper Devonian Catskill Formation (Hampshire Formation in West Virginia), which is characterized by red beds with caliche, suggesting that deposition occurred under semiarid conditions (high pressure, consistent with paleolatitude). The ESI and the overlying Lower Mississippian formations at this stop and elsewhere contain plant debris and coal, indicating that deposition occurred under a humid climate (low pressure, inconsistent with paleolatitude). However, the humid climate that dominated the region during the Devonian-Mississippian transition is consistent with the development of a subpolar low-pressure system that was associated with a polar front along the northern edge of the ice. Aridosols and

other features of aridity in Osagean red beds that overlie the Pocono Group indicate that high pressure and aridity returned to the study region once global warming and ice melting caused a poleward migration of the subpolar low-pressure system.

A cold climate in the Appalachian basin also is indicated by the paleoecology of marine fauna (D.K. Brezinski, unpub. data). First, the latest Devonian sea floor fauna in western Pennsylvania and southern New York known from these strata is unusual, even though the epeiric seas of the time were some of the shallowest waters in the Late Devonian and Early Mississippian in the Appalachian basin. The fauna is composed of cold-water siliceous sponges, not shallow warm-water calcareous sponges. This exotic fauna has, for nearly a century, perplexed paleontologists by virtue of the paradox of a demonstrably "deep water" (cold) fauna dominating shallow-water environments. Clearly the Appalachian basin, during this time, contained very cold waters allowing deep water faunas to migrate to shallow waters. Second, there is a clear empirical correlation between brachiopod diversity through the Late Devonian and Early Mississippian of North America and its relation to both sea-level fluctuations and glacial episodes on Gondwanaland. Overall brachiopod diversity dips in the latest Famennian and climbs back to high levels during the Kinderhookian. Copper (1998) recognized that certain families of Late Devonian brachiopods (spiriferids, athyrids, rhynchonelids, and terebratulids) were eurythermal (not affected by temperature changes). When those groups are taken as a percentage of the total brachiopod fauna, it is apparent that the eurythermal groups dominated during the latest Devonian, a time known to have seen glaciation in the southern hemisphere. This glacial episode is coincident with a period of sea-level draw down at the Devonian-Carboniferous boundary. This glacial episode also is coincident with the long-term humid period during the Devonian-Mississippian transition in the Appalachian basin. The succeeding arid climate is coincident with global warming and sea-level rise. As noted above, the long-term humid period during the Devonian-Mississippian transition is best explained by the close proximity of a polar front that was associated with the northern edge of ice as indicated by features contained within the ESI.

Stop 12. U.S. Silica property along Sandy Mile Road.

Lat 39°42.72′ N., long 78°13.82′ W., Hancock, Md., 7.5-minute quadrangle.

Leaders: Dave Brezinski, John Repetski, and Blaine Cecil

Introduction

At this stop we will examine the Silurian-Devonian contact interval. The main units exposed are the Keyser

Formation, which occurs in an abandoned quarry just to the east, and the Lower Devonian Oriskany Sandstone. The Keyser Formation is predominantly a limestone unit and represents a Late Silurian submergence of the Appalachian basin. The Oriskany on the other hand is a carbonate-cemented sandstone, grading laterally in some places into an arenaceous limestone. The Oriskany has been one of the most prolific gas-producing units in the central Appalachians.

Lithostratigraphy

Helderberg Group

Although much of the Helderberg Group is encompassed by this stop, only about 65 m (213 ft) of the lower part of the basal unit, the Keyser Formation, are accessible (Brezinski, 1996). The Keyser Formation is exposed in the abandoned quarry located east of the road. At this location the Keyser Formation is predominantly composed of nodular-bedded, argillaceous, fossiliferous lime wackestone. This interval contains thin (<5 cm) pelmatozoan packstone or grainstone intervals that are commonly graded and exhibit hummocky cross-stratification. The uppermost 10 m (33 ft) of the exposure becomes more regularly bedded and contains noticeably more and thicker layers of grainstone-packstone. The lithologies exposed at this location are included within the nodular facies of Head (1969) and the shaly/nodular-bedded/cherty limestone facies of Dorobek and Read (1986).

Although these strata are highly fossiliferous, most faunal components have been comminuted. The most common faunal components include abundant ramose and fenestrate bryozoans, rugose corals, tabulate corals, trilobites, brachiopods, and pelmatozoans. The regularly bedded intervals near the top of the exposure contain brachiopod coquinas and more pervasive indications of current activity such as crossbedding and graded beds.

On the basis of conodont ranges, the Silurian-Devonian contact can be placed within the upper Keyser near the contact with the overlying New Creek Limestone (Denkler and Harris, 1988). Consequently, the Keyser Formation here is almost totally Silurian (Pridolian) in age. Between the Keyser exposure and the outcrop of the overlying Oriskany Sandstone is a covered interval approximately 35 m (115 ft) thick. On the basis of regional stratigraphic relations this covered interval contains the intervening units of the New Creek Limestone, Corriganville Limestone, Mandata Shale, and Shriver Chert. The New Creek Limestone consists of thick-bedded lime grainstone that is intensely crossbedded. The Corriganville Limestone is characterized by nodular-bedded, shaly limestone. The Mandata Shale and Shriver Chert are composed of dark-gray, calcareous shale, chert, and siliceous shale and siltstone. All of these intervening units are Early Devonian in age.

Oriskany Sandstone

Regionally, the Oriskany Sandstone is underlain and overlain by marine cherty units and black shales, respectively.

Unit	Lithology	Environment	Sea level
Oriskany Sandstone	white sandstone	shallow marine	
Shriver Chert	black shaly siltstone	basinal	
Mandata Shale	black shale	basinal	
Corriganville Limestone	nodular-bedded limestone	deep ramp	
New Creek Limestone	crossbedded encrinites	tidally dominated shelf	
Keyser Formation	nodular-bedded limestone	deep ramp	deeper

Figure 32. Relations between stratigraphy and sea-level curve at Stop 12. Modified from Dorobek and Read (1986).

These chert-bearing units are indicative of a high silica input into the basin just prior to and immediately following deposition of the Oriskany Sandstone. C.B. Cecil (unpub. data) has attributed the source of the silica to wind-blown dust from coeval nearby warm-arid sand seas. At this location, the Oriskany Sandstone is approximately 50 m (164 ft) thick and consists of light-gray, medium-bedded, fine- to medium-grained, carbonate-cemented quartz sandstone. Crossbedding is prevalent in only a few intervals. To the south in West Virginia, U.S. Silica mines this unit for use in the manufacture of glass. As a consequence of the carbonate cementation, this sandstone is easily leached on exposed surfaces, leaving behind a residue of pure quartz sand.

The Oriskany Sandstone is highly fossiliferous in some intervals. These fossiliferous intervals are concentrated near the top of the formation and the fossils occur in the form of internal and external molds. The faunal components are primarily large, thick-shelled, coarsely plicate brachiopods, and, more rarely, large, platyceratid gastropods. These coarsely plicate brachiopods are indicative of turbulent, current-swept environments. The preponderance of brachiopod valves are disarticulated and convex-up indicating that they have been rearranged post-mortem by traction currents.

Depositional Environments

Dorobek and Read (1986) examined the Helderberg Group from a regional perspective. Their interpretations are summarized in figure 32. From their interpretations it is possible to recognize two separate transgressive-regressive episodes within the Helderberg Group of the central Appalachians. The first of these episodes is manifested in the Late Silurian Keyser Formation. This deepening episode submerged the tidal flat facies of the underlying Tonoloway Limestone as seen at Stop 10 and continued into the latest Silurian, completely drowning the Appalachian basin. At maximum deepening, the center of the basin was the site of deposition of nodular-bedded, argillaceous lime wackestone as seen at this stop. Dorobek and Read (1986) interpreted this facies as a deep ramp deposit formed below fair-weather wave base. The burrowed character of the sediments and the paucity of shallow water features suggested water depths of up to 50 m (164 ft).

Head (1969) also interpreted these lithologies as occurring near the center of the Keyser seaway. The increased numbers of crossbedded intervals near the top of the exposure suggest regression.

The overlying New Creek Limestone marks the base of the second of the two transgressive episodes and is interpreted as a skeletal sand bank that formed in water depths of less than 15 m (49 ft) (Dorobek and Read, 1986). The upsection transition of the New Creek encrinites into the nodular-bedded Corriganville Limestone indicates a continued deepening of the Early Devonian sea. Like the Keyser lithologies at this stop, the Corriganville nodular-bedded lithologies are interpreted as deep ramp deposits. Upsection, the Corriganville Limestone passes into the Mandata Shale and Shriver Chert. These two lithologies represent basinal lithologies that formed at the apex of the Helderberg transgression. Water depths are estimated in excess of 50 m (164 ft) (Dorobek and Read, 1986).

Presumably the regressive phase of this episode resulted in the shallow water deposition of the Oriskany Sandstone. The presence of crossbedding, coarsely plicate and thick-shelled brachiopods, and the disarticulated, convex-up brachiopod valves suggest strong, current-swept conditions.

Paleoclimate

During the Late Silurian and Early Devonian, the Appalachian basin was in the vicinity of lat 30° to 40° S. in a belt analogous to modern-day aridity and high pressure. Paleoclimate indicators suggest that the climate was arid (Scotese, 1998). Unlike the limestone intervals at this stop, the origin of the highly siliceous Lower Devonian strata remains speculative. On a regional scale, the siliceous strata consist of the following in ascending order: (1) the Shriver Chert, (2) the Oriskany Sandstone, and (3) the Huntersville Chert. The Shriver Chert consists predominantly of decimeter-scale interbedded chert and silty limestone. The overlying Oriskany Sandstone contains rounded sand grains floating in a carbonate matrix and rounded to subrounded quartz grains in quartz arenite. Grabau (1932, 1940) and Cecil and others (1991) proposed an eolian provenance for the Oriskany sand; the quartz sand was either blown into the carbonate environments of the Oriskany seaway or the sand was derived from ergs that were reworked during sea-level rise. Shinn (1973) has described a similar set of conditions in the modern Persian Gulf where dust and sand are blown into modern carbonate environments. The Huntersville Chert (not present at this stop) grades from impure chert in West Virginia into the cherty Onondaga Limestone in Pennsylvania and New York (Dennison, 1961). Sheppard and Heald (1984) described the following seven lithotypes in the Huntersville Chert in West Virginia: (1) clean chert, (2) chert with organic material, (3) spicular chert, (4) dolomitic chert, (5) glauconitic chert, (6) silty, argillaceous chert, and (7) dolomitic, silty, argillaceous chert. They pointed out that all lithotypes in the Huntersville contain some dolomite and silt-size (quartz) detritus.

The source of silica for the Shriver and Huntersville Cherts (and equivalent cherty limestones) has previously been attributed to the biotic extraction of silica from seawater derived from the dissolution of volcanic ash (Dennison, 1961; Sheppard and Heald, 1984). Although minor amounts of biotic components have been recognized in the cherts, and volcanic ash (bentonite) occurs near the top of the Huntersville, the lithologies of the siliceous stratigraphic interval considered herein appear to be best explained by eolian sand and dust as the predominant source of silica. The coarsest silt fraction accounts for the quartz silt noted in the cherts as well as the quartz silt in interbedded limestone, whereas the finer size fraction of quartz dust readily provided an ample supply of soluble silica and residual particles that are equivalent in size to quartz crystallites in chert. Thus, the Early and early Middle Devonian sequence in the Appalachian basin can be readily explained by temporal and spatial variations in eolian processes in a warm arid climate. In contrast, it is unclear how the enormous amounts of Devonian chert can be accounted for by either silica derived from dissolution of volcanic ash or biotic extraction of silica from normal seawater.

Stop 13. Ordovician Beekmantown through Chambersburg Limestone.

Lat 39°36.99′ N., long 77°52.99′ W., C&O Canal Towpath, milepost 103, Hedgesville, W. Va., 7.5-minute quadrangle.

Leaders: Dave Brezinski and John Repetski

Introduction

At this stop we are on the western flank of the Massanutten synclinorium, a broad fold that is bordered on the east by the South Mountain anticlinorium and generally coincides with the Great Valley section of the Valley and Ridge physiographic province. The section here begins in the Lower Ordovician Stonehenge Limestone and continues eastward (and upsection) along the C&O Canal through the Lower to lower Middle Ordovician Rockdale Run Formation, the lower Middle Ordovician Pinesburg Station Dolomite into Middle Ordovician St. Paul Group, and Upper Ordovician Chambersburg Limestone. The basal strata of the Upper Ordovician Martinsburg Formation are the uppermost strata exposed. We will concentrate on the lower part of this section, which records the final regressive phase of the Sauk Sequence (Brezinski and others, 1999).

The widespread marine facies that existed in North America during the Cambrian and Early Ordovician is known as the Sauk Sequence (named by Sloss, 1963). Vail and others (1977) proposed that the Sauk Sequence was a first-order deepening episode. Palmer (1981) subdivided the Sauk Sequence into three sequences, Sauk I, Sauk II, and Sauk III.

Each of these subsequences represents a separate transgressive and regressive episode that is interpreted as third-order in magnitude (Brezinski and others, 2002).

Lithostratigraphy

The lowest strata encountered are assignable to the Stonehenge Limestone. The Stonehenge is 150 to 250 m (492–820 ft) thick, although only the upper 30 m (98 ft) are exposed at this location. Three members of the Stonehenge are recognized. The basal member, the Stoufferstown Member, is composed of ribbony limestone interbedded with thin intraclastic grainstones, 3 to 6 cm (1–2 in) thick. The middle member of the Stonehenge, unnamed, consists of thick-bedded, thrombolitic algal limestone and, rarely, ribbony limestone. The upper member is also unnamed and is lithologically similar to the Stoufferstown Member. The contact between the Stonehenge and the overlying Rockdale Run Formation is generally placed at the lowest tan-weathering, laminated dolomitic limestone. This dolomite reflects the onset of peritidal cyclic sedimentation that characterizes the Rockdale Run Formation.

The Rockdale Run Formation is approximately 850 m (279 ft) thick and consists mostly of 1- to 5-m (3–16 ft)-thick peritidal carbonates that are probably fifth-order in magnitude. The lithologic character of these cycles varies upsection with certain intervals containing thick limestone and thin dolomite subcycles and other intervals containing thicker dolomite and thin limestone subcycles (fig. 33A, B).

Sando (1957) recognized three subdivisions of the Rockdale Run Formation in this region. He noted that the basal 30 to 50 m (100–160 ft) contained large, silicified algal masses. Above these basal cherty beds, the Rockdale Run Formation contained abundant oolitic beds. Much higher in the formation a thick dolomite interval is prevalent. Sando (1957, pl. 4) also recognized a number of vertically distributed faunas. These faunas include the *Bellefontia* fauna within the upper Stonehenge Limestone and macrofaunas characterized by *Lecanospira*, *Archaeoscyphia*, *Diparelasma*, and *Syntrophopsis-Clelandoceras* in the Rockdale Run Formation, in ascending order (fig. 34). Hardie (1989) interpreted the faunas within the Stonehenge and lower Rockdale Run Formations to represent large-scale deepening episodes that he believed were third-order in magnitude. Brezinski and others (1999) showed that there were several different orders of sea-level cycles displayed within this stratigraphic section (fig. 34). The variations between limestone-dominated and dolomite-dominated cycles are the result of the large-scale deepening episodes as recognized by Hardie (1989). It appears that the fifth-order cycles, which formed near or at the transgressive apex of the larger scale cycles are limestone dominated, whereas fifth-order cycles that have been interpreted to have formed during regression or at the regressive nadir are dolomite dominated. Our observations in the Rockdale Run, however, indicate that regression was rapid

and resulted in exposure surfaces at the top of the subtidal limestone units rather than at the top of the peritidal dolomite. Exposure at the top of the subtidal limestones is indicated by pedogenic brecciation and subaerial crusts (fig. 33B). These subaerial exposure surfaces represent fourth- or fifth-order sequence boundaries. The peritidal dolomite formed during relatively slow transgression and is part of the transgressive systems tract.

Within the dolomite member of the upper Rockdale Run (*sensu* Sando, 1957), cycles are difficult to recognize inasmuch as diagenetic overprinting has obliterated many of the internal features. However, it does seem likely that this dolomite tongue was deposited during a major sea-level lowstand or slowly rising sea level during transgression.

Overlying the Rockdale Run Formation is the Pinesburg Station Dolomite, which is the uppermost formation of the Beekmantown Group. The Pinesburg Station Dolomite is 120 to 160 m (394–525 ft) thick and consists of cherty, laminated dolomite and burrow-mottled dolomite. The Pinesburg Station Dolomite is unfossiliferous, save for conodonts and many stromatolitic intervals. The Pinesburg Station Dolomite is overlain by a Middle Ordovician succession of interbedded limestone and dolomite, termed the St. Paul Group by Neuman (1951). Neuman subdivided the St. Paul Group into two units, the lower Row Park Limestone and the upper New Market Limestone. The Row Park Limestone consists of light-gray, massive, micritic to fenestral limestone with thin interbeds of laminated dolomitic limestone. It is approximately 85 m (279 ft) thick. The overlying New Market Limestone is characterized by interbedded, medium-bedded, light-gray, burrow-mottled limestone; stromatolitic limestone; and gray and tan, laminated dolomite and dolomitic limestone. It is capped by a light- to medium-gray, micritic limestone. The New Market is approximately 67 m (220 ft) thick. Fossils are not common in either of the St. Paul Group Formations; however, they are present within horizons in the upper part of the New Market Limestone. The main macrofaunal components are macluritid snails. Conodonts occur throughout these units. Overlying the St. Paul Group is an interval of medium- to dark-gray, medium- to wavy bedded and even nodular-bedded, shaly, fossiliferous limestone termed the Chambersburg Limestone.

Depositional Environments

The Stonehenge Limestone was deposited during a major deepening episode that was probably third-order in magnitude and appears to exhibit a symmetrical facies distribution (Hardie, 1989; Taylor and others, 1993). The sea-level drop that was concurrent with the regression at the termination of Stonehenge deposition also produced the fifth-order depositional peritidal cycles in the basal Rockdale Run Formation. The peritidal mud flats that existed throughout most of the Rockdale Run deposition were periodically submerged by shallow subtidal waters, indicating that larger
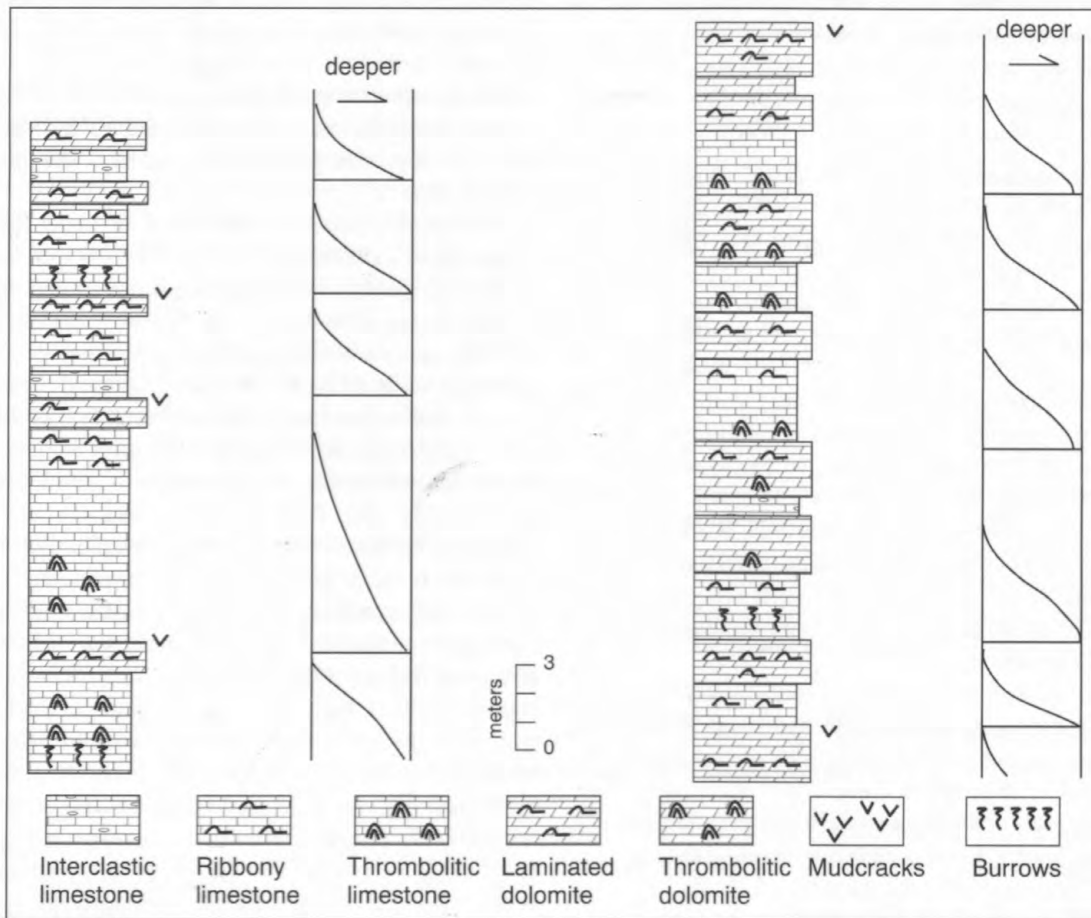
Figure 33. A, Fifth-order(?) cycle variations within the Rockdale Run Formation at Stop 13. Left column shows limestone-dominated subcycles with interpreted sea-level curve (Hardie, 1989). Maximum water depth is during limestone deposition shallowing upward to peritidal conditions during dolomite deposition. Right column shows dolomite-dominated subcycles. B (facing page), Fifth-order(?) cycle variations within the Rockdale Run Formation at Stop 13. Left column shows limestone-dominated subcycles with re-interpreted sea-level curve based on exposure surfaces at the top of the limestone beds. Right column shows dolomite-dominated subcycles.

scale cycles of a fourth- or third-order are superimposed on the sequence. The thick dolomite in the upper part of the Rockdale Run Formation was previously thought to record a significant shallowing episode for the central Appalachians. Our observations, however, indicate that at the scale of the fifth-order lithologic cycles, subtidal limestone deposition was followed by abrupt regression and subaerial exposure. Primary dolomite was deposited on the exposure surfaces during subsequent transgression and deepening. This cyclic sedimentation continued during the deposition of the Pinesburg Station Dolomite at the end of Beekmantown Limestone deposition.

Mitchell (1982) discussed in detail the vertical arrangement of lithologies within the St. Paul Group of Maryland. The vertical arrangement of lithologies within the Pinesburg Station

Dolomite to New Market Limestone led Mitchell to interpret the sequence as two separate transgressive and regressive pairs.

The deepening event at the end of the Middle Ordovician of the central Appalachian basin produced the Chambersburg Limestone. This deepening episode resulted from the downwarping that occurred with the onset of the Taconic orogeny. This deepening provided the accommodation space for the graptolitic black shales of the overlying Martinsburg Formation.

Climate of the Early and Middle Ordovician

In contrast to the moist subhumid climate of the Late Precambrian and Early Cambrian as discussed at Stop 14, long-term aridity prevailed during deposition of Early
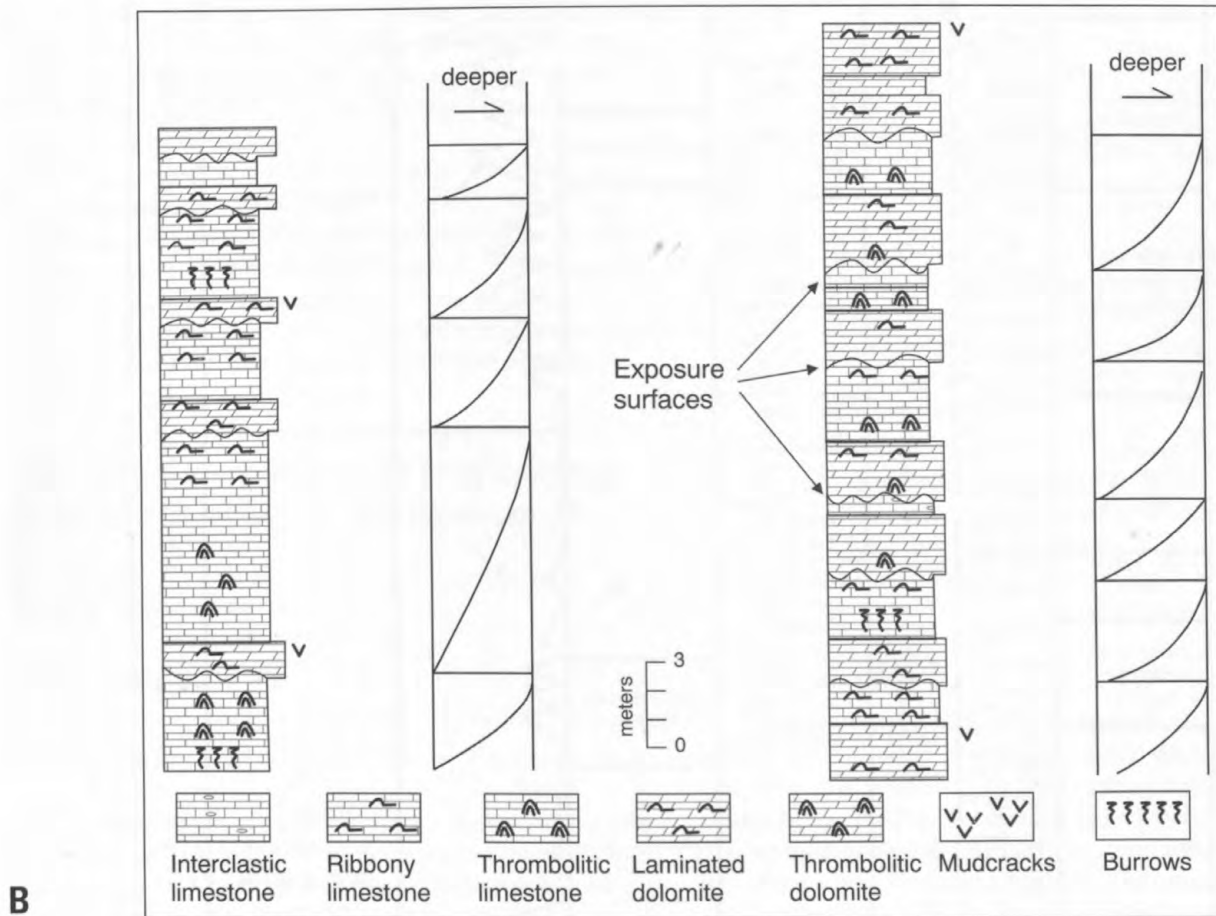
Figure 33. Continued

Ordovician strata (Stop 13). Intermediate- to short-term climates fluctuated from arid to semiarid. Paleogeographic reconstructions indicate that deposition at Stop 13 occurred in the arid high-pressure belt at approximately lat 30° S. Indications for long-term aridity at Stop 2 include (1) the lack of fluvial siliciclastic influx, (2) stratigraphically equivalent evaporites to the west in the depocenter of the basin (Ryder and others, 1992), (3) intervals of nodular chert that presumably are replacements of gypsum or anhydrite, and (4) primary dolomite resulting from probable hypersaline conditions in peritidal environments. Localized evaporate casts within the subjacent Conococheague Formation (Demicco and Mitchell, 1982) corroborate these interpretations.

At a continental scale, the eolian St. Peter Sandstone of the midcontinent also was being deposited during part of this time (coeval with the mid-St. Paul Group and younger strata). Contemporaneous deposition in the sediment starved Ouachita basin consisted of deep water shale, chert, and limestone (Stone and others, 1986, p. 19). Sediment starvation in the deep water Ouachita basin during the Ordovician is consistent with low fluvial sediment supply to continental margins under arid conditions (fig. 1A). Interestingly, the pulses

of quartz sand deposition in the Ouachita trough represented by the Crystal Mountain and Blakely Sandstones appear well correlated with the central Appalachian shallowing episodes represented by the initiation of Rockdale Run deposition and the peritidal dolomite deposition of the upper Rockdale Run through Pinesburg Station, respectively.

The interpreted sea-level history at Stop 2 is best explained by a glacial model even though direct evidence for Early and early Middle Ordovician glaciation is lacking (Frakes and others, 1992). The third-order cycle of subtidal deposition of the Stonehenge followed by deposition of the Rockdale Run in peritidal environments may be best explained by greenhouse followed by ice house conditions. The fourth- or fifth-order cycles within the Rockdale Run have inferred sea-level curves (fig. 33B) that are similar to glacial-interglacial cycles. Exposure surfaces at the top of subtidal limestone beds represent fourth- or fifth-order sequence boundaries. Following subaerial exposure in the fourth- or fifth-order cycles of the Rockdale Run, sea level appears to have slowly risen during deposition of the peritidal dolomite followed by subtidal carbonates which, in turn, was followed by a rapid fall and subaerial exposure (fig. 33B). If the third- through fourth-order
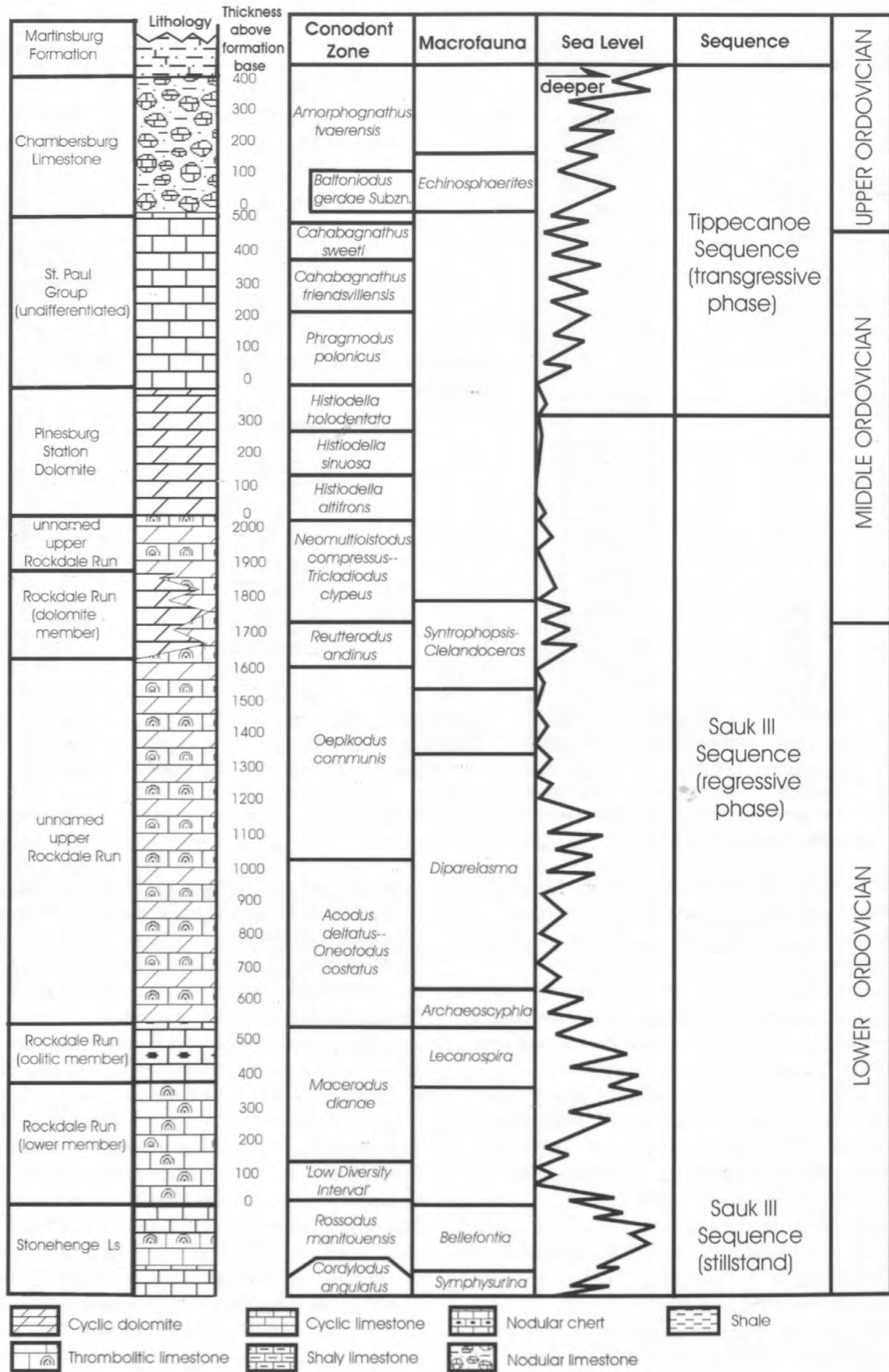
Figure 34. Relations among stratigraphy, faunas, and transgressive-regressive packages for the Early Ordovician Stonehenge and Rockdale Run Formations. Modified from Brezinski and others (1999).

cycles were driven by the presence or absence of continental glaciation, then the third-order Stonehenge deepening is likely the result of greenhouse conditions, whereas the fourth- and fifth-order cycles of the Rockdale Run and Pinesburg Station may be the product of long-term ice house conditions and intermediate- to short-term glacial cycles and the accompanying sea-level and climate cycles.

From a practical perspective, climate considerations become important in predicting porosity and permeability in carbonates and sandstones. Primary dolomitization in carbonates as well as texturally and mineralogically mature quartz arenites deposited by eolian processes may be the result of arid conditions. Both dolomitized limestone and quartz arenites (Stops 3, 6) are often targeted as potential petroleum reservoirs.

Stop 14. Late Precambrian and Early Cambrian Chilhowee Group on U.S. 340, Weverton, Md.

Lat 77°40.47' N., long 39°19.29' W., Harpers Ferry, W. Va., 7.5-minute quadrangle.

Leader: Dave Brezinski

Introduction

At this stop we will examine the Chilhowee Group of the northern Blue Ridge physiographic province. The Chilhowee Group, the basal Cambrian clastic unit in the northern Blue Ridge, is a main ridge-forming unit of the Blue Ridge. The Blue Ridge of northern Virginia, Maryland, and Pennsylvania consists of a large overturned fold called the South Mountain anticlinorium (Cloos, 1971). The South Mountain anticlinorium contains Grenville basement (1.1 b.y.) at its core and is flanked by Chilhowee strata. The eastern flank, known as Catoctin Mountain in Maryland and the Bull Run Mountains in Virginia, is the normal limb of the South Mountain anticlinorium and dips southeastward at approximately 35°. The western limb of the anticlinorium, known as South Mountain in Maryland and Short Hill in Virginia, is overturned and also dips to the southeast, but at a much steeper angle than the eastern limb (Catoctin Mountain). The Grenville basement complex is overlain, in ascending order, by Late Proterozoic sediments of the Swift Run Formation, basaltic lava flows of the Catoctin Formation, and clastics of the Chilhowee Group. These units are generally termed the Blue Ridge cover sequence. Both the Swift Run and Catoctin Formations exhibit considerable syndepositional thickness variation. Their geometries suggest that they were deposited in linear basins presumably formed by attenuation of the underlying basement complex (Schwab, 1972). Most of the Chilhowee units, on the other hand, appear to be more or less continuous throughout the northern Blue Ridge, indicating that much of the Late Precambrian topography had been filled prior to its deposition.
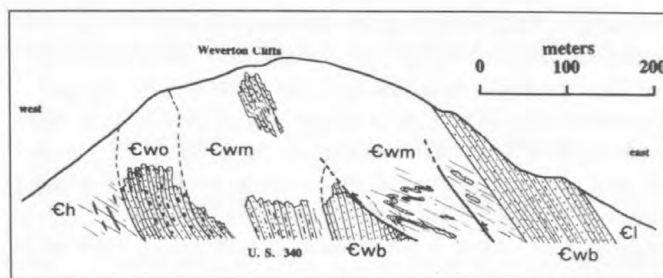
Figure 35. Diagrammatic sketch showing stratigraphy and structure of the Weverton Formation at the Maryland Heights section at the terminus of South Mountain, Md. €wb, Buzzard Knob Member; €wm, Maryland Heights Member; €wo, Owen Creek Member, all of the Weverton Formation. €h, Harpers Formation; €l, Loudoun Formation.

At this stop we will examine the type section of the Weverton Formation at the southern terminus of South Mountain and discuss the Sauk I transgression and its initial deposition within the Appalachian basin (fig. 35).

Lithostratigraphy

The Chilhowee Group in the northern Blue Ridge consists of the following in ascending order: the Loudoun, Weverton, Harpers, and Antietam Formations. These units generally overlie the Catoctin Formation, but at this location the Catoctin is absent, and the Chilhowee units sit directly on top of the Grenville basement strata. The basal unit of the Chilhowee Group, the Loudoun Formation, consists of intercalated black tuffaceous phyllites and polymictic conglomerate. The Loudoun Formation exhibits considerable variation in thickness and extent. This patchy distribution has led some workers to abandon the name Loudoun and assign the conglomeratic intervals to the Weverton Formation and the tuffaceous phyllites to the underlying Catoctin Formation (see Nunan, 1979). The Loudoun can vary in thickness from as little as 2 m (7 ft) to more than 70 m (230 ft). At Stop 14 the Loudoun is represented by several loose blocks of gray, tuffaceous phyllite, and it is estimated that more than 30 m (98 ft) of the formation is present.

Weverton Formation

The Weverton Formation, unlike its subjacent units, is relatively continuously distributed throughout the northern Blue Ridge. The Weverton has been subdivided into three members in ascending order as follows: (1) Buzzard Knob, (2) Maryland Heights, and (3) Owens Creek (fig. 35).

Buzzard Knob Member

The Buzzard Knob Member of the Weverton Formation is the single most significant ridge-forming unit in the northern Blue Ridge. The Buzzard Knob Member consists of medi-

um-bedded, light-gray to greenish-gray, chloritic, coarse-grained to very coarse grained, subarkose to quartzose arenite. The crossbedding within this unit is poorly defined and consists mainly of tabular to planar sets as well as horizontally stratified beds. At this location the basal 10 m (33 ft) consist of a very coarse grained sandstone to granular, feldspathic arenite. The upper 35 m (115 ft) comprise a resistant, light- to medium-gray, coarse-grained quartzite with dusky-blue, grayish-olive, and grayish-yellow bands. Trough crossbedding is much more prevalent in this part of the unit, although crossbed foresets are restricted to individual beds. Separating the two resistant intervals is approximately 10 m (33 ft) of interbedded, light-gray to dusky-yellow, platy, micaceous sandstone and light-olive-gray, quartzose siltstone. This interval weathers more readily than do the surrounding quartzite layers, and thus gives the member an apparent bifurcation that is manifested in less well-exposed areas of the two separate arenite units.

Maryland Heights Member

The middle member of the Weverton Formation, named the Maryland Heights Member, is difficult to accurately and thoroughly describe, and varies from 100 to 150 m (328–492 ft) in thickness. The unit is strongly deformed and less resistant to weathering than the massive units that make up the upper and lower parts of the Weverton. The Maryland Heights Member is generally composed of alternating medium-dark-gray, conglomeratic graywacke and dark-gray phyllite and metasiltstone. The incompetent phyllite and metasiltstone, being situated stratigraphically between the underlying and overlying resistant members, are deformed to the degree that stratigraphic characteristics are obscured.

At this location the Maryland Heights Member consists of olive-gray, grayish-black, and olive-black, quartzose metasiltstones that contain thin intervals, 0.33 to 0.6 m (1–2 ft) thick, of conglomerate with white quartz pebbles and 1- to 10-m (3–33 ft)-thick intervals of gray and greenish-gray arenite and graywacke. The thicknesses of the metasiltstone intervals are obscured by isoclinal folds and pervasive foliation. Near the middle of the unit is a 25-m (82-ft)-thick interval of medium-gray quartzite, which is nearly identical to the upper resistant quartzite of the underlying Buzzard Knob Member exposed at another point in the roadcut. Folding can be observed within these units. This quartzite, which is truncated above road level by a small fault, has been interpreted to be a fragment of the Buzzard Knob Member (Southworth and Brezinski, 1996; fig. 35).

Owens Creek Member

The upper member of the Weverton consists of another ledge-forming quartzite termed the Owens Creek Member (Brezinski, 1992). Although this member is more resistant and much better exposed than the Maryland Heights Member, rarely does it form the prominent ledges and ridge crests

common to the Buzzard Knob Member. At this location, more than 35 m (115 ft) of the Owens Creek Member crops out. The lower 25 m (82 ft) consist of medium- to medium-dark-gray, medium-bedded, coarse-grained, crossbedded conglomeratic sandstone with many interbeds of dark-gray, sandy siltstone as well as conglomerate, which contains white, pink, and bluish quartz pebbles. Many of the beds in this interval fine upward. The upper 7 to 10 m (23–33 ft) are composed of medium-light-gray to greenish-gray, medium-bedded, coarse-grained sandstone that is typically trough crossbedded. The contact with the overlying Harpers Formation is not exposed at this location. From other locations the contact is gradational, with progressively thicker interbeds of shaly Harpers punctuating the sandstones of the upper Weverton.

Harpers Formation

Overlying the Weverton Formation is an interval of shale, siltstone, sandstone and quartzite called the Harpers Formation. The Harpers Formation is characterized by dark-gray to olive-black, medium-grained sandstone and siltstone in the lower 30 to 50 m (98–164 ft). Above this basal sandy interval, the Harpers consists of greenish-black to brownish-black, highly cleaved siltstone, fine-grained sandstone, and some silty shale. Somewhat higher in the stratigraphic section the first distinct trace fossils are present. These are mainly in the form of the vertical burrow *Skolithos*.

Several small exposures of the lower Harpers Formation are evident to the west. However, these are intensely sheared owing to the proximity of these exposures to a large thrust fault that is present approximately 200 m (656 ft) to the west of the Weverton-Harpers contact.

Depositional Environments

No detailed depositional studies have been conducted on the Chilhowee strata of the northern Blue Ridge of northern Virginia and Maryland. However, the similarity of vertically juxtaposed lithologies between the Weverton at this location and the correlative Unicoi Formation of central and southern Virginia allows extrapolation of correlative depositional processes. The following discussion is based on the work of Schwab (1972) and Simpson and Eriksson (1989) and their studies on the coeval Unicoi Formation of Virginia. From these studies it can be inferred that the Chilhowee of the northern Blue Ridge represents a preserved rift-to-drift sequence. Moreover, the deepening episode that is preserved within these strata represents the initial submergence of the North American craton during the early Paleozoic and, thus, marks the onset of the Sauk transgression.

The underlying Swift Run and Catoctin Formations represent rift sedimentation and volcanism that filled grabens within the basement complex during extension (Wehr and Glover, 1985). The lack of Catoctin basalts at this location indicates that this site was located on an erosional horst between the

Table 3. Interpreted stratigraphic relations at Stop 14 and proposed depositional environments extrapolated from Schwab (1971, 1972), Simpson and Eriksson (1989) and interpreted tectonic regimes from Wehr and Glover (1985, table 2) and Fichter and Diecchio (1986, fig. 1)

Unit	Lithology	Environment	Tectonic regime
Harpers Formation	Dark silty shale and thin sandstone	Shallow marine	Transgressive
Weverton Formation	Crossbedded arkosic and conglomeratic sandstones	Meandering fluvial Braided fluvial	Trailing margin deposition
Loudoun Formation	Tuffaceous shale and conglomerate	Alluvial fan–rift valley	
Catoctin Formation	Basaltic lava flows	Extensional, rift volcanics	Extension and rifting
Swift Run Formation	Arkosic sandstone and varved shales	Rift valley	

southern Pennsylvanian graben and the central Virginia graben. The patchy distribution of the Loudoun Formation, as well as the apparent interfingering of the tuffaceous shales of the formation with the lavas of the underlying Catoctin Formation, suggests that these two formations may have been, in part, coeval. The localized distribution of the cobble conglomeratic facies of the Loudoun appears to reflect localized depocenters, probably within small fault-created basins in the underlying Proterozoic strata. The coarseness of these strata suggests deposition by high-gradient streams. An alluvial fan environment of deposition is suggested for this unit.

The planar bedded and trough crossbedded facies of the Buzzard Knob Member of the Weverton Formation appears to be similar to facies association C of the Unicoi Formation (Simpson and Eriksson, 1989). These lithologies were interpreted to be consistent with a distal facies of a braided fluvial plain.

The interbedded shale and thin sandstone lithologies of the Maryland Heights Member are interpreted to represent alluvial plain deposition. In this scenario the shaly strata, including the thin (<1 m; <3 ft) sandy conglomerates, are suggestive of overbank deposits and the thicker sandstone (>10 m; >33 ft) are channel deposits. The Owens Creek Member is much coarser grained and exhibits thicker, trough crossbedded sandstones than does any subjacent unit of the Weverton. A similar relation is present in the upper Unicoi of Virginia. This association of lithologies indicates deposition in a shoreface or tidal setting (Simpson and Eriksson, 1989). Schwab (1972) interpreted this part of the stratigraphic section to be fluvial channel sandstones.

The Harpers Formation exhibits a vertical arrangement of lithologies that suggests a transgressive relation (Schwab, 1971, 1972). The lower Harpers contains many, *Skolithos*-burrowed sandstone intervals, which are suggestive of littoral and sublittoral deposition (Brezinski, 1992). The increase in shaly strata upsection suggests a progression from nearshore to more offshore deposition within the lower Harpers.

Tectonics and Depositional Sequences

The late Precambrian to Early Cambrian depositional pattern of the central Appalachians suggests that the late Precambrian volcaniclastic and overlying Chilhowee Group represents the progression of depositional environments from rift basin alluvial fan (Loudoun) to braided and meandering fluvial (Weverton) to nearshore marine (upper Owens Creek Member, lower Harpers) and deeper shelf environments (Harpers) (table 3). This vertical sequence and the resulting environmental progression indicates a depositional onlap. The resulting transgressive episode, which began in the latest Precambrian, is equivalent to the Sauk I Sequence of Palmer (1981) and Sequence 1 of Read (1981). This apparent third-order eustatic event and the late Precambrian rift-basins and their accumulated sediments, resulted in the transitions from rift sedimentation to trailing margin sedimentation (Fichter and Diecchio, 1986).

Climate of the Late Precambrian and Early Cambrian

Climate interpretations of the late Precambrian and the Early Cambrian presented herein are primarily based on interpretations of lithologies and the depositional environment interpretations cited above. The massive influx of siliciclastic material that comprises the Chilhowee Group is consistent with a moist subhumid climate (fig. 1A, table 1). Such a climate is compatible with a paleogeographic location of approximately lat 40° S. (Scotese, 1998). The subarkosic sediments within the Weverton Formation are indicative of a dryer, perhaps subarid climate. However, the paucity of calcareous materials in Chilhowee strata indicates a subhumid or wetter climate setting where fluvial systems were low in dissolved solids precluding syndepositional precipitation of calcareous materials.

Field Trip Summary and Discussion

This trip traversed and included stops in Paleozoic strata from the latest Pennsylvanian to the earliest Cambrian within the central Appalachian basin. The Early Cambrian illustrates the tectonic influence of rifting and siliciclastic sediment supply in response to a long-term, dry subhumid to subhumid climate (table 1), which is consistent with a paleolatitude location of approximately 40° S. In contrast, Early Ordovician strata at Stop 13 consist of carbonates that were deposited in response to allocyclic changes in sea level. Sea level fluctuated from subtidal to total withdrawal with protracted subaerial exposure. By the Early Ordovician, the region was located in the high-pressure climate zone near lat 30° S., which is consistent with inferred climate ranges of arid to semiarid conditions.

As a result of the Taconic orogeny, the Appalachian foreland basin was well developed by the Late Ordovician and the red continental siliciclastic strata of the Juniata Formation (Stop 9) were deposited in response to semiarid to dry subhumid conditions. The depositional hiatus at the end of the Ordovician was succeeded by transgression and deposition of the Early Silurian Tuscarora Sandstone. The origin of the Tuscarora (Stop 9) remains enigmatic even though most workers agree that both marine and fluvial processes contributed to its deposition; neither process adequately explains the textural and mineralogical maturity of the Tuscarora. This maturity, however, can be attributed to mechanical weathering by eolian processes in an arid environment, which resulted in sand seas that were reworked and redeposited by hydraulic processes during sea-level rise in the Early Silurian.

The long-term climate remained arid throughout the remainder of the Silurian and into the Devonian. Regional-scale Upper Silurian peritidal carbonates (Stop 10) with abundant halite casts are indicative of these dry conditions. Latest Silurian and earliest Devonian sea-level rise resulted in subtidal carbonate deposition (Stop 3) throughout the central Appalachian basin. Such deposition is consistent with long-term aridity and very low fluvial siliciclastic sediment supply.

The textural and mineralogical maturity of the Lower Devonian Oriskany Sandstone (Stop 12) may be best explained by continuation of Silurian long-term aridity and mechanical weathering by eolian processes. The lithology of the Oriskany, which regionally ranges from a pure quartz arenite to an arenaceous limestone, may indicate the predominance of eolian transport of sand into the carbonate environments of the Early Devonian seaway. Similarly, the Lower Silurian Tuscarora Sandstone was the result of transgressive reworking of an eolian regolith. Both the Tuscarora and the Oriskany owe their textural maturity to eolian processes.

Following deposition of the Oriskany Sandstone, there was an apparent deepening of the Appalachian foreland basin as indicated by widespread deposition of finer grained silici-

clastic materials, including black shale. The deepening of the foreland basin was likely in response to the Acadian orogeny. Abundant terrestrial organic matter in some black shale facies appears to indicate high terrestrial organic productivity in response to a wetter paleoclimate. Following black shale deposition, basin filling materials coarsened upward, culminating in a major influx of sand in the Late Devonian and Early Mississippian (Stops 4, 8). The widespread distribution of this sand, from New York to Tennessee, is indicative of a climate control on sediment supply. The amount of sand and the types of paleosols, including coal, associated with these sands indicates that the long-term climate was moist subhumid. Based on the occurrence of coal and variation in siliciclastic sediment supply, the intermediate- to short-term climate fluctuations ranged from dry subhumid to humid during the Devonian-Mississippian transition in response to the proximity of glacial ice.

The influx of sand in the Early Mississippian was followed by a return to aridity as evidenced by deposition of evaporites throughout much of North America including southwest Virginia. Coeval terrestrial red beds containing Aridisols occur in southern West Virginia (informally referred to as the Pocahontas basin). Late Mississippian transgression under these arid conditions resulted in deposition of the overlying Greenbrier Formation. In the vicinity of the field trip route, the lowstand Loyalhanna Limestone Member eolianite(?) further indicates Late Mississippian aridity. Latest Mississippian strata are missing in the vicinity of the field trip route as a result of the worldwide mid-Carboniferous unconformity. However, relatively rapid subsidence in the Pocahontas basin resulted in nearly continuous deposition during the Late Mississippian and Early Pennsylvanian. In the Pocahontas basin, Late Mississippian deposition was only interrupted by eustatic drops in sea level that resulted in lowstand pedogenesis of regional subaerial exposure surfaces. These paleosols record both eustatic cycles and climate cycles that ranged from semiarid to humid. The influx of sediment and deposition of Late Mississippian red beds reflects the onset of global ice house conditions that spanned the Devonian-Mississippian transition.

Although Lower Pennsylvanian strata also are missing in the vicinity of the field trip route, deposition in the Pocahontas basin recorded a fluctuating water table, probably related to eustatic changes in sea level, and climate cycles that were much wetter than those of the Late Mississippian. Paleosols in the Early Pennsylvanian of the Pocahontas basin, as well as those at the Mississippian-Pennsylvanian unconformity (Stop 11), indicate that the climates of the Early Pennsylvanian ranged from humid to perhumid. These climate cycles and sea-level cycles appear to have been driven by glacial-interglacial conditions.

By the late Middle Pennsylvanian (Desmoinesian of the United States; Westphalian D of Europe), the long-term climate shifted from humid to moist subhumid conditions. Intermediate- to short-term climate cycles ranged from perhu-

mid to dry subhumid conditions as evidenced by a marked but cyclic change in the sedimentary geochemistry of nonmarine strata. Dry subhumid conditions are indicated by increased siliciclastic flux, abundant pyrite and calcite, including nonmarine limestone (Stops 10, 12). In contrast, humid to perhumid conditions produced chemically weathered and highly leached mineral paleosols and coal beds during lowstands.

A pronounced long-term dry subhumid climate developed in the early Late Pennsylvanian (Missourian) as evidenced by lowstand calcic-Vertisols, calcareous red beds, and far fewer economic coal deposits (Stop 13). A shift toward moist subhumid conditions during deposition of uppermost Pennsylvanian strata (Virgilian) in the central Appalachian basin resulted in increased coal formation (Stop 14) under moist subhumid conditions. Peat developed in topographic lows while coeval Ultisols formed around the basin margins. Moist subhumid conditions were followed by dry subhumid conditions that led to clastic influx and burial of the underlying peat. The driest parts of climate cycles, which were dry subhumid to semiarid, were conducive to nonmarine limestone deposition in topographic lows in the basin, while coeval calcic-Vertisols formed around the basin margins. Climate change, therefore, was the primary control on the lithostratigraphy of Upper Pennsylvanian strata in the Appalachian basin.

Paleoclimate and the Origin of Paleozoic Quartzose Sandstones

The origin of quartz-rich sandstones in Paleozoic strata in the Appalachian basin is generally attributed to multicycles of sedimentation, reworking within aqueous depositional environments, and (or) diagenesis. However, weathering within tropical paleoclimates appears to provide a explanation for the textural and mineralogical maturity of Paleozoic quartz arenites. From the Ordovician through the Early Devonian, the Eastern United States was in the southern hemisphere tropical dry belt and moved northward into the equatorial tropical rainy belt in the latest Mississippian and Pennsylvanian. Texturally mature quartz and trace amounts of unaltered detrital feldspars in Late Cambrian through Devonian quartz arenites are indicative of mechanical weathering by eolian processes in an arid or semiarid climate rather than chemical weathering in a humid tropical climate (Cecil and others, 1991). Grabau (1940, p. 220) suggested that the Oriskany Sandstone was an eolian deposit that was reworked by a marine transgression. An eolian component may be equally viable for the origin for the Silurian Tuscarora Sandstone as noted at Stop 9. Furthermore, the Oriskany and Tuscarora are associated with other strata that appear to be the result of deposition under arid conditions. Although both

the Oriskany and parts of the Tuscarora Sandstones were deposited in aqueous environments, they may have been blown into a marine environment analogous to the modern Persian Gulf where massive amounts of sand are being blown into a marine carbonate environment (Shinn, 1973).

In contrast, Late Mississippian and Pennsylvanian quartz arenites in the Appalachian basin tend to be texturally immature and nearly devoid of feldspars and, therefore, appear to be products of chemical weathering under humid conditions rather than mechanical weathering under arid conditions. Regional occurrences of residual kaolin deposits of latest Mississippian and Early Pennsylvanian age, which result from chemical weathering in humid tropical environments, are consistent with this interpretation. Thus, mature sandstones in Cambrian through Devonian strata may, in part, be the result of mechanical processes in eolian environments, prior to deposition in aqueous systems, whereas chemical weathering appears to have been a primary factor in the genesis of quartz arenites in Mississippian and Pennsylvanian strata.

Conclusions

By the examples included herein, we have attempted to illustrate the relative importance of allocyclic and autocyclic processes as controls on sedimentation and stratigraphy in the central Appalachian basin. Allocyclic processes appear to be the dominant control on lithostratigraphy. Autocyclicity seems to control facies relations within allocyclic packages. Clearly long-term tectonic subsidence was a primary control on accommodation space. Tectonic influence on fluvial sediment supply, while commonly suggested, is unclear and may be highly over emphasized. Intermediate- to short-term eustatic changes in sea level were also important controls on accommodation space but probably had little influence on sediment supply. Global long- to short-term changes in climate, however, were the primary controls on variation in sediment supply, both chemical and siliciclastic, and the predominant control on lithostratigraphy.

References Cited

Adams, R.W., 1970, Loyalhanna Limestone-crossbedding and provenance, *in* Fisher, G.W., Pettijohn, F.J., Reed, J.C., and Weaver, K.N., eds., Studies of Appalachian geology: central and southern: New York, John Wiley and Sons, p. 83–100.

Ahlbrandt, T.S., 1995, The Mississippian Loyalhanna Limestone (Formation)—A Paleozoic eolianite in the Appalachian basin: U.S. Geological Survey Open-File Report 95–240, 25 p.

Allings, H.I., and Briggs, L.I., 1961, Stratigraphy of Upper Silurian Cayugan Evaporites: American Association of Petroleum Geologists Bulletin, v. 45, p. 515–547.

Beerbower, 1964, Cyclothems and cyclic deposition mechanisms in alluvial plain sedimentation: Kansas Geological Survey Bulletin 169, 169 p.

Berg, T.M., 1999, Devonian-Mississippian transition, in Shultz, C.H., ed., The geology of Pennsylvania: Pennsylvania Geological Survey and Pittsburgh Geological Society Special Publication 1, p. 129–137.

Beuthin, J.D., 1986a, Lower Pocono coastal embayments, in western Maryland and vicinity, related to latest Devonian eustatic sea level rise [abs.]: American Association of Petroleum Geologists Bulletin, v. 70, no. 5, p. 565.

Beuthin, J.D., 1986b, Paleogeography of the uppermost Devonian-lowermost Mississippian lower Pocono Formation; Garrett County, Maryland [abs.]: SEPM annual midyear meeting, Abstracts Meeting, v. 3, p. 10.

Beuthin, J.D., 1986c, Facies interpretation of the lower Pocono Formation (Devonian-Mississippian); Garrett County, Maryland, and vicinity: Chapel Hill, University of North Carolina, M.S. thesis, 91 p.

Bjerstedt, T.W., 1986a, Stratigraphy and deltaic depositional systems of the Price Formation (Upper Devonian-Lower Mississippian) in West Virginia: Morgantown, West Virginia University, Ph.D. dissertation, 730 p.

Bjerstedt, T.W., 1986b, Regional stratigraphy and sedimentology of the Lower Mississippian Rockwell Formation and Purslane Sandstone based on the new Sideling Hill road cut, Maryland: Southeastern Geology, v. 27, p. 69–94.

Bjerstedt, T.W., 1987, Latest Devonian-earliest Mississippian trace-fossil assemblages from West Virginia, Pennsylvania, and Maryland: Journal of Paleontology, v. 61, p. 865–889.

Bjerstedt, T.W., and Kammer, T.W., 1988, Genetic stratigraphy and depositional systems of the Upper Devonian-Lower Mississippian Price-Rockwell deltaic complex in the central Appalachians, U.S.A.: Sedimentary Geology, v. 54, p. 265–301.

Brett, C.E., Tepper, D.H., Goodman, W.M., LoDuca, S.T., and Echert, B-Y., 1995, Revised stratigraphy and correlations of the Niagaran Provincial Series (Medina, Clinton, and Lockport Groups) in the type area of western New York: U.S. Geological Survey Bulletin 2086, 66 p.

Brezinski, D.K., 1983, Developmental model for an Appalachian Pennsylvanian marine incursion: Northeastern Geology, v. 5, p. 92–95.

Brezinski, D.K., 1989a, Mississippian foreland basin deposits of western Maryland: Field Trip Guidebook T226 for the 28th International Geological Congress: Washington, D.C., American Geophysical Union, 13 p.

Brezinski, D.K., 1989b, The Mississippian System in Maryland: Maryland Geological Survey Report of Investigations 52, 75 p.

Brezinski, D.K., 1989c, Late Mississippian depositional patterns in the north-central Appalachian basin and their implications to Chesterian hierarchal stratigraphy: Southeastern Geology, v. 30, p.1–23.

Brezinski, D.K., 1992, Lithostratigraphy of the western Blue Ridge cover rocks in Maryland: Maryland Geological Survey Report of Investigations 55, 69 p.

Brezinski, D.K., 1996, Carbonate ramps and reefs, Paleozoic stratigraphy and paleontology of western Maryland: Field Trip for the North American Paleontological Convention VI, Maryland Geological Survey Geologic Guidebook 6, 25 p.

Brezinski, D.K., Repetski, J.R., and Taylor, J.F., 1999, Stratigraphic and paleontologic record of the Sauk III regression in the central Appalachians, in Santucci, V., and McCelland, L., eds., National Park Service Paleontological Research, Geological Resources Division Technical Report NPS/NRGRD/GRDTR–03, v. 4, p. 32–41.

Brezinski, D.K., Repetski, J.E., and Taylor, J.F., 2002, Middle Cambrian to Upper Ordovician stratigraphy and paleontology along the Chesapeake & Ohio Canal National Historical Park, western Maryland [abs.]: Geological Society of America Abstracts with Programs, v. 34, no. 6, p. 423.

Buol, S.W., Hole, F.D., and McCracken, R.D., 1989, Soil genesis and classification, 3d ed.: Ames, Iowa State University Press, 446 p.

Caputo, M.V., and Crowell, J.C., 1985, Migration of glacial centers across Gondwana during Paleozoic era: Geological Society of America Bulletin, v. 96, no. 8, p. 1020–1036.

Carter, J.L., and Kammer, T.W., 1990, Late Devonian and Early Carboniferous brachiopods (Brachiopoda, Articulata) from the Price Formation of West Virginia and adjacent areas of Pennsylvania and Maryland: Annals of Carnegie Museum, v. 59, p. 77–103.

Cecil, C.B., 1990, Paleoclimate controls on stratigraphic repetition of chemical and siliciclasitic rocks: Geology, v. 18, p. 533–536.

Cecil, C.B., 2003, The concept of autocyclic and allocyclic controls on sedimentation and stratigraphy, emphasizing the climate variable, in Cecil, C.B., and Edgar, N.T., eds., Climate controls on stratigraphy: SEPM Special Publication 77, SEPM (Society for Sedimentary Geology), p. 13–20.

Cecil, C.B., and Dulong, F.T., 2003, Precipitation models for sediment supply in warm climates, in Cecil, C.B., and Edgar, N.T., eds., Climate controls on stratigraphy: SEPM Special Publication 77, SEPM (Society for Sedimentary Geology), p. 21–27.

Cecil, C.B., Stanton, R.W., Neuzil, S.G., Dulong, F.T., Ruppert, L.F., and Pierce, B.S., 1985, Paleoclimate controls on late Paleozoic sedimentation and peat formation in the central Appalachian basin (U.S.A.): International Journal of Coal Geology, v. 5, p. 195–230.

Cecil, C.B., Ahlbrandt, T.S., and Heald, M.T., 1991, Paleoclimatic implications for the origin of Paleozoic quartz arenites in the Appalachian basin [abs.]: Geological Society of America Abstracts with Programs, v. 23, no. 5, p. A72.

Cecil, C.B., Dulong, F.T., Cobb, J.C., and Supardi, 1993, Allogenic and autogenic controls on sedimentation in the central Sumatra basin as an analogue for Pennsylvanian coal-bearing strata in the Appalachian basin, in Cobb, J.C., and Cecil, C.B., eds., Modern and ancient coal-forming environments: Geological Society of America Special Paper 286, p. 3–22.

Cecil, C.B., Dulong, F.T., and Brezinski, D.K., 1998, Allocyclic controls on Paleozoic sedimentation in the Appalachian basin; Geological Society of America Field Trip No. 4 Guidebook: U.S. Geological Survey Open-File Report 98-577, 75 p.

Cecil, C.B., Skema, V., Stamm, R., and Dulong, F.T., 2002, Evidence for Late Devonian and Early Carboniferous global cooling in the Appalachian basin [abs.]: Geological Society of America Abstracts with Programs, v. 34, no. 7, p. 500.

Cecil, C.B., Dulong, F.T., Harris, R.A., Cobb, J.C., Gluskoter, H.G., and Nugroho, H., 2003a, Observations on climate and sediment discharge in selected tropical rivers, Indonesia, in Cecil, C.B., and Edgar, N.T., eds., Climate controls on stratigraphy: SEPM Special Publication 77, SEPM (Society for Sedimentary Geology), p. 29–50.

Cecil, C.B., Dulong, F.T., West, R.R., Stamm, R., Wardlaw, B., and Edgar, N.T., 2003b, Climate controls on the stratigraphy of a Middle Pennsylvanian cyclothem in North America, in Cecil, C.B., and Edgar, N.T., eds., Climate controls on stratigraphy: SEPM Special Publication 77, SEPM (Society for Sedimentary Geology), p. 151–180.

Cloos, E., 1971, Microtectonics along the western edge of the Blue Ridge, Maryland and Virginia: Baltimore, Johns Hopkins Press, 234 p.

Copper, P., 1998, Evaluating the Frasnian-Fammenian mass extinction; Comparing brachiopod faunas: Acta Palaeontologia Polonica, v. 43, p. 137–154.

Cotter, E., 1983, Shelf, paralic, and fluvial environments and eustatic sea-level fluctuations in the origin of the Tuscarora Formation (Lower Silurian) of central Pennsylvania: Journal of Sedimentary Petrology, v. 53, no. 1, p. 25–49.

Cotter, E., 1993, Overview of geology of central Pennsylvania, in Driese, S.G., ed., Paleosols, Paleoclimate, and Paleoatmospheric CO_2: International Association of Geochemistry and Cosmochemistry—3d International

Symposium on Geochemistry of the Earth's Surface and SEPM (Society for Sedimentary Geology) Field Trip: University of Tennessee, Knoxville publication EO1–1040–001–94, p. 1–22.

Cross, A.T., 1952, The geology of the Pittsburg coal: Nova Scotia Department of Mines second conference on the origin and constitution of coal, p. 32–111.

Demicco, R.V., and Mitchell, R.W., 1982, Facies of the Great American Bank in the central Appalachians, in Lyttle, P.T., Central Appalachian geology; Field trip guidebook for the joint meeting of the Northeastern and Southeastern Sections of the Geological Society of America, Washington, D.C., 1982: Falls Church, Va., American Geological Institute, p. 171–266.

Denkler, K.E., and Harris, A.G., 1988, Conodont-based determination of the Silurian-Devonian boundary in the Valley and Ridge province, northern and central Appalachians: U.S. Geological Survey Bulletin 1837, p. B1–B13.

Dennison, J.M., 1961, Stratigraphy of the Onesquethaw stage of Devonian in West Virginia and bordering states: West Virginia Geological and Economic Survey Bulletin 22, 87 p.

Dennison, J.M., 1976, Appalachian Queenston delta related to eustatic sea-level drop accompanying Late Ordovician glaciation centered in Africa, in Bassett, M.G., ed., The Ordovician System: Cardiff, University of Wales Press, p. 107–120.

Dennison, J.M., 1982, Uranium favorability of nonmarine and marginal-marine strata of late Precambrian and Paleozoic age in Ohio, Pennsylvania, New Jersey, and New York: U.S. Department of Energy National Uranium Resource Evaluation Report GJBX–50 (82), 254 p.

Dennison, J.M., and Head, J.W., 1975, Sea level variation interpreted from the Appalachian basin Silurian and Devonian: American Journal of Science, v. 275, p. 1089–1120.

Dennison, J.M., and Jolley, R., 1979, Devonian shales of south-central Pennsylvania and Maryland: Guidebook for the Annual Field Conference of Pennsylvania Geologists, v. 44, p. 67–90.

Dennison, J.M., Beuthin, J.D., and Hasson, K.O., 1986, Latest Devonian-earliest Carboniferous marine transgressions, central and southern Appalachians, USA, in Bless, M.J.M., and Streel, Maurice, eds., Late Devonian events around the Old Red Continent; Field conference in Aachen (FGR), with excursions in the Ardenne (Belgium), the Rheinisches Schiefergebirge (FRG) and in Moravia (CSSR): Annales de la Société Géologique de Belgique, v. 109, p. 123–129.

De Witt, Wallace, Jr., 1970, Age of the Bedford Shale, Berea Sandstone, and Sunbury Shale in the Appalachian and Michigan basins: U.S. Geological Survey Bulletin 1294–G, 11 p.

Donaldson, A.C., and Schumaker, R.C., 1981, Late Paleozoic molasse of the central Appalachians, in Miall, A.D., ed.,

Sedimentation and tectonics in alluvial basins: Geological Association of Canada Special Paper 23, p. 99–124.

Dorobek, S.L., and Read, J.F., 1986, Sedimentology and basin evolution of the Siluro-Devonian Helderberg Group, central Appalachians: Journal of Sedimentary Petrology, v. 56, p. 601–613.

Drake, A.A., Jr., Sinha, A.K., Laird, Jo, and Guy, R.E., 1989, The Taconic orogen, *in* Hatcher, R.D., Jr., Thomas, W.A., and Viele, G.W., eds., The Appalachian-Ouachita orogen in the United States, v. F–2 *of* The geology of North America: Boulder, Colo., Geological Society of America, p. 101–177.

Eames, L.E., 1974, Palynology of the Berea Sandstone and Cuyahoga Group of northeastern Ohio: East Lansing, Michigan State University, Ph.D. dissertation, 215 p.

Eble, C.F., 1994, Palynostratigraphy of selected Middle Pennsylvanian coal beds in the Appalachian basin, *in* Rice, C.L., ed., Elements of Pennsylvanian stratigraphy, central Appalachian basin: Geological Society of America Special Paper 294, p. 55–68.

Eble, C.F., 2003, Palynological perspectives of late Middle Pennsylvanian coal beds, *in* Cecil, C.B., and Edgar, N.T., eds., Climate controls on stratigraphy: SEPM Special Publication 77, SEPM (Society for Sedimentary Geology), p. 123–135.

Edmunds, W.E., and Eggleston, J.R., 1993, Unconformable Mississippian-Pennsylvanian contact (Mauch Chunk, Pottsville, and Allegheny Formations), *in* Shaulis, J.R., Brezinski, D.K., Clark, G.M., and others, Geology of the southern Somerset County region, southwestern Pennsylvania: 58th Annual Field Conference of Pennsylvania Geologists, Somerset, Pa., Guidebook, p. 82–88.

Ferm, J.C., and Horne, J.C., 1979, Carboniferous depositional environments in the Appalachian region: Columbia, Department of Geology, University of South Carolina, 760 p.

Fichter, L.S., and Diecchio, R.J., 1986, Stratigraphic model for timing the opening of the Proto-Atlantic Ocean in northern Virginia: Geology, v. 14, p. 307–309.

Flint, N.K., 1965, Geology and mineral resources of southern Somerset County, Pennsylvania: Pennsylvania Topographic and Geologic Survey, 4th Series, County Report 56 A, 267 p.

Frakes, F.A., Frances, J.E., and Syktus, J.I., 1992, Climate modes of the Phanerozoic: Cambridge, United Kingdom, Cambridge University Press, 274 p.

Grabau, A.W., 1932, Principles of stratigraphy: 3d ed., New York, A.G. Seiler, 1185 p.

Grabau, A.W., 1940, The rhythm of the ages: Peking, China, Henri Vetch, 561 p.

Hardie, L.A., 1989, Cyclic platform carbonates in the Cambro-Ordovician of the central Appalachians, *in* Walker, K.R., Read, J.F., and Hardie, L.A., leaders, Cambro-Ordovician banks and siliciclastic basins of the United States Appalachians: Field Trip Guidebook T161 for the 28th International Geological Congress: Washington, D.C., American Geophysical Union, p. 51–78.

Harper, J.A., and Laughrey, C.D., 1989, Upper Devonian and Lower Mississippian stratigraphy and depositional systems, *in* Harper, J.A., ed., Geology in the Laurel Highlands of southwestern Pennsylvania: 54th Annual Field Conference of Pennsylvania Geologists, Johnstown, Pa., Guidebook, p. 35–62.

Head, J.W., 1969, The Keyser Limestone at New Creek, West Virginia; An illustration of Appalachian early Devonian depositional basin evolution, *in* Donaldson, A.C., ed., Some Appalachian coals and carbonates; Models of ancient shallow water deposition: Geological Society of America field trip guidebook, p. 323–355.

Hoque, M., 1975, Paleocurrent and paleoslope—A case study: Palaeogeography, Palaeoclimatology, Palaeoecology, v. 17, p. 77–85.

Johnson, J.G., Klapper, G., and Sandberg, C.A., 1985, Devonian eustatic fluctuations in Euramerica: Geological Society of America Bulletin, v. 95, no. 5, p. 567–587.

Kammer, T.W., and Bjerstedt, T.W., 1986, Stratigraphic framework of the Price Formation (Upper Devonian-Lower Mississippian) in West Virginia: Southeastern Geology, v. 27, p. 13–32.

Kosanke, R.M., 1973, Palynological studies of the coals of the Princess Reserve district in northeastern Kentucky: U.S. Geological Survey Professional Paper 839, 24 p.

Kosanke, R.M., 1984, Palynology of selected coal beds in the proposed Pennsylvanian System stratotype in West Virginia: U.S. Geological Survey Professional Paper 1318, 44 p.

Kosanke, R.M., and Cecil, C.B., 1996, Late Pennsylvanian climate changes and palynomorph extinctions, *in* Wnuk, C., and Pfefferkorn, H.W., eds.: Review of Palaeobotany and Palynology, v. 90, no. 1–2, p. 113–140.

Krumbein, W.C., and Garrels, R.M., 1952, Origin and classification of chemical sediments in terms of pH and oxidation potentials: American Association of Petroleum Geologists Bulletin, v. 60, p. 1–33.

Kuenen, PH.H., 1960, Experimental abrasion 4; Eolian action: Journal of Geology, v. 68, no. 4, p. 427–449.

Laughrey, C.D., Harper, J.A., and Kaktins, U., 1989, Upper Devonian and Lower Mississippian (Stop 4): 54th Annual Field Conference of Pennsylvania Geologists, Johnstown, Pa, Guidebook, p. 183–205.

McBride, E.F., 1963, A classification of common sandstones: Journal of Sedimentary Petrology, v. 33, p. 664–669.

Meckel, L.D., 1967, Origin of Pottsville conglomerates (Pennsylvanian) in the central Appalachians: Geological Society of America Bulletin, v. 78, p. 223–258.

Mitchell, R.W., 1982, Middle Ordovician St. Paul Group, in Lyttle, P.T., Central Appalachian geology; Field trip guidebook for the joint meeting of the Northeastern and Southeastern Sections of the Geological Society of America, Washington, D.C., 1982: Falls Church, Va., American Geological Institute p. 175–216.

Neuman, R.B., 1951, St. Paul Group; A revision of the "Stones River" Group of Maryland and adjacent states: Geological Society of America Bulletin, v. 62, no. 3, p. 267–324.

Nunan, W.E., 1979, Stratigraphy of the Weverton Formation, northern Blue Ridge anticlinorium: Chapel Hill, University of North Carolina, Ph.D. dissertation, 215 p.

Palmer, A.R., 1981, Subdivision of the Sauk Sequence, in Taylor, M.E., ed., Short Papers for the Second International Symposium on the Cambrian System: U.S. Geological Survey Open-File Report 81–742, p. 160–161.

Pepper, J.F., de Witt, W., Jr., and Demarest, D.F., 1954, Geology of the Bedford Shale and Berea Sandstone in the Appalachian basin: U.S. Geological Survey Professional Paper 259, 111 p.

Peppers, R.A., 1970, Correlation and palynology of coals in the Carbondale and Spoon Formations (Pennsylvanian) of the northeastern part of the Illinois basin: Illinois State Geological Survey Bulletin 93, 173 p.

Platt, Franklin, and Platt, W.G., 1877, Report of progress in the Cambria and Somerset district of the bituminous coal fields of western Pennsylvania; Part II, Somerset: Pennsylvania Geological Survey Report of Progress, 2d Series, v. HHH, 348 p.

Presley, M.W., 1979, Facies and depositional systems of the Upper Mississippian and Pennsylvanian strata in the central Appalachians, in Donaldson, A.C., Presley, M.W., and Renton, J.J., eds., Carboniferous coal guidebook: West Virginia Geological and Economic Survey Bulletin B–37–1, p. 1–50.

Ravn, R.L., 1986, Palynostratigraphy of the Lower and Middle Pennsylvanian coals of Iowa: Iowa Geological Survey Technical Paper No. 7, 245 p.

Read, J.F., 1981, Carbonate platform slopes of extensional continental margins: American Association of Petroleum Geologists Bulletin, v. 65, no. 5, p. 976.

Read, J.F., 1989, Controls on evolution of Cambrian-Ordovician passive margin, U.S. Appalachians, in Crevello, P.D., Wilson, J.L., Sarg, J.F., and Read, J.F., eds., Controls on carbonate platform and basin development: Society of Economic Paleontologists and Mineralogists Special Publication 44, p. 147–165.

Retallack, G.J., 1989, Soils of the past; An introduction to paleopedology: Winchester, Massachusetts, Unwin Hyman, 520 p.

Retallack, G.J., 1993, Late Ordovician paleosols in the Juniata Formation near Potters Mills, PA, in Driese, S.G., ed., Paleosols, Paleoclimate, and Paleoatmospheric CO_2: International Association of Geochemistry and Cosmochemistry—3d International Symposium on Geochemistry of the Earth's Surface and SEPM (Society for Sedimentary Geology) Field Trip: University of Tennessee, Knoxville publication EO1–1040–001–94, p. 33–50.

Ross, C.A., and Ross, J.R.P., 1988, Late Paleozoic transgressive-regressive deposition, in Wilgus, C.K., Hastings, B.S., Ross, C.A., Posamentier, H., Van Wagoner, J., and Kendall, C.G.St C., Sea-level changes; An integrated approach: Society of Economic Paleontologists and Mineralogists Special Publication 42, p. 227–247.

Rowley, D.B., Raymond, A., Parrish, J.T., Lottes, A.L., Scotese, C.R., and Ziegler, A.M., 1985, Carboniferous paleogeographic, phytographic and paleoclimatic reconstructions: International Journal of Coal Geology, v. 5, no. 1–2, p. 7–43.

Ryder, R.T., Harris, A.G., and Repetski, J.E., 1992, Stratigraphic framework of Cambrian and Ordovician rocks in the central Appalachian basin from Medina County, Ohio, through southwestern and south-central Pennsylvania to Hampshire County, West Virginia: U.S. Geological Survey Bulletin 1839–K, 32 p.

Saunders W.B., and Ramsbottom, W.H.C., 1986, The mid-Carboniferous eustatic event: Geology, v. 14, p. 208–212.

Sando, W.J., 1957, Beekmantown Group (Lower Ordovician) of Maryland: Geological Society of America Memoir 68, 161 p.

Schwab, F.L., 1971, Harpers Formation, central Virginia: A sedimentary model: Journal of Sedimentary Petrology, v. 41, p. 139–149.

Schwab, F.L., 1972, The Chilhowee Group and the late Precambrian-early Paleozoic sedimentary framework in the central and southern Appalachians, in Lessing, P., Hayhurst, R.I., Barlow, J.A., and Woodfork, L.D. eds., Appalachian structures origin, evolution, and possible potential for new exploration frontiers: West Virginia University and West Virginia Geological and Economic Survey Seminar, p. 59–101.

Scotese, C.R., 1998, Quicktime computer animations, PALEOMAP project: Arlington, Texas, Department of Geology,

University of Texas at Arlington.

Sevon, W.D., 1969, The Pocono Formation in northeastern Pennsylvania: 34th Annual Field Conference of Pennsylvania Geologists, Hazelton, Pa., Guidebook, 129 p.

Sheppard, S.J., and Heald, M.T., 1984, Petrology of the Huntersville Chert: Southeastern Geology, v. 25, no. 1, p. 37–47.

Shinn, E.A., 1973, Sedimentary accretion along the leeward, SE coast of Qatar Peninsula, Persian Gulf, *in* Purser, B.H., ed., The Persian Gulf: New York, Springer-Verlag, p. 199–209.

Simpson, E.L., and Eriksson, K.A., 1989, Sedimentology of the Unicoi Formation in southern and central Virginia; Evidence for Late Proterozoic to Early Cambrian rift-to-passive margin transition: Geological Society of America Bulletin, v. 101, no. 1, p. 42–54.

Sloss, L.L., 1963, Sequences in the cratonic interior of North America: Geological Society of America Bulletin, v. 74, p. 93–113.

Soil Survey Staff, 1975, Soil taxonomy: U.S. Department of Agriculture Handbook Number 436, 754 p.

Southworth, S., and Brezinski, D.K., 1996, Geology of the Harpers Ferry quadrangle, Virginia, Maryland, and West Virginia: U.S. Geological Survey Bulletin 2123, 33 p.

Smosna, R., and Patchen, D., 1978, Silurian evolution of the central Appalachian basin: American Association of Petroleum Geologists Bulletin, v. 62, p. 2308–2328.

Stamm, R.G., and Wardlaw, B.R., 2003, Conodont faunas of the late Middle Pennsylvanian (Desmoinesian) lower Kittanning cyclothem, U.S.A., *in* Cecil, C.B., and Edgar, N.T., eds., Climate controls on stratigraphy, SEPM Special Publication 77, SEPM (Society for Sedimentary Geology), p. 95–121.

Stevenson, J.J., 1873, Notes on the geology of West Virginia: American Philosophical Society Transactions, new series, v. 15, p. 15–32.

Stevenson, J.J., 1876, Report of progress in the Greene and Washington district of the bituminous coal fields of western Pennsylvania: Pennsylvania Geological Survey Report of Progress, 2d Series, v. K, 419 p.

Stevenson, J.J., 1878, Report of progress in the Fayette and Westmoreland district of the bituminous coal fields of western Pennsylvania; Part II, The Ligonier Valley: Pennsylvania Geological Survey Report of Progress, 2d Series, v. KKK, 331 p.

Stone, C.G., Howard, J.M., and Haley, B.R., 1986, Sedimentary and igneous rocks of the Ouachita Mountains of Arkansas; A guidebook with contributed papers: Little Rock, Arkansas Geological Commission, 151 p.

Streel, Maurice, 1986, Miospore contribution to the upper Famennian-Strunian event stratigraphy, *in* Bless, M.J.M., and Streel, Maurice, eds., Late Devonian events around the Old Red Continent; Field conference in Aachen (FGR), with excursions in the Ardenne (Belgium), the Rheinisches Schiefergebirge (FRG) and in Moravia (CSSR): Annales de la Société Géologique de Belgique, v. 109, no. 1, p. 75–92.

Suter, T.D., 1991, The origin and significance of Mississippian polymictic diamictites in the central Appalachian basin: Morgantown, West Virginia University, Ph.D. dissertation, 369 p.

Swartz, C.K., 1923, Stratigraphic and paleontologic relations of the Silurian strata of Maryland: Maryland Geological Survey Systematic Report, p. 25–50.

Taylor, J.F., Repetski, J.E., and Orndorff, R.C., 1993, The Stonehenge Limestone; Anatomy of a third-order transgressive-regressive cycle in the Lower Ordovician of the central Appalachians [abs.]: Geological Society of America Abstracts with Programs, v. 24, no. 3, p. 80.

Thompson, A.M., 1999, Ordovician, *in* Shultz, C.H., ed., The geology of Pennsylvania: Pennsylvania Geological Survey and Pittsburgh Geological Society Special Publication 1, p. 75–89.

Thompson, A.M., and Sevon, W.D., 1982, Comparative sedimentology of Paleozoic clastic wedges in the central Appalachians, U.S.A.: Hamilton, Ontario, Eleventh International Congress on Sedimentology, Excursion 19B, Guidebook, 136 p.

Thornthwaite, C.W., 1948, An approach toward a rational climate classification: Geographical Review, v. 38, p. 55–94.

Vail, P.R., Mitchum, R.M., and Thompson, S., 1977, Seismic stratigraphy and global changes of sea level, *in* Payton, C.E., ed., Seismic stratigraphy—Applications to hydrocarbon exploration: American Association of Petroleum Geologists Memoir 26, p. 53–62.

Veevers, J.J., and Powell, M., 1987, Late Paleozoic glacial episodes in Gondwanaland reflected in transgressive-regressive depositional sequences in Euramerica: Geological Society of America Bulletin, v. 98, no. 4, p. 475–487.

Waagé, K.M., 1950, Refractory clays of the Maryland coal measures: Maryland Geological Survey Bulletin 9, 182 p.

Wehr, F., and Glover, L., III, 1985, Stratigraphy and tectonics of the Virginia-North Carolina Blue Ridge; Evolution of a Late Proterozoic-early Paleozoic hinge zone: Geological Society of America Bulletin, v. 96, no. 3, p. 285–295.

White, I.C., 1878, Report of progress in the Beaver River district of the bituminous coal fields of western Pennsylvania, with analyses of coal, cannel, coke, clay, limestone, and ore, from Butler and Beaver Counties, Pennsylvania by A.S. McCreath: Pennsylvania Geological Survey Report of Progress, 2d Series, v. Q, 337 p.

White, I.C., 1891, Stratigraphy of the bituminous coal field of Pennsylvania, Ohio, and West Virginia: U.S. Geological Survey Bulletin 65, 212 p.

White, I.C., 1903, The Appalachian coal field, the Conemaugh series: West Virginia Geological Survey Report, v. 2, p. 225–332.

Wilmarth, M.G., 1938, Lexicon of geologic names of the United States (including Alaska): U.S. Geological Survey Bulletin 896, pt. 1, A–L, p. 1–1244; pt. 2, M–Z, p. 1245–2396.

Ziegler, A.M., Raymond, A.L., Gierlowski, T.C., Horrell, M.A., Rowley, D.B., and Lottes, A.L., 1987, Coal, climate and terrestrial productivity; The present and Early Cretaceous compared, *in* Scott, A.C., ed., Coal and coal-bearing strata; Recent advances: Geological Society of London Special Publication, v. 32, p. 25–49.

PLATE FOLLOWS

PLATE 1.
[Conodonts from the Deer Valley and Loyalhanna Limestone Members of the Mauch Chunk Formation]

FIGURES 1, 2.   Conodonts from the Deer Valley Member of the Mauch Chunk Formation, Keystone quarry, Pa. This collection (93RS–79c) is from the lower 10 cm of the Deer Valley Member. Note the non-abraded, although slightly broken, conodont elements of the high-energy oolitic marine facies of the Deer Valley Member.

      1. *Kladognathus* sp., Sa element, posterior view, X140.

      2. *Cavusgnathus unicornis*, gamma morphotype, Pa element, lateral view, X140.

    3–9.   Conodonts from the uppermost Loyalhanna Limestone Member of the Mauch Chunk Formation, Keystone quarry, Pa. This collection (93RS–79b) is from the upper 10 cm of the Loyalhanna Member. Note the highly abraded and reworked aeolian forms.

      3, 4. *Kladognathus* sp., Sa element, lateral views, X140.

      5. *Cavusgnathus unicornis*, alpha morphotype, Pa element, lateral view, X140.

      6, 7. *Cavusgnathus* sp., Pa element, lateral view, X140.

      8. *Polygnathus* sp., Pa element, upper view, reworked Late Devonian to Early Mississippian morphotype, X140.

      9. *Gnathodus texanus*?, Pa element, upper view, X140.

   10–14.   Conodonts from the basal 20 cm of the Loyalhanna Limestone Member of the Mauch Chunk Formation, Keystone quarry, Pa. (93RS–79a), and Westernport, Md. (93RS–67). Note the highly abraded and reworked aeolian forms.

      10. *Polygnathus* sp., Pa element, upper view, reworked Late Devonian to Early Mississippian morphotype, 93RS–79a, X140.

      11. *Polygnathus* sp., Pa element, upper view, reworked Late Devonian to Early Mississippian morphotype, 93RS–67, X140.

      12. *Gnathodus* sp., Pa element, upper view, reworked Late Devonian(?) through Mississippian morphotype, 93RS–67, X140.

      13. *Kladognathus* sp., M element, lateral views, 93RS–67, X140.

      14. *Cavusgnathus* sp., Pa element, lateral view, 93RS–67, X140.
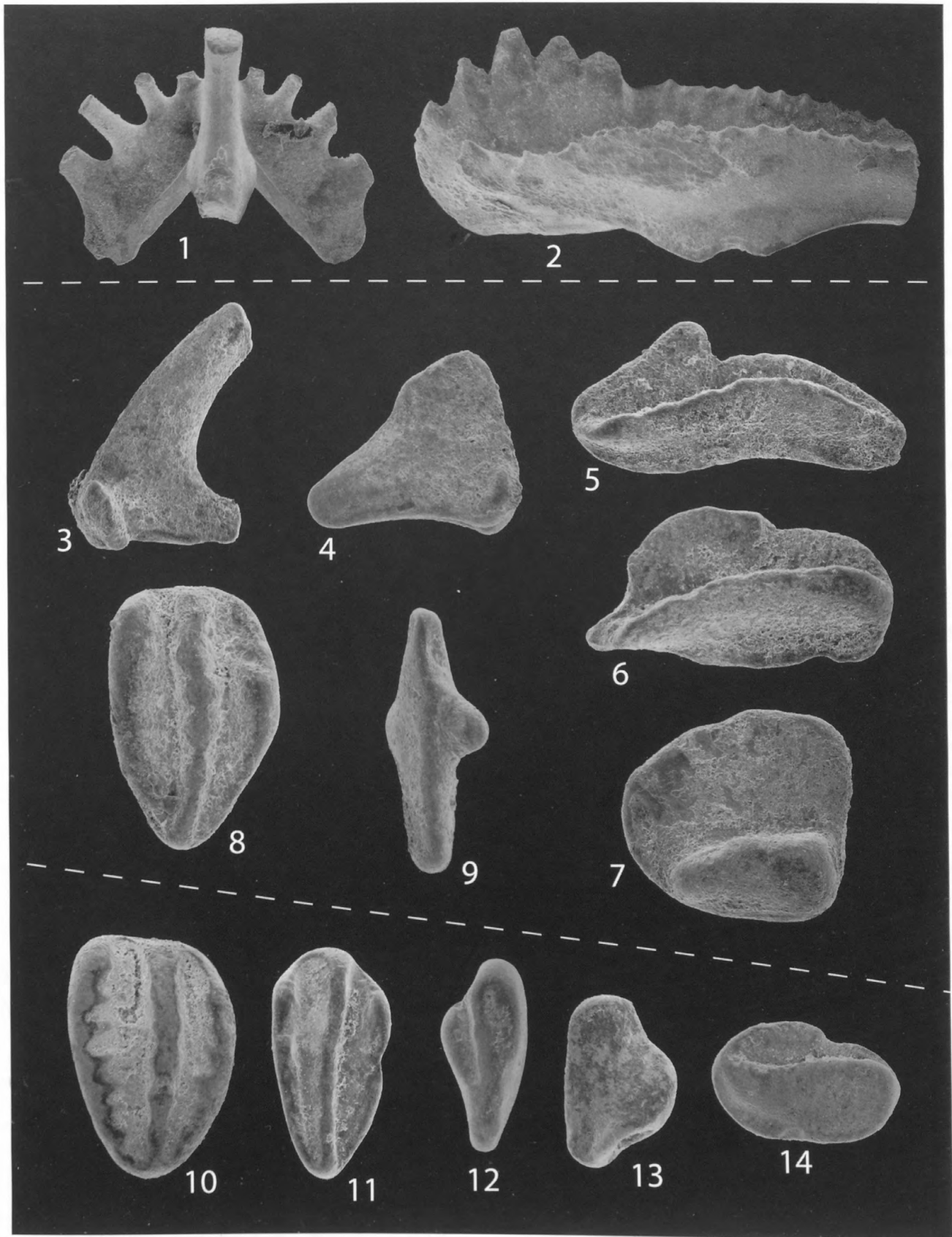
4. Middle Eocene Igneous Rocks in the Valley and Ridge of Virginia and West Virginia

By Jonathan L. Tso,[1] Ronald R. McDowell,[2] Katharine Lee Avary,[2] David L. Matchen,[2] and Gerald P. Wilkes[3]

Introduction

The igneous rocks of Highland County, Va., and Pendleton County, W. Va., have fascinated and puzzled geologists since the 19th century. The rocks form a series of bodies, ranging from dikes and sills only a half-meter (m) (1.6 feet (ft)) or so wide (Stop 3), to larger necks and diatremes, such as Trimble Knob (Stop 2), with a diameter of approximately 150 m (500 ft). The bodies are found over a widespread area that tends to concentrate around two centers: Trimble Knob in Highland County and Ugly Mountain in southern Pendleton County (fig. 1).

The igneous rocks contrast sharply with their geological surroundings. Highland and Pendleton Counties lie within the Valley and Ridge physiographic province, a region dominated by folded and faulted Paleozoic clastic and carbonate sedimentary rocks (Butts, 1940; Woodward, 1941, 1943). The igneous rocks of the area intrude and crosscut the sedimentary rocks, which range in age from Ordovician through Devonian, and the Alleghanian-age regional folding (Rader and Wilkes, 2001).

The anomalous nature of these rocks has been recognized for at least a century. N.H. Darton (1894, 1899) described and mapped a number of occurrences of exposed igneous rocks in the area and described their petrology and petrography (Darton and Diller, 1890; Darton and Keith, 1898). Watson and Cline (1913) described the igneous rocks of Augusta County, Va. Over the years, these rocks have been the subject of numerous thesis projects (Dennis, 1934; Garnar, 1951; Kapnicky, 1956; Kettren, 1970; Hall, 1975). In later years, detailed field guides and petrologic descriptions were published in the scientific literature by Garnar (1956) and by Johnson and others (1971).

Prior to 1969, the precise age of the rocks was unknown. It was inferred that they were late Paleozoic or younger, based on crosscutting relations observed in the field (Garnar,

1956). Prior to studies employing radiometric methods, these rocks were thought to be of Mesozoic age (Darton and Diller, 1890; Johnson and Milton, 1955; Zartman and others, 1967), and related to rifting as the Atlantic Ocean basin opened.

However, using K-Ar and Rb-Sr isotopic techniques to date rocks that they thought were temporally related the Devonian Tioga Bentonite, Fullagar and Bottino (1969), came to the surprising conclusion that the rocks were a much younger age of approximately 47 Ma, placing them in the Eocene. This Eocene age is quite significant, making these rocks the youngest known igneous rocks in the Eastern United States.

This discovery sparked more research and speculation about the origin of the rocks. Southworth and others (1993), attempting to synthesize what was known about the rocks, employed isotopic and geochemical methods on both Eocene and Mesozoic igneous rocks over a wide area in Highland, Rockingham, and Pendleton Counties. They came to the following conclusions: (1) the Eocene rocks are bimodal in composition and include mafic (basalt, picrobasalt, and basanite) and felsic (trachyte, trachydacite, and rhyolite) members (fig. 2); (2) radiometric dates combined with paleomagnetic dates are consistently middle Eocene, at around 48 Ma (Trimble Knob in Highland County is the youngest at 35 Ma); (3) the igneous activity was generally short-lived, with the bulk of it occurring within a span of perhaps a few million years; (4) isotopic evidence does not indicate significant crustal assimilation, suggesting that the magmas moved rapidly upward, possibly through deep-seated fractures; and (5) chemical plots of major and minor elements indicate that the mafic and felsic rocks had a common source, possibly in the mantle, and their tectonic environment was consistent with within-plate continental extension. Of note was the discovery that not all the igneous rocks in the region are Eocene. A sample of mica pyroxenite from Pendleton County was dated at 143.8 Ma.

As a result of these studies, several questions, with no scientific consensus, remain. First, the Eocene epoch in eastern North America is not generally known to be a time of great tectonic activity. Poag and Sevon (1989), studying the sediments on the Atlantic Continental Shelf, Slope, and Rise, document relatively low sedimentation rates during the Eocene, with low stream gradients, high sea level, and a trop-

[1]Department of Geology, Radford University, Radford, VA 24141.

[2]West Virginia Geological and Economic Survey, Morgantown, WV 26507.

[3] Virginia Department of Mines, Minerals and Energy, Division of Mineral Resources, Charlottesville, VA 22903.
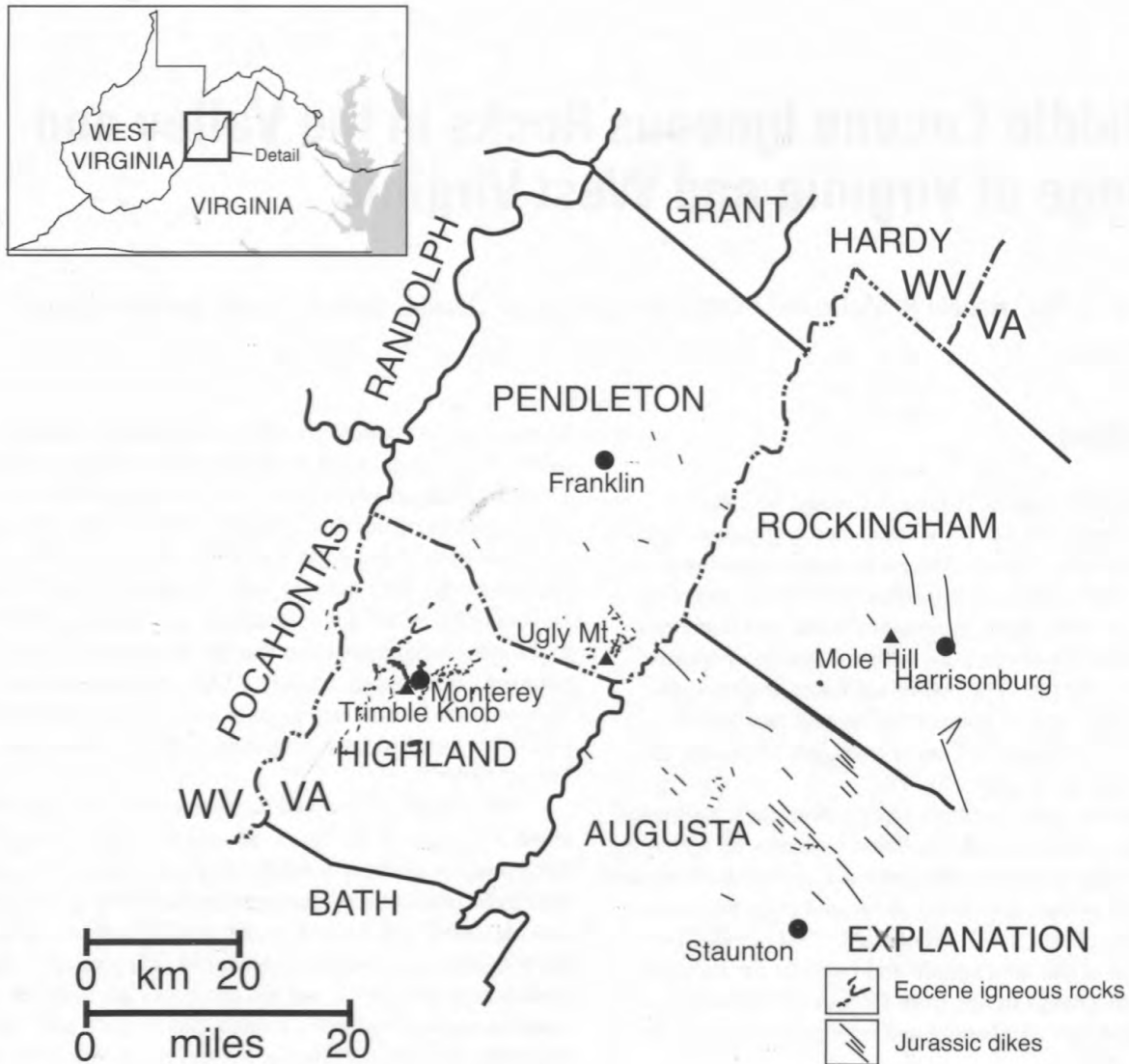
Figure 1. Regional map showing the location of the field trip area (in the central box in the upper left inset), the distribution of Jurassic dikes in a part of the Shenandoah Valley, Va., and the middle Eocene igneous rocks in the central Appalachian Valley and Ridge province (modified from Southworth and others, 1993).

ical rainforest environment. In this setting, what caused the igneous activity?

Of the numerous theories that have been proposed, some suggest that (1) a regional basement fracture zone, the 38th Parallel lineament, provided a focus for igneous activity (Fullagar and Bottino, 1969; Dennison and Johnson, 1971); (2) a still-cooling intrusion is responsible for the regional uplift of the "Virginia Highlands" and the nearby hot springs of Bath County (Dennison and Johnson, 1971); (3) a global shift in plate tectonic motion occurred during the Eocene, which resulted in the formation of the Bermuda Rise and was also responsible for igneous activity as far inland as Highland County (Vogt, 1991); (4) the transition between thin Atlantic lithosphere and thick North American lithosphere created a small-scale downwelling convection current, and the Eocene

igneous activity was a result of an upwelling return flow (Gittings and Furman, 2001, citing King and Ritsema, 2000); and (5) the North American plate at this time overrode the hinge of the subducting Pacific plate, which reactivated pre-existing structures and produced magmatism (Grand, 1994). Southworth and others (1993) summarized the merits of many of the theories and concluded that a combination of causes (a reactivation of basement fracture zones and a plate-tectonical-ly driven extension of North America, possibly associated with a shift in plate tectonic direction in the Eocene) provided the right conditions to form magma.

A second unresolved question involves how the magma or magmas evolved to form the bimodal compositional range that varies from olivine-bearing basalt to rhyolite. Although the actual relative percentage of mafic rocks versus felsic

TOTAL-ALKALI-SILICA DIAGRAM
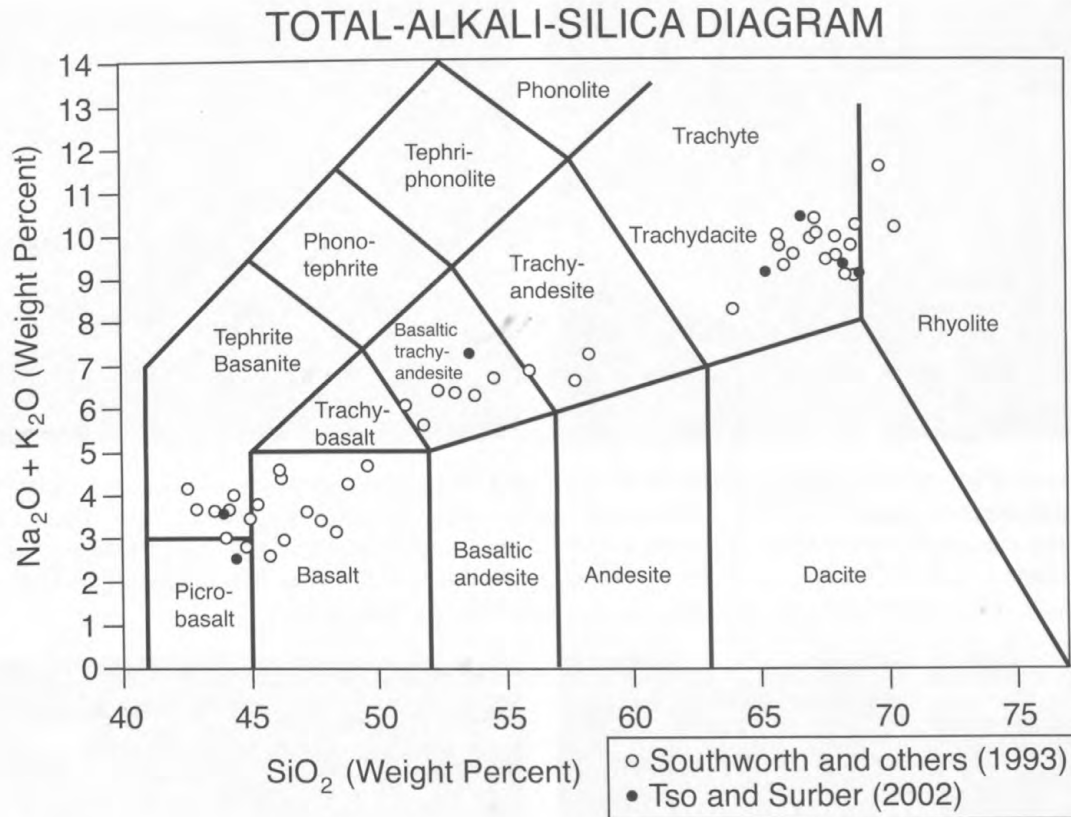
Figure 2. Major-element chemical classification based on $Na_2O + K_2O$ against SiO_2, based on the method of Le Bas and others (1986). The open circles are analyses from Southworth and others (1993), and the closed circles are from Tso and Surber (2002).

rocks is not known, known exposures (Johnson and others, 1971) suggest that they are present in roughly equal proportions. Southworth and others (1993) concluded that both magma types intruded in approximately the same timeframe. Both magma types can be found in very close proximity, although crosscutting relations are commonly obscured. We will consider this problem further as we visit sites during this field trip. There is much in the way of conflicting data. At the Hightown Quarry in Highland County, a mafic dike cuts across a felsic dike (Rader and others, 1986). Any petrologic model must include a common source for all the Eocene intrusives (Hall, 1975; Southworth and others, 1993) and provide a deep source and minimal assimilation of the continental crust (Southworth and others, 1993).

## Petrology

Mafic Rocks

The mafic rocks are dark gray to black in color. They range from aphanitic to porphyritic with phenocrysts that include plagioclase, clinopyroxene, and occasionally olivine and biotite (fig. 3). Matrix minerals include abundant thin laths of plagioclase, opaque (magnetite) and clinopyroxene.

Some rocks show a parallel alignment of matrix plagioclase, indicating a flow texture. Amygdules may also be present, with zeolite, calcite, and quartz the principal minerals filling the cavities. Xenoliths of country rock are common, and will be observed at Stop 7.
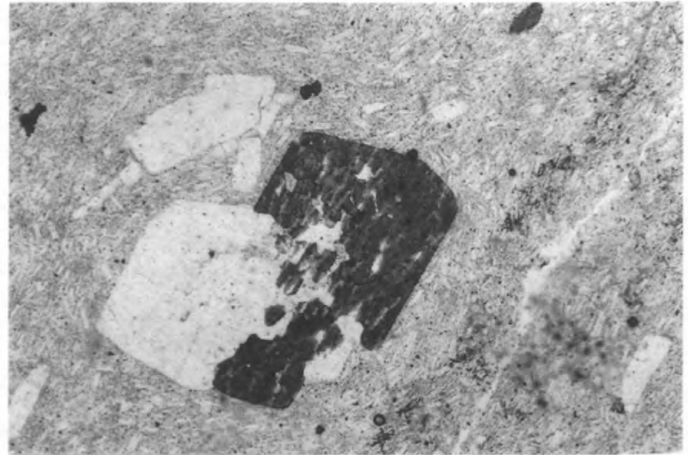
Felsic Rocks

Compared to mafic rocks, the felsic rocks are more mineralogically variable and texturally complex, and provide more details of their eruptive history. They contrast in the field from the mafic rocks by their light- to medium-gray color when fresh, which weathers to buff to pink. The most abundant mineral in all felsic rocks is plagioclase, which composes 80 to 95 percent of the rock. Matrix textures commonly show parallel alignments of feldspar laths. Most felsic rocks are porphyritic with phenocrysts that include plagioclase (most common), biotite, hornblende, orthopyroxene (rare), and orthoclase (rare) (fig. 4). Amygdules are observed in felsic rocks as well, but less commonly than in mafic rocks.

Felsic rocks can show textural complexity. Felsic rocks observed near Stop 3 contain inclusions of older felsic rock, seen as parallel lenses on the centimeter scale (fig. 5). In thin section, these inclusions are observed as elliptical areas showing internal flow banding in orientations slightly different
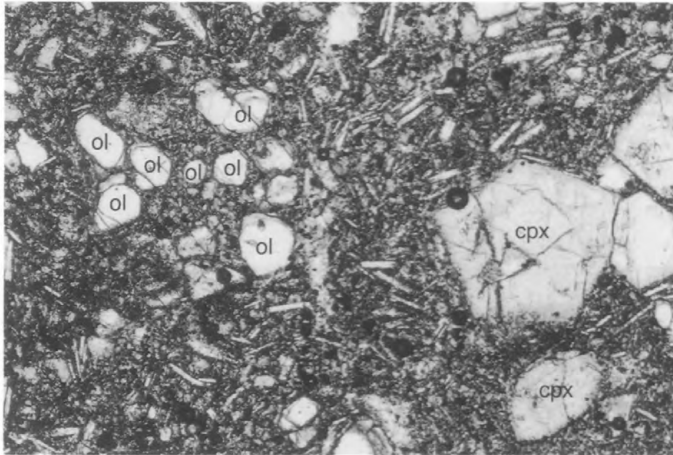
Figure 3. Photomicrograph of a porphyritic-aphanitic basalt. Clinopyroxene (cpx) and altered olivine (ol) phenocrysts are set in a fine matrix that contains thin laths of plagioclase. Plain polarized light; length of photo is 2.6 mm.

Figure 4. Photomicrograph of a porphyritic-aphanitic felsic rock. Plagioclase phenocrysts (white) and hornblende phenocryst (dark; intergrown with plagioclase) are set in a fine matrix of plagioclase laths that show flow structure. Plain polarized light; length of photo is 2.6 mm.
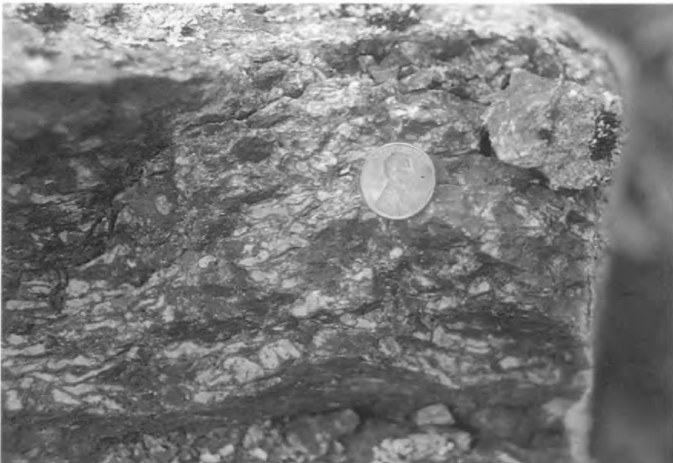
Figure 5. Photograph of a felsic rock composed of lens-shaped inclusions of older felsic rock. The inclusions are parallel, imparting a strong flow structure to the rock. Within the lenses, on the microscopic scale, plagioclase laths also show a strong flow structure parallel to the lengths of the lenses.

Figure 6. Photograph of volcaniclastic unit at Stop 4 described previously as a diatreme (Kettren, 1970) or volcanic breccia. The elongate clast in the center of the photograph is porphyritic basalt similar to dikes seen elsewhere on the Hull property. See figures 20 and 21 for closer views. Rock hammers for scale.

from the flow banding of the matrix. Felsic rocks may contain xenoliths of sedimentary country rocks. Rocks containing these xenoliths have a finer grained matrix than other felsic rocks, indicating that they cooled more quickly and probably formed near the margin of the body next to the country rock.

Breccias

A third type of igneous rock is breccia, or diatreme. Unlike mafic and felsic rocks that formed in dikes or sills, the breccias are commonly found in circular bodies that we interpret to represent cross-sectional views of diatreme pipes. The sizes of these bodies range from a few meters in diameter to

approximately 150 m (500 ft) (Rader and others, 1986) at Trimble Knob.

In general, breccias contain abundant xenoliths of older igneous rocks, sedimentary country rocks, and individual crystals of various minerals such as plagioclase, olivine, clinopyroxene, hornblende, and biotite, embedded in a fine, highly altered, vesicular matrix. The xenoliths range in size from a few millimeters to approximately 1.25 m (4 ft) in diameter at the Hull Farm (Stop 4; fig. 6) and are typically subrounded in shape. In general, the xenoliths appear unlayered and unsorted. However, in a few places, a crudely developed size sorting is observed as a weak layering of the coarse xenoliths (fig. 7). At Stop 3, the layering is on a scale of 4 to 10 centimeters (cm) (1.6–3.9 inches (in)), and its N. 45° W.

Figure 7. Photograph of "Breccia no. 1" at Stop 3. Note the weakly developed beds of coarser clasts that occur below and above the quarter at the left-center of the picture and parallel to the long dimension of the picture.
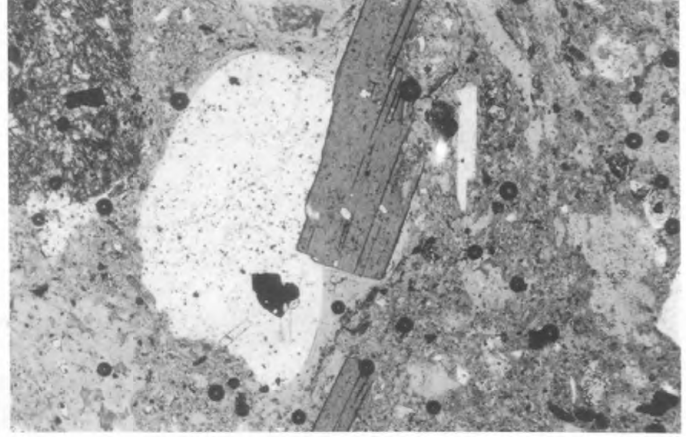

Figure 8. Photomicrograph from "Breccia no. 2" (near Stop 3) showing a rounded abraded plagioclase xenocryst with attached biotite. The morphological similarity between single crystals in breccias and those as phenocrysts within xenoliths suggests that many xenocrysts are derived from xenoliths. Other thin sections show various stages of phenocrysts separating out of xenoliths. A mafic xenolith is in the upper left corner. Plain polarized light; length of photo is 2.6 mm.

strike with steep southwest dip runs counter to the predominantly northeast strike of the bedding of the surrounding rocks. Typically, matrices are fine grained, highly altered, vuggy, and generally indecipherable in thin section.

As a general rule, the sedimentary xenoliths are a reflection of the identity of the immediate wall rock. Thus, at Stop 4, clasts of Helderberg Group and Oriskany Sandstone are indicative of the local bedrock, and similarly, at Stop 3, limestone and calcareous shale xenoliths are similar to the Wills Creek and Tonoloway Formations that dominate the area.

Diatremes are typically found in direct association with nearby mafic or felsic dikes or sills, with the overall composition of the diatreme and its igneous xenoliths reflecting the composition of these dikes and sills. We will see two mafic diatremes at Stops 3 and 4. Basalt xenoliths and xenocrysts of clinopyroxene and olivine embedded in a dark, nearly black matrix are common within these diatremes.

On the other hand, diatreme compositions can be complex, with contributions from multiple compositions of igneous rock. Although we will not visit this locality, a dominantly felsic diatreme ("Breccia no. 2") occurs near Stop 3. There, the overall color of the matrix is medium gray, with abundant felsic xenoliths and xenocrysts of plagioclase, biotite, and hornblende reflecting the felsic dikes nearby. However, this diatreme is unusual in that it also contains basalt xenoliths and clinopyroxene and olivine xenocrysts despite the fact that mafic rocks are uncommon in the immediate surrounding area. An implication is that here, the felsic magma that powered the diatreme postdated the mafic intrusion that formed the xenoliths.

Individual crystals are a ubiquitous feature of all diatremes. Many grains are broken fragments of once larger

crystals. However, many crystals preserve euhedral shapes. Two sources for these individual crystals are (1) as phenocrysts from the magmas that powered the formation of the breccia pipes and (2) as xenocrysts derived from xenoliths (Mitchell, 1986). In the former situation, these crystals provide an important clue as to the identity of the magma that was active during the emplacement of the diatreme. In the latter case, the xenocrysts are derived from older igneous rock that had become fragmented and disaggregated during the eruption of the diatreme. One sample from a diatreme near Stop 3 shows evidence for this mechanism (fig. 8). There, a biotite-plagioclase xenocryst shows the biotite nearly separated from the plagioclase. The common similarity between xenocrysts in diatremes and phenocrysts in xenoliths suggests that many of these crystals are ones disaggregated from xenoliths, and several thin sections show phenocrysts that were in the process of separating from xenoliths

Geochemistry

In general, trace element geochemical analyses of the middle Eocene igneous rocks of the area indicate enrichment of lighter elements and depletion of heavier elements compared to the midocean ridge basalt (MORB) standard of Taylor and McLennan (1985; see also fig. 9). Compared to Taylor and McLennan's (1985) chondrite standard, mafic rocks of the area are enriched in all trace elements except scandium (fig. 10). Trace element analyses of the felsic and volcaniclastic (diatreme) rocks of the area show the same trend (figs. 11 and 12) when compared to the chondrite standard.

Mafic rocks REE ppm/MORB ppm
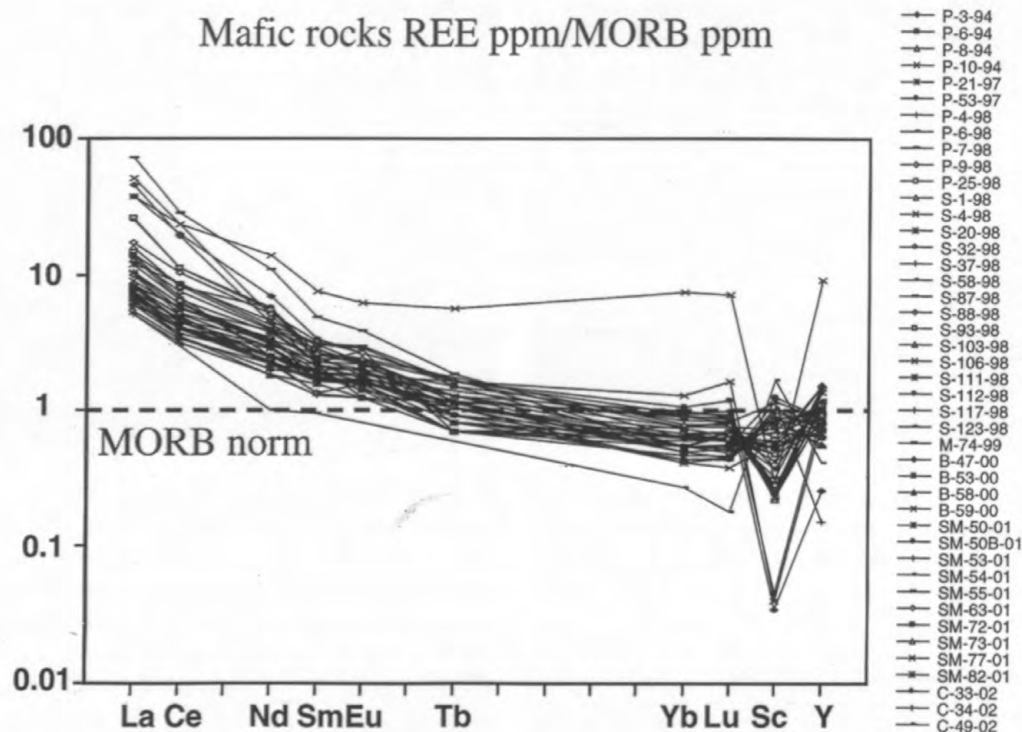
Figure 9. Normative plot showing normalized rare-earth-element (REE) concentrations from 44 mafic rock samples plotted against midocean ridge basalt (MORB) standard of Taylor and McLennan (1985). Lighter trace elements are enriched; heavier trace elements are depleted relative to the standard. Refer to McDowell (2001) for sample locations and analytical results.

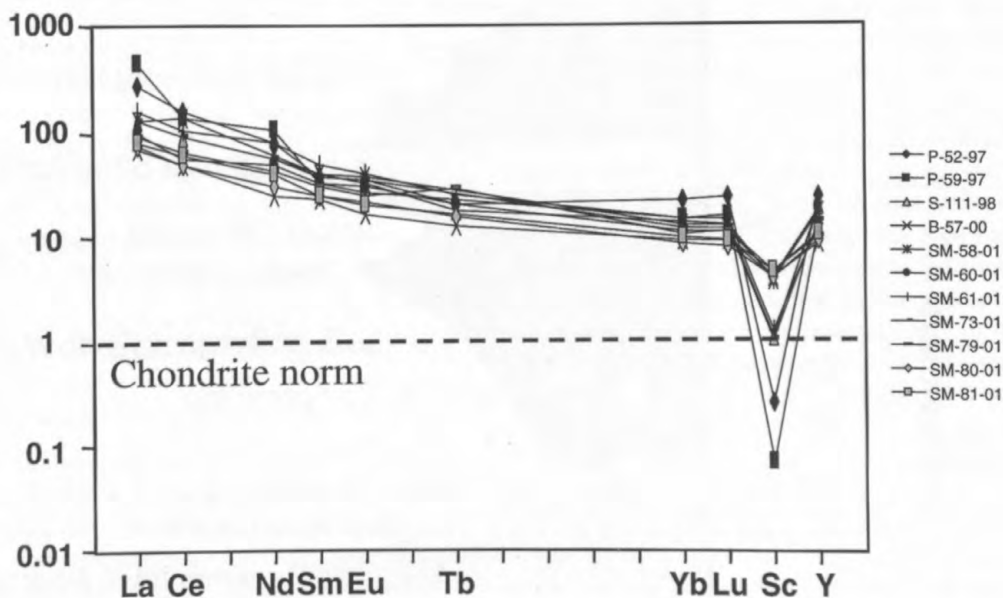## Mafic rocks REE ppm/Chondrite ppm
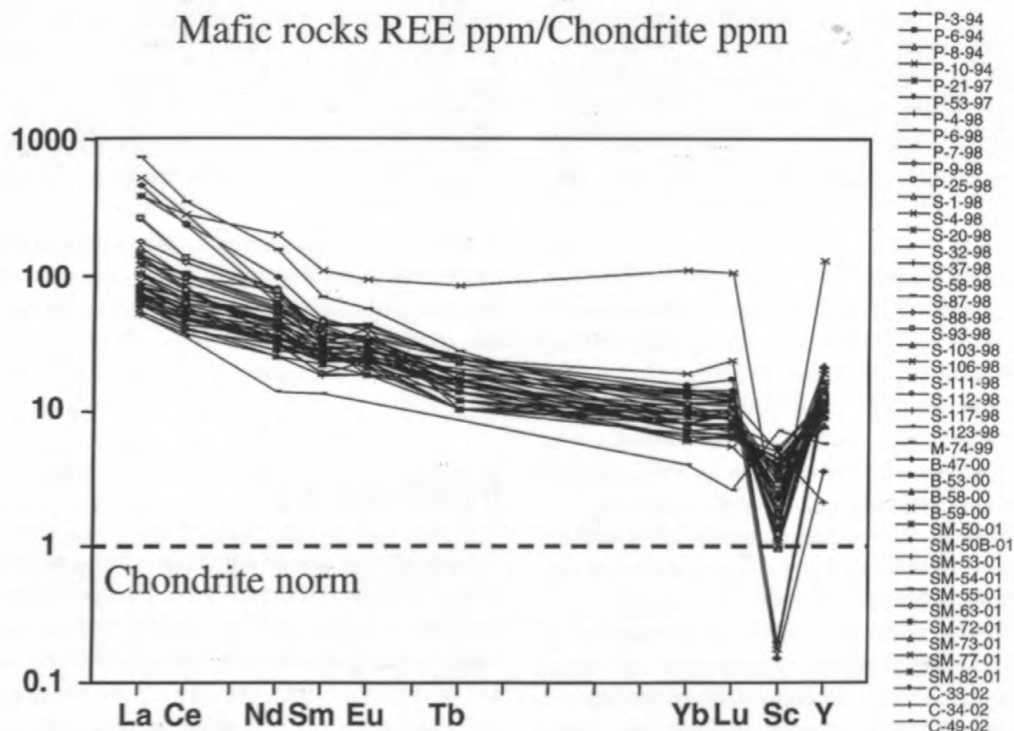
Figure 10. Normative plot showing normalized REE concentrations from 44 mafic rock samples plotted against chondrite standard of Taylor and McLennan (1985). Lighter trace elements are enriched; heavier trace elements are depleted relative to the standard. Refer to McDowell (2001) for sample locations and analytical results.

Felsic rocks REE ppm/Chondrite ppm
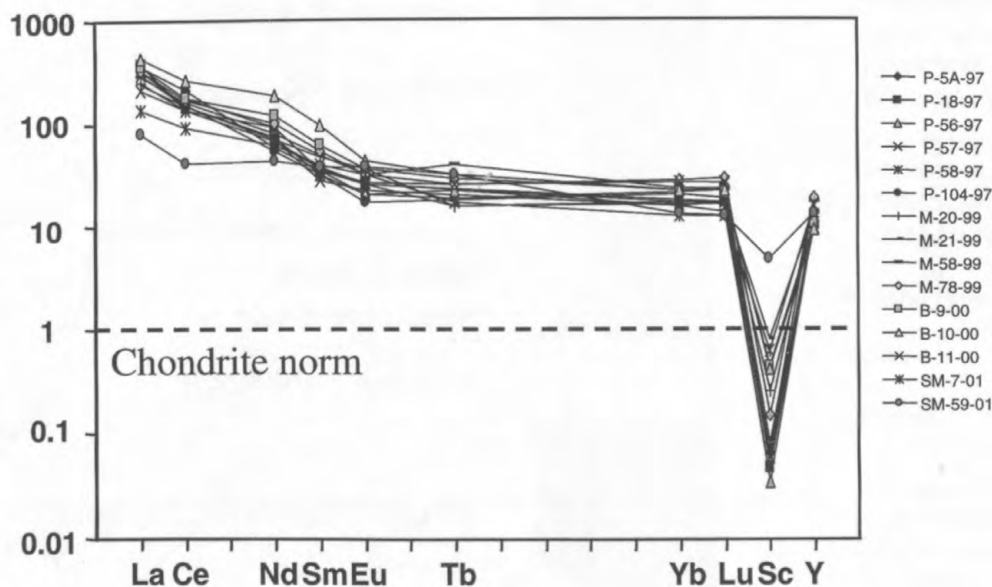
Figure 11. Normative plot showing normalized REE concentrations from 15 felsic rock samples plotted against chondrite standard of Taylor and McLennan (1985). All elements except scandium are enriched compared to the standard. Refer to McDowell (2001) for sample locations and analytical results.

Diatreme REE ppm/Chondrite ppm

Figure 12. Normative plot showing normalized REE concentrations from 11 diatreme samples plotted against chondrite standard of Taylor and McLennan (1985). In general, all elements except scandium are enriched compared to the standard. Refer to McDowell (2001) for sample locations and analytical results.
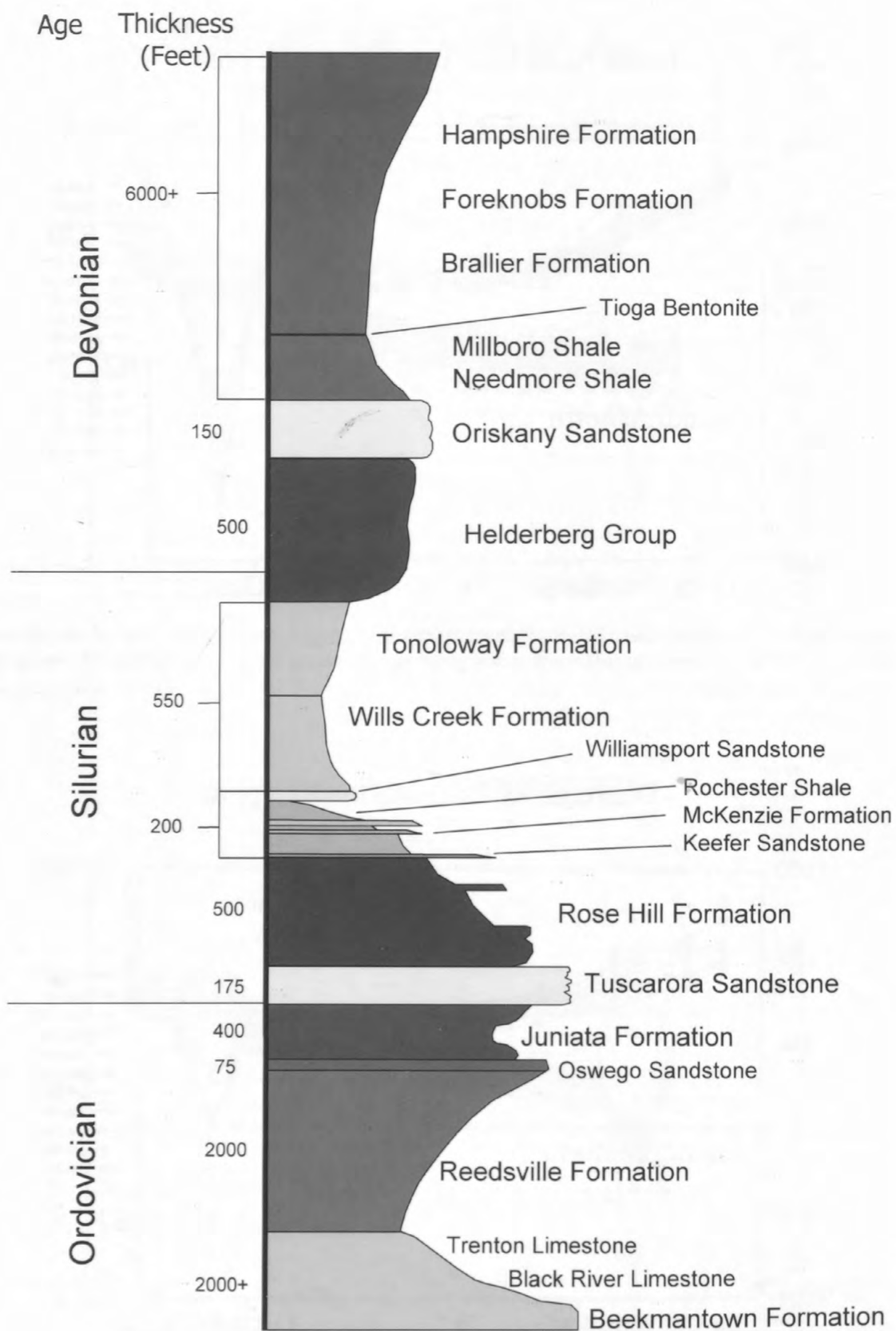
Age   Thickness
         (Feet)

Devonian

6000+

Hampshire Formation

Foreknobs Formation

Brallier Formation

— Tioga Bentonite

Millboro Shale
Needmore Shale

150   Oriskany Sandstone

500   Helderberg Group

Silurian

Tonoloway Formation

550   Wills Creek Formation

— Williamsport Sandstone

— Rochester Shale

200   — McKenzie Formation
            — Keefer Sandstone

500   Rose Hill Formation

175   Tuscarora Sandstone

400   Juniata Formation
75   Oswego Sandstone

Ordovician

2000   Reedsville Formation

Trenton Limestone
2000+   Black River Limestone
            Beekmantown Formation

Figure 13. Generalized stratigraphic column of the Highland County–Pendleton County area. Stratigraphic thicknesses are in feet and are approximate; column is not drawn to scale.
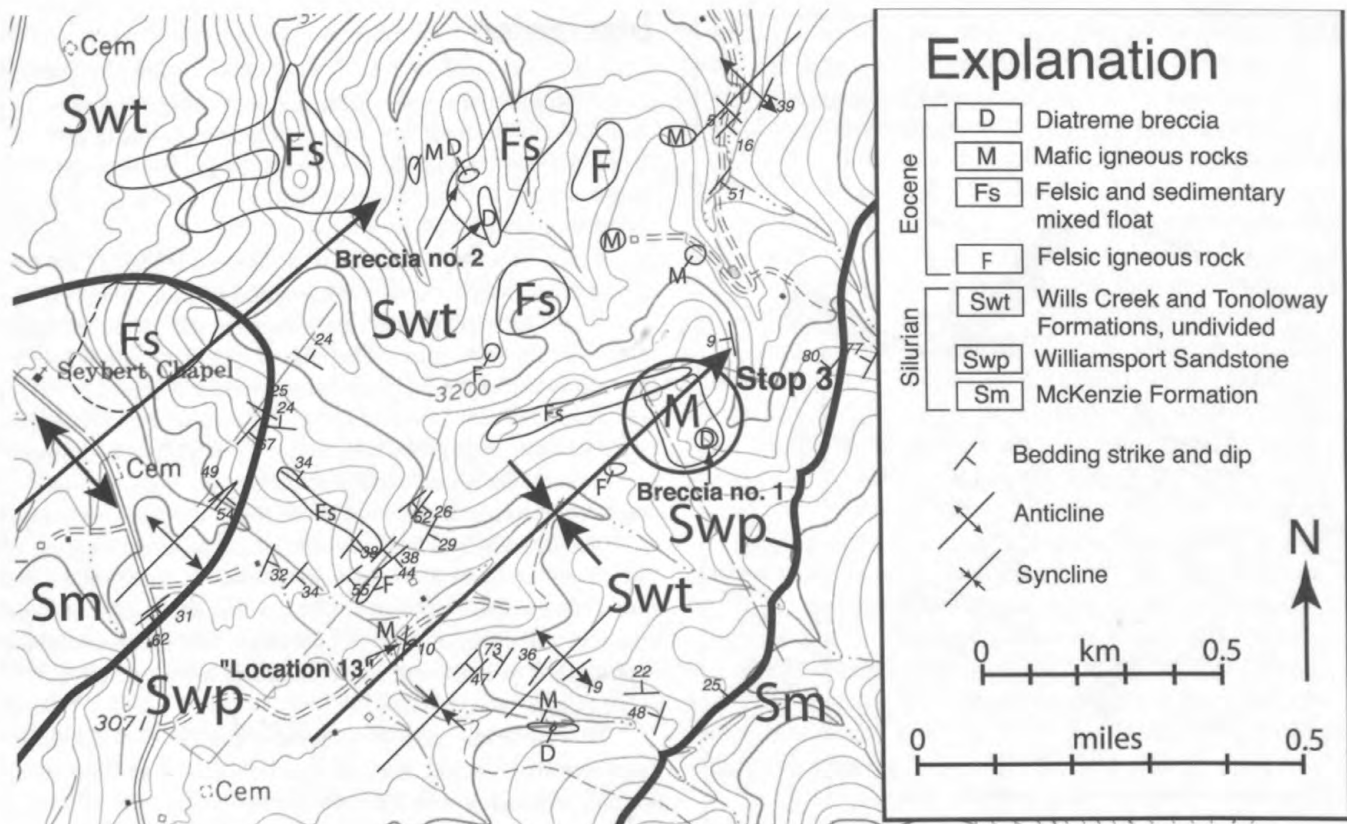
Figure 14. Bedrock geology of the area surrounding Stop 3 (the Beverage Farm), modified from Tso and Surber (2002). The circled area is the location of Stop 3. Note the location of two prominent diatremes, "Breccia no. 1" and "Breccia no. 2." Area is located in the Monterey, Va., 7.5-minute quadrangle, approximately 5.6 km (3.5 mi) east of Monterey.

Major elements barium, chromium, sodium, zinc, manganese, strontium, calcium, aluminum, and potassium are enriched (4 to 55 X) in the area's igneous rocks compared to background values (McDowell, 2001) for sedimentary country rocks in the area. The major element thorium is depleted (0.5 X) in the igneous rocks. In general, there appears to have been little transfer of metals from the igneous intrusives into the sedimentary country rocks. This suggests a *dry* emplacement of many of the intrusives, with the fluid phase in the magma being gases rather than liquids like water.

Interactions with Surrounding Bedrock Geology

The igneous bodies are observed to intrude rocks of the Ordovician Beekmantown Formation through the Devonian Foreknobs Formation (fig. 13). Broad anticlines and synclines dominate the regional structure, with Ordovician rocks found in the cores of the anticlines and Devonian rocks found in the cores of synclines. The regional strike is northeast-southwest, giving the region a strong structural and topographic grain in those directions.

Tso and Surber (2002, 2003) undertook a detailed field

study of a small (1 mi²; (2.6 km²) area of intrusions east of Monterey, Va., in the vicinity of Stop 3 (fig. 14). As is typical of this region, bedrock exposure consists of isolated outcrops, and it is rare to find well-exposed contacts between igneous rocks and the surrounding bedrock. Commonly, igneous bodies consist of a patchy distribution of small outcrops exposed in fields, or areas of igneous float, often mixed with sedimentary float. The general outlines of the igneous bodies are commonly surmised by groupings of float patches, or in the case of dikes, linear float trends of similar rock combined with topographic hints such as low ridges and knolls.

Joint data were collected on the outcrops in the area near Stop 3 and along the main roads nearby (fig. 15). Joint strikes have two very strong orientations: in the cross-strike direction of N. 40°–60° W., and in the direction of N. 60°–80° E. Note that this latter joint orientation is not parallel to the overall strike of the bedding (which is approximately N. 45° E.). At "Location 13" (fig. 14), a mafic dike has intruded into the Tonoloway Formation along a joint set which trends N. 78° E. Elsewhere, the trends of the dikes are inferred from the geologic map. Inspection of figure 14 reveals that all the prominent linear igneous bodies in the study area follow the dominant joint sets. Several felsic bodies have linear trends that parallel the northeast joint direction, and there is one prominent felsic dike that parallels the northwest joint direction.
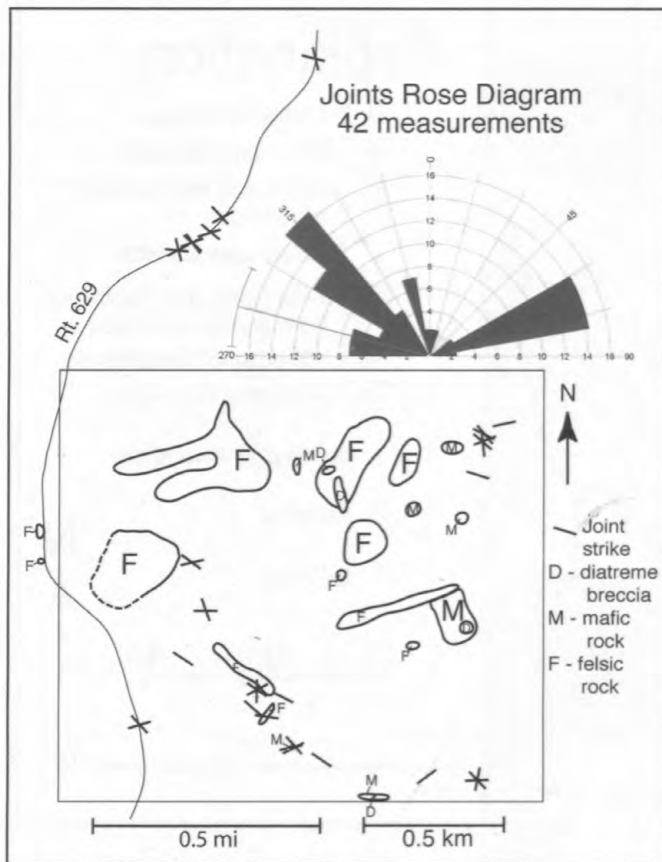
Figure 15. Rose diagram of joints and map of joint measurements of the Stop 3 area and along nearby major road (modified from Tso and Surber, 2002).

Where contacts between the dikes and sills and the country rock are exposed, xenoliths are common, but obvious chemical alteration of either intrusion or wall rock is not widespread except for a minor zone of contact metamorphism. Evidence for contact metamorphism will be observed at Stop 7, where a mafic sill/dike has intruded the Millboro Shale, leaving a harder phyllitic zone right at the contact. Another notable locality is at the previously mentioned Hightown Quarry, where the contact was first described by Giannini and others (1987), and in great detail by Good (1992). There, the igneous rocks intrude the Beekmantown Formation, causing a contact zone containing brucite marble.

Exposed contacts between diatremes and country rocks are exceedingly rare. However, at Stop 4 (the Hull Farm), we will have the chance to observe such a locality. In the contact zone, hot fluids have leached carbonate from the country rock, leaving behind only a siliceous "skeleton."

Discussion

Although the causes of the magmatism and the geochemical evolution of the magma or magmas remain as debated issues, certain inferences can be made about the eruption history on the basis of fieldwork, geochemical data, and petrographic study.

From joint data, field observation, and mapping, it appears that the dominant joint sets and bedding planes in the region provided the primary pathways for the ascent of both mafic and felsic magmas. The lack of extensive alteration of the wall rocks along dikes and sills where the common aphanitic rocks are in contact with the surrounding sedimentary rocks does not provide evidence of extensive hydrothermal interactions. Geochemical trace element analysis indicates that the emplacement of these rocks was relatively dry.

The diatreme bodies, however, tell a different history. The extensive hydrothermally altered matrix, the dissolved contact in evidence at Stop 4, and the rounded nature of xenoliths indicate either a dynamic, abrasive, water-rich environment for the formation of these bodies or a very reactive vapor phase.

The consensus of how diatremes form has evolved since they were first studied. Early theories called for an "explosive boring" process, in which pulses of magma from the mantle or lower crust rapidly rise through fractures, shattering the country rock until the magma reaches a critical depth where reduced pressures allow dissolved gases (H_2O and CO_2) to separate from the magma and violently blow out (Mitchell, 1986). The gas streams upward, mixing with rock in a process called "fluidization," forming an abrasive stream that "sandblasts" its way upward with enough force that solid particles are held in suspension by the "fluid" stream of gas, enlarging conduits and forming much of the breccia in the pipe.

In the last several decades, the role of "hydrovolcanism" has become increasingly recognized as a key player in diatreme formation (Mitchell, 1986; Lorenz, 1986). In this process, magma moves upward through joints until it reaches a rich source of ground water. At the contact between the hot magma and cooler ground water, the water flashes to steam, shattering the bedrock while incorporating some of the magma. The material is then expelled upward, breaching the ground surface and becoming airborne. The material falls around the vent to form a ring of tuff with a central crater ("maar"). There are two points to emphasize: (1) the eruption lasts as long as there is an adequate supply of ground water and not when magma runs out and (2) the eruption begins at shallow depths (200–300 m; 650–1,000 ft). Shallow depths

and low pressure are necessary in order for water vapor explosions to occur (Lorenz, 1986). Once the eruption gets going and as long as the water supply lasts, the crater propagates downward, using up the water and creating an increasingly deeper "cone of depression" in the ground water table, thus allowing the pipe to deepen (fig. 16). As the pipe propagates downward, normal faulting occurs along the sides, thus allowing the pipe to widen while the sides collapse. The eruption style is both pyroclastic in nature and episodic. Thus, not only will ejected material form layers of tuff around the maar, it will also fall back into the crater itself, causing pyroclastic bedding within the pipe. Layered kimberlitic diatremes in western Montana that contain graded beds on scale of 1.2 to 30.5 cm (0.5–12.0 in) have been described by Hearne (1968). As the diatreme propagates downward, older bedrock clasts will increasingly be found in the higher beds of tuff surrounding the maar. During the pauses between eruptions, the tuff forming the walls of the central depression may slide back into the crater in the form of lahars. These deposits may become interlayered with pyroclastic beds within the diatreme. Once the water supply is used up, the hydrovolcanic phase of the eruption ends and later magmas may work their way up the pipe to form dikes that crosscut the previously deposited breccia.

Important to the hydrovolcanic model of diatreme formation is the fact that this is a relatively low-temperature process. Thus, hydrovolcanic diatremes do not show extensive contact metamorphism of the country rock. The formation of the diatreme walls is predominantly one of collapse, not of outward explosion. For this reason, extensive faulting of the bedrock outside of the diatreme is not commonly observed. Within the diatreme, along the walls, concentric normal faults form as the sides collapse down.

The diatremes of Highland and Pendleton Counties have much in common with the hydrovolcanic model. The abundance of xenoliths of country rock, crude layering observed in some localities, lack of contact metamorphism with the country rock, lack of strong deformation of the country rock, and the hydrothermal alteration of the matrix are similar to hydrovolcanism described in other parts of the world (Mitchell, 1986; Lorenz, 1986).

An interesting aspect to this mechanism is the fact that as material collapses into the pipe, rocks from higher in the stratigraphic section may fall into lower levels of the pipe and be preserved. Thus, it is possible to preserve younger rocks, which elsewhere have been eroded away, as xenoliths in diatremes. This situation has been observed at a diatreme near Stop 3 (labeled "Breccia no. 2" in figure 14). The surrounding

bedrock is limestone and shaly limestone of the Silurian Wills Creek and Tonoloway Formations. However, in addition to these formations, this diatreme also contains xenoliths of black shale. The shale is found within the breccia both as clasts 2 to 3 cm (0.8–1.2 in) in diameter and as weathered-out chips in the soil overlying the diatreme. The lithology, color, and weathering characteristics of these chips do not resemble what is found in the surrounding Wills Creek and Tonoloway Formations, but are more similar to younger shales within the Devonian rocks such as the Millboro Shale. Kettren (1970), in his study of rocks in Highland County, reported a similar situation. In a breccia body, he found a Lower to Middle Devonian pelecypod from a black shale xenolith that he identified as possibly being from the Marcellus Shale. Kettren (1970) identified the surrounding host bedrock as lowest Devonian Keyser or Coeymans Limestone of the Helderberg Group, suggesting to him there was "at least 500 ft of vertical mixing." Alternatively, younger xenoliths can also originate from units embedded in a thrust sheet deeper in the crust. This would require a major subsurface thrust fault placing older rocks over younger rocks such as the Millboro Shale. However, geologic cross sections constructed through the region (Shumaker, 1985; Kulander and Dean, 1986) show no indication of such a fault under the field area.

In "Breccia no. 2," the minimum distance to the source of these xenoliths can be estimated by calculating the stratigraphic thickness between the bottom of the Millboro Shale and the top of the Tonoloway Formation, assuming no structural complications. Various workers have made differing estimates on the stratigraphic thickness. Figure 13 gives an estimate of at least 650 ft (198 m), although using the data from Butts (1940), the thickness estimate is 1,100 ft (335 m). Mitchell (1986) notes that in diatremes associated with kimberlites, inclusions have been demonstrated to have descended as much as 1,000 m (3,280 ft). This intriguing observation then provides a minimum estimate as to how much overlying rock has been eroded away since the Eocene, providing independent confirmation about the erosion rate of this region of the Appalachians since the Eocene. Using the range of stratigraphic thickness, the estimate of 198 to 335 m (650–1,100 ft) from Highland County diatremes is well within estimates of erosion for other localities in the southern Appalachians. For example, Mathews (1975) estimated 2,000 m (6,600 ft) of erosion since the beginning of the Cenozoic on the basis of sediment volumes in the Atlantic Ocean, and Matmon and others (2003), using [10]Be techniques, estimated an erosion rate of approximately 30 m/m.y. for the Mesozoic and Cenozoic.
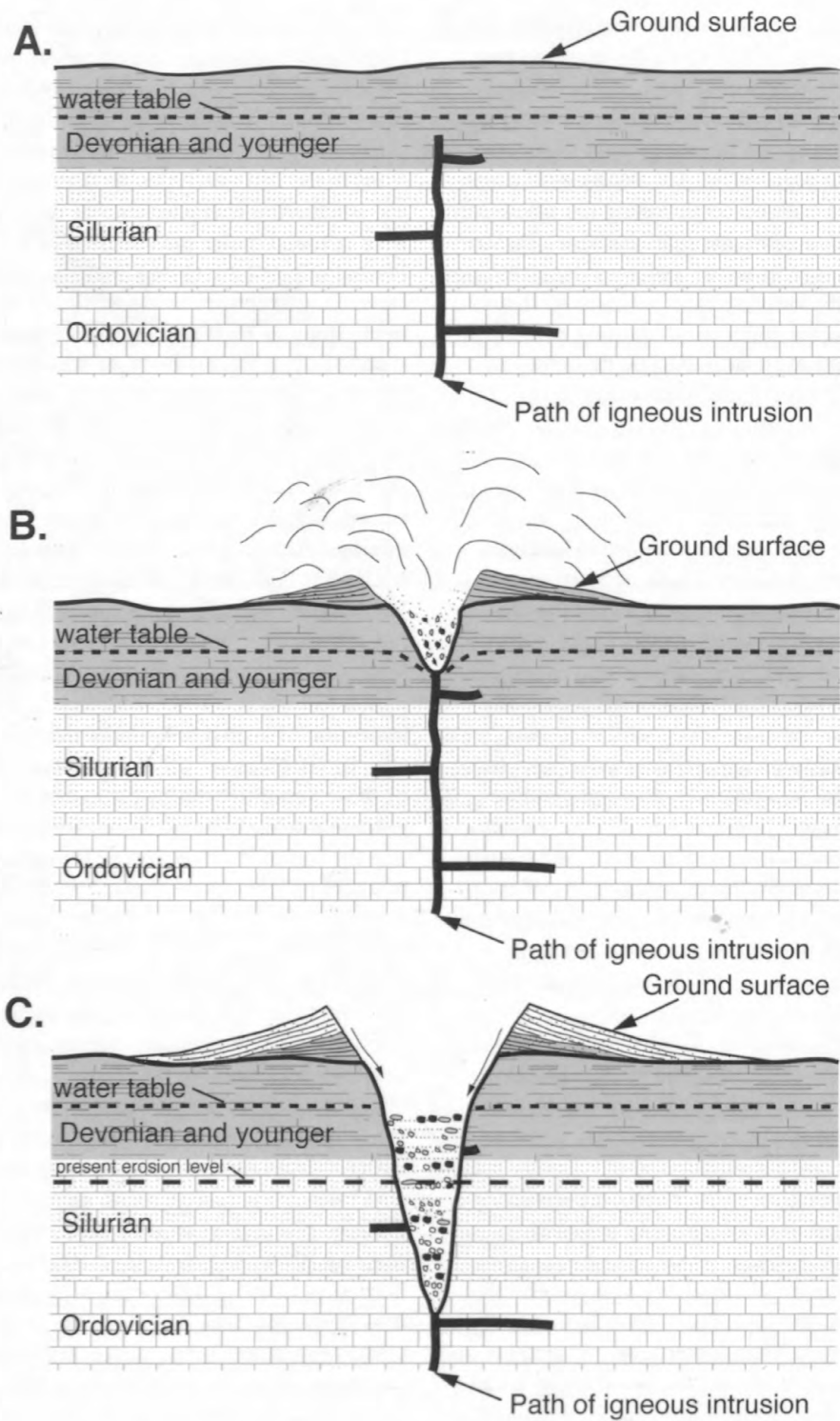
Figure 16. Eruption sequence of an Eocene diatreme following the hydrovolcanic model. A, Eruption commences when an intrusion reaches shallow depths and encounters a rich source of ground water; B, the breccia pipe propagates downward, creating a cone of depression of the water table, while a tuff ring forms around the central crater and the walls of the pipe collapse downward; C, material collapses into the pipe, allowing rocks from higher in the stratigraphic sequence to fall to lower levels, while forming some crude layering. Debris flows away from the crater walls to form volcaniclastic layering.

Figure 17. Photograph of Trimble Knob, a basaltic volcanic neck or plug, near Monterey, Va. View is to the south.

Figure 18. Photograph of the area of Stop 3, looking northwest. The dark patches in the center of the picture are exposures of "Breccia no. 1." Mafic rock dominates the area immediately surrounding the breccia to the line of grassy knolls behind and uphill from the breccia. Running along the crest of the line of knolls is a northeast-trending felsic dike. The large ridge in the background is Monterey Mountain. Grazing cows provide scale.

Stop Descriptions

Stop 1. Confederate breastworks on Shenandoah Mountain.

The roadside historical park offers exceptional scenery from the overlook. The high ridge on the straight skyline 11 miles (18 km) to the west is in Highland County; Jack Mountain is formed by tilted strata of the Silurian Tuscarora Sandstone. The slightly higher knob on this skyline ridge is Sounding Knob (elevation 1,308 m; 4,291 ft), an Eocene basalt plug that happens to rise up through the high ridge of Jack Mountain. The low mountain with a building having a prominent light-colored roof is Bullpasture Mountain. The Battle of McDowell on May 8, 1862, was fought mainly on the northwestern side of that mountain, and it resulted in a Confederate victory that prevented Union forces from penetrating eastward toward the Shenandoah Valley.

Contributed by Dr. John M. Dennison, Professor Emeritus of Geology, University of North Carolina, Chapel Hill, N.C.

Stop 2. View of Trimble Knob.

Trimble Knob (fig. 17) has been variously described as a volcanic neck, a plug, and as a diatreme (Rader and others, 1986). Although in shape this feature resembles basaltic cinder cones in the Western United States, no cinders, ash beds, or lava flows are present.

Like many of the igneous bodies you will see today, the basalt core of Trimble Knob is surrounded or mantled by

lithified volcaniclastic material, hence the interpretation of the feature as a diatreme. The suggestion is that rapid and violent emplacement of the basalt to a near-surface position, associated with the rapid release of fluids, shattered the country rock adjacent to the basalt body. This produced a chaotic collection of fragments of country rock, basalt, and a finely comminuted matrix of rock flour, all of which lithified. Southworth and others (1993) give a date of 35.0±0.5 Ma for the basalt of Trimble Knob, making it the youngest of all igneous rock units you will see today.

Stop 3. Beverage Farm diatreme, basalt, and felsic rock.

All three igneous types (diatreme, mafic, and felsic rocks) are exposed on the rolling hills of the Beverage Farm (see fig. 14). The small knolls and subtle ridgelines are typical of how the igneous bodies influence the topography and crop out, as scattered patches of exposed rock and areas of mixed igneous and sedimentary float (fig. 18). Soil cover and grass make it difficult to precisely determine the boundaries of these bodies, and contact relations with the surrounding rock are only rarely observed. Many isolated smaller bodies are mapped as having a circular or oval shape based on single outcrops and patches of float, but the true shapes of these bodies are unknown. In some cases, dike-like shapes may be inferred from linear trends of outcrop and float of similar rock. Although dikes can be observed in roadcuts or quarry walls, attempts to trace them away from where they are exposed are difficult.

Near the farmhouse, an outcrop of the Wills Creek or Tonoloway Formation contains a typical mafic dike that follows the N. 78° E. trend of the regional joints ("Location 13"

Figure 19. Photograph of an older breccia inclusion in "Breccia no. 1" at Stop 3. The dark angular grains are clinopyroxene crystals, and the lighter rounded features are vugs. Quarter for scale.

of figure 14). The highly weathered, narrow dike is not traceable for any significant distance in the field behind the outcrop nor does it provide any topographic expression, thus causing speculation that perhaps the region is crisscrossed by an untold number of bodies that have yet to be found.

Hike the farm roads to visit a concentrated group of exposures on the small knoll 0.7 km (0.4 mi) to the northeast of the farmhouse.

"Breccia no. 1" crops out on the side of a small knoll where the pasture grass gives way to a black-brown rocky rubble and soil. This body is characterized by a chaotic assortment of angular to rounded xenoliths of mafic igneous and sedimentary country rock and sizes (up to 15 cm; 5.9 in), with single crystals (xenocrysts) embedded in a fine powdery matrix with up to 70 percent of the rock composed of xenoliths and xenocrysts. Xenoliths identifiable in the field include red iron-stained aphanitic mafic rock, gray limestone, chips of shaly limestone, and earlier-formed breccia.

By means of a hand corer, fresh breccia was recovered for thin sectioning. Thin section analysis reveals that: (1) igneous xenoliths include both finer grained (0.1 mm) vesicular aphanitic plagioclase—clinopyroxene basalt and slightly coarser grained (0.2 mm), non-vesicular aphanitic plagioclase-clinopyroxene basalt; (2) xenocrysts (augite, olivine, and rare hornblende) are commonly 1- to 2-mm size, and bounded by both well-defined crystal faces and broken and fragmented surfaces; (3) the matrix is highly altered, fine grained, and basically indecipherable, although there are areas of sheet silicate that resemble chlorite and fibrous zeolite; (4) samples commonly contain numerous rounded vugs that are filled with carbonate or zeolite; and (5) some of the vugs, judging from their shapes, are replaced xenocrysts and xenoliths.

By brushing the rubble away, relatively fresh breccia can be observed. Although most of the diatreme is highly unsorted, crude layering in the form of beds of coarser xenoliths on the 4- to 10-cm scale (1.6–3.9 in) (see fig. 7) is observed. The strike of the layers (N. 45° W.) cuts sharply against the regional northeast strike of the surrounding beds of sedimentary rock.

A feature of this diatreme is the presence of xenoliths composed of older breccia (fig. 19). A thin section reveals that it differs from the usual breccia in that it contains single crystals of well-terminated 2- to 5-mm clinopyroxene that are much coarser than those from the surrounding mafic rock, and that it lacks xenoliths of any type.

"Breccia no. 1" sits at the edge of a larger area of aphanitic mafic rock. The mafic rock consists of aphanitic, vuggy plagioclase-clinopyroxene basalt and porphyritic basalt with olivine, augite, and plagioclase phenocrysts.

Just north of the diatreme, following the crest of a small ridge that trends approximately N. 72° E. (along one of the dominant joint directions) is a series of small patchy outcrops that expose a felsic dike. The rock is light gray with plagioclase and rare hornblende and biotite phenocrysts in a plagioclase-dominated matrix that commonly has parallel laths.

Stop 4. Hull Farm basalt and diatreme.

Exposed in the creek bed to the north of the road is an unusual rock unit previously described as a volcanic breccia (Garnar, 1951, 1956) and as a diatreme breccia (Kettren, 1970). A volcanic breccia is a deposit of angular pieces of volcanic and country rock that can form in several ways. The more common of these are described below.

(1) A gas or steam explosion ejects shattered bedrock fragments, volcanic rock, and ash into the air which subsequently fall back into the crater—the material is still hot and is typically welded together because the volcanic rock fragments and ash may be close to melting temperature. This volcanic breccia is called an explosion, fallback, or diatreme breccia, and it is extrusive in nature;

(2) A sudden withdrawal of magma from beneath a volcano can stress the country rock and any volcanic deposits on top of it so that the entire structure collapses into the magma chamber. The jumble of angular debris may be welded together. This is a collapse breccia, and it has no extrusive component to its formation.

The key feature of these types of volcanic deposits is the *angular* pieces of volcanic and country rock (making it a breccia rather than conglomerate), the presence of ash, and the lack of any evidence of flow—either flow layering or flow lineations.

The dark-colored rock unit in the streambed has several features that appear to be at odds with the interpretation of the unit as a diatreme breccia. The rock itself is a boulder mudstone or volcaniclastic conglomerate consisting of a dark matrix of very fine grained material surrounding and support-

Figure 20. Closeup photograph of the volcaniclastic unit at Stop 4 exposed in the streambed just south of the Hull residence. Rounded to subrounded clasts of basalt, Oriskany Sandstone, and limestone from the Helderberg Group are identified (arrows). Margin of large basalt clast shown in figure 6 is marked by a dashed line. Rock hammer for scale.

ing a large of number of rock fragments. These rock fragments are polymict and most are rounded. The most obvious fragment is a boulder of porphyritic basalt approximately 1.2 m (4 ft) in length (see fig. 6). Also present are cobbles and pebbles (fig. 20) of the porphyritic basalt, clasts of the fine-grained matrix material, clasts of light-gray limestone (Silurian-Devonian Helderberg Group), and clasts of light-gray quartz sandstone (Devonian Oriskany Sandstone); in general, these are subrounded to rounded. There are weak indications of flow in the unit in the form of surfaces covered with small (less than 1 cm (0.4 in) in diameter) pebbles (fig. 21). These concentrations of pebbles appear on only the east side of the large basalt clast seen in figure 6 and may represent a lag deposit deposited on the leeward or *downstream* side of the basalt clast.

McDowell speculates that this unit might be the lithified remains of a lahar deposit. A *lahar* is a debris or mudflow produced contemporaneously (usually) with extrusive volcanic activity. Volcanic events typically create a strongly localized weather anomaly associated with violent rainfall in the vicinity of the volcano. Heavy rainfall mixes with volcanic ash and any loose volcanic debris and soon produces a gravity flow having the consistency of wet concrete and as much momentum as the gradient of the volcano's slope will allow. Modern lahars incorporate trees, buildings, houses, and pieces of country rock as they move rapidly downhill. Because a lahar can contain a large amount of freshly erupted volcanic material, the temperature of the lahar deposit may be

close to the boiling point of water. A solidified lahar should be a collection of fragments of various sizes and shapes (both rounded and angular), including boulders, caught up in a very fine grained matrix, lithified into a material resembling concrete, and perhaps showing some flow structures. That description seems to fit this outcrop.

Extrusive volcanic activity associated with the middle Eocene igneous rocks in this area has not been documented. The presence of a possible lahar deposit suggests otherwise. Drilling or geophysical survey work may be required to determine the exact nature of this material.

In the hillside just to the east of the Hull residence, the contact between volcaniclastic material and country rock (Oriskany Sandstone) is exposed. All calcite cement has been removed from the rock, leaving only the original quartz grains in a clay-rich matrix that crumbles in the hand. This suggests that the interaction between country rock and volcaniclastic material was a reactive one. The volcaniclastic material may have been very hot and contained acidic fluids.

A porphyritic basalt dike is exposed in the small valley to the north of the Hull residence (fig. 22). This igneous body protrudes from the ground to a height of approximately 1.2 m (4 ft) and is roughly 0.6 m (2 ft) wide. Abundant, large pyroxene phenocrysts up to 0.6 cm (0.2 in) in diameter are visible. In thin section, these phenocrysts may be euhedral or corroded.

Typical of most of the igneous bodies in the area, this dike is surrounded by volcaniclastic material. Clasts within this material may be rounded or angular and the matrix mate-

Figure 21. Closeup photograph of the volcaniclastic unit at Stop 4 exposed in the streambed just south of the Hull residence. Concentrations of small pebbles are observed only on the east side of the large basalt clast (margin marked by dashed line) shown in figure 6. This suggests that the pebbles represent a lag deposited from horizontal flow on the leeward side of the large clast. Rock hammer for scale.

rial typically weathers to irregular rubble less than 1 cm (0.4 in) in diameter. Is the volcaniclastic material an emplacement breccia as suggested at Trimble Knob, making it essentially contemporaneous with the dike? Did the dike intrude existing volcaniclastic debris? Is the volcaniclastic material part of a lahar deposit that flowed around the dike? What was the surface topography like here in the Eocene? Are these the remnants of an extrusive igneous event?

Stop 5. Ugly Mountain overview.

Brushy Fork Dam, on the right, was constructed by the U.S. Soil Conservation Service (now the Natural Resources Conservation Service) for local flood control. In 1996, heavy rain in the aftermath of Hurricane Fran caused the dam to be overtopped and the spillway stripped to bare bedrock. Reclamation has since recovered the site. Ugly Mountain, visible to the south of the reservoir, has the highest topographic relief in the immediate area.

Stop 6. Brushy Fork albitite dike.

*The dike is exposed in the streambed and water may be high so **be prepared to get your feet wet.***

Ugly Mountain to the west is a middle Eocene plug or volcanic neck with a diatreme breccia near its top and on its west flank (Garnar, 1951, 1956). The rock that you are stand-

ing on is one of several dikes that radiate out in an easterly direction from Ugly Mountain. The dike (fig. 23) here is approximately 9 m (30 ft) wide, trends N. 83° E., and has been dated at 42.8±0.5 Ma (Southworth and others, 1993). The light-orange to pinkish color of the dike is a product of weathering. If you break off a piece of the rock, you will see that it has a thick, brown weathering rind with occasional dark-blue or steel-gray mineralized bands. The latter are probably pyrolusite, a common secondary mineral in this area; it precipitates out of near-surface ground water. Fresh samples of this rock are nearly white or yellowish white. The texture is aphanitic and resembles a very fine grained quartz sandstone. In thin section, this unusual rock consists almost entirely (>95 percent) of a felted mat of equigranular, euhedral crystals of albite (sodium plagioclase), a smattering of small, euhedral biotite? crystals, and rare ilmenite. The absence of quartz, the small number of mafic minerals, and the fine grain size suggest that this rock is properly named a rhyolite or dacite, but because of the unusually high content of sodium plagioclase, the rock was termed an *albitite* by Garnar (1951, 1956).

Another interesting feature of this rock is the presence of parallel foliations resembling sedimentary bedding. In reality, these layers are shrinkage cracks resulting from differential cooling. The country rock here consists of shales and siltstones of the Devonian Brallier Formation. The Brallier, visible approximately 15 m (50 ft) downstream, is dipping steeply toward the southeast at 50°. The albitite dike intruded a fracture and cuts across strike at an angle of 52°.

Figure 22. Dike of porphyritic basalt exposed at Stop 4 just north of the Hull residence. Co-author (Matchen) visible in the photograph is 1.8 m (5.9 ft) tall.

Figure 23. Dike of albitite (>95 percent sodium plagioclase) exposed in Brushy Fork Creek at Stop 6 shows cooling fractures that resemble sedimentary bedding. Unit trends N. 83º E. and is approximately 9 m (30 ft) wide.

Also of note here are a number of core holes drilled for paleomagnetic analysis (Ressetar and Martin, 1980), which confirmed the middle Eocene age of this igneous body.

Optional Stop. Wilfong Church gabbro.

The igneous rock exposed here is coarser grained than at Stop 7 and probably should be classified as a gabbro on the basis of its texture. Garnar (1951, 1956) referred to it as a diabase because of the predominance of calcium plagioclase over pyroxene (fig. 24). Both euhedral and corroded pyroxenes are present in this rock, suggesting two stages of precipitation of these minerals, with the euhedral crystals representing the later stage. This igneous material has not been dated but is assumed to belong to the middle Eocene group.

NOTE: A mica pyroxenite dike dated at 143.8±1.8 Ma (Southworth and others, 1993) is present 1.6 km (1 mi) to the east.

The very poorly exposed country rock here is Devonian Brallier Formation, an interbedded shale, siltstone, and sandstone unit that directly overlies the Devonian Millboro Shale. In fact, the contact between the two units is probably within 15 m (50 ft) of the dike.

Stop 7. Sugar Grove sill-dike.

The hillside in front of you is formed by the silty shales of the Devonian Millboro Shale (section described in Woodward, 1943). Originally flat-lying strata of the Millboro have been folded into the steep east limb of a broad syncline whose axis is centered along the crest of Shenandoah Mountain, visible to the east. Here, the Millboro is dipping approximately 60° to the southeast. The folding of the syncline occurred while the Millboro was buried thousands of
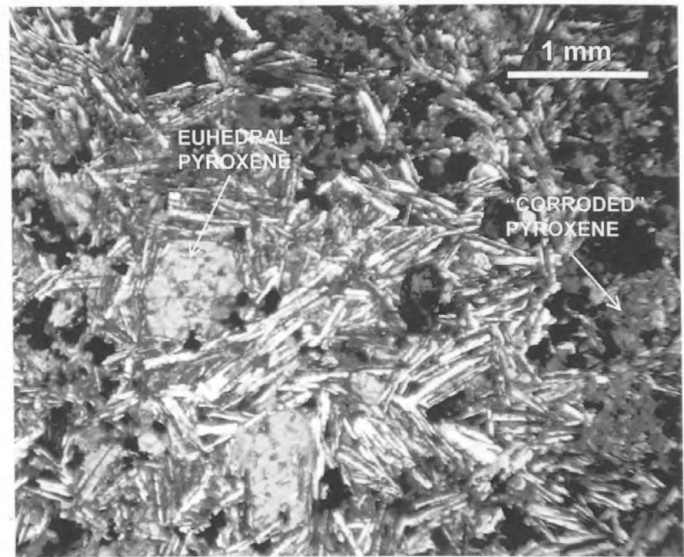
Figure 24. Photomicrograph of gabbro from Wilfong Church (Optional Stop). Pyroxenes suggest different times of precipitation. Euhedral crystals are late; corroded crystals are early. Crossed polars.

meters below the land surface. We believe this to be true because when rocks are subjected to compression, they are more likely to bend if they are confined or surrounded by an equally strong pressure. This confining pressure corresponds to the weight of overlying rocks.

The Millboro also exhibits another kind of deformation. A number of nearly vertical joints cut across the rock and intersect to form two distinct sets at a 30° angle. These brittle fractures form when rocks are subjected to extensional forces that tend to pull them apart *or* to compressional forces with greatly reduced confining pressure. Without confining pres-

Figure 25. Contact between the Millboro Shale and the dike portion of the Sugar Grove basalt sill-dike at Stop 7. Basalt intruded along a joint (dashed line). Notice that a second joint set intersects the first at a 30° angle. Also notice the 0.25- to 0.5-m (0.8–1.6-ft)-diameter xenoliths of Millboro Shale in the basalt and the apparent flow foliation in the basalt.

sure, rocks will break and move relative to each other (faulting); when minimal confining pressure is present, rocks will fracture without movement (jointing). This suggests that the joint sets were formed by the compression of Millboro strata overlain by a greatly reduced thickness of rock—decidedly after folding had occurred.

Today, the Millboro has been exposed by an extensive period of erosion that has removed several thousand meters of Devonian through Mississippian sedimentary rock overburden. The exposed Millboro here is a geological hazard because the steeply dipping and fractured rock spalls off and slides down the dip surface into the roadbed at the foot of the slope. You can see that the highway at this point and at other spots along our travel route has been built up on artificial fill and shows evidence of recent landslides and rock fall.

An additional geologic event has affected the rocks at this outcrop. Long after the Millboro was tilted, jointed, and much of the overlying strata removed, magma with a basaltic composition migrated upward toward the surface and intruded these rocks. The dark-reddish-brown rock unit exposed before you is not part of the Millboro Shale. It is a *sill-dike* of mid-

dle Eocene basalt dated at 43.1±2.1 Ma (Southworth and others, 1993).

The shales of the Millboro immediately adjacent to the basalt have a phyllitic sheen due to contact metamorphism. In addition, you will find small- and large-diameter (up to 1 m; 3 ft), irregularly shaped pieces of Millboro Shale within the basalt. These xenoliths clearly postdate the structural deformation of the Millboro.

The body of igneous rock observed here is unusual in that it changes *character* over the width of the outcrop. Igneous material first reached the near surface by moving upward along one of the large joints within the Millboro (fig. 25). At this point, the igneous body is a dike that cuts across the bedding of the Millboro at approximately right angles. As the igneous material got closer to the surface, it intruded between the bedding of the Millboro by simply pushing the strata apart. This portion of the igneous body is a sill because it parallels the bedding of the country rock. During the latter stages of intrusion, broken pieces of Millboro Shale were picked up and included in the molten material as xenoliths. The igneous material cooled and the remainder of overlying sedimentary rock eroded away, leaving the exposed sill-dike we see today.

There is another apparent paradox here. The igneous rock making up the sill-dike is a porphyritic, amygdaloidal basalt. It has the aphanitic groundmass of an extrusive volcanic rock as might be associated with a lava flow, yet we believe that it is intrusive. When igneous intrusions occur within a few meters to a few hundreds of meters of the surface, cooling occurs rapidly at rates similar to those experienced by lava. This is especially true when ground water is present in the near-surface rock. The end result is a very fine grained igneous rock texture such as is seen here.

Basaltic magmas typically melt at 1,000 to 1,300°C (1,800–2,300°F) depending on depth of burial and water and gas content (Hyndman, 1972). The slightly phyllitic nature of the Millboro near the basalt indicates contact metamorphism. It should be noted, however, that metamorphic alteration does not appear extensive here, and it is possible that the temperature of the molten material was significantly cooler than those listed above. The north end of the sill is in direct contact with the underlying Millboro. A zone of alteration 10 cm (0.3 ft) wide is present and is marked by a slight yellow coloration of the rock material. The underlying Millboro shows little alteration other than the phyllitic sheen observed elsewhere in the outcrop. More important, geochemical analyses of samples from the basalt of the sill-dike, the contact zone, and the adjacent Millboro Shale do not indicate any wholesale transfer of trace or other metals from the basalt into the country rock, which would be the case if a large volume of liquid were present in the magma or if a large volume of ground water were present in the country rock. Here, we see the effects of a *dry* emplacement. The resulting contact metamorphic features are related primarily to heating rather than to hydrothermal alteration of the country rock.

There are a number of vesicles and amygdules present in the basalt. Many of the amygdules have been filled with crystals of calcite, quartz, and zeolites (see Kearns, 1993) after the basalt was emplaced and was cooled or cooling. The number and size of vesicles and amygdules appear to increase upward toward the exposed upper surface of the sill. The basalt itself consists of an equigranular, aphanitic groundmass of calcium plagioclase crystals, with phenocrysts of euhedral biotite and euhedral to corroded pyroxenes, probably augite (fig. 26). The phenocrysts indicate that the magma stopped its ascent to the surface long enough for the larger crystals to begin to precipitate. The corrosion of the pyroxene crystals indicates that they were in disequilibrium with the rest of the magma as it rose closer to the Earth's surface; they are partly resorbed. The aphanitic, *felted* groundmass of calcium plagioclase is the result of a final, relatively rapid stage of cooling near the surface.
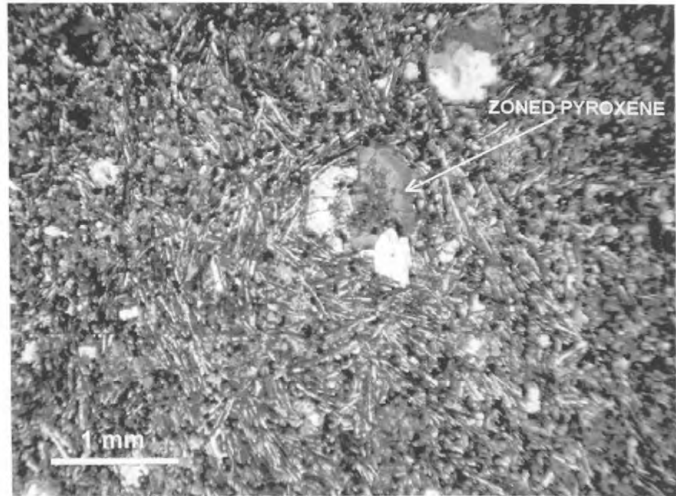
Last, notice the cylindrical holes drilled into the surface of the sill-dike. Small cores were taken from the basalt (Ressetar and Martin, 1980) using a diamond coring drill. These samples, carefully marked with their compass orientation with respect to the Earth's magnetic north pole, were subjected to paleomagnetic analysis which yielded a middle Eocene date and confirmed the results of radiometric dating.

Figure 26. Photomicrograph of amygdaloidal basalt from Sugar Grove, Stop 7. Euhedral pyroxene with compositional zonation is visible, as is the groundmass of plagioclase with felted texture. Crossed polars.

Acknowledgments

References Cited

Butts, C., 1940, Geology of the Appalachian Valley in Virginia: Virginia Geological Survey Bulletin 52, 568 p.

Darton, N.H., 1894, Description of the Staunton sheet: U.S. Geological Survey Geological Atlas, Folio 14.

Darton, N.H., 1899, Description of the Monterey quadrangle: U.S. Geological Survey Geological Atlas, Folio 61.

Darton, N.H., and Diller, J.S., 1890, On the occurrence of basalt dikes in the upper Paleozoic series in the central Appalachian Virginias: American Journal of Science, v. 139, p. 269–271.

Darton, N.H., and Keith, A., 1898, On dikes of telsophyre and Paleozoic rocks in central Appalachian Virginia: American Journal of Science, v. 156, p. 305–315.

Dennis, W.C., 1934, Igneous rocks of the valley of Virginia: Charlottesville, University of Virginia, unpublished M.S. thesis, 76 p.

Dennison, J.M., and Johnson, R.W., Jr., 1971, Tertiary intrusions and associated phenomena near the thirty-eighth parallel fracture zone in Virginia and West Virginia: Geological Society of America Bulletin, v. 82, p. 501–508.

Fullagar, P.D., and Bottino, M.L., 1969, Tertiary felsite intrusions in the Valley and Ridge province, Virginia: Geological Society of America Bulletin, v. 80, no. 9, p. 1853–1858.

Garnar, T.E., 1951, The igneous rocks of Pendleton County, West Virginia: Morgantown, W. Va., West Virginia University, unpublished M.S. thesis, 67 p.

Garnar, T.E., 1956, The igneous rocks of Pendleton County, West Virginia: West Virginia Geological and Economic Survey, Report of Investigations No. 12, 31 p.

Giannini, W.F., Mitchell, R.S., and Mann, R.W., 1987, Mineral update; Brucite from Highland County, Virginia: Virginia Minerals, v. 33, no. 1, p. 11.

Gittings, H.E., and Furman, T., 2001, Eocene basalt volcanism in central Virginia; Implications for Cenozoic tecton-

ism [abs.]: Geological Society of America Abstracts with Programs, v. 33, no. 2, p. A–5.

Good, R.S., 1992, Brucite marble occurrences along Ordovician Beekmantown dolomite and Eocene basalt and andesite dike contacts, Highland County, Virginia: Virginia Division of Mineral Resources Publication 119, p. 143–151.

Grand, S.P., 1994, Mantle shear structure beneath the Americas and surrounding oceans: Journal of Geophysical Research, v. 99, p. 11,591–11,621.

Hall, S.T., 1975, Mineralogy, chemistry, and petrogenesis of some hypabyssal intrusions, Highland County, Virginia: Blacksburg, Va., Virginia Polytechnic Institute and State University, unpublished M.S. thesis, 71 p.

Hearne, B.W., Jr., 1968, Diatremes with kimberlitic affinities in north-central Montana: Science, v. 159, p. 622–625.

Hyndman, D.W., 1972, Petrology of igneous and metamorphic rocks: New York, McGraw-Hill, 533 p.

Johnson, R.W., and Milton, C., 1955, Dike rocks of central-western Virginia [abs.]: Geological Society of America Abstracts with Programs, v. 66, no. 1, p. 1689–1690.

Johnson, R.W., Milton, C., and Dennison, J.M., 1971, Field trip to the igneous rocks of Augusta, Rockingham, Highland, and Bath Counties, Virginia: Virginia Division of Mineral Resources, Information Circular 16, 68 p.

Kapnicky, G.E., 1956, Petrology and contact effects of igneous rocks in Pendleton County, West Virginia: Morgantown, W. Va., West Virginia University, unpublished M.S. thesis, 67 p.

Kearns, L.E., 1993, The minerals of Sugar Grove, West Virginia: Rocks and Minerals, v. 68, no. 3, p. 158–167.

Kettren, L.P., 1970, Relationship of igneous intrusions to geologic structures in Highland County, Virginia: Blacksburg, Va., Virginia Polytechnic Institute and State University, unpublished M.S. thesis, 45 p.

King, S.D., and Ritsema, J., 2000, African hot spot volcanism; Small-scale convection in the upper mantle beneath cratons: Science, v. 290, p. 1137–1140.

Kulander, B.R., and Dean, S.L., 1986, Structure and tectonics of the central and southern Appalachian Valley and Ridge and Plateau provinces, West Virginia and Virginia: American Association of Petroleum Geologists Bulletin, v. 70, p. 1674–1684.

Le Bas, M.J., Le Maitre, R.W., Streckeisen, A., and Zanettin, B., 1986, A chemical classification of volcanic rocks based on the total alkali-silica diagram: Journal of Petrology, v. 27, p. 745–750.

Lorenz, V., 1986, On the growth of maars and diatremes and

its relevance to the formation of tuff rings: Bulletin of Volcanology, v. 48, p. 265–274.

Mathews, W.H., 1975, Cenozoic erosion and erosion surfaces of eastern North America: American Journal of Science, v. 275, p. 818–824.

Matmon, A., Bierman, P.R., Larsen, J., Southworth, S., Pavich, M., and Caffee, M., 2003, Temporally and spatially uniform rates of erosion in the southern Appalachian Great Smoky Mountains: Geology, v. 31, p. 155–158.

McDowell, R.R., comp., 2001, Stratigraphic geochemical database for portions of Pendleton County, West Virginia, and adjacent Virginia counties, covering portions of Pendleton County, West Virginia, Highland County, Virginia, and Augusta County, Virginia: West Virginia Geological and Economic Survey, Report of Investigations RI-34, computer diskette.

Mitchell, R.H., 1986, Kimberlites; Mineralogy, geochemistry, and petrology: New York, Plenum Press, 442 p.

Poag, C.W., and Sevon, W.D., 1989, A record of Appalachian denudation in postrift Mesozoic and Cenozoic sedimentary deposits of the U.S. Middle Atlantic continental margin: Geomorphology, v. 2, p. 119–157.

Rader, E.K., Gathright, T.M., and Marr, J.D., 1986, Trimble Knob basalt diatreme and associated dikes, Highland County, Virginia, in Neathery, T.L., ed., Geological Society of America Centennial Field Guide; Southeastern Section: Geological Society of America, p. 97–100.

Rader, E.K., and Wilkes, G.P., 2001, Geologic map of the Virginia portion of the Staunton 30 x 60 minute quadrangle: Virginia Division of Mineral Resources, Publication 163.

Ressetar, R., and Martin, D.L., 1980, Paleomagnetism of Eocene igneous intrusions in the Valley and Ridge province, Virginia and West Virginia: Canadian Journal of Earth Science, v. 17, p. 1583–1588.

Shumaker, R.C., 1985, Geologic cross-section 12, in Woodward, N.B., ed., Valley and Ridge thrust belt; Balanced structural sections, Pennsylvania to Alabama: Appalachian Basin Industrial Associates, University of Tennessee, Knoxville, Department of Geological Sciences, Studies in Geology, v. 12, 64 p.

Southworth, C.S., Gray, K.J., and Sutter, J.F., 1993, Middle Eocene intrusive igneous rocks of the central Appalachian Valley and Ridge province; Setting, chemistry, and implications for crustal structure: U.S. Geological Survey Bulletin 1839, p. J1–J24.

Taylor, S.R., and McLennan, S.M., 1985, The Continental crust; Its composition and evolution: Oxford, United Kingdom, Blackwell Scientific, 312 p.

Tso, J.L., and Surber, J.D., 2002, Eocene igneous rocks near Monterey, Virginia; A field study: Virginia Minerals, v. 48, p. 25–40.

Tso, J.L., and Surber, J.D., 2003, A field study of Eocene intrusive rocks and their surroundings in Highland County, Virginia [abs.]: Geological Society of America Abstracts with Programs, v. 35, no. 1, p. 69.

Vogt, P.R., 1991, Bermuda and Appalachian-Labrador Rises; Common non-hotspot processes?: Geology, v. 19, p. 41–44.

Watson, T.L., and Cline, J.H., 1913, Petrology of a series of igneous dikes in central western Virginia: Geological Society of America Bulletin, v. 24, p. 301–334.

Woodward, H.P., 1941, Silurian System of West Virginia: West Virginia Geological Survey Reports, v. 14, 326 p.

Woodward, H.P., 1943, Devonian System of West Virginia: West Virginia Geological Survey Reports, v. 15, 655 p.

Zartman, R.E., Brock, M.R., Heyl, A.V., and Thomas, H.H., 1967, K-Ar and Rb-Sr ages of some alkaline intrusive rocks from central and eastern United States: American Journal of Science, v. 265, no. 10, p. 848–870.

ROAD LOG FOLLOWS
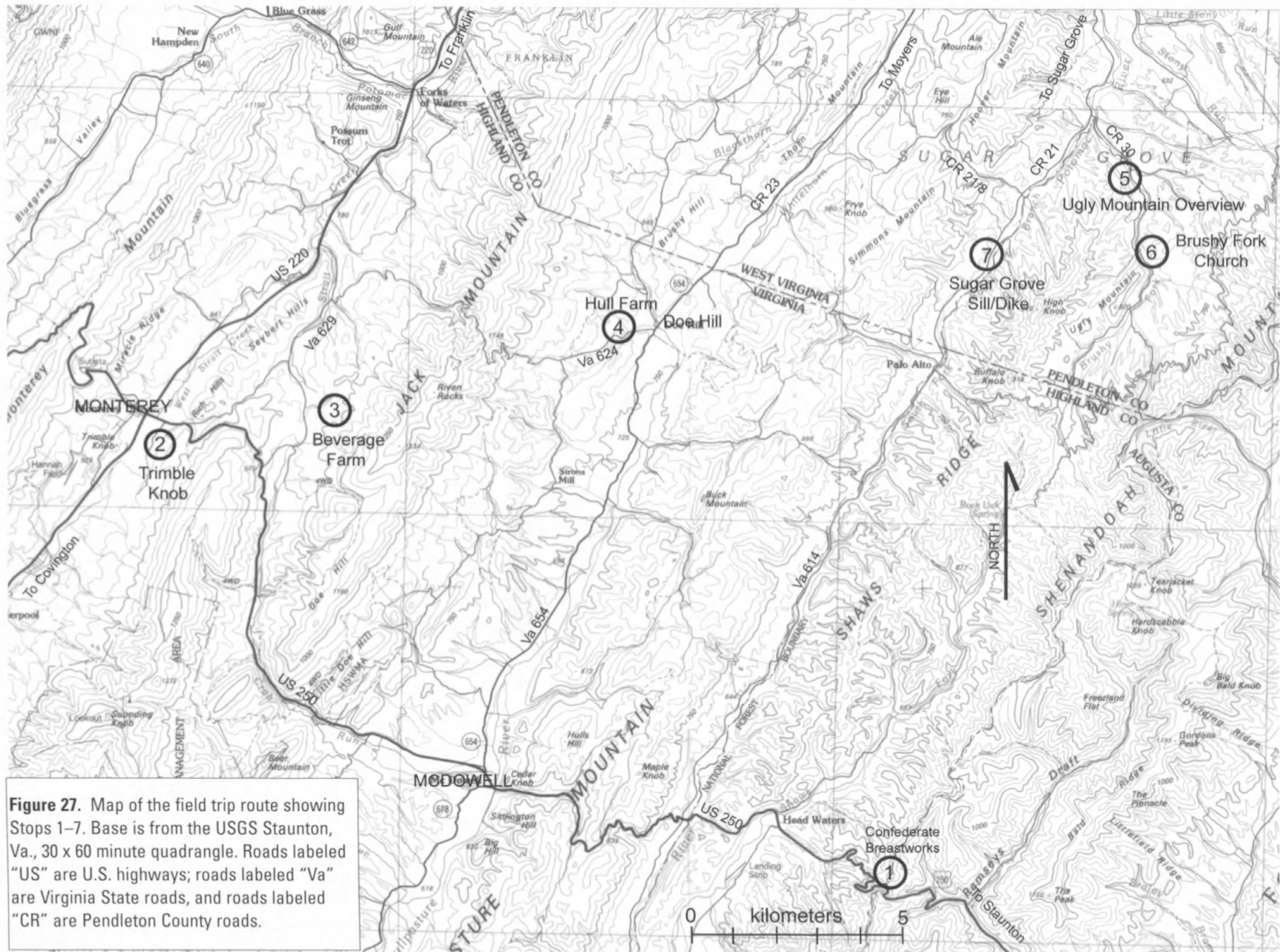
Figure 27. Map of the field trip route showing Stops 1–7. Base is from the USGS Staunton, Va., 30 x 60 minute quadrangle. Roads labeled "US" are U.S. highways; roads labeled "Va" are Virginia State roads, and roads labeled "CR" are Pendleton County roads.

Road Log

See text for description of each stop, and figure 27 for stop locations.

Day 1

From Washington, D.C., travel west on I-66 to junction with I-81. Turn south on I-81.

Mileage

Incremental	Cumulative	
0.0	0.0	Junction of I-81 and Va. 275 (Woodrow Wilson Parkway) in Staunton. Turn right (west) onto Va. 275.
1.3	1.3	Cross U.S. 11, continue west on Va. 275.
3.6	4.9	Junction of Va. 275 and U.S. 250. Turn right (west) onto U.S. 250.
4.6	9.5	Craigsville.
9.9	19.4	West Augusta.
6.2	25.6	Shenandoah Mountain. Turn into parking area at Confederate breastworks.

Stop 1. Confederate breastworks on Shenandoah Mountain (elevation 893 m; 2,930 ft).

Mileage

Incremental	Cumulative	
		Turn right (west) from breastworks parking area onto U.S. 250.
2.9	28.5	Village of Head Waters.
0.7	29.2	Crest of Shaws Ridge (elevation 701 m; 2,300 ft).
1.1	30.3	This landslide occurred in 1998 and was seated in one of the ash beds of the Devonian Tioga Bentonite. The subsequent remediation by Virginia Department of Transportation can be seen.
1.3	31.6	Top of Bullpasture Mountain (elevation 835 m; 2,740 ft).
2.7	34.3	Village of McDowell.
7.2	41.5	Top of Jack Mountain (elevation 1,038 m; 3,406 ft).
1.7	43.2	Downtown Monterey.

End of Day 1.

Day 2

Mileage

Incremental	Cumulative	
0.0	0.0	Junction of U.S. 250 and 220 in Monterey. Travel east on U.S. 250.
0.2	0.2	Junction of Va. 649 and U.S. 250. Turn right (south) onto Va. 649.
0.5	0.7	Travel south on Va. 649, past high school, to "End State Maintenance" sign and stop.

Stop 2. View of Trimble Knob.

Mileage

Incremental	Cumulative	
		Retrace route back to U.S. 250.
0.5	1.2	Junction of Va. 649 and U.S. 250. Turn left (west) onto U.S. 250.
0.2	1.4	Junction of U.S. 250 and U.S. 220. Turn right (north) onto U.S. 220.
3.6	5.0	Junction of U.S. 220 and Va. 629 (Strait Creek Road). Turn right (east) onto Va. 629.
2.7	7.7	Turn left into entrance to Beverage Farm.
		Park at main house.

Stop 3. Beverage Farm diatreme, basalt, and felsic rock.

Observe the rocks near the main house, then hike northeast approximately 0.7 km (0.4 mi) along the farm road to the small knoll that exposes "Breccia no. 1" and surrounding mafic and felsic rocks (fig. 14). *Note: As this location is on private property,* **obtain permission from the landowners** *before visiting the stop.*

Mileage

Incremental	Cumulative	
		Board vehicles, return to Va. 629 and turn left (south).
1.1	8.8	Junction of Va. 629 and U.S. 250. Turn left (east) onto U.S. 250.
6.4	15.2	Junction of U.S. 250 and Va. 654 in McDowell. Turn left (north) onto Va. 654.
7.1	22.3	Junction of Va. 654 and Va. 624 in the village of Doe Hill. Turn left (west) onto Va. 624.
1.3	23.6	Turn right into Hull Farm. Pull into driveway and park.

Stop 4. Hull Farm basalt and diatreme.

Note: As this location is on private property, **obtain permission from the landowners** *before visiting the stop.*

Mileage

Incremental	Cumulative	
		Board vehicles, turn left (east) onto Va. 624, and return to Va. 654 in Doe Hill.
1.3	24.9	Junction of Va. 624 and Va. 654 in Doe Hill. Turn left (north) onto Va. 654.
1.2	26.1	State line. Leave Highland County, Va., and enter Pendleton County, W. Va. Va. 654 becomes Doe Hill Road (County Road (CR) 23).
5.5	31.6	Junction of Doe Hill Road and Simmons Mountain Road (CR 23/2). Turn right (east) onto Simmons Mountain Road.
2.9	34.5	Simmons Mountain Road becomes Crummets Run Road (CR 21/8). Continue straight (east) on Crummets Run Road.
1.7	36.2	Junction of Crummets Run Road and Sugar Grove Road (CR 21). Turn left (north) onto Sugar Grove Road.
1.5	37.7	Junction of Sugar Grove Road and Brushy Fork Road (CR 30). Turn right (east) onto Brushy Fork Road.
1.1	38.8	Pull off in parking area to right of road at the junction of Fleisher Run Road (CR 30/2).

Stop 5. Ugly Mountain overview.

Mileage

Incremental	Cumulative	
		Continue ahead on Brushy Fork Road.
1.6	40.4	Park near, but do not block, church driveway.

Stop 6. Brushy Fork albitite dike.

Walk downstream (west) 69 m (75 yards) to streambed outcrop of albitite dike. Use caution in stream as rocks are slippery and the water is cold. Please take samples from rock already broken.

Mileage

Incremental	Cumulative	
		Board vehicles and retrace route on Brushy Fork Road back to Sugar Grove Road.
2.6	43.0	Junction of Brushy Fork Road and Sugar Grove Road.
		Turn left onto Sugar Grove Road.
0.2	43.2	Park on east side of the road and walk across road to outcrop.
		Use caution as outcrop is close to road.

Optional Stop. Wilfong Church gabbro.

Mileage

Incremental	Cumulative	
		Continue south on CR 21.
2.3	45.5	Park on the west (left) next to the outcrop. *Use caution as outcrop is close to road.*

Stop 7. Sugar Grove sill-dike.

Mileage

Incremental	Cumulative	
		Turn around and travel north on Sugar Grove Road.
5.2	50.7	Junction of Sugar Grove Road and Moyer Gap Road (CR 25) in the village of Sugar Grove.
		Continue right on Sugar Grove Road.
10.0	60.7	Junction of Sugar Grove Road and U.S. 33 in Brandywine.
		Turn right (east) onto U.S. 33.
7.6	68.3	State line and top of Shenandoah Mountain (elevation 1,052 m; 3,452 ft).
10.4	78.7	Rawley Springs.
9.8	88.5	Harrisonburg city limits.
0.6	89.1	Junction of U.S. 33 and High Street.
		Turn right onto High Street.
0.4	89.5	Junction of High Street and Cantrell Avenue.
		Turn left onto Cantrell Avenue.
0.3	89.8	Cross U.S. 11. Continue straight on Cantrell Avenue.
1.2	91.0	Junction of Cantrell Avenue and East Market Street.
		Turn right onto East Market Street.
0.5	91.5	Junction of East Market Street and I-81.
		Turn north onto I-81 and return to Washington, D.C.

End of Day 2.

5. Multiple Paleozoic Metamorphic Histories, Fabrics, and Faulting in the Westminster and Potomac Terranes, Central Appalachian Piedmont, Northern Virginia and Southern Maryland

By Michael J. Kunk,[1] Robert P. Wintsch,[2] C. Scott Southworth,[3] Bridget K. Mulvey,[2] Charles W. Naeser,[3] and Nancy D. Naeser[3]

Introduction

This field trip is a progress report of research on the complex rocks of the Westminster and Potomac terranes (Horton and others, 1991) of Maryland, Virginia, and Washington, D.C. (fig. 1). The study of these rocks was begun more than 60 years ago with work by Jonas and Stose (1938), Cloos and Broedel (1940), Stose and Stose (1946), and Cloos and Cooke (1953). Research continued with Fisher (1963, 1970, 1971), Hopson (1964), and Drake (1986, 1989, 1994, 1998), and continues today. Geologic mapping at a scale of 1:24,000 by the U.S. Geological Survey (USGS) in this region was begun by Avery Drake in the 1970s and resulted in a number of novel concepts and interpretations, and the publication of a large number of geologic quadrangle maps (Drake, 1986, 1994, 1998; Drake and Froelich, 1986, 1997; Drake and Lee, 1989; Fleming and others, 1994; Drake and others, 1999; Southworth, 1999). Compilations of these data at a scale of 1:100,000 were recently published (Southworth and others, 2002; Davis and others, 2002) and constitute a summary of the latest understanding of the distribution of the rocks.

During the map compilation phase of the study, rocks were sampled for $^{40}Ar/^{39}Ar$ and fission-track dating to better understand the chronology of the tectonic assemblage in the region. Specifically, rocks were sampled across the major faults along an east to west transect along the Potomac River and its tributaries. Results of the recent argon and fission-track dating compel us to reconsider many earlier interpretations and are the motivation for this field trip. In particular, $^{40}Ar/^{39}Ar$ and fission-track data identify age and thermal discontinuities that give added significance to mapped faults and identify unmapped faults and shear zone boundaries.

Geologic Setting

The Westminster and Potomac terranes are exposed in southern Maryland, northern Virginia, and Washington, D.C. (fig. 1). Drake and others (1989) and Horton and others (1989) proposed that the Potomac terrane was thrust onto the Westminster terrane along the Pleasant Grove fault, and that the Westminster terrane was thrust westward along the Martic fault onto Cambrian and Ordovician continental margin strata, during the Ordovician Taconian orogeny. Horton and others (1989) also speculated that both thrust faults were reactivated with dextral strike-slip motion during the late Paleozoic Alleghanian orogeny.

Westminster terrane

The rocks of the Westminster terrane are dominated by phyllites and have been correlated with the Hamburg klippe in Pennsylvania and higher slices of the Taconic allochthon in New England and New York (Knopf, 1935; Lyttle, 1982; Drake, 1986; Drake and others, 1989; Horton and others, 1989). Both the Westminster and Hamburg terranes are considered to represent offshore, deepwater, post-rift deposits with no direct stratigraphic ties to Laurentia (Horton and others, 1989). The low-grade, polymetamorphic, and polydeformed rocks previously mapped by Jonas and Stose (1938), Cloos and Broedel (1940), Cloos and Cooke (1953), Hopson (1964), Froelich (1975), Fisher (1978), and Edwards (1986, 1988, 1994), have been mapped, compiled, and summarized by Southworth and others (2002). We will examine part of the terrane that is dominated by rocks assigned to the Marburg Formation.

[1]U.S. Geological Survey, Denver, CO 80225.

[2]Department of Geological Sciences, Indiana University, Bloomington, IN 47405.

[3]U.S. Geological Survey, Reston, VA 20192.
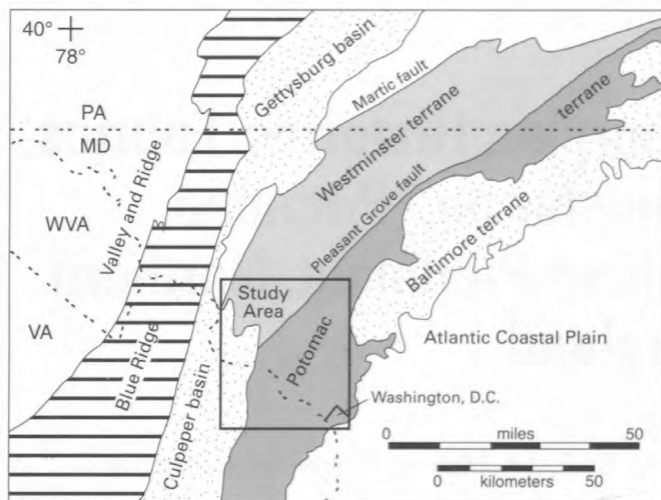
Figure 1. Terrane map of the south-central Appalachians. Box indicates the area of figures 2 and 6. Modified from Horton and others (1991).

Marburg Formation

The Marburg Formation contains primarily phyllite, metasiltstone, and quartzite. The protolith of the metasiltstone with quartz ribbons within the Marburg Formation has been interpreted to be turbidites by Southworth (1999). A few lenses of quartzite and rare greenstone have been interpreted to reflect an influx of channel deposits and volcanic sediments. Because the Marburg Formation contains some rocks that are similar to those in the Ijamsville Phyllite to the west, Marburg Formation rocks are interpreted to be composed of deepwater-rise deposits beneath and eastward of the Ijamsville Phyllite. Rocks of the Marburg Formation have been thrust onto the rocks of the Sams Creek Formation to the west along the Hyattstown fault (fig. 2). Rocks of the Marburg Formation collectively constitute a wide fault zone with multiple foliations, retrogressive phyllonites, and polydeformed vein quartz between the Hyattstown fault and the Pleasant Grove fault.

Potomac terrane

The Potomac terrane is bounded on the west by the Pleasant Grove fault and covered by Cretaceous and Tertiary Coastal Plain deposits to the east (fig. 1). The mapped units of the Potomac terrane, from west to east, are the Mather Gorge, Sykesville, and Laurel Formations (Drake and Froelich, 1997; Drake, 1998) (fig. 2). The protoliths of these rocks are interpreted to be Neoproterozoic to Early Cambrian distal slope deposits and olistostromes (Drake, 1989). These formations include mélanges that contain ultramafic rocks, and they are intruded by Early to Middle Ordovician tonalitic to granodioritic rocks (Aleinikoff and others, 2002). The three formations are separated by major faults that trend northward. The Plummers Island fault separates rocks of the Mather

Gorge Formation on the west from rocks of the Sykesville Formation on the east (Drake, 1989). The Rock Creek shear zone separates rocks of the Sykesville Formation intruded by Ordovician plutons on the west from diamictite of the Laurel Formation on the east (Fleming and others, 1994; Drake and Froelich, 1997; Fleming and Drake, 1998) (fig. 2). Multiple foliations in the rocks are common, and composite foliations are strongest in phyllonitic rocks in fault zones.

Regional aeromagnetic data reflect this complex geology (Southworth and others, 2002). Pronounced patterns of magnetic highs and lows define the Mather Gorge Formation (€Zmg, fig. 2) and the presence of ultramafic and mafic rocks. A broad low magnetic anomaly defines the rocks of the Sykesville Formation, and magnetic lineaments mark the Rock Creek shear zone.

Mather Gorge Formation

Rocks defined as the Mather Gorge Formation by Drake and Froelich (1997) consist of the metamorphosed equivalents of well-bedded graywacke and mudstone, which are now granofelsic metagraywackes and quartz-mica schists and higher grade equivalents (€Zmg, fig. 2). This north-northeast-striking belt of rock includes poorly exposed map-scale bodies of amphibolite, serpentinite, and talc schist that have been collectively mapped as ultramafic rocks (um, fig. 2). Both the metasedimentary rocks and amphibolite are intruded by the Ordovician Bear Island Granodiorite and associated pegmatites, and Devonian lamprophyre dikes intrude the schist. An apparent Barrovian metamorphic sequence of chlorite to sillimanite grade has been described that extends from the phyllitic rocks near the margin of the Culpeper basin eastward to the migmatites on Bear Island near Great Falls (Fisher, 1970; Drake, 1989). East of Great Falls (fig. 2, Stop 4), migmatitic rocks occur in a belt and grade eastward into a zone of retrograded chlorite-sericite phyllonites (Fisher, 1970) that are truncated on the east by the Plummers Island fault (Drake and Froelich, 1997) (fig. 2). The metagraywacke near Great Falls preserves bedding and soft-sedimentary slump features (Hopson, 1964; Fisher, 1970), and the package of rocks is interpreted to have been deposited as a sequence of turbidites (Drake and Froelich, 1997).

In this study, the rocks included in the Mather Gorge Formation are subdivided into three domains that are defined on the basis of lithology, metamorphic history, structure, and geochronology. From west to east, these are the Blockhouse Point, Bear Island, and Stubblefield Falls domains (fig. 2). The Blockhouse Point domain is characterized by chlorite-sericite phyllonites and some ultramafic rock bodies. The Bear Island domain is characterized by garnet-sillimanite-grade metagraywacke and schist that is migmatitic near the eastern boundary. Well-bedded metagraywacke (type locality of the Mather Gorge Formation), large ultramafic rock bodies, migmatite, granodiorite and pegmatite closely associated with amphibolite, and lamprophyre dikes characterize this domain.
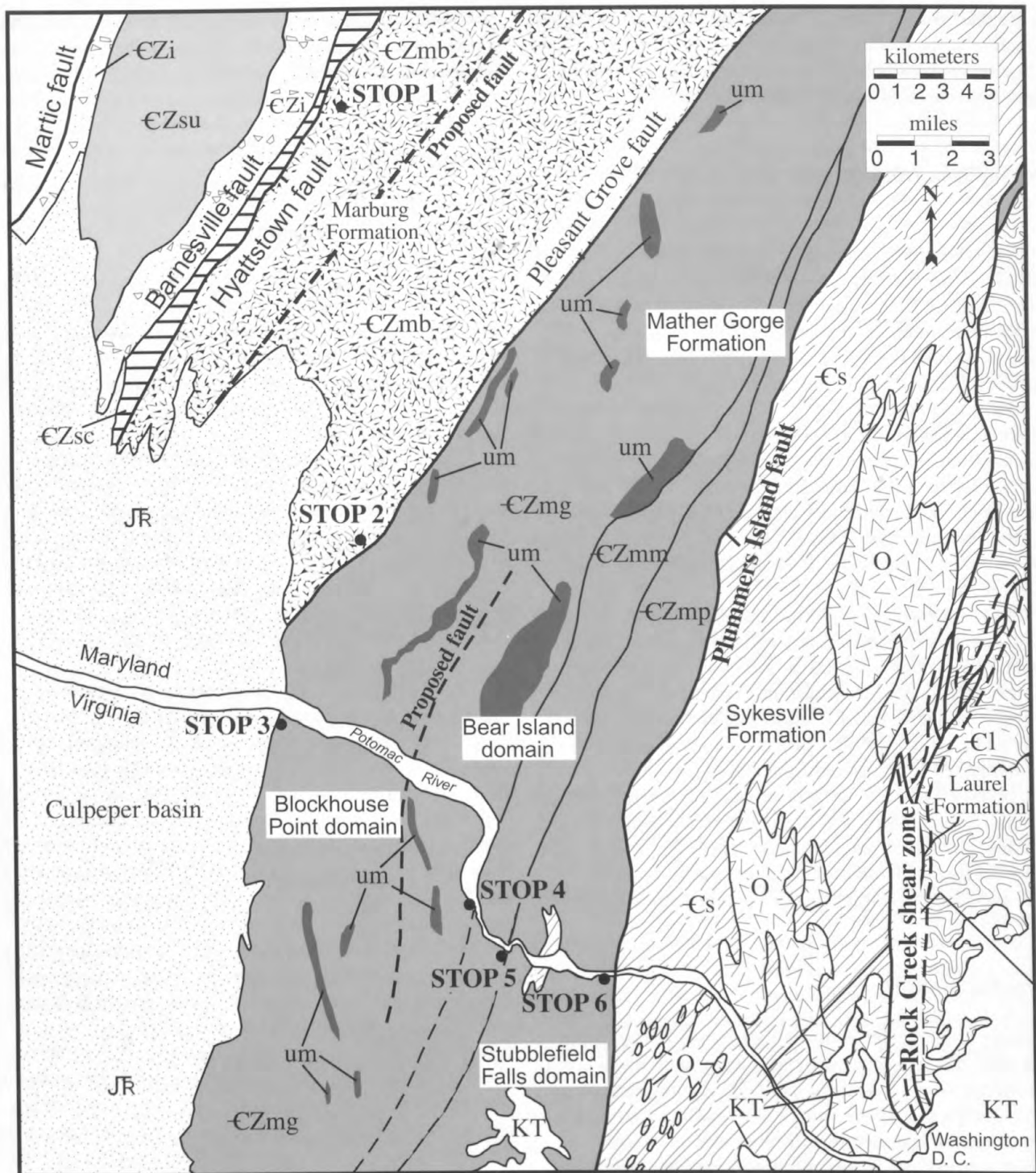
Figure 2. Geologic map of parts of the Westminster and Potomac terranes, Maryland, Virginia, and Washington, D.C. The Pleasant Grove fault separates the Westminster terrane on the west from the Potomac terrane on the east. Geologic map-unit symbols are as follows: €Zmg, Mather Gorge Formation; €Zmp, chlorite-sericite phyllonite of the Mather Gorge Formation; €Zmm, migmatitic Mather Gorge Formation; €Zi, Ijamsville Phyllite; €Zmb, Marburg Formation; €Zsc, Sams Creek Formation; €Zsu, undifferentiated metasilt-stone, phyllite, quartzite, and metagraywacke; €s, Sykesville Formation; €l, Laurel Formation; O, Ordovician plutons; um, ultramafics; J₮, Late Triassic and Early Jurassic rocks; KT, Cretaceous and Tertiary Coastal Plain deposits. Faults are as indicated and are dashed where inferred. Modified from Davis and others (2002).

The Stubblefield Falls domain to the east is characterized by migmatitic schist that has been retrograded to chlorite-sericite phyllonitic schist, small bodies of amphibolite, very minor granodiorite, and a few areas mapped as diamictite.

Sykesville Formation and Ordovician Plutonic Rocks

The Sykesville Formation of Hopson (1964) is a belt of metasedimentary rocks east of the Plummers Island fault and west of the Rock Creek shear zone (€s, fig. 2). These rocks have been metamorphosed to upper amphibolite facies, and intruded by a suite of Ordovician tonalitic to granodioritic rocks (O, fig. 2). Aleinikoff and others (2002) used U-Pb zircon techniques to date intrusive rocks including the Norbeck, Falls Church, Dalecarlia, and Georgetown Intrusive Suites and the Kensington Tonalite. Rocks of the Sykesville Formation have been interpreted to structurally underlie rocks of the Mather Gorge Formation under the Plummers Island fault along the Potomac River (Drake, 1989) (fig. 2), but to overlie them southwest of Baltimore to the north (Muller and others, 1989).

The sedimentary protoliths of the Sykesville Formation were diamictites and sedimentary mélanges containing clasts of amphibolite, migmatite, schist, metagraywacke, gabbroic granofels, phyllonite, greenstone, and vein quartz supported in a matrix of quartz-feldspar-muscovite granofels and schist (Drake and Froelich, 1997). Clasts within the diamictite have been interpreted to be derived from already deformed and metamorphosed rocks of the Mather Gorge Formation (Drake, 1989; Muller and others, 1989), and map-scale bodies of migmatite, phyllonite, and ultramafic schists that appear to be surrounded by diamictite have been interpreted by Drake (1989) and Fleming and others (1994) to be large olistoliths.

Laurel Formation

Rocks of the Laurel Formation are considered by Drake (1989) to be part of a separate motif (Laurel-Loch Raven), east of the Mather Gorge-Sykesville motif. The Laurel Formation (€l, fig. 2) (Hopson, 1964) forms a north-northeast-striking belt of diamictite that superficially resembles that of the Sykesville Formation. To the east it is covered by Cretaceous and younger Coastal Plain sediments, and to the west it is separated from the Sykesville Formation and Ordovician plutons by the Rock Creek shear zone (Fleming and others, 1994). These rocks were metamorphosed to upper amphibolite facies, then retrograded to phyllitic and mylonitic schists in the Rock Creek shear zone (Fleming and Drake, 1998).

In spite of the metamorphism, the protolith of the Laurel Formation is recognizably a diamictite, a sedimentary mélange with clasts of vein quartz, meta-arenite, biotite schist, actinolite schist, and local amphibolite supported by a

quartzofeldspathic matrix (Fleming and others, 1994). The unit is similar to the Sykesville Formation but contains a greater number and variety of olistoliths (Drake, 1998).

Geochronology

Previous geochronology

U-Pb zircon ages reflect the time of igneous crystallization and later metamorphic overgrowths, and K-Ar, ^{40}Ar/^{39}Ar, and Rb-Sr mica ages have been interpreted to reflect the time of cooling and, in some cases, muscovite growth. Published data are not complete enough to constrain metamorphic histories in our field area, but they provide important additional ages in our study area.

Earlier attempts at U-Pb dating of zircons in this complex setting (Davis and others, 1958, 1960; Wetherill and others, 1966; Fisher, 1970; Sinha and others, 1989) are difficult to interpret in light of recent advances in our understanding of U-Pb systems, and they will not be discussed here. U-Pb SHRIMP and TIMS analyses of zircons from plutonic rocks that intruded the Sykesville Formation in our field area (Aleinikoff and others, 2002) reveal Early to Late Ordovician ages of emplacement.

Reed and others (1970) dated two biotite separates from a lamprophyre dike at Great Falls (Stop 4) at 360±13 Ma and 363±13 Ma (2σ) using conventional K-Ar techniques. Muth and others (1979) dated muscovite cooling from the Bear Island Granodiorite within the Mather Gorge Formation, at 469±20 Ma and 469±12 Ma (2σ) using Rb-Sr techniques. Becker and others (1993) report ^{40}Ar/^{39}Ar ages of amphibole and muscovite from migmatitic rocks along Difficult Run (Stop 5, fig. 2) of 490 Ma and 422 Ma, respectively. They interpreted the amphibole age to represent cooling from the Cambrian-Ordovician, Penobscottian orogeny. We reinterpret the spectrum age as being the result of extraneous argon. Their muscovite age spectrum is sigmoidal because of the presence of more than one generation of muscovite, so the minimum apparent cooling age probably reflects a mixture of muscovite populations. Krol and others (1999) used ^{40}Ar/^{39}Ar dating of muscovite and biotite from rocks within the Pleasant Grove fault "zone." Their study did not provide any ages from the Mather Gorge, Sykesville, or Laurel Formations. They interpreted their ^{40}Ar/^{39}Ar data from muscovite to indicate a possible thermotectonic event between 368 and 348 Ma (Acadian), and dextral shearing of the central and northern parts of the Pleasant Grove fault "zone" at 311 Ma (Alleghanian).

New geochronology

New argon and fission-track data from the Westminster and Potomac terranes (Mulvey, 2003; Kunk and others, in press; and M.J. Kunk, unpub. data) together with published data require modifications of the previously interpreted

regional framework. A summary of these data is presented in figure 3. Our sampling strategy was designed to take advantage of detailed geologic mapping summarized by Southworth and others (2002), along a traverse that extends (west to east) from near the Hyattstown fault in Maryland (Stop 1) across the Rock Creek shear zone in the District of Columbia.

Amphibole ^{40}Ar/^{39}Ar ages

All amphibole samples were collected from rocks that experienced upper amphibolite facies metamorphism (Drake, 1989). They contain more than 50 percent coarse-grained amphibole coexisting with, and locally including, plagioclase, magnetite, biotite, and epidote. Many samples also contain retrograde epidote and chlorite that may or may not define a late fabric. In most rocks the amphiboles define at least one foliation. In some samples, a coarser grained gneissosity is overprinted by a more pervasive schistosity, and one sample appears to retain an igneous texture. Amphibole in metagabbro intrusive to the Laurel Formation is typical, containing equant grains of amphibole up to 0.5 mm in diameter that are overgrown by acicular needles that define a second foliation (S$_2$, fig. 4A). The high metamorphic grade of the samples is supported by the amphibole textures which indicates temperatures >600°C (Poirier, 1985).

The time of cooling of each of the three high-grade domains of figure 2 is estimated by at least two amphibole analyses. Three samples from the Bear Island domain contain excess argon, with two samples yielding minimum and isochron ages of 475 Ma (Stops 4 and 5). The third sample produces an overlapping isochron age of 455±23 Ma. These ages are consistent with the Rb-Sr ages of muscovite of 469±12 Ma and 469±20 Ma (Muth and others, 1979), which are also considered to have a closure temperature of ~500°C (Jäeger, 1979). The ~455- to 475-Ma age range of these samples is accepted as the best estimate for the time of cooling of the Bear Island domain through ~500°C.

Two samples of amphibole from rocks that intrude the Sykesville Formation also agree with each other within analytical uncertainty. A sample from the Falls Church pluton produced a near-plateau age spectrum with a minimum age of 401 Ma. This amphibole probably had a relatively simple igneous crystallization history, followed by slow cooling with relatively little deformation. The 405-Ma isochron age of a sample from the Georgetown Intrusive Suite confirms the time of cooling. Hence the Early Devonian age of ~401 Ma is a reasonable estimate of the time of regional cooling of the intrusive rocks and the country rocks of the Sykesville Formation through 500°C.

Two amphibole samples from rocks that intrude the Laurel Formation have minimum ages of 404 Ma and 398 Ma. This indicates Early Devonian cooling through 500°C for the intrusive rocks and rocks of the Laurel Formation. These ages are indistinguishable from the amphibole cooling ages of the Sykesville Formation.

Muscovite ^{40}Ar/^{39}Ar ages

The rocks of the Westminster terrane (Stops 1 and 2) never exceeded lower greenschist facies conditions, and thus were always below the closure temperature for diffusion of argon in muscovite (~350°C). Many of the muscovite separates (and one whole-rock sample) produced either sigmoidal or climbing age spectra (Mulvey, 2003). The shapes of these age spectra can be caused by (1) the presence of a (usually) very small population of much older detrital muscovite in the sample, (2) the presence of multiple generations of metamorphic muscovite in the sample, and (3) the presence of inseparable, intimately intergrown chlorite. Because of these complications, the muscovite age spectra provide only approximations of the maximum ages of the most recent muscovite growth and minimum ages of earlier muscovite foliations or detrital components in the Westminster terrane (Mulvey, 2003). These results are nonetheless useful at the orogenic level.

Three samples collected from the western part of the Marburg Formation in the Westminster terrane gave ages of ~435 to 430 Ma, whereas two samples from the eastern part of the Marburg Formation gave ages of ~382 to 375 Ma (Stops 1 and 2) (fig. 2) (Mulvey, 2003; M.J. Kunk, unpub. data). All of these ages are interpreted to approximate the time of growth of cleavage-forming muscovite in these samples.

All of the rocks in the Potomac terrane have been metamorphosed to at least biotite grade (Kunk and others, in press), thus any detrital muscovite in sedimentary protoliths has been either recrystallized or thermally reset. In addition, we were able to separate muscovite that was free of chlorite intergrowths in all but one of the samples from the Potomac terrane (Kunk and others, in press. Nonetheless, most of the muscovite samples from the Potomac terrane also have sigmoidal or climbing age spectra. In these rocks, older (S$_1$) high-grade mineral assemblages have been partly overprinted by younger (S$_2$), lower grade foliation(s) (crystallized below the muscovite closure temperature for argon diffusion). For these samples we have interpreted the minimum age in the spectrum as the maximum age of muscovite growth below closure, and the maximum age in the spectrum as a minimum age for cooling of the higher grade muscovite through 350°C. These age pairs for each sample are plotted in figure 3, and rocks of the Mather Gorge Formation are summarized as follows:

(1) The westernmost muscovite sample from the Blockhouse Point domain (figs. 2 and 3) produced a plateau age of 362±2 Ma (1σ) that we interpret as the time of white mica growth (S$_2$) in the sample. Two samples farther to the east gave ~371 Ma cooling ages (S$_1$) and ~362 Ma growth ages (S$_2$).
(2) In the Bear Island domain, cooling-age estimates from the muscovite age spectra range from 422 to 411 Ma (S$_1$), and below-closure growth-age estimates range from 385 to 373 Ma (S$_2$).
(3) In the Stubblefield Falls domain, cooling-age estimates
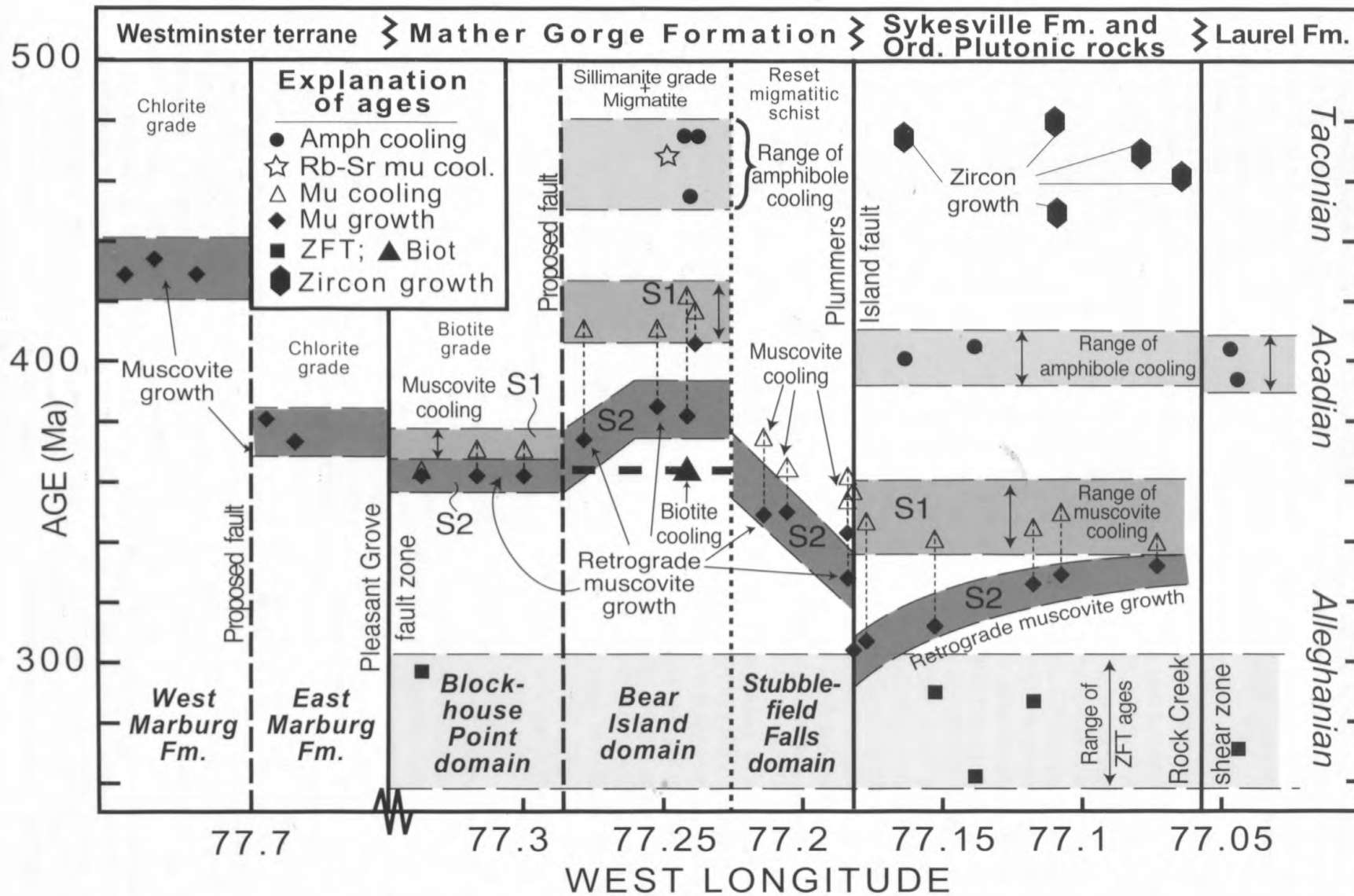
Figure 3. Diagram plotting age against sample location along west-to-east transect for parts of the Westminster and Potomac terranes. Ages are based on ⁴⁰Ar/³⁹Ar data (Kunk and others, in press; Mulvey, 2003; and M.J. Kunk, unpub. data), U-Pb data (Aleinikoff and others, 2002), Rb-Sr data (Muth and others, 1979), K-Ar data (Reed and others, 1970), and zircon fission-track data (Kunk and others, in press). The five zircon fission-track ages from the Potomac terrane are statistically indistinguishable, with a mean of 282±13 Ma, suggesting that these rocks all cooled through the ~235°C zircon closure temperature (Brandon and others, 1998) in earliest Permian time. See text for additional discussion. Modified from Kunk and others (in press). ZFT, zircon fission track; Amph, amphibole; mu, muscovite; biot, biotite; Ord., Ordovician; Fm, Formation.

from the muscovite age spectra range from 375 to 354 Ma (S₁), and growth-age estimates range from 350 to 328 Ma (S₂).

East of the Mather Gorge Formation and Plummers Island fault, cooling-age estimates from the muscovite age spectra from the Sykesville Formation range from 354 to 340 Ma (S₁), and growth-age estimates range from 332 to 304 Ma (S₂).

Biotite ^{40}Ar/^{39}Ar ages

Only one biotite sample was dated because of the dearth of unaltered biotites in the field area. The biotite (Stop 5, fig. 2) is from the Bear Island Granodiorite in the Bear Island domain and produced a ^{40}Ar/^{39}Ar total fusion age of 364±2 Ma. This age is the same, within the limits of analytical precision, as K-Ar ages reported by Reed and others (1970) for two biotite samples (360±13 Ma and 363±13 Ma) collected nearby from a lamprophyre dike (Stop 4, fig. 2). Because the biotite from our sample grew in a metamorphic environment well above its argon closure temperature, we interpret both this age and the ages from the dike to represent the timing of cooling of the biotite through ~300°C in a regional thermal gradient.

Zircon fission-track ages

Zircon fission-track ages determined for five samples from the Potomac terrane (one sample from the Blockhouse Point domain of the Mather Gorge Formation, three samples from the Sykesville Formation, and one sample from the Laurel Formation), are statistically indistinguishable, suggesting that the rocks cooled through the zircon fission-track closure temperature (~235°C; Brandon and others, 1998) from 298±46 Ma to 262±20 Ma (±2 standard errors of the mean; fig. 3). The mean zircon age calculated for the five samples is 282±13 Ma, suggesting that the rocks cooled through ~235°C in earliest Permian time.

Apatite fission-track ages

Seven samples yielded sufficient apatite for fission-track analysis. The samples span most of the Potomac composite terrane, from the shear zone separating the Blockhouse Point and Bear Island domains in the Mather Gorge complex in the west to Rock Creek Park (Laurel Formation) in the east. Apatite fission-track ages range from 198±21 Ma to 131±16 Ma (±2σ), with ages generally becoming younger to the west. The apatite fission-track age and track-length data indicate that rocks presently exposed at the surface cooled through the
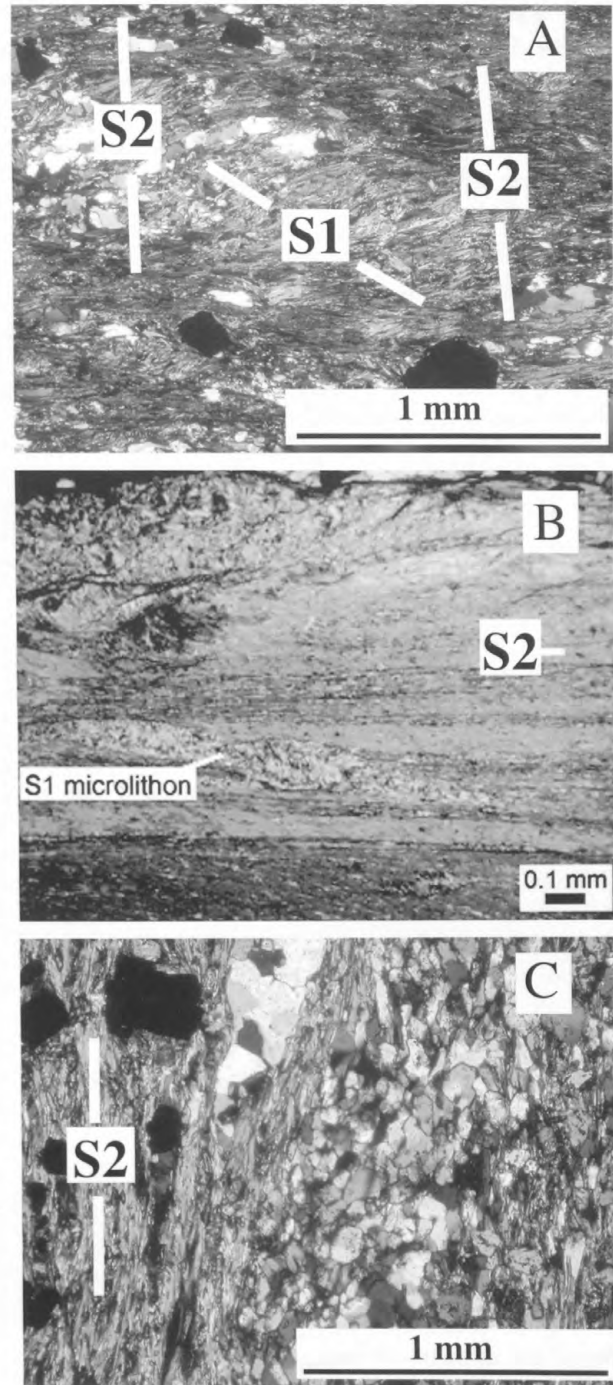
Figure 4. Photomicrographs in cross polarized light from (A) a metagabbro in the Laurel Formation, (B) the eastern Marburg Formation, and (C) the Blockhouse Point domain of the Mather Gorge Formation. See text for discussion.

apatite fission-track closure temperature (~90°C–100°C in these rocks) from the Early Jurassic to the Early Cretaceous, with the time of cooling becoming younger to the west.

Summary of recent studies

The rocks of the Potomac terrane have been metamorphosed to at least biotite grade, and contain one or more higher grade schistosities (collectively called "S_1"), which formed above the ~350°C closure temperature of muscovite. The $^{40}Ar/^{39}Ar$ ages recorded by S_1 muscovites should represent the time of their passage through ~350°C. In addition, most of these rocks and the rocks of the Marburg Formation in the Westminster terrane also contain one or more younger schistosities (collectively called "S_2"), that grew below ~350°C in the greenschist facies; their $^{40}Ar/^{39}Ar$ muscovite ages should record the time of these muscovites' crystallization. S_1 and S_2 as referred to here are clearly not the same in the various tectonic blocks that are discussed. While S_1 ages represent only the last passage of the rocks through the ~350°C isotherm, S_2 ages can represent composite schistosities and multiple episodes of mineral growth.

Westminster terrane

The muscovite growth-age estimates in the western part of the Marburg Formation (Stop 1) are ~435 to 430 Ma, in contrast to those in the eastern part of the Marburg Formation (Stop 2) where they range from 382 to 375 Ma (fig. 3). The ~50 m.y. discontinuity in age between these two groups of samples is most easily explained by a fault within the Marburg Formation between Stops 1 and 2.

Potomac terrane

Mather Gorge Formation

Blockhouse Point domain

Maximum estimates of muscovite growth ages of two samples are 362 Ma, and a third sample in the westernmost part of the Blockhouse Point domain has a plateau age of 362±2 Ma. We interpret 362 Ma as the age of the lower greenschist facies muscovite growth (Stop 3). Because the metamorphic grade of these rocks reached biotite-grade conditions in the Middle Devonian, any argon isotopic evidence of an earlier metamorphic event in these muscovites has been reset.

Bear Island domain

Higher metamorphic temperatures here resulted in formation of migmatite (Stops 5 and 6). Our amphibole data indicate that cooling through 500°C occurred between 475

and 455 Ma (fig. 3). The estimate from muscovite data for the timing of cooling through 350°C (S_1) is >422 Ma. Maximum age estimates for below-closure-temperature growth of muscovite (S_2) range from 385 to 373 Ma. A comparison with the muscovite samples of the Blockhouse Point domain shows a striking difference in the estimated time of cooling through 350°C (371 Ma versus 422 Ma), suggesting the presence of a fault zone between the two domains.

Stubblefield Falls domain

The rocks west of the Plummers Island fault were migmatitic (Stop 6), but they were later retrograded to a chlorite-sericite phyllonite (Fisher, 1970). We extend the Ordovician cooling history of the Bear Island domain here based on that earlier high-temperature history. Muscovite age spectra indicate minimum estimates for cooling through 350°C that range from 375 Ma to 354 Ma, younging to the east, suggesting reheating in the Devonian to reset the muscovite ages. Maximum estimates for the time of subsequent growth below closure of S_2 muscovite also show a general pattern of younging to the east, and range from 350 Ma in the western part of the domain to 328 Ma near the Plummers Island fault.

#### Sykesville Formation and Ordovician intrusive rocks

The rocks of the Sykesville Formation were intruded by Middle to Late Ordovician plutonic rock (Aleinikoff and others, 2002) prior to or during peak amphibolite facies metamorphic conditions. Amphibole samples from the Falls Church pluton and the Dalecarlia Intrusive Suite have disturbed $^{40}Ar/^{39}Ar$ ages of 401 Ma and 405 Ma, respectively, indicating cooling through 500°C in the Early Devonian. The muscovite age spectra from the Sykesville Formation give minimum estimates for cooling through 350°C that range from 357 to 340 Ma (S_1). Maximum age estimates for subsequent muscovite below-closure growth (S_2) range from 304 Ma in the Plummers Island fault to 332 Ma near the Rock Creek shear zone, and show a dramatic decrease in age to the west (fig. 3). We interpret the 304-Ma age to represent a maximum age for the time of final Alleghanian movement on the Plummers Island fault.

Laurel Formation and intrusive rocks

Two amphiboles were dated from rocks that intrude the Laurel Formation. Both had relatively flat age spectra and suggest an age of ~400 Ma for their time of cooling through 500°C.

Thermal Histories Across the Plummers Island Fault

Cooling curves provide comparison of the thermal history across the Plummers Island fault (fig. 5). The best estimate for
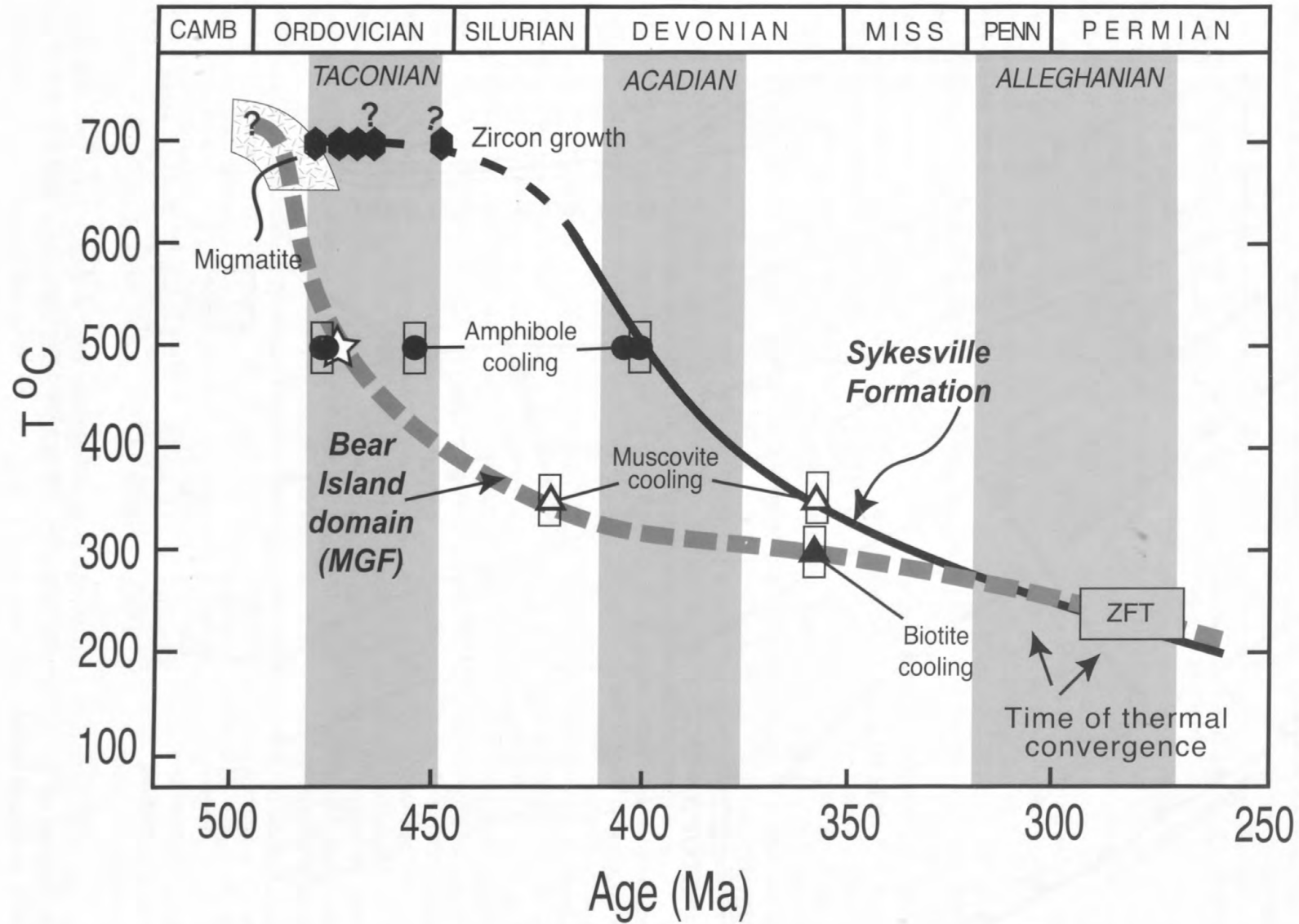
Figure 5. Cooling curves for the Bear Island domain of the Mather Gorge Formation and for the Sykesville Formation. Filled circle represents $^{40}Ar/^{39}Ar$ amphibole cooling age; open star, Rb-Sr muscovite cooling ages; open triangle, $^{40}Ar/^{39}Ar$ muscovite cooling age; filled triangle, $^{40}Ar/^{39}Ar$ biotite cooling age; filled hexagon, U-Pb zircon growth age; ZFT, zircon fission-track cooling ages; MGF, Mather Gorge Formation. Open rectangles denote error bars. All U-Pb zircon age data are on the Sykesville Formation cooling curve. Modified from Kunk and others (in press).
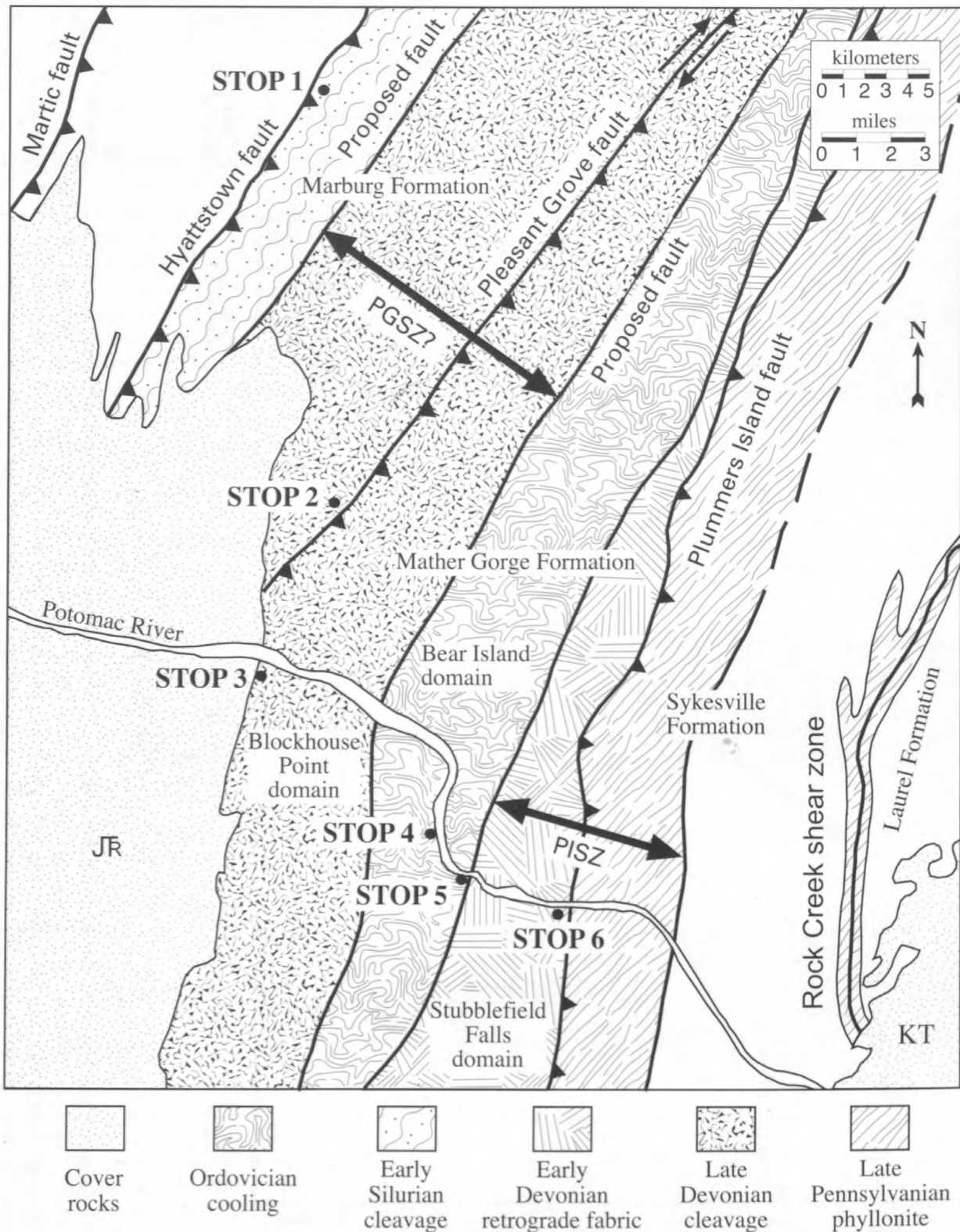
Figure 6. Tectonic domain map modified from figure 2 in response to existing lithologic and geochronologic data. The tectonic boundaries do not appear to be coincident with the formation boundaries. PISZ, Plummers Island shear zone; PGSZ, Pleasant Grove shear zone. For definitions of other symbols see figure 2.

the time of cooling of the Bear Island domain through ~500°C is 475 to 455 Ma, obtained from the three amphibole $^{40}Ar/^{39}Ar$ ages and two Rb-Sr muscovite ages. The minimum age estimate for cooling of muscovite through its closure temperature, 422 Ma, provides a data point at ~350°C. Our biotite $^{40}Ar/^{39}Ar$ age of 364±2 Ma adds a point on the curve at ~300°C. Regional zircon fission-track ages of ~280 Ma add a point at ~235°C. Together these points generate the concave-up cooling trend (fig. 5) typical of many metamorphic terranes. Extrapolating back from this curve, migmatitic conditions of 650 to 700°C appear to have occurred in these rocks in the Early Ordovician (migmatite patterned polygon, fig. 5). This cooling curve also shows that metamorphic conditions did not exceed greenschist facies after mid-Paleozoic times. The planar lamprophyre dikes in fractures suggests no significant contractional deformation occurred after about 365 Ma.

Migmatitic textures in the diamictite of the Sykesville Formation indicate upper amphibolite facies metamorphism. The Ordovician ages of the five dated plutonic rocks (Aleinikoff and others, 2002) provide data points at the near-solidus temperatures of ~700°C. Our ~400-Ma cooling ages of amphiboles provide a point at ~500°C. The minimum cooling-age estimate from the muscovite data provides a data point at 357 Ma and ~350°C, and a fourth point is established by the zircon fission-track data at 280 Ma and 235°C.

The cooling curves show independent paths throughout the Paleozoic that do not converge until ~300 to 280 Ma (fig. 5). In particular, migmatitic rocks of the Bear Island domain had cooled to greenschist-facies conditions by the time that the Sykesville Formation was still at upper amphibolite facies in the Late Silurian. These temperature contrasts reflect 3 to 6 km of net vertical displacement, depending on the geothermal gradients in the two blocks of rock. Vertical displacement may have been accompanied by an unknown, but possibly considerable, component of strike-slip movement. This difference in cooling history is not consistent with the interpretation of a Cambrian-age premetamorphic Plummers Island fault that shed clasts of metamorphosed Mather Gorge Formation into sediments that became the Sykesville Formation (Drake, 1989). Muller and others' (1989) interpretation of the Sykesville Formation being deposited in late Cambrian to Early Ordovician time from erosion of an uplifted Mather Gorge Formation (their Morgan Run Formation) is also unlikely, based on the difference in cooling histories during much of the Paleozoic.

Rocks of the Bear Island domain cooled continuously from Middle Ordovician to Late Carboniferous time, and were cooler at any given time than the rocks of the Sykesville Formation (fig. 5). Nonetheless, the cooling rate of the Sykesville Formation exceeded that of the Bear Island domain from the middle Silurian through the Pennsylvanian (fig. 5). The net crustal displacement across the fault from the Ordovician through Pennsylvanian is east side up.

Interpreted Tectonic Assemblage

By the Early to Middle Ordovician, the rocks of the Bear Island domain and, by inference, also the Stubblefield Falls domain in the Mather Gorge Formation, had been metamorphosed and were cooling through ~500°C (fig. 5), while the Sykesville Formation was still at upper amphibolite-facies prograde metamorphic conditions and was being intruded by plutons (Aleinikoff and others, 2002). The metamorphic and necessarily structural divergence precludes a geological connection between the formations in the Ordovician. Rocks of the Blockhouse Point domain had not been detectably metamorphosed, so they were also physically separated from the Bear Island domain.

By the Early Silurian the rocks of the westernmost Marburg Formation had been metamorphosed to lower greenschist facies when an S_1 cleavage was produced, while the eastern Marburg Formation apparently remained unmetamorphosed. During the Early Devonian (figs. 5, 6), hot rocks of the Sykesville Formation and associated plutons were being thrust over the Stubblefield Falls domain, heating the muscovite to temperatures well above argon closure, along an early Plummers Island shear zone (Schoenborn, 2002). At ~400 Ma, the Laurel and Sykesville Formations simultaneously cooled through 500°C, the closure temperature for argon diffusion in amphibole, suggesting that they were at the same structural level at that time.

By the Late Devonian, the Blockhouse Point domain had cooled from biotite-grade metamorphism (>400°C). A shear zone with strain distributed over a zone as much as 12 km wide, from the Blockhouse Point domain west into the Westminster terrane, produced S_2 cleavage defined by muscovite that crystallized below its closure temperature. At about the same time, rocks of the Stubblefield Falls domain, and later of the Sykesville Formation, cooled through ~350°C while the rocks of the Bear Island domain cooled through 300°C, demonstrating that these blocks were at different structural levels at the time (figs. 5, 6).

In the Late Pennsylvanian, the rocks of the Stubblefield Falls domain of the Mather Gorge Formation moved up relative to the Sykesville Formation on the steep, west-dipping Plummers Island fault and mylonite zones (Schoenborn, 2001) within an existing Plummers Island shear zone (figs. 5, 6). Shearing formed S_2 cleavage with below-closure muscovite growth and more pervasive S_2 cleavage in the Sykesville Formation. By the earliest Permian, all of the rocks in the Potomac terrane had cooled through 235°C (figs. 3, 5). Apatite fission-track data indicate cooling through ~90°C to 100°C in Early Jurassic to Early Cretaceous time, with increasing ages to the east, suggesting kilometer-scale rotation of the Potomac terrane in the Cretaceous and (or) Tertiary, with the west side up.
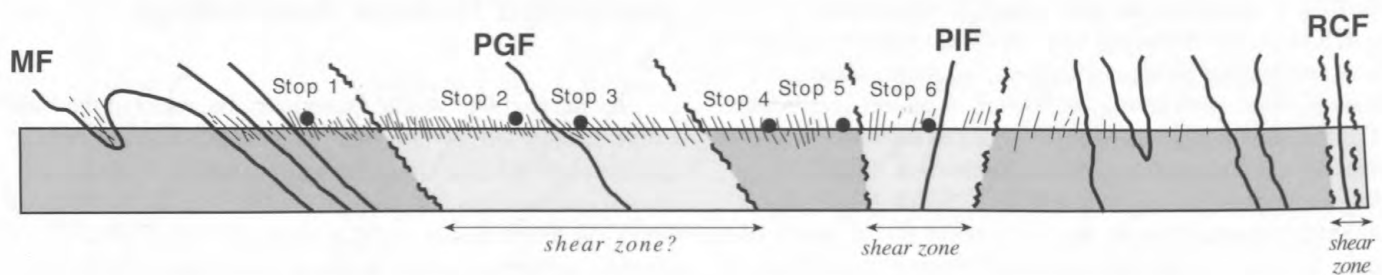
Figure 7. Tentative, conceptual cross section of study area showing the Ordovician Potomac River fan structure of Drake (1989). The data discussed in this study indicate that the Potomac River fan structure is a composite of foliations formed throughout the Paleozoic. Approximate locations of field stops are indicated. MF, Martic fault; PGF, Pleasant Grove fault; PIF, Plummers Island fault; RCF, Rock Creek fault.

Faults and Shear Zones: Plummers Island, Pleasant Grove, and Rock Creek

In summary, the assemblage of the rocks of the Potomac and Westminster terranes occurred during the Acadian orogeny in the Devonian, with fault reactivation during the Alleghanian orogeny in Pennsylvanian time. The apparent Barrovian metamorphic sequence of chlorite to sillimanite grade (west to east) (Fisher, 1970), and the Potomac River fan structure (fig. 7) (Drake, 1989), both interpreted to be of Ordovician age (Drake, 1989), are obviously a composite of different events throughout the Paleozoic.

If our analysis is correct, the 5-km-wide Early Devonian (Acadian) Plummers Island shear zone was reactivated in the Carboniferous (Alleghanian) under lower greenschist-facies conditions as the Plummers Island fault (fig. 6). The muscovite cooling (S_1) and growth ages (S_2) in the Blockhouse Point domain are similar to growth ages in the eastern part of the Westminster terrane. Therefore, Late Devonian (Acadian) deformation in a 12-km-wide Pleasant Grove shear zone may have extended from the Blockhouse Point domain west *across* the Pleasant Grove fault into the Marburg Formation of the Westminster Terrane. There is no isotopic evidence of pre-Devonian or significant post-Devonian movement on this part of the Pleasant Grove fault. However, shear-band cleavage with dextral strike-slip kinematics supports Alleghanian movement of unknown significance within the Pleasant Grove shear zone.

References Cited

Aleinikoff, J.N., Horton, J.W., Jr., Drake, A.A., Jr., and Fanning, C.M., 2002, Shrimp and U-Pb ages of Ordovician granites and tonalites in the central Appalachian Piedmont; Implications for Paleozoic tectonic events: American Journal of Science, v. 302, p. 50–75.

Becker, J.L., Kunk, M.J., Wintsch, R.P., and Drake, A.A., Jr., 1993, Evidence for pre-Taconic metamorphism in the Potomac terrane, Maryland and Virginia; Hornblende and muscovite $^{40}Ar/^{39}Ar$ results: Geological Society of America Abstracts with Programs, v. 25 no. 2, p. A5.

Brandon, M.T., Roden-Tice, M.K., and Garver, J.I., 1998, Late Cenozoic exhumation of the Cascadia accretionary wedge in the Olympic Mountains, northwest Washington State: Geological Society of America Bulletin, v. 110, no. 8, p. 985–1009.

Cloos, Ernst, and Broedel, C.H., 1940, Geologic map of Howard County: Maryland Geological Survey, scale 1:62,500.

Cloos, Ernst, and Cooke, C.W., 1953, Geological map of Montgomery County and the District of Columbia: Maryland Department of Geology, Mines, and Water Resources, scale 1:62,500.

Davis, A.M., Southworth, C.S., Reddy, J.E., and Schindler, J.S., 2002, Geologic map database of the Washington, D.C. area featuring data from three 30- x 60-minute quadrangles, Frederick, Washington West, and Fredericksburg: U.S. Geological Survey Open-File Report 01–227.

Davis, G.L., Tilton, G.R., Aldrich, L.T., and Wetherill, G.W., 1958, The age of rocks and minerals: Carnegie Institute of Washington Yearbook 57, p. 176–181.

Davis, G.L., Tilton, G.R., Aldrich, L.T., Wetherill, G.W., and Bass, M.N., 1960, The age of rocks and minerals: Carnegie Institute of Washington Yearbook 59, p. 147–158.

Drake, A.A., Jr., 1986, Geologic map of the Fairfax quadrangle, Fairfax County, Virginia: U.S. Geological Survey Geologic Quadrangle Map GQ–1600, scale 1:24,000.

Drake, A.A., Jr., 1989, Metamorphic rocks of the Potomac terrane in the Potomac Valley of Virginia and Maryland, *in* International Geological Congress, 28th, Field Trip Guidebook T202: Washington, D.C., American Geophysical Union, 22 p.

Drake, A.A., Jr., 1994, The Soldier's Delight Ultramafite in the Maryland Piedmont, *in* Stratigraphic Notes, 1993: U.S. Geological Survey Bulletin 2076, p. A1–A14.

Drake, A.A., Jr., 1998, Geologic map of the Kensington quadrangle, Montgomery County, Maryland: U.S. Geological Survey Geologic Quadrangle Map GQ–1774, scale 1:24,000.

Drake, A.A., Jr., and Froelich, A.J., 1986, Geologic map of the Annandale quadrangle, Fairfax and Arlington Counties, and Alexandria City, Virginia: U.S. Geological Survey Geologic Quadrangle Map GQ–1601, scale 1:24,000.

Drake, A.A., Jr., and Froelich, A.J., 1997, Geologic map of the Falls Church quadrangle, Fairfax and Arlington Counties and the City of Falls Church, Virginia, and Montgomery County, Maryland: U.S. Geological Survey Geologic Quadrangle Map GQ–1734, scale 1:24,000.

Drake, A.A., Jr., and Lee, K.Y., 1989, Geologic map of the Vienna quadrangle, Fairfax County, Virginia, and Montgomery County, Maryland: U.S. Geological Survey Geologic Quadrangle Map GQ–1670, scale 1:24,000.

Drake, A.A., Jr., and Morgan, B.A., 1981, The Piney Branch Complex—A metamorphosed fragment of the central Appalachian ophiolite in northern Virginia: American Journal of Science, v. 281, p. 484–508.

Drake, A.A., Jr., Sinha, A.K., Laird, J., and Guy, R.E., 1989, The Taconic orogen, in Hatcher, R.D., Jr., Thomas, W.A., and Viele, G.W., eds., The Appalachian-Ouachita orogen in the United States: Boulder, Colorado, Geological Society of America, The Geology of North America, v. F-2, p. 101–177.

Drake, A.A., Jr., Southworth, S., and Lee, K.Y., 1999, Geologic map of the Seneca quadrangle, Montgomery County, Maryland, and Fairfax and Loudoun Counties, Virginia: U.S. Geological Survey Geologic Quadrangle Map GQ–1802, scale 1:24,000.

Edwards, Jonathan, Jr., 1986, Geologic map of the Union Bridge quadrangle, Carroll and Frederick Counties, Maryland: Maryland Geological Survey, scale 1:24,000.

Edwards, Jonathan, Jr., 1988, Geologic map of the Woodsboro quadrangle, Carroll and Frederick Counties, Maryland: Maryland Geological Survey, scale 1:24,000.

Edwards, Jonathan, Jr., 1994, Geologic map of the Libertytown quadrangle, Carroll and Frederick Counties, Maryland: Maryland Geological Survey Open-File, scale 1:24,000.

Fisher, G.W., 1963, The petrology and structure of crystalline rocks along the Potomac River near Washington, D.C.: Baltimore, The Johns Hopkins University, Ph.D dissertation, 241 p.

Fisher, G.W., 1970, The metamorphosed sedimentary rocks along the Potomac River near Washington, D.C., in Fisher, G.W., Pettijohn, F.J., Reed, J.C., and Weaver, N.K., eds., Studies of Appalachian geology; Central and southern: New York, Interscience, p. 299–315.

Fisher, G.W., 1971, The Piedmont crystalline rocks at Bear Island, Potomac River, Maryland: Maryland Geological Survey Guidebook 4, 32 p.

Fisher, G.W., 1978, Geologic map of the New Windsor quadrangle, Maryland: U.S. Geological Survey Miscellaneous Investigations Map I–1037, scale 1:24,000.

Fleck, R.J., Sutter, J.F., and Elliot, D.H., 1977, Interpretation of discordant $^{40}Ar/^{39}Ar$ age spectra of Mesozoic tholeiites from Antarctica: Geochimica et Cosmochimica Acta, v. 41, p. 15–32.

Fleming, A.H., and Drake, A.A., Jr., 1998, Structure and tectonic setting of a multiply reactivated shear zone in the Piedmont near Washington, D.C., and vicinity: Southeastern Geology, v. 38, no. 3, p. 115–140.

Fleming, A.H., Drake, A.A., Jr., and McCartan, L., 1994, Geologic map of the Washington West quadrangle, District of Columbia, Montgomery and Prince Georges Counties, Maryland, and Arlington and Fairfax Counties, Virginia: U.S. Geological Survey Geologic Quadrangle Map GQ–1748, scale 1:24,000.

Froelich, A.J., 1975, Bedrock map of Montgomery County, Maryland: U.S. Geological Survey Miscellaneous Investigations Map I–920–D, scale 1:62,500.

Haugerud, R.A., and Kunk, M.J., 1988, ArAr*, a computer program for reduction of $^{40}Ar/^{39}Ar$: U.S. Geological Survey Open-File Report 88–261, 68 p.

Hopson, C.A., 1964, The crystalline rocks of Howard and Montgomery Counties, in The geology of Howard and Montgomery Counties: Baltimore, Maryland Geological Survey, p. 27–215

Horton, J.W., Drake, A.A., Jr., and Rankin, D.W., 1989, Tectonostratigraphic terranes and their Paleozoic boundaries in the central and southern Appalachians, in Dallmeyer, R.D., ed., Terranes in the circum-Atlantic Paleozoic orogens: Geological Society of America Special Paper 230, p. 213–245

Horton, J.W., Jr., Drake, A.A., Jr., Rankin, D.W., and Dallmeyer, R.D., 1991, Preliminary tectonostratigraphic terrane map of the central and southern Appalachians: U.S. Geological Survey Miscellaneous Investigations Series Map I–2163, scale 1:2,500,000.

Jäeger, E., 1979, The Rb-Sr Method, in Jäeger, E., and Hunziker, J.C. eds., Lectures in isotope geology: Springer, Berlin Heidelberg New York, p. 13–26.

Jonas, A.I., and Stose, G.W., 1938, Geologic map of Frederick County and adjacent parts of Washington and Carroll Counties: Maryland Geological Survey, scale 1:62,500.

Knopf, E.B, 1935, Recognition of overthrusts in metamorphic terranes: American Journal of Science, v. 30, p. 198–209.

Krol, M.A., Muller, P.D., and Idelman, B.D., 1999, Late Paleo-

zoic deformation within the Pleasant Grove shear zone, Maryland; Results from $^{40}Ar/^{39}Ar$ dating of white mica, *in* Valentino, W.D., and Gates, A.E., eds., The Mid-Atlantic Piedmont; Tectonic missing link of the Appalachians: Geological Society of America Special Paper 330, p. 93–111.

Kunk, M.J., Wintsch, R.P., Naeser, C.W., Naeser, N.D., Southworth, S., Drake, A.A., Jr., and Becker, J.L., in press, Multiple Paleozoic metamorphic histories in the Potomac composite terrane, Virginia and Maryland; Discrimination of ages of multiple generations of muscovite with Ar/Ar: Geological Society of America Bulletin.

Lyttle, P.T., 1982, The South Valley Hills phyllites; A high Taconic slice in the Pennsylvanian Piedmont: Geological Society of America Abstracts with Programs, v. 14, p. 37.

Muller, P.D., Candela, P.A., and Wylie, A.G., 1989, Liberty Complex; Polygenetic melange in the central Maryland Piedmont, *in* Horton, J.W., Jr., and Rast, N., eds., Melanges and olistostromes of the U.S. Appalachians: Geological Society of America Special Paper 228, p. 113–134.

Mulvey, B.K., 2003, Devonian recrystallization of Silurian white mica in the Westminster terrane of Maryland, identified by petrography and $^{40}Ar/^{39}Ar$ analyses: Bloomington, Indiana University, Master's thesis, 55 p.

Muth, K.G., Arth, J.G., and Reed, J.C., Jr., 1979, A minimum age for high-grade metamorphism and granitic intrusion in the Piedmont of the Potomac River gorge near Washington, D.C.: Geology, v. 7, p. 349–350.

Poirier, J.P., 1985, Creep of crystals; high-temperature deformation processes in metals, ceramics and minerals: New York, Cambridge University Press, 260 p.

Reed, J.C., Jr., Marvin, R.F., and Mangum, J.H., 1970, K-Ar ages of lamprophyre dikes near Great Falls, Maryland-Virginia: U.S. Geological Survey Professional Paper 700–C, p. C145–C149.

Reed, J.C., Jr., Sigafoos, R.S., and Fisher, G.W., 1980, The river and the rocks; the geologic story of Great Falls and the Potomac River gorge: U.S. Geological Survey Bulletin 1471, 75 p.

Schoenborn, W.A., 2001, Structural geometry, kinematics, and strain in Piedmont rocks, southwestern Maryland and northern Virginia: Geological Society of America Abstracts with Programs, v. 33, no. 1, p. A–4.

Schoenborn, W.A., 2002, Conditions of deformation in the Mather Gorge and Sykesville Formations, Potomac River, SW Maryland and N Virginia: Geological Society of America Abstracts with Programs, v. 34, no. 1, p. A–19.

Sinha, A.K., Hund, E.A., and Hogan, J.P., 1989, Paleozoic accretion of the North American plate margin (central and southern Appalachians); Constraints from the age, origin and distribution of granitic rocks, *in* Hillhouse J.W., ed., Deep structure and post kinematics of accreted terranes: American Geophysical Union Geophysical Monograph 50, p. 219–238.

Southworth, Scott, 1999, Geologic map of the Urbana quadrangle, Frederick and Montgomery counties, Maryland: U.S. Geological Survey Geologic Quadrangle Map GQ–1768, scale 1:24,000.

Southworth, Scott, Brezinski, D., Drake, A., Burton, W., Orndorff, R., Froelich, A., Reddy, J., and Daniels, D., 2002, Digital geologic map of the Frederick 30 by 60 minute quadrangle, Maryland, Virginia, and West Virginia: U.S. Geological Survey Open-File Report 02–437.

Stose, A.J., and Stose, G.W., 1946, Geology of Carroll and Frederick Counties, *in* The physical features of Carroll County and Frederick County: State of Maryland Department of Geology, Mines, and Water Resources, p. 11–131.

Wetherill, G.W., Tilton, G.R., Davis, G.L., Hart, S.R., and Hopson, C.A., 1966, Age measurements in the Maryland Piedmont: Journal of Geophysical Research, v. 71, no. 8, p. 2139–2155.

ROAD LOG AND STOP DESCRIPTIONS FOLLOW

Road Log and Stop Descriptions

This trip transects the Piedmont beginning with Stops 1 and 2 in the chlorite-grade rocks of the Westminster terrane west of the Pleasant Grove fault. The remainder of the trip will be in several different tectonothermal domains of the Potomac composite terrane east of the Pleasant Grove fault. Stop 3 is in biotite-grade rocks of the Blockhouse Point domain, the westernmost part of the Potomac terrane. Stop 4 and lunch is in kyanite-grade rocks of the western Bear Island domain. Stop 5 is in staurolite-sillimanite-grade rocks of the eastern Bear Island domain. Stop 6 is in sillimanite-grade rocks retrograded to chlorite grade in the Stubblefield Falls domain in the Plummers Island fault zone.

Mileage

Incremental	Cumulative	
0.0	0.0	Depart from back door, Tysons Corner Hilton.
		Drive around front, and turn right on Jones Branch Road.
1.2	1.2	Turn right on Spring Hill Road.
0.1	1.3	Turn right on Va. 267 east, Dulles Toll Road.
1.1	2.4	Exit to I-495 north.
7.2	9.6	Exit to I-270 north.
21.4	31.0	Exit to Md. 109 (Exit 22, Hyattstown, Barnesville).
0.2	31.2	Turn left on Md. 109 north.
0.5	31.7	Turn right on Md. 355.
0.1	31.8	Turn left on Frederick Road–Hyattstown Mill Road.
0.7	32.5	Use parking area by rusty footbridge at junction of Hyattstown Mill Road and Prescott Road to turn around and head back westbound on Hyattstown Mill Road.
0.3	32.8	Pull off to the right at trailhead to Dark Branch Trail.
		Outcrop is on north side of road, on small hill on the right side (east) of small valley of Dark Branch.

Stop 1. Hyattstown.

Western Westminster terrane above Hyattstown thrust fault, in metasiltstone and phyllite of the Marburg Formation, Urbana, Md., 7.5-minute quadrangle (Southworth, 1999).

The rocks at this stop are chlorite-grade metasiltstone, phyllite, and thin quartzite assigned to the Neoproterozoic and Early Cambrian Marburg Formation (Southworth, 1999). The foliation regionally and in the rocks here strikes northeast and dips steeply to the southeast. This foliation is a composite of nearly coplanar cleavages, bedding, and transposed vein quartz. Where bedding is at a high angle to cleavage it can be conspicuous, as it is on the left side of the knoll here as we climb up from the parking area. Here, graded beds of metasiltstone strike northwest and dip moderately to the southwest. Bedding is made conspicuous by beds that are relatively rich and poor in hematite, giving the rock a strikingly banded appearance (fig. 8A). Also visible here are isoclinally folded quartz veins (fig. 8B). These are significant in that they cut older foliation, but have limbs transposed into the schistosity, and axial planes parallel to the later composite foliation. They thus demonstrate the composite nature of the foliation here. Late quartz veins do exist, however, that are relatively undeformed and cut this cleavage at moderately high angles.

Regionally, similar Marburg Formation rocks comprise a ~12-km-wide lithotectonic belt in the eastern part of the Westminster terrane. The belt is separated from the Potomac composite terrane to the east by the Pleasant Grove fault zone. To the west 4.7 km, the 50-km-long Hyattstown thrust fault places rocks of the Marburg Formation above greenstone and phyllite of the Sams Creek Formation. Rocks of the Marburg Formation are distinctively different from the rocks to the west of the Hyattstown thrust fault, which are a diverse assem-

Figure 8. Photographs of rocks of the Marburg Formation at Stop 1. *A*, Intersection of laminated bedding (trending upper left to lower right) with cleavage that is parallel to the outcrop face and page; both are cut by vein quartz that is transposed (upper left). View is to the east on the face of an outcrop. Pen segment shown is 10 cm long. *B*, Steep downdip view (to the southeast) of northeast-striking cleavage and transposed vein quartz with dextral kinematic motion. Pen is 1 cm in diameter.

blage of phyllite, phyllonite, metasiltstone, quartzite, metagraywacke, greenstone, marble, and metalimestone (Southworth and others, 2002). In contrast to the fine-grained rocks of the Sams Creek Formation and Ijamsville Phyllite immediately west of the fault, the phyllite and metasiltstone of the Marburg Formation locally contain paragonite as well as porphyroblasts of albite and chloritoid. The metasiltstone commonly has a distinctive pinstriped appearance of quartz laminae and ribbons interlayered with chlorite phyllite; a later crenulation cleavage crinkles these ribbons, in many places to produce a characteristic texture. The quartz laminae may represent thin turbidites or metamorphic segregations. Within the 12-km-wide belt of the Marburg Formation there are a few meter-thick beds of metagraywacke and pebbly quartzite, and rare bodies of greenstone. To the northeast about 25 km, rocks of the Prettyboy Schist are in gradational contact with rocks of the Marburg Formation.

Age spectra from three samples from this part of the Westminster terrane (Kunk, unpub. data; Mulvey, 2003) give ages of ~435 to 430 Ma. These samples all contain muscovite preserved in multiple generations of spaced cleavage. Typically, older generations contain muscovite intergrown with chlorite, whereas later generations contain primarily chlorite. We interpret the reproducible early Silurian ages of muscovites from several samples, including a marble, to be a close approximation to the time of S_2 muscovite growth, thus indicating a Silurian cleavage-forming event.

Mileage

Incremental	Cumulative	
0.5	33.3	Return to vehicles and head west on Frederick Road. Turn right at stop sign onto Md. 355.
0.1	33.4	Turn left on Md. 109 south.
0.6	34.0	Turn left on I-270 south.
7.3	41.3	Exit to Md. 118 south (Exit 15A).
6.2	47.5	Turn right on Md. 28 west.
1.0	48.5	Turn right on Black Rock Road.
0.6	49.1	Park in lot on left at Black Rock Mill.
		Walk across bridge of Great Seneca Creek and walk left (west) about 15 m to large bluff.

Stop 2. Black Rock Mill.

Metagraywacke and phyllite of the Marburg Formation, eastern part of Westminster terrane, Damascus, Md., 7.5-minute quadrangle (A.A. Drake, Jr., unpub. data; Southworth and others, 2002).

The rocks exposed on the north bank of Great Seneca Creek are metagraywacke interbedded with phyllite and metasiltstone assigned to the Marburg Formation by A.A. Drake, Jr. (unpub. data) and Southworth and others (2002). At this location we are about 1.75 km west of the Pleasant Grove fault zone. Like the rocks at Stop 1, the regional foliation here strikes northeast, dips steeply to the southeast and locally is vertical. Well-cemented metagraywacke beds are relatively resistant, and probably are responsible for the exposure here. They form rapids in the streambed, and are well exposed in a bluff across and downstream from the mill. There the nearly vertical schistosity of the rocks is axial planar to vertical isoclinal folds (fig. 9A). Note also that the phyllitic limbs of these folds contain lozenges or boudins of quartz, undoubtedly representing dismembered lenses of once-continuous quartz veins (fig. 9B)

In thin section (fig. 4B) the phyllites are composed of phyllosilicate-rich layers (~60 percent) separated by quartz microlithons and veins (~40 percent). The phyllosilicate-rich layers contain ~90 percent muscovite flakes up to 80 μm long. Accessory minerals include 10- to 100-μm grains of chlorite (5 percent), rutile (5 percent), and quartz (<1 percent). The quartz microlithons and veins are elongate parallel to compositional layering and range in thickness from 1 to 9 mm. Although several generations of white mica can be identified, by far the dominant and coarsest mica is S_2. Because of its coarse grain size, it is also the mica that is concentrated in the sample analyzed isotopically. Replicate analyses of two different
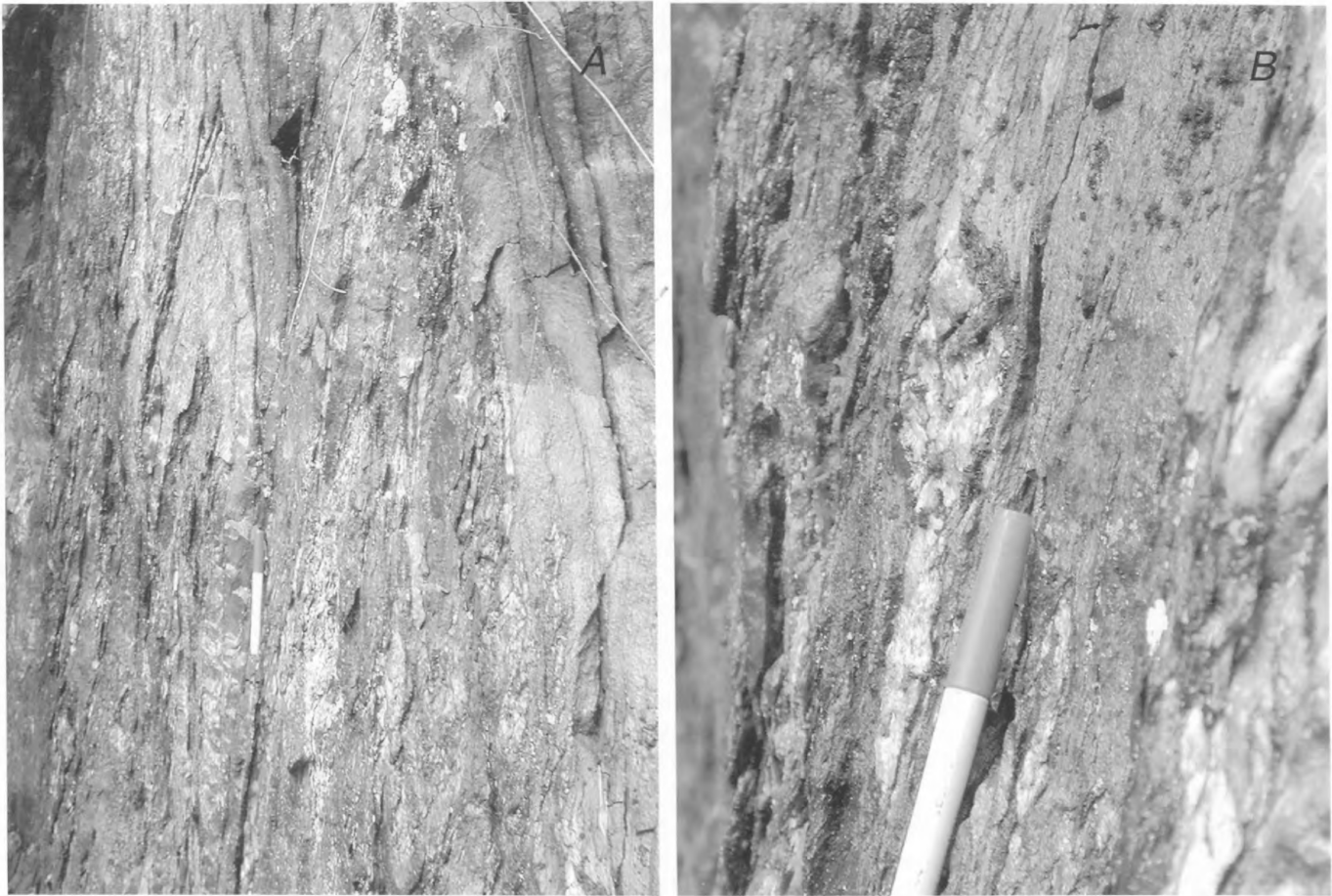
Figure 9. Photographs of rocks of the Marburg Formation at Stop 2, looking north. *A*, Isoclinal folds of thin metagraywacke and phyllite (with axial plane cleavage?) are transected by cleavage that dips steeply to the northwest (left). Pen is 14 cm long. *B*, Closeup view of vein quartz transposed in the early folds and foliation. Pen segment shown is 10 cm long.

samples both record an age of ~375 Ma, approximately the age of S_2 mica. This age is distinct from the age determined for the samples at Stop 1, and clearly reflects a Middle Devonian cleavage-forming event that was not recorded in the phyllites of Stop 1. This is the basis for interpreting a fault or boundary of a shear zone between Stops 1 and 2.

Mileage

Incremental	Cumulative	
0.0	49.1	Return to vehicles and go north on Black Rock Road.
1.9	51.0	Turn left on Md. 118 north.
3.6	54.6	Bear right onto entrance ramp to I-270 south.
11.7	66.3	Bear right onto I-495 south.
6.4	72.7	Exit to Va. 193; bear left to avoid Exit 43.
0.7	73.4	Bear right and take Exit 44.
0.1	73.5	Turn right at traffic light onto Georgetown Pike, Va. 193 west.
9.3	82.8	Turn right onto Seneca Road, Va. 602.
2.3	85.1	Continue straight at No Outlet sign.
1.4	86.5	At end of road, park on right of roadside.
		Walk north along paved road (gated) to the bottom of the hill and follow the gravel road to the right (east) for about 10 m.
		Outcrops are on forested bluff on the right.

Stop 3. Seneca Road/Northern Virginia Regional Park.

Chlorite phyllonite of Mather Gorge Formation, western Blockhouse Point domain, Potomac terrane, Seneca, Va.-Md., 7.5-minute quadrangle (Drake and others, 1999).

The rocks exposed here are chlorite phyllite and phyllonite with transposed and folded vein quartz speckled with magnetite. These chlorite-grade rocks were called the Upper Pelitic Schist of the Wissahickon Formation by Fisher (1970), chlorite schist and lesser metasiltstone of the Peters Creek Schist (Drake, 1989), and later were assigned to the metagraywacke and lesser semi-pelitic schist unit of the Mather Gorge Formation by Drake and others (1999). This is the westernmost part of the Blockhouse Point domain in the western part of the Potomac terrane of Kunk and others (in press) and is Stop 1 of Drake (1989).

The regional composite foliation strikes northeast and dips gently to moderately to the southeast. The eastern margin of the Mesozoic Culpeper basin unconformably overlies these rocks about 0.5 km to the west beneath Quaternary alluvium. The southwestward projection of the Pleasant Grove fault is about 1.5 km to the west but is also unconformably overlain by Late Triassic rocks of the Culpeper basin and by alluvium.

At this stop, we can recognize both muddy and gritty protoliths, now phyllites and thin lenses of lithic and arkosic quartzites. These are intruded by several generations of quartz veins, and deformed and folded by several cleavage-forming events. A composite cleavage composed of S_1 and S_2 (at least) gives the overall steep cleavage of the outcrop (fig. 10). This composite cleavage contains transposed bedding, intrafolial folds, and dismembered quartz veins, and shear-band cleavage records a dextral, transpressive fabric. An S_3 cleavage anastomoses across this structure, giving the composite cleavage a wavy fabric. Finally, there is a late, gently dipping discontinuous cleavage, S_4, that locally cuts all previous structures.

In thin section our nearby analyzed sample (Kunk and others, in press) (fig. 4C) is a differentiated quartz-muscovite phyllonite. Most phyllosilicate layers are dominated by muscovite (>90 percent), but contain ~10 percent chlorite, with accessory sphene, magnetite, and albite, and trace amounts of epidote. Most of the muscovite grains that define the foliation in these layers are 200 to 400 μm long and 50 μm thick, but some are over 500 μm long and 100 μm thick.

The age spectrum of this sample is very slightly sigmoidal, but forms an age plateau (Fleck and others, 1977; Haugerud and Kunk, 1988) at 362±2 Ma that contains 70 percent of the ^{39}Ar released from the sample. The vast majority of the gas released from the sample is from muscovite flakes that together with chlorite define S_2. The muscovite-chlorite association is interpreted to reflect below-closure growth, and the plateau age is interpreted to represent the age of this cleavage-forming event. By this analysis, the younger cleavages, S_3 and S_4, must be Carboniferous or younger. This interpretation is completely consistent with our results from the Plummers Island fault (Stop 6).

Return to vehicles, retrace route south on Seneca Road, and turn left (east) on Georgetown Pike, Va. 193.

Mileage

Incremental	Cumulative	
8.7	95.2	Turn left into Great Falls Park.
1.0	96.2	Park entrance. Park in parking lot.

Lunch Stop. Restrooms are available at the Visitor Center en route to Overlook 2, which affords a view of the Great Falls of the Potomac River. Bag lunches can be eaten at the overlook or at the picnic tables to the south.

Figure 10. Photograph of chlorite metasiltstone and phyllonite of the Blockhouse Point domain of the Mather Gorge Formation, Stop 3, looking east into the foliation. Thin layers of metagraywacke, metasiltstone, and vein quartz dipping to the northeast (left) are domains cut by anastomosing shear-band cleavage with dextral kinematic indicators (lower center). Pen is 14 cm long.

Stop 4. Great Falls Park.

Metagraywacke and staurolite schist of the Mather Gorge Formation, Bear Island domain, Vienna and Falls Church, Va.-Md., 7.5-minute quadrangles (Drake and Lee, 1989; Drake and Froelich, 1997).

The level ground of the parking area and Visitor Center is a bedrock strath terrace of the Potomac River that may be as young as 30 ka (Bierman and others, this volume). The current position of the Great Falls of the Potomac River is situated at perhaps the thickest section of metagraywacke exposed in the Potomac River valley (fig. 11A). Formerly called the Wissahickon Formation and Peters Creek Schist, these rocks were renamed the Mather Gorge Formation by Drake and Froelich (1997), based on this type locality, and are in the
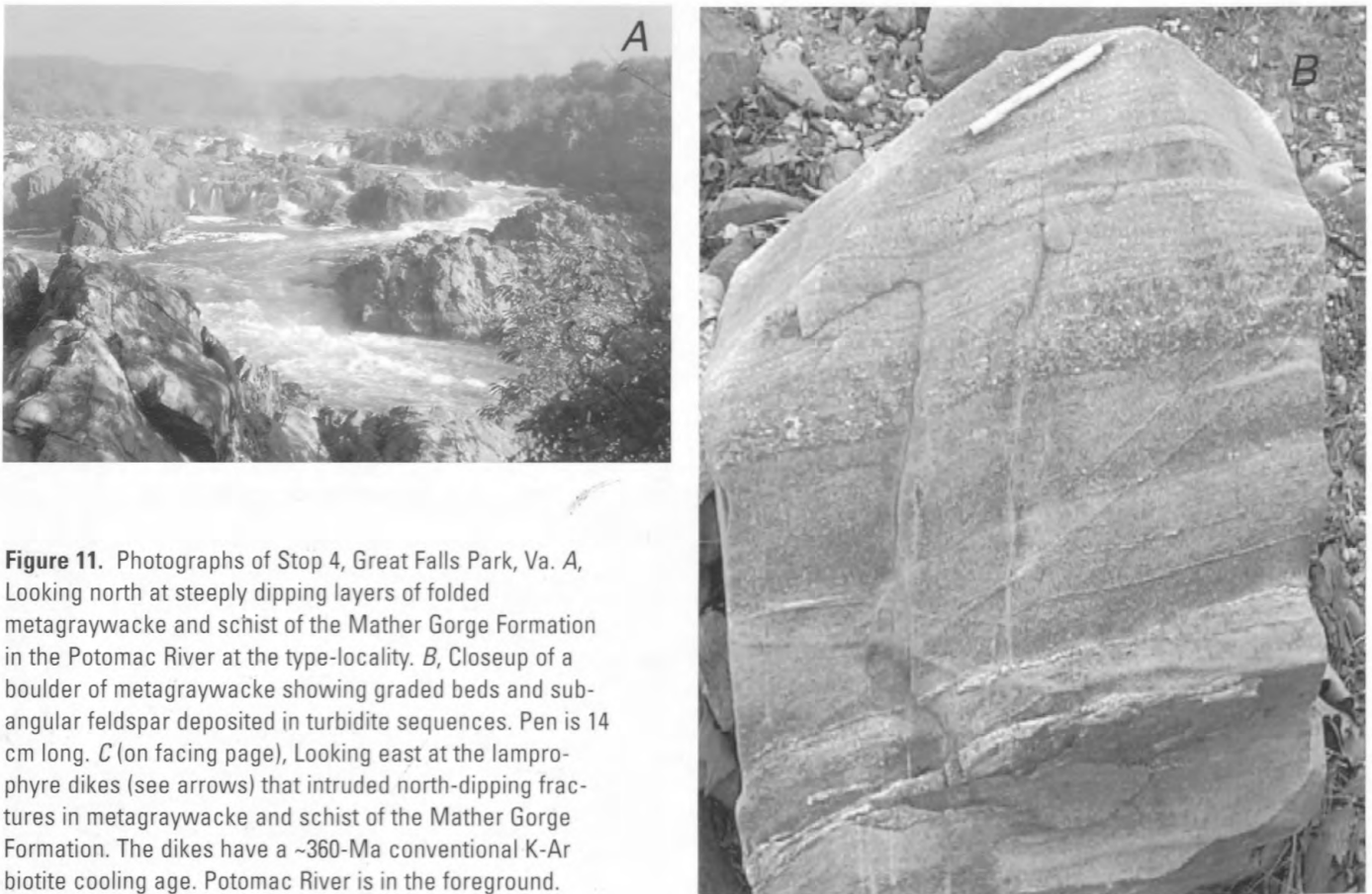
Figure 11. Photographs of Stop 4, Great Falls Park, Va. *A*, Looking north at steeply dipping layers of folded metagraywacke and schist of the Mather Gorge Formation in the Potomac River at the type-locality. *B*, Closeup of a boulder of metagraywacke showing graded beds and sub-angular feldspar deposited in turbidite sequences. Pen is 14 cm long. *C* (on facing page), Looking east at the lamprophyre dikes (see arrows) that intruded north-dipping fractures in metagraywacke and schist of the Mather Gorge Formation. The dikes have a ~360-Ma conventional K-Ar biotite cooling age. Potomac River is in the foreground.

Bear Island domain of Kunk and others (in press). In general, rocks mapped as Mather Gorge Formation are dominantly schist interbedded with metagraywacke; metagraywacke interbedded with schist is subordinate but best exposed here. The metagraywacke consists of well-graded beds of quartz and detrital feldspar (fig 11B). Soft-sedimentary features exposed along Bear Island to the east support the interpretation that these are turbidite deposits (Hopson, 1964; Drake and Morgan, 1981). Isoclinal recumbent folds of metagraywacke and schist are locally refolded upright. About 1 km to the west are bodies of ultramafic rocks, and about 1.5 km to the east are bodies of amphibolite and granodiorite/pegmatite. Immediately east of the overlook along the bluffs is one of the northwest-dipping, undeformed lamprophyre dikes that has conventional K-Ar biotite cooling ages of ~360 Ma (Reed and others, 1970), similar to the dikes shown in figure 11C.

Mileage

| Incremental	Cumulative	
1.4	97.6	Return to vehicles, leave park, and turn left (east) on Georgetown Pike, Va. 193.
0.6	98.2	Turn right into parking lot of Difficult Run.
		Follow the trail at the south end of the parking area around the meander.
		Go under the bridge carrying Va. 193.
		Continue along trail on the north side of the creek for about 500 m
		to a broad outcrop on the bank near a sharp north bend in Difficult Run.

Figure 11. Continued

Stop 5. Difficult Run.

Migmatitic schist of the Mather Gorge Formation, amphibolite, and Bear Island Granodiorite, eastern boundary of Bear Island domain, Potomac terrane, Falls Church, Va.-Md., 7.5-minute quadrangle (Drake and Froelich, 1997)

This outcrop of a variety of rocks was scoured clean by the floods of Hurricane Agnes in 1972, and was Virginia stop 8 of Reed and others (1980) and stop 5 of Drake (1989). These sillimanite-grade rocks were called the Upper Pelitic Schist of the Wissahickon Formation (Fisher, 1970) and the metagraywacke and semipelitic schist of the Mather Gorge Formation (Drake and Froelich (1997); they are the Bear Island domain of the Mather Gorge Formation of Kunk and others (in press). The dominant rock is gray coarsely mottled mica schist that contains conspicuous dark-green 1- to 2-cm-diameter crystals of garnet, staurolite, cordierite(?), and shimmer aggregates. The schist also contains segregated leucosomes of quartz and albite or sodic oligoclase, forming a wavy migmatite. Several 2-m-thick layers of dark-green, fine-grained epidote-plagioclase-hornblende amphibolite are found within the schist, and are probably gabbro sills or basalts whose origin may have been either intrusive, extrusive, or as olistoliths. Drake (1989) suggests that the amphibolite intruded the schist prior to deformation. The known distribution of amphibolite is restricted to the sillimanite-grade migmatites of the eastern part of the Bear Island domain.

Both the amphibolite and schist are cut by tabular dikes of light-gray granite and granodiorite called the Bear Island Granodiorite (fig. 12). Streaks of biotite define flow foliation in these dikes. The largest dike here is cut by a pegmatite 5 to 15 cm thick. Small bod-
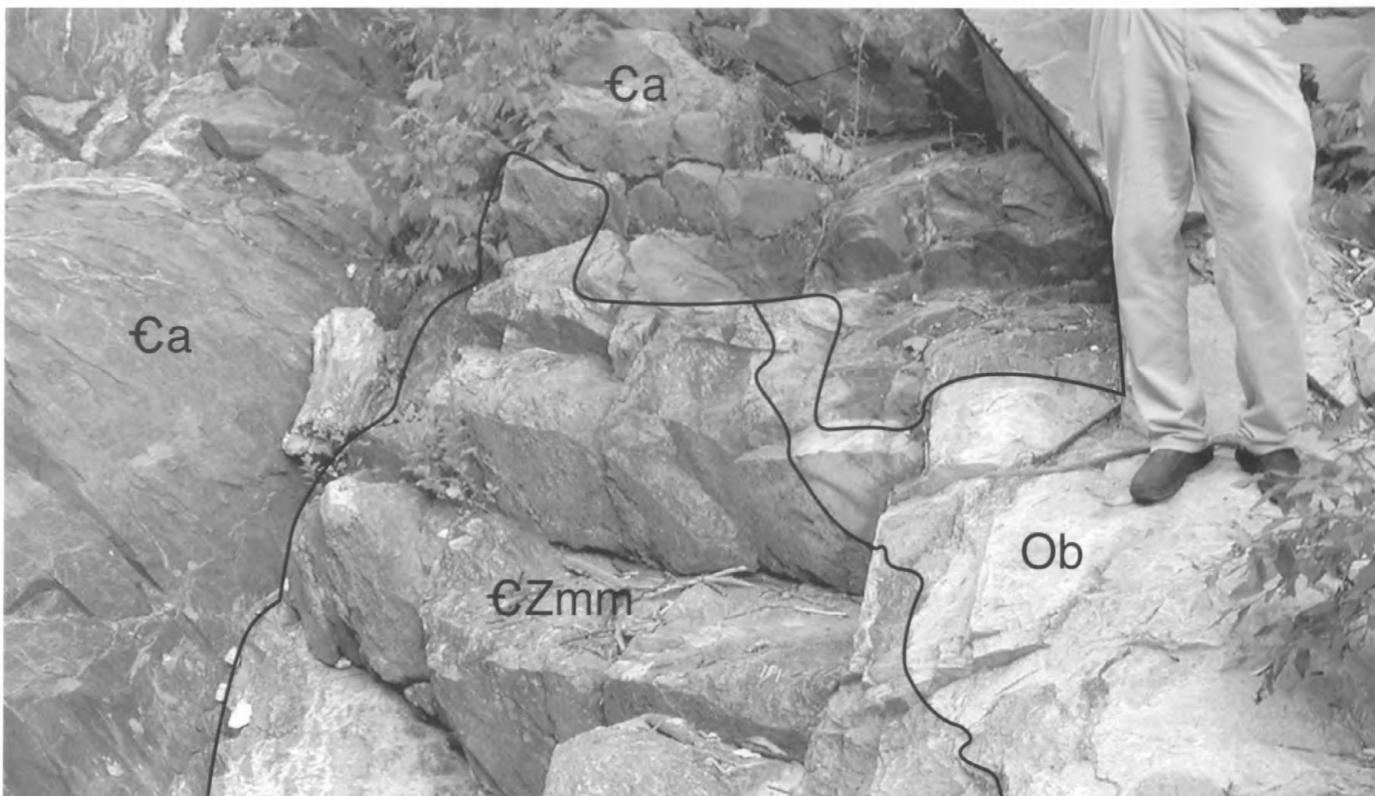
Figure. 12. Photograph of rocks along Difficult Run, Stop 5, looking north at east-dipping foliated rocks. The person is standing on Ordovician Bear Island Granodiorite (Ob) (east dipping) which intrudes both amphibolite (Єa) and migmatitic schist of the Mather Gorge Formation (ЄZmm). Man's foot is 28 cm long.

ies of Bear Island Granodiorite are abundant in the migmatites of the Bear Island domain and in the deformed schists of the Stubblefield Falls domain. The distribution of these dikes seems to be structurally controlled, in that dikes are most common cutting fractures and boudin necks in the amphibolite. It is possible that these dikes were passively injected into dilational sites caused by breakup of the competent amphibolite layer within ductile schist under anatectic conditions. The Bear Island Granodiorite is commonly seen associated with amphibolite, but it is recognized only where metamorphic grade reached at least sillimanite zone, an area that spans both east and west of the known distribution of amphibolite. Most of the dikes are undeformed as they are here, but similar dikes are locally folded. Muscovite from this pegmatite yielded the 469-Ma Rb-Sr cooling ages (Muth and others, 1979). Fisher (1963, 1970), Hopson (1964), and Drake (1989) suggest that the granodiorite had a source at depth, and was emplaced well after the climax of regional metamorphism and deformation.

Amphibole from an outcrop near here yielded a disturbed $^{40}Ar/^{39}Ar$ age spectrum with an isochron age of 475 Ma, which is interpreted as the time of cooling through 500°C. Further cooling below 500°C (staurolite to biotite grade) was complete by the end of the Devonian. With this Early Ordovician amphibole cooling age, the highest metamorphic grade and melting of these rocks (T>650°C) could very possibly be older than Ordovician and thus predate the classic Taconian orogeny.

Mileage

Incremental	Cumulative	
0.0	98.2	Return to vehicles, turn right (east) on Georgetown Pike, Va. 193.
3.7	101.9	Drive past I-495 overpass and turn left at traffic light onto Balls Hill Road.
0.4	102.3	Turn left on Live Oak Drive, cross over I-495, and continue north.

| 0.9 | 103.2 | Park on right at neck of cul-de-sac next to the trailhead of the National Park Service Potomac Heritage Trail. Follow the trail down to within sight of the Potomac River (do not take the footbridge right across the culvert and go under I-495). Take the foot trail into the woods and walk west along the river to the large outcrops beneath the cliffs. |

Stop 6. Plummers Island Shear Zone.

Phyllonitic schist and migmatite, and migmatitic phyllonitic schist, Mather Gorge Formation, eastern boundary of Stubblefield Falls domain of the Mather Gorge Formation, Potomac terrane, Falls Church, Va.-Md., 7.5-minute quadrangle (Drake and Froelich, 1997).

The rocks seen at this stop are very difficult to interpret (Drake, 1989, Stop 6). Fisher (1970) mapped these sillimanite- to staurolite-grade rocks as the Upper Pelitic Schist of the Wissahickon Formation. Beneath the American Legion (I-495) Bridge, he mapped a transitional contact with the diamictite of the Sykesville Formation. Fisher (1963, 1970) and Hopson (1964) describe the transition between Peters Creek Schist and Sykesville diamictite as containing a decreasing amount of olistoliths in the Sykesville Formation. Drake (1989) described these rocks as retrograded chlorite-sericite phyllonite of the quartzose schist of the Peters Creek Schist, and called Fisher's (1963, 1970) contact with the rocks of the Sykesville Formation the Plummers Island fault. He suggested that the Sykesville is choked with olistoliths of Peters Creek Schist near its contact with that unit. Drake and Froelich (1997) later classified rocks at this stop as the upper part of the Sykesville Formation, with the upper part containing 50 percent or more phyllonite olistoliths, interpreted as having been derived from rocks of the Mather Gorge Formation. Drake and Froelich (1997) placed the Plummers Island fault, the contact between phyllonite of the Mather Gorge Formation and the rocks of the upper part of the Sykesville Formation, about 0.5 km to the west of this stop.

We retain the original contact of Fisher (1963, 1970) as the Plummers Island fault of Drake (1989), but suggest that this linear fault was reactivated as a wide Alleghanian shear zone. The major (Alleghanian) foliation in rocks across the fault strikes northeast and dips steeply to the northwest. This steep northwest-dipping to near-vertical foliation begins in the Stubblefield Falls domain and continues with a decreasing amount of muscovite recrystallization for 11 km east, to the Rock Creek shear zone. To the west of the Plummers Island fault of Fisher (1963, 1970), the rocks exposed on scoured outcrops on the south side of the Potomac River appear to be a phyllonitized migmatite that has been later remigmatized and sheared and retrograded. Blocks and rafts of the disrupted phyllonitic migmatite appear as "olistoliths," along with subrounded quartz "cobbles" and rootless quartz veins that are transposed (fig. 13). The blocks and rafts of first-generation phyllonitic migmatite contain foliations that strike in many different directions, and are supported by a matrix of feldspathic second-generation migmatite (fig. 12). The matrix is migmatitic, not granular quartzofeldspathic like the Sykesville. Overprinted on this is a strong north-south foliation that is subparallel to the late (Alleghanian) movement on the Plummers Island fault.

$^{40}Ar/^{39}Ar$ age spectra of muscovites from the Stubblefield Falls domain provide estimates of the minimum time of cooling (S_1) through 350°C, decreasing from 375 Ma to the west to 354 Ma here at the Plummers Island fault. $^{40}Ar/^{39}Ar$ age spectra of muscovites from the rocks of the Sykesville Formation to the east give an estimate of the minimum time of cooling through 350°C at 357 Ma. This age is virtually identical to the time of cooling on the eastern side of the Stubblefield Falls domain, and is interpreted as a minimum age for thrusting of the Sykesville Formation over the Mather Gorge Formation in the Devonian (Acadian).

Estimates of the time of below-closure growth of muscovite (S_2) also decrease from west to east in the Stubblefield Falls domain, to a minimum of 328 Ma at the Plummers Island fault. In Sykesville Formation rocks to the east, on the other side of the fault, the below-closure ages increase dramatically from 304 Ma at the fault to 332 Ma near the Rock Creek shear zone. The ~304-Ma age within the fault is a maximum estimate of the time of the last Alleghanian movement on the fault.
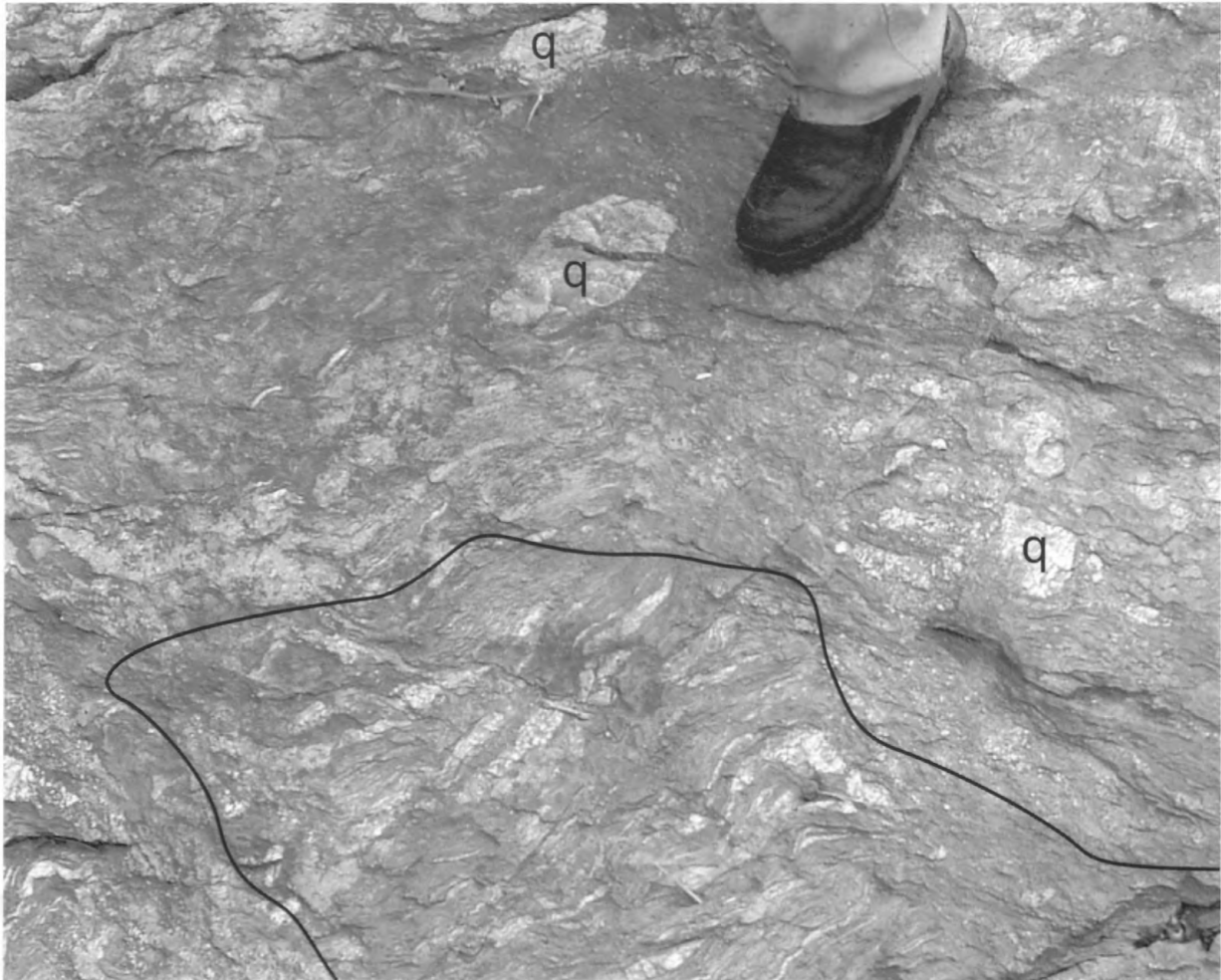
Figure 13. Photograph of complex rocks exposed at Stop 6 immediately west of the American Legion (I-495) Bridge on a scoured section along the Potomac River, in the Stubblefield Falls domain. These rocks were interpreted by Drake and Froelich (1997) to be olistoliths of Mather Gorge Formation and quartz cobbles in a Sykesville Formation matrix. The outcrop consists of disrupted, foliated blocks of Mather Gorge Formation (outlined in lower part of photograph) and dis-membered quartz veins (q) associated with a small amount of migmatite. Man's foot is 10 cm wide. Potomac River is to the right of the photographed area.

Return to vehicles and retrace route back to Georgetown Pike, Va. 193.

Mileage

Incremental	Cumulative	
1.3	104.5	Turn right on Georgetown Pike, Va. 193.
0.7	105.2	Turn left on Swinks Mill Road, Va. 685.
1.6	106.8	Turn right on Lewinsville Road.
0.9	107.7	Turn left at traffic light on Spring Hill Road, Va. 694.
0.4	108.1	Turn left at traffic light on Jones Branch Drive.
1.2	109.3	Turn left into Tysons Corner Hilton.
0.1	109.4	End of Field Trip.

6. The Incision History of a Passive Margin River, the Potomac Near Great Falls

By Paul Bierman,[1] E-an Zen,[2] Milan Pavich,[3] and Luke Reusser[1]

Introduction

This field trip focuses on the emerging significance of complex geomorphic processes that have operated in a passive margin setting in the mid-Atlantic region (fig. 1A). The application of cosmogenic exposure dating to understanding the responses of rivers to Quaternary tectonic, eustatic, and climatic variations is providing unprecedented information about landscape histories. This trip presents new information about the response of the Potomac River to regional variability in sea level and climate over the late Pleistocene and Holocene. We present a regional framework, field observations of the morphology of the Potomac River gorge below Great Falls (fig. 1B), and data on the age relations of strath terraces associated with the Potomac River gorge.

Acknowledgments

Regional Framework: The Complexity of Passive Margin Settings

Passive margins, the trailing edges of continental plates, are geomorphically complex. Despite the absence of active tectonics, passive margins exhibit features such as great escarpments (Matmon and others, 2002; Bank and others, 2001), river gorges, and marine terraces (Flint, 1940; Cooke, 1952). New analytical techniques, such as fission track thermochronology (Naeser and others, 2001) and cosmogenic isotope exposure dating (Bierman and others, 2002) are providing insights into the processes that control passive margin evolution. Passive margins exhibit both stable and active features. Recent analyses of great escarpments (Matmon and others, 2002) provide evidence that "…the locations of great escarpments bordering passive margins are exceptionally stable and are probably determined by crustal structure." By contrast, this trip will focus on active rock erosion in the Potomac River gorge, particularly the formation processes and ages of strath terraces and knickpoints. Fluvially eroded straths and knickpoints provide direct evidence for river channel adjustments to climate, discharge, and crustal motion. They form one set of datable surfaces that will help unravel the complexities of passive margins.

Geologic Setting

The geomorphology of the Potomac River valley as it enters the Coastal Plain is a complex series of terraces and channels. The terrace morphology between Great Falls and the Coastal Plain is distinct and mappable, but the age is not well understood. Investigations of bedrock strath terraces (Zen, 1997a,b; Bierman and others, 2002) and fill terraces show that there has been significant modification of the

[1]University of Vermont, Burlington, VT 05405.

[2]University of Maryland, College Park, MD 20742.

[3]U.S. Geological Survey, Reston, VA 20192.
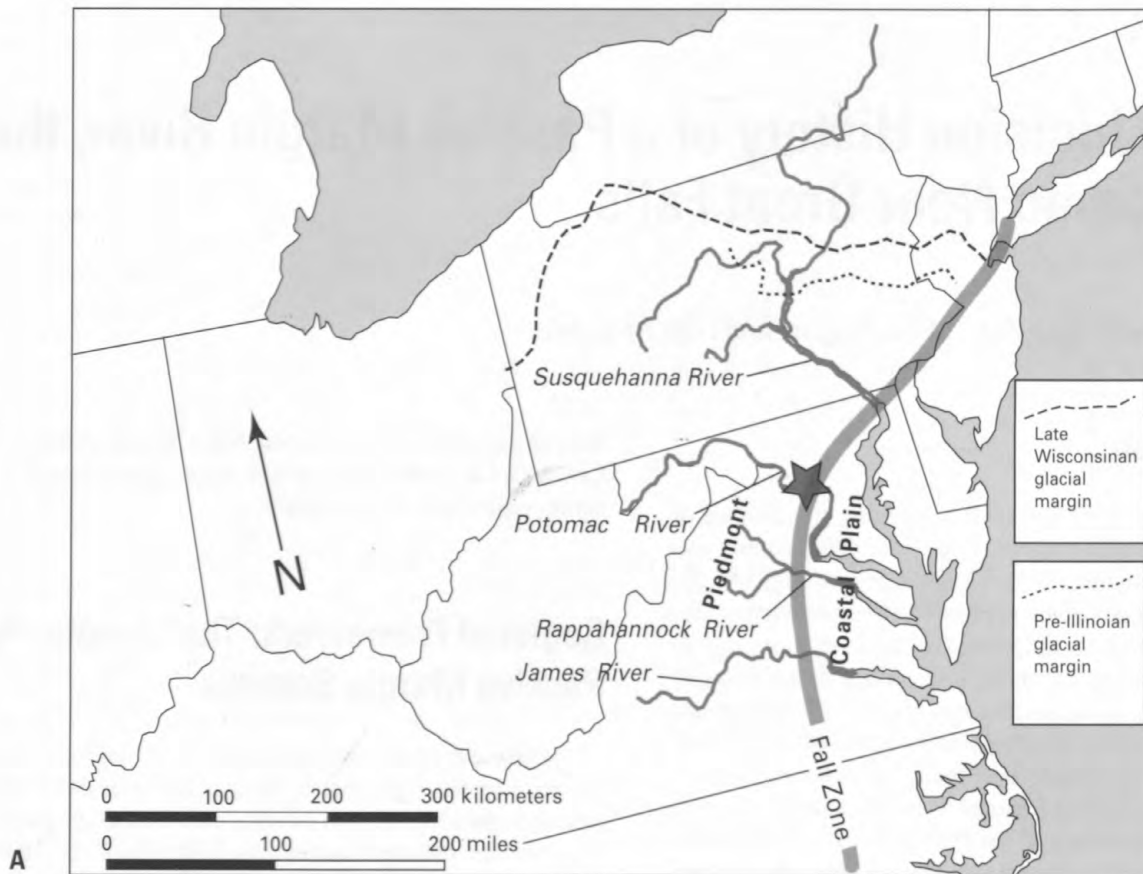
Figure 1. A, Index map of the Eastern United States showing the location of the field trip (star) near Great Falls of the Potomac River. Regional features include the Fall Zone, separating the Piedmont and Coastal Plain provinces, and the Pleistocene glacial borders north of the Potomac River drainage basin. B (facing page), Location map of the Potomac River in the vicinity of Great Falls, showing the areas to be visited on Days 1 and 2 of this field trip.

Potomac River valley and tributaries to the Potomac over the past half-million years. The stratigraphy of upland sedimentary deposits on the Piedmont (Fleming and others, 1994) indicates that the Potomac River has incised into a Miocene-to-Pliocene landscape of fluvial to nearshore marine deposits. The ages assigned to upland gravel deposits (Fleming and others, 1994) are based on correlation with downdip Coastal Plain units. There is no direct dating of fluvial gravels that underlie the highest elevations, but Tertiary ages are consistent with rates of topographic inversion resulting from bedrock weathering, saprolite formation, and soil erosion (Pavich and others, 1985). The fluvial incision and topographic inversion relative to upland gravels is attributed primarily to eustatic sea-level drop since the Miocene.

There is direct evidence along the Atlantic Coast for higher than present sea level in the late Tertiary to the last interglacial period (MIS 5). The basal elevations of fluvial gravels and sands adjacent to the Potomac River suggest significant downcutting of the river since late Tertiary time, perhaps over the last 5 Ma. A series of fill terraces can be mapped below the highest level at Tysons Corner, Va. (fig. 2). The fluvial gravel deposit at Tysons Corner is possibly older

than 5 Ma based on identification of late Tertiary-age fossils (A.J. Froelich, USGS, oral commun., 1980). These gravels may be age-equivalent to the Bryn Mawr Gravels mapped by Pazzaglia (1993) in the upper Chesapeake Bay area.

There are many fluvial features that invite more detailed analysis and explanation. Prominent features include the bedrock channel and strath terraces of the Potomac River near Great Falls. Lacking tectonic forcing, except for possible forebulge uplift (Douglas and Peltier, 2002), it is likely that climatic and sea-level variations have played major roles in the modification of this landscape during the late Quaternary. There are no numerical age measurements for the upland sedimentary units, but new age data for the Potomac River bedrock strath terraces (Bierman and others, 2002) are presented here. One of the major observations from the new data is that rates of bedrock gorge cutting can be very rapid; the fluvial incision relative to remnant fluvial gravel deposits may have occupied a small fraction of the total time since the Miocene (~5 Ma). This highlights the need for improved age-control on the youngest of the sedimentary units in order to understand the dynamics of transgressive deposition and regressive erosion during eustatic cycles.

B
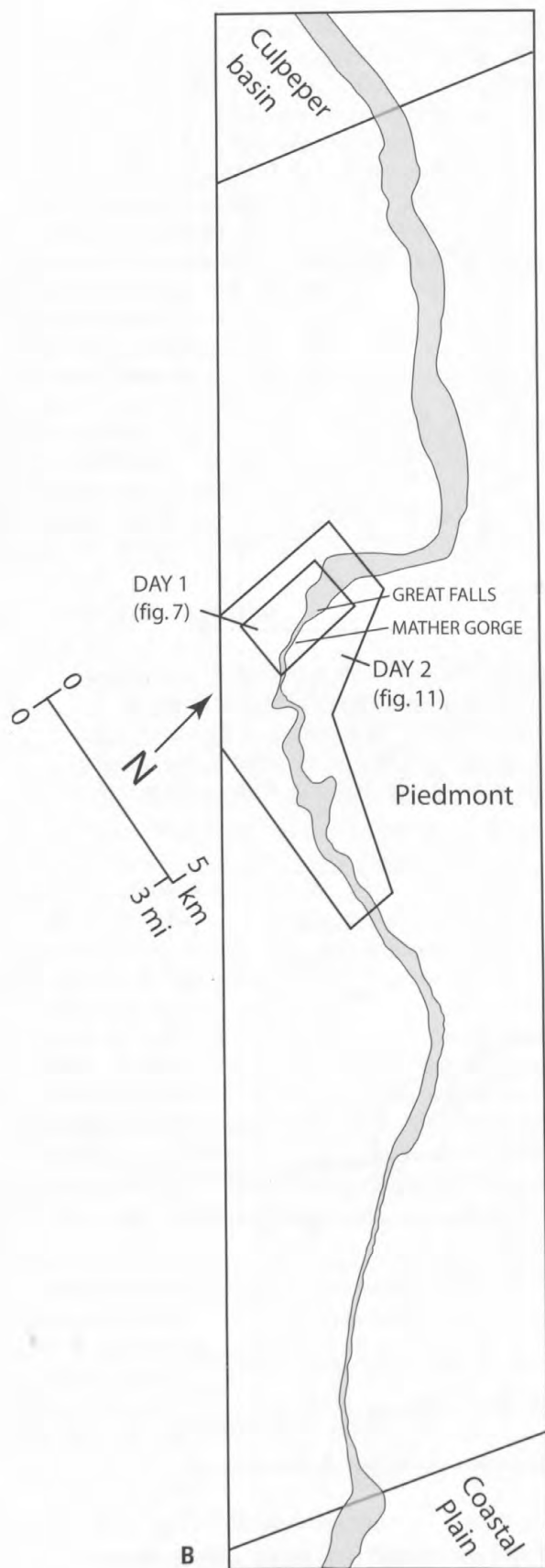
Day 1

The Potomac River Gorge Below Great Falls: Field Observations and Inferred Processes of Excavation

Introduction

The Potomac River flows across the Piedmont physiographic province between Blockhouse Point, Maryland (opposite the Fairfax-Loudoun County boundary), and tidewater at Georgetown, Washington, D.C., a distance of about 35 river kilometers. About one-third of the way across the Piedmont, the river makes a sudden drop of about 50 ft (feet) (15 m (meters)) in a distance of 500 ft (150 m), through a series of cascades collectively called the Great Falls of the Potomac, and enters Mather Gorge. This gorge, excavated out of thoroughly fractured Neoproterozoic and Early Cambrian metamorphic rocks, consists of several rectilinear segments. The gorge extends for about 3 km (kilometers) (1.9 miles (mi)), then makes a sharp turn to the left below a rock promontory in which Black Pond is nestled. Beyond the nearby Sherwin Island, the valley opens up somewhat. Remnants of bedrock straths (in other words, abandoned channels) are recognized all the way to tidewater (Zen, 1997a; Southworth and others, 2000). The gorge is as narrow as 30 m (100 ft) at its entrance; the most scenic part, between the entrance and Sandy Landing, is 70 m (230 ft) wide and as much as 30 m (100 ft) deep to water level.

At low flow, Great Falls consists of three channels: Maryland Falls, The Streamers, and The Spout (fig. 3). Each channel has 10- to 15-ft (3–5 m)-high cataracts separated by pool reaches. Maryland Falls and The Streamers have three cataracts each, and The Spout has four. The Great Falls Water Intake Dam is located between 0.6 and 1 mi (1 and 1.6 km) above the Falls, and provides engineering data on the 3,300-ft (1-km)-wide channel. The dam has a recorded elevation of 150.5 ft (45.9 m) above sea level (asl). As its height varies between 6 ft (2 m) near the ends and a maximum of 10 ft (3 m) (Hahn, 1992, p. 46), the channel is flat to 1.5 parts per thousand except for some protruding rock islands. Below Great Falls, the remnants of this channel form a strath that is readily traceable to Plummers Island just inside the Capital Beltway American Legion Bridge, 5.6 mi (9 km) downstream, and it might exist all the way to Key Bridge at the original Fall Line at tidewater (Zen, 1997a).

Below the Water Intake Dam, the modern river has four knickpoints: Great Falls (top, ~140 ft (43 m) above sea level), Yellow Falls (top, ~ 68 ft (21 m) above sea level), Stubblefield Falls (top, ~ 57 ft (17 m) above sea level), and
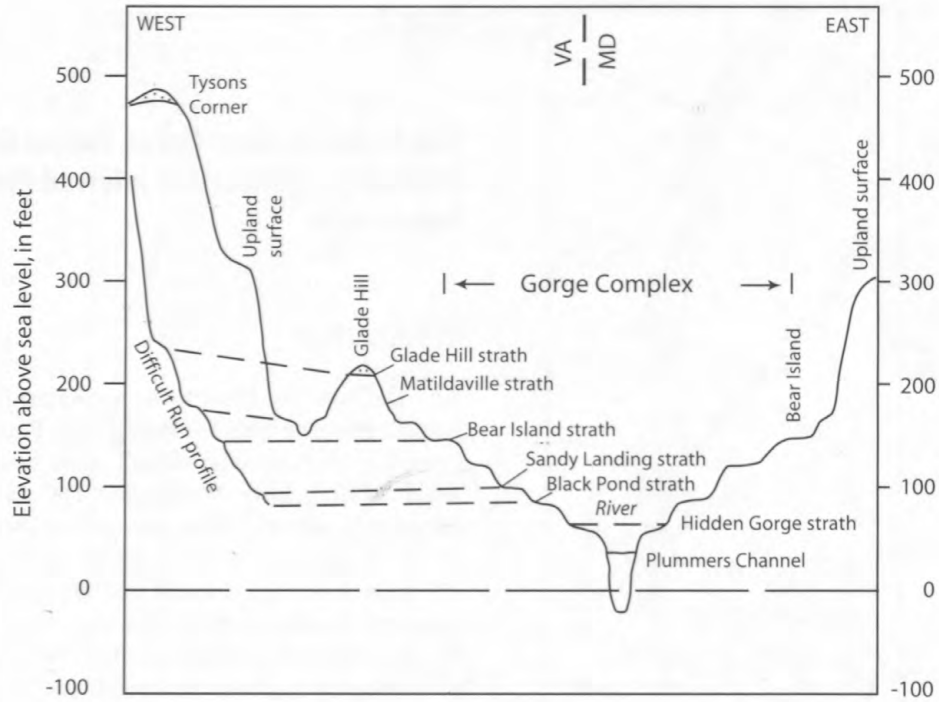
Figure 2. Synoptic and schematic cross section of the nested straths (Zen, 1997a). Elevations are appropriate for the entrance to Mather Gorge. Also shown are the upland surface and the Miocene-Pliocene fluvial deposit sequence found at Tysons Corner. Elevations of features are approximate. The profile of Difficult Run, a tributary entering the river near the end of Mather Gorge, is schematic except for the elevations of the knickpoints; these have been adjusted for the effect of longitudinal declinations of the straths. Horizontal distance not to scale.
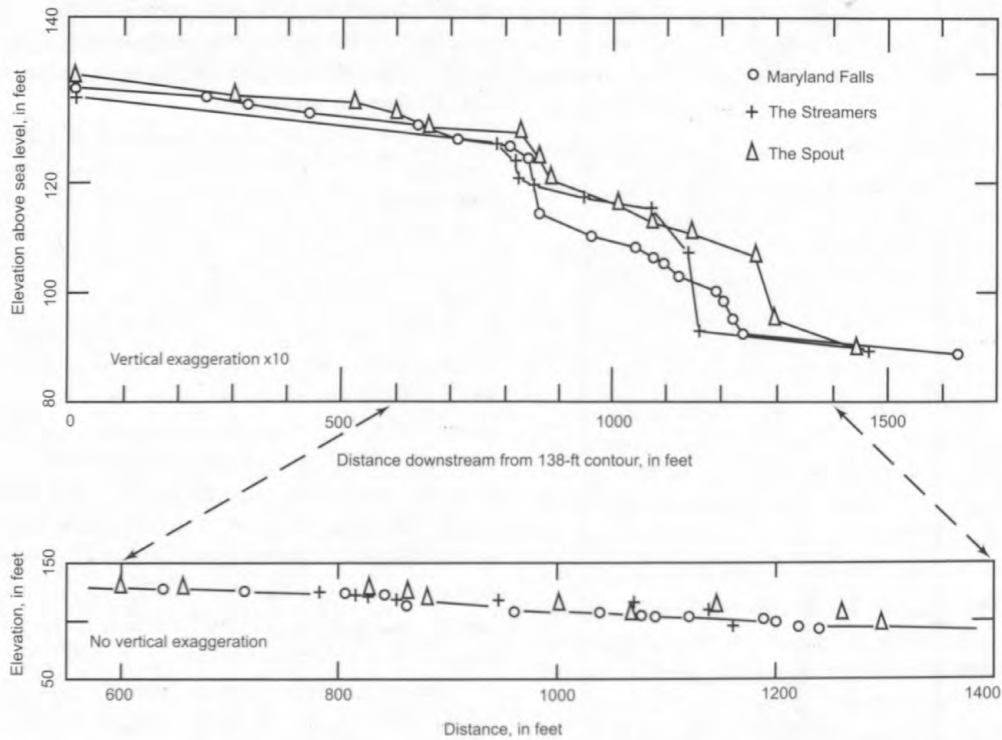
Figure 3. Longitudinal profile of Potomac River water surface at Great Falls (Zen, 1997a). From east to west, the three strands are Maryland Falls, The Streamers, and The Spout. Upper profile, vertical exaggeration 10x. Lower profile, expanded view of the main drop, no vertical exaggeration.

Little Falls (top, ~ 40 ft (12 m) above sea level). Tidewater is the lowest base-level. The bedrock gradient between Blockhouse Point and the Water Intake Dam is 0.07 percent (Zen, 1997b); within the gorge complex and between knickpoints it is typically about 0.06 percent. I have used this "default" gradient to reconstruct the paleochannels.

As the bounding knickpoints retreat, a given channel reach is constantly being eroded at the lower terminus but also extended by erosion at the higher terminus (fig. 4). The record of a strath, thus, is diachronous; it is, in general, younger at its upper end, and the contiguous straths are nested within one another.

Between Great Falls and Sherwin Island, the gorge system contains many channels at different levels. Several, including one that separates Olmsted Island from the mainland (the "fishladder channel") by-pass Great Falls, have their own cascades, and are active today. Some others become active only during floods; yet others serve no modern river function even during the highest recorded flood levels.

Straths of the Potomac Gorge

Evidence for straths of the Potomac River gorge complex (Zen, 1997a) includes three large data sets: (1) "concordant summits," which are surfaces of former channel floors; (2) "rock benches," which are similar features preserved as erosional remnants of limited areal extent, mostly on sides of younger straths; (3) "channels and ponds" incised into earlier straths and their associated scour ponds (the outlet sill levels are recorded); and two small data sets: (4) the levels of aligned lateral potholes (Zen and Prestegaard, 1994); and (5) outlet sills of plunge pools. All these recorded features show evidence of wear by running water (for example, flutes, sculptured p-forms, and potholes); fig. 5A plots strath elevations against measured river distances.

Using a default gradient of 0.06 percent to connect the datapoints and to guide the reconstruction of the other straths (fig. 5B), seven tiered straths are recognized within the Potomac River gorge complex. For ease of reference, these straths are here informally given geographic names (highest/oldest first); the elevations shown are the actual or projected elevations asl at or near the entrance to Mather Gorge.

1. Glade Hill level: 200 ft (61 m)
2. Matildaville level: 155 ft (47 m)
3. Bear Island level: 140 ft (43 m)
4. Sandy Landing level: 115 ft (35 m)
5. Black Pond level: 95 ft (29 m)
6. Hidden Gorge level: 77 ft (23 m)
7. Plummers Channel level: 53 ft (16 m) (observed, not projected).

As Mather Gorge is incised into what is the modern river channel above Great Falls, the level of that channel becomes the Bear Island strath below Great Falls, dry except during decadal floods. This strath forms much of Great Falls Park in
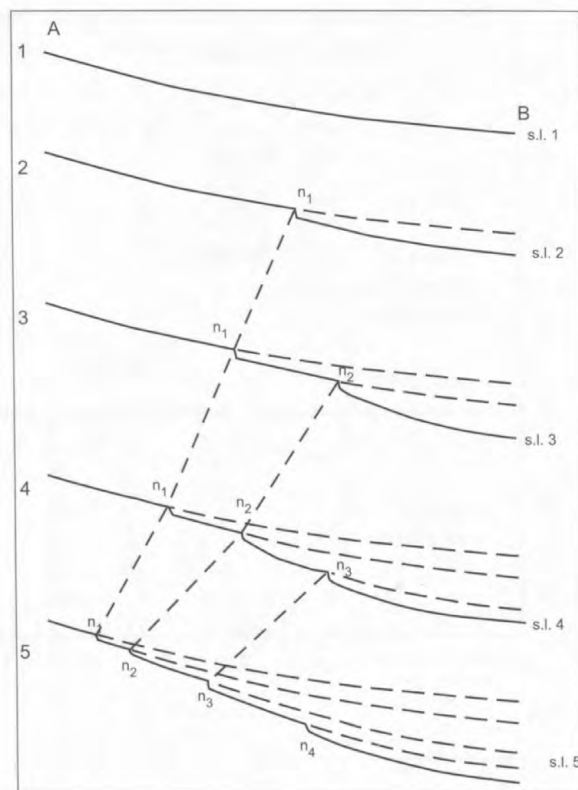
Figure 4. Schematic interpretation of formation of straths through retreat of knickpoints. The knickpoints between points A and B, designated n_1, n_2, and so forth, move upstream with the passage of time, indicated by 1, 2, and so forth, in response to successive drops in sea level (s.l. 1, s.l. 2, and so forth). As a result, the younger and lower straths become entrenched within the older straths.

Virginia, as well as the high points of Olmsted Island, Rocky Island, Bear Island, and Sherwin Island in the Chesapeake and Ohio Canal National Historical Park in Maryland. A diagrammatic cross section of the nested straths is shown in figure 2. Added here are the upland surface at about 350 ft (107 m) asl and the presumed Miocene-Pliocene fluvial deposit at 450 ft (137 m) asl at Tysons Corner, Va., interpreted as the oldest record of the paleo-Potomac River (Zen, 1997b).

The best record of the highest strath, the Glade Hill (fig. 6), is a fluvial boulder bed resting directly on unweathered schist on the flat top of Glade Hill at 200 ft (61 m) asl (Stop 1). The well-rounded boulders are varieties of quartzite. The nearest source of similar quartzite is the west limb of the Blue Ridge anticlinorium (Nickelsen, 1956; Southworth and Brezinski, 1996) at Harpers Ferry, W. Va. Geomorphic features, mostly knickpoints on entrenched tributaries, allowed extension of this level between Glade Hill and Harpers Ferry (Zen, 1997b).

The next lower strath, Matildaville (fig. 6), forms a rock bench near the ruins of that hamlet in Great Falls Park (Stop 4). This strath can be traced as far as the Water Intake Dam as waterworn summits of rock islands rising above the Bear
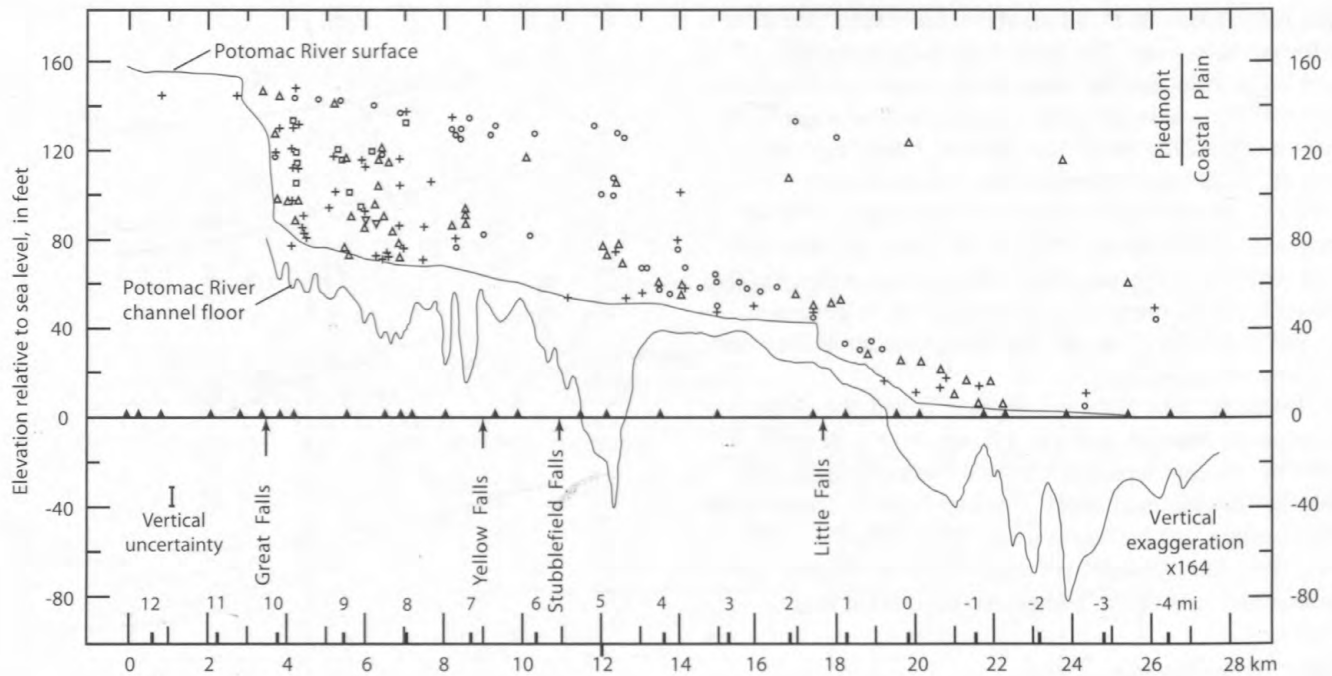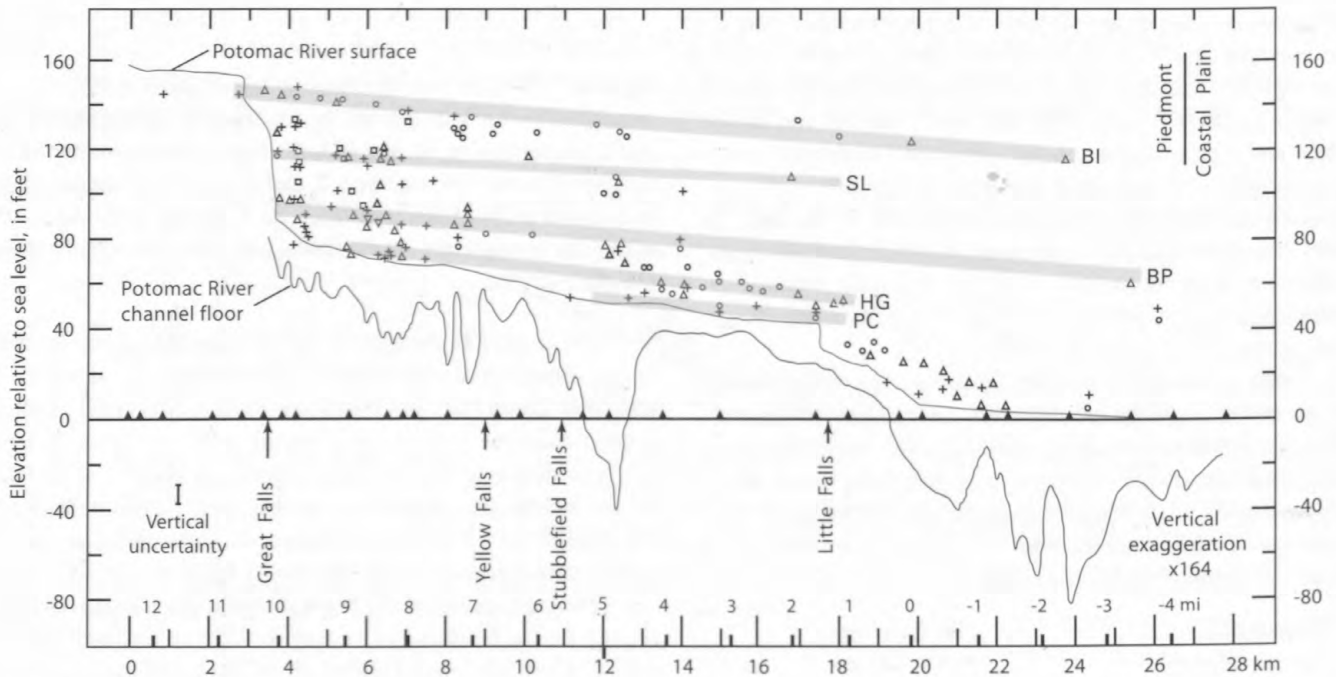
Figure 5. Composite record of strath elevations along the Potomac River gorge complex, Great Falls to tidewater. Kilometer scale is measured from Gladys Island. Miles scale is measured from Chain Bridge, as originally used by Reed and others (1980). Vertical uncertainty refers to the uncertainty in location of individual outcrops during mapping. A, Data: circles, rock summits; crosses, channels and scour ponds; up-pointing triangles, rock benches; down-pointing triangles, outlets of plunge pools; squares, lateral potholes. Profile of channel floor based on sounding by J.C. Reed, Jr. (written commun., 1993). B, Interpretation of data as strath levels (Zen, 1997a), not including Glade Hill and Matildaville straths that are higher than the Bear Island level. BI, Bear Island; SL, Sandy Landing; BP, Black Pond; HG, Hidden Gorge; PC, Plummers Channel.
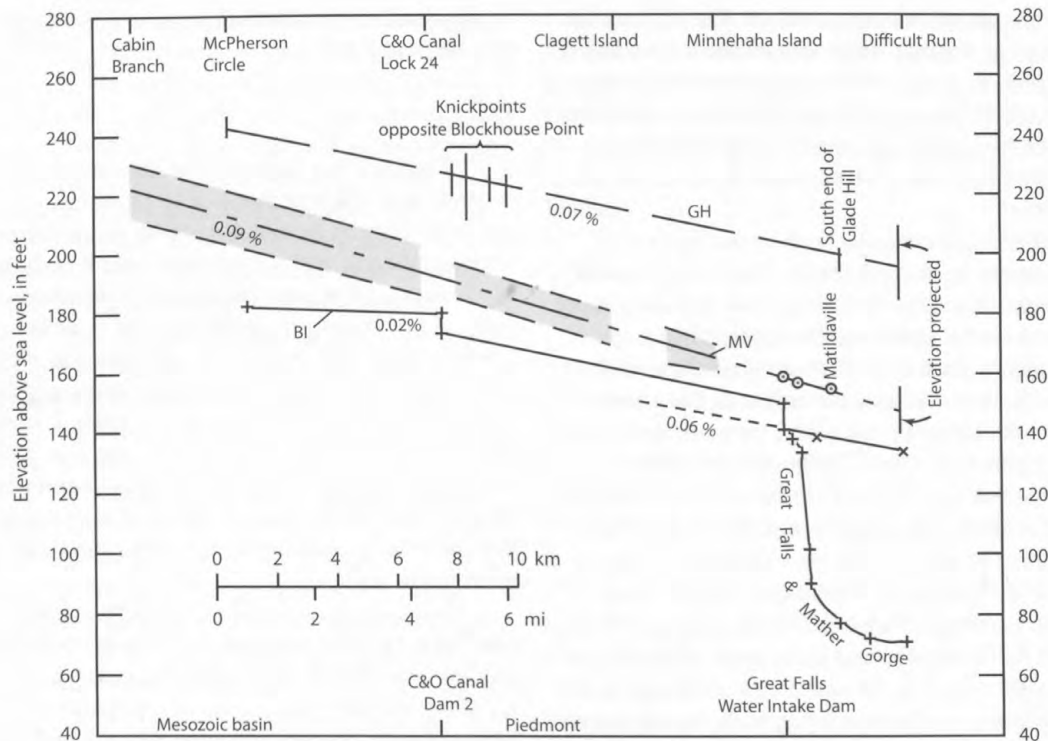
Figure 6. Comparison of the profiles for Glade Hill (GH), Matildaville (MV) (screened area represents vertical uncertainty), and Bear Island (BI) straths with the modern river channel. Solid lines designate BI and the modern river channel above the Great Falls Water Intake Dam. Projection of modern river channel is indicated by dashed line. Circled points and vertical bars show selected data (Zen, 1997b). The elevations at Difficult Run are projected (Zen, 1997a). The BI profile drops 6 ft at the dam because below this point the elevations refer to the rock floor but above this point they refer to the water surface. +, water surface elevations; x, channel floor elevations. Distances are measured along the river. Vertical exaggeration 328x.

Island level, as well as lateral potholes on the sides of water-worn outcrops. Upriver from the dam and as far as the western edge of the Piedmont, it is recognized as waterworn islands, *p*-forms, and sharp erosional benches where spurs of Piedmont hills are trimmed (Zen, 1997b). These benches can be recognized even in the early Mesozoic Culpeper basin as far as the mouth of Cabin Branch near the site of Edwards Ferry, Md.

The Glade Hill strath has an inferred gradient of 0.07 percent between Glade Hill and Harpers Ferry. This result is consistent with hydraulic demands for moving the boulders to Glade Hill (Zen, 1997a). The Matildaville strath has an inferred steeper gradient of 0.09 percent (fig. 6); this higher value may explain its disappearance upstream of Cabin Branch. Curiously, neither strath seems to show lower gradients within the early Mesozoic Culpeper basin, across which the modern gradient is 0.02 (fig. 6; Zen, 1997a).

Modes of Gorge Excavation

Abrasion, quarrying, and drilling are among the possible modes of excavation for the Potomac River gorge (see also

Tinkler and Wohl, 1998a,b).

Abrasion

The importance of abrasion is attested by the abundance of *p*-forms, flutes, and water-rounded rock surfaces. Abrasion should be especially powerful at knickpoints (Hancock and others, 1998) where flow is vigorous; yet abrasion, by itself, could not account for the excavation of Mather Gorge, particularly in view of the age constraints discussed on Day 2. Abrasion is likely important in molding the fractured albeit initially flat rock surfaces as seen below the Water Intake Dam into the breadloaf shapes of the Bear Island strath.

Quarrying

The ability of flood discharge to loosen blocks of rocks at the lips of knickpoints might be the key step in the *en bloc* removal, or quarrying, process and could be the major cause of excavation of Mather Gorge (Zen, 1997a; see also Seidl and Dietrich, 1992; Tinkler and Wohl, 1998a). Block loosening could be by hydraulic impact or by gravity and thawing

and freezing during more quiescent periods. The efficacy of freezing and thawing depends on annual temperatures, and if river flow continues during cold seasons the process might only marginally affect the main channel. Hancock and others (1998) mentioned hydraulic wedging; for that to promote block removal, however, the wedged material must first be removed by a flood.

In fractured bedrock channels such as the Potomac, another process might be at work. At the lip of a knickpoint, the pressure exerted at the top of a rock is the normal component of the water column (ignoring the atmospheric pressure!). At the under surface of the fracture-bounded block, the upward pressure is augmented by the height of the intermediate water column but this difference does no work. If, however, the fracture is part of a hydraulically connected fracture system, then the upward pressure could be sensitive to hydrological events elsewhere. Specifically, just below the Water Intake Dam, within the very flat bedrock channel, during periods of low flow water pours vigorously into the steeply dipping fractures. A connectivity of hydraulic signals within the fractures just below the channel floor seems plausible. In filled fractures, such signals would propagate at the speed of sound, about 1.5 km/second in water. Slight as the effect must be, it would push the rock slab upward, unopposed, during the entire period of waxing flood.

The distance between the Water Intake Dam and the top of Great Falls varies between 1 and 1.5 km (0.6–0.9 mi). During an onset of flooding, the crest passes downriver at about 2 m/s (meters/second) (E-an Zen, unpub. data), and so a pressure change due to increased water depth at the top of the rock block would take above 500 to 700 seconds to travel the distance between the dam and the lip of Great Falls. However, the same change transmitted through the fracture system would take only about 1 second (albeit probably attenuated by leakage). For about 10 minutes, the pulse of flood would exert small but unopposed upward pressure on the underside of the rock block. By extension, during waxing flood there could be sustained unbalanced upward thrust lasting hours to days. Could this hydraulic jacking loosen a block and ready it for eventual tumbling over the knickpoint within the main channels?

The process of quarrying is episodic. It occurs only during floods that had adequate power. Further, a given point along the river remains immune to quarrying except during the upriver passage of a knickpoint. Yet another possible source of episodicity is that excavation probably was most effective during glacial periods with greater runoff relative to seepage into the ground. Today, the Great Falls-Mather Gorge system might be only marginally active, awaiting the next cold epoch.

The rate of knickpoint retreat is not likely to be constant and also differs for different knickpoints. Thus, cataracts could bunch and transiently create large declivities (for example, the modern Great Falls; for past records, see Zen, 1997a),

or disperse into "rapids" such as at Yellow Falls and Stubblefield Falls.

Drilling

"Drilling" is a subset of the abrasion process but merits separate discussion because of its importance. As here used, the term refers to erosion caused by local turbulence, including formation of both vertical and lateral potholes (Zen and Prestegaard, 1994; see also Hancock and others, 1998, p. 40). Vertical potholes form on the channel floor but lateral potholes form in response to flow separation at rock obstacles. Formation of lateral potholes can be quite rapid: a few centimeters per year or more (Gregory, 1950; Putzer, 1971; Vivian, 1970; Bloom, 1998, p. 205; see Zen, 1997a). Because the vortex forming a lateral pothole is produced by a physical obstacle and not by chance encounter with a free vortex, vortices will form at the same sites when the flood reaches an appropriate level.

Coalescence of lateral potholes thus could widen the channel between knickpoints. A plausible example of such a process is a field of lateral potholes, some as high as 2 m (7 ft), along the Billy Goat Trail on the Bear Island side of Mather Gorge, formed when the Sandy Landing strath was the active channel (Stop 2).

Neither quarrying nor drilling automatically leads to bedrock channels that have the inferred strath gradients. This is troublesome because during floods, the water surface gradient in the upper reaches of Mather Gorge is as much as 0.6 percent (E-an Zen, unpub. data), several times that of the straths. Some other process must have intervened to "ream out" the longitudinal profile to those of the straths. How and why this occurred remains a puzzle; hydraulic jacking down to the level of the base of the knickpoint-defining cascades might be one mechanism.

Shoestring Channels on the Potomac: Modern and Ancient

The modern channel as well as paleochannels of the Potomac River contain records of multiple channels stacked in time and space. Particularly intriguing are "shoestring channels" (Zen, 1997a) that are straight or smoothly arcuate in plan view, narrow, have a nearly constant width (typically 15 m; 50 ft), and a shallow depth. A modern shoestring channel that may provide a conceptual template is the channel bounding Cabin John Island, entirely in alluvial cover, having a length of 0.5 km (0.3 mi), a sinuosity less than 1.1, and a length/width aspect ratio of 40. Its upstream end is arcuate. By comparison, a 0.6-km (0.4-mi)-long active shoestring channel incised in bedrock, also ending headward in an arcuate reach, bounds the east side of Plummers Island. It has a sinuosity of 1.05 and a length/width aspect ratio of 40.

Networks of shoestring channels of similar length and aspect ratios are preserved on several straths; some are active during floods. Examples include the heads of Vaso Island, Sherwin Island, incised channels at the south end of Bear Island, and the complex, multi-tiered network of channels around Rocky Island (Zen, 1997a). At Rocky Island, both straight and arcuate channels, the latter mimicking a meander, had formed in an alternating time sequence, crossing and beheading one another. Comparison of the configurations of these channels suggests that the bedrock shoestring channels might be imprinted from preexisting alluvial channels. If so, we might infer that during quiescent periods, the Potomac channel and straths were veneered with alluvium. Floods would remove this material to expose the rock floor to erosion. We see these latter records, but miss the alluvial parts of the story (see also Howard, 1998, p. 307). Inheritance from vanished alluvial regimes might have played a major role in the alignment of modern channels, including Mather Gorge itself.

An illustrative shoestring channel near Lock 12 of the Chesapeake and Ohio Canal opposite Plummers Island is an oxbow having a sinuosity of 2.4 (defining nearly three-quarters of a circle), about 15 ft (5 m) deep and 25 ft (8 m) wide, cut into the Hidden Gorge strath. Its configuration seems to require an origin through superimposition from an alluvial mantle where meander loops could develop. Thus, comparison of the alluvial and bedrock channels suggests their common origin.

Is the Gorge Erosion Still Active?

The age of the Potomac River gorge complex, including Mather Gorge, is being measured by the cosmogenic nuclide method and the results are a major focus of Day 2. We now know that for the upper reaches of Mather Gorge, the Bear Island strath became substantially dry by about 35 ka (Bierman and others, 2002) implying an average gorge incision rate of about 2.5 ft/1000 yr (0.8 m/1000 yr) (the modern submerged gorge floor has sill elevations at about 70 ft (21 m) asl between deeps; J.C. Reed, Jr., USGS, oral commun., 1993). The young date suggests that gorge incision and knickpoint retreat at Great Falls are active, but do the hydraulics of the recorded floods support this idea?

We can estimate the water gradient during floods near the entrance to Mather Gorge. For the largest recorded flood, that of 1936, a minimum estimate of the gradient, based on data in Grover (1937), is 0.3 percent; for the January 1996 flood Zen measured a gradient of 0.6 percent near the marker post (this may be anomalous; see discussion for Stop 9) but 0.3 percent along Mather Gorge. In what follows, I used a gradient of 0.3 percent. For the 1996 flood, I estimated a flow speed of 15±3 ft/s (5±1 m/s) at the entrance to Mather Gorge 46 hours after the peak; and a flow speed of 9±1.5 ft/s (3±0.5 m/s) at Sandy Landing. Leopold and others (1964) cited a

value of 22 ft/s (6.7 m/s) at Little Falls Gauge Station for the 1936 flood but this seems improbable; the average speed of passage of the crest of that flood between Great Falls and Little Falls was 6 ft/s (2 m/s), the same as what Zen obtained for the 1996 flood by dividing the discharge, Q, by an accurately constructed cross section area of the channel across Mather Gorge.

These parameters lead to an estimated unit stream power within the main channel of about 2 to 3 kilowatts per square meter (kW/m^2) (Williams, 1983). Extrapolation from Williams (1983) suggests that blocks as much as 6 ft (2 m) in diameter could be moved. This estimate is consistent with the preserved evidence of movement of 1-m (3-ft) blocks at Stop 8. As a dimension of 1 m is comparable to the spacings of fractures and joints in the bedrock near Great Falls, the headward retreat of Great Falls and the resulting extension of Mather Gorge could occur during decadal floods even though the evidence for the process is largely hidden from our view.

The Little Falls gauge record goes back only to 1930. However, in May 1994 the Great Falls Park posted notes on some post-1773 floods, including those post-1930, that rose "above drought level" below Great Falls. Comparison between these values and the flood levels recorded on that marker post (which has a base elevation of 146 ft (44 m) asl; Stop 9) shows that "drought level" is 65 ft (20 m) asl. Calculated pre-1930 flood records are shown in table 1.

If the tabulations are reliable, then a striking feature is that since 1773 only the 1785 and 1889 floods have topped the Bear Island strath. Even if the itemized 19th-century floods were all underestimates, there were fewer 19th-century floods of comparable magnitude. This deficit is compatible with the climate record since 1730 based on a tree-ring study at Point of Rocks (Cook and Jacoby, 1983). However, the extant post-1773 flood records are consistent with the idea that headward migration of Mather Gorge through knickpoint retreat is still episodically active. The modern process, however, may be slower than its counterpart during the glacial intervals and, with our short historical and hydrological records, humans would hardly notice the landscape modifications caused by knickpoint retreat at Great Falls.

Day 1 Trip Route and Stop Descriptions (fig. 7)

Leaving the McLean Hilton, turn left on Jones Branch Drive.

Turn right (north) on International Drive/Spring Hill Road.

Proceed about 0.5 mi, then turn left (west) onto Old Dominion Drive.

Continue on Old Dominion Drive (west) about 3 mi. Enter Great Falls Park.

Pass the park entrance and park in the farthest parking area about 0.5 mi past the guard station.

Table 1. Major floods at Great Falls since 1773.

[Abbreviations are as follows: ft, feet; m, meters; asl; above sea level)]

Date	Flood height above "drought level," in ft	Known/calculated elevation above sea level, in ft	Discharge, in 1000 ft³/s (1000 m³/s) at Little Falls
Sept. 1996	—	146	314 (8.89)
Jan. 1996	—	148	347 (9.82)
Nov. 1985	82	147	317 (8.98)
June 1972	87	151	359 (10.16)
Oct. 1942	90	155	447 (12.66)
Apr. 1937	85	150	347 (9.82)
Mar. 1936	91	156	484 (13.70)
Mar. 1924	>65	139[1]	
1889	>73	>138[2]	
1877	70	135	
1870	≥60	≥125	
1857	≥60	≥125	
1852	64	129	
1847	≥58	≥123	
1785	≥80	≥145	
1773	≥75	≥138	

[1]This is the level based on the photographic record at Lock 17 on the C&O Canal (National Park Service, 1991, p. 59). Lock 17 is directly across from the lower observation platform (140 ft (43 m) asl) in Great Falls Park.

[2]Notes on the U.S. Geological Survey's Little Falls Gauge Station (01646500) webpage say that the "flood of June 2, 1889, was approximately the same magnitude as that of March 19, 1936."

Stop 1. Lower observation platform.

The horizontal line at the upstream end of the visible river is the Water Intake Dam, built on a flat bedrock channel floor. Below Great Falls, this floor forms the principal rock benches visible to the right. It is hummocky as a result of subsequent erosion, mainly along fractures. Great Falls is a series of cataracts, each 10 to 15 ft (3–5 m) high, separated by pools (fig. 3). Immediately below the observation platform on the Maryland side (if water level permits viewing) is a large rock bench with a sharp peak at about 100 ft (30 m) asl. The base of this peak, at about 95 ft (29 m) asl, is ringed by lateral potholes; it was a rock obstacle when the channel was at the Black Pond level (here at 95 ft; 29 m). Another preserved bench of this strath is downriver, on the Virginia side, across from the fishladder. Looking at Rocky Island, its top is the Bear Island strath (here at 140 ft; 43 m). The transverse, arcuate channel at its north (left) side has a rock sill at 77 ft (24 m) (the Hidden Gorge strath). Hidden Gorge is an erosion channel that at high water bisects Rocky Island; it is a wetland area during periods of low to medium flow.

Walk along footpath that parallels the ruins of the Patowmack Canal, to the edge of the clearing.
Cross small wooden bridge to right.
Take the Carriage Road to the right of the building to follow the base of Glade Hill.

The swamp to the right occupies a former channel of the Bear Island strath. Milton (1989) reports that bedrock is a few feet below the muck surface; this is confirmed by Lee (1993) using a portable seismograph. The bedrock here is about 140 ft (43 m) asl, confirming that the valley is a part of the Bear Island strath. The upper end of the valley is partly filled by colluvium, which prevented even the 1936 flood to enter; nor could it have backed up beyond the abandoned quarry (en route to Stop 3) from Sandy Landing (see also Milton, 1989). This wetland area thus is fed by rainwater and seepage. The Carriage Road follows a regional sewer interceptor (from whence cometh the odor in warm weather).

Stop 2. Glade Hill.

Ascend at the point opposite a weir in the swampy valley. Notice outcrops of fresh schist to about 200 ft (61 m) (top elevation, 210 ft; 64 m), as well as scattered boulders of quartzite. The hill is flat-topped; it has no saprolite or streams running off its side. It is set within the incised upland whose top is about 350 ft (107 m). Glade Hill is not a Piedmont hill; instead, it is the oldest recognized strath of the Potomac River (Glade Hill level; see also Reed and others, 1980) preserved through topographic inversion. It is capped by a boulder bar in the former channel.

The boulders are various types of quartzite that can be
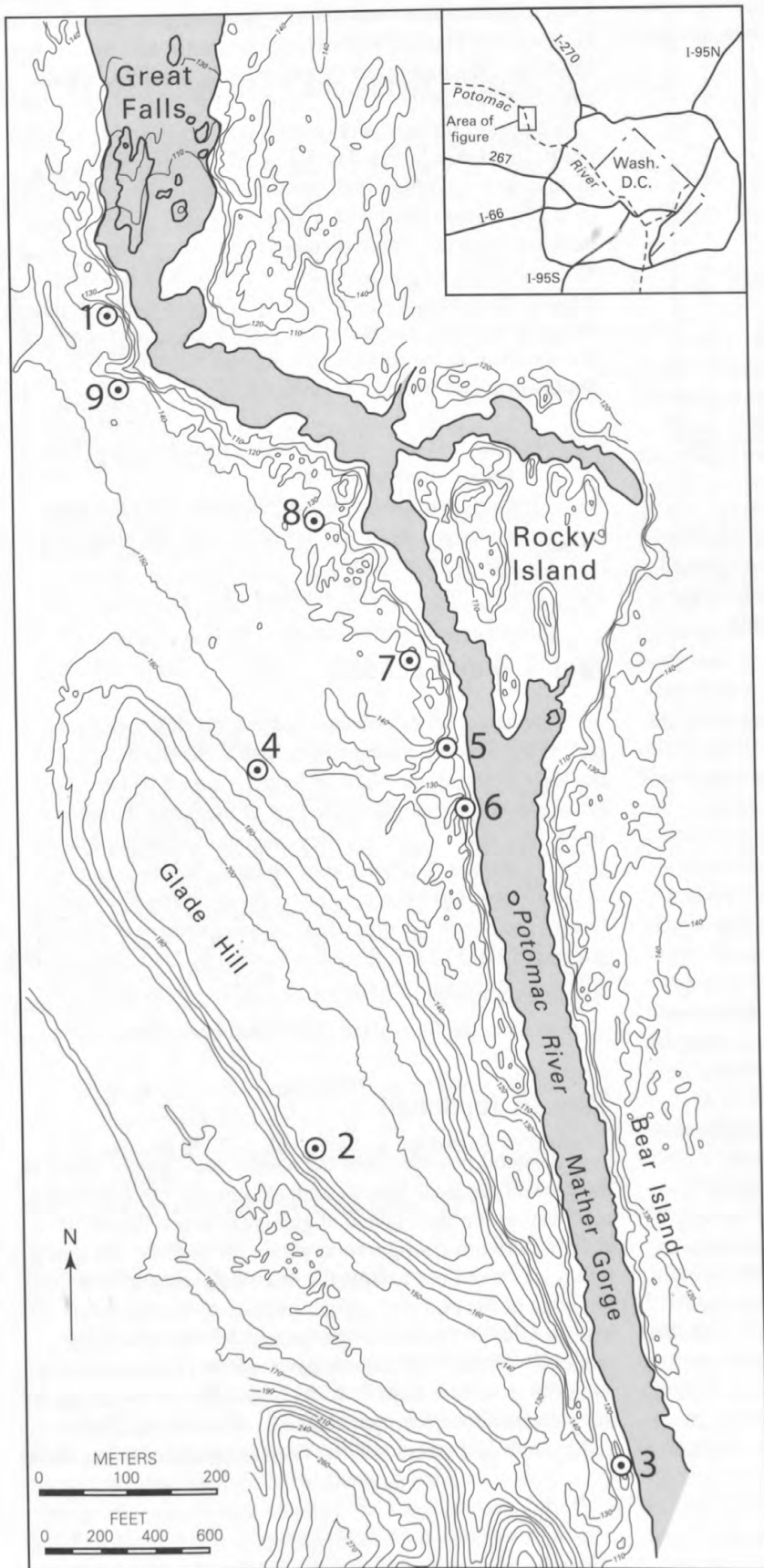
Figure 7. Day 1 field trip stops. Inset shows location of figure area in regional setting. Topographic contours in feet.
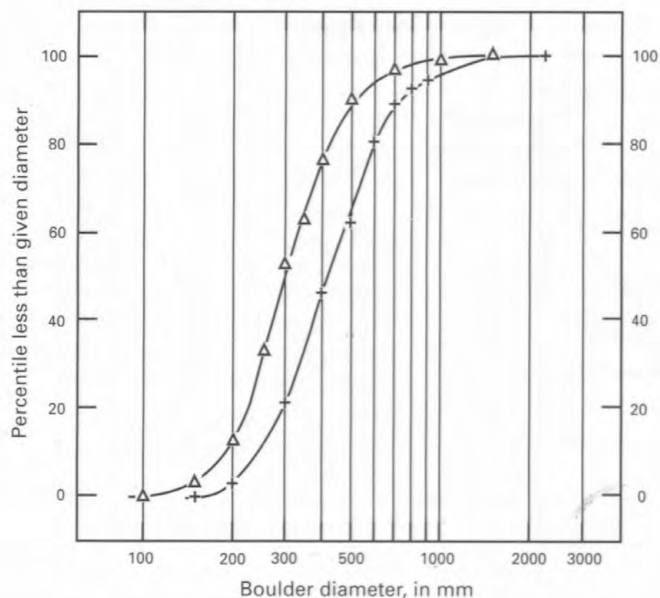
Figure 8. The Glade Hill boulder count, showing both the maximum (crosses) and median (triangles) diameters for all located unbroken boulders. n = 280. The lines are interpolations of the actual points. See Zen (1997a) for data and discussions.

matched with the Lower Cambrian Weverton Formation on the west flank of the Blue Ridge province, exposed along the Potomac River just below Harpers Ferry, 45 mi (72 km) (river distance) away. The absence of clasts of Piedmont rocks (and extreme rarity of Mesozoic rocks from the intervening Culpeper basin) makes it unlikely that these boulders were transported incrementally; one or a few large floods must have brought them here in brief, but violent, flood events.

We do not know the paleowidth of the Glade Hill strath. It could have been as wide as 1,800 ft (600 m), which is the maximum possible width for the 200-ft (61-m) level, or as narrow as Glade Hill, about 300 ft (100 m). Zen (1997b) estimated the Glade Hill channel gradient, as far west as Harpers Ferry, at about 0.07 percent. As the hydraulic conditions have allowed transport of boulders as much as 2-1/4 m (~7 ft) across all the way from Harpers Ferry, but stopped them here, we can place some constraints on the flood magnitude on a per-unit width basis by means of the unit stream-power relations (Williams, 1983). Such a flood would require about twice the discharge of the 1936 flood. The regression data of Hoyt and Langbein (1955, p. 20) and of Zawada (1997) both suggest that for the Potomac River having a drainage area down to this point of about 10,000 square miles (mi²) (26,000 square kilometers (km²)), a maximum flood discharge of 1 million cubic feet per second (ft³/s), or twice that of March 1936, is reasonable; if the paleochannel was as wide as the modern one, the discharge per unit width would also be dou-

ble the modern value. I speculate that the boulders originated from a debris apron between Maryland Heights and Loudoun Heights near Harpers Ferry (see Southworth and Brezinski, 1996, fig. 26), mobilized by exceptional, possibly climate-triggered, floods.

Some of the boulders contain still recognizable feldspar grains in arkosic layers. The frequency distribution of the median and maximum diameters of all the unbroken boulders (n = 280) is consistent with a single population; the largest boulders have maximum diameters exceeding 2 m (7 ft) (fig. 8; data in Zen, 1997a; assumes the unobserved boulder dimensions were the shortest). A large boulder of vein quartz might be from the Piedmont but large bodies of vein quartz are abundant in the rocks near Loudoun Heights (see Southworth and Brezinski, 1996, fig. 23).

> Follow first the ridgeline south, then the bridle trail back to the swamp valley.
> The original hilltop beyond the bridle trail has been destroyed by quarry operation, and the sharp ridgeline is an artifact.
> Follow trail to Sandy Landing.

Stop 3. Sandy Landing.

The large, water-polished and p-form-rich rock bench is part of the Sandy Landing strath; here it crowds the edge of the Bear Island strath. View of large (~ 2 m; 7 ft) lateral potholes across the river, likewise part of the Sandy Landing strath. The small hanging valley diagonally entering Mather Gorge is another Sandy Landing channel, but its elevation near the gorge has been reamed by downcutting to lower base levels. The Sandy Landing strath is quite wide near the southern end of Bear Island; there it is incised by later channels. We will discuss the straight section of Mather Gorge at Stop 6.

> Follow the blue-blaze River Trail back north.

Stop 3A. (optional).

A lateral pothole along the narrow rock bench, which is the edge of the Bear Island strath (Mather Gorge cuts diagonally across the Bear Island alignment). Notice the small-scale waterworn configuration within the pothole: the quartz-rich layers stand out against the mica-rich layers. From the left edge of the pothole, a small muscovite-bearing pegmatite was sampled in the late 1970s for age determination. The model Rb-Sr "age" of the muscovite, 469±12 Ma assuming an initial strontium ratio of 0.707, was taken to be the age of the peak metamorphism and anatexis of the schist (Fisher, 1970; Muth and others, 1979). The sampled spot is beginning

to be colonized by crustose lichens after about a quarter century; 10 years ago, the chipped surface was still shiny.

Stop 3B. (optional; Reed and others, 1980, p. 31).

A well-preserved vertical pothole, bottom not exposed. In the Great Falls area, the depth/width aspect ratio of vertical potholes rarely exceeds 1.5; frictional energy loss probably controlled the erosional reach (see Alexander, 1932). Two well-preserved vertical potholes (one 0.2 m (0.7 ft) and the other 1 m (3 ft) across at the bottom) have double basins separated by a water-sculpted ridge. Could it be that the tip of the vortex was bi-stable (Jonathan Tuthill, oral commun., 2000)?

> Follow the path along the canal locks.
> Take the path left to ascend toward the ruins of Matildaville.

The footpath roughly follows the alignment of Canal Street. The large building was the Superintendent's House, and the glass-and-crockery-littered ground at Stop 4 marks the site of Dickey Inn, which existed until the early 20th century. The foundation with a curious alcove was the spring house (Garrett, 1987).

Stop 4. Matildaville.

This hamlet for canal keepers was sited at 155 ft (47 m) level on the Matildaville level strath. The site was safely above even the 1936 flood. The exposure is waterworn; large lateral potholes, belonging to the 140-ft (43-m) or Bear Island strath, occur at its northeastern base and establish the chronological sequence of the Bear Island and Matildaville straths. A lateral pothole consistent with the Matildaville strath can be seen on the side of a waterworn rock prominence west of the picnic area, near the small parking lot.

> Go across the alluvium-filled holding basin of the Patowmack Canal.
> Go east on the trail that parallels the basin's outflow channel.
> Turn right onto the blue-blaze River Trail.

Stop 5. Trestle over small stream.

This miniature gorge in the small stream which we first crossed at the holding basin seems much too large for a watershed area of about 0.5 km² (0.2 mi²). Milton (1989) suggests that the channel is sited on lamprophyre dikes. I found no dike within the channel; at the channel mouth, dikes are exposed off the side (see photograph in Reed and others, 1980, p. 27). This robust channel is a fossil strand of the Potomac River when the paleo-Great Falls was just upriver from the mouth, abandoned when further knickpoint retreat

deprived this stream of its flow. The flat stretch of the channel below the trestle is consistent with its being part of the Sandy Landing strath.

> Go south and cross the trestle.
> Peel off immediately to the left, and climb up a large rock at the top of the cliffs above Mather Gorge.
> *Watch out for rock climbers!*
> *Do not fall into the river!*

Stop 6. View above Mather Gorge.

Across the river, on the Maryland side of Mather Gorge, at least three lamprophyre dikes, each no thicker than 1 ft (0.3 m), are aligned with the small valley (part of the Sandy Landing strath). These dikes are weathered back from the more resistant schist and follow parallel joints that dip steeply downriver. Biotite in dikes just like these, near Stop 1, yielded 363–360±13 Ma by the K-Ar method (Reed and others, 1970), showing that not only had rock deformation and metamorphism ceased, but that some joints had already formed. On the Virginia side, a triplet of lamprophyre dikes are assumed to be the same dikes as those visible on the Maryland side. If true, then projecting their strikes across the 70-m (230-ft)-wide gorge would show a dextral offset of 25 m (82 ft), a point used as evidence (for example, Reed and others, 1980, see photograph on p. 27) that a fault is responsible for this straight 1.4-km (0.9-mi) reach of the gorge (sinuosity <1.01). However, this evidence is permissive, because the dikes might have jumped across preexisting fractures (indeed, the just-mentioned photograph of the dikes shows two of the dikes to pinch out). As the strike of the dikes is visible only for a couple of meters, their straight extension across the gorge is an assumption. No fault could be identified along its expected on-land continuation on Rocky Island. Detailed landform analysis of the Bear Island strath shows no preferred thalweg; yet 25 ft (8 m) lower, the Sandy Landing channel closely followed the Mather Gorge alignment (Stops 3, 5, 6, 8). A fault that did not affect the Bear Island strath would have to become the controlling structure within that short vertical distance.

Another possible cause of the straight gorge is control by fractures. Tormey (1980) reported concentration of fractures in a direction parallel to the gorge. Again, the evidence is permissive because the fractures could be the result of stress release, analogous to the formation of sheeting fractures in quarries (Jahns, 1943). One joint-bounded cliff face just up river shows a lateral pothole at the Sandy Landing level, so at least some of the gorge-parallel joints dated back to when the gorge excavation was just beginning.

The rocks here are mica schists and graywackes metamorphosed in the Ordovician. Sillimanite, andalusite, and large pseudomorphs of cordierite are present, as well as disputed pseudomorphs of kyanite (which may be that of sillimanite; see Hopson, 1964; and Fisher, 1970). The metamor-

phic pressure was likely in the 2 to 4 kilobar range (lower if the identification of kyanite was invalid). As the granite and pegmatite show that the temperature must have reached 700°C (Stop 3A), the average vertical thermal gradient must have been 60–70°C/km. This is unlikely for an "upstroke" P-T trajectory in a subduction zone; more likely the setting was back-arc extension. These rocks must have been elsewhere during the Taconian deformation.

> Return to the River Trail. Recross the trestle bridge. Go past the bronze plaque marked Mather Gorge Overlook to a large rock outcrop on the left about 500 ft (150 m) beyond the plaque.

Stop 7. Lateral pothole.

Three aligned potholes on a large rock obstacle within the Bear Island strath. The pothole farthest upriver (north) is about 4 m (13 ft) from the rock's prow (Zen and Prestegaard, 1994, figs. 3, 4). Note that the potholes are not nucleated on fractures. Note the overhanging alcove, the shallow and simple basin, and the downstream inclination of the potholes. The plans of these potholes are far from circular; they terminate sharply in the downstream direction but taper on the upstream side. The waterworn sloping downstream edges of the potholes are integral parts of the architecture. They are not broken edges of former vertical potholes.

Lateral potholes form where vortices are created by flow separation at rock obstacles. The process can be observed during floods on many rivers, including the Mather Gorge reach (see also Zen and Prestegaard, 1994, p. 50). The overhangs mark levels of water-air intersection during "average" eroding floods. The asymmetry results from the tip of the eroding vortex being anchored in the pothole but the top being swept downstream by the current; in the absence of other indications, they can give the paleoflow direction.

The processes of removal of rock material during pothole drilling include hydraulic impact, cavitation, and blasting by suspended load. The interiors of the potholes show strong material control (see also Stop 3A): millimeter-thick quartz-rich layers stand out in relief, and the ridges smoothly grade into recessed unweathered mica-rich layers. The millimeter-scale selectivity rules out large "grinders" as the principal agent of erosion (see Alexander, 1932; see Wentworth, 1924). Large grinders found in fossil potholes may have choked the hydrodynamic process, contrary to the intuitive inference.

Reliable data on the rates of pothole formation are scanty. The available data from natural settings, however, yield consistent values on the order of 1 in (2–3 cm) per yr (Gregory, 1950; Putzer, 1971; Bloom, 1998). A pothole of the size seen here could be formed within a human lifespan. The interior of the potholes on high level straths are commonly coated with colonies of crustose lichens whose enlargement rate is a fraction of a mm per yr (Lawrey and Hale, 1977).

Their presence shows that the occasional inundations during decadal floods do not modify the potholes.

> Continue on the River Trail to where the gravel path splits near the edge of the open area.
> Take the right split for about 70 ft (20 m).
> Go right on an unimproved trail for 100 ft (30 m).
> Opposite a low rock on the right, bear left on an obscure path toward the river, emerging in the open area above an abandoned plunge pool.

Stop 8. Plunge pool of a fossil cascade.

The outlet is at 115 ft (35 m), part of the river's Sandy Landing strath. The cascade formed when the paleo-Great Falls was near the head of Rocky Island, subsequent to its residence near Stop 5. The top of this fossil falls is about 130 ft (40 m) asl, incised about 10 ft (3 m) into the Bear Island level.

During the waning stage of the January 1996 flood, the river current damaged and bent every tree within the amphitheater; their direction of bend described a large clockwise gyre (looking down) that persisted for some hours. A rampart fronting the reshaped debris apron was about 9 ft (3 m) high and sloped 20° towards the pond. This rampart was formed of blocks of local schist mixed with blocks of concrete and a few blocks of sandstone. The blocks were as much as 2 m (7 ft) across and showed a tendency for the long dimension to be aligned with the strike of the rampart. The top of the reshaped apron consisted of sand draped over the blocks, introduced at a later and lower stage from a side channel, as well as artifacts, such as a 10-ft (3-m) section of 2-in (5-cm) diameter iron pipe, the working end of a rusted manual lawnmower, and other objects whose shapes provide little or no hydrodynamic lift. These may have been "lags" from earlier events. One block of concrete, 42 by 27 by 8 in (1.1 by 0.7 by 0.2 m), bent a standing iron fence post (a piece of old detritus) and rested in its crook, demonstrating that blocks of this size were moved by the flood, which at this point should have generated unit stream power of about 1 kW (Williams, 1983).

> Return to the River Trail and onto the picnic ground.

Stop 9. Flood marker post.

The water levels for six post-1930 floods are shown on figure 9. These, plus a seventh flood that just touched the base of the post, together yielded a regression relation between these local elevations and Q values recorded at the Little Falls Gauge Station (Bob Ridky, USGS, oral commun., 2002). The Little Falls Q value needed to first dissect the Bear Island level (here at about 140 ft (43 m) asl) into islets, then to completely inundate it, is about 220,000 to 230,000

ft³/s (6,200–6,500 m³/s) In addition to the seven post-1930 floods (and probably two others in 1785 and 1889) that inundated Bear Island and other parts of the "flood plain," four high flows since 1930 (dated Aug. 1955, Oct. 1977, Feb. 1979, Feb. 1984) exceeded 200,000 ft³/s and were nearly brimful to the Bear Island strath. These floods must have moved blocks more than 1 m (3 ft) across (as attested by the record at Stop 8) but we cannot see the results. The location of the marker post, just downstream from the transverse rock wall athwart the main flow down the falls, however, cautions us that superelevation could have caused reproducible but anomalous flood levels as well as water-surface slopes here.

End of Day 1.

Day 2

## Cosmogenic Dating of Strath Surfaces of the Potomac River near Great Falls

Introduction

Resolving the age of bare bedrock strath terraces bordering the Potomac River and other rivers draining the central Appalachian Mountains (fig. 1A) is key to understanding the nature of bedrock channel incision along the Atlantic passive margin. Until recently, direct dating of such erosional surfaces has not been possible. Over the past decade, the development and application of surface exposure dating methods (Bierman, 1994; Gosse and Phillips, 2001), particularly the application of in situ produced cosmogenic nuclides such as ¹⁰Be, now allows dating of exposed bedrock surfaces, including bare-rock strath terraces.

This field trip presents data that we have gathered over the last 4 years from terraces along the Potomac River. We have taken a similar approach to studying terraces of the Susquehanna River (Reusser and others, 2003). We will visit sample sites near the Potomac River and discuss how the data collected and analyzed so far help us to understand better the timing and spatial pattern of channel incision upstream, within, and downstream of Great Falls and Mather Gorge. The fundamental geomorphology of the gorge/falls/strath-terrace complex is discussed in detail in Day 1 of this guidebook.

Background Information—Cosmogenic nuclides and terrace dating

Cosmogenic nuclides, produced in rock and soil near and on the Earth's surface, have seen increasing use in geomorphic studies since their first applications in the late 1980s
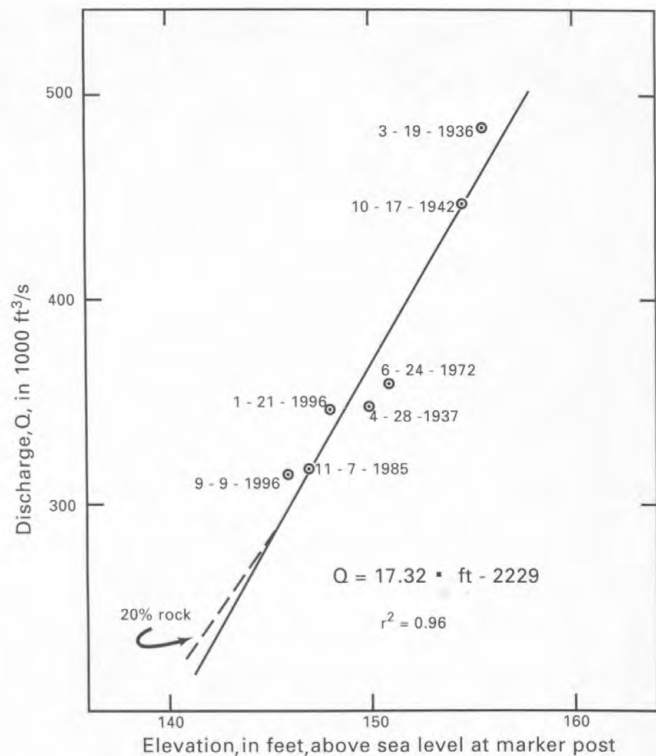
Figure 9. Regression of the seven post-1930 flood levels, in feet asl, at the marker post near the scenic overlook at Great Falls Park against the discharge, Q in 1000 cubic feet per second (1000 ft³/s), as recorded at the Little Falls Gauge Station. Dashed line shows the relation that would obtain if 20 percent of the space between 140 ft and 146 ft were occupied by rocks.

(Craig and Poreda, 1986; Kurz, 1986; Nishiizumi and others, 1986; Phillips and others, 1986). Although the use of such nuclides for dating was first suggested almost half a century ago (Davis and Schaeffer, 1955), widespread application happened only after the more recent development of accelerator mass spectrometry (Elmore and Phillips, 1987). Hundreds of studies have now been published that rely, at least in part, on such nuclides either for age estimates or for estimating rates of surface processes. Reviews pertinent to both the cosmogenic literature and cosmogenic techniques are provided by several authors: Bierman and Nichols (2004); Bierman (1994); Bierman and others (2003); Gosse and Phillips (2001); Kurz and Brooke (1994); Zreda and Phillips, (1998).

Cosmogenic nuclides have not been widely applied to bedrock exposed by fluvial erosion. To date, most cosmogenic dating of strath terraces has been done along rivers draining active margins (Hancock and others, 1998; Leland and others, 1998; Pratt and others, 2002) and only a handful of analyses have been published. Some work has been done on rock exposed in channels to estimate rates of bedrock lowering and knickpoint retreat (Hancock and others, 1998; Seidl and others, 1997), and alluvial terraces have been dated in several locations (Burbank and others, 1996; Hancock and
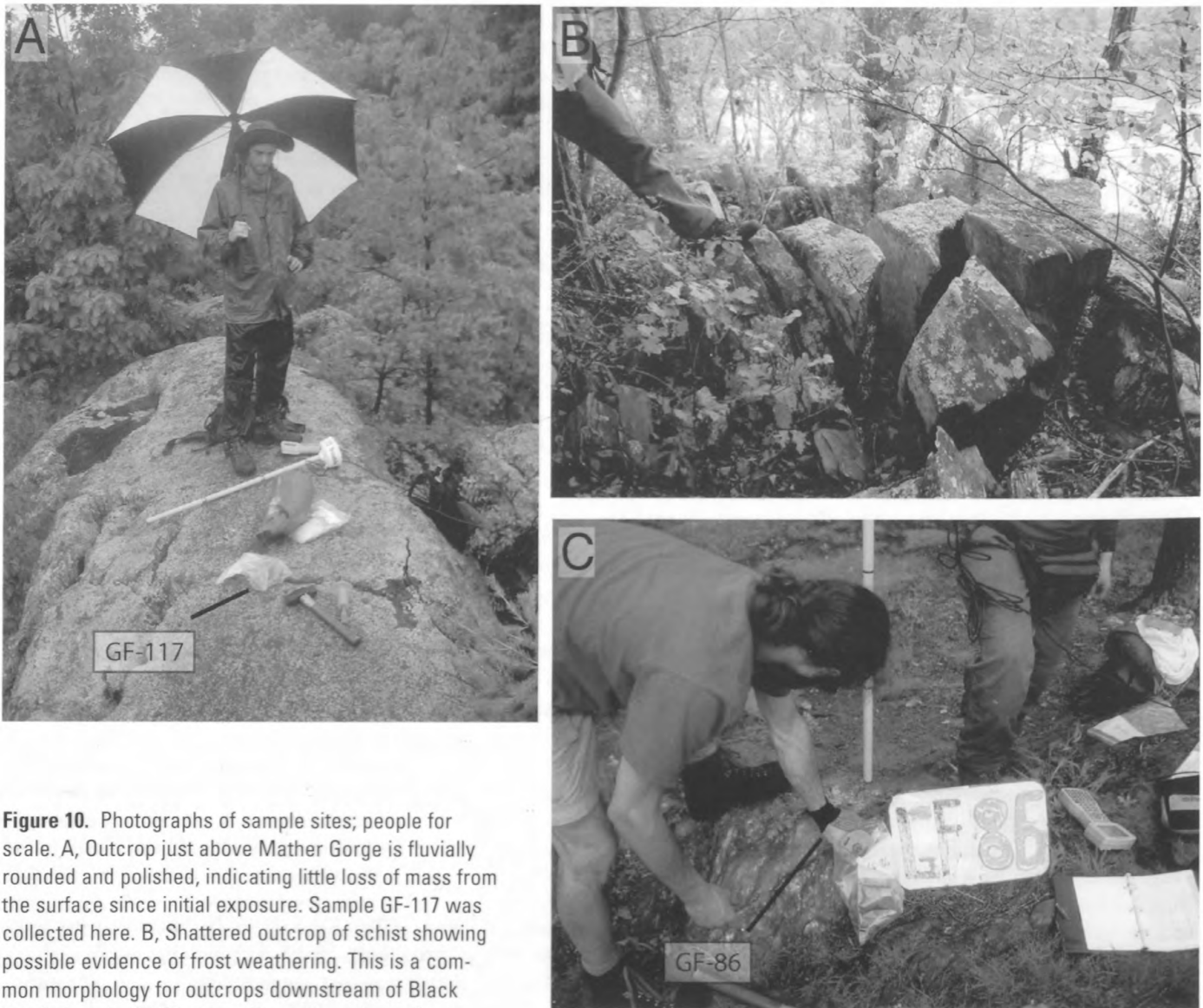
Figure 10. Photographs of sample sites; people for scale. A, Outcrop just above Mather Gorge is fluvially rounded and polished, indicating little loss of mass from the surface since initial exposure. Sample GF-117 was collected here. B, Shattered outcrop of schist showing possible evidence of frost weathering. This is a common morphology for outcrops downstream of Black Pond. Sample GF-75 was collected near here. C, Outcrop from which sample GF-86 was collected is covered for the most part by fine-grained sediment. Fine-grained red soil is exposed behind the outcrop, which stands only 20 cm (8 in) above the ground surface.

others, 1999; Repka and others, 1997; Schildgen and others, 2002). In some cases, alluvial terrace dating has used a technique that accounts explicitly for inheritance of nuclides from prior periods of exposure upstream (Anderson and others, 1996). Cosmogenic data are just starting to be collected for bedrock terraces bounding passive margin rivers, such as the Potomac (Bierman and others, 2003; Bierman and others, 2002; Reusser and others, 2003).

The basic premise of the cosmogenic method is the accumulation of nuclides over time in response to cosmic-ray dosing, the result primarily of neutrons splitting target atoms in minerals (Lal and Peters, 1967). Measuring nuclide concentration is now a relatively straightforward but time con-

suming procedure. Interpreting measured nuclide concentrations provides the greatest challenge in many situations. Nuclide concentrations can be interpreted confidently as exposure ages only if several conditions are met: rapid exposure of rock from a depth of several meters, no cover by soil, sediment, or water since initial exposure, and no erosion of the rock surface. Violations of these conditions can result in age overestimates (inheritance; Colgan and others, 2003) or age underestimates (stripping of soil or erosion of rock; see Bierman and Gillespie, 1991).

Field observations suggest that most samples collected from bedrock surfaces along the Potomac River meet the requisite conditions for dating. All but a few sampled outcrops

preserve intact fluvial forms (sculpting, potholes, and polish), implying little erosion since abandonment (fig. 10A). Several samples collected from below mean low water have nuclide concentrations equivalent to only several thousand years of continuous surface exposure suggesting that most nuclides measured in currently exposed outcrops resulted from subaerial cosmic-ray dosing rather than from exposure under river water (Bierman and others, 2003). For 3 km (2 mi) downstream of Great Falls, most outcrops we sampled stand greater than 1 m (3 ft) above their surrounding rock or soil; thus, we conclude the likelihood of extended burial by soil or overbank sediments is low. However, 3 km (2 mi) downstream of Great Falls there is a dramatic change in the appearance of the most prominent strath terrace surface. Here and farther downstream, most outcrops are heavily weathered both chemically and by what appears to be frost shattering (fig. 10B); these downstream outcrops are much more deeply immersed in alluvium and may well have been covered at sometime in the past (fig. 10C). Thus, model dates on most downstream outcrops are likely minima.

Calculations, made for the Susquehanna River, suggest that occasional inundation of sampled outcrops by floodwaters probably has little effect (an error at the percent level) on model ages except for samples within 1 m (3 ft) of mean river level. Large flows are so rare and short-lived that their waters intercept few neutrons and thus have little effect on cosmogenic model age estimates; common flows in today's channel geometry do not raise river stage enough to submerge many sampled outcrops. Prior to or at the beginning of incision, outcrops which today are inundated only every decade were likely flooded multiple times each year. The vertical incision rates we calculate are sufficiently rapid (0.5 to 0.8 m/1000 yr) that annual water cover and neutron absorption would rapidly be reduced for outcrops within the gorge just several thousand years after incision begins. However, for samples collected from outcrops on the broad strath terrace, incision rates were presumably much lower as the strath was being beveled; thus, inundation of outcrops by floodwaters likely absorbed some neutrons. Of course, we have no way of estimating flows in the past when climate was different nor can we know paleochannel geometry. In any case, the effect of floodwater absorption of neutrons would be to reduce the model ages we report.

Sampling and Analysis Strategy

Our sampling strategy is designed to provide age estimates for exposed bedrock surfaces at different elevations along the Potomac River from above Great Falls to Plummers Island at the I-495 American Legion Bridge, 6.25 mi (10 km) downstream (fig. 11). Samples collected along the length of the most prominent morphological feature, a broad bedrock strath called the Bear Island level by Zen (1997a) dominate the sample population. Examining sample age, as a function of distance downstream, allows us to speculate about the tim-

ing and horizontal rate of incision along the river (fig. 12). At eight places along the river, we collected vertical transects of samples, which allow us to estimate rates of vertical incision. Two of those transects are shown in figure 13.

We collected samples, using a hammer and chisel, from the best-preserved outcrops we could identify in the field. Such identification was based on the presence of water-polished rock, potholes, fluvially shaped and streamlined outcrops, and the absence of surface weathering. If quartz veins were present, we sampled them; otherwise, we sampled schist. Sample elevation was measured using a global positioning system (GPS). At open-sky sample sites, differential GPS (Trimble 4400) provided centimeter-scale precision. Under tree cover, a Trimble ProXR using Coast Guard beacon correction provided elevations with 1- to 2-m precision. We processed samples at the University of Vermont using standard methods (Bierman and Caffee, 2001). Isotope ratios were measured at Livermore National Laboratory and model exposure ages were calculated by using an integrated ^{10}Be production rate of 5.2 atoms g^{-1} y^{-1} adjusted for the elevation and latitude of the sample sites considering the neutron-only corrections provided by Lal (1991).

Field Observations

We have identified three morphologically distinct sections of the Potomac River separated by the present and a proposed paleo knickpoint in the 10-km (6-mi) reach that extends from just above Great Falls to Plummers Island. Three sections are separated by the current knick zone (Great Falls) and what we interpret as the paleo knick zone (Black Pond). A brief description of the two knick zones and three morphologically distinct sections follows.

1. The Potomac River above the knick zone: Above Great Falls, the river occupies a wide channel in which water-rounded rock crops out in isolated knobs mostly within the river but also along the shore. Soil-mantled slopes extend nearly to the channel margin in most places; there are restricted areas of overbank deposition in other locations. Little bare rock is exposed except at and near the channel margins. We view this section of the river as a modern analog of the paleo-Potomac River downstream, before significant incision of the channel. If the river were to incise significantly above Great Falls, sections of the present-day channel bottom would become terrace surfaces and the in-channel rock outcrops here would become isolated high knobs.

2. The current knick zone (Great Falls): At Great Falls, the river has incised deeply, leaving waterworn, fluvially rounded outcrops high and dry above the modern channel. The water moves through Great Falls in distinct channels rather than moving over a single waterfall; this pattern of erosion isolates a series of high points in the knick zone that are above the water level (and thus continually exposed to cosmic
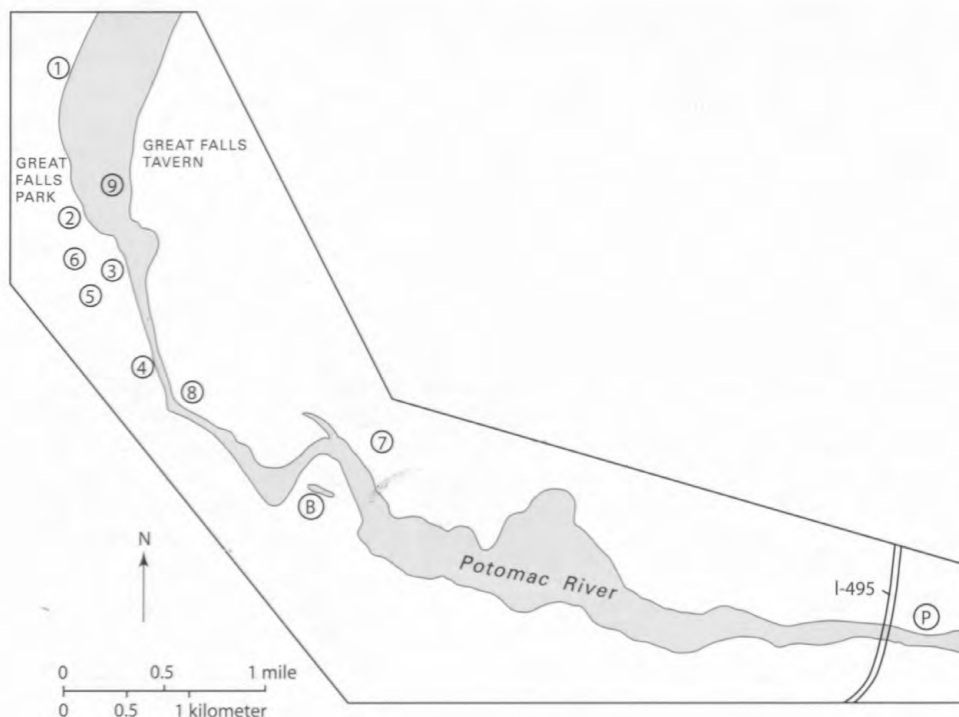
Figure 11. Day 2 field trip stops and location of sample sites. Black Pond, B, is the site of paleo-Great Falls; P, Plummers Island.

radiation) at most river stages (fig. 14). Conversely, at the base of the channels, there is outcropping rock that sees little if any cosmic-ray dosing. As one approaches the falls from upstream, the river has begun to incise about 1 km (0.6 mi) before the falls, leaving increasing amounts of rock and a greater vertical extent of rock exposed in the channel and along its margins than farther upstream.

3. The young terrace landscape: Immediately downstream of Great Falls and adjacent to Mather Gorge on both the Maryland and Virginia banks of the river is a wide strath terrace of fresh bedrock, mantled by thin sediment in places. This surface extends 3 km (2 mi) on the Virginia bank from Great Falls to Cow Hoof Rock. Bedrock forms on what we term the young terrace landscape are well rounded and water sculpted; most appear fresh and only lightly weathered. The majority of our samples have been collected on and below this surface. Many of these samples were collected near the edge of the terrace overlooking the gorge where very little sediment covers the bedrock.

4. The last paleo-falls (pre-Great Falls) knick zone (Black Pond): The area surrounding Black Pond on the Virginia bank is one of transition where the riverside landscape of the Potomac changes dramatically, suggesting that this was the location of a long-lasting stand of a paleo-Great Falls, occupied until the Potomac began incising Mather Gorge. Upstream of the Black Pond area, the young terrace landscape is dominated by exposed, fresh rock outcrops, the result of this downcutting. Downstream, the old terrace landscape is soil mantled; outcrops are isolated and usually heavi-

ly weathered. The morphology upstream of Black Pond is similar to the present-day Great Falls. There are isolated high points separated by deep channels (fig. 15). Channel bottoms, meters above the waters of the Potomac, are cluttered with boulders. The Black Pond area has been left high and isolated by incision of the Potomac River. The upstream end of this peninsula is bare rock, water polished, and fluvially rounded from the tops of the highest isolated knobs to the base of the now-abandoned channels. The highest outcrops likely stood above all but the highest flows while the channels were usually submerged; rock on these high points is more weathered than rock at the channel bottoms, implying a longer period of exposure. On the uplands south and east of Black Pond, rock exposed on the uplands becomes extremely weathered 200 m (650 ft) downstream and 10 m (33 ft) in elevation.

5. The old terrace landscape: Downstream of Black Pond, the wide strath terrace continues on the Maryland side to the American Legion Bridge, but little rock crops out—a dramatic change from the young terrace landscape upstream where rock outcrops dominate the terrace surface. Most rock on what we term old terrace landscape is buried by a thick (up to 5 m (16 ft) in stream cuts) cover of red, fine-grained sediment that could be overbank material or loess. There are two exceptions—just below and just above the American Legion Bridge are Plummers Island and an unnamed island, respectively. Both are isolated bedrock hills and both have little to no fine-grained sediment cover and an assortment of fluvial forms (heavily weathered) extending to their summits (fig. 16). The outcrops on the old terrace landscape were
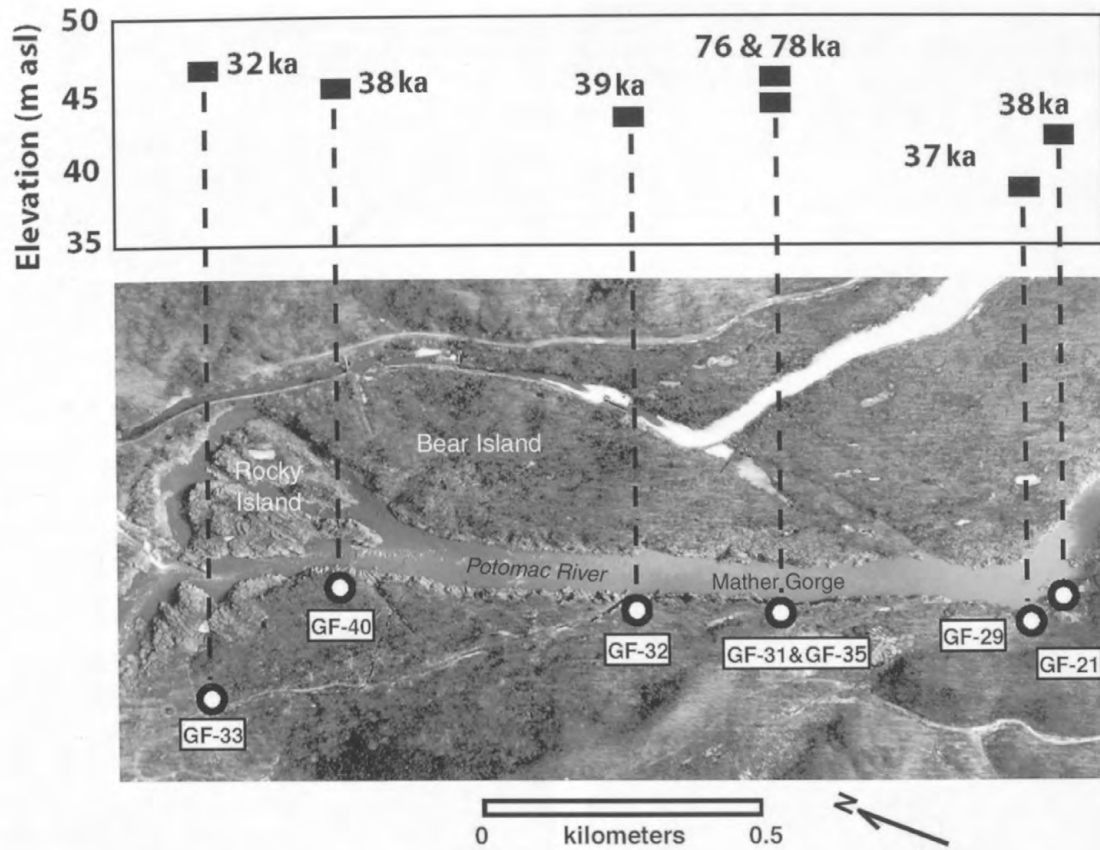
Figure 12. Samples collected from the Bear Island surface along the Virginia side of the Potomac River show no trend of age with distance downstream. m asl, meters above sea level.
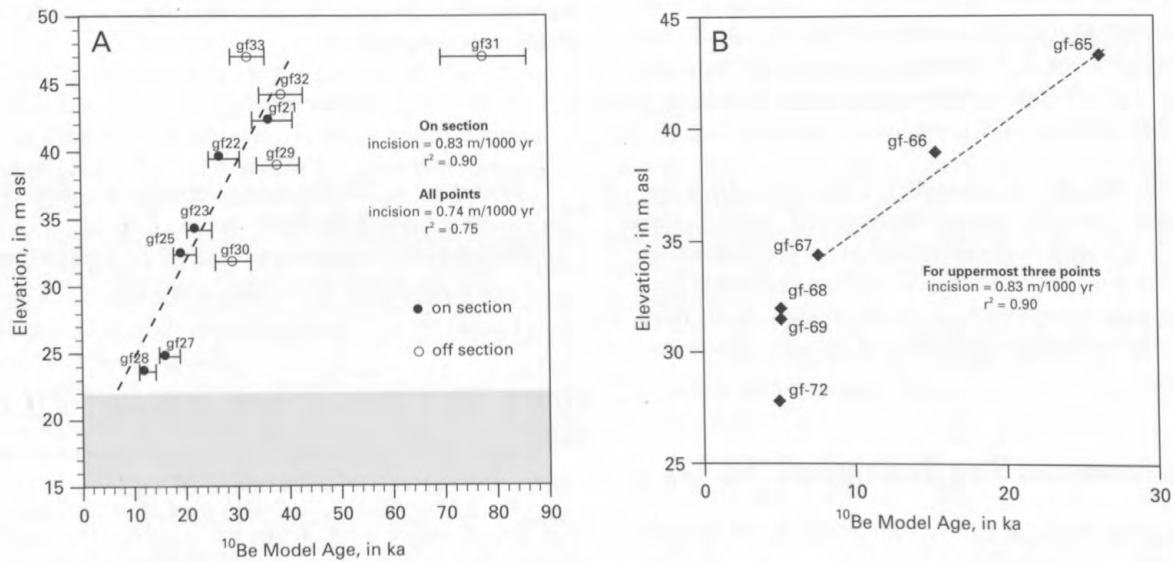
Figure 13. The model age of samples collected along vertical transects is related to elevation above the river channel. This relation can be used to estimate effective vertical incision rates at several places. A, Transect at Cow Hoof Rock (Stop 8). B, Transect at the Maryland viewing platform (Stop 9). "On section" are samples collected on the Cow Hoof Rock vertical transect. "Off section" are samples not collected on that transect but at other locations along and below the 140-ft strath.
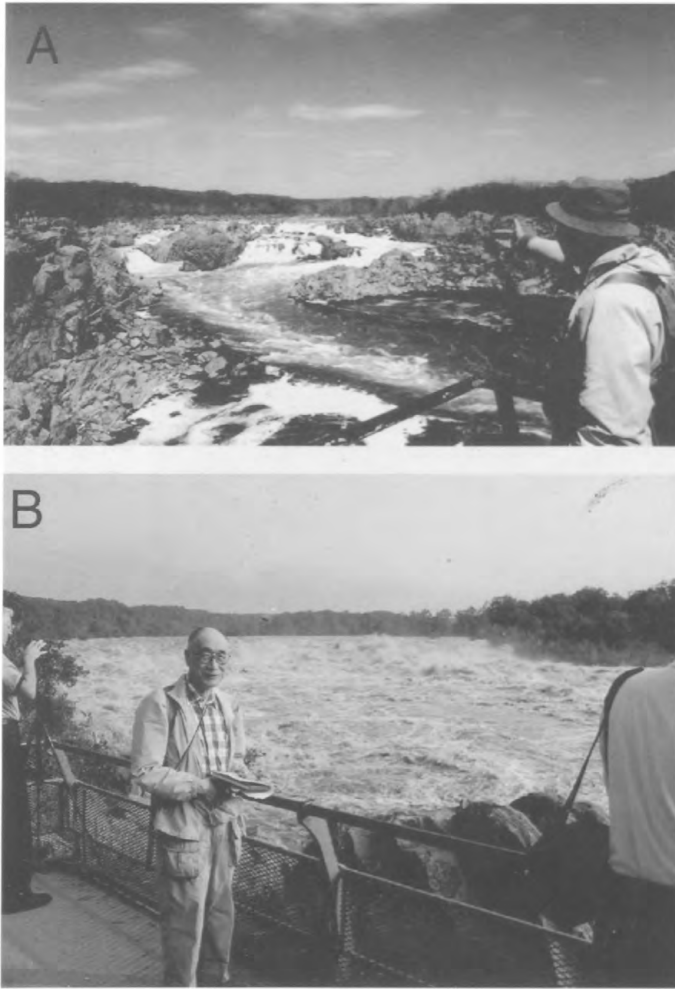
Figure 14. High points in the channel remain exposed to cosmic radiation during all but the largest floods. A, Photograph of Great Falls from downstream viewing platform on the Virginia side during low-flow conditions. B, Photograph of Great Falls from same viewpoint during high-flow conditions after Hurricane Isabel, September 2003 (flow ~165,000 cubic feet per second).

Figure 15. At Black Pond, paleochannels are exposed including the high points and the channel bottoms. Photograph taken from a high point looking toward another high point. Main channel of present-day river is in distance. Looking toward Maryland from the Virginia side of the river. Person for scale in upper center of photo.

heavily weathered, pitted, and shattered (fig. 10B). In many places, trees are growing through cleaved rock. Most outcrops are at most a few meters above the soil and were exposed at the terrace margin or near drainages. All sampled outcrops preserved at least a suggestion of fluvial erosion. Some have degraded potholes nearby; others appear rounded or streamlined by water.

Day 2 Trip Route and Stop Descriptions (fig. 11)

Leaving the McLean Hilton, turn left on Jones Branch Drive.

Turn right (north) on International Drive/Spring Hill Road.

Proceed about 0.5 mi, then turn left (west) onto Old Dominion Drive.

Continue on Old Dominion Drive (west) about 3 mi and enter Great Falls Park.

Pass the park entrance and park in the farthest parking area about 0.5 mi past the guard station.

Stop 1. The Potomac River upstream of Great Falls.

This stop illustrates the broad channel morphology of the river prior to major incision that has modified that morphology downstream. Note the isolated islands of rock exposed in the channel here and along the channel margin. Rock exposed on these islands is dosed by cosmic radiation; however, rock exposed on the channel bottom is largely shielded from cosmic rays by water.

Figure 16. Sample GF-60 was collected from this outcrop at the top of Plummers Island. The outcrop is smooth and includes a remnant of a pothole suggesting that erosion has been minimal.

Find the trail head at the upstream end of the parking lot.

Walk along the gravel trail by the river until the Great Falls aqueduct dam is reached.

Go past the dam to examine the channel morphology (considering that the dam ponds water about 1.5 m (5 ft) higher than the natural river level). About 1 km (0.6 mi) farther upstream, we collected two samples from outcrops adjacent to the channel (fig. 17A). The lower outcrop (GF-53) gave a ^{10}Be model age of 31 ka. The outcrop about 1 m (3 ft) higher (GF-54) gave a slightly older model age (33 ka). Both ages suggest that incision between 35 and 30 ka was not limited to Mather Gorge but extended upstream past Great Falls, albeit to a much lesser depth.

Return to just downstream of the dam site to examine the vertical transect of samples GF-55 to GF-58. We collected four samples here at different elevations (fig. 17B). Ages range from 22 to 38 ka. The ages of the upper three samples, which span an elevation range of 4 m (13 ft), are very similar (38, 35, and 36 ka in decreasing elevation). Such similar ages imply rapid incision occurring about 35 ka, very similar to the age at which Mather Gorge begins to incise several kilometers downstream. The lowest sample (GF-58) gives a model age of 22 ka. Because this lowest sample sat just 10 cm above the water level the day we sampled (flow = 11,000

ft^3/s), the model age for this sample is a minimum estimate, the result of shielding by water during floods. Because the discharge the day we sampled was nearly two times median flow, the impact of flood-induced neutron absorption is likely to be minimal, even here.

The lowermost two samples were completely covered by floodwaters of Hurricane Isabel, for which the Little Falls gauge, 14 km (9 mi) downstream, recorded a peak discharge of 167,000 ft^3/s. This flood represented the 28th highest daily maximum flow in 73 years (yr) of record, a 2.6-yr recurrence in the partial duration series and the 13th largest annual flow, a 5.7-yr recurrence in the annual maximum series. For more information on flood flows, see the discharge values in table 1 (Day 1).

To view Great Falls and several sample sites near the falls, walk past the Visitor Center.

Take the footpath to the most upstream overlook platform.

Stop 2. Great Falls overlook.

When standing on the overlook, look back at the outcrop in the woods (fig. 18A; GF-37) which gave ^{10}Be model ages of 25.9 ka and 25.5 ka (two laboratory replicates), suggesting that significant incision here, at Great Falls, took place prior to the last glacial maximum.

Across the river is Olmsted Island and the viewing plat-
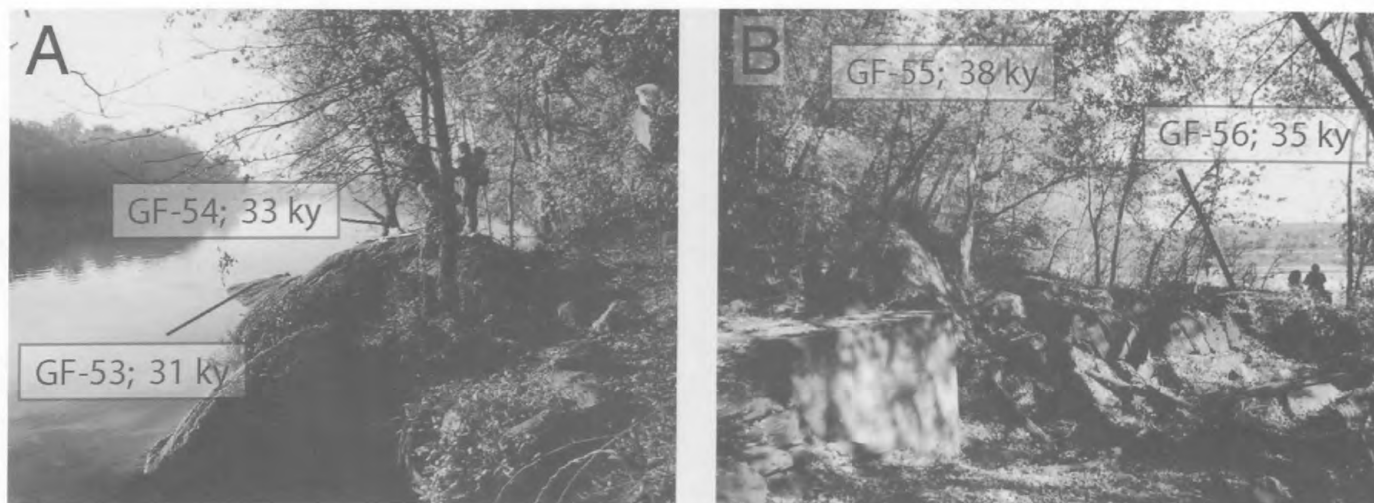
Figure 17. Sample sites upstream of Great Falls at Stop 1 (Day 2). A, Samples GF-53 and GF-54 were collected from fluvially rounded and polished outcrops along the Virginia side of the river upstream of the aqueduct dam. B, Samples GF-55 and GF-56 were collected as the two highest samples of a four-sample transect downstream of the aqueduct dam.

form. Upstream of the viewing platform, in the woods, we sampled one of the highest outcrops on Olmsted Island (GF 46). The outcrop was hard, fresh, and fluvially eroded (fig. 18B). It gave a model ^{10}Be age of 30 ka. Downstream of the viewing platform on the Maryland side of the river channel, we collected a vertical transect of eight samples (GF-65–GF-72) from the highest point (fig. 18C) to the water's edge at low flow, a span of 15.4 m (50.5 ft) elevation. The uppermost sample (GF-65) on the Maryland side has an age of 27 ka, similar to the exposure age of the outcrop here. Several samples lower on the vertical transect have shorter model exposure ages ranging from 16 to 5 ka, the latter age common to three samples collected within 2 m (7 ft) of flow at 11,000 ft^3/s (fig. 13) implying very rapid incision of greater than 4 m (13 ft) in the mid-to-late Holocene. The apparent incision rate reflected by this profile is about 50 cm/1000 yr between 27 and 12 ka, increasing to nearly 100 cm/1000 yr during the middle Holocene.

This age similarity, for samples collected from rock surfaces bordering Great Falls, suggests that the falls we see today began to take on their modern character at this location between 25 and 30 ka. Since that time, the falls have deepened and steepened but there is no cosmogenic dating evidence for steady, ongoing knickpoint retreat.

> To explore the channel of the Potomac River prior to the last glacial maximum, walk downstream from Stop 2.
> Pass the grassy picnic areas, to the River Trail through the woods that parallels the river's edge.

Along this trail, which winds along the terrace margin, are many bedrock outcrops, many of which preserve evidence of fluvial rounding and erosion. There is significant relief on this surface with some outcrops standing several meters

above the general terrace level. By analogy to the modern river, we suggest that these same higher outcrops stood above the most common flows of the river when the Bear Island level was the bottom of the river channel.

Stop 3. The dominant strath terrace: the Bear Island level.

This is the largest and most continuous strath terrace of the Potomac River near Great Falls, encompassing both the less-extensive Matildaville level and the more-extensive Bear Island level of Zen (1997a). This broad, composite surface ranges in elevation from 140 ft (43 m) to 155 ft (47 m) asl at Great Falls and dips gently downstream. Exposure ages on this strath are multi-modal with a cluster of four ages between 86 and 62 ka on high, isolated, and weathered outcrops; two ages for adjacent high outcrops at 53 and 55 ka; and another cluster of five ages from 39 to 32 ka on lower, better-preserved rock surfaces. We interpret the older ages on higher surfaces as minimum limits for an initial period of channel-bottom erosion (>75,000 yr) that lowered but did not dissect the terrace. The younger ages, which cluster between 32 and 39 ka with no clear pattern upstream or downstream, indicate the timing of terrace abandonment and the rapid incision of Mather Gorge starting about 38 ka. The age-clustering represents the time at which the Potomac River incised a narrow channel (Mather Gorge) of sufficient depth to carry the most common flows. When this occurred, the Bear Island level was abandoned. What was once the broad, inundated channel bottom was then left exposed more or less continuously to cosmic radiation.

Sample site GF-33 is found just after the trail enters the woods (fig. 19A). This is a lightly weathered outcrop of schist that stands about 1 m (3 ft) above the soil around it.
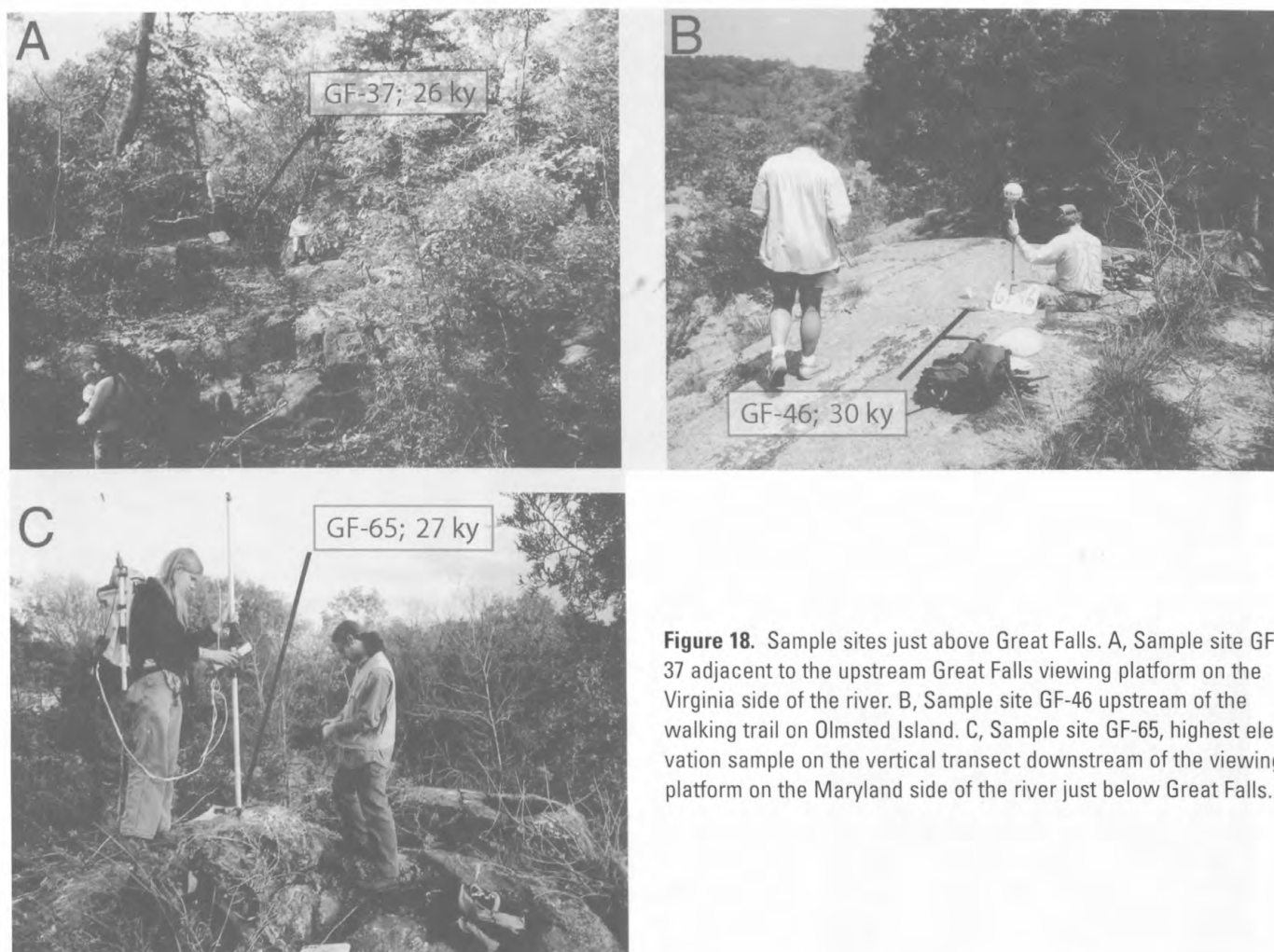
Figure 18. Sample sites just above Great Falls. A, Sample site GF-37 adjacent to the upstream Great Falls viewing platform on the Virginia side of the river. B, Sample site GF-46 upstream of the walking trail on Olmsted Island. C, Sample site GF-65, highest elevation sample on the vertical transect downstream of the viewing platform on the Maryland side of the river just below Great Falls.

The model ^{10}Be age is 32 ka. Farther down the trail, sample GF-40 has a model exposure age of 38 ka. Samples GF-42 and -43 (figs. 19B, C) have very similar exposure ages of 56 and 53 ka respectively, with the slightly higher outcrop having the slightly older age. GF-32 (fig. 19D), collected from a broad expanse of bare rock just above the walls of Mather Gorge, gives a model ^{10}Be exposure age of 39 ka. Farther downstream, sample GF-30 (fig. 19E) was collected from an outcrop topographically lower than the others, and it has a model ^{10}Be exposure age of 29 ka consistent with exposure after incision of the Bear Island level strath had already begun. This sample site was just inundated by the flood resulting from Hurricane Isabel in September 2003, whereas all other sample sites on the Bear Island level were not. Farther downstream, samples GF-29 (fig. 19F) and GF-21, have model exposure ages of 38 and 37 ka, respectively.

Proceed uphill from GF-21 to an abandoned quarry.

Stop 4. Older, higher outcrops—Paleo islands?

Climbing to the top of the quarry wall, we will examine several outcrops that form another, albeit short, vertical transect. The highest of these outcrops, from which sample GF-31 was collected, is quite weathered, suggesting that it has been exposed longer than the other lower outcrops surrounding it. This field observation is confirmed by ^{10}Be measurements, which suggest that the two higher outcrops (GF-31 and GF-35, within 1 or 2 m (0.35–0.6 ft) of elevation and above the general Bear Island level) record 76,000 and 78,000 yr of exposure, respectively. Nearby, the outcrop from which GF-36 was collected is 7 m (23 ft) lower than the older outcrops, several meters below the general Bear Island level, and records an age of only 23 ka. This young age makes sense as this outcrop could only have been exposed after the incision of Mather Gorge had begun.

GF-33; 32 ky

GF-42; 56ky

GF-43; 53 ky

GF-32; 39 ky

GF-30; 29 ky

GF-29; 38 ky
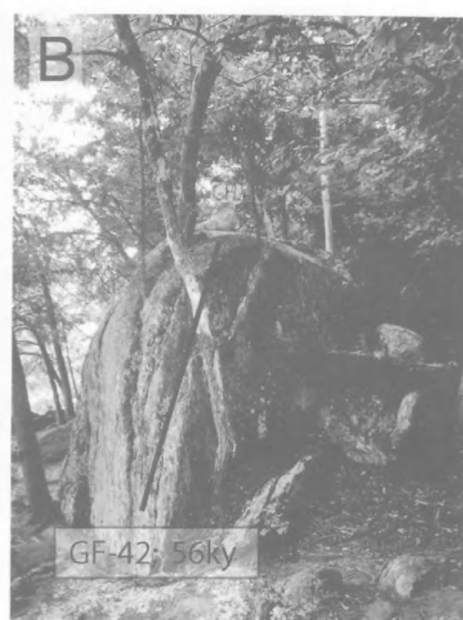
Stop 5. Glade Hill boulder bed.

From the abandoned quarry, we will walk back to the parking area along the service road. Just before the service road opens into the field with picnic tables, it ascends the upstream end of Glade Hill. Here, we will turn off the trail and climb Glade Hill, which stands above the Bear Island level and was clearly an island during fluvial erosion of the Bear Island and Matildaville levels more than 90,000 ka. Glade Hill is underlain by schist, outcrops of which can be seen as we walk up the hill. However, the top of the hill is mantled by a boulder bed that is overlain by fine-grained, reddened material, probably loess. These bouldery deposits are unique in the vicinity of Great Falls and Mather Gorge.

On top of the hill are large boulders of far-traveled quartzite (discussed in detail at Stop 2, Day 1). Both ^{10}Be and ^{26}Al have been measured in one of these boulders. The ^{26}Al and ^{10}Be model ages are both high (253 and 228 ka, respectively), but they are discordant suggesting either measurement error or a complex history of exposure either before or during burial (Bierman and others, 2003). There is no unique inverse solution to the measured nuclide activities; therefore, we discuss several end-member interpretations below, the calculations for which are based on the production rate estimates of Bierman and others (1996) and Stone (2000). Because the sample was taken from a quartzite boulder fluvially transported to its current location on a high terrace above the Potomac River, there is the added complexity of considering where the boulder received some or all of its cosmic-ray dosing. With only one sample from this deposit, its history remains uncertain.

The simplest and shortest duration scenarios involve a period of exposure followed by deep burial, as explained in Bierman and others (1999). Another possible scenario begins with the boulder accumulating initial nuclide activity upstream, either by a period of surface exposure or from slow, steady erosion on the basin hill slopes, before being deposited in the boulder bar. Because we do not know the elevation at which such dosing might have occurred, we can set only an upper limit for the duration of this initial exposure period, considering the elevation and corresponding nuclide production at the site where the boulder was sampled. Because the sample site must be equal or lower in elevation than where the dosing occurred, the calculated production rates are also lower limits.

Initial boulder exposure of ≤280,000 yr or erosion at >2.2 m/m.y. are consistent with a two-step model in which the boulder is then buried for a period ranging from 170,000 yr in the exposure case or 70,000 yr in the erosion case,

before being rapidly exposed and then sampled. Such burial might have been caused by the loess that currently covers the boulder bed in places; perhaps, the boulder we sampled was exposed as the loess was eroded in response to Holocene-Pleistocene climate change. These exposure-prior-to-delivery scenarios suggest that the boulder bed was deposited between 70 and 170 ka. Conversely, we could assume that the boulder arrived on the bar with a negligible inventory of cosmogenic nuclides; such a scenario might imply that it was delivered to the Potomac channel by rock fall and rapidly moved downstream. Once deposited, the boulder might have been irradiated before being deeply buried by loess and recently re-exposed; if this were the case, then the boulder was deposited about 450 ka (280±170 ka).

From Glade Hill, go down the hill and toward the picnic area.

Stop 6. More older, higher outcrops.

At the downstream end of the picnic area, one can examine several outcrops in the woods that also stand several meters above the Bear Island level. The outcrops are weathered but still preserve fluvial forms. Samples GF-38 and GF-39 were collected from these outcrops and give ages of 86 and 62 ka, respectively (fig. 20). Considering the possible loss of mass from the surface of these outcrops by erosion, their ages are similar to those visited at Stop 4 and suggest a minor period of incision that left these higher outcrops exposed. The date of incision is uncertain, but likely it was prior to 76 ka and if erosion has been minimal, not much earlier than 86 ka.

Return to the parking area. (As you return to the parking lot, restrooms are on the lower floor level of the Visitor Center and at the upstream (north) end of Glade Hill.)

From the parking area, drive to Old Dominion Drive (1 mi).

Turn left (south) on Georgetown Pike for 4 mi.

Enter I-495 northbound.

Cross the American Legion Bridge; stay in right lane.

Take the Clara Barton Parkway exit (right lane) at the far end of the bridge.

Immediately bear left on exit ramp toward Carderock.

Follow Clara Barton Parkway until it ends.

Turn left onto MacArthur Boulevard.

Figure 19 (facing page). Sample sites on the Bear Island strath terrace surface, downstream of Great Falls. A, GF-33 was collected from an isolated outcrop less than 1 m (3 ft) high. B, GF-42 was collected from a tall outcrop within 10 m (33 ft) of GF-43. C, GF-43 was collected from a shorter outcrop adjacent to GF-42. D, GF-32 was collected from a broad expanse of rock. E, GF-30 is topographically lower than the other pictured samples and overlooks Mather Gorge. This outcrop was submerged during the peak flooding of Hurricane Isabel (~165,000 ft³/s). F, GF-29 was collected from an isolated outcrop of rock farther downstream than the other samples.

Figure 20. Panoramic photograph of sample sites GF-38 and GF-39 on the Bear Island surface. Both outcrops are weathered and are separated by about 30 m (100 ft).

Go 1 mi to the Old Anglers Inn (on your right).

Turn left into one of the dirt parking lots.

Lunch is by the C&O Canal, a several minute walk from the parking lot. There are usually porta-potties near the parking lot.

Stop 7. The old terrace surface.

Here, we examine the highly weathered outcrops and the mature, reddened soils of the old terrace surface. Outcrops are few and far between. Bedrock is shattered and shows significant physical, granular weathering. Such shattering may be the result of tree roots that wedge outcrops apart or the effect of freeze-thaw processes more active during glacial times than under present climate conditions. Most bedrock outcrops along this section of terrace are isolated knobs standing just above the blanket of fine-grained material that covers the terrace. The fine-grained material is very red, clay rich, and can be several meters deep. It is best observed where tree throws have exposed the soil. The presence of this sedimentary cover smoothes the surface and makes smooth, flat, easily walked trails.

Although we are walking on the Bear Island level at an elevation just below Stops 1 through 6, and just several kilometers downstream, the character of the surface has changed dramatically. We are now just downstream of Black Pond, the area we interpret as the paleo-Great Falls. Upstream of Black Pond, the Bear Island level is dominated by outcrops that are largely intact, exposed, and lightly weathered. Downstream of Black Pond, outcrops are few, deeply weathered, and mantled with reddened soil. We interpret this change in geomorphic character as an indication of surface age; thus, the Bear Island level is time transgressive. Upstream the surface is young; downstream the surface is old. We believe this change in character reflects the episodic nature of knickpoint retreat along the Potomac River; in other words, the knick zone is stable for thousands to tens of thousands of years and then moves rapidly upstream presumably in response to some external forcing such as climate and (or) land-level change relative to base level.

Sample site GF-73 (fig. 21) is a weathered, but still fluvially rounded, outcrop just above a cliff on the Potomac

River. As of November 2003, no isotopic data are available for GF-73, nor for the samples farther downstream along this surface. However, we do have data for a single sample (GF-60, fig. 16) collected from the top of Plummers Island, just below the American Legion Bridge, 4 km (2.5 mi) downstream. The age for this sample is greater than 202 ka, supporting the geomorphically based inference that at least some surfaces downstream of Black Pond are much older than those upstream of the pond. This age also implies very low rates of erosion for metadiamictite (≤ 3 m/m.y.) despite the humid climate of northern Virginia.

If time allows, walk upstream along the C&O Canal towpath.

Turn off on the "escape" trail about halfway along Widewater, the area where the canal widens significantly and occupies an abandoned channel of the paleo-Potomac (Southworth and others, 2001).

Stop 8. Cow Hoof Rock view (optional).

At this stop, we will examine the Cow Hoof Rock vertical transect from afar and note the dramatic change in the landscape (rock outcrops predominate and soil cover is minimal) just 1 km (0.6 mi) upstream of Stop 7. At Cow Hoof Rock, vertical incision from the time of initiation of Mather Gorge (GF-21, 37 ka) until about 13 ka (GF-28), proceeded at about 80 cm/1000 yr (fig. 13). This rate is lower than incision rates estimated in tectonically active areas (Burbank and others, 1996; Leland and others, 1998), similar to rates estimated over the same timeframe on the Susquehanna River, 100 km (62 mi) north (Reusser and others, 2003), and higher than those estimated for the Rocky Mountains (Schildgen and others, 2002).

Retrace route to the parking area opposite the Old Anglers Inn.

Drive 2 mi north on MacArthur Boulevard to the C&O Canal National Historical Park.

Park in parking lot adjacent to Great Falls Tavern.

From the parking area upriver from the tavern, walk downstream along the towpath to the bridge leading across an incised rock channel to Olmsted Island.

Figure 21. Sample GF-73 was collected from a low outcrop alongside the Billy Goat trail downstream of the Old Anglers Inn. It is weathered and stands just proud of the fine-grained sediment covering the Bear Island surface in this locale. No age data were available at the time this guide was written.

Stop 9. Great Falls overlook, the Maryland view.

Along the path and under the bridges, note the series of bedrock channels separated by bedrock islands elongated in the direction of river flow. The channels are dry at low flow, allowing one to see a series of small knickpoints within the channels. At higher flows, water begins to fill these channels, isolating and eventually flooding the islands (fig. 22). The rock surfaces on these islands are water polished and rounded. Two samples from Olmsted Island give ages of 30 ka (GF-46, upstream of path) and 27 ka (GF-65, downstream of path).

The end of the trail is an overlook of Great Falls. This is the main channel of the Potomac River and carries most of the flow. The width and depth of the main channel suggest that the smaller, ephemeral channels are inactive except during the highest flows and will likely carry less flow over time as the main stem Potomac continues to incise and the falls retreat. It is interesting to note that these small channels (and their knick zones) occur at approximately the same point in the channel of the Potomac as the larger Great Falls. Maybe this spatial coincidence means that most of the erosion is done by flows so large that all islands are covered and the entire Great Falls area acts as one channel, instead of what we see today under lower flow conditions?

At Black Pond (the area we interpret as the paleo-Great Falls), the geometry is similar with isolated high points and incised channels but the abandoned channels are subaerially exposed. There, the main channel of the Potomac is on the Maryland side of the river and the channel-island complex is on the Virginia side (fig. 15).

Conclusions

Fieldwork along the Potomac River, in conjunction with many measurements of cosmogenic nuclides in samples collected from fluvially eroded surfaces, suggests that:

(1) The most distinct bedrock strath terrace bordering the Potomac River downstream of Great Falls is a time transgressive feature. Between Black Pond and Great Falls, this terrace surface, the Bear Island level, was first exposed about 38 ka, coincident with the onset of the latest Laurentide ice advance. Downstream of Black Pond, the same terrace surface is considerably older.

(2) Terrace formation and knick zone retreat appear to be episodic with long stillstands and rapid periods of retreat.

Figure 22. View looking upstream of one channel cutting Olmsted Island. Photograph was taken from Park Service walkway bridge at flow of 60,000 cubic feet per second (ft³/s). This channel is dry at low flow and was bank full at ~165,000 ft³/s.

Both field and cosmogenic data argue against steady knick zone retreat over time.

(3) Great Falls first formed between 25 and 30 ka as indicated by the exposure ages of several samples collected just above the knick zone.

(4) Two vertical transects of samples suggest that Mather Gorge was steadily incised at a rate between 0.5 and 0.8 m/1000 yr over much of the late Pleistocene.

References Cited

Alexander, H.S., 1932, Pothole erosion: Journal of Geology, v. 40, p. 305–337.

Anderson, R.S., Repka, J.L., and Dick, G.S., 1996, Explicit treatment of inheritance in dating depositional surfaces using in situ ^{10}Be and ^{26}Al: Geology, v. 24, no. 1, p. 47–51.

Bank, G.C., Spotila, J.A., and Reiners, P.W., 2001, Origin of an eastern North America great escarpment, based on (U-Th)/He dating and geomorphic analysis [abs.]: Eos, Transactions, American Geophysical Union, v. 82, no. 19, fall meeting supplement, 10–14 December 2001, Abstract T52C-0957. (Also available online at http://www.agu.org/meetings/waisfm01.html)

Bierman, P.R., 1994, Using in situ produced cosmogenic isotopes to estimate rates of landscape evolution; A review from the geomorphic perspective: Journal of Geophysical Research, B, Solid Earth and Planets, v. 99, no. 7, p. 13,885–13,896.

Bierman, Paul, and Gillespie, Alan, 1991, Range fires; A significant factor in exposure-age determination and geomorphic surface evolution: Geology, v. 19, no. 6, p. 641–644.

Bierman, P.R., and Caffee, M.W., 2001, Slow rates of rock surface erosion and sediment production across the Namib Desert and escarpment, Southern Africa: American Journal of Science, v. 301, no. 4–5, p. 326–358.

Bierman, P., and Nichols, K., 2004, Rock to sediment–Slope to sea with ^{10}Be; Rates of landscape change: Annual Review of Earth and Planetary Sciences, v. 32, p. 215–255.

Bierman, Paul, Larsen, Patrick, Clapp, Erik, and Clark, Douglas, 1996, Refining estimates of ^{10}Be and ^{26}Al production rates [abs.], in Gosse, J.C., Reedy, R.C., Harrington, C.D., and Poths, Jane, eds., Workshop on secular variations in production rates of cosmogenic nuclides on Earth: Radiocarbon, v. 38, no. 1, p. 149.

Bierman, P.R., Marsella, K.A., Patterson, C., Davis, P.T., and Caffee, M., 1999, Mid-Pleistocene cosmogenic minimum-age limits for pre-Wisconsinan glacial surfaces in southwestern Minnesota and southern Baffin Island; A multiple nuclide approach: Geomorphology, v. 27, no. 1-2, p. 25–39.

Bierman. P.R., Caffee, M.W., Davis, P.T., Marsella, Kim, Pavich, Milan, Colgan, Patrick, Mickelson, David, and Larsen, Jennifer, 2002, Rates and timing of earth surface processes from in-situ produced cosmogenic Be-10, in Grew, E.S., ed., Beryllium; Mineralogy, petrology and geochemistry: Reviews in Mineralogy and Geochemistry, v. 50, p. 147–205.

Bierman, P.R., Reusser, Lucus, Pavich, Milan, Zen, E-an, Finkel, Robert, Larsen, Jennifer, and Butler, E.M., 2002, Major, climate-correlative incision of the Potomac River gorge at Great Falls about 30,000 years ago [abs.]: Geological Society of America Abstracts with Programs, v. 34, p. 127.

Bloom, A.L., 1998, Geomorphology: A systematic analysis of Late Cenozoic landforms: Upper Saddle River, N.J., Prentice Hall, 510 p.

Burbank, D.W., Leland, J., Fielding, E., Anderson, R.S., Brozovic, N., Reid, M.R., and Duncan, C., 1996, Bedrock incision, rock uplift and threshold hillslopes in the northwestern Himalayas: Nature, v. 379, p. 505–510.

Colgan, P.M., Bierman, P.R., Mickelson, D.M., and Caffee, M.W., 2003, Variation in glacial erosion near the southern margin of the Laurentide Ice Sheet, south-central Wisconsin, USA; Implications for cosmogenic dating of glacial terrains: Geological Society of America Bulletin, v. 114, p. 1581–1591.

Cook, C.W., 1952, Sedimentary deposits of the Prince Georges County and the District of Columbia, in Cooke, C.W., Martin, R.O.R., and Meyer, G., Geology and water resources of Prince Georges County: Maryland Department of Geology, Mines, and Water Resources Bulletin 10, 270 p.

Cook, E.R., and Jacoby, G.C., 1983, Potomac River streamflow since 1730 as reconstructed by tree rings: Journal of Climate and Applied Meteorology, v. 22, p. 1659–1672.

Craig, H., and Poreda, R.J., 1986, Cosmogenic ^{3}He in terres-

trial rocks; The summit lavas of Maui: Proceedings of the National Academy of Science, v. 83, p. 1970–1974.

Davis, R., and Schaeffer, O.A., 1955, Chlorine-36 in nature: Annals of the New York Academy of Science, v. 62, p. 105–122.

Douglas, B.C., and Peltier, W.R., 2002, The puzzle of global sea-level rise: Physics Today, v. 55, p. 35–40.

Elmore, D., and Phillips, F., 1987, Accelerator mass spectrometry for measurement of long-lived radioisotopes: Science, v. 236, p. 543–550.

Fisher, G.W., 1970, The metamorphosed sedimentary rocks along the Potomac River near Washington, D.C., in Fisher, G.W., and others, eds., Studies in Appalachian geology; Central and southern: New York, Wiley-Interscience, p. 299–315.

Fleming, A.H., Drake. A.A., Jr., and McCartan, Lucy, 1994, Geologic map of the Washington West quadrangle, District of Columbia, Montgomery and Prince Georges Counties, Maryland, and Arlington and Fairfax Counties, Virginia: U.S. Geological Survey Geologic Quadrangle Map GQ–1748, scale 1:24,000.

Flint, R.F., 1940, Pleistocene features of the Atlantic Coastal Plain: American Journal of Science, v. 238, no. 11, p. 757–787.

Garrett, W.E., 1987, George Washington's Patowmack Canal: National Geographic Magazine, v. 171, no. 6, p. 716–753.

Gosse, J.C., and Phillips, F.M., 2001, Terrestrial in situ cosmogenic nuclides; Theory and application: Quaternary Science Reviews, v. 20, no. 14, p. 1475–1560.

Gregory, H.E., 1950, Geology and geography of the Zion Park region, Utah and Arizona: U.S. Geological Survey Professional Paper 220, 200 p.

Grover, N.C., 1937, The floods of March 1936, part 3, Potomac, James, and upper Ohio Rivers: U.S. Geological Survey Water Supply Paper 800, 351 p.

Hahn, T.F., 1992, Towpath guide to the C&O Canal: Freemansburg, Pennsylvania, American Canal and Transportation Center, 226 p.

Hancock, G.S., Anderson, R.S., and Whipple, K.X., 1998, Beyond power; Bedrock river incision process and form, in Tinkler, K.J., and Wohl, E.E., eds., Rivers over rock; Fluvial processes in bedrock channels: American Geophysical Union Geophysical Monograph 107, p. 35–60.

Hancock, G.S., Anderson, R.S., Chadwick, O.A., and Finkel, R.C., 1999, Dating fluvial terraces with [10]Be and [26]Al profiles; Application to the Wind River, Wyoming: Geomorphology, v. 27, no. 1–2, p. 41–60.

Hopson, C.A., 1964, The crystalline rocks of Howard and Montgomery Counties, in The geology of Howard and Montgomery Counties: Maryland Geological Survey, p. 27–336.

Howard, A.D., 1998, Long profile development of bedrock channels; Interaction of weathering, mass wasting, bed erosion, and sediment transport, in Tinkler, K.J., and Wohl, E.E., eds., Rivers over rock; Fluvial processes in bedrock channels: American Geophysical Union Geophysical Monograph 107, p. 297–319.

Hoyt, W.G., and Langbein, W.B., 1955, Floods: Princeton, N.J., Princeton University Press, 469 p.

Jahns, R.H., 1943, Sheeting structure in granites; Its origin and use as a measure of glacial erosion in New England: Journal of Geology, v. 51, p. 71–98.

Kurz, M.D., 1986, Cosmogenic helium in a terrestrial igneous rock: Nature, v. 320, no. 3, p. 435–439.

Kurz, M.D., and Brooke, E.J., 1994, Surface exposure dating with cosmogenic nuclides, in Beck, C., ed., Dating in exposed and surface contexts: Albuquerque, N.M., University of New Mexico Press, p. 139–159.

Lal, D., 1991, Cosmic ray labeling of erosion surfaces; In situ nuclide production rates and erosion models: Earth and Planetary Science Letters, v. 104, no. 2-4, p. 424–439.

Lal, D., and Peters, B., 1967, Cosmic ray produced radioactivity on the earth, in Sitte, K., ed., Handbuch der Physik: New York, Springer-Verlag, p. 551–612.

Lawrey, J.D., and Hale, Mason E., Jr., 1977, Natural history of Plummers Island, Maryland, XXIII. Studies on lichen growth rate at Plummers Island, Maryland: Biological Society of Washington, Proceedings, v. 90, no. 3, p. 698–725.

Lee, Jennifer, 1993, Bankfull discharge estimates for reconstructed paleochannels of a Potomac River meander at Great Falls, Virginia: College Park, University of Maryland, unpub. Senior thesis, 30 p.

Leland, J., Reid, M.R., Burbank, D.W., Finkel, R., and Caffee, M., 1998, Incision and differential bedrock uplift along the Indus River near Nanga Parbat, Pakistan Himalaya, from [10]Be and [26]Al exposure age dating of bedrock straths: Earth and Planetary Science Letters, v. 154, no. 1–4, p. 93–107.

Leopold, L.B., Wolman, M.G., and Miller, J.P., 1964, Fluvial processes in geomorphology: San Francisco, W.H. Freeman and Co., 522 p.

Matmon, Ari, Bierman, Paul, and Enzel, Yehouda, 2002, Pattern and tempo of great escarpment erosion: Geology, v. 30, no. 12, p. 1135–1138.

Milton, N.M., 1989, Geomorphology, vegetation, and Patowmack Canal construction problems, Great Falls Park, Potomac River, Virginia: Field Trip Guidebook T236 for the 28th International Geological Congress: Washington, D.C., American Geophysical Union, 8 p.

Muth, K.G., Arth, J.G., and Reed, J.C., Jr., 1979, A minimum age for high-grade metamorphism and granite intrusion in

the Piedmont of the Potomac River gorge near Washington, D.C.: Geology, v. 7, no. 7, p. 349–350.

Naeser, C.W., Naeser, N.D., Kunk, M.J., Morgan, B.A., III, Schultz, A.P., Southworth, C.S., and Weems, R.E., 2001, Paleozoic through Cenozoic uplift, erosion, stream capture, and depositional history in the Valley and Ridge, Blue Ridge, Piedmont and Coastal Plain provinces of Tennessee, North Carolina, Virginia, Maryland and District of Columbia [abs.]: Geological Society of America Abstracts with Programs, v. 33, no. 6, p. A312.

National Park Service, 1991, Chesapeake and Ohio Canal: National Park Service Handbook 142, 111 p.

Nickelsen, R.P., 1956, Geology of the Blue Ridge near Harpers Ferry, West Virginia: Geological Society of America Bulletin, v. 67, p. 239–270.

Nishiizumi, K., Lal, D., Klein, J., Middleton, R., and Arnold, J.R., 1986, Production of ^{10}Be and ^{26}Al by cosmic rays in terrestrial quartz in situ and implications for erosion rates: Nature, v. 319, no. 6049, p. 134–136.

Pavich, M.J., Brown, Louis, Valette-Silver, J.N., Klein, Jeffrey, and Middleton, Roy, 1985, ^{10}Be analysis of a Quaternary weathering profile in the Virginia Piedmont: Geology, v. 13, no. 1, p. 39–41.

Pazzaglia, F.P., 1993, Stratigraphy, petrography and correlation of late Cenozoic middle Atlantic Coastal Plain deposits; Implications for late stage passive margin geologic evolution: Geological Society of America Bulletin, v. 105, p. 1617–1634.

Phillips, F.M., Leavy, B.D., Jannik, N.O., Elmore, D., and Kubik, P.W., 1986, The accumulation of cosmogenic chlorine-36 in rocks; A method for surface exposure dating: Science, v. 231, no. 4733, p. 41–43.

Pratt, Beth, Burbank, D.W., Heimsath, A.M., and Ojha, Tank, 2002, Impulsive alluviation during early Holocene strengthened monsoons, central Nepal Himalaya: Geology, v. 30, no. 10, p. 911–914.

Putzer, Hannfrit, 1971, Kolke im Cabora-Bassa-Canyon des mittleren Sambesi: Zeitschrift fur Geomorphologie, bd. 15, hft. 3, p. 330–338.

Reed, J.C., Jr., 1981, Disequilibrium profile of the Potomac River near Washington, D.C.—A result of lowered base level or Quaternary tectonics along the Fall Line?: Geology, v. 9, no. 10, p. 445–450.

Reed, J.C., Jr., Marvin, R.F., and Mangum, J.H., 1970, K-Ar ages of lamprophyre dikes near Great Falls, Maryland-Virginia: U.S. Geological Survey Professional Paper 700-C, p. 145–149.

Reed, J.C., Jr., Sigafoos, R.S., and Fisher, G.W., 1980, The river and the rocks: U.S. Geological Survey Bulletin 1471, 75 p.

Repka, J.L., Anderson, R.S., and Finkel, R.C., 1997,

Cosmogenic dating of fluvial terraces, Fremont River, Utah: Earth and Planetary Science Letters, v. 152, no. 1–4, p. 59–73.

Reusser, L., Bierman, P.R., Pavich, M., Butler, E., Larsen, J., and Finkel, R., 2003, Late Pleistocene bedrock channel incision of the lower Susquehanna River; Holtwood Gorge, Pennsylvania, in Merritts, D., Walter, R., and de Wet, A., eds., Channeling through time; Landscape evolution, land use change, and stream restoration in the lower Susquehanna Basin: Southeastern Friends of the Pleistocene guidebook (2003), p. 41–45.

Schildgen, T., Dethier, D., Bierman, P.R., and Caffee, M., 2002, ^{26}Al and ^{10}Be dating of late Pleistocene fill terraces; A record of glacial and non-glacial fluvial deposition and incision, Colorado Front Ranges and Landforms: Earth Surface Processes and Landforms, v. 27, p. 773–787.

Seidl, M.A., and Dietrich, W.E., 1992, The problem of channel erosion into bedrock, in Schmidt, K.H., and de Ploey, J., eds., Functional Geomorphology: Catena Supplement 23, p. 101–124.

Seidl, M.A., Finkel, R.C., Caffee, M.W., Hudson, G.B., and Dietrich, W.E., 1997, Cosmogenic isotope analyses applied to river longitudinal profile evolution; Problems and interpretations: Earth Surface Processes and Landforms, v. 22, no. 3, p. 195–209.

Southworth, Scott, and Brezinski, D.K., 1996, Geology of the Harpers Ferry quadrangle, Virginia, Maryland, and West Virginia: U.S. Geological Survey Bulletin 2123, 33 p., 1:24,000-scale plate.

Southworth, S., Fingeret, C., and Weik, T., comps., 2000, Geologic map of the Potomac River gorge; Great Falls Park, Virginia, and part of the C&O Canal National Historical Park, Maryland: U.S. Geological Survey Open-File Report 00–264.

Southworth, C.S., Brezinski, D.K., Orndorff, R.C., Chirico, P.G., and Legueux, K.M., 2001, Geology of the Chesapeake and Ohio Canal National Historical Park and Potomac River corridor, District of Columbia, Maryland, West Virginia, and Virginia: U.S. Geological Survey Open-File Report 01–188, 2 CD-ROMS.

Stone, J., 2000, Air pressure and cosmogenic isotope production: Journal of Geophysical Research, v. 105, no. b10, p. 23,753–23,759.

Tinkler, K.J., and Wohl, E.E., 1998a, A primer on bedrock channels, in Tinkler, K.J., and Wohl, E.E., eds., Rivers over rock; Fluvial processes in bedrock channels: American Geophysical Union Geophysical Monograph 107, p. 1–18.

Tinkler, K.J., and Wohl, E.E., 1998b, Field studies of bedrock channels, in Tinkler, K.J., and Wohl, E.E., eds., Rivers over rock; Fluvial processes in bedrock channels: American Geophysical Union Geophysical Monograph 107, p. 261–278.

Tormey, B.B., 1980, Geomorphology of the falls stretch of the Potomac River: State College, The Pennsylvania State University, D.Ed. thesis, 287 p.

Vivian, Robert, 1970, Hydrologie et erosion sous-glaciaires: Revue de géographie alpine, v. 58, p. 241–264.

Wentworth, C.K., 1924, Note on a cobble of peculiar shape: Journal of Geology, v. 32, p. 524–528.

Williams, G.P., 1983, Paleohydrological methods and some examples from Swedish fluvial environments. I. Cobble and boulder deposits: Geografiska Annaler, v. 65A, p. 227–243.

Zawada, P.K., 1997, Palaeoflood hydrology; Method and application in flood-prone southern Africa: South African Journal of Science, v. 93, p. 111–132.

Zen, E-an, 1997a, The seven-storey river; Geomorphology of the Potomac River channel between Blockhouse Point,

Maryland, and Georgetown, District of Columbia, with emphasis on the gorge complex below Great Falls: U.S. Geological Survey Open-File Report 97–60, 142 p.

Zen, E-an, 1997b, Channel geometry and strath levels of the Potomac River between Great Falls, Maryland and Hampshire, West Virginia: U.S. Geological Survey Open-File Report 97–480, 92 p.

Zen, E-an, and Prestegaard, K.L., 1994, Possible hydraulic significance of two kinds of potholes; Examples from the paleo-Potomac River: Geology, v. 22, no. 1, p. 47–50.

Zreda, M., and Phillips, F., 1998, Quaternary dating by cosmogenic nuclide buildup in surficial materials, *in* Sowers, J.M., Noller, J.S., and Lettis, W.R., eds., Dating and earthquakes; Review of Quaternary geochronology and its application to paleoseismology: U.S. Nuclear Regulatory Commission, p. 2-101–2-127.

7. The Goochland-Chopawamsic Terrane Boundary, Central Virginia Piedmont

By David B. Spears,[1] Brent E. Owens,[2] and Christopher M. Bailey[2]

Introduction

The southern Appalachian hinterland is composed of a number of terranes with distinctly different geologic histories. Some terranes, such as the central and northern Virginia Blue Ridge, are clearly of North American or Laurentian affinity (Rankin and others, 1989; Horton and others, 1989). Others, such as the Carolina slate belt, are demonstrably exotic with respect to Laurentia (Secor and others, 1983; Hibbard and others, 2002). Still others, such as the Goochland and Chopawamsic terranes, are, because of a lack of definitive evidence, of uncertain affinity and considered to be "suspect" with respect to Laurentia. While it is generally understood that these exotic and suspect terranes were accreted to the Laurentian margin during Paleozoic orogenesis, major unresolved questions remain, including (1) the origin and affinity of such terranes, (2) the timing of their accretion, and (3) the kinematics of deformation along terrane boundaries.

In central Virginia, at the northern end of the southern Appalachians, exposed terranes include, from west to east, the Blue Ridge, the Western Piedmont, the Chopawamsic, the Goochland, and the Southeastern Piedmont (fig. 1). They are separated from each other by major fault systems along which multiple generations of motion are recognized. The present state of these boundaries holds clues to the past relations of the adjacent terranes. Understanding the affinity of these terranes and the kinematics and timing of their juxtaposition is a prerequisite for accurately describing the tectonic history of the Virginia Piedmont.

The Goochland and Chopawamsic terranes have markedly different geologic histories (fig. 2). The Goochland terrane, in the eastern Piedmont, has been described as a Middle to Late Proterozoic basement massif with relict granulite-facies mineral assemblages (Glover and others, 1982; Farrar, 1984; Farrar and Owens, 2001). The Chopawamsic terrane, in the central Piedmont, is an Ordovician volcanic-plutonic arc complex (Pavlides, 1981; Coler and others, 2000). The

boundary between the Goochland and Chopawamsic terranes coincides with a pronounced northeast-trending aeromagnetic and aeroradiometric feature known as the Spotsylvania lineament. Neuschel (1970) first recognized this geophysical boundary before mapping, geochronology, and tectonic models provided an adequate framework for understanding its significance. Later workers described this discontinuity as a brittle thrust fault (Pavlides and others, 1980a), a mylonite zone (Farrar, 1984; Brown, 1986), and a "major suture" (Marr, 1991). Recent workers have named this zone the Spotsylvania high-strain zone (Spears and Bailey, 2002; Bailey and others, in press).

The purpose of this field trip is to focus on new research within and along the boundary between the Goochland and Chopawamsic terranes in central Virginia. We present new evidence describing the kinematics of deformation in the Spotsylvania high-strain zone with indications of large-scale relative displacement between the terranes. Surprising new geochronology in the Goochland terrane challenges long-standing assumptions about its history. We also examine two enigmatic fault slices and a suite of unusual mafic to ultra-mafic igneous rocks and speculate as to their origin. This work provides new insights into the spatial and temporal relation of the terranes, with implications for the tectonic assembly of the Piedmont.

Geology

Goochland Terrane

The Goochland terrane is composed of multiply deformed and metamorphosed gneiss, amphibolite, granite, and anorthosite (fig. 2). The oldest and structurally lowest unit in the Goochland terrane is the State Farm Gneiss (Brown, 1937), a coarse-grained granitic gneiss that crops out in a series of domes (fig. 3) that are overlain by the Sabot Amphibolite and the heterogeneous Maidens Gneiss (Poland, 1976). Both the Sabot and the Maidens are intruded by the Montpelier Anorthosite (Aleinikoff and others, 1996). U-Pb zircon analyses of the State Farm Gneiss and Montpelier
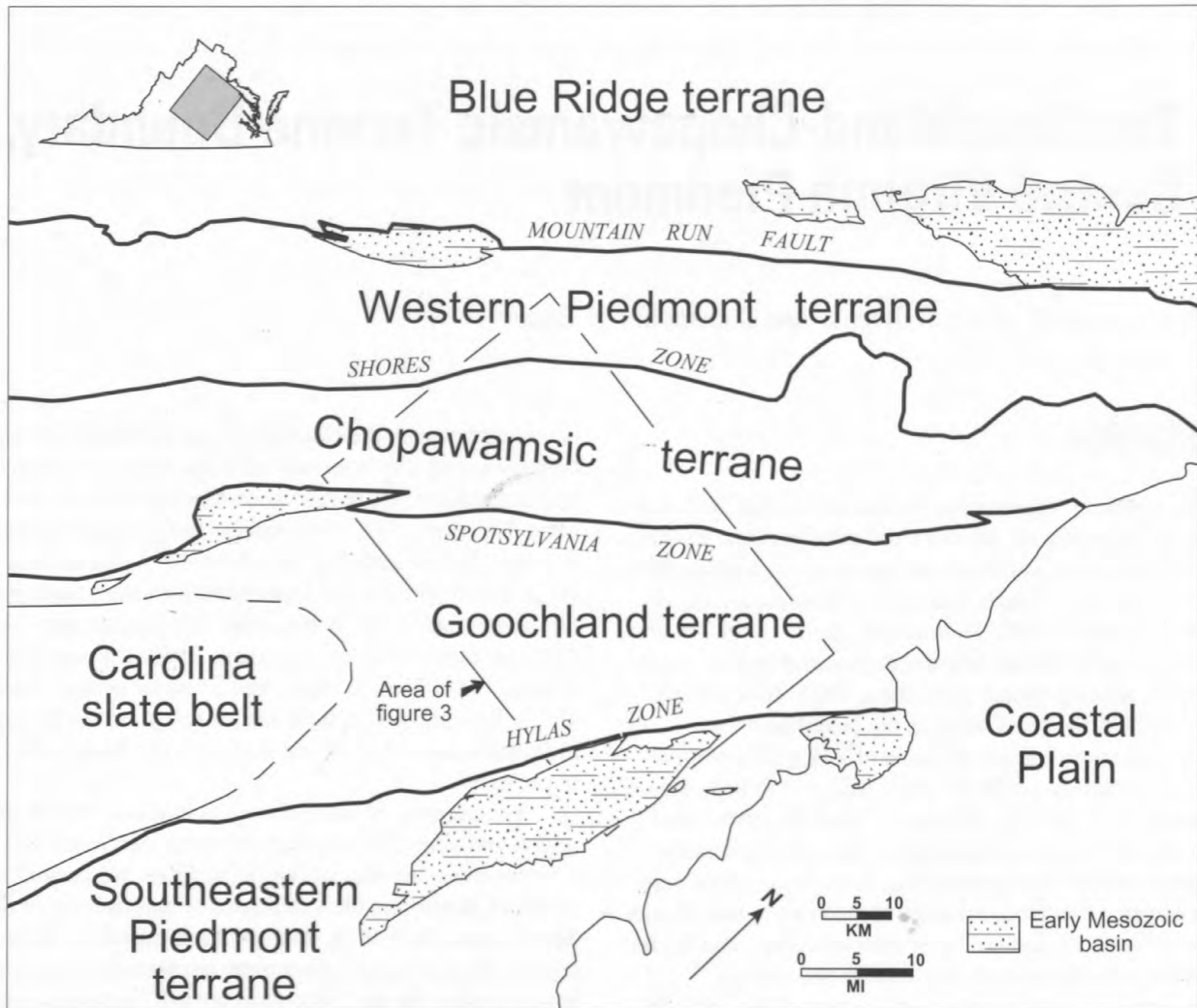
Figure 1. Map showing geologic terranes and their boundaries in central Virginia.

Anorthosite yield Mesoproterozoic ages of 1,050 to 1,020 Ma (Aleinikoff and others, 1996; Owens and Tucker, 1999). A suite of small A-type granitoid plutons with U-Pb zircon ages of ~630 Ma intrudes the State Farm Gneiss (Owens and Tucker, 2000). The Maidens, the most extensive map unit in the Goochland terrane, is dominantly pelitic (biotite-garnet and muscovite-sillimanite gneiss) with some granitic gneiss.

Rocks of the Goochland terrane experienced an early granulite-facies metamorphic event that was overprinted by a later amphibolite-facies event (Farrar, 1984; Farrar and Owens, 2001). Farrar (1984) interprets the early granulite-facies metamorphism as Mesoproterozoic and the amphibolite-facies event as Alleghanian (~300–250 Ma). The origin of the Goochland terrane is unclear; the Mesoproterozoic rocks and A-type Neoproterozoic granitoids are similar to Laurentian basement in the Blue Ridge (Glover and others, 1978; Farrar, 1984; Glover and others, 1989; Aleinikoff and others, 1996). New Nd-isotopic results reported by Owens

and Samson (2001, in press) for the State Farm Gneiss and Montpelier Anorthosite show that these units are isotopically similar to other blocks of Mesoproterozoic crust along the eastern and southern margins of Laurentia (for example, Adirondacks, Blue Ridge, Llano uplift); however, other workers have suggested that the Goochland terrane may be of peri-Gondwanan affinity (Rankin and others, 1989; Hibbard and Samson, 1995).

Previously, the entire Goochland terrane was considered to be a coherent block of Mesoproterozoic crust. Mesoproterozoic crystallization ages based on modern U-Pb zircon methods have been confirmed for both the Montpelier Anorthosite (1,045±10 Ma; Aleinikoff and others, 1996) and the State Farm Gneiss (~1,046–1,023 Ma; Owens and Tucker, 2003). In addition, Horton and others (1995) reported a U-Pb zircon age of 1,035±5 Ma for a granitic gneiss within the Maidens Gneiss near Amelia Courthouse, possibly indicating that the Maidens is also Mesoproterozoic. However, new results based on electron

microprobe dating of monazite in more typical Maidens lithologies (metapelites, and so forth) have thus far revealed no ages older than about 420 Ma (R.J. Tracy, B.E. Owens, and C.R. Shirvell, unpub. data). If these monazite ages reflect the timing of granulite-facies metamorphism (a plausible interpretation), the long-held assumption that the high-grade event was Grenvillian is clearly incorrect (see Burton and Armstrong, 1997). Furthermore, new U-Pb zircon results for a probable metaigneous variety of Maidens Gneiss (Stop 3) indicate a Paleozoic age, suggesting that at least some portions of the Maidens Gneiss are younger than Mesoproterozoic. An interesting additional point in this regard is that Neoproterozoic granitoids have thus far not been recognized within the Maidens Gneiss; in other words, they appear to be restricted to the State Farm Gneiss (Owens and Tucker, 2003). These points suggest the possibility of a previously unrecognized unconformity or structural discontinuity between at least the western part of the Maidens Gneiss and the more easterly (State Farm, Sabot, and Montpelier) portion of the Goochland terrane.

Chopawamsic Terrane

The Chopawamsic terrane is composed of metamorphosed volcanic and sedimentary rocks with a suite of associated granitoid plutons, all of Middle to Late Ordovician age (fig. 2). The most widespread unit is the Chopawamsic Formation, a suite of mafic and felsic metavolcanic rocks dated at ~470 Ma (Horton and others, 1998; Coler and others, 2000). In central Virginia, the Chopawamsic is intruded by the Columbia pluton (fig. 3), a granite to granodiorite body that yielded a U-Pb SIMS (secondary ion mass spectrometry) zircon age of 457±7 Ma (Wilson, 2001). In the western part of the Chopawamsic terrane, both the Chopawamsic Formation and the Columbia pluton are unconformably overlain by the Arvonia Formation (figs. 2, 3), a metasedimentary package that contains Late Ordovician fossils (Darton, 1892; Watson and Powell, 1911; Tillman, 1970). The northeastern part of the terrane contains a similar metasedimentary unit, the Quantico Formation, which may be partly interlayered with the Chopawamsic Formation. Late Ordovician fossils also are present in the Quantico Formation (Pavlides and others, 1980b).

Rocks of the Chopawamsic terrane preserve evidence of one regional metamorphic event. Metamorphic mineral assemblages indicate that greenschist-facies conditions were reached along the northwest side of the terrane; these grade into amphibolite-facies assemblages in the southeast part of the terrane. Metamorphic hornblende from the Chopawamsic Formation dated by $^{40}Ar/^{39}Ar$ methods yielded ages of 318 to ~284 Ma (Burton and others, 2000). The Chopawamsic terrane is interpreted to be an Ordovician volcanic arc complex developed on continental crust outboard of Laurentia (Coler and others, 2000) and later accreted during the Late Ordovician Taconic orogeny (Glover and others, 1989).
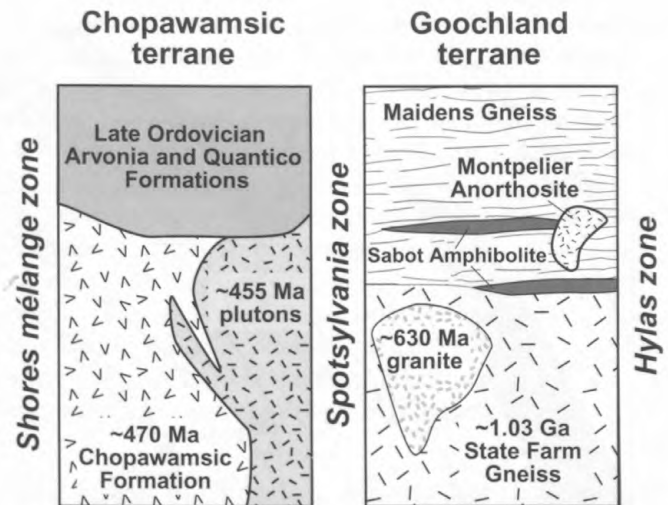
Figure 2. Generalized stratigraphy of the Chopawamsic and Goochland terranes.

Spotsylvania High-Strain Zone

The Spotsylvania high-strain zone (SHSZ) forms the boundary between the early Paleozoic Chopawamsic terrane and the Mesoproterozoic-Paleozoic(?) Goochland terrane in the central Virginia Piedmont (fig. 3). This boundary was originally recognized as a sharp geophysical (aeromagnetic and aeroradiometric) lineament (Neuschel, 1970) and interpreted as a brittle fault. In the Piedmont of southern Virginia, the SHSZ appears to connect with the Hyco shear zone, a component of the Alleghanian-age central Piedmont shear zone, a major boundary traceable for over 500 km (kilometers; 300 mi (miles)) in the southern Appalachians (Hibbard and others, 1998; Wortman and others, 1998). Hibbard and others (1998) interpreted the Hyco zone in southern Virginia to be a ductile thrust that emplaced the Carolina terrane over the Chopawamsic terrane. Farrar (1984), Pratt and others (1988), and Glover and others (1989) interpreted the Spotsylvania zone as a significant thrust fault (not a suture) along which granulite/amphibolite-facies rocks of the Goochland belt were emplaced to the northwest in the late Paleozoic. In north-central Virginia, Pavlides and others (1980a) interpreted the Spotsylvania zone to be a 2- to 3-km (1–2 mi)-wide zone of predominantly brittle en-echelon faults. In central Virginia, Marr (1991) reported the presence of a tectonic mélange zone within the SHSZ and suggested it may represent a suture. Bourland (1976) and Spears and Bailey (2002) recognized brittle fault rocks in the SHSZ and interpreted these to have formed during Mesozoic reactivation of the Paleozoic high-strain zone. The Spotsylvania zone is located within the central Virginia seismic zone (Bollinger and others, 1986; Çoruh and others, 1988) and as recently as 2003, small earthquakes have occurred at depth along this structure.

We define the SHSZ as a ~15-km (~9-mi)-wide belt of heterogeneously deformed mylonitic rocks that typically lacks

Chopawamsic terrane

Oa	Arvonia Formation
Ocg	Columbia pluton
Ocv	Chopawamsic Formation

Pegmatite belt

| mpx | Metapyroxenite |
| pg | Pegmatite and granitic gneiss |

Elk Hill Complex

| eh | Elk Hill Complex, undivided |
| dg | Diorite gneiss |

Goochland terrane

PzYm	Maidens Gneiss
Zgr	A-type granites
Yma	Montpelier Anorthosite
Ysa	Sabot Amphibolite
Ysf	State Farm Gneiss

Southeastern Piedmont terrane

| Tr | Early Mesozoic basin |
| Mpg | Petersburg Granite |

Legend:
- 9 ● Field trip stop
- Mylonitic rocks in high-strain zone
- ↔ Doubly plunging antiform
- ⊢ Plunging synform

N

0 ———— 9 km
0 ———— 9 mi

Figure 3. Generalized geologic map of the central Virginia Piedmont showing locations of field trip stops.

distinct boundaries (fig. 3). Its northwestern boundary is defined by the geophysical lineament at the contact between amphibole-rich gneisses of the Elk Hill Complex to the northwest and m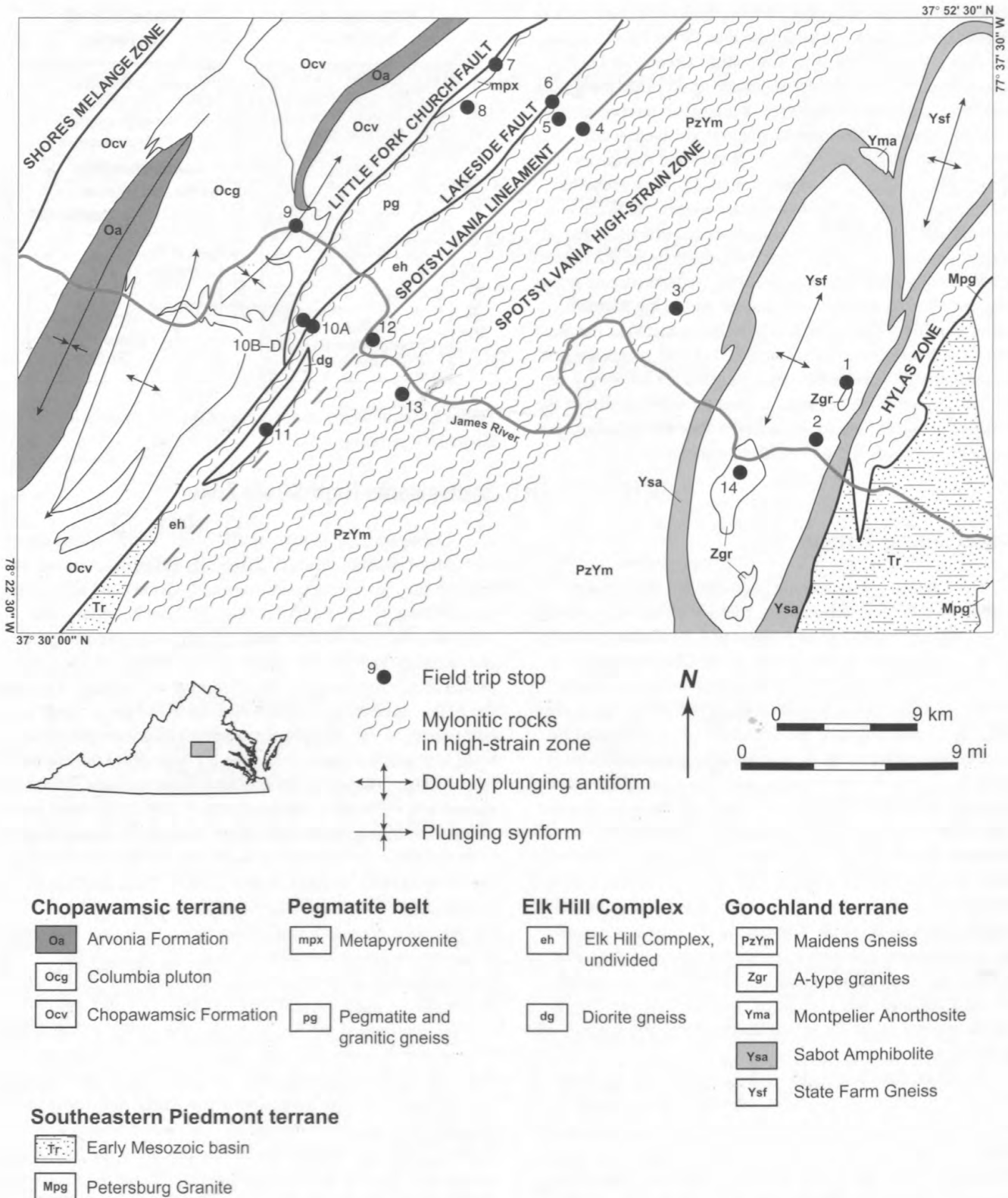ylonitic rocks derived from more granitic to pelitic protoliths to the southeast. Gneissic rocks to the southeast of the Spotsylvania lineament are strongly deformed well into the Goochland terrane. Mylonitic biotite schist, granitic mylonite, biotite-rich ultramylonite, amphibolite, and protomylonitic pegmatite are the most common rock types in the SHSZ. Foliation in the SHSZ strikes to the northeast and generally dips moderately to gently to the southeast. At some locations, where SHSZ is located in the hanging wall of listric Mesozoic normal faults, dips of mylonitic foliations flattened out due to horizontal axis rotations associated with normal faulting. Lineations (both elongation and mineral) plunge shallowly to the northeast and southwest in the plane of the foliation. Asymmetric porphyroclast tails and boudins from surfaces normal to foliation and parallel to lineation consistently exhibit a strike-parallel dextral asymmetry across the SHSZ. Pegmatite dikes are commonly folded and boudinaged in a geometry consistent with bulk constrictional strain ($K > 1$) (Bailey and others, in press). Folded dikes are asymmetric; the folds generally verge to the northwest. The geometry of asymmetric structures, both parallel and normal to the elongation lineation, is consistent with a modest triclinic deformation symmetry (Bailey and others, in press).

Minimum sectional strains, estimated from boudinaged and folded dikes on lineation-parallel surfaces, range from 8:1 to >20:1. Feldspar porphyroclasts, pegmatitic boudins, and amphibolite boudins are superficially similar to clasts or blocks in a mélange, but exhibit consistent dextral asymmetries and at many locations occur as tabular bodies with a pinch-and-swell character (Stops 3, 4, 8). Backward-rotated porphyroclasts are common in SHSZ ultramylonites and vorticity analysis yields W_n-values between 0.8 and 0.4, indicating general shear deformation that significantly deviated from simple shear (Bailey and others, in press).

Quartz grains in mylonitic rocks from the SHSZ are completely recrystallized, straight extinction is common, and strong crystallographic preferred orientations are well developed. Feldspar porphyroclasts display core and mantle structures and strong undulose extinction. In mylonites and ultramylonites, myrmekite and flame perthite are localized along high-strain grain boundaries. Synkinematic metamorphic minerals include biotite, garnet, epidote, and staurolite. Microstructures preserved in mylonitic rocks from the SHSZ are consistent with deformation conditions in the upper greenschist to lower amphibolite facies (450–500°C).

In order to better constrain the kinematics and tectonic significance of the SHSZ, Bailey and others (in press) used estimated values for vorticity and three-dimensional strain to restore the Goochland terrane to its paleogeographic position prior to dextral transpression. Deformation in the SHSZ produced significant thinning (~40–70 percent) normal to the zone and up to 500 percent stretching parallel to the zone

boundaries. With the Chopawamsic terrane fixed in position, the Goochland terrane is retrodeformed to a predeformation position 80 to 300 km (50–186 mi) northeast of its present location. These displacement estimates are minimum values because strains were calculated from boudinaged and folded dikes that are, in themselves, minimum strain indicators. Furthermore, the Brookneal/Shores high-strain zone and the Mountain Run fault zone, more westerly structural discontinuities in the Virginia Piedmont (fig. 1), also exhibit dextral motion (Gates and others, 1986; Bobyarchick, 1999). Thus, the Goochland terrane, relative to the more western elements in the Virginia Piedmont, experienced significant southwestern translation during the Alleghanian orogeny.

Fault Slices of Uncertain Affinity Associated with the Terrane Boundary

Two narrow belts of rocks originally described by Taber (1913) are now recognized to be fault-bounded blocks of unknown affinity (Spears and Bailey, 2002). Although well documented by Taber (1913) and Brown (1937), the pegmatite belt and Elk Hill Complex were excluded from map compilations in the second half of the twentieth century (for example, Virginia Division of Mineral Resources, 1993). We find that both blocks exist as mappable fault-bounded units spatially associated with the terrane boundary. No published geochronology exists for any of the rocks in these two fault blocks. Comparison of these rocks to the Goochland and Chopawamsic terranes does not yield obvious correlations to units in either of the adjacent terranes.

Pegmatite Belt

Taber (1913) used the term "pegmatite belt" to describe an area underlain by pegmatite and granite in western Goochland and northern Cumberland Counties. Some later workers (Jonas, 1932; Brown, 1937) honored Taber's nomenclature and included a similar area of pegmatite on their geologic maps. However, the 1963 geologic map of Virginia (Virginia Division of Mineral Resources, 1963) depicts this area as an extension of the Columbia granite. Farrar (1984) recognized pegmatite in this area and interpreted it to be associated with the intrusion of the Columbia pluton. However, on the 1993 geologic map of Virginia (Virginia Division of Mineral Resources, 1993), this area was mapped as biotite gneiss with small intrusions of biotite granite, all within the Chopawamsic terrane.

We find that these rocks are lithologically distinct and separated by faults from the Chopawamsic Formation and the Elk Hill Complex (fig. 3). The recently described Little Fork Church fault, mappable by a lithologic discontinuity coincident with both ductile and brittle fault rocks (Spears and Bailey, 2002) forms the western boundary of the pegmatite belt (fig. 3). The eastern boundary is defined by the Lakeside
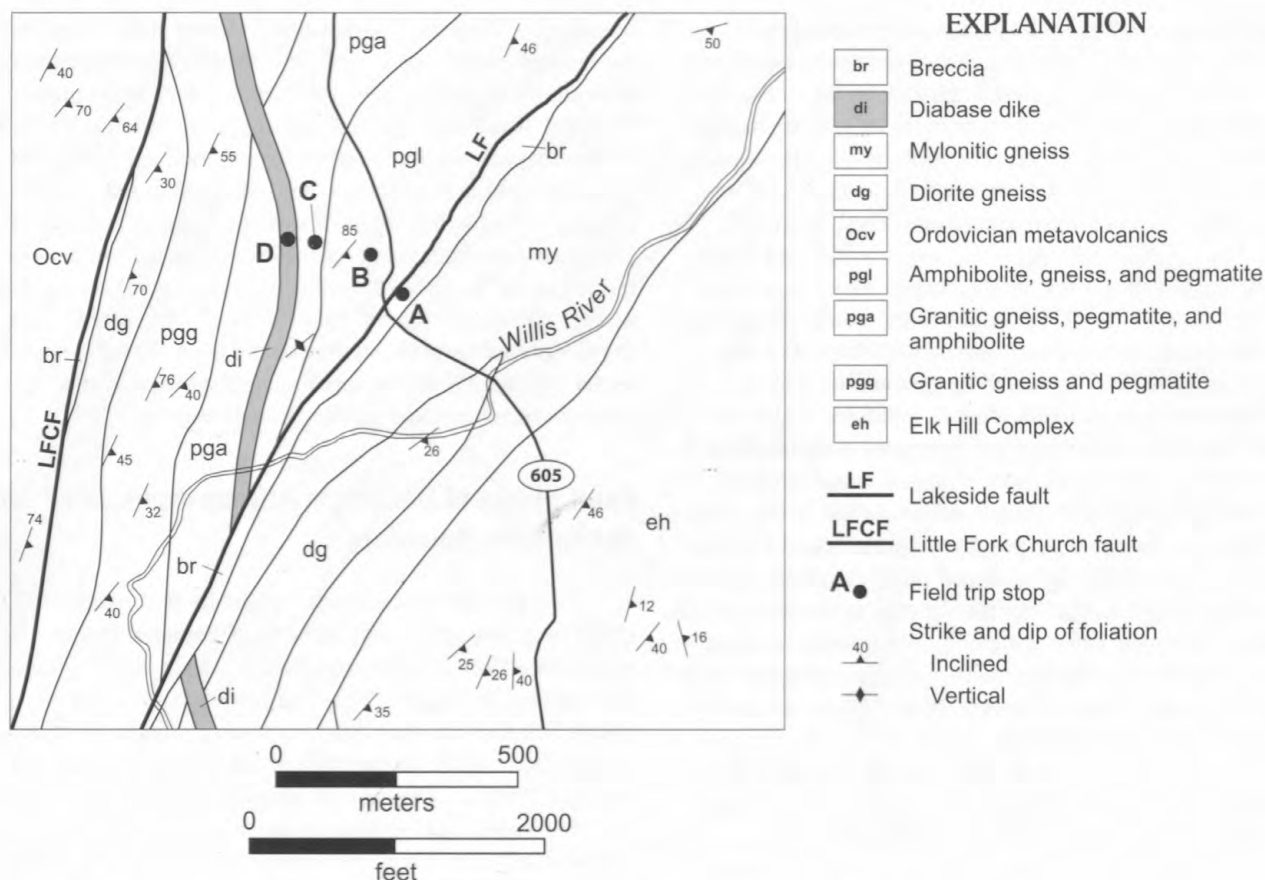
EXPLANATION

br	Breccia
di	Diabase dike
my	Mylonitic gneiss
dg	Diorite gneiss
Ocv	Ordovician metavolcanics
pgl	Amphibolite, gneiss, and pegmatite
pga	Granitic gneiss, pegmatite, and amphibolite
pgg	Granitic gneiss and pegmatite
eh	Elk Hill Complex

LF ——— Lakeside fault

LFCF ——— Little Fork Church fault

A● Field trip stop

Strike and dip of foliation

40 ⊥ Inclined

✦ Vertical

Figure 4. Bedrock geologic map of the area around Stops 10A–D, Cumberland County, Va.

fault, which separates the pegmatite belt from the Elk Hill Complex (Stops 6, 10) (fig. 3). The belt can be separated into three distinct lithologic packages from west (structurally lowest) to east (structurally highest). The structurally lowest unit (pgg) is composed of light-gray, fine-grained, weakly layered micaceous granitic gneiss with abundant white to pink potassium feldspar-quartz-muscovite pegmatite (Stop 8; fig. 4). The pegmatite is concordant with the foliation in the surrounding gneiss and is commonly deformed into lens-shaped domains containing potassium feldspar porphyroclasts in a fine-grained matrix of muscovite, quartz, and microcline. Large feldspars are commonly kaolinized and display throughgoing brittle fractures. The middle unit (pga, fig. 4) is composed of weakly layered granitic gneiss similar to the lower unit, with less pegmatite, and generally concordant bodies of fine-grained amphibolite that are commonly deformed into boudins (Stop 10C). The upper unit (pgl) is strongly compositionally layered amphibolite, biotite gneiss, and minor pegmatite (Stop 10B, fig. 4).

Elk Hill Complex

The Elk Hill Complex was named by Taber (1913) for exposures in cuts along the railroad southeast of Elk Hill plan-

tation in western Goochland County. At its type locality, the Elk Hill is dominated by strongly compositionally layered hornblende gneiss with lesser amounts of biotite gneiss and pegmatite. We find that, in addition to these lithologies, the Elk Hill contains gneissic diorite, talc-chlorite soapstone, and, especially south of the James River, distinctive phenocrystic felsic rocks resembling pinkish, fine-grained granite in outcrop.

Brown (1937) recognized the Elk Hill Complex on his geologic map of Goochland County, but the name was excluded from the literature for the rest of the 20th century. A hornblende gneiss unit was indicated in this area on the 1963 geologic map of Virginia (Virginia Division of Mineral Resources, 1963); however, on the 1993 geologic map of Virginia (Virginia Division of Mineral Resources, 1993), rocks in this area were mapped as "biotite gneiss" contiguous with the Central Virginia volcanic-plutonic belt, which at that time was a synonym for the Chopawamsic terrane.

Our work demonstrates that the Elk Hill Complex is distinct and separated by faults from both the Chopawamsic and the Goochland terranes. The Lakeside fault, previously mapped from the early Mesozoic Farmville basin northeastward to a point just south of the James River (Virginia Division of Mineral Resources, 1993), in fact extends farther northeastward across the James River and across western Goochland County at least as far north as I-64. This fault sep-

arates the Elk Hill Complex from the pegmatite belt and the Chopawamsic Formation throughout the area mapped. The eastern boundary of the Elk Hill is marked by the strongly mylonitic rocks of the Spotsylvania high-strain zone.

Although the Elk Hill Complex and the Chopawamsic Formation are superficially similar in that they are both dominated by mafic metavolcanic rocks, we note certain dissimilarities. The Elk Hill includes, particularly south of the James River, distinctive fine-grained felsic metavolcanic rocks interlayered with amphibolite. The felsic rocks contain concentrically zoned plagioclase phenocrysts, presumably of primary volcanic origin; such phenocrysts are not observed in the Chopawamsic Formation at this latitude. Geophysically, the Chopawamsic Formation is characterized by a high-amplitude, short-wavelength pattern on total intensity aeromagnetic maps; the pattern over the Elk Hill Complex is lower amplitude and longer wavelength. Furthermore, the Chopawamsic Formation contains substantial deposits of precious metals and massive sulfides. These well-known deposits were heavily exploited beginning in the early 19th century, to the point that a well-defined band of rocks now recognized as the Chopawamsic terrane was known as the "gold-pyrite belt" (Lonsdale, 1927; Spears and Upchurch, 1997). Despite intense prospecting by gold seekers, adjacent parts of the Piedmont remained largely unproductive. The Elk Hill (as well as the pegmatite belt and the Goochland terrane) is apparently barren of metallic mineralization, as demonstrated by the total absence of known mines.

These dissimilarities raise suspicions that the Elk Hill Complex and the Chopawamsic Formation, while both ostensibly of volcanic origin, may be of different ages and affinities. Additional work is needed to fully characterize the differences between these two blocks, and to establish the possible relation of the Elk Hill to other metavolcanic units in the Piedmont.

Conclusions

The Goochland and Chopawamsic terranes have markedly different histories that indicate that they developed independently and were not juxtaposed until post-Late Ordovician. Unpublished monazite ages in the Goochland terrane, referred to above, raise the intriguing possibility that they were separate until even later, post ~420 Ma (Silurian), and that the granulite-facies metamorphic event may be middle Paleozoic. While the basement rocks of the Goochland terrane, including the State Farm Gneiss, superficially resemble Laurentian rocks of the Virginia Blue Ridge, our work on the kinematics of its western boundary indicates that it originated far to the north. Quantitative understanding of the kinematics does not resolve whether the Goochland is a native Laurentian or an exotic terrane; however it does place meaningful limits on its pre-Alleghanian position in the Appalachian orogen. If the Goochland terrane is Laurentian,

it originated somewhere between the Pennsylvania reentrant and the New York promontory, not outboard of the Virginia Blue Ridge.

The Elk Hill Complex and the pegmatite belt form two fault slices of uncertain affinity between the Goochland terrane and the Chopawamsic terrane proper. In addition, we recognize an unusual suite of mafic to ultramafic rocks associated with faults along the terrane boundary. Further work is needed to establish the significance of these units and their relation to adjacent terranes. These previously unrecognized crustal elements must be considered in future models for the tectonic assembly of the southern Appalachian Piedmont.

Acknowledgments

References Cited

Aleinikoff, J.N., Horton, J.W., Jr., and Walter, M., 1996, Middle Proterozoic age for the Montpelier Anorthosite, Goochland terrane, eastern Piedmont, Virginia: Geological Society of America Bulletin, v. 108, p. 1481–1491.

Bailey, C.M., Francis, B.E., and Fahrney, E.E., in press, Strain and vorticity analysis of transpressional high-strain zones from the Virginia Piedmont, USA: Geological Society of London Special Paper.

Bobyarchick, A.R., 1999, Kinematics of the Mountain Run fault zone, Virginia [abs.]: Geological Society of America Abstracts with Programs, v. 31, no. 3, p. 6.

Bollinger, G.A., Snoke, J.A., Sibol, M.S., and Chapman, M.C., 1986, Virginia regional seismic network; Final Report (1977–1985): Washington, D.C., U.S. Nuclear Regulatory Commission, NUREG/CR–4502, 57 p.

Bourland, W.C., 1976, Tectonogenesis and metamorphism of the Piedmont from Columbia to Westview, Virginia, along the James River: Blacksburg, Virginia Polytechnic Institute and State University, M.S. thesis, 105 p.

Brown, C.B., 1937, Outline of the geology and mineral resources of Goochland County, Virginia: Virginia Geological Survey Bulletin, v. 48, 68 p.

Brown, W.R., 1986, Shores complex and mélange in the central Virginia Piedmont, in Neathery, T.L., ed., Southeastern Section of the Geological Society of America: Geological Society of America Centennial Field Guide, v. 6, p. 209–214.

Burton, W.C., and Armstrong, T.R., 1997, Structural and ther-

mobaric history of the western margin of the Goochland terrane, Virginia [abs.]: Geological Society of America Abstracts with Programs, v. 29, no. 3, p. 7–8.

Burton, W.C., Kunk, M.J., and Marr, J.D., Jr., 2000, $^{40}Ar/^{39}Ar$ age constraints on the timing of Alleghanian metamorphism in the central and southern Virginia Piedmont [abs.]: Geological Society of America Abstracts with Programs, v. 32, no. 2, p. A–8.

Coler, D.G., Wortman, G.L., Samson, S.D., Hibbard, J.P., and Stern, R., 2000, U-Pb geochronology, Nd isotopic, and geochemical evidence for the correlation of the Chopawamsic and Milton terranes, Piedmont zone, southern Appalachian orogen: Journal of Geology, v. 108, p. 363–380.

Çoruh, C., Bollinger, G.A., and Costain, J.K., 1988, Seismogenic structures in the central Virginia seismic zone: Geology, v. 16, p. 748-751.

Darton, N.H., 1892, Fossils in "Archean" rocks of the central Piedmont, Virginia: American Journal of Science, Series 3, v. 44, p. 50–52.

Farrar, S.S., 1984, The Goochland granulite terrane; Remobilized Grenville basement in the eastern Virginia Piedmont: Geological Society of America Special Paper 194, p. 215–227.

Farrar, S.S., and Owens, B.E., 2001, A north-south transect of the Goochland terrane and associated A-type granites—Virginia and North Carolina (field trip guide), in Field Trip Guidebook, Southeastern Section 50th Annual Meeting: Geological Society of America, p. 75–92.

Gates, A.E., Simpson, C., and Glover, L., III, 1986, Appalachian Carboniferous dextral strike slip faults; An example from Brookneal, Virginia: Tectonics, v. 5, p. 119–133.

Glover, Lynn, III, Mose, D.G., Poland, F.B., Bobyarchick, A.R., and Bourland, W.C., 1978, Grenville basement in the eastern Piedmont of Virginia; Implications for orogenic models [abs.]: Geological Society of America Abstracts with Programs, v. 10, no. 4, p. 169.

Glover, Lynn, III, Mose, D.G., Costain, J.K., Poland, F.B., and Reilly, J.M., 1982, Grenville basement in the eastern Piedmont of Virginia; A progress report [abs.]: Geological Society of America Abstracts with Programs, v. 14, no. 1 and 2, p. 20.

Glover, Lynn, III, Evans, N.H., Patterson, J.G., and Brown, W.R., 1989, Tectonics of the Virginia Blue Ridge and Piedmont: Field Trip Guidebook T363 for the 28th International Geological Congress: Washington, D.C., American Geophysical Union, 59 p.

Goodman, M.C., Dubose, J., Bailey, C.M., and Spears, D.B., 2001, Petrologic and structural analysis of the Columbia pluton, central Virginia Piedmont [abs.]: Geological Society of America Abstracts with Programs, v. 33, no. 2, p. 4.

Hibbard, J.P., 2000, Docking Carolina; Mid-Paleozoic accretion in the southern Appalachians: Geology, v. 28, no. 2, p. 127–130.

Hibbard, J.P., and Samson, S.D., 1995, Orogenesis exotic to the Iapetan cycle in the southern Appalachians, in Hibbard, J.P., van Staal, C.R., and Cadwood, P.A., eds., Current perspectives in the Appalachian-Caledonian orogen: Geological Society of America Special Paper 241, p. 191–205.

Hibbard, J.P., Shell, G., Bradley, P., Samson, S.D., and Wortman, G., 1998, The Hyco shear zone in North Carolina and southern Virginia; Implications for the Piedmont zone-Carolina zone boundary in the southern Appalachians: American Journal of Science, v. 298, p. 85–107.

Hibbard, J.P., Stoddard, E.F., Secor, D.T., and Dennis, A.J., 2002, The Carolina zone; Overview of Neoproterozoic to early Paleozoic peri-Gondwanan terranes along the eastern flank of the southern Appalachians: Earth Science Reviews, v. 57, p. 299–339.

Horton, J.W., Jr., Aleinikoff, J.N., and Burton, W.C., 1995, Mesoproterozoic and Neoproterozoic terranes in the eastern Piedmont of Virginia, implications of coordinated field studies and U-Pb geochronology [abs.]: Geological Society of America Abstracts with Programs, v. 27, no. 6, p. A–397.

Horton, J.W., Jr., Aleinikoff, J.N., Drake, A.A., Jr., and Fanning, M.C., 1998, Significance of Middle to Late Ordovician volcanic-arc rocks in the central Appalachian Piedmont, Maryland and Virginia [abs.]: Geological Society of America Abstracts with Programs, v. 30, no. 7, p. 125.

Horton, J.W., Jr., Drake, A.A., Jr., and Rankin, D.W., 1989, Tectonostratigraphic terranes and their Paleozoic boundaries in the central and southern Appalachians, in Dallmeyer, R.D., ed., Terranes in the Circum-Atlantic Paleozoic orogens: Geological Society of America Special Paper 230, p. 213–245.

Jonas, A.I., 1932, Structure of the metamorphic belt of the southern Appalachians: American Journal of Science, v. 24, p. 228–243.

Lonsdale, J.T., 1927, Geology of the gold-pyrite belt of the northeastern Piedmont, Virginia: Virginia Geological Survey Bulletin 30, 110 p.

Marr, J.D., Jr., 1991, The Ca Ira mélange—Indicator of a major suture in the Piedmont of Virginia [abs.]: Geological Society of America Abstracts with Programs, v. 23, no. 1, p. 62.

Murray, J.D., and Owens, B.E., 2002, Field, mineralogical, and geochemical constraints on the origin of a metapyroxenite dike(?), central Piedmont province, Virginia [abs.]: Geological Society of America Abstracts with Programs, v. 34, p. 23.

Neuschel, S.K., 1970, Correlation of aeromagnetics and aeroradioactivity with lithology in the Spotsylvania area, Virginia: Geological Society of America Bulletin, v. 81, p. 3575–3589.

Owens, B.E., and Samson, S.D., 2001, Nd-isotopic con-
straints on the magmatic history of the Goochland terrane,
easternmost Grenville crust in the southern Appalachians
[abs.]: Geological Society of America Abstracts with
Programs, v. 33, no. 6, p. 28.

Owens, B.E., and Samson, S.D., in press, Nd-isotopic con-
straints on the magmatic history of the Goochland terrane,
easternmost Grenvillian crust in the southern Appalachians,
in Tollo, R.P., Corriveau, L., McLelland, J.B., and
Bartholomew, M.J., eds., Proterozoic tectonic evolution of
the Grenville orogen in North America: Geological Society
of America Memoir 197.

Owens, B.E., and Tucker, R.D., 1999, New U-Pb zircon age
constraints on the age of the State Farm Gneiss, Goochland
terrane, Virginia [abs.]: Geological Society of America
Abstracts with Programs, v. 31, no. 3, p. 58.

Owens, B.E., and Tucker, R.D., 2000, Late Proterozoic plu-
tonism in the Goochland terrane, Virginia; Laurentian or
Avalonian connection? [abs.]: Geological Society of
America Abstracts with Programs, v. 32, no. 2, p. 65.

Owens, B.E., and Tucker, R.D., 2003, Geochronology of the
Mesoproterozoic State Farm Gneiss and associated
Neoproterozoic granitoids, Goochland terrane, Virginia:
Geological Society of America Bulletin, v. 115, p. 972–982.

Pavlides, Louis, 1981, The central Virginia volcanic-plutonic
belt; An island arc of Cambrian(?) age: U.S. Geological
Survey Professional Paper 1231–A, 34 p.

Pavlides, Louis, Bobyarchick, A.R., and Wier, K.E., 1980a,
Spotsylvania lineament of Virginia: U.S. Geological
Survey Professional Paper 1175, p. 73.

Pavlides, Louis, Pojeta, John, Jr., Gordon, Mackenzie, Jr.,
Parsley, R.L., and Bobyarchick, A.R., 1980b, New evi-
dence for the age of the Quantico Formation of Virginia:
Geology, v. 8, p. 286–290.

Poland, F.B., 1976, Geology of the rocks along the James
River between Sabot and Cedar Point, Virginia:
Blacksburg, Virginia Polytechnic Institute and State
University, M.S. thesis, 98 p.

Pratt, T., Çoruh, C., Costain, J.K., and Glover, L., III, 1988, A
geophysical study of the earth's crust in central Virginia;
Implications for Appalachian crustal structure: Journal of
Geophysical Research, v. 93, p. 6649–6667.

Rankin, D.W., Drake, A.A., Jr., Glover, L., III, Goldsmith, R.,
Hall, L.M., Murray, D.P., Ratcliffe, N.M., Read, J.F., Secor,

D.T., Jr., and Stanley, R.S., 1989, Pre-orogenic terranes, in
Hatcher, R.D., Jr., Thomas, W.A., and Viele, G.W., eds.,
The Appalachian-Ouachita orogen in the United States, v.
F–2 of The geology of North America: Boulder, Colo.,
Geological Society of America, p. 7–100.

Secor, D.T., Jr., Samson, S.D., Snoke, A., and Palmer, A.,
1983, Confirmation of the Carolina slate belt as an exotic
terrane: Science, v. 221, p. 649–651.

Smith, J.W., Milici, R.C., and Greenberg, S.S., 1964, Geology
and mineral resources of Fluvanna County: Virginia
Division of Mineral Resources Bulletin 79, 62 p.

Spears, D.B., and Bailey, C.M., 2002, Geology of the central
Virginia Piedmont between the Arvonia syncline and the
Spotsylvania high-strain zone: Guidebook, 33rd Annual
Virginia Geological Field Conference, 36 p.

Spears, D.B, and Upchurch, M.L., 1997, Metallic mines,
prospects and occurrences in the gold-pyrite belt of
Virginia: Virginia Division of Mineral Resources
Publication 147, 73 p.

Taber, S., 1913, Geology of the gold belt in the James River
basin: Virginia Geological Survey Bulletin 7, 271 p.

Tillman, C.G., 1970, Metamorphosed trilobites from Arvonia,
Virginia: Geological Society of America Bulletin, v. 81, no.
4, p. 1189–1200.

Virginia Division of Mineral Resources, 1963, Geologic map
of Virginia: Charlottesville, Virginia Division of Mineral
Resources, scale 1:500,000.

Virginia Division of Mineral Resources, 1993, Geologic map
of Virginia: [Richmond], Virginia Division of Mineral
Resources, scale 1:500,000.

Watson, T.L., and Powell, S.L., 1911, Fossil evidence of the
age of the Virginia Piedmont slates: American Journal of
Science, Series 4, v. 31, p. 33–44.

Wilson, J., 2001, U/Pb zircon ages of plutons from the central
Appalachians and GIS-based assessment of plutons with
comments on their regional tectonic significance:
Blacksburg, Virginia Polytechnic Institute and State
University, M.S. thesis 121 p.

Wortman, G.L., Samson, S.D., and Hibbard, J.P., 1998,
Precise U-Pb timing constraints on the kinematic develop-
ment of the Hyco shear zone, southern Appalachians:
American Journal of Science, v. 298, p. 108–130.

ROAD LOG AND STOP DESCRIPTIONS FOLLOW

Road Log and Stop Descriptions

Day 1 (Sunday, March 28, 2004)

The field trip begins at the I-64/I-295 interchange west of Richmond.

Mileage

Incremental	Cumulative	
4.5	4.5	Proceed west on I-64 for 4.5 miles (mi) to Exit 173.
1.2	5.7	Turn left and go south on Va. 623 for 1.2 mi to stop sign.
0.7	6.4	Turn right (west) on U.S. 250 for 0.7 mi to Va. 621.
2.3	8.7	Turn left (south) on Va. 621 for 2.3 mi to Va. 644.
0.75	9.45	Turn right (west) and follow Va. 644 for 0.75 mi to third driveway on left after crossing Dover Creek.
0.15	9.6	Follow driveway 0.15 mi to creek crossing. Park along driveway.

Stop 1. Neoproterozoic granitoid along unnamed, east-flowing tributary of Dover Creek.

Outcrop in creek upstream (west) of driveway.

The slopes and creek bed here contain excellent exposures of a distinctive type of Neoproterozoic granitoid (Zgr) within the State Farm Gneiss (fig. 3). The rock here is characterized by a somewhat spotted appearance, reflecting oriented clusters of biotite+amphibole. This same rock type also occurs as a small body some 10 km (6 mi) to the north (not shown on figure 3 because of scale). Although the full dimensions of this pluton have not been completely mapped out, it is exposed in several drainages to the west of Dover Creek covering an area of at least 2 × 0.5 km (1–0.3 mi) (A.K. Teepe, 2001, undergraduate geology thesis, College of William and Mary). Thin sections show that the rock is dominated by microcline, plagioclase, and quartz; dark-green amphibole, yellow-brown biotite, allanite, and sparse garnet are accessory minerals. Samples from this pluton are typically quartz syenite, with SiO_2 ranging from 60 to 69 weight percent in four samples (Owens and Tucker, 2003). One sample (south of this stop) yielded a U-Pb zircon age of 588+9/-12 Ma (Owens and Tucker, 2003).

Mileage

Incremental	Cumulative	
0.15	9.75	Retrace route back to Va. 644. Turn left (west).
3.7	13.45	Follow Va. 644 for 3.7 mi to stop sign. Turn right (west) on Va. 6.
0.1	13.55	Proceed west on Va. 6 for 0.1 mi. Park on shoulder of road.

Stop 2. State Farm Gneiss and Neoproterozoic granitoid in roadcut on north side of Va. 6.

Outcrop is in roadcut on north side of road.

This location represents one of the few actual roadcuts in this part of the Goochland terrane. Although highly iron-stained, this exposure shows a key intrusive relation between a mafic variety of the State Farm Gneiss (~57 weight percent SiO_2) and a leucocratic variety of Neoproterozoic granite (~70 weight percent SiO_2). Both rock types are exposed at various places in the roadcut, but the west end shows that a number of small (centimeter-

scale) dikes of granite have intruded the gneiss. These dikes also are folded, indicating deformation following emplacement. A larger mass of the granite is exposed near the east end of the main roadcut, and here shows only a faint foliation. The granite here is more leucocratic than it is at Stop 1, but is mineralogically similar. Some differences include more abundant garnet, local occurrences of distinctive euhedral magnetite, and the presence of sphene. Samples from this roadcut give U-Pb zircon ages of 1039+18/-11 Ma for the State Farm Gneiss and ~654 Ma for the Neoproterozoic granite. The poorly constrained age for the granite is based on a single concordant zircon analysis, with five additional analyses showing considerable scatter (see Owens and Tucker, 2003, for additional discussion). Pegmatites of Paleozoic age, common throughout the Goochland terrane, also are present in this roadcut.

Mileage

| Incremental	Cumulative	
10	23.55	Continue west on Va. 6 for 10 mi, through village of Goochland Courthouse to traffic light.
0.35	23.9	Turn right (north) on U.S. 522. Go 0.35 mi and turn right (east) on Va. 632.
0.9	24.8	Follow Va. 632 for 0.9 mi to entrance of Hidden Rock Park on left.
0.3	25.1	Turn into park, drive 0.3 mi to end of driveway and park in parking lot.

Stop 3. Maidens Gneiss at Hidden Rock Park.

Outcrops in whaleback exposures near bathrooms.

This locality contains some of the best exposures (outcrops and large blocks) of the Maidens Gneiss in this area. The gneiss here is a medium-grained, biotite plagioclase+quartz gneiss, with additional amphibole and (or) clinopyroxene present in some samples. All samples also contain sphene. The gneiss has obviously been highly injected by pegmatites for pegmatite is present in most exposures of the Maidens in this area. The protolith of the Maidens Gneiss is uncertain, but work is in progress to help answer this question on the basis of chemical compositions. Analyses of rocks from this park and several other locations (six samples, including the type locality at Maidens Cave, 4 km (2 mi) to the south) show a narrow range of bulk compositions: SiO_2=~55–62 weight percent; CaO=~4.2–6.8 weight percent; and K_2O=~2.7–4.0 weight percent (B.E. Owens, unpub. data). In addition, one sample from this locality has yielded a well-constrained U-Pb zircon age of 407±2 Ma (B.E. Owens and R.D. Tucker, unpub. data). The nearly concordant nature of the zircon analyses, in conjunction with the chemical compositions, suggests that this variety of Maidens Gneiss may have originated from an igneous protolith of intermediate composition (quartz monzodiorite to quartz monzonite or volcanic equivalents). The significance of the Paleozoic age is unclear at the present time, but work is in progress on additional samples to evaluate this surprising result.

The penetrative foliation in the gneiss, defined by amphibolite-facies minerals and microstructures, is folded into a series of northwest-verging, gently plunging, overturned antiforms and synforms (fig. 5). Burton and Armstrong (1997), in a study approximately on strike about 50 km (30 mi) southwest of this locality, interpret this fabric to be of Alleghanian age. Some pegmatitic dikes are discordant to the foliation whereas other pegmatitic dikes are folded and boudinaged in dramatic fashion. We interpret these dikes to have intruded throughout the deformation. These dikes serve as minimum strain markers and record sectional strains of ~15:1 to 20:1. Elongation lineations, where discernible, plunge gently to both the northeast and southwest parallel to fold axes. Kinematic indicators are compatible with dextral transpressive shear. These exposures are ~10 km (~6 mi) southeast of the Spotsylvania geophysical lineament at the western edge of the Goochland
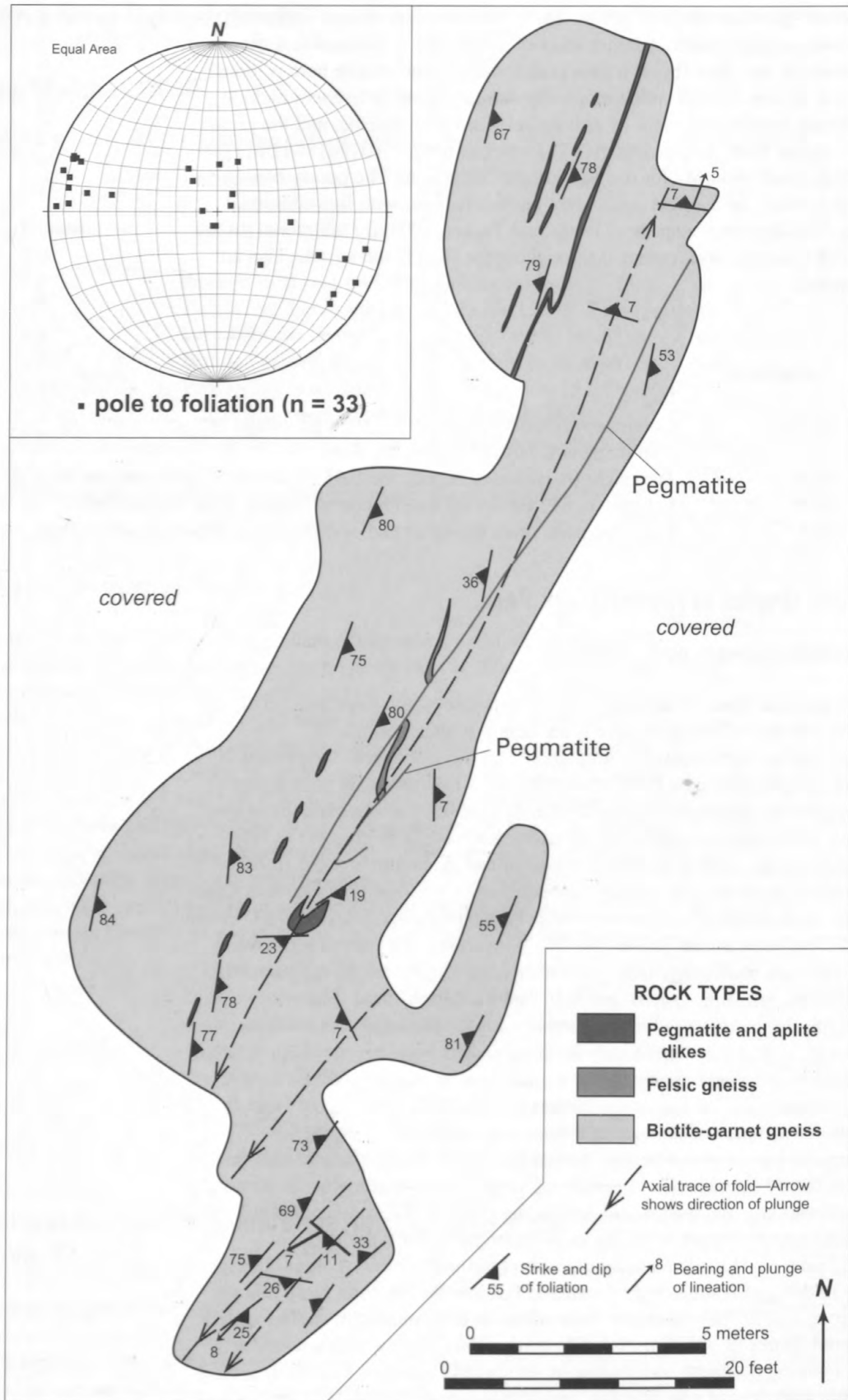
Figure 5. Outcrop map with stereogram (inset) of large whaleback exposure of mylonitic Maidens Gneiss at Hidden Rock Park, Goochland County, Va. (Stop 3). n, number of measurements.
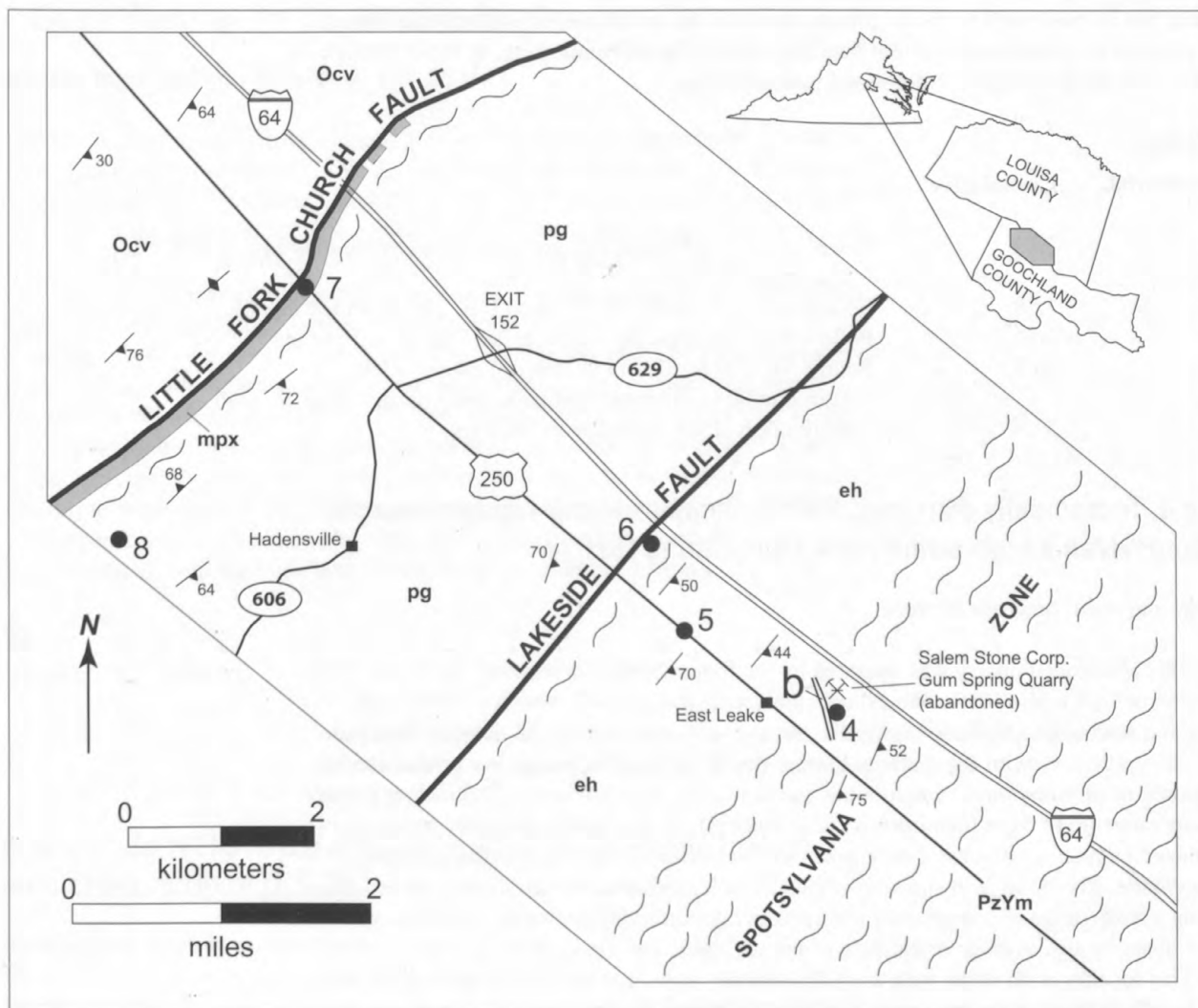
EXPLANATION

Ocv	Chopawamsic Formation
mpx	Metapyroxenite
pg	Pegmatite belt, undivided
eh	Elk Hill Complex
PzYm	Maidens Gneiss
b	Siliceous breccia

6●   Field trip stop

〰〰〰   Mylonitic rocks in high-strain zone

Strike and dip of foliation
40   Inclined
◆   Vertical

Figure 6. Generalized geologic map along I-64 and U.S. 250 in Goochland and Louisa Counties, Va., showing the locations of Stops 4 through 8.

terrane, but as evidenced by the pegmatite markers, the rocks are very strongly deformed. It is difficult to place a southeastern boundary on the Spotsylvania zone, as rocks throughout the Goochland terrane are deformed in this fashion.

Mileage

Incremental	Cumulative	
1.2	26.3	Retrace route back to Va. 632 and turn right (west), returning to U.S. 522. Turn right (north).
6.5	32.8	Follow U.S. 522 north for 6.5 mi to U.S. 250. Turn left (west).
3.3	36.1	Follow U.S. 250 west for 3.3 mi to Va. 700. Turn right (east).
0.1	36.2	Follow Va. 700 for 0.1 mi to first driveway on left. Turn around in driveway and park along north side of Va. 700. Walk north along driveway for 0.25 mi.

Stop 4. Tectonically disrupted Elk Hill Complex along western margin of Spotsylvania high-strain zone, Gum Spring Quarry.

Blocks and small outcrops in creek.

This abandoned quarry was operated by the Salem Stone Corporation during the construction of I-64 in the 1960s. We cannot safely visit the pit itself, which is filled with water and surrounded by steep highwalls, but the large quarried blocks dumped here provide an excellent view of the material blasted out of the pit. The blocks are predominantly composed of protomylonitic amphibolite and porphyroclastic mylonite. Plagioclase porphyroclasts range up to 5 cm (centimeters) (2 in (inches)) in diameter, apparently remnants of tectonized pegmatite. Blocks of dark-green to black amphibolite form tectonic inclusions in the mylonite. These range in shape from blocky to lens-shaped to extremely flattened, suggesting a wide range of competency contrasts in relation to the enclosing mylonitic gneiss. In the quarry walls, average orientation of the mylonitic foliation is 035° 42° SE.

This locality is on strike with and lithologically similar to the Ca Ira mélange of Marr (1991). While these rocks are certainly highly deformed, we note the lack of truly exotic blocks; virtually all observable tectonic inclusions are varieties of amphibolite, the dominant rock type in the nearby Elk Hill Complex. Therefore, we interpret this locality not as true mélange, but as highly deformed Elk Hill lithologies in the footwall of the Spotsylvania high-strain zone (fig. 6). Just east of here, the presence of strongly pelitic rocks (muscovite-sillimanite-garnet schist) marks the transition into the Maidens Gneiss protolith of the Goochland terrane.

A narrow zone of poorly exposed siliceous breccia trends north-northwest across the south slope of this small valley. Lithologically, the rock is similar to the breccia along the Lakeside fault: nearly white, massive cryptocrystalline silica with both quartz-filled and open fractures enclosing angular clasts of the same lithology. The siliceous breccia can be traced from the crest of a low hill on the quarry entrance road in a north-northwesterly direction for at least 500 meters (m) (1,600 feet (ft)) (fig. 6). The re-brecciated breccia indicates multiple episodes of Mesozoic brittle reactivation along the western margin of the Spotsylvania high-strain zone, although at an angle oblique to the original mylonitic foliation.

Mileage

Incremental	Cumulative	
0.1	36.3	Return to vehicles and return on Va. 700 west to U.S. 250. Turn right (west).
1.2	37.5	Follow U.S. 250 west for 1.2 mi. Park on grassy shoulder at crest of hill.

Stop 5. Elk Hill Complex on U.S. 250 near East Leake.

Small outcrops in roadcut on north side of U.S. 250.

Small outcrops of the Elk Hill Complex here were fresh and more extensive when photographed by C.B. Brown in 1937 (his pl. 7). We can still observe the general nature of the complex, compositionally layered amphibolite interlayered with biotite gneiss, as it is expressed north of the James River. The compositional layering here is parallel to a moderately developed foliation that strikes 040° and dips 70° SE. A weak mineral lineation (mostly hornblende) plunges gently northeast (20°–48°). On the north side of the road, outcrops display northeast-plunging Z-shaped refolded folds.

The main purpose of this stop is to demonstrate that the Elk Hill Complex is a coherent body of relatively undeformed amphibolitic rocks between two parallel high-strain zones (fig. 6). It is bounded on the east by the Spotsylvania high-strain zone (Stop 4) and on the west by mylonitic rocks in the hanging wall of the Lakeside fault (Stop 6). Our mapping indicates that the Elk Hill extends from here at least as far as the Farmville basin, 40 km (25 mi) to the southwest. Its northeastward extent has not been determined. While these rocks superficially resemble amphibolites in the Chopawamsic Formation, they are structurally separated from the main body of the Chopawamsic Formation to the west.

Mileage

Incremental	Cumulative	
0.4	37.9	Continue west on U.S. 250 for 0.4 mi. At bottom of hill, park on grassy shoulder. Walk through woods following creek north-northeast, about 0.3 mi.

Stop 6. Mylonitic rocks in the hanging wall of the Lakeside fault in unnamed creek north of U.S. 250.

Creek pavement outcrops near I-64 culvert.

Exposures in this streambed give us a view of mylonitic rocks in the hanging wall of the Lakeside fault (fig. 6). A fine-grained matrix of biotite, muscovite, and quartz encloses abundant porphyroclasts of plagioclase feldspar. Plagioclase-quartz pegmatite layers have been deformed into lens-shaped, generally foliation-parallel domains of various sizes. Foliation trends 042° with an average dip of 50° SE. Preliminary analysis of porphyroclast asymmetry indicates dextral oblique motion on this mylonitic zone, similar to that in the Spotsylvania high-strain zone. Creeks crossing this zone at a high angle yield outcrops that indicate a width of nearly 900 m (3,000 ft). Elsewhere, the trace of the Lakeside fault is marked by extensive development of siliceous breccia (for example, Stop 10A), an indication of Mesozoic brittle reactivation of this Paleozoic ductile fault zone. The outcrops here represent part of the case for extending the Lakeside fault northeast of the terminus shown in northern Cumberland County on the geologic map of Virginia (Virginia Division of Mineral Resources, 1993). Its northeastern termination has not yet been determined.

Mileage

Incremental	Cumulative	
2.9	40.8	Return to vehicles and continue west on U.S. 250 for 2.9 mi. Turn vehicles around in driveway near top of hill and park on south shoulder of road.

Stop 7. Amphibole-rich metapyroxenite at Hadensville, U.S. 250.

Roadcut at crest of hill on south side of U.S. 250.

This roadcut exposes one of the most prominent mafic to ultramafic dike-like bodies in the Piedmont province of Virginia. It was originally mapped as pyroxenite by Brown (1937), but labeled as hornblende gabbro on the 1963 geologic map of Virginia. Curiously, the body was omitted from the 1993 geologic map of Virginia (Virginia Division of Mineral Resources, 1993). The body is well exposed in outcrop or float for about 5.5 km (3 mi), ranges up to ~200 m (~660 ft) wide, and is oriented ~040° (Murray and Owens, 2002). Most exposures are dominated by green, medium- to coarse-grained (≤1 cm), blocky calcic amphibole, and textures range from massive to slightly foliated. The blocky shapes may reflect pseudomorphic replacement of pyroxene by amphibole. In thin section, the rocks typically consist of ~85 to 90 percent calcic amphibole (actinolite to actinolitic hornblende to magnesio-hornblende), minor epidote and quartz, and rare talc (and even rarer cumming-tonite). Clinopyroxene (relict igneous?) occurs in small amounts in a few samples as ragged grains within amphibole. Eight samples from along the length of the body show similar whole-rock SiO_2 (50–55 weight percent), Al_2O_3 (3–7 weight percent), and Mg# (73–82), but a range in MgO (14–23 weight percent) and CaO (5–14 weight percent). Normative mineralogy of typical samples is dominated by clinopyroxene and orthopyroxene; all are quartz normative. These observations and data suggest that the body represents a pyroxenite metamorphosed at middle- to upper-amphibolite-facies conditions, and that the protolith was a cumulate consisting largely of two pyroxenes and minor plagioclase. The mode of emplacement is an unresolved issue. The body clearly has a dike-like form, but its original cumulate character suggests that it could not have been emplaced as a liquid. In addition, no other indicators of intrusive emplacement (chilled margins, contact metamorphism, xenoliths) have been observed. Alternatively, the body was emplaced tectonically. Its proximity to the Little Fork Church fault (fig. 6) may be significant in this regard, but no clear field evidence linking these features has thus far been observed. [Much of this information is from the 2002 undergraduate geology thesis by J.D. Murray, College of William and Mary; see also Murray and Owens (2002)].

Mileage

Incremental	Cumulative	
0.9	41.7	Return east on U.S. 250 for 0.9 mi to Va. 606. Turn right (south).
1.8	43.5	Follow Va. 606 for 1.8 mi to Va. 609. Turn right (west).
1.0	44.5	Follow Va. 609 for 1.0 mi to Mill Creek.
		Park in driveway on left.

Stop 8. Granitic gneiss, mylonitized pegmatite, and breccia in the pegmatite belt near Mill Creek.

Outcrops on hillside north of road.

This leucocratic, fine-grained, weakly layered granitic gneiss with thin pegmatites is typical of the structurally lowest unit of the pegmatite belt (fig. 3). The pegmatites are composed mostly of pinkish-white microcline with lesser quartz and muscovite, and are typically deformed into lens-shaped bodies. Pegmatite bodies are parallel to the foliation, which strikes 052° and dips 68° NW. "Floating" porphyroclasts surrounded by fine-grained gneiss suggest that some of the granitic gneiss may be derived from extreme deformation of pegmatite. Pegmatites in this unit are the coarsest grained rocks seen in this part of the Piedmont, with individual microcline crystals up to 15 cm (6 in) long. Feldspars in the pegmatite are strongly fractured, with development of subgrains having nearly parallel crystal-

lographic axes. Float blocks on the slope to the northeast include re-brecciated breccia similar to that found along the Lakeside fault and the western margin of the Spotsylvania high-strain zone. These blocks suggest the presence of an unmapped breccia zone, perhaps related to the Little Fork Church fault.

This locality is about 700 m (2,300 ft) southeast of the mapped trace of the Little Fork Church fault (fig. 6). Considering the high degree of deformation apparent in these rocks, and the presence of possibly tectonically separated, enigmatic, mafic to ultramafic rocks nearby (Stop 7), we must consider the possibility that the Little Fork Church fault is a major structural discontinuity.

Mileage

Incremental	Cumulative	
0.2	44.7	Continue west on Va. 609 for 0.2 mi. At stop sign, turn left (still Va. 609).
1.1	45.8	Continue on Va. 609 for 1.1 mi to stop sign. Turn left (south) on Va. 603.
3.6	49.4	Follow Va. 603 for 3.6 mi to stop sign at Va. 610.
		Turn left (east) for 60 yards (yd) then right (south) on Va. 603.
2.3	51.7	Follow Va. 603 for 2.3 mi to stop sign at Va. 667. Turn right (west).
4.6	56.3	Follow Va. 667 for 4.6 mi to village of Columbia.
8.0	64.3	At blinking light, turn right (west) on Va. 6 and
		proceed 8 mi to village of Fork Union for overnight stay.

End of Day 1.

## Day 2 (Monday, March 29, 2004)

Mileage

Incremental	Cumulative	
8.0	72.3	Return east on Va. 6 for 8 mi to village of Columbia.
		Park in lot on right side of road 50 yd past blinking light.

Stop 9. L-tectonites in Columbia pluton at Cowherd quarry, Va. 6, Columbia.

Old dimension stone quarry on north side of Va. 6.

Granodioritic gneiss of the Columbia pluton is exposed in this old roadside quarry (fig. 3). Wilson (2001) obtained a U-Pb zircon SIMS age of 457±7 Ma on rock from this locality. The Columbia pluton ranges from granite to quartz diorite in composition and intrudes metavolcanic rocks of the Chopawamsic Formation (Smith and others, 1964; Goodman and others, 2001) (fig. 3). The Columbia pluton is part of a suite of Ordovician plutons that record magmatic activity associated with the Taconic orogeny. These plutons may have originated above a subduction zone associated with the accretion of the Carolina zone to Laurentia (Hibbard, 2000).

At the Cowherd quarry the granodioritic gneiss contains plagioclase, quartz, biotite, potassium feldspar, and epidote with minor amounts of garnet, muscovite, and opaque minerals. Feldspar and quartz microstructures are consistent with recrystallization under amphibolite-facies conditions. This rock forms a distinctive L-tectonite (fig. 7). The penetrative fabric is defined by aligned biotite and quartz aggregates. The lineation plunges ~25° towards ~050° and a very weak foliation strikes ~055° and dips ~80° NW (fig. 8A–C). Poles to biotite cleavage form a strong great circle girdle normal to the lineation (fig. 8B, C). Three-dimensional quartz fabrics in the XZ section range from 2.7 to 3.4 with K-values of 4 to 12 (strongly constrictional) (fig. 8D). Locally, L-tectonites are restricted to the nose of a map-scale northeast-plunging synform (fig. 3). Three-dimensional quartz fabrics in the Columbia pluton exhibit a complete range from L- to L/S- to S-tectonites.
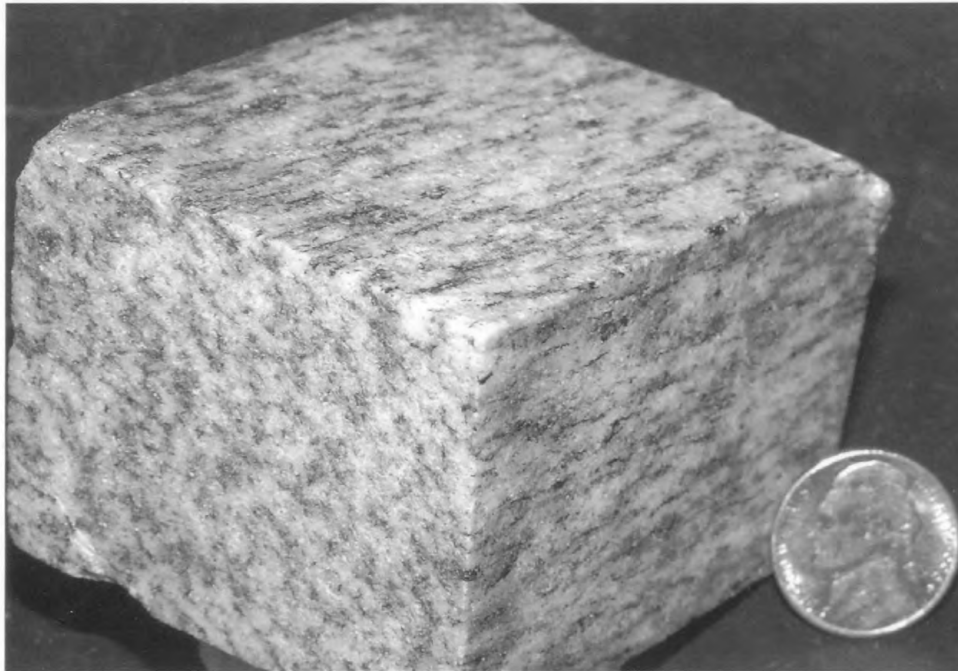
Figure 7. Photograph of polished block of L-tectonite from the Columbia pluton, Cowherd quarry, Fluvanna County, Va. (Stop 9).
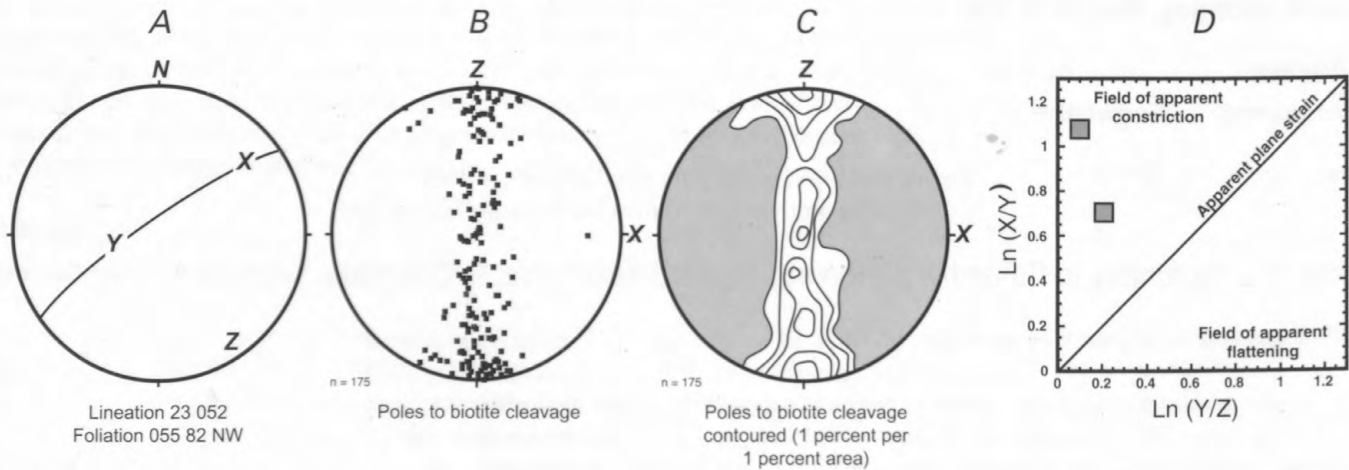
Figure 8. Synoptic diagram for fabric elements in the Columbia granodiorite gneiss at Cowherd quarry; poles and contoured poles to biotite cleavage; and logarithmic Flinn diagram for quartz grain shapes (n = 40 to 64 measurements per sample).

We view the L-tectonite as the product of cumulative deformation. At the map scale, the foliation is folded into a series of asymmetric northeast-plunging folds with axes that parallel the elongation lineation, suggesting a post-foliation deformation event. However, there is no microstructural evidence for two deformational events in these rocks. Although the quartz fabrics do not, in a strict sense, record the finite strain, they are a measure of the approximate overall strain. Here at the Cowherd quarry and at many locations in the central Piedmont, crustal rocks were apparently elongated in an orogen-parallel direction late in the Paleozoic.

Mileage

Incremental	Cumulative	
		Retrace route 50 yd back to blinking light. Turn left (south) on Va. 690.
3.1	75.4	Follow Va. 690 for 3.1 mi to Va. 602. Turn left (east).
1.0	76.4	Follow Va. 602 for 1.0 mi to Va. 605. Turn right (south).
2.1	78.5	Follow Va. 605 for 2.1 mi to edge of flood plain at bottom of hill. Park on side of road.

Stop 10. Fault breccia, pegmatite belt, and diabase at "Bodatious" race track.

A. Breccia associated with the Lakeside fault.

Outcrops on hillside northeast of road.

This prominent northeast-trending ridge is underlain by erosionally resistant siliceous fault breccia, which marks the trace of the Lakeside fault (fig. 4). This fault forms the western bounding normal fault of the Farmville basin, 20 km (12 mi) to the southwest. From here, the fault continues northeastward, crossing the James River between Columbia and Cartersville. Our mapping extends the fault at least as far north as I-64 in Goochland County (fig. 6, Stop 6).

Breccia occurs discontinuously along the fault trace. This, the largest mapped breccia body, is about 8 km (5 mi) long. The breccia is composed of cherty, cryptocrystalline silica with multiple generations of partly to fully filled fractures. Some fractures are filled with microbreccia, but more commonly they are fully or partly healed with crystalline quartz; partly open fractures display terminated quartz crystals. Angular clasts displaying truncated internal fractures are common; they are either supported by microbreccia, by other clasts, or completely surrounded by cherty silica. Bourland (1976) reports zeolite minerals and prehnite from fractures associated with this fault. The breccia apparently formed from silica-rich hydrothermal fluids migrating along the fault in the early Mesozoic; the still-active fault fractured the hydrothermal deposits repeatedly during their formation.

Cross road and enter "Bodatious" race track complex. Walk 250 yd to the northwest to dirt drag strip.

B. Structural complex in upper unit of pegmatite belt.

Large saprolite cut along north side of drag strip.

This large saprolite cut provides a rare view of the structure of the eastern part of the pegmatite belt in the footwall of the Lakeside fault (fig. 4). The strongly compositionally layered gneiss consists of amphibolite, quartzofeldspathic biotite gneiss, and thin concordant pegmatites. These lithologies are typical of the structurally highest lithologic unit in the pegmatite belt (pgl, fig. 4). Layers have been deformed into a series of upright outcrop-scale folds that plunge steeply to the northeast. The folds are cut by two families of younger normal faults, one dipping steeply to the southeast and one dipping gently to the northwest. The faults commonly contain thin discontinuous fills of vein quartz. Crosscutting relations at most fault intersections indicate that the northwest-dipping set is younger, but a few examples can be found in which the southeast-dipping set displays more recent movement.

Follow creek upstream (west) for 100 yd.

C. Granitoid gneiss and amphibolite in middle unit of pegmatite belt.

Creek pavement outcrops west of race track.

In this outcrop, light-gray, fine-grained granitoid gneiss is intruded by a 1.5-m (5-ft)-thick amphibolite dike. The irregular boundaries of the dike cut and trend more easterly than weak compositional layering in the granitoid gneiss. Foliation dips steeply to the southeast (038° 80° SE) and cuts both the dike and the country rock. The amphibolite has been deformed into Z-shaped folds and is locally stretched into boudins of various size. The presence of amphibolite boudins within granitoid gneiss is a characteristic feature of the middle unit of the pegmatite belt (pga, fig. 4). Fine brittle fractures in both lithologies, apparently related to Mesozoic deformation, are filled with epidote and zeolite minerals.

Continue upstream (west) on path along north bank for 50 yd.

D. Large diabase dike.

Stream pavement, boulders, and blocks in ruins of mill dam.

This old mill dam, now in ruins, was built of local boulders placed on top of stream pavement composed of diabase. The boulders themselves are primarily diabase, but light-gray granitic gneiss and white siliceous breccia also are evident. This diabase, one of several large, north-trending Jurassic dikes in the Virginia Piedmont, can be traced on aeromagnetic maps for at least 80 km (50 mi) to the south. To the north, this dike crosses the James River 2 km (1 mi) east of Columbia, where Brown (1937) measured its width at 75 m (250 ft).

South of this outcrop (1.2 km; 0.75 mi), the dike intersects the trace of the Lakeside fault near the Willis River (fig. 4). Although the intersection of the dike with the fault is beneath the flood plain of the river, mapping indicates that where the dike emerges from the flood plain in the hanging wall of the fault, it displays an apparent right-lateral offset of 600 m (2,000 ft) (fig. 4). This evidence suggests a degree of dextral offset on the Lakeside fault after intrusion of the diabase in Early Jurassic time.

Mileage

Incremental	Cumulative	
2.1	80.6	Return to vehicles and go south on Va. 605 for 2.1 mi to stop sign at Va. 690.
0.7	81.3	Turn left (southeast) and follow Va. 690 for 0.7 mi to stop sign at Va. 45.
4.7	86.0	Turn right (south) on Va. 45 and travel for 4.7 mi to Va. 615. Turn right (west).
1.7	87.7	Follow Va. 615 for 1.7 mi to Va. 663. Turn right (north).
1.2	88.9	Follow Va. 663 for 1.2 mi to end of gravel. Park vehicles and walk down old road to creek.

Stop 11. Gneissic diorite near Whiteville.

Outcrops and blocks in creek.

This coarse-grained melanocratic gneiss (dg), described here for the first time, occupies an area of 6 km² (2 mi²) in northern Cumberland County (fig. 3). It forms an elongate fault block bounded on the west by mylonitic rocks in the hanging wall of the Lakeside fault, and on the east by a narrow band of mylonitic biotite schist that separates it from metavolcanic rocks in the Elk Hill Complex (fig. 3). Composition is dominantly hornblende+plagioclase with minor clinopyroxene, quartz, titanite, and epidote. Foliation strikes 042° and is nearly vertical; hornblende defines a mineral lineation plunging 12° and bearing 042°. The weak to moderate gneissic layering seen here (fig. 9) is quite variable, with some outcrops showing no layering or foliation. Superficially, this unit resembles dioritic rocks identified as high-grade equivalents of the Carolina slate belt generally on strike to the south (W.C. Burton, written commun., 2003). When considered with the metapyroxenite in western Goochland County (Stop 7) and poorly exposed talc-chlorite soapstone about 3 km (2 mi) to the north-east (D.B. Spears, unpub. field data), all spatially associated with mapped faults, we can
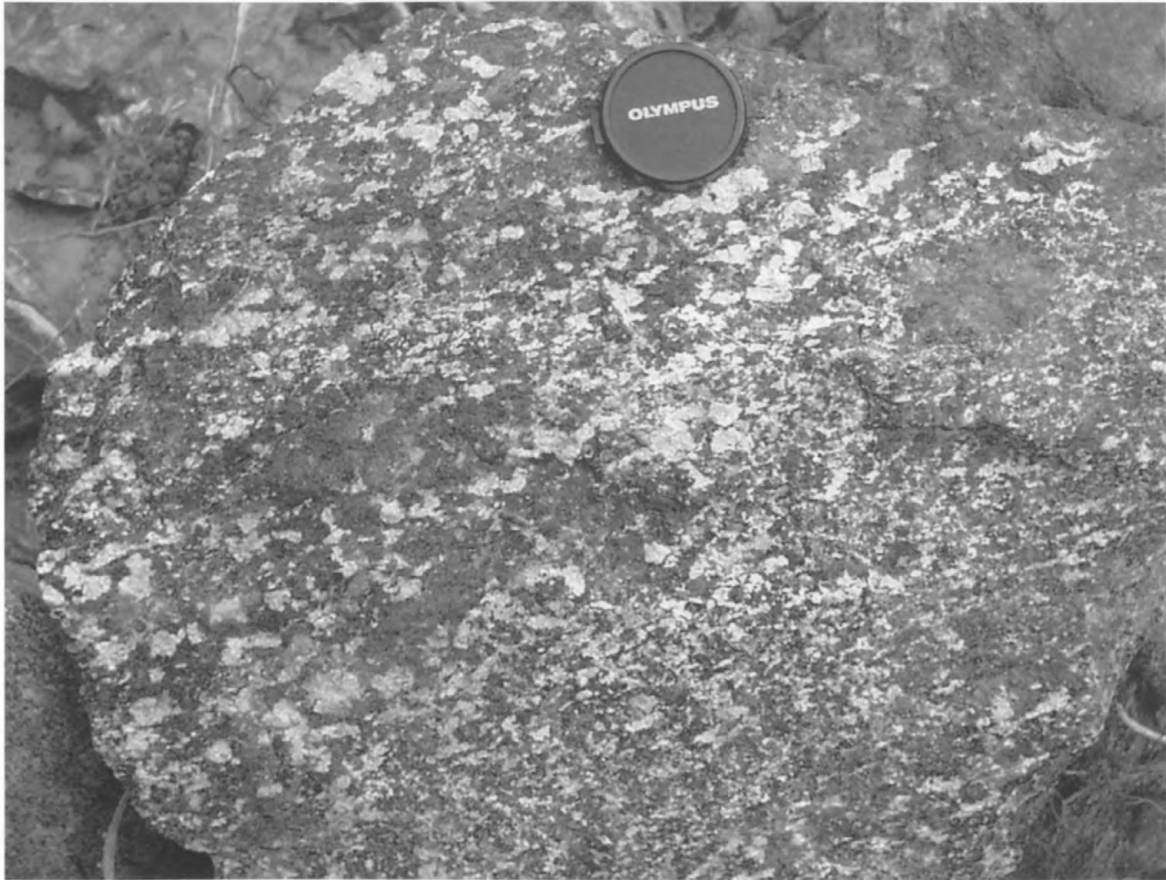
Figure 9. Photograph of block of weakly gneissic coarse-grained diorite from an outcrop near Whiteville, Cumberland County, Va. Lens cap is 4.5 cm (1.75 in) in diameter.

speculate that we are seeing the remains of a tectonically dismembered mafic-ultramafic complex. More work is needed to establish the affinity of these units and their significance with respect to the terrane boundary.

Mileage

Incremental	Cumulative	
9.9	98.8	Retrace route back to Va. 45. Turn left (north) and follow Va. 45 for 7 mi to village of Cartersville, Va.
1.25	100.05	Continue north on Va. 45, crossing James River (0.5 mi), then 0.75 mi farther to driveway of Howard's Neck Plantation on left.
1	101.05	Turn left (west) into driveway. Drive ~1 mi west on driveway and park near house. Walk westward across pasture toward James River, approximately 800 yd.

Stop 12. Mylonitic rocks along west edge of Spotsylvania high-strain zone at Howard's Neck Plantation.

Large natural pavement exposure on south side of small valley east of railroad.

This large natural outcrop exposes rocks and structures typical of the Spotsylvania high-strain zone. The country rock is a mica-rich mylonitic gneiss that has been intruded by dikes of medium-grained granitic gneiss and pegmatite. These dikes are variably dismembered; some retain a tabular shape and others form lozenge-shaped asymmetric boudins. It is possible that the granitic intrusions occurred prior to and during ductile defor-

mation. Foliation strikes to the northeast and dips moderately to gently southeast; elongation lineations plunge subhorizontally in the plane of foliation. Asymmetric structures consistently display a dextral sense of shear. Minimum strain estimates based on boudinaged and folded pegmatites are in excess of 10:1 on lineation parallel faces. The Spotsylvania lineament is located within a few hundred meters to the west and is defined on the ground by a transition to amphibole-rich gneisses of the Elk Hill Complex that do not display a mylonitic texture.

Mileage

Incremental	Cumulative	
1	102.05	Retrace route back to Va. 45. Turn right (south).
2.25	104.3	Follow Va. 45 south for 1.25 mi, back through Cartersville, then continue south 1.0 mi to Va. 684. Turn left (east).
1.1	105.4	Follow Va. 684, 1.1 mi to road sign saying "Tam Worth."
0.25	105.65	Turn left onto gravel road, follow 0.25 mi to end. Turn vehicles around and park.

Stop 13. Maidens Gneiss at Tamworth.

Roadcuts along west side of gravel road and outcrop on east bank of Muddy Creek at mill dam.

This small roadcut contains fine-grained, weakly layered, moderately foliated quartzo-feldspathic gneiss with finely disseminated biotite. A few thin, coarse-grained quartz-feldspar-muscovite-garnet pegmatites are present, concordant with the compositional layering. This locality falls into an area defined as the "Central Piedmont" terrane on the most recent geologic map of Virginia (Virginia Division of Mineral Resources, 1993), but no other reference to this terrane appears in the literature. Farrar (1984) included this area in his mapping of the Maidens Gneiss and reported high-grade pelitic assemblages (sillimanite+potassium feldspar±muscovite; sillimanite+staurolite+muscovite) from outcrops nearby. Outcrops adjacent to the mill dam are more typical Maidens biotite-hornblende gneiss with feldspar porphyroclasts showing strong dextral asymmetry.

Mileage

Incremental	Cumulative	
7.55	113.2	Retrace route back to Va. 684. Turn left (east) and travel 7.3 mi to crossroads at Provost. Continue straight (east). Road becomes Va. 621.
4	117.2	Follow Va. 621 for 4 mi to stop sign at Va. 711. Turn left (east).
5.7	122.9	Follow Va. 711 for 5.7 mi to Fine Creek Mills. Turn left (north) on Va. 628.
0.1	123.0	Follow Va. 628 for 0.1 mi and park at sharp bend. After gaining permission from landowner, walk west to Fine Creek.

Stop 14. Fine Creek Mills Granite.

Stream pavement exposures along Fine Creek.

Although this stop has been included on at least one other field trip (Farrar and Owens, 2001), it is one of the more spectacular outcrops in this part of the Piedmont province (and therefore worth re-visiting!). The Neoproterozoic Fine Creek Mills Granite (629+4/-5 Ma; Owens and Tucker, 2003) intrudes the Middle Proterozoic State Farm Gneiss. It is well exposed here along both sides of Fine Creek. This medium- to coarse-grained granite is mineralogically similar to the other Neoproterozoic granitoids previously visited. The dark minerals include both biotite and amphibole. Discrete, narrow shear zones

cut a moderately developed foliation in the granite, but these have not been systematically examined.

Mileage

Incremental	Cumulative	
29.1	152.1	Retrace route back to Va. 711 and turn left (east).
		Follow Va. 711 approximately 15 mi back to suburban Richmond.
		Turn left (north) on Va. 147. Follow signs to I-64/I-295 interchange.

End of field trip.

End of Day 2.

8. Terrain and the Battle of Fredericksburg, December 13, 1862

By Judy Ehlen[1]

Introduction

The area around Fredericksburg, Va., was a major theater of operations in the American Civil War (1861–1865), beginning with the Battle of Fredericksburg in December 1862. The city and its environs along the Rappahannock River in north-central Virginia were significant obstacles to Union advances on Richmond, the Confederate capital. The battlefield consists of a series of flood plains and river terraces with gentle slopes paralleled by north-south ridges that provide structural boundaries on either side, all composed of Tertiary and Quaternary Coastal Plain sediments. The Confederates, led by General Robert E. Lee, effectively used natural terrain features to impede attacks made by the Union army. Tactical benefits were also accrued by the Confederates from manmade obstacles on the battlefield, such as stone walls and fences. After crossing the Rappahannock River, the Union army, led by Major General Ambrose E. Burnside, was forced to attack uphill with little cover in its unsuccessful attempts to dislodge the Confederates. Effective use of the terrain thus enabled Confederate forces to defeat the Union army at the Battle of Fredericksburg, which helped delay Union capture of Richmond for almost three years.
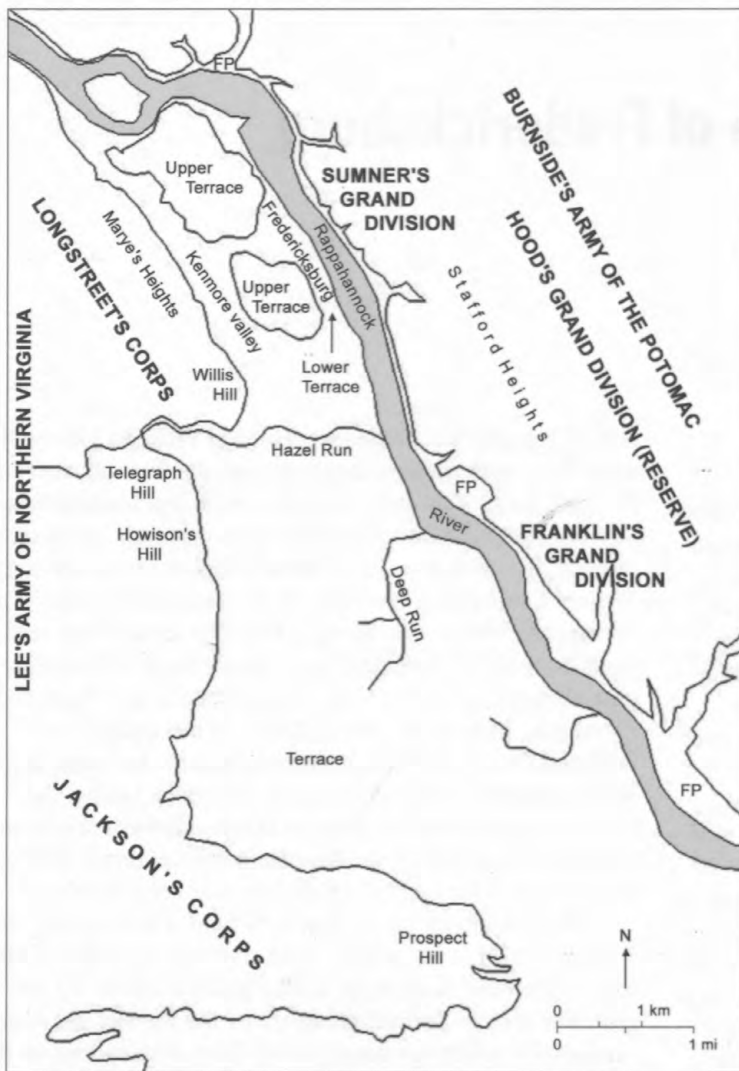
Battlefield Terrain

Fredericksburg is located on the west side of the Rappahannock River, partly on flood plain and partly on terraces about 6 to 15 meters (m) (20–50 feet (ft)) or more above the river (fig. 1). The city is about 1,800 m (1.1 miles (mi)) southeast of the Fall Line. The materials forming the terraces are Pleistocene sediments—clay, sandy silt, sand, with some gravel—of the Shirley, Chuckatuck, and Charles City Formations (Mixon and others, 2000). Although only about 1 kilometer (km) (0.62 mi) wide in the vicinity of the city, the terraces widen considerably to the south. High ridges parallel the river on both sides—Stafford Heights to the east and Marye's Heights and a series of hills, including Willis

Hill, Telegraph Hill, Howison's Hill and Prospect Hill, to the west. This western ridge curves toward the river about 6 km (3.7 mi) south of the city, forming a wide, open amphitheater. Stafford Heights is formed of the same materials as the terraces in Fredericksburg, and Marye's Heights is composed of Tertiary sands and gravels and the Cretaceous Potomac Formation (Mixon and others, 2000). The terraces are separated from Marye's Heights by a narrow band of Quaternary gravelly sand, sandy silt, and clay (primarily the Chuckatuck Formation; Mixon and others, 2000). In the vicinity of Fredericksburg, the Rappahannock is narrow but quite deep, and is treacherous to cross even at low water. During the Civil War, there were no fords or bridges downstream from Fredericksburg, and by the time the battle occurred, bridges that existed in the city before the war had been destroyed.

In the southern part of the battlefield, a low terrace about 3.2 km (2.0 mi) wide slopes uphill from the west bank of the river to the base of the ridge with a grade of about 4.5 percent. The ridge is formed primarily by the Calvert and Aquia Formations, which are mainly sand. Deep Run and Hazel Run flow across the terrace to the river. During the Civil War, the land was cultivated and ". . . much cut up by hedges and ditches" (U.S. War Department, 1888, p. 449). Other obstacles on the terrace included the main road south to Richmond, a railroad embankment, fences, ditches, and a stone wall. Trees were present only in the ravines formed by Hazel and Deep Runs and near the river (O'Reilly, 1993). In this area, the ridge, which is heavily wooded, curves toward the river and is about 60 m (200 ft) above the terrace at Prospect Hill.

The northern part of the battlefield consists of the terraces upon which Fredericksburg is located, a swampy valley to the west (herein called Kenmore valley for ease of reference) occupied by a ditch or millrace that drained the canal network in the industrial section of the city to the north, and a sloping terrace that ends against Marye's Heights. The 150-m (500-ft)-wide lower terrace is about 6 m (20 ft) above the river, and the upper terrace, about 9 m (30 ft) higher than the lower terrace and 600 m (660 yards (yd)) wide, is west of town. The millrace in Kenmore valley was about 4.5 m (15 ft) wide and between 1.5 and 1.8 m (5 and 6 ft) deep (Whan, 1961), and could be crossed by bridges that carried the main streets. The west side of the valley in this area is a steep, 6-m

[1]1408 William Street, Fredericksburg, VA 22401.

Figure 1. Map showing the distribution of major terrain features in the vicinity of Fredericksburg and the two armies on the battlefield. FP refers to the flood plain of the Rappahannock River, which, although present, is not apparent on the west side of the river at this scale. This map is based on 30-m (98-ft)-resolution digital elevation data. Terrain features having dimensions smaller than 30 m (98 ft), such as much of the flood plain on the west bank of the Rappahannock River, are therefore not shown.

(20-ft)-high bluff. The 275-m (300-yd)-wide, sloping terrace leading up to Marye's Heights has a grade of about 3 percent and consisted of open fields with isolated houses and gardens (Stackpole, 1991). Telegraph Road, a sunken road with stone walls on both sides at the time of the battle, ran parallel to Marye's Heights at the base of the ridge.

The Battle

In early November 1862, Major General Ambrose E. Burnside, recently appointed commander of the Union Army of the Potomac, proposed to take Richmond using the shortest, most direct route from Washington. This route went through the city of Fredericksburg (fig. 2). Burnside's army was located at this time near Warrenton, and the Confederate Army of Northern Virginia, commanded by General Robert E. Lee, was located on both sides of the Blue Ridge—in the Shenandoah Valley and near Culpeper. As supplies were moved south from Washington by boat and rail, the two armies moved southeast, meeting at Fredericksburg.

Burnside's army consisted of more than 110,000 men separated into three "Grand Divisions" commanded by Major Generals Edwin V. Sumner, William B. Franklin, and Joseph Hooker. When the army reached Fredericksburg between November 15 and 20, it took positions along Stafford Heights east of Fredericksburg and the Rappahannock River. Franklin was on the left flank to the south; Sumner on the right flank to the north; and Hooker, in reserve, behind Sumner (Esposito, 1959).

Lee's army consisted of two corps comprising about 80,000 soldiers commanded by Lieutenant Generals Thomas "Stonewall" Jackson and James Longstreet. When Lee realized Burnside had sent his army to Fredericksburg, he ordered Longstreet's corps to the Fredericksburg area to protect the route to Richmond and safeguard the rich agricultural area near Fredericksburg (Stackpole, 1991; O'Reilly, 2003). Both Confederate corps were in position on the ridge west of the city by December 5. Longstreet occupied the northern part of the ridge west of town opposite Sumner, and Jackson occupied the southern end of the ridge opposite Franklin (Esposito, 1959). Jackson's line extended some distance

Figure 2. Historical photograph of Fredericksburg from the east bank of the Rappahannock River, looking northwest, in 1863. The structures in the river are the supports for the railway bridge that was destroyed earlier in the war. Source: National Archives Still Photo Unit, College Park, Md.; Timothy O'Sullivan, photographer.

downriver: Lee was not sure where Burnside's attack would occur, so he extended Jackson's line to cover all possibilities.

The Battle of Fredericksburg, which occurred on December 13, 1862, has been well described in numerous books, including Whan (1961), Stackpole (1991), O'Reilly (1993), Gallagher (1995), Rable (2002), and O'Reilly (2003), in addition to Volume 21 of the Official Records (U.S. War Department, 1888), newly released in its entirety on CD-ROM. Sections on the battle can also be found in Esposito (1959) and Johnson and Buel (1956). In addition, Luvaas and Nelson (1994) have prepared an excellent guide to the battle for use with military staff rides. Because the battle is so well described in easily accessible publications, only the highlights will be described here.

Burnside intended to attack across the Rappahannock using pontoon bridges. Although ordered long in advance, the pontoons did not arrive until late November (Stackpole, 1991); crossing points were not selected until December 10, after the Confederate army was in position. Preparations for battle thus began on December 10 with the construction of pontoon bridges at three locations: two at the north end of Fredericksburg (fig. 3), one at the south end (fig. 4), and three farther south beyond Deep Run. On December 11, construc-

tion of the upper and middle pontoon bridges was disrupted by Confederate sharpshooters deployed in houses connected with trenches on the river edge of the lower terrace (Whan, 1961). The formidable Union artillery on Stafford Heights could not provide adequate protection for the engineers due to heavy fog (U.S. War Department, 1888) and because the gun crews could not depress the barrels of their cannons sufficiently. Federal artillery on Stafford Heights comprised 147 guns, many of large caliber, including 20-pounder Parrotts and 4.5 inch (in) siege rifles (O'Reilly, 2003). After the fog lifted, nine unsuccessful attempts were made to complete the upper bridges (McLaws, 1956). Eventually, volunteers forced a bridgehead, allowing the engineers to complete the bridges and the infantry to cross the river (Rable, 2002). The Confederates were slowly forced back to the upper terrace. The fierce hand-to-hand fighting along city streets and between buildings was one of the few instances of urban warfare during the Civil War (O'Reilly, 2003). Union bridge builders faced only minimal opposition during construction of the middle bridge because the terrain beyond the bluff, consisting of open fields sloping gently upward to the base of the western ridge, exposed Confederate defenders to the Union artillery on Stafford Heights. There was also little opposition

Figure 3. Historical photograph of the upper pontoon bridges at the north end of Fredericksburg, looking east toward Stafford Heights. Date unknown. Source: National Archives Still Photo Unit, College Park, Md.; Timothy O'Sullivan, photographer.

to construction of the lower bridges for the same reason—there was no cover to protect Confederate troops from the Union artillery. By nightfall on December 12, Burnside's army had crossed the Rappahannock River and was on the flood plain and on the lower terrace throughout Fredericksburg.

The Union attack began mid-morning on December 13 (McLaws, 1956). Burnside's battle plan called for Franklin to attack first and seize Prospect Hill, the right flank of Jackson's line. Once this had been accomplished, Sumner was to attack and seize Marye's Heights from Longstreet's corps. Hooker's corps was held in reserve.

Franklin's attack began about 1000 (10:00 a.m.) with an artillery barrage. One gun, a 12-pounder Napoleon (fig. 5), from Confederate Lieutenant General J.E.B. Stuart's Horse Artillery, slowed the initial infantry attack that began about an hour later by enfilading the Union line (firing on the line of advancing troops at an angle to their front) from a depression near Hamilton's Crossing (O'Reilly, 1993). Union artillery soon forced the gun to retire, but the delay allowed Jackson to clearly see the Union position (O'Reilly, 1993). The Confederate artillery, concealed by woods, withheld fire during the Union artillery barrage, and did not open fire until the advancing infantry were well within range, about 720 m (790

yd) from the Confederate guns (U.S. War Department, 1888; O'Reilly, 1993, 2003). As a result, Franklin's generals did not know exactly where the Confederate forces were when the infantry attack began. Union Major General George Meade's division spearheaded the attack, beginning about 1300. Confederate artillery fire from three sides funneled the Union infantry toward dense woods in the center of the Confederate line. Jackson had assumed the woods were impenetrable, and as a result, they were inadequately defended. Meade was thus able to penetrate the Confederate line at this point. He was unable to hold the position (Smith, 1956), even with support from a second division, and his forces were eventually pushed back. About 1430, Franklin received orders to attack with his entire force (Whan, 1961). Franklin's new attack was to serve as a diversion to the heavy fighting west of town (Whan, 1961). Franklin had already deployed in a defensive position (O'Reilly, 2003), so was unable to provide relief for Sumner.

Burnside ordered Sumner to attack the Confederate position west of Fredericksburg shortly after 1030 (Whan, 1961), regardless of his earlier orders and without knowing the status of Franklin's attack. He merely assumed that Franklin had been successful and that Lee had weakened his left flank to support his right (Freeman, 1943). Burnside should have known this was not the case, because by this time the fog had

Figure 4. Photograph showing the location of the former middle pontoon bridge at the south end of Fredericksburg. Ferry Farm, boyhood home of George Washington, is above the open grassy area on the opposite side of the river.

Figure 5. Cast bronze "Light" 12-pounder gun-howitzer, or Napoleon, at Howison's Hill. This gun was made in 1864 by James R. Anderson and Co., Tredegar Foundry, Richmond, Va. (Hazlett and others, 1988). Although cast long after the battle, this gun is virtually identical to Napoleons that would have been used during the Battle of Fredericksburg.

Figure 6. Historical photograph of Hanover Street looking west across the Kenmore valley. One of the bridges used by Union infantry can be seen in the center of the photo (x). Source: National Archives Still Photo Unit, College Park, Md.; Matthew Brady studio, photographers.

lifted and reports from his reconnaissance balloons above Stafford Heights would have indicated that Lee had not done so. Longstreet expected the main attack to occur on his right near Telegraph Hill, which was Lee's headquarters (Luvaas and Nelson, 1994), but the attack was made against his center along the base of Marye's Heights.

Union infantry marshalled in the city and on the upper terrace about 550 m (600 yd) from the base of Marye's Heights. The advance was slowed by the millrace in Kenmore valley; the water was deep, covered by ice, and surrounded by marshy ground, and the walls of the millrace were lined with stone and with wooden boards (O'Reilly, 2003), so the only practical crossing points were the road bridges (Couch, 1956; fig. 6). This funneled the infantry toward the sunken part of Telegraph Road along the base of Marye's Heights (fig. 7) and considerably restricted troop movements (U.S. War Department, 1888). As the Union skirmishers approached Marye's Heights, they were hit by a wall of musket fire from the sunken road which they were unable to see (U.S. War Department, 1888; McLaws, 1956; Whan, 1961), and were forced back. Six attempts were made to take the Confederate position (Longstreet, 1956), but all failed, in part because of the difficulties caused by the terrain—that is, crossing the millrace.

At the end of the day, Union and Confederate infantry in the southern sector of the battlefield occupied the same positions they had occupied at the beginning of the day. West of town, Sumner's infantry spent the night where they lay. Lee did not counterattack for several reasons. First, it was dark, and he expected Burnside to renew his attack the next day, so he did not want to lose his good defensive positions. Second, he was well aware of the devastation his army would face from the Union artillery on Stafford Heights if he did attack. Burnside, however, did not attack on December 14, although heavy skirmishing occurred throughout the day on both flanks. He in fact moved most of his army back from the front line and continued to fortify the city. Both armies now maintained defensive postures. The next day, Burnside requested a truce to care for the wounded and bury the dead. That night he moved his army across the Rappahannock under cover of a violent storm and removed the pontoon bridges (Freeman, 1943). On the morning of December 16, Lee was surprised to see no Union troops on the western side of the river, and knew then that although the battle was a defensive victory for the Army of Northern Virginia, it had gained them nothing. Although damaged, Burnside's army was still intact and in position on Stafford Heights.

Figure 7. Photograph of Telegraph Road, the sunken road, looking south. The wall on the left behind the fence is the only section of the original wall still extant.

Effective Use of Terrain

Terrain was a crucial factor in the progress and outcome of the Battle of Fredericksburg. The favorable terrain was under Confederate control, whereas the terrain over which the Union infantry advanced was generally disadvantageous. As the battle progressed on December 13, the balance for the Confederates shifted from more vulnerable terrain south of Fredericksburg to superior terrain below Marye's Heights west of Fredericksburg. The southern terrain was heavily defended, but here the Union forces had some freedom of movement and protection from Confederate infantry and artillery fire. The terrain below Marye's Heights was less heavily defended, but Union forces in this area had no room to maneuver and little protection from Confederate fire. The main Union advantage in both sectors of the battlefield was the formidable heavy artillery on Stafford Heights (Rable, 2002; O'Reilly, 2003).

Lee's Army of Northern Virginia occupied a defensive position on high ground, and Burnside's Army of the Potomac was forced to attack uphill over lower ground. In addition, Union troops had numerous obstacles to negotiate—not least of which was the Rappahannock River. On Burnside's left flank, these included, in addition to the river, the open nature of the terrace and deep ravines, numerous hedges and ditches in the open farmland, a railroad embankment, and the Richmond Road. In addition, the curved shape of the ridge gave Confederate artillery good positions for enfilading fire. On Burnside's right flank the most significant obstacles, in addition to the river and the city itself, were the frozen millrace; limited space for troop deployments; the smooth, open ground below Marye's Heights; numerous fences, houses and gardens; marshy areas both north and south of the main point of attack; the shape of the ridge that allowed Confederate enfilading fire; and most important, the sunken road and its stone walls.

Stackpole (1991) contends that the tactical Confederate success at Fredericksburg was based on Lee's ". . . keen sense of terrain appreciation" (p. 172). Lee took a defensive position because ". . . the natural features of the ground were made to order for the purpose . . ." (p. 271). Lee's judgment, confidence, and effective use of terrain, coupled with Burnside's incompetence, indecision, and limited knowledge of the battlefield, appear to have been instrumental factors controlling the battle which thus contributed in no small part toward the final outcome.

Acknowledgments

References Cited

Couch, D.N., 1956, Sumner's "Right Grand Division," *in* Johnson, R.U., and Buel, C.C., eds., Battles and leaders of the Civil War; v. 3, Retreat from Gettysburg: New York, Castle Books, p. 105–120.

Ehlen, J., and Abrahart, R.J., 2002, Effective use of terrain in the American Civil War; The Battle of Fredericksburg, December 1862, *in* Doyle, P., and Bennett, M.B., eds., Fields of battle; Terrain in military history: Dordrecht, The Netherlands, Kluwer Academic Publishers, p. 63–97.

Esposito, Col. V.J., 1959, The West Point atlas of American wars; v. 1, 1689–1900: New York, Frederick A. Praeger Publishers, Maps 70–73.

Freeman, D.S., 1934, R.E. Lee, a biography; v. 2: New York, Charles Scribner's Sons, p. 415–474.

Freeman, D.S., 1943, Lee's lieutenants; v. 2, Cedar Mountain to Chancellorsville: New York, Charles Scribner's Sons, p. 269–396.

Gallagher, G.W., ed., 1995, The Fredericksburg campaign; Decision on the Rappahannock: Chapel Hill, N.C., The University of North Carolina Press, 243 p.

Hazlett, J.C., Olmstead, E., and Parks, M.H., 1988, Field artillery weapons of the Civil War (2d ed.): Newark, Del., University of Delaware Press, 322 p.

Johnson, R.U., and Buel, C.C., eds., 1956, Battles and leaders of the Civil War; v. 3, Retreat from Gettysburg: New York, Castle Books, p. 70–147.

Longstreet, J., 1956, The Battle of Fredericksburg, *in*

Johnson, R.U., and Buel, C.C., eds., Battles and leaders of the Civil War; v. 3, Retreat from Gettysburg: New York, Castle Books, p. 70–85.

Luvaas, J., and Nelson, H.W., eds., 1994, Guide to the Battles of Chancellorsville and Fredericksburg: Lawrence, Kans., University of Kansas Press, p. 1–128.

McLaws, L., 1956, The Confederate Left at Fredericksburg, *in* Johnson, R.U., and Buel, C.C., eds., Battles and leaders of the Civil War; v. 3, Retreat from Gettysburg: New York, Castle Books, p. 86–94.

Mixon, R.B., Pavlides, L., Powars, D.S., Froelich, A.J., Weems, R.E., Schindler, J.S., Newell, W.L., Edwards, L.E., and Ward, L.W., 2000, Geologic map of the Fredericksburg 30' x 60' quadrangle, Virginia and Maryland: U.S. Geological Survey Geologic Investigations Series Map I–2607, 2 sheets and pamphlet, scale 1:100,000.

O'Reilly, F.A., 1993, "Stonewall" Jackson at Fredericksburg; the Battle of Prospect Hill, December 13, 1862 (2d ed.): Lynchburg, Va., H.E. Howard, Inc., 243 p.

O'Reilly, F.A., 2003, The Fredericksburg campaign; Winter war on the Rappahannock: Baton Rouge, La., Louisiana State University Press, 630 p.

Rable, G.C., 2002, Fredericksburg! Fredericksburg!: Chapel Hill, N.C., The University of North Carolina Press, 671 p.

Reardon, C., 1995, The forlorn hope; Brig. Gen. Andrew A. Humphreys's Pennsylvania Division at Fredericksburg, *in* Gallagher, G.W., ed., The Fredericksburg campaign; Decision on the Rappahannock: Chapel Hill, N.C., The University of North Carolina Press, p. 80–112.

Smith, W.F., 1956, Franklin's "Left Grand Division," *in* Johnson, R.U., and Buel, C.C., eds., Battles and leaders of the Civil War; v. 3, Retreat from Gettysburg: New York, Castle Books, p. 128–138.

Stackpole, E.J., 1991, The Fredericksburg campaign (2d ed.): Mechanicsburg, Pa., Stackpole Books, 312 p.

U.S. War Department, 1888, The war of the rebellion; A compilation of the official records of the Union and Confederate Armies: Washington, Government Printing Office, Series 1, v. 21, 1280 p.

Whan, V.E., Jr., 1961, Fiasco at Fredericksburg: Gaithersburg, Md., Olde Soldiers Books, Inc., 159 p.

ROAD LOG AND STOP DESCRIPTIONS FOLLOW
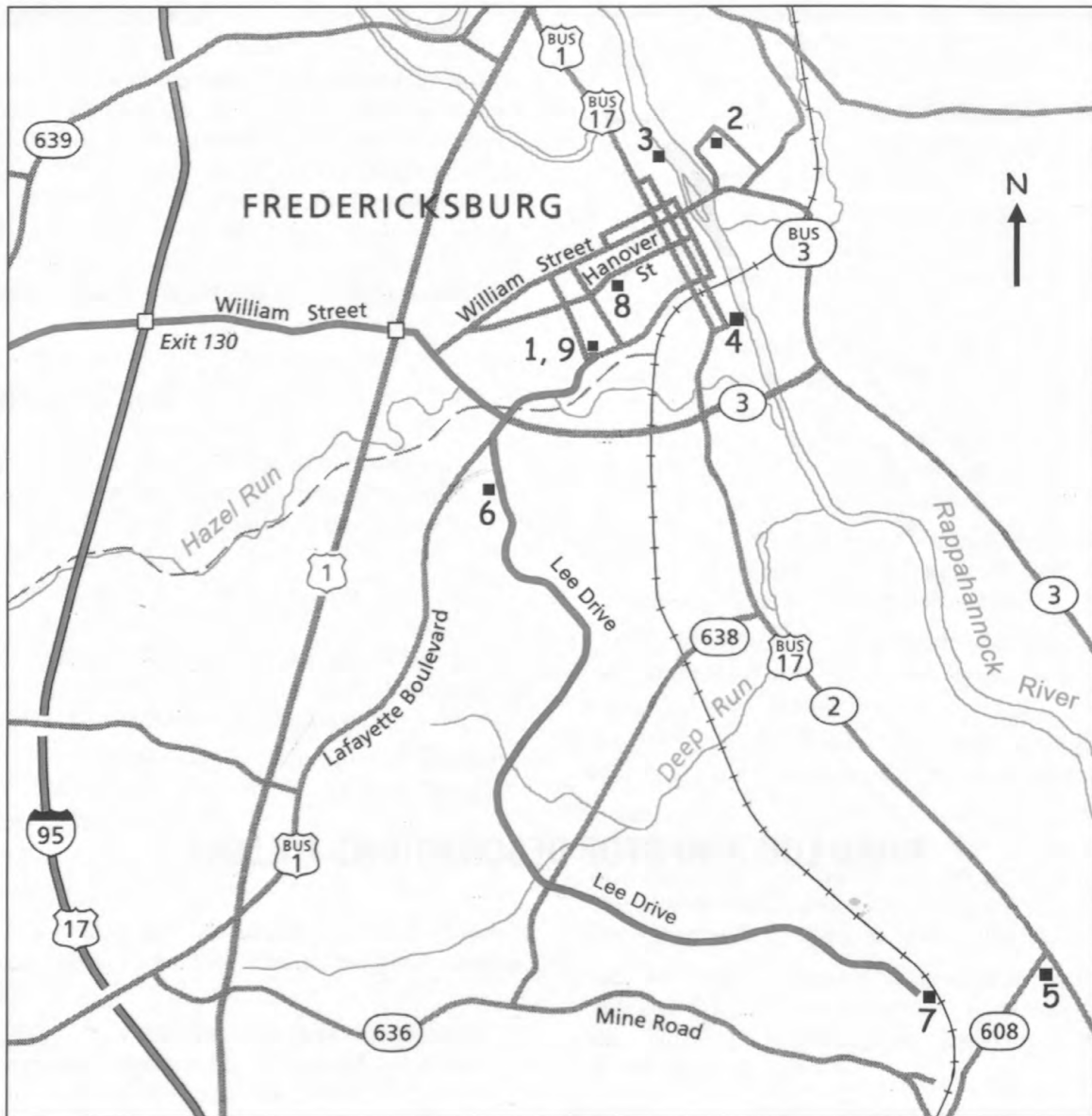
Figure 8. Map of the Fredericksburg area showing field trip stops. Modified from map in the National Park Service battlefield brochure.

Road Log and Stop Descriptions

See figure 8 for field-trip stop locations.

Take I-95 South from the Capital Beltway, I-495.

Mileage

Incremental	Cumulative	
0.0	0.0	Take Exit 130-A (Fredericksburg) onto Va. 3 East; turn left on Lafayette Boulevard.
2.5	2.5	Park and go to Visitor Center.

Stop 1. Visitor Center, Fredericksburg and Spotsylvania National Military Park.

View the park video and visit the museum. Restrooms available.

Mileage

Incremental	Cumulative	
		Turn left on Lafayette Boulevard.
		Go nine blocks and turn left on Caroline Street.
		Go five blocks and turn right on William Street.
		Cross the river, then turn left on Chatham Heights Road.
1.8	4.3	Following brown signs to Chatham Manor, turn left on Chatham Lane.
		Caroline Street in this area is on the lower terrace.

Stop 2. Chatham Manor, Fredericksburg and Spotsylvania National Military Park Headquarters.

Chatham Manor, located on Stafford Heights and the home of the Lacy family, was General Sumner's headquarters during the battle. The Union army had heavy artillery deployed along Stafford Heights, which commanded the battlefield, from Falmouth to just across the river from the Confederate right flank. One hundred forty-seven heavy guns were deployed in four sections (Rable, 2002; O'Reilly, 2003). The location of the former upper pontoon bridges is clearly visible from the terraces on the river side of the house. Restrooms available.

Mileage

Incremental	Cumulative	
		Exit Chatham Manor and turn left on River Road.
		Turn right on Va. 3 (William Street), crossing the river.
		Turn right on Sophia Street.
0.9	5.2	Go four blocks to the historical marker on the right. River Road is on the flood plain of the Rappahannock and Sophia Street is on the lower terrace.

Stop 3. Upper Pontoon Bridge crossing.

There were three pontoon bridge sites across the Rappahannock River. This upper crossing (fig. 3), which consisted of two bridges, was the most strongly contested by the Confederate army. Sharpshooters positioned themselves in houses and in basements along the edge of the lower terrace, and defeated nine attempts by Union engineers to complete

construction of the pontoon bridge. The Union artillery on Stafford Heights was unable to depress the barrels of the guns sufficiently to fire upon the sharpshooters and provide cover for the bridge builders. The tenth attempt, carried out by volunteers, was successful, and Union infantry were able to cross the river during the night of December 11. This was the first bridgehead landing ever secured under fire by U.S. forces (O'Reilly, 2003). Once Union troops crossed the river, they had to traverse the very small flood plain in this area under fire, and force themselves up the 10-m (33-ft)-high bluff to the lower terrace. The Confederate sharpshooters—Barksdale's Mississippians—withdrew slowly from the terrace edge, which resulted in fierce hand-to-hand fighting in this area of the city. This was one of the few occurrences of urban warfare in the Civil War.

Mileage

Incremental	Cumulative	
		Continue north one block on Sophia Street.
		Turn left on Pitt Street.
		Go two blocks and turn left on Princess Anne Street.
		Turn left on Frederick Street.
		Go one block and turn right on Sophia Street.
1.3	6.5	Proceed to the Public Boat Landing (City Dock; dead end).

Stop 4. Middle Pontoon Bridge crossing.

This is the flood plain of the Rappahannock River, with the lower terrace to the west. Although the terrain in this area provided superior defensive positions for Confederate sharpshooters, bridge building was not strongly opposed, because the terrain above and west of the bluff was exposed to the full firepower of Union artillery on Stafford Heights across the river. One bridge was built in this location (fig. 4). This area also was the location of the historic ferry crossing from Stafford County to the city of Fredericksburg. Ferry Farm, from which the ferry crossed, was the boyhood home of George Washington. It is said that the cherry tree incident occurred on Ferry Farm and that it was really this part of the Rappahannock across which George Washington threw his dollar, not the Potomac River.

Mileage

Incremental	Cumulative	
		Go north one block on Sophia Street.
		Turn left on Frederick Street.
		Go three blocks and turn left on Charles Street.
		Turn right on Dixon Street (Va. 2 and U.S. Bus. 17), which becomes Tidewater Trail.
		Turn right on Va. 608, Benchmark Road.
4.0	10.5	Pull into the gravel lane immediately on the left.

On the horizon to your right as you drive south along Tidewater Trail is the ridge upon which the Confederate army was deployed. At the time of the Civil War, the terrace to the right was treeless and used for farming.

Stop 5. "The Gallant Pelham."

Grove of cedar trees from which "The Gallant Pelham" (Major John Pelham, commander of Stuart's Horse Artillery) distracted the Union army at the beginning of Franklin's attack against Jackson's position along the ridge to the west. Pelham received this sobriquet from Lee because of his action here. Pelham's fire, initially with only one gun, a 12-pounder Napoleon (fig. 5), delayed the Union attack and also revealed the Union

position to Jackson, giving him an even greater advantage than what he derived from his excellent position. As a result, Jackson was able to withhold both his artillery and small arms fire until the Union infantry were well within range, giving the Confederate army a significant advantage in this part of the battle.

Mileage

Incremental	Cumulative	
		Turn right on Va. 608.
		Turn left on Tidewater Trail/Dixon Street (Va. 2 and U.S. Bus. 17).
		At first stop light after going under the Va. 3 overpass, turn left on Charles Street.
		At next stop light, turn left on Lafayette Boulevard.
5.1	15.6	Turn left at the brown National Park sign (Lee Drive).

Stop 6. Lee's Hill.

This was Lee's headquarters during the battle (National Park driving tour stop 2). From this point in the center of the Confederate lines, he could clearly view action on both flanks. It was here that he made his famous statement, "It is well that war is so terrible - we should grow too fond of it" (Freeman, 1934, p. 462). At the time of the Civil War, this hill was called Telegraph Hill. The two cannons beyond the shelter serve as examples of artillery pieces that might have been used during the battle. The 30-pounder Parrott rifle on the left would most likely not have been present on the battlefield; Parrotts used in the field were typically 10-pounders. Parrott rifles represented state-of-the-art, cutting-edge technology in 1862. They were first introduced in 1861 and were the first American rifled cannon. They were also the first truly successful rifled cannon because of the method used for reinforcement. The cannon on the left is a smoothbore "Light" 12-pounder gun-howitzer, or Napoleon (fig. 5). This was the most common weapon in northern arsenals, and the preferred smoothbore cannon for both Union and Confederate armies.

Mileage

Incremental	Cumulative	
4.5	20.1	Continue south on Lee Drive.

Stop 7. Prospect Hill.

This was the far right flank of Jackson's line. Meade's attack came from the east toward the left where the woods reach the railway track. The pyramidal monument in the distance was built by railroad men in honor of this attack. Meade's men advanced through the woods and up the hill to your left before they were stopped and then pushed back. The artillery positions in this area are typical of artillery positions of the time, and the cannon displayed are also typical. These include, from right to left facing east, an iron 3-in ordnance rifle, which was the most popular rifle in Union artillery batteries during the war; a bronze 14-pounder James rifle (fig. 9); and two bronze 6-pounders. Six-pounders were the most common Confederate artillery pieces. They were relatively ineffective against Napoleons and Union rifles, however, because of their short range. A number of six-pounders, including these two, were thus returned to the foundries for rifling in the hope that this would increase their effectiveness. Any such increase did not last long, however, because the lands and grooves wore down too rapidly due to the twisting action of the projectiles in the barrels.

Figure 9. Cast bronze 14-pounder (3.8-in) James rifle at Prospect Hill. This gun was made in 1861 by Ames Co., Chicopee, Mass. (Hazlett and others, 1988).

Return to Lafayette Boulevard, viewing entrenchments on the right (east) side of Lee Drive.

The first organized use of "hasty" entrenchments in warfare occurred during the Battle of Fredericksburg in this area (Luvaas and Nelson, 1994). Prior to this time, entrenchments were built only around permanent fortifications. The landscape to the east just before crossing Lansdown Road is considered to be very similar to the landscape in the area at the time of the battle.

Mileage

Incremental	Cumulative	
		Turn right on Lafayette Boulevard.
		Turn left on Kenmore Avenue.
6.2	26.3	Go four blocks and park just before the stop light on Hanover Street.

Stop 8. Kenmore valley.

You are now in the Kenmore valley in the vicinity of the millrace. To the east is the upper terrace; this is the direction from which the Union army advanced on Marye's Heights. The bridge in figure 6 must have been very near this spot. Just beyond Kenmore Cleaners on your right is the bluff beneath which Union infantry found cover after crossing the millrace. Because the area was swampy and the millrace was covered with ice, the only feasible crossing points were bridges on Hanover, William, and Prussia Streets (O'Reilly, 2003). At the time of the battle, the area west of the bluff was open, with scattered houses and fences. Other than the small bluff and a swale that extended across the front, there was no cover for the attacking Union infantry. Crossing Kenmore valley at this point, however, was far better than to the north where swampy areas were more extensive. The area to the north was also crossed by numerous canals, which would have complicated traversing the swamp even more.

Mileage

Incremental	Cumulative

		Turn left on Lee Avenue (almost a U-turn).
		Go one long block and turn right on Charlotte Street.
		Go two blocks and turn left on Littlepage Street.
		Go two blocks and turn right on Lafayette Boulevard.
0.5	26.8	Turn right into the National Park Visitor Center parking lot.

The area you are driving through is the ground over which the Union army advanced. Littlepage Street marks the approximate location of the swale.

Stop 9. Visitor Center, Fredericksburg and Spotsylvania National Military Park.

This area below Marye's Heights was the focus of Major General Sumner's "Grand Division's" attack on Longstreet's corps. The foundations of several houses are preserved, and one house from the 1860s still stands. The wall along the north end of the sunken road is the only part of the original wall extant (fig. 7). Confederate infantry and artillery were deployed along the top of the ridge, and additional infantry, several men deep, were behind the stone wall. Union infantry advanced across the open fields, and most attacks got no closer than 100 m (110 yd) to the Confederate line. One bayonet charge, that of Humphrey's Division, did get within about 25 m (80 ft), resulting in hand-to-hand fighting (Reardon, 1995). The Marye House of Civil War fame is now Brompton, the home of the president of Mary Washington College. Confederate infantry repulsed six attacks on their position during the battle. The National Cemetery just west of the Visitor Center is located on Willis Hill, from which the best views of the city and this part of the battlefield can be obtained. Restrooms available.

> Turn right out of the parking lot onto Lafayette Boulevard.
> Turn right on Va. 3 (Blue-Gray Parkway).
> Turn right onto I-95 North and return to Northern Virginia.

9. Tertiary Lithology and Paleontology, Chesapeake Bay Region

By Lauck W. Ward[1] and David S. Powars[2]

Introduction

Tertiary beds exposed along the Chesapeake Bay and Potomac River southeast of Washington, D.C., have been studied since the early 1800s. Because of their relative proximity to that city, where both the U.S. Geological Survey and the Smithsonian Institution are housed, many geologists and paleontologists have worked on the stratigraphy and fossils. Most of the earliest efforts were taxonomic ones, but Rogers (for a summary see Rogers, 1884) described the Paleocene and Eocene deposits of Virginia. Later work by Darton (1891) drew from these earlier investigations and he proposed the primary lithic division of Coastal Plain sediments in Virginia and Maryland. The term "Pamunkey Formation" was proposed for the glauconitic units, and the overlying shelly sands and marls were named the "Chesapeake Formation." Since then, a steady refinement of the units has led to the present stratigraphic framework.

Geologic Setting

Stratigraphic units exposed in the Chesapeake Bay area consist of Mesozoic and Cenozoic Coastal Plain beds deposited in a tectonic downwarp known as the Salisbury embayment (fig. 1). The Salisbury embayment includes parts of Virginia, Maryland, Delaware, and southern New Jersey and is bordered on the north and south by the South New Jersey arch and the Norfolk arch, respectively. Subsurface data indicate that these arches are characterized by stratigraphic thinning or truncation of formations of Cretaceous and Tertiary age. The basement complex underlying the embayment includes Precambrian and Paleozoic age crystalline rocks and Mesozoic age rift-basin fill. The Salisbury embayment was the site of intermittent marine overlap and deposition during the Early and Late Cretaceous and most of the Tertiary. Beds are of fluvial, deltaic, and open-shelf origin and were deposit-

ed in a wedge-like configuration with their thin, westward edge overlapping the Piedmont. To the east, the Coastal Plain deposits thicken to several thousand feet.

The lithology, thickness, and dip of the various formations deposited in the Salisbury embayment are, to a great extent, structurally controlled. This tectonism occurred at several local and regional scales. Tectonism on a regional scale involved tilting of the entire Atlantic continental margin. Of lesser importance was the independent structural movement of the various basins, or depocenters, and the intervening arches, or high areas. These high and low areas moved independently of each other, creating a stratigraphic mosaic that is unique from basin to arch. Various tectonic models include block faulting and possible movement of the landward portions of the Coastal Plain. Parts of oceanic transform faults have been suggested as causes for the arch-basin configuration. Variations in the distribution and thickness of Cretaceous and Tertiary deposits also suggest the gradual migration of basins through time. Other structural deformation in the Salisbury embayment consists of localized, downdropped grabens that occur along northeast-trending lineaments. These grabens are related to early Mesozoic rifting and caused certain areas to be unstable. These areas were reactivated during the Cretaceous and Tertiary, possibly due to sediment loading. The presence of the grabens resulted in structural highs behind which finer sediments accumulated. Thus, each of these various structural elements contributed to the overall depositional patterns on the Coastal Plain and in the Salisbury embayment.

Lower Tertiary deposits consist of glauconitic silty sands containing varying amounts of marine shells. The Tertiary beds are principally marine-shelf deposits. Fluvial, deltaic, and nearshore-shelf facies are generally lacking. The same is true for the upper Tertiary marine beds, which consist of diatomaceous silts and silty and shelly sands. However, sands and gravels of fluvial and deltaic origin cap most of the higher inteffluves in the Salisbury embayment area and are thought to be Miocene, Pliocene, and (or) Pleistocene.

The Salisbury embayment had a warm-temperate to subtropical marine setting throughout much of its history. During the late Tertiary, a portion of the temperate molluscan fauna became endemic. Abrupt cooling in the late Pliocene caused a major local extinction involving these taxa that had been successful since the Oligocene.

[1]Virginia Museum of Natural History, Martinsville, VA 24112.

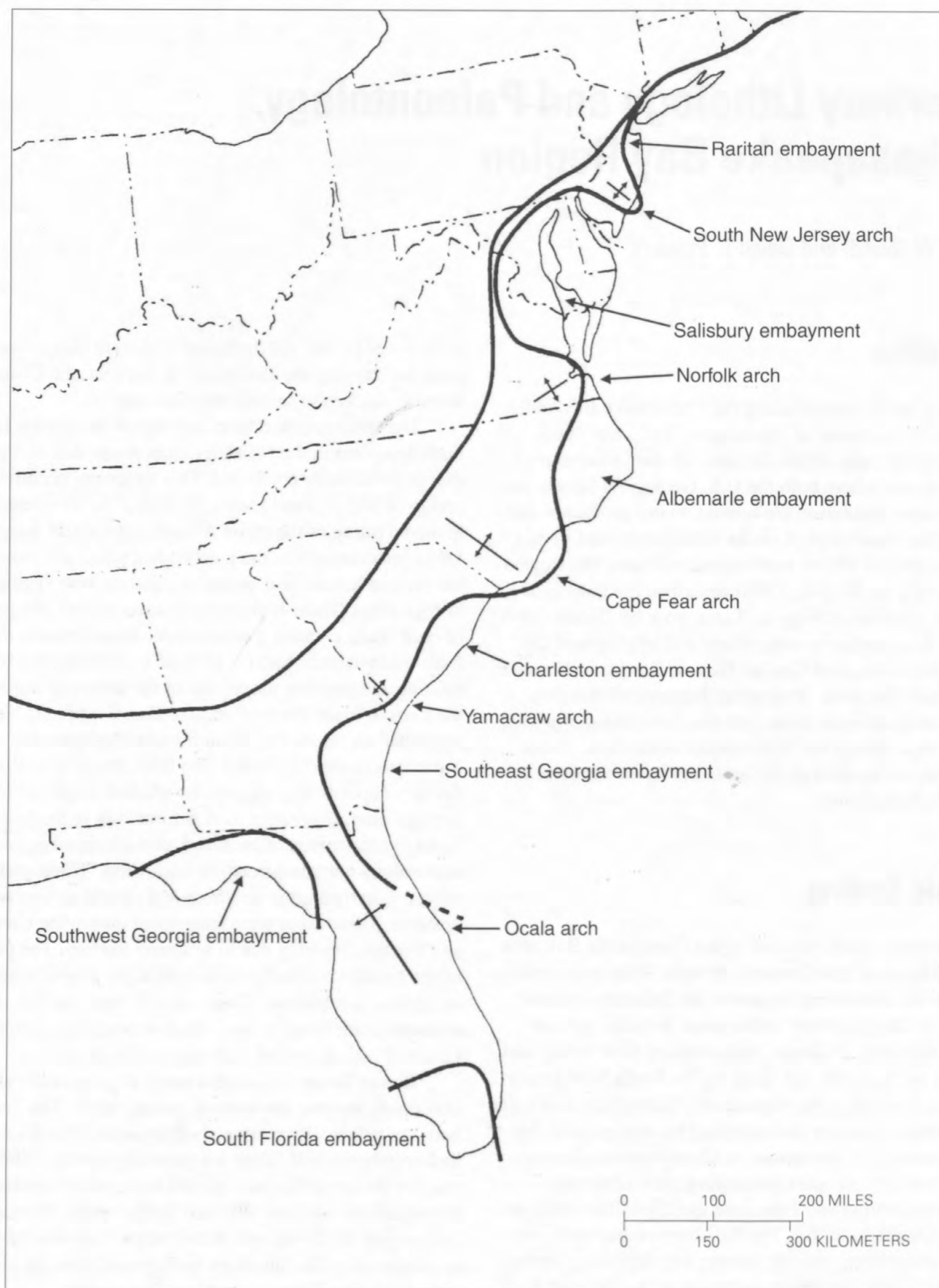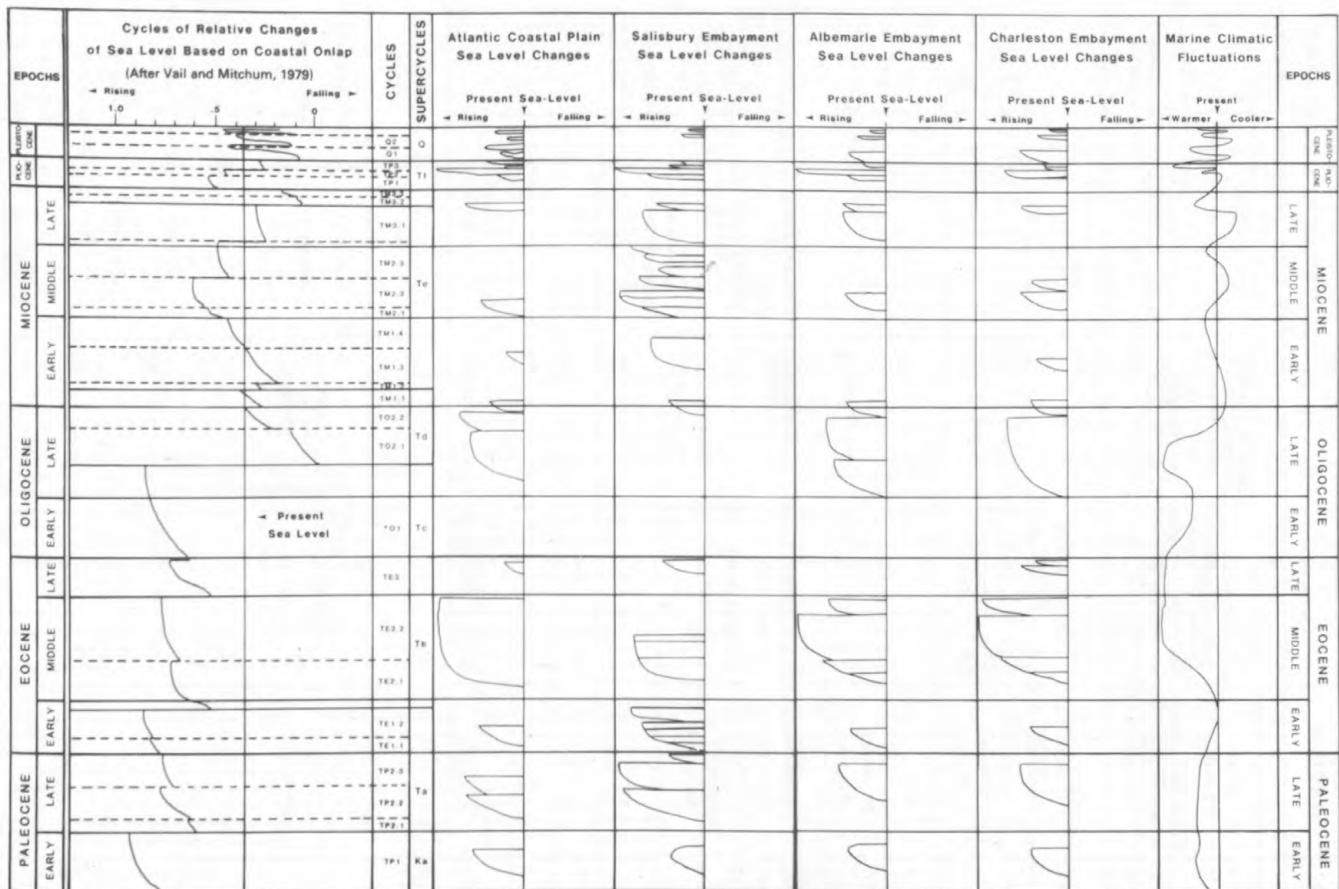[2]U.S. Geological Survey, Reston, VA 20192.

Figure 1. Map showing principal basins and arches of the Atlantic Coastal Plain.

Figure 2. Onlap-offlap history of the Atlantic Coastal Plain, based on onshore outcrop and subsurface data. Sea-level fluctuations in the Salisbury, Albemarle, and Charleston embayments are plotted against a chart of cycles and supercycles by Vail and Mitchum (1979). Data from the basins are combined to approximate global sea-level events as seen along the Atlantic Coastal margin. The marine climate curve represents conditions in the Salisbury embayment and is based on data from fossil molluscan assemblages.

Tertiary History of the Salisbury Embayment

The Salisbury embayment and the entire Atlantic Coastal Plain have had a complex history. In contrast to "passive margin" descriptions, this was a structurally dynamic area whose sedimentary history clearly shows the effects of structural movement as well as of global sea-level events. To identify and eliminate local tectonic "noise" and detect actual global sea-level changes, one must compare the detailed stratigraphic records of several embayments. In figure 2, the sea-level curves of three principal Atlantic Coastal Plain basins (Salisbury embayment, Albemarle embayment, and Charleston embayment) are summarized. A fourth curve for the Atlantic Coastal Plain combines the data obtained in the three basins and attempts to show the actual record of sea-level fluctuations. These curves are plotted against the cycles and supercycles of Vail and Mitchum (1979). The curves are based on our interpretations of onshore outcrop and subsurface data. We have made no attempt to plot sea-level changes beyond the pres-

ent coastline. The following trends occur and are based on the onlap relations of formations in the three basins.

Paleocene

In the middle early Paleocene, there is agreement for a moderately strong marine pulse. This pulse is evidenced by the Brightseat Formation in the Salisbury embayment (figs. 3, 4A), the Jericho Run Member of the Beaufort Formation in the Albemarle embayment, and the Black Mingo Formation in the Charleston embayment. Another strong onlap sequence occurred during the late Paleocene and lasted almost that entire period. In the Salisbury embayment, beds associated with the event are included in the Aquia Formation (fig. 4B). There are at least two recognizable sea-level pulses, represented by the Piscataway and Paspotansa Members, involved in that sequence. A final small transgression, probably only in the Salisbury embayment, resulted in the deposition of the Marlboro Clay (fig. 4C).

SERIES	STAGE		NEW JERSEY	DELAWARE	MARYLAND	VIRGINIA	NORTH CAROLINA	SOUTH CAROLINA	GEORGIA	ALABAMA
PLEISTOCENE				Columbia Formation	Columbia Formation	Norfolk Formation	Norfolk Formation	Socastee Formation / Canepatch Formation		
PLIOCENE							James City Formation / Waccamaw Formation	Waccamaw Formation		
	UPPER					Chowan River Formation	Chowan River Formation	Bear Bluff Formation / Goose Creek Limestone		Citronelle Formation
	LOWER					Yorktown Formation	Yorktown Formation	Raysor Formation	Raysor Formation	
MIOCENE	UPPER	MESSINIAN			Cobham Bay Member	Cobham Bay Member	Cobham Bay Member			
		TORTONIAN			Eastover Formation / Claremont Manor Member	Eastover Formation / Claremont Manor Member	Eastover Formation / Claremont Manor Member			
	MIDDLE	SERRAVALIAN			St. Marys Formation "Windmill Point Mbr." "Little Cove Point Mbr." Conoy Member Boston Cliffs Mbr. St. Leonard Mbr. Drumcliff Mbr.	St. Marys Formation		Coosawhatchie Clay Member	Coosawhatchie Clay	
		LANGHIAN	Cohansey Formation	Choptank Formation	Choptank Formation	Choptank Formation	Pungo River Formation		Marks Head Formation	
	LOWER	BURDIGALIAN	Kirkwood Formation	Calvert Formation / Kirkwood Formation	Calvert Formation / Calvert Beach Mbr. / Plum Point Member / Fairhaven Member	Calvert Formation		Hawthorn Formation	Hawthorn Formation	
		AQUITANIAN	Old Church(?) Formation	Old Church(?) Formation	Old Church Formation	Old Church Formation	Belgrade Formation / Pollocksville Mbr. / Haywood Landing Mbr.	Edisto Formation	Tampa Formation	
OLIGOCENE	UPPER	CHATTIAN / CHICKASAWHAN					River Bend Formation	Cooper Marl / Ashley Member	Suwannee Limestone	Chickasawhay Limestone
	LOWER	RUPELIAN / VICKSBURGIAN							Bridgeboro Limestone	Bryam Formation
										Marianna Limestone
									Bumpnose Limestone	Red Bluff Formation

Figure 3. *Continued.*

EOCENE / PALEOCENE				Formations
EOCENE	UPPER	PRIABONIAN	JACKSONIAN	Chickahominy Formation · Chickahominy Formation · Cooper Marl · Parkers Ferry Mbr. / Harleyville Member · Sandersville Limestone / Twiggs Clay / Tivola Limestone · Ocala Limestone
EOCENE	MIDDLE	BARTONIAN	CLAIBORNIAN	Piney Point Formation · Piney Point Formation · Piney Point Formation · Castle Hayne Formation (Spring Garden Member, Comfort Member, New Hanover Member) · Santee Limestone · Cross Member / Moultrie Member · Gosport Sand / Lisbon Formation · Gosport Sand / Lisbon Formation
EOCENE	MIDDLE	LUTETIAN	CLAIBORNIAN	Tallahatta Formation · Tallahatta Formation
EOCENE	LOWER	YPRESIAN	SABINIAN	Shark River Formation / Manasquan Formation · Nanjemoy Formation (Woodstock Member, Potapaco Member) · Fishburne Formation · Hatchetigbee Formation · Hatchetigbee Formation
PALEOCENE	UPPER	THANETIAN	SABINIAN / MIDWAYAN	Marlboro Clay · Aquia Formation (Paspotansa Member, Piscataway Member) · Beaufort Formation · Tuscahoma Formation / Nanafalia Formation · Tuscahoma Formation / Nanafalia Formation / Naheola Formation
PALEOCENE	UPPER	THANETIAN	MIDWAYAN	Vincentown Formation · Vincentown Formation · Black Mingo Formation · Porters Creek Clay · Porters Creek Clay
PALEOCENE	LOWER	DANIAN	MIDWAYAN	Hornerstown Formation · Hornerstown Formation · Brightseat Formation · Brightseat Formation · Beaufort Formation / Jericho Run Member · Clayton Formation · Clayton Formation

A

Middle early Paleocene   Brightseat Formation

B

Late Paleocene   Aquia Formation

C
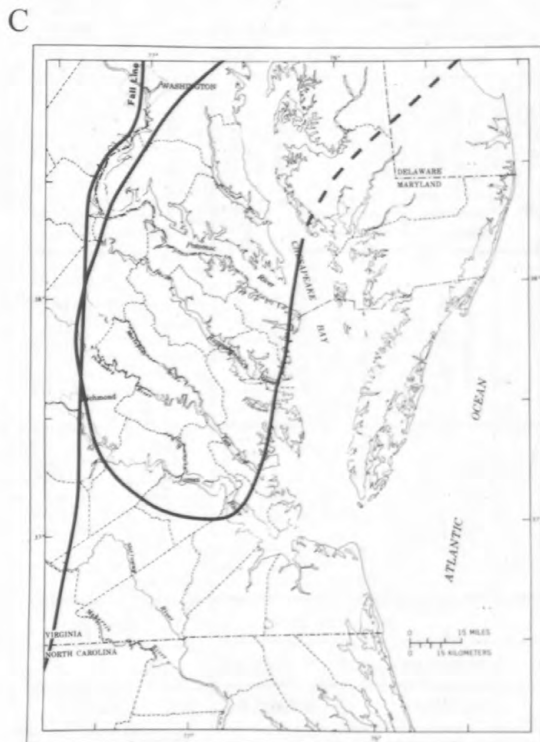
Late Paleocene   Marlboro Clay

Figure 4. Maps showing depositional basins in the Salisbury embayment during the Paleocene. Dashed lines indicate areas where boundary data are lacking.

A

Early Eocene   Nanjemoy Formation
                                Potapaco Member

B

Late Eocene   Nanjemoy Formation
                                Woodstock Member

C

Middle Eocene   Piney Point Formation

D

Late Eocene   Chickahominy Formation
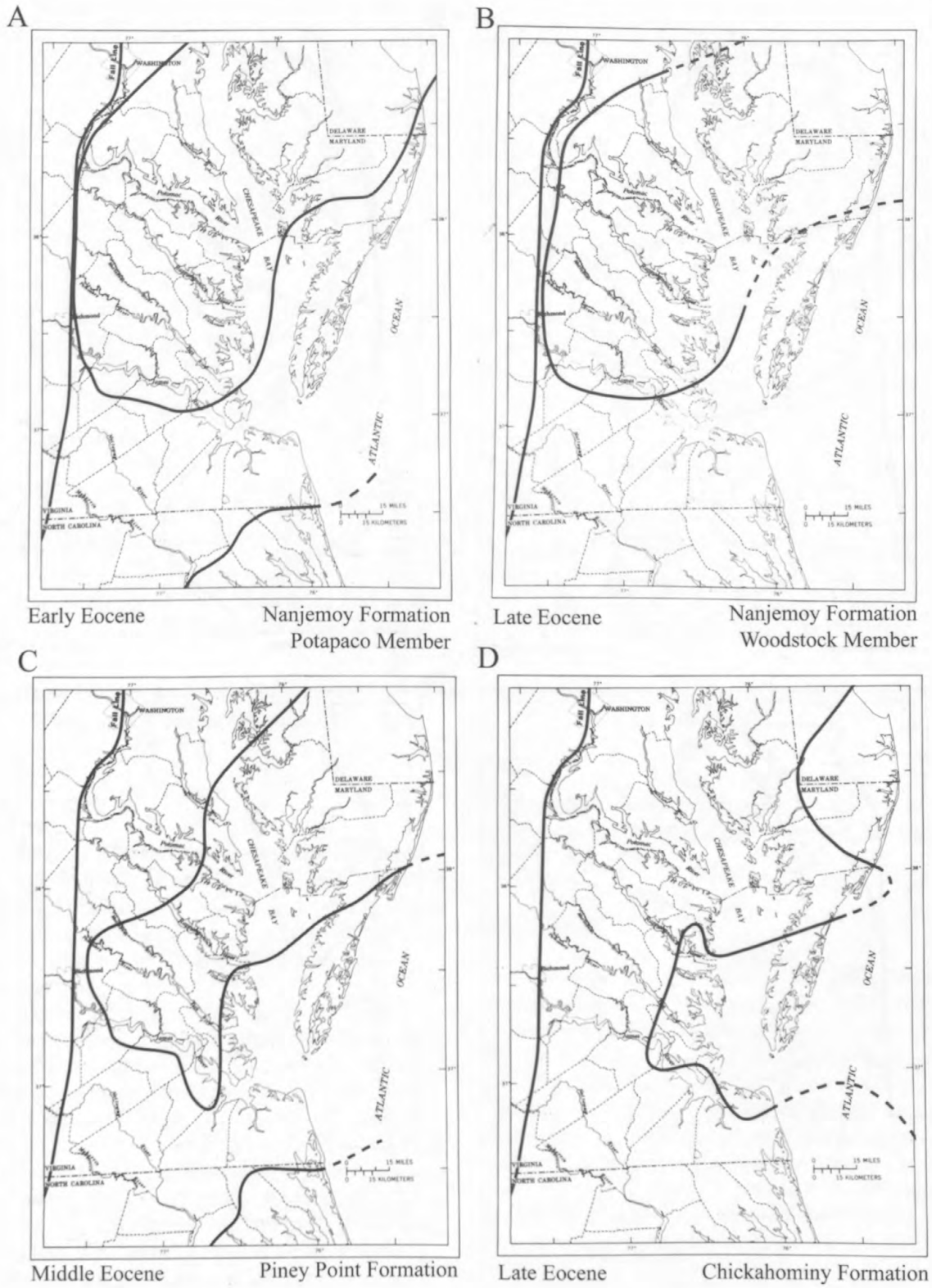
Figure 5. Maps showing depositional basins in the Salisbury embayment during the Eocene. Dashed lines indicate areas where boundary data are lacking.

A

Late Oligocene   Old Church Formation

B

Early to middle Miocene   Calvert Formation

C

Middle Miocene   Choptank Formation

D

Early Miocene   St. Mary's Formation

Figure 6. Maps showing depositional basins in the Salisbury embayment from the late Oligocene through the middle Miocene. Dashed lines indicate areas where boundary data are lacking.

A

B

Late Miocene   Eastover Formation
                                Claremont Manor Member

Late Miocene   Eastover Formation
                                Cobham Bay Member
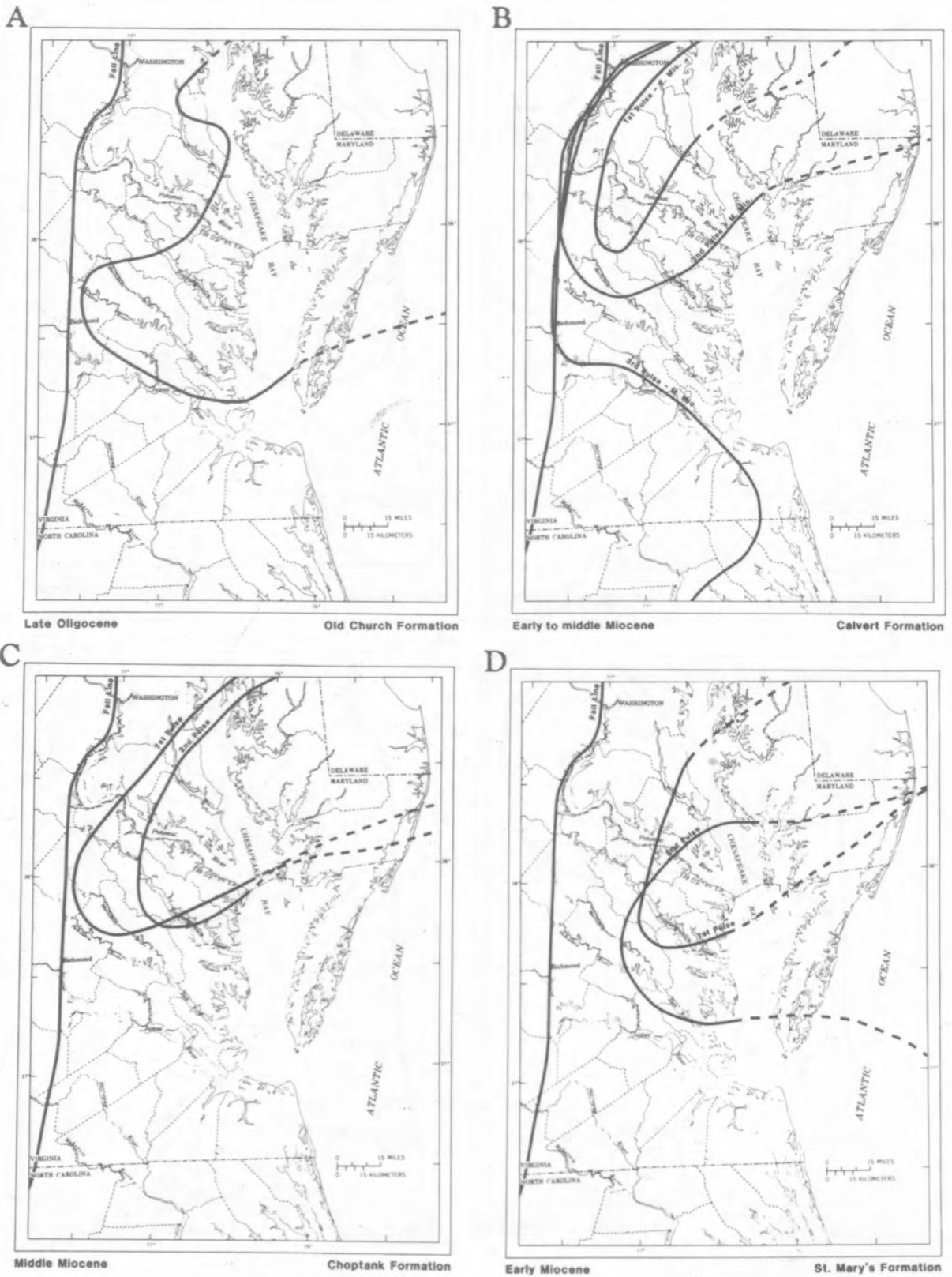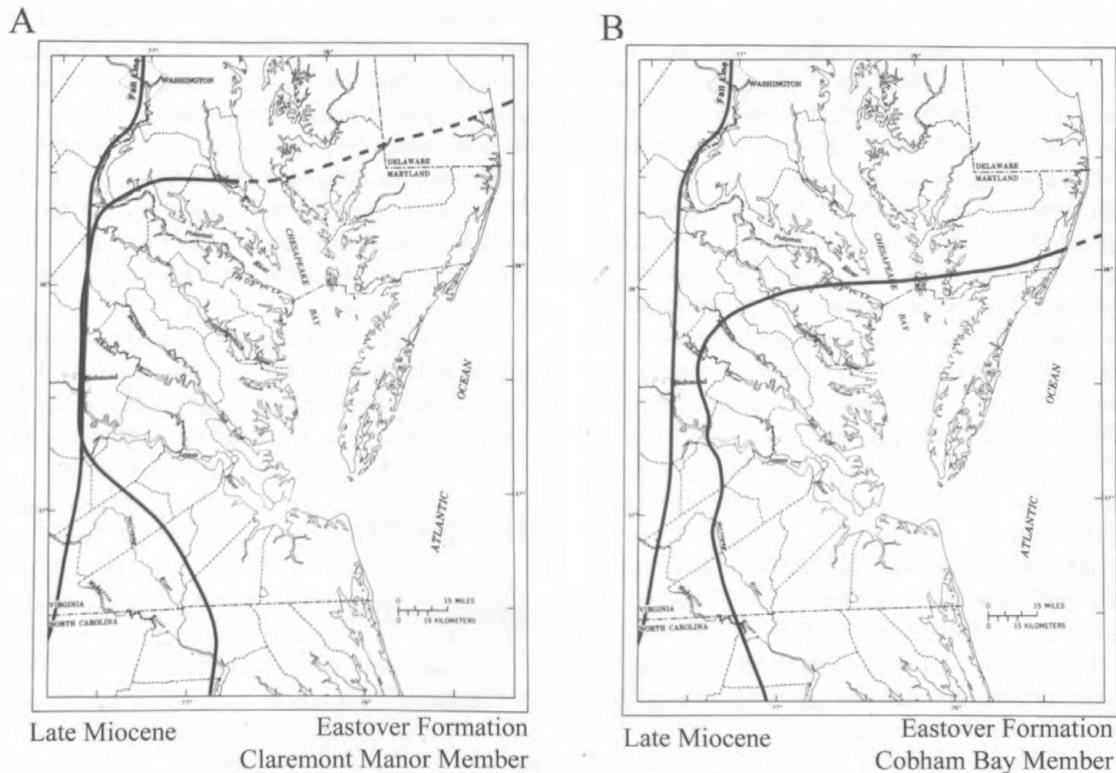
Figure 7. Maps showing depositional basins in the Salisbury embayment during the late Miocene. Dashed lines indicate areas where boundary data are lacking.

Eocene

During the early Eocene a moderately strong transgression occurred in the Salisbury embayment (Potapaco Member of the Nanjemoy Formation, fig. 5A). In the late early Eocene a second transgression occurred, which is reflected in the Salisbury embayment by the Woodstock Member of the Nanjemoy Formation (fig. 5B).

The most extensive transgression during the Tertiary occurred in the middle Eocene. In Virginia and Maryland it took place during the middle middle Eocene and resulted in the deposition of the Piney Point Formation (fig. 5C). To the south, this transgression consists of carbonate beds: Castle Hayne Formation in North Carolina; Moultrie Member of the Santee Limestone and McBean Formation in South Carolina and Georgia; and Lisbon Formation in Georgia and Alabama. Beds associated with this event are present in all areas of the Gulf Coastal Plain. It is clear that these deposits record a global sea-level rise. At least five small transgressions are reflected in the middle Eocene sequence, but they are plotted as a single event in figure 2 because of the lack of correlative data. During the late Eocene, a small-scale transgression took place in Virginia (the Chickahominy Formation of Cushman and Cederstrom, 1945; fig. 5D). This thin unit contrasts with the thick stratigraphic sequence deposited in the Gulf area at that time. That record suggests a high sea-level stand, but the

meager upper Eocene record in the Atlantic basins indicates a general sea-level lowering, unless most of that area was tectonically emergent.

Oligocene

During the early Oligocene, a thick sequence of beds was deposited in the Gulf, while in the Atlantic region there are only thin subsurface units of that age. In the late Oligocene, data indicate a relative highstand, which resulted in the deposition of beds in the Charleston embayment, Albemarle embayment, and the Gulf. During the very late Oligocene or very early Miocene a brief, small-scale, high stand left a sedimentary record in the Salisbury embayment (Old Church Formation, fig. 6A). In spite of the thinness of these deposits, their widespread occurrence is good evidence for a global sea-level rise and the submergence of much of the Atlantic Coastal Plain (Ward, 1985).

Miocene

Following the Old Church transgression and a brief regression, onlap in the Salisbury embayment during the Miocene is characterized by nearly continuous sedimentation punctuated by short breaks, resulting in a series of thin,

unconformity-bounded beds. Three of these transgressions produced the silty sands and diatomaceous clays of the Calvert Formation (Shattuck, 1902, 1904; fig. 6B). The diatom assemblages indicate the first and second transgressions occurred in the late early Miocene, and the third in the early middle Miocene (Abbott, 1978; Andrews, 1978). The axis of the depocenter was still to the northeast and it was apparently a restricted basin. Diatomaceous clays accumulated deep in the embayment while coarser grained, sandy deposits predominated in a seaward direction. Small-scale marine pulses brought coarser sediments deep into the embayment and stillstands resulted in clay accumulations. This formed cyclic deposits of alternating thick beds of clay and sand. Each of the Calvert pulses was successively more extensive; the third pulse partially overlapped the Norfolk arch and extended into the Pungo River Formation sea in the Albemarle embayment.

In the middle and late middle Miocene, the Salisbury embayment was again the site of two brief transgressions. Both were less extensive than the earlier Calvert seas and brought coarser sediments deeper into the embayment (fig. 6C). Beds of the first transgression, including the Drumcliff and St. Leonards Members (of Gernant, 1970) of the Choptank Formation, unconformably overlie the Calvert Formation. The second pulse of the Choptank, which corresponds to the Boston Cliffs Member of Gernant (1970), unconformably overlies beds of the first pulse. Molluscan assemblages indicate cool-temperate to warm-temperate, shallow-shelf, open-marine conditions.

In the early late Miocene, another pair of marine transgressions occurred in the Virginia-Maryland area (fig. 6D). Predominantly clayey sands were deposited, with some beds containing a prolific and diverse molluscan assemblage. These beds, which have been assigned to the St. Marys Formation, conformably overlie the Choptank Formation and, in turn, are unconformably overlain by beds of the second pulse, which corresponds to Shattuck's (1904) "Zone 24." Both units contain abundant and diverse molluscan assemblages that indicate shallow-shelf, open-marine, warm-temperate to subtropical conditions. During the second pulse, the locus of marine deposition shifted substantially to the south. This shift indicates an end of the northeast depositional alignment that appeared to have dominated in the Salisbury embayment from the Paleocene to the middle Miocene. After the shift, the principal basinal area was centered in Virginia, while Maryland was largely emergent.

After a break of approximately 1.5 to 2.0 m.y., marine sedimentation resumed with a large-scale transgression in the late late Miocene (fig. 7A). It began with localized subsidence in central Virginia that caused the deposition of a thick sequence of inner-bay, shallow-shelf sediments, termed the Claremont Manor Member of the Eastover Formation (Ward and Blackwelder, 1980). The Claremont Manor Member is a poorly sorted mixture of clay and sand with the finer material concentrated in the westward portion of the basin. Toward the center, fine-grained sands dominate and contain large concentrations of mollusks in the beds. Some of the nearshore clays deposited at that time contain appreciable concentrations of diatoms. Molluscan assemblages found in the Claremont Manor Member are less diverse than in either of the previous pulses in the St. Marys Formation and are less diverse than the subsequent Cobham Bay Member of the Eastover Formation. The composition of the fauna suggests cool to mild temperature conditions in a somewhat protected and restricted embayment.

After a brief lowstand, a high sea-level pulse in the late Miocene resulted in a very thin, but widespread, marine deposit termed the Cobham Bay Member of the Eastover Formation (Ward and Blackwelder, 1980; fig. 7B).

Stratigraphy

Pamunkey Group

Brightseat Formation

The Brightseat Formation, named by Bennett and Collins (1952) for outcrops in Prince George's County, Maryland, consists of olive-black (5Y 2/1), micaceous, clayey and silty sands. Ward (1985) reported that the Brightseat Formation crops out as far south as the Rappahannock River in Virginia. The Brightseat sea occupied principally the northeastern portion of the Salisbury embayment and was separated from the Albemarle embayment to the south by the Norfolk arch (fig. 4A). In its type area, 1.0 mile (mi) west-southwest of Brightseat, Prince Georges County, Md., mollusks are abundant, but only the calcitic forms are well preserved. Away from the type area, the macrofossils are leached, leaving only molds and casts. In the Prince Georges County area, the Brightseat Formation unconformably overlies marine deposits of the Severn Formation (Upper Cretaceous). To the south, on the Potomac and Rappahannock Rivers, it overlies fluvial deposits of the Potomac Group (Lower Cretaceous). Beds now placed in the Brightseat Formation were originally assigned, with some reservations, to "Zone 1" of the Aquia Formation (Clark and Martin, 1901).

On the right bank of Aquia Creek (Stop 1) (see figure 8 for locality map), the Brightseat Formation unconformably overlies the Patapsco Formation of the Potomac Group. The Brightseat Formation is, in turn, unconformably overlain by the Aquia Formation. Macrofossils at the locality are leached and are present only as rare molds and casts, but the micaceous silty sand, nearly devoid of glauconite, distinguishes the unit. The Brightseat Formation is not known to either crop out or exist in the subsurface south of the Rappahannock River exposures; however, it has been identified in cores from the Dismal Swamp area near Norfolk.

Hazel (1968, 1969), studying the ostracodes of the

Brightseat Formation in the type area, found the unit to be equivalent to the upper part of the Clayton Formation in Alabama, and placed it in the *Globoconusa daubjergensis-Globorotalia trinidadensis* zone on the basis of planktic foraminifers. He showed the Brightseat Formation to be early Paleocene in age and placed it in the upper part of the Danian Stage. According to Gibson and Bybell (1984), calcareous nannofossils present in the Brightseat Formation indicate its placement in nannoplankton zone NP 3 (of Martini, 1971).

Aquia Formation

The use of the term "Aquia" as a stratigraphic unit was first introduced by Clark (1896). He gave the name "Aquia Creek Stage" to beds that crop out in the vicinity of Aquia Creek, Stafford County, Va. The concept of the unit was soon revised, and it was renamed the Aquia Formation by Clark and Martin (1901). Bennett and Collins (1952) restricted Clark's and Martin's (1901) earlier definition of the Aquia Formation when beds placed in "Zone 1" by Clark and Martin were designated the Brightseat Formation. It is the Aquia Formation, in this restricted sense, that unconformably overlies the Brightseat Formation in the northeastern area of its range and unconformably overlies Lower Cretaceous deposits south of the Rappahannock River. The Aquia Formation consists of clayey, silty, very shelly, glauconitic sand. It crops out in a continuous arc from the upper Chesapeake Bay to the area around Hopewell, Va., on the James River. Both members of the Aquia Formation, the Piscataway and Paspotansa, are recognized along the Potomac, Rappahannock, Mattaponi, Pamunkey, and James Rivers, and both are extremely fossiliferous (see figure 4B for the basinal outline of the Aquia).

Macrofossils in the Aquia Formation locally are well preserved but more commonly are leached, making recovery difficult. Microfossil groups consist of ostracodes, foraminifers, pollen, dinoflagellates, and calcareous nannofossils. Microfossil work has indicated placement of the Aquia Formation in the upper Paleocene. Gibson and Bybell (1984), on the basis of calcareous nannofossils, placed the Aquia Formation in zones NP 5–9.

Piscataway Member

The Piscataway Member of the Aquia Formation was named by Clark and Martin (1901) from exposures along Piscataway Creek, Prince Georges County, Md. It included seven "zones," which were traceable along the Potomac River in the type area of the Aquia Formation. "Zone 1" of Clark and Martin (1901) has since been recognized as a distinct unit by Bennett and Collins (1952) and was termed the Brightseat Formation. Study of the lectostratotype section (principal reference section designated by Ward, 1985; Stop 2) of the Aquia Formation and the Piscataway and Paspotansa Members has revealed the most significant lithic change to be at the "Zone 5"-"Zone 6" contact of Clark and Martin (1901). There it changes from a poorly sorted, clayey sand to a very

well sorted, micaceous, silty, fine-grained sand. Ward (1985) proposed that the boundary between the two members be placed between Beds 5 and 6 and that the base of the Paspotansa be extended downward to include "Zones 6 and 7" of Clark and Martin (1901). Beds 2 to 5, assigned to the Piscataway Member, consist of clayey, silty, poorly sorted glauconitic sands containing large numbers of macrofossils, principally mollusks. The mollusks are concentrated in beds of varying thicknesses and are cemented at several intervals into locally traceable indurated ledges. Large bivalves, which include *Cucullaea*, *Ostrea*, *Dosiniopsis*, and *Crassatellites* (see pl. 1), are the most conspicuous taxa. The quartz sand present in the Piscataway Member is usually poorly sorted, angular, and clear. Glauconite is extremely abundant, ranging from sand-size pellets to coatings on and in molluscan fossils. The sand, glauconite, and mollusks are interspersed in a clayey, silty matrix producing a very tough, olive-gray (5Y 4/1) calcareous marl. Glauconite percentages range from a low of 20 percent in far updip localities to 70 percent or more in the more seaward parts of the basin.

Paspotansa Member

The Paspotansa Member of the Aquia Formation, described by Clark and Martin (1901), received its name from Passapatanzy Creek, a tributary of the Potomac River in Stafford County, Va. As originally defined, the Paspotansa included "Zones 8 and 9" of Clark and Martin (1901). However, as previously discussed, Ward (1985) recommended that Beds 6 and 7 also be included in the Paspotansa Member. Bed 6 consists of an olive-gray (5Y 4/1), very fine grained, micaceous, glauconitic sand containing large numbers of *Turritella mortoni*. Beds 7 and 8 consist of olive-black (5Y 2/1), fine-grained, glauconitic sand, with scattered, thin *Turritella* beds. Bed 9 is an olive-black (5Y 2/1), fine-grained, glauconitic sand containing large numbers of closely packed *Turritella* in beds of varying thickness. The thicknesses of the units, as well as their fossil content, vary from locality to locality, but several characteristics are internally consistent. The Paspotansa Member consists of fine- to very fine grained, silty, well-sorted, micaceous, glauconitic and quartzose sand in massive or very thick beds. This texture is strikingly different from the underlying poorly sorted, clayey, shelly, glauconitic and quartzose sand of the Piscataway Member. The Paspotansa Member is usually overlain by a gray (N 7, when fresh), tough clay termed the Marlboro Clay. This bed, where present, makes the recognition of the upper boundary of the Paspotansa Member relatively easy. Where the Marlboro Clay is absent, the well-sorted, fine-grained sands of the Paspotansa Member may be distinguished from the overlying, clayey, highly bioturbated, poorly sorted glauconitic sands of the Potapaco Member of the Nanjemoy Formation.

As in all formations in the Pamunkey Group, the glauconite content of the Paspotansa Member of the Aquia Formation varies with proximity to the paleoshoreline. Percentages are much

lower near the perimeter of the basin, in some areas less than 10 percent. Seaward, in an eastward direction, the glauconite content may reach 90 percent. The nature of the shell deposits within the Paspotansa Member further serves to distinguish that unit from the underlying Piscataway Member and the overlying Nanjemoy Formation. Massive glauconitic sands containing considerable numbers of large *Turritella* in thin beds or lenses characterize the Paspotansa Member, in striking contrast to the very shelly, silty sands of the Piscataway Member, which are usually dominated by loosely packed, medium-size to large bivalves. Also notable is the massive nature of the Paspotansa Member, often exposed in the high vertical walls of bluffs along the Potomac, Rappahannock, and Pamunkey Rivers. Where very fresh, the unit is dark-olive-black (5Y 2/1). Where partially weathered, it is grayish-orange (10YR 7/4), and where very weathered, it appears yellowish-orange (10YR 7/6), because of the oxidation of iron in the glauconite.

The Paspotansa Member apparently disconformably overlies the Piscataway Member, but the nature of the contact is commonly obscured. Clark and Martin (1901) described the nature of the contact between "Zones 6 and 8" along the bluffs below Aquia Creek, but the most notable lithic change occurs at the contact between their "Zones 5 and 6" (Ward, 1985). On the Rappahannock and Mattaponi Rivers, the contact between the two members is obscured by slumping and poor outcrops. Along the Potomac River, however, the contact between the two members is sharp and undulating. No phosphate accumulations or burrows are present, indicating only a brief period of nondeposition.

The Paspotansa Member crops out in a broad arc from the Eastern Shore of Maryland to the James River in Virginia (see fig. 4B). Clark and Martin (1901, p. 73) described the Paspotansa Member from the Chester River in Kent County, Md., and their descriptions of the sections on the Severn and South Rivers in Anne Arundel County, Md., indicate the presence of the unit there. Additional sections are described in the Upper Marlboro area of Prince Georges County, where the Paspotansa Member includes a heavy concentration of bryozoans. The most extensive outcrops of the member extend along the Virginia shore of the Potomac River from the mouth of Aquia Creek to below Fairview Beach. Between Potomac Creek and Aquia Creek (Stop 2), 61.5 feet (ft) (18.8 meters (m)) of the Paspotansa Member occurs in steep, almost vertical bluffs, which have been weathered to a reddish-orange color. This section was designated the principal reference section (lectostratotype locality) of the Paspotansa Member by Ward (1985). Several distinct shell beds are present, as well as several discontinuous ledges of boulder-size concretions. Other shell concentrations, consisting principally of large, current-oriented *Turritella mortoni* (see pl. 2), occur in lens-shaped masses.

Marlboro Clay

Clark and Martin (1901, p. 65) first applied the term

"Marlboro clay" to sediments included in "Zone 10" of Clark (1896, p. 42). The name was derived from exposures of that unit near Upper Marlboro, Prince Georges County, Md. Clark and Martin (1901) considered this unit to be the basal unit of the Potapaco Member of the Nanjemoy Formation. Clark and Miller (1906) briefly described the outcrop area of the "Marlboro clay" across Maryland and Virginia and included it in the basal bed of the Nanjemoy Formation. Clark and Miller (1912) again included the pink clay as the basal bed in the Nanjemoy Formation. However, at only one locality, below Hopewell, Va., on the James River (Clark and Miller, 1912, p. 115), is a specific outcrop section described. Darton (1948), in a short note, described the areal extent of the Marlboro Clay and referred to that unit as the basal member of the Nanjemoy Formation. This had the effect of formalizing the name. A more detailed study, including a detailed geologic map by Darton (1951), also placed the Marlboro Clay as the basal bed of the Nanjemoy Formation. Glaser (1971), however, was the first to formally propose the elevation of the Marlboro Clay to formational rank. This restricted the original concept of the Nanjemoy Formation and, more specifically, that of the Potapaco Member. This treatment of the Marlboro Clay, as a separate formation, was continued by Reinhardt and others (1980).

Glaser (1971, p. 14) characterized the Marlboro Clay as "a silvery-gray to pale-red plastic clay interbedded with much subordinate yellowish-gray to reddish silt." Glaser noted that both the lower and upper contacts of the Marlboro Clay were sharp and nongradational and probably represented at least a brief hiatus between the underlying and overlying units. A more recent study by Reinhardt and others (1980) on a core from Westmoreland County, Va., concluded that the Aquia-Marlboro contact was somewhat gradational, whereas the upper Marlboro-Nanjemoy contact was sharp and was marked by burrows into the underlying Marlboro Clay.

The areal distribution of the Marlboro Clay was mapped by Darton (1951) and schematically shown by Glaser (1971), but no detailed study of the formation has been made in much of the Virginia Coastal Plain. Outcrops of the Marlboro Clay examined by us have been limited to those found on the Potomac, Mattaponi, Pamunkey, and James Rivers. Outcrop patterns indicate a spotty, although widespread, occurrence of the unit.

Because of the lack of calcareous fossils, the age of the Marlboro Clay has been assigned principally on the fact that it occurs between the Aquia and Nanjemoy Formations. This brackets its age but does not afford primary evidence. A detailed study of a core from Oak Grove, Westmoreland County, Va., by Gibson and others (1980) and Frederiksen (1979) afforded the best paleontologic evidence of its age. The consensus of pollen and dinoflagellate data suggested an age of very late Paleocene and possibly very early Eocene. Mixing of the two floral assemblages may have occurred through reworking and bioturbation or the unit may contain the Paleocene-Eocene boundary.

Nanjemoy Formation

Beds now included in the Nanjemoy Formation were first studied in detail by Clark (1896), who divided them (along with those now included in the Aquia Formation) into "zones." Those "zones" above the "Aquia Creek Stage" of Clark (1896) were numbered 10 through 17. "Zone 17" was named the "Woodstock Stage." Clark and Martin (1901) revised this terminology and placed their "Zones 10 through 17" in the "Nanjemoy Formation or Stage." The Nanjemoy Formation was divided into the "Potapaco Member or substage" including "Zones 10–15" and the Woodstock Member including "Zones 16 and 17." In this same publication Clark and Martin (1901, p. 65) introduced the term "Marlboro clay," informally, for part of their "Zone 10." In a brief, preliminary report on the stratigraphy of the Virginia Coastal Plain, Clark and Miller (1906) dropped the stage and substage terminology and referred only to the Aquia and Nanjemoy Formations. Clark and Miller (1912) continued this usage and retained both as formations. The "Marlboro clay" was briefly mentioned again (Clark and Miller, 1912, p. 103) but was specifically reported from only one locality (Clark and Miller, 1912, p. 115). The zonation of beds and their breakdown into members was retained only for those well-studied exposures along the Potomac River. South of the Potomac, assignment only to formation was attempted. The term "Marlboro Clay" was finally formalized by Darton (1948), but the unit was retained as a basal member of the Nanjemoy. This removed the Marlboro Clay ("Zone 10," in part, of Clark) from beds previously included in the Potapaco Member. The Marlboro Clay was retained as a member of the Nanjemoy until Glaser (1971) elevated it to formational rank. This, in effect, restricted the original concept of the Nanjemoy Formation, and only part of "Zone 10" and "Zones 11–17" remained in that formation. Beds younger than "Zone 17" were not included in the original description or sections of the Nanjemoy Formation but were later lumped under the term "Nanjemoy Formation" by Clark and Miller (1912).

Potapaco Member

The Potapaco Member of the Nanjemoy Formation was described by Clark and Martin (1901, p. 65) and received its name from "...the word Potapaco found on the (Captn. John) Smith and others early maps..." The Potapaco Member included "Zones 10 to 15" of Clark and Martin (1901). Part of their "Zone 10" included the Marlboro Clay. Clark (1896), Clark and Martin (1901), and Clark and Miller (1912) described the beds ("Zones") found in the Potapaco Member at sections upriver from Popes Creek on the left bank of the Potomac River, Charles County, Md. The section described by Clark and Martin (1901, p. 70, Section VIII) was designated the principal reference section (lectostratotype) of the Nanjemoy Formation and the Potapaco Member by Ward (1985). The exposure is just downstream of Stop 6 in this report.

The following terminology is used for the series of four beds that have been recognized in the Potapaco Member (lettered from oldest to youngest) (from Ward, 1984, 1985):
Bed D—Concretion-bed Potapaco
Bed C—Burrowed Potapaco
Bed B—Bedded Potapaco
Bed A—Nonbedded Potapaco

Bed A—Nonbedded Potapaco

Bed A is found on the Potomac, Rappahannock, Mattaponi, and Pamunkey Rivers. It consists of a clayey, silty, fine-grained sand that contains scattered, small mollusks including *Venericardia potapacoensis* Clark and Martin, 1901 (see pl. 3). Glauconite occurs in relatively small amounts in the sand-size fraction in updip areas, but glauconite percentages increase in a seaward direction. Small phosphate pebbles are common. The bed is estimated to be 15 to 20 ft (4.6–6.1 m) thick and, in most places, unconformably overlies the Marlboro Clay. Bed A is distinguishable from Bed B by its darker color, lack of bedding, and less clayey texture. Calcareous fossils are generally leached, leaving only molds and casts. The unit is present on the right bank of the Potomac River 1.75 mi (2.8 km) below Fairview Beach in King George County, Va. (Stop 4).

The lithic and faunal makeup of Bed A suggests an initial marine pulse and basal transgression in contrast to the quiet, protected embayment indicated by the Marlboro Clay. Physical and paleontologic evidence indicates that little time occurred in the break between the Marlboro Clay and Bed A of the Potapaco Member.

Low molluscan diversity and small glauconite percentages suggest restricted conditions during the deposition of Bed A. In spite of this evidence, renewed marine influence is apparent. Dinoflagellate assemblages are marked by reduced diversity; the flora is dominated by a single taxon, indicating restricted marine conditions (L.E. Edwards, written commun., 1984). Mollusks, in general, are poorly preserved but where present are low in diversity.

Calcareous nannofossils found in the Oak Grove core in Westmoreland County (Gibson and others, 1980), from the interval just above the Marlboro Clay, probably come from Bed A and indicate the placement of that bed in calcareous nannoplankton zone NP 10 (early Eocene). Assemblages of pollen, dinoflagellates, foraminifers, and ostracodes substantiate this placement.

Bed B—Bedded Potapaco

Bed B, the most striking unit in the Potapaco Member, is easily recognized by its thinly bedded appearance. This appearance is due to the accumulation of a small bivalve, *Venericardia potapacoensis* Clark and Martin, 1901, in vast numbers along many discontinuous, thin bedding planes. Bed B varies in thickness from locality to locality. Its exact thickness in surface exposures is difficult to determine because of

poor outcrops. It is estimated to range from only a few feet (about 1 m) to more than 15 ft (4.6 m) thick. The sediment in Bed B consists of olive-gray (5Y 4/1), very clayey, glauconitic sand to sandy clay. The clay, when fresh, appears to be grayish orange pink in color (5YR 7/2) and contains varying amounts of fine- to medium-size glauconite and quartz sand. Glauconite content ranges from less than 10 percent in the westernmost exposures to more than 75 percent with increasing distance eastward (seaward). Bedded concretions ranging up to boulder size are common in Bed B. These nodules, although sometimes regionally traceable, are not sufficiently stratigraphically continuous to be used as marker beds.

Sedimentological and faunal characteristics of Bed B indicate deposition in a shallow, somewhat restricted embayment. Glauconite grains, which appear to be concentrated in burrows, are common. The burrows and the concentrations of abraded bivalves along bedding planes suggest shallow depths, probably not below wave base. Glauconite-coated, worn, disarticulated valves of *Venericardia* indicate periods of slow sediment accumulation. Bivalves may be concentrated along those winnowed zones because of intermittently favorable bottom conditions or storms. Elsewhere in the section, where soft clays inhabited by burrowing organisms predominated, the bottom may not have been suitable for the settlement of bivalve larvae. The molluscan assemblage of Bed B is dominated (up to 95 percent of the assemblage) by *Venericardia potapacoensis* Clark and Martin, 1901 (pl. 3).

Bed C—Burrowed Potapaco

Above the thin-bedded clayey sand of Bed B is a series of sandy clays to clayey sands that are easily recognizable by their intensely burrowed appearance. Bedding, if it was ever present, has been obscured by bioturbation except along a few very thin planes. Along those surfaces sedimentation appears to have been interrupted and is marked by local diastems, by a concentration of glauconitic sand, and by glauconite-filled burrows extending down into the underlying sediment. These stratigraphic breaks, if that is what they are, have not been traced over a wide area and may be only local, possibly current-scoured surfaces. The dominant lithic characteristic of Bed C is its very clayey texture; grains of fine- to medium-grained sand-size glauconite are interspersed in a grayish-orange-pink (5YR 7/2) clay matrix. In some areas, the concentration of glauconite is such that the lithology is best described as a clayey sand. This very clayey, glauconitic texture is typical of the entire Potapaco Member, but the intensely burrowed nature of the unit is unique to Bed C. The macrofossil component of Bed C consists principally of small or broken, poorly preserved mollusks that are concentrated in burrows and make up a small percentage of the bed. Thicknesses of as much as 20 ft (6.1 m) have been observed in outcrop.

Bed C overlies Bed B with no distinct contact between the two, suggesting a gradation from one environmental regime to another. In most of its outcrop area, Bed C is over-lain by the Woodstock Member of the Nanjemoy Formation. On the Pamunkey River, at least, Bed C is overlain by a thin bed (Bed D), 1.5 to 3.0 ft (0.5–0.9 m) thick, of clayey, very glauconitic sand marked by a series of boulder-size concretions. The contact between Bed C and this younger unit, Bed D, is abrupt and is marked by a sharp, but burrowed, contact indicating a probable diastem. Elsewhere, where Bed D is missing, the Bed C-Woodstock boundary is disconformable and is marked by an abrupt change in lithology, a lag deposit of phosphate, bone, pebbles, and wood in the lower part of the Woodstock Member, and burrows containing Woodstock sediment extending several feet into the underlying Bed C. The olive-black (5Y 2/1), very fine grained, well-sorted, micaceous, glauconitic sand of the Woodstock Member is easily distinguishable from the very clayey, burrowed sand of Bed C. This contact has been observed on the Patuxent, Potomac, Mattaponi, and Pamunkey Rivers. Upriver of Popes Creek on the left bank of the Potomac River, Charles County, Md., the area in which Bed C should descend to water level is slumped and obscured by weathering of the cliff face.

Dinoflagellate assemblages indicate near-shore or high-energy conditions that had an abundant source of nutrients (L.E. Edwards, written commun., 1984). On the basis of the dinoflagellate flora, Bed C may be correlated with calcareous nannoplankton zone NP 10 or 11.

Bed D—Concretion-bed Potapaco

Bed D crops out only along the Pamunkey River below the mouth of Totopotomoy Creek in Hanover County, Va., and therefore is discussed only briefly here. Bed D, in its small outcrop area, consists of 1.5 to 3.0 ft (0.5–0.9 m) of clayey, very glauconitic sand and has sharp upper and lower contacts. Both the upper and lower contacts are marked by abrupt changes in lithology and color and contain concentrations of quartz and phosphate pebbles, and wood. Burrows at both contacts extend down into the underlying beds. The high glauconite content of Bed D makes it easily distinguishable from the lighter colored clays of Bed C and the less glauconitic silty sand of the basal portion of the overlying Woodstock Member. The bed is marked by a line of boulder-size concretions, which occur in the middle of the unit.

Woodstock Member

The Woodstock Member of the Nanjemoy Formation was first proposed by Clark and Martin (1901, p. 66) for beds of glauconitic sand exposed near Woodstock, "an old estate situated a short distance above Mathias Point," King George County, Va. The term "Woodstock" had previously been used by Clark (1896) to describe the Woodstock Stage, a unit defined principally by its fauna. Clark and Martin (1901) described the Woodstock Member as consisting of their "Zones 16 and 17." The bluff described by Clark (1896, p. 40, Pl. IV, Section III) and Clark and Martin (1901, p. 70, Section IX) exhibits both the Potapaco and Woodstock

Members. Stop 5 of this guidebook was designated the lectostratotype section by Ward (1985).

The Woodstock Member consists of olive-black (5Y 2/1), very fine grained, well-sorted, silty, glauconitic sands. The glauconite content increases markedly from a low of 10 to 15 percent in its most inland outcrops to 70 to 80 percent in its most seaward exposures. Carbonaceous material in the form of logs, branches, and nuts is abundant. The Woodstock Member unconformably overlies the Potapaco Member and is unconformably overlain either by the Piney Point Formation in the James and Pamunkey River areas or by younger beds on the Mattaponi, Rappahannock, and Potomac. The lower contact with the Potapaco Member is an easily recognized feature that may be seen from the Patuxent River to the Pamunkey River. There is a significant faunal and floral change at this boundary, although it represents only a relatively brief hiatus. The Woodstock Member may be distinguished from the underlying Potapaco Member by its fine-textured, micaceous, massive appearance, which differs from the very clayey, poorly sorted, bioturbated texture of the underlying Potapaco Member.

Molluscan assemblages in the Woodstock Member are diverse and abundant and are scattered throughout the fine matrix (pl. 4). Many of the taxa are new, and their stratigraphic significance is, at present, poorly understood. A number of species were listed by Clark and Martin (1901) as being present in the Woodstock Member, but the list is in serious need of updating. Large valves of *Venericardia ascia* Rogers and Rogers, 1839, are concentrated along bedding planes in some areas but are easily distinguished from the much smaller *Venericardia potapacoensis* found in the Potapaco Member. Along the Potomac River above Mathias Point on the right bank (Stop 5) and below Popes Creek on the left bank (Stop 6), the Woodstock Member is overlain by transgressive sediments of the Calvert Formation that range from early to middle Miocene in age. The contact is marked by a basal lag concentration of phosphate and quartz pebbles, a burrowed surface, and an abrupt lithic change from glauconitic sand to olive-brown, clayey, phosphatic sand. At the end of the bluffs, downriver from Popes Creek (below Stop 6), a very thin tongue of burrowed, gray clay and a bed of glauconitic sand occur between the typical, easily recognized Woodstock Member and the Calvert Formation. These two beds thicken downstream but are beveled off upstream south of Popes Creek. Macrofossils are leached from the beds, but dinoflagellates indicate that they are early Eocene in age (L.E. Edwards, written commun., 1984). Therefore, we include them in the Woodstock Member in spite of their different lithologies. We believe that these units are represented in the Oak Grove core by the clay and sand beds shown as occurring in the upper part of the Nanjemoy by Reinhardt and others (1980, fig. 1).

Best evidence, at this time, of the age and correlation of the Woodstock Member is found in the dinoflagellate and calcareous nannofossil assemblages. Calcareous nannofossils in the Putney Mill core, New Kent County, Va., indicate an approximate equivalence with nannofossil zone NP 12 (L.M. Bybell, written commun., 1984). This zone also was reported in the Oak Grove core (Gibson and others, 1980) in the interval between 227.0 and 269.4 ft (69.2 and 82.1 m). L.M. Bybell (written commun., 1984) now believes that only the 69.2- to 82.1-m interval in the Oak Grove core contains calcareous nannofossils indicative of nannoplankton zone NP 12.

The Woodstock sea occupied a broad embayment reaching from at least the Patuxent River in Maryland to a short distance south of the James River in Virginia (fig. 5B). The locus of the embayment was somewhat south of the Potomac River.

Chesapeake Group

The term "Chesapeake Formation" was introduced by Darton (1891, p. 433) for a series of beds in southeastern Maryland and Virginia that consists of sands, clays, marls, diatomaceous clays, and shell fragments. Dall and Harris (1892) elevated the unit to group status and included all stratigraphically equivalent beds at the same horizon from Delaware to Florida. Shattuck (1902) subdivided the Chesapeake Group in Maryland into (in ascending order) the Calvert Formation, Choptank Formation, and St. Marys Formation. Shattuck (1904) greatly expanded this work and described the units, and their contained molluscan fauna, in detail. Clark and Miller (1906) expanded the definition of the Chesapeake Group by including the Yorktown Formation in Virginia. Clark and Miller (1912) included beds along the Chowan River in Bertie County, N.C., in the Yorktown Formation. Mansfield (1944) also included the Chowan River beds in the Yorktown. Blackwelder (1981) named those beds the Chowan River Formation; he split the unit into two members, the Edenhouse Member (lower) and the Colerain Beach Member (upper), and included this new formation in the Chesapeake Group.

Ward (1985) recommended that a new unit, the Old Church Formation, be included in the Chesapeake Group. The Old Church Formation is a calcareous, shelly sand that contains only small amounts of glauconite. It unconformably underlies the Calvert Formation and unconformably overlies the Piney Point Formation. It is easily differentiated from the underlying, very glauconitic beds of the Pamunkey Group. It is unclear whether Darton (1891) or Clark and Miller (1912) actually observed the unit that Ward (1985) termed the Old Church. Therefore, where they would have placed the Old Church Formation is unclear.

The following units constitute the Chesapeake Group:

Chowan River Formation
    Colerain Beach Member (upper Pliocene)
    Edenhouse Member (upper Pliocene)
Yorktown Formation
    Moore House Member (upper Pliocene)
    Morgarts Beach Member (upper Pliocene)

Rushmere Member (upper Pliocene)
Sunken Meadow Member (lower Pliocene)

Eastover Formation
Cobham Bay Member (upper Miocene)
Claremont Manor Member (upper Miocene)

St. Marys Formation
Windmill Point Member (upper Miocene)
Little Cove Point Member (upper Miocene)
Conoy Member (lower upper Miocene)

Choptank Formation
Boston Cliffs Member (upper middle Miocene)
St. Leonard Member (middle middle Miocene)
Drumcliff Member (middle middle Miocene)

Calvert Formation
Calvert Beach Member (lower middle Miocene)
Plum Point Marl Member (lower middle Miocene)
Fairhaven Member (lower and lower middle
Miocene)

Old Church Formation (upper Oligocene and lower
Miocene)

Only beds of the Calvert, Choptank, St. Marys, and Eastover Formations crop out in the field trip area and are described here.

Calvert Formation

The Calvert Formation was named and described by Shattuck (1902, 1904) for Miocene beds exposed along the Calvert Cliffs in Calvert County, Md. Sections for the Calvert Formation were given by that author, principally along the Chesapeake Bay, but he described a few other localities in Maryland. The Calvert Formation in Virginia was first mentioned by Clark and Miller (1906), and it was soon thereafter mapped in the Richmond area by Darton (1911). Clark and Miller (1912) documented, rather completely, the extent of the Calvert and other Coastal Plain units; no such exhaustive treatment has since been attempted. More recently, descriptions have been published in guidebooks, treating exposures described by Clark and Miller (1912) (see Stephenson and others, 1933; Ruhle, 1962). Shattuck (1904) described 15 "zones" or beds in the Calvert Formation.

Fairhaven Member

The Fairhaven Member of Shattuck (1904) included "Zones 1–3." "Zones 1 and 2" are two basal transgressive sands that accumulated during the first Calvert pulse or sea-level rise (see fig. 6B). "Zone 3," a massive series of diatomaceous clays, includes most of the Fairhaven Member. "Zone

3" contains two distinct marine pulses (Beds 3–A, 3–B), which exhibit basal transgressive lags and fining-upward sequences. Exposures at the Kaylorite pit on Ferry Road, Calvert County, Md. (Bed 3–A), and the lower 10 ft (3.0 m) of the Fairhaven Member below Popes Creek, Charles County, Md. (Bed 1), contain beds associated with the first pulse of the Calvert. At Popes Creek, this bed is separated from the remaining, upper portion of the Fairhaven Member by a phosphate pebble lag indicating an unconformity or at least a diastem. This lower unit (Bed 1) was named the Popes Creek Sand Member by Gibson (1982, 1983) and was excluded from the Fairhaven even though it was included in that unit by Shattuck (1904) as "Zone 1" (Bed 1). Beds associated with the first transgression can be found as far south as the area of Wilmont on the Rappahannock River, Westmoreland County, Va. Beds of the second pulse are known as far south as the vicinity of Reedy Mill on the Mattaponi River, Caroline County, Va.

Plum Point Marl Member

The Fairhaven Member is overlain, unconformably, by a series of shelly sands that is interbedded with diatomaceous clays and grouped under the term Plum Point Marl Member. This series contains a number of identifiable pulses: the first pulse includes "Zones 4 to 9" (of Shattuck, 1904), the second pulse includes "Zones 10 and 11," the third pulse includes "Zones 12 and 13," and the fourth pulse includes "Zones 14–16." The pulses are included in the area plotted as the third pulse on figure 6B. "Zone 16," as exposed at Calvert Beach, Calvert County, Md. (Stop 10), was originally included in the Choptank Formation by Shattuck (1904). This miscorrelation and the fact that "Zone 16" contains "Choptank fossils" led to its inclusion in that unit despite its very different lithology and the presence of a striking unconformity. Mollusks that characterize "Zones 17 and 19" of the Choptank Formation make their first appearance at least as far down in the sequence as "Zone 14," and some taxa may be present in "Zone 12." It was recommended that "Zones 14–16" be included in the Calvert Beach Member and kept in the Calvert Formation (Ward, 1984). The Plum Point Marl Member, as a lithic entity, is recognizable only as far south as the Westmoreland Cliffs in Westmoreland County, Va. Farther to the southeast, beds equivalent to the Plum Point Marl Member grade into silty, diatomaceous clays that resemble the Fairhaven.

Mollusks are common in the Calvert Formation but are well preserved only in beds along the Chesapeake Bay in Calvert County, Md. Some of the common forms are (pl. 5)

Astarte cuneiformis
Bicorbula idonea (Conrad, 1833)
Cyclocardia sp.
Ecphora tricostata Martin, 1904
Lirophora latilirata (Conrad, 1841)

Lucinoma contracta (Say, 1824)
Marvacrassatella melinus (Conrad, 1832)
Melosia staminea (Conrad, 1839)
Mercenaria sp.
Pecten humphreysii Conrad, 1842

Choptank Formation

The Choptank Formation was named and described by Shattuck (1902, 1904) for the shelly, sandy Miocene beds exposed along the Choptank River, Talbot County, Md., and in the Calvert Cliffs in Calvert County, Md. The Choptank was originally composed of "Zones 16 through 20" of Shattuck (1904). Ward (1984) recommended the placement of "Zones 14–16" in the Calvert Beach Member, as defined by Gernant (1970), and expanded by Ward (1984). Blackwelder and Ward (1976) recommended that "Zone 20," or the Conoy Member of Gernant (1970), be removed from the Choptank Formation and placed in the St. Marys Formation. Distribution of the Choptank beds is shown in figure 6C.

The Choptank Formation consists of three members (in ascending order): the Drumcliff (Bed 17), St. Leonard (Bed 18), and Boston Cliffs (Bed 19). The Drumcliff and St. Leonard Members are best seen along the Chesapeake Bay in Calvert County from Scientists Cliffs to the Baltimore Gas and Electric Powerplant. On the Patuxent River they are best seen in the vicinity of Drumcliff (Jones Wharf) in St. Marys County. Mollusks commonly found in the Choptank Formation are shown in plate 6.

St. Marys Formation

The St. Marys Formation was named and described by Shattuck (1902, 1904) for Miocene beds exposed along the Calvert Cliffs in Calvert County, Md., and along the St. Marys River, St. Marys County, Md. The St. Marys can be seen overlying the Choptank Formation (Bed 19) in the Westmoreland Cliffs on the Potomac River. There, the Eastover Formation unconformably overlies the St. Marys. The St. Marys was divided into three members by Ward (1984): Conoy Member ("Zone 20" of Shattuck, 1904), Little Cove Point Member ("Zones 21–23" of Shattuck, 1904), Windmill Point Member ("Zone 24" of Shattuck, 1904). The Windmill Point Member can be identified near Tappahannock on the Rappahannock River and at White Oak Landing on the Mattaponi River. Mollusks commonly found in the St. Marys Formation are shown on plate 7. The distribution of the St. Marys beds is shown in figure 6D.

Eastover Formation

The Eastover Formation of Ward and Blackwelder (1980) was named for shelly sands on the James River in Surry County, Va. These beds are present in the uppermost portion (top 50 ft; 15 m) of the Westmoreland Cliffs on the Potomac River. Some of the upper beds in the southern Calvert Cliffs may represent a marginal-marine, inner bay facies of the Eastover Formation. The Eastover Formation was divided into the Claremont Manor and Cobham Bay Members by Ward (1980).

Claremont Manor Member

Two facies of the Claremont Manor Member are very evident: a sandy, basal transgressive portion which grades into a silty clay containing many diatoms and an overlying clayey sand. Mollusks in the Claremont Manor Member are low in diversity and are usually poorly preserved (pl. 8). The distribution of the Claremont Manor Member is shown in figure 7A.

Cobham Bay Member

The Cobham Bay Member consists of very shelly, well-sorted sand and unconformably overlies the Claremont Manor Member. The unit is quite thin and is approximately 12.0 ft (3.6 m) thick at Cobham Wharf, Surry County, Va., the type area. The distribution of the Cobham Bay Member is shown in figure 7B.

Mollusks in the Cobham Bay Member are much more diverse than those in the Claremont Manor Member and probably represent open-shelf, warm conditions.

Acknowledgments

References Cited

Abbott, W.H., 1978, Correlation and zonation of Miocene strata along the Atlantic margin of North America using diatoms and silicoflagellates: Marine Micropaleontology, v. 3, p. 15–34.

Andrews, G.W., 1978, Marine diatom sequence in Miocene strata of the Chesapeake Bay region, Maryland: Micropaleontology, v. 24, p. 371–406.

Bennett, R.R., and Collins, G.G., 1952, Brightseat Formation, a new name for sediments of Paleocene age in Maryland: Journal of the Washington Academy of Science, v. 42, no. 4, p. 114–116.

Blackwelder, B.W., 1981, Stratigraphy of upper Pliocene and lower Pleistocene marine and estuarine deposits of northeastern North Carolina and southeastern Virginia: U.S. Geological Survey Bulletin 1502–B, 16 p.

Blackwelder, B.W., and Ward, L.W., 1976, Stratigraphy of the

Chesapeake Group of Maryland and Virginia; Geological Society of America, Joint Northeastern-Southeastern Section Meeting Guidebook, Field Trip 7b: Arlington, Va., 55 p.

Clark, W.B., 1896, The Eocene deposits of the middle Atlantic slope in Delaware, Maryland, and Virginia: U.S. Geological Survey Bulletin 141, p. 1–67.

Clark, W.B., and Martin G.C., 1901, The Eocene deposits of Maryland: Maryland Geological Survey, Eocene, p. 1–91, 122–204, 258–259.

Clark, W.B., and Miller, B.L., 1906, A brief summary of the geology of the Virginia Coastal Plain: Virginia Geological Survey Bulletin 2, pt. 1, p. 11–24.

Clark, W.B., and Miller, B.L., 1912, The physiography and geology of the Coastal Plain province of Virginia: Virginia Geological Survey Bulletin 4, p. 1–58, 88–222.

Cushman, J.A., and Cederstrom, D.J., 1945, An upper Eocene foraminiferal fauna from deep wells in York County, Virginia: Virginia Geological Survey Bulletin 67, 58 p.

Dall, W.H., and Harris, G.D., 1892, Correlation papers; Neogene: U.S. Geological Survey Bulletin 84, 349 p.

Darton, N.H., 1891, Mesozoic and Cenozoic formations of eastern Virginia and Maryland: Geological Society of America Bulletin, v. 2, p. 431–450.

Darton, N.H., 1911, Economic geology of Richmond, Virginia, and vicinity: U.S. Geological Survey Bulletin 483, 48 p.

Darton, N.H., 1948, The Marlboro Clay: Economic Geology, v. XLIII, no. 2, p. 154–155.

Darton, N.H., 1951, Structural relations of Cretaceous and Tertiary formations in parts of Maryland and Virginia: Geological Society of America Bulletin, v. 62, p. 745–780.

Frederiksen, N.O., 1979, Sporomorph biostratigraphy, northeastern Virginia: Palynology, v. 3, p. 129–167.

Gernant, R.E., 1970, Paleoecology of the Choptank Formation (Miocene) of Maryland and Virginia: Maryland Geological Survey Report of Investigations 12, 90 p.

Gibson, T.G., 1982, Depositional framework and paleoenvironments of Miocene strata from North Carolina to Maryland, in Scott, J.M., and Upchurch, S.B., eds., Miocene of the southeastern United States: Florida Bureau of Geology, Special Publication 25, p. 1–22.

Gibson, T.G., 1983, Stratigraphy of Miocene through lower Pleistocene strata of the United States central Atlantic Coastal Plain, in Ray, C.E., ed., Geology and paleontology of the Lee Creek mine, North Carolina, I: Smithsonian Contributions to Paleobiology 53, p. 35–80.

Gibson, T.G., Andrews, G.W., Bybell, L.M., Frederiksen, N.O., Hansen, Thor, Hazel, J.E., McLean, D.M., Witmer, R.J., and Van Nieuwenhuise, D.S., 1980, Biostratigraphy of the Tertiary strata of the core, in Geology of the Oak Grove core: Virginia Division of Mineral Resources Publication 20, pt. 2, p. 14–30.

Gibson, T.G., and Bybell, L.M., 1984, Foraminifers and calcareous nannofossils of Tertiary strata in Maryland and Virginia; A summary, in Frederiksen, N.O., and Krafft, Kathleen, eds., Cretaceous and Tertiary stratigraphy, paleontology, and structure, southwestern Maryland and northeastern Virginia; Field trip volume and guidebook [for field trip held October 17, 1984]: Reston, Va., American Association of Stratigraphic Palynologists, p. 181–189.

Glaser, J.D., 1971, Geology of mineral resources of southern Maryland: Maryland Geological Survey Report of Investigations 15, 84 p.

Hazel, J.E., 1968, Ostracodes from the Brightseat Formation (Danian) of Maryland: Journal of Paleontology, v. 42, p. 100–142.

Hazel, J.E., 1969, Faunal evidence for an unconformity between the Paleocene Brightseat and Aquia Formations (Maryland and Virginia): U.S. Geological Survey Professional Paper 650–C, p. 58–65.

Mansfield, W.C., 1944, Stratigraphy of the Miocene of Virginia and the Miocene and Pliocene of North Carolina: Pt. 1, Pelecypoda: U.S. Geological Survey Professional Paper 199–A, p. 1–19.

Martini, E., 1971, Standard Tertiary and Quarternary calcareous nannoplankton zonation, in Farinacci, A., ed., Proceedings of the second planktonic conference: Roma, Edizioni Tecnoscienza, v. 2, p. 739–785.

Reinhardt, Juergen, Newell, W.L., and Mixon, R.B., 1980, Tertiary lithostratigraphy of the core, in Geology of the Oak Grove core: Virginia Division of Mineral Resources Publication 20, pt. 1, p. 1–13.

Rogers, W.B., 1884, A reprint of annual reports and other papers on the geology of the Virginias: New York, D.A. Appleton and Company, 832 p.

Ruhle, J.L., 1962, Guidebook to the Coastal Plain of Virginia north of the James River: Virginia Division of Mineral Resources Information Circular 6, 46 p.

Shattuck, G.B., 1902, The Miocene formations of Maryland [abs.]: Science, v. XV, no. 388, p. 906.

Shattuck, G.B., 1904, Geological and paleontological relations, with a review of earlier investigations, in Clark, W.B., Shattuck, G.B., and Dall, W.H., The Miocene deposits of Maryland: Maryland Geological Survey, Miocene, v. 1, p. xxxiii–cxxxvii.

Stephenson, L.W., Cooke, C.W., and Mansfield, W.C., 1933, Chesapeake Bay region, International Geological Congress, XVI session, United States, 1933: Guidebook 5, Excursion A–5, 49 p.

Vail, P.R., and Mitchum, R.M., Jr., 1979, Global cycles of rel-

ative changes of sea level from seismic stratigraphy, *in* Geological and geophysical investigations of continental margins: American Association of Petroleum Geologists Memoir 29, p. 469–472.

Ward, L.W., 1984, Stratigraphy and paleontology of the outcropping Tertiary beds along the Pamunkey River-central Virginia Coastal Plain, *in* Ward, L.W., and Krafft, Kathleen, eds., Stratigraphy and paleontology of the outcropping Tertiary beds in the Pamunkey River region, central Virginia Coastal Plain—Guidebook for Atlantic Coastal Plain Geological Association 1984 field trip: Atlantic Coastal Plain Geological Association, p. 11–17, 240–280.

Ward, L.W., 1985, Stratigraphy and characteristic mollusks of the Pamunkey Group (lower Tertiary) and the Old Church Formation of the Chesapeake Group—Virginia Coastal Plain: U.S. Geological Survey Professional Paper 1346, 78 p., 6 pls.

Ward, L.W., and Blackwelder, B.W., 1980, Stratigraphic revision of upper Miocene and lower Pliocene beds of the Chesapeake Group, middle Atlantic Coastal Plain: U.S. Geological Survey Bulletin 1482–D, 61 p., 5 pls.

FIELD TRIP STOP DESCRIPTIONS FOLLOW

Figure 8. Map showing location of field trip stops.

Field Trip Stop Descriptions

Potomac River Sections

Stop 1. Aquia Creek.

Right bank of Aquia Creek, 0.5 mi (0.8 km) above Thorney Point, Stafford County, Va.

	ft	m
Sloped and covered by vegetation	3.0	0.9
Paleocene		
Aquia Formation		
Piscataway Member		
Sand, grayish-orange (10YR 7/4), silty, fine-grained, very glauconitic, poorly sorted, weathered, and leached; some molds and casts	9.0	2.7
—Unconformity—		
Brightseat Formation		
Sand, dark-olive-black (5Y 2/1), micaceous, clayey, silty, very fine grained, well-sorted in the lower half, weathered to grayish-orange in the upper half; an 8-in (20-cm)-thick indurated capping present at the lower end of the exposure but beveled off at the upper end of the exposure	7.0	2.1
—Unconformity—		
Lower Cretaceous		
Patapsco Formation		
Sand, well-consolidated, clayey, silty, light-blue-gray (5B 7/1); burrowed and eroded upper surface	0.0–1.0	0.0–0.3
—Sea Level—		

Below the mouth of Aquia Creek, most of the good exposures are on the Virginia shore for the next 5.0 mi (8.0 km). The bluffs immediately downriver of the mouth of Aquia Creek are the site of the lectostratotype section of the upper Paleocene Aquia Formation. Ward (1985, p. 62) described the section as follows.

Stop 2. Aquia Creek.

Right bank of the Potomac River, 1.5 mi (2.4 km) below the mouth of Aquia Creek, Stafford County, Va.

	ft	m
Covered	5.0	1.5
Eocene		
Nanjemoy Formation		
Sand, yellowish-gray (5Y 8/1), weathered, moderately glauconitic, fine-grained	5.0	1.5
Paleocene		
Marlboro Clay		
Clay, light-gray (N 8), weathered; where this bed is absent there is a distinct line between the Aquia Formation and the overlying bed of Nanjemoy Formation	0.0–0.75	0.0–0.23
Aquia Formation		
Paspotansa Member		
Sand, weathered, grayish-orange (10YR 7/4), glauconitic, fine-grained; contains large number of *Turritella* in lenses, bands, and large indurated masses	35.0	10.7

		ft	m
Sand, olive-black (5Y 2/1), fine-grained, well-sorted, silty; scattered, poorly preserved *Turritella*		25.0	7.6
Sand, olive-black (5Y 2/1), glauconitic, very fine-grained, well-sorted; many *Turritella* ("Zone 6" of Clark and Martin, 1901)		1.5	0.5

—Unconformity—

Aquia Formation
    Piscataway Member

		ft	m
Sandstone, light-olive-gray (5Y 6/1), indurated, glauconitic: many molds and casts, some siliceous replacements ("Zone 5" of Clark and Martin, 1901)		2.0	0.6
Sand, olive-gray (5Y 4/1), very glauconitic, silty, clayey, very shelly, poorly sorted; packed with large bivalves and *Turritella*. Appears light-olive-gray (5Y 6/1) from a distance because of large numbers of mollusks present; preservation, poor to moderate; irregularly indurated in beds where *Ostrea* are concentrated		12.0	3.7

—Sea Level—

Stop 3. Belvedere Beach.

Right bank of the Potomac River, 0.3 mi (0.5 km) above Belvedere Beach, King George County, Va.

		ft	m
Covered		5.0	1.5

Paleocene
    Aquia Formation
        Paspotansa Member

		ft	m
Sand, olive-black (5Y 2/1), fine-grained, well-sorted, silty, micaceous, glauconitic; many *Turritella*, scattered as well as in distinct bands; common *Ostrea sinuosa*; moderate molluscan diversity		12.0	3.7

—Sea Level—

Stop 4. Fairview Beach Marina

Right bank of the Potomac River, just 100 yd below the Fairview Beach Marina, King George County, Va. (Ward, 1985, p. 64).

		ft	m
Sloped and covered		5.0	1.5

Eocene
    Nanjemoy Formation
        Potapaco Member (Bed A)

		ft	m
Sand, grayish-yellow (5Y 8/4), weathered, clayey, fine-grained, poorly sorted, glauconitic		6.0	1.8

—Unconformity—

Paleocene
    Marlboro Clay

		ft	m
Clay, light-gray (N 7), somewhat weathered, blocky		6.0	1.8

Aquia Formation
    Paspotansa Member

		ft	m
Sand, grayish-yellow, silty, very weathered; molds of *Turritella mortoni*		2.5	0.8

—Sea Level—

Stop 5. Woodstock Member lectostratotype.

Right bank of the Potomac River (high bluffs), 2.0 mi (3.2 km) above Mathias Point, King George County, Va.

	ft	m
Pleistocene		
Sand, orange, coarse-grained	5.0	1.5
Conglomerate, sand, gravel, cobbles, boulders	3.0	0.9
—Unconformity—		
Miocene		
Calvert Formation		
Fairhaven Member		
Clay, yellowish-gray (5Y 8/1), silty, somewhat sandy near base, weathered, blocky, diatomaceous, phosphate pebbles and coarse-grained sand along basal contact	17.0	5.2
—Disconformity—		
Eocene		
Nanjemoy Formation		
Woodstock Member		
Sand, pale-greenish-yellow (10Y 8/2), weathered, fine-grained, micaceous; molds and casts; upper surface very eroded and burrowed with as much as 3 ft (0.9 m) of relief	25.0	7.6
Sand, olive-black (5Y 2/1), silty, very fine grained, micaceous, glauconitic; small mollusks with moderate preservation	15.0	4.6
—Sea Level—		

Stop 6. Popes Creek.

Left bank of the Potomac River, 0.95 mi (1.5 km) below the mouth of Popes Creek, Charles County, Md.

	ft	m
Pleistocene		
Conglomerate, yellowish-orange, weathered; gravel, sand, cobbles, boulders	25.0	7.6
Miocene		
Calvert Formation		
Fairhaven Member		
Clay, light-yellowish-gray (5Y 9/1), blocky, diatomaceous	10.0	3.0
Sand, yellowish-gray (5Y 8/1), silty	2.0	0.6
—Disconformity—		
Clay, light-yellowish-gray (5Y 9/1), blocky	0.5	0.2
Sand, yellowish-gray (5Y 8/1), silty	5.0	1.5
Sand, olive-brown (5Y 4/4), silty, phosphatic, pebbles	1.5	0.5
Sand, yellowish-gray (5Y 7/2), silty	2.5	0.8
Sand, olive-brown (5Y 4/4), silty, phosphatic, pebbles	2.0	0.6
—Unconformity—		
Eocene		
Nanjemoy Formation(?) The following unit is provisionally placed in the Woodstock Member.		
Sand, olive-gray (5Y 4/1), medium-grained, very glauconitic; many molds and casts; unit becoming thicker downstream	0.75	0.23
—Disconformity—		

Nanjemoy Formation
    Woodstock Member

	ft	m
Sand, olive-black (5Y 2/1), very fine grained, micaceous, silty, glauconitic; many small mollusks, poorly preserved	5.0	1.5
Concretions, olive-gray (5Y 4/1), calcareous, sandy, glauconitic, rounded	5.0	1.5
Sand, olive-black (5Y 2/1), very fine grained, micaceous, silty, glauconitic; many small mollusks, moderately preserved	5.0	1.5

—Sea Level—

Chesapeake Bay Section

Stop 7. Randle Cliffs (northern end).

High bluff just south of Chesapeake Beach, Calvert County, Md.

	ft	m
Soil	2.0	0.6
—Unconformity—		
Miocene		
Choptank Formation		
Boston Cliffs Member		
Silt, sandy, blocky (Bed 19)	7.0	2.1
—Unconformity—		
Drumcliff and St. Leonard Members, undivided		
Silt, sandy, blocky (Beds 17, 18)	10.0	3.0
Calvert Formation		
Calvert Beach Member		
Silt, clayey, blocky (Bed 15)	6.0	1.8
Sand, silty, shelly (Bed 14)	17.0	5.2
Plum Point Member		
Silt, clayey, blocky (Bed 13)	6.0	1.8
Sand, silty; poorly preserved shells (Bed 12)	3.0	0.9
Silt, clayey, blocky (Bed 11)	2.0	0.6
Sand, silty; very shelly (Bed 10)	10.0	3.0
—Unconformity—		
Sand, silty; many Corbulids concentrated in bands (Beds 4–9)	35.0	10.7
Fairhaven Member		
Silt, clayey, blocky, burrowed (Bed 3)	2.0	0.6

—Sea Level—

Stop 8. Camp Roosevelt.

3.7 mi south of the mouth of Fishing Creek at Chesapeake Beach, Calvert County, Md.

	ft	m
Soil	2.0	0.6
—Unconformity—		
Miocene		
Choptank Formation		
Boston Cliffs Member		

	ft	m
Silt, sandy, fine-grained, with sand near base (Bed 19)	14.0	4.3
Drumcliff Member		
Sand, silty, clayey; poorly preserved shells (Bed 17)	1.0	0.3
—Unconformity—		
Calvert Formation		
Calvert Beach Member		
Silt, clayey, blocky (Bed 15)	10.0	3.0
Sand, silty, clayey; poorly preserved shells (Bed 14)	10.0	3.0
Plum Point Member		
Silt, clayey, blocky (Bed 13)	7.0	2.1
Sand, silty, shelly (Bed 12)	4.0	1.2
—Unconformity—		
Silt, clayey, blocky (Bed 11)	4.0	1.2
Sand, silty; very shelly (Bed 10)	12.0	3.7
—Unconformity—		
Sand, silty; many small *Varicorbula* concentrated in several distinct bands (Beds 4–9)	25.0	7.6

Stop 9. Plum Point.

1.0 mi (1.6 km) south of Plum Point, Calvert County, Md.

	ft	m
Miocene		
Choptank Formation		
Boston Cliffs Member		
Silt, clayey, blocky (Bed 19)	17.0	5.2
St. Leonard Member		
Silt, clayey, blocky (Bed 18)	9.0	2.7
Drumcliff Member		
Sand, silty, clayey; some preserved shells (Bed 17)	4.0	1.2
Calvert Formation		
Calvert Beach Member		
Silt, clayey, blocky, laminated (Bed 15)	10.0	3.0
Sand, silty, clayey; moderately shelly (Bed 14)	15.0	4.6
Plum Point Member		
Silt, clayey, blocky (Bed 13)	13.5	4.1
Sand, silty, clayey; poorly preserved mollusks (Bed 12)	2.5	0.8
Silt, clayey, blocky (Bed 11)	10.0	3.0
Sand, silty; very shelly (Bed 10)	9.0	2.7
—Sea Level—		

Stop 10. Parkers Creek.

Just above Scientists Cliffs, Calvert County, Md.

	ft	m
Covered with vegetation	1.5	0.5
Miocene		
St. Marys Formation		
Clay, silty	4.9	1.5
Choptank Formation		
Boston Cliffs Member		
Sand, silty, fine-grained; many mollusks	13.1	4.0

St. Leonard Member		
Sand, clayey, silty, well-burrowed; some molds of mollusks	14.7	4.5
Drumcliff Member		
Sand, very shelly, fine-grained; many large mollusks, well-preserved	13.1	4.0
Calvert Formation		
Calvert Beach Member		
Sand, silty, fine-grained; scattered, small, poorly preserved mollusks	6.5	2.0
Sand, shelly, silty; many mollusks, especially *Glossus*	4.9	1.5
Plum Point Member		
Clay, blocky, silty	9.8	3.0
Sand, shelly, silty; many, poorly preserved mollusks	0.9	0.3
Clay, blocky, silty	4.2	1.3

—Sea Level—

Stop 11. Baltimore Gas and Electric Powerplant.

The section given below, now inaccessible, was described from a bluff just upbay from the powerplant, Calvert County, Md. A similar section near Rocky Point, below the plant site, will be visited instead.

	ft	m
Pleistocene(?)		
Miocene		
St. Marys Formation		
Little Cove Point Member		
Soil	1.5	0.5
Sand, pebbly, coarse-grained	10.0	3.0
Sand, silty, fine-grained; molluscan molds	14.7	4.5
Sand, fine-grained, burrowed, clean, well-sorted	3.2	1.0
Sand, medium-grained, well-sorted	3.2	1.0
Shell hash, clayey, sandy; very worn mollusks	1.9	0.6
Clay, sandy; scattered, small fragmented mollusks	4.9	1.5
Clay, sandy; scattered, small, poorly preserved mollusks	1.3	0.4
Clay, sandy; scattered, small shells	4.9	1.5
Sand, shelly, fine-grained	1.5	0.5
Clay, blocky; molluscan molds	1.9	0.6
Sand, clayey, fine-grained	5.1	1.6
Clay, blocky; molluscan molds abundant along thin horizontal planes	5.1	1.6
Choptank Formation		
Boston Cliffs Member		
Sand, shelly, fine-grained; abundant large mollusks, upper 1.0 m (3.3 ft) indurated	5.1	1.6
St. Leonard Member		
Sand, silty, fine-grained, very burrowed; mollusks scarce, scattered, poorly preserved	5.1	1.6
Drumcliff Member		
Sand, shelly, silty, fine-grained; abundant mollusks, cetacean remains common	10.4	3.2

Stop 12. Little Cove Point.

Bluff, 0.6 mi (1.0 km) downbay from Little Cove Point, Calvert County, Md.

	ft	m
Pliocene(?)		
Sand, grayish-orange (10*YR* 7/4), interbedded with thin clay layers, flaser-bedded, ripple-marked	30.0	9.1
Sand, reddish-orange (10*YR* 5/6) medium- to coarse-grained, burrowed, crossbedded, with pebbles and cobbles at base	5.0	1.5
Miocene		
St. Marys Formation		
Little Cove Point Member		
Sand, yellow-orange (10*YR* 5/6), poorly sorted, burrowed	13.0	4.0
Sand, olive-gray (5*Y* 4/1), fine-grained, silty, interbedded with silty clay	15.0	4.6
Sand, olive-gray (5*Y* 4/1), silty, fine-grained; molluscan molds only	11.0	3.4
Sand, olive-gray (5*Y* 4/1), silty, fine-grained, glauconitic; abundant mollusks	5.0	1.5
Sand, olive-gray (5*Y* 4/1), silty, fine-grained; few mollusks	6.0	1.8
Sand, olive-gray (5*Y* 4/1), fine-grained, very shelly; mollusks dominated by *Turritella*, many worn	1.0	0.3
Sand, grayish-olive-gray (5G 4/1), silty, fine-grained, burrowed; small, fragile mollusks	3.0	0.9

PLATE 1.

[Mollusks common in the Piscataway Member of the Aquia Formation. All specimens were collected from the Pamunkey River 0.5 mi (0.8 km) east of Wickham Crossing, Hanover County, Va. (USGS Locality 26337)]

FIGURE 1, 2, 4, 5. *Ostrea alepidota* Dall, 1898.

      1. Left valve of specimen (USNM 366570); length 73.5 mm, height 85.1 mm.

      2. Right valve of specimen (USNM 366470); length 65.4 mm, height 82.6 mm.

      4. Left valve of specimen (USNM 366472); length 58.9 mm, height 74.3 mm.

      5. Left valve of specimen (USNM 366473); length 36.3 mm, height 44.6 mm.

   3. *Turritella humerosa* Conrad, 1835.

      Apertural view of an incomplete specimen (USNM 366471); height 32.5 mm.

   6. *Turritella mortoni* Conrad, 1830.

      Apertural view of incomplete specimen (USNM 366474); height 35.8 mm.

   7. *Cucullaea gigantean* Conrad, 1830.

      Left valve of specimen (USNM 366475); length 42.4 mm, height 27.4 mm.

   8. *Pitar pyga* Conrad, 1845.

      Left valve of a double-valved specimen (USNM 366476); length 46.3 mm, height 38.9 mm.

   9. *Crassatellites capricranium* (Rogers, 1839).

      Left valve of specimen (USNM 366477); length 59.1 mm, height 38.6 mm.

  10. *Dosiniopsis lenticularis* (Rogers, 1839).

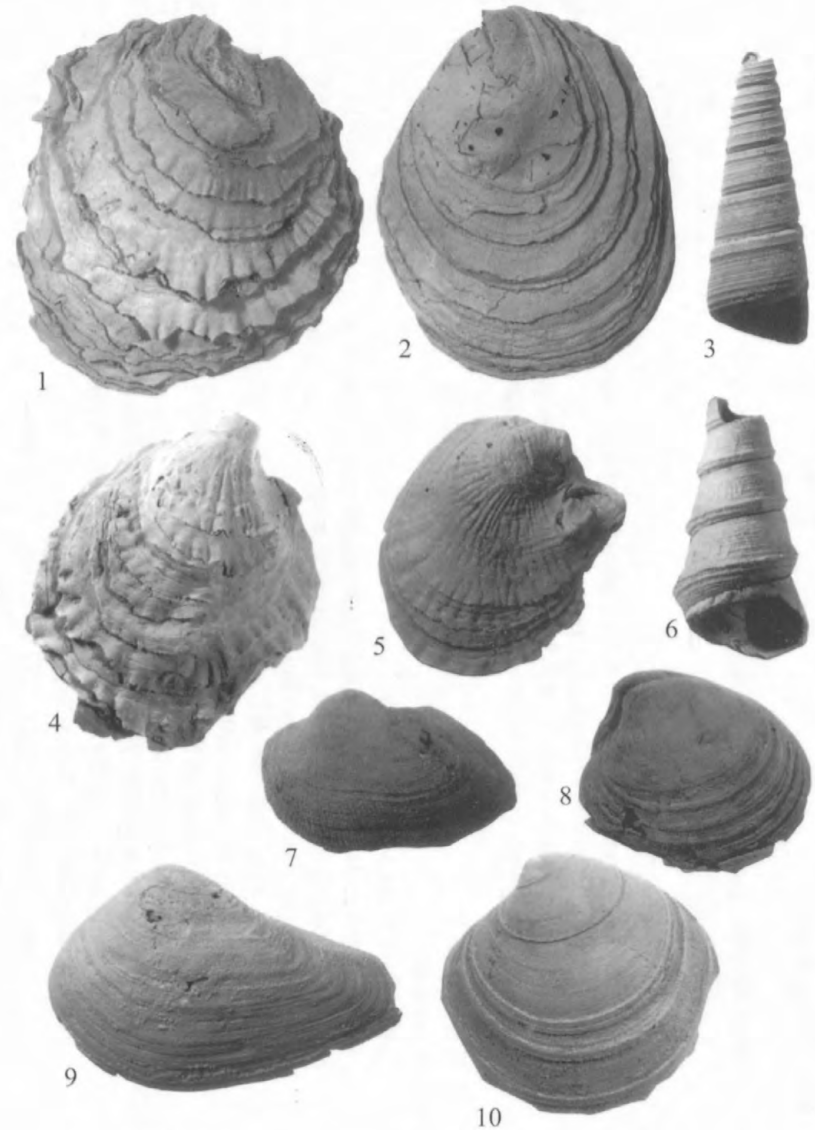   Left valve of specimen (USNM 366478); length 47.1 mm, height 44.5 mm.

PLATE 2.

[Mollusks common in the Paspotansa Member of the Aquia Formation. All except figure 5 were collected from the Potomac River, 0.3 mi (0.5 km) above Belvedere Beach, King George County, Va.]

FIGURE

1. *Cucullaea gigantea* Conrad, 1830.
   Left valve of specimen (USNM 366479); length 83.3 mm, height 71.8 mm.
2. *Pycnodonte* sp.
   Left valve of specimen (USNM 366480); length 74.2 mm, height 74.6 mm.
3. *Turritella mortoni* Conrad, 1830.
   Apertural view of specimen (USNM 366481); height 105.0 mm.
4, 8. *Ostrea sinuosa* Rogers and Rogers, 1837.
   4. Left valve of specimen (USNM 366482); length 152.8 mm, height 134.3 mm.
   8. Right valve of specimen (USNM 366482); length 98.8 mm, height 118.3 mm.
5. *Venericardia regia* Conrad, 1865.
   Left valve of specimen (USNM 366483) from the Potomac River, 0.1 mi (0.3 km) below the mouth of Passapatanzy Creek, King George County, Va. USGS Locality 26341); length 75.4 mm, height 71.7 mm.
6. *Turritella mortoni* Conrad, 1830.
   Apertural view of nearly complete specimen (USNM 366484); height 92.3 mm.
7. *Crassatellites alaeformis* Conrad, 1830.
   Right valve of specimen (USNM 366485); length 51.9 mm, height 22.7 mm.
9. *Pitar pyga* Conrad, 1845.
   Right valve of specimen (USNM 366486); length 33.6 mm, height 28.1 mm.
10. *Turritella humerosa* Conrad, 1835.
   Apertural view of an incomplete specimen (USNM 366487); height 49.8 mm.
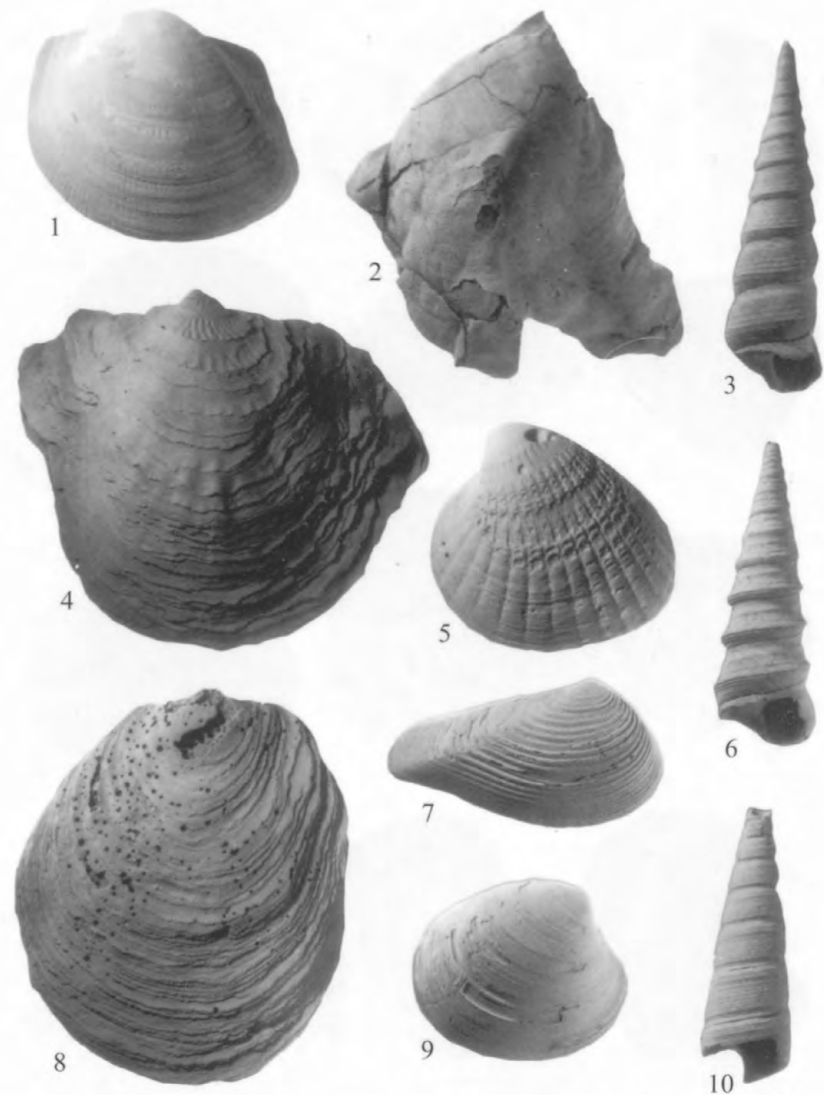
PLATE 3.

[Mollusks common in the Potapaco Member of the Nanjemoy Formation. Figures 1, 3, and 5 from the Pamunkey River, 0.8 mi (1.3 km) below Hanovertown, Hanover County, Va. (USGS Locality 26377). Figures 2, 4, and 6 from the Pamunkey River, 0.45 mi (0.72 km) above the mouth of Millpond Creek on the right bank, Hanover County, Va. (USGS Locality 26424). Figures 7–9, 11, and 12 from the Potomac River, 2.3 mi (3.9 km) above Popes Creek, Charles County, Md. (USGS Locality 26425). Figure 10 from the Rappahannock River, opposite Goat Island, Caroline County, Va. (USGS Locality 26360)]

FIGURE   1. *Cubitostrea* sp.

Left valve of specimen (USNM 366488); length 48.5 mm, height 51.6 mm.

2. *Cubitostrea* sp.

Left valve of specimen (USNM 366489); length 35.7 mm, height 50.4 mm.

3. *Cubitostrea* sp.

Left valve of specimen (USNM 366490); length 37.7 mm, height 58.5 mm.

4. *Cubitostrea* sp.

Left valve of specimen (USNM 366491); length 18.7 mm, height 27.6 mm.

5. *Cubitostrea* sp.

Right valve of specimen (USNM 366492); length 47.9 mm, height 56.2 mm.

6. *Cubitostrea* sp.

Right valve of specimen (USNM 366493); length 18.8 mm, height 21.4 mm.

7. *Venericardia potapacoensis* Clark and Martin, 1901.

Left valve of specimen (USNM 366494); length 29.0 mm, height 24.1 mm.

8. *Nuculana parva* (Rogers, 1837).

Right valve of specimen (USNM 366495); length 4.62 mm, height 2.85 mm.

9. *Vokesula* sp.

Right valve of specimen (USNM 366496); length 4.48 mm, height 4.20 mm.

10. *Lucina* sp.

Right valve of specimen (USNM 366497); length 5.14 mm, height 4.66 mm.

11. *Vokesula* sp.

Right valve of specimen (USNM 366498); length 4.29 mm, height 3.65 mm.

12. *Cadulus* sp.

Lateral view of incomplete specimen (USNM 366499); length 3.45 mm.
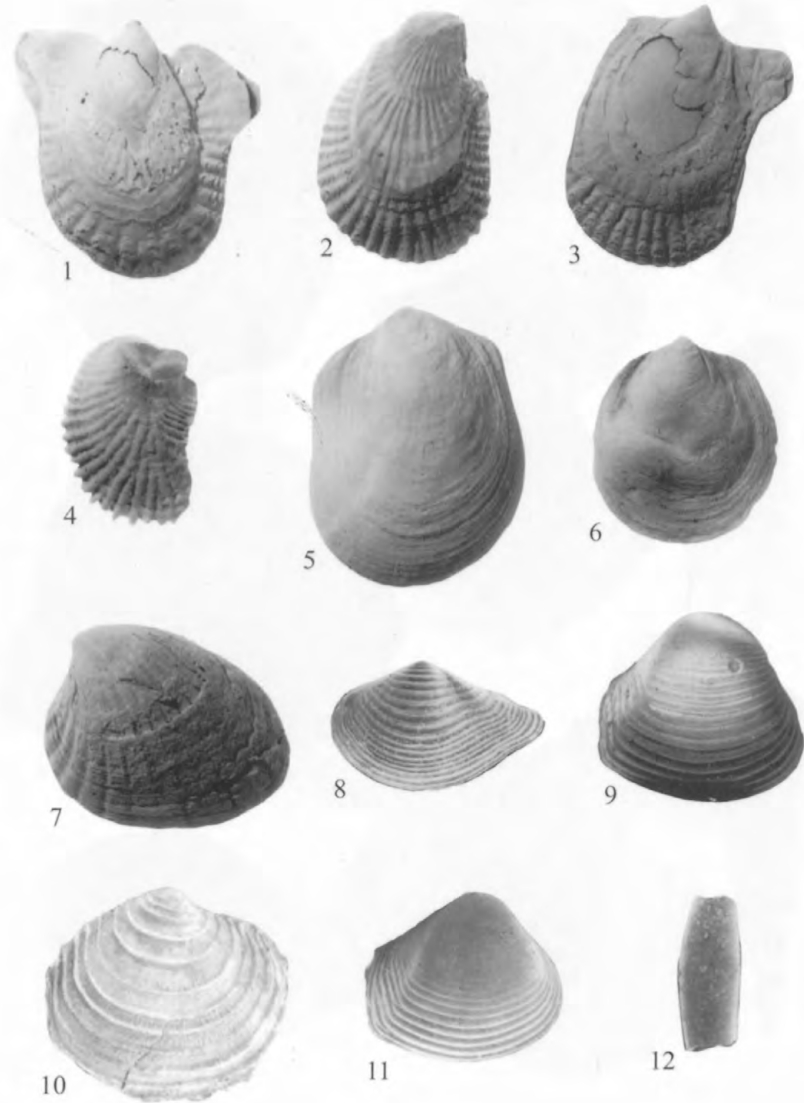
PLATE 4.

[Mollusks common in the Woodstock Member of the Nanjemoy Formation. Figures 5, 6, and 10–14 from the Pamunkey River, in a small ravine, 0.63 mi (1.01 km) south-southeast of the mouth of Totopotomoy Creek, Hanover County, Va. (USGS Locality 26403). Other localities are as described below]

FIGURE 1. *Glycymeris* sp.

  Right valve of specimen (USNM 366500) from the Pamunkey River at the termination of Va. 732, Hanover County, Va. (USGS Locality 26393); length 22.0 mm, height 21.0 mm.

2–4. Specimens from the Potomac River, 0.95 mi (1.53 km) below the mouth of Popes Creek, Charles County, Md. (Stop 6) (USGS Locality 26397).

  2. *Cubitostrea* sp.

   Left valve of specimen (USNM 366501); length 13.8 mm, height 20.2 mm.

  3. *Cubitostrea* sp.

   Left valve of specimen (USNM 366502); length 11.8 mm, height 17.0 mm.

  4. *Cubitostrea* sp.

   Right valve of specimen (USNM 366503); length 12.0 mm, height 22.0 mm.

 5. *Nuculana* sp.

  Right valve of specimen (USNM 366504); length 4.14 mm, height 2.56 mm.

 6. *Macrocallista subimpressa* (Conrad, 1848).

  Left valve of specimen (USNM 366505); length 21.3 mm, height 13.9 mm.

7–9. Specimens from the Pamunkey River, just upstream of the old Newcastle Bridge, Hanover County, Va. (USGS Locality 26405).

  7. *Corbula aldrichi* Meyer, 1885.

   Right valve of specimen (USNM 366506); length 10.0 mm, height 7.5 mm.

  8. *Venericardia ascia* Rogers and Rogers, 1839.

   Right valve of specimen (USNM 366507); length 41.4 mm, height 37.5 mm.

  9. *Venericardia ascia* Rogers and Rogers, 1839.

   Right valve of specimen (USNM 366508); length 62.6 mm, height 54.1 mm.

 10. *Lucina dartoni* Clark, 1895.

  Left valve of specimen (USNM 366509); length 6.1 mm, height 5.2 mm.

 11. *Lunatia* sp.

  Apertural view of specimen (USNM 366510); height 14.2 mm.
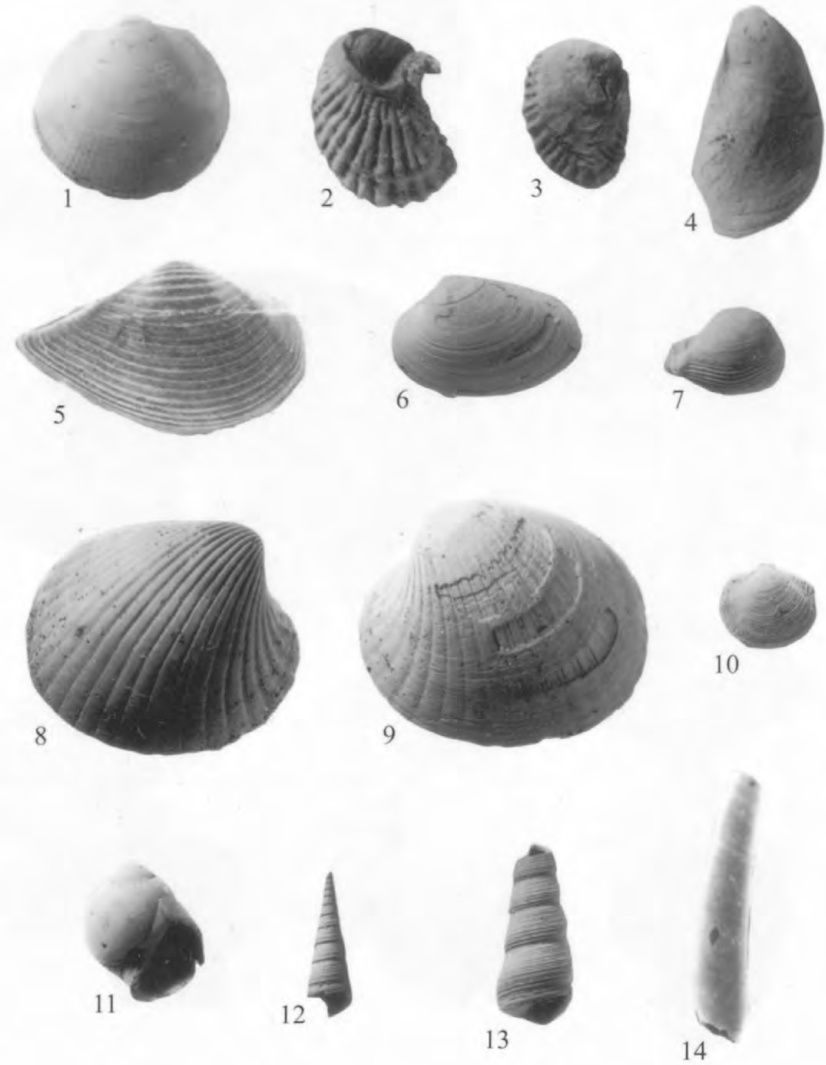
 12. *Turritella* sp.

  Apertural view of incomplete specimen (USNM 366511); height 12.2 mm.

 13. *Turritella* sp.

  Apertural view of incomplete specimen (USNM 366512); height 14.4 mm.

 14. *Cadulus* sp.

  Lateral view of nearly complete specimen (USNM 366513); height 4.93 mm.

PLATE 5.

[Mollusks common in the Calvert Formation. Figures 1, 3, 4, and 9 are from Plum Point, on the Chesapeake Bay, Calvert County, Md. (Stop 9). Figures 2, 5, 6,and 8 are from Camp Roosevelt, on the Chesapeake Bay, Calvert County, Md. (Stop 8). Figure 7 is from Mrs. Anderson's Cottages, near Plum Point, on the Chesapeake Bay, Calvert County, Md.]

FIGURE

1. *Pecten humphreysii* Conrad, 1842.
   Right valve of specimen (USNM 380693); length 52.2 mm, height 47.6 mm.
2. *Bicorbula idonea* (Conrad, 1833).
   Right valve of specimen (USNM 380694); length 28.0 mm, height 24.9 mm.
3. *Pecten humphreysii* Conrad, 1842.
   Left valve of specimen (USNM 380695); length 48.4 mm, height 35.5 mm.
4. *Lirophora latilirata* (Conrad, 1841).
   Right valve of specimen (USNM 380696); length 19.9 mm, height 15.6 mm.
5. *Melosia staminea* (Conrad, 1839).
   Right valve of specimen (USNM 380697); length 30.0 mm, height 28.0 mm.
6. *Astarte cuneiformis* Conrad, 1840.
   Left valve of specimen (USNM 380698); length 35.6 mm, height 25.0 mm.
7. *Mercenaria* sp.
   Right valve of specimen (USNM 380699); length 92.5 mm, height 91.4 mm.
8. *Marvacrassatella melinus* (Conrad, 1832).
   Left valve of specimen (USNM 280700); length 80.9 mm, height 51.8 mm.
9. *Ecphora tricostata pamlico* Wilson, 1987.
   Apertural view of specimen (USNM 280701); height 73.6 mm.
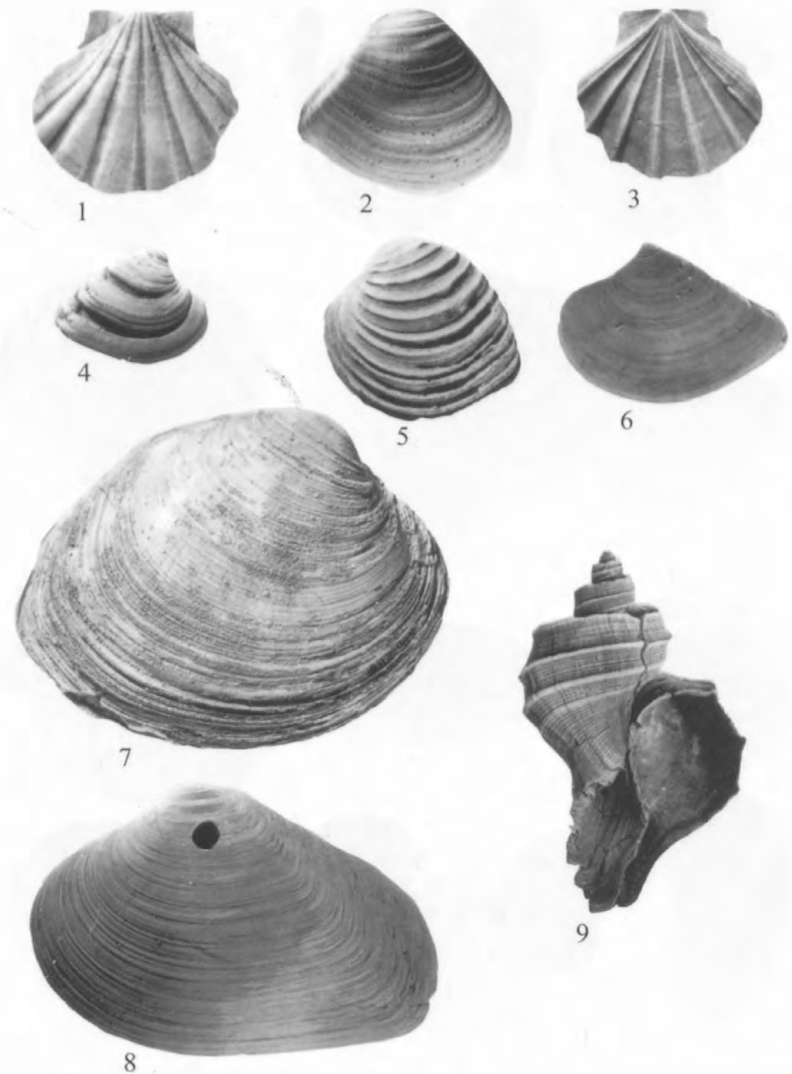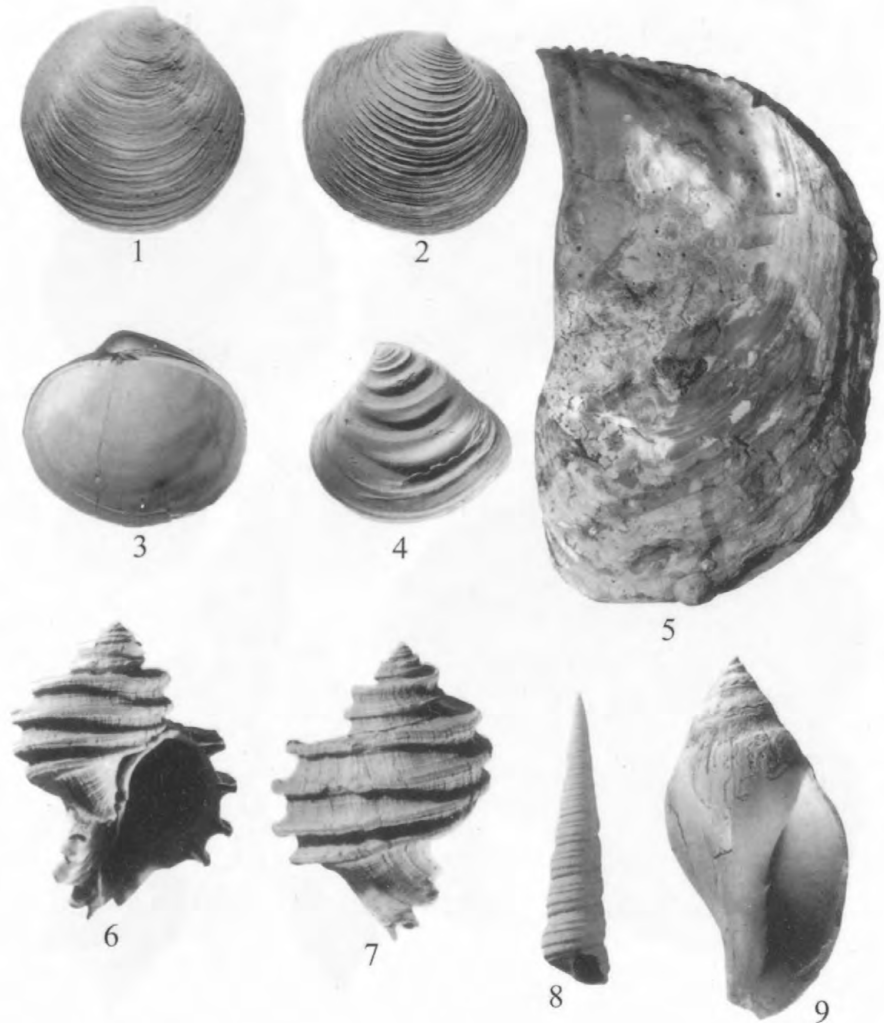
PLATE 6.

[Mollusks common in the Choptank Formation]

FIGURE

1. *Stewartia anodonta* (Say, 1824).

    Right valve of specimen (USNM 405221) from Drumcliff (Jones Wharf), on the Patuxent River, St. Marys County, Md. (USGS Locality 26557); length 46.2 mm, height 49.0 mm.

2. *Lucinoma contracta* (Say, 1824).

    Right valve of specimen (USNM 405225) from Calvert Beach, on the Chesapeake Bay, Calvert County, Md.; length 37.8 mm, height 34.0 mm.

3. *Timothynus subvexa* (Conrad, 1838).

    Right valve of specimen (USNM 405227) from Calvert Beach, on the Chesapeake Bay, Calvert County, Md.; length 35.6 mm, height 32.1 mm.

4. *Astarte thisphila* Glenn, 1904.

    Left valve of holotype specimen (USNM 405239) from Drumcliff (Jones Wharf), on the Patuxent River, St. Marys County, Md. (USGS Locality 26557); length 27.0 mm, height 25.3 mm.

5. *Isognomon (Hippochaeta)* sp.

    Left valve of nearly complete specimen (USNM 405192) from Long Beach, on the Chesapeake Bay, Calvert County, Md.; length 105.0 mm.

6, 7. *Ecphora meganae* Ward and Gilinsky, 1988.

    6. Apertural view of holotype (USNM 405320) from Drumcliff (Jones Wharf), on the Patuxent River, St. Marys County, Md. (USGS Locality 26557); height 64.6 m.

    7. Posterior view of the same specimen.

8. *Turritella* sp.

    Apertural view of specimen (USNM 405306) from Drumcliff (Jones Wharf), on the Patuxent River, St. Marys County, Md. (USGS Locality 26557); height 21.4 mm.

9. *Scaphella virginiana* Dall, 1890.

    Apertural view of neotype (USNM 405342) from Drumcliff (Jones Wharf), on the Patuxent River, St. Marys County, Md. (USGS Locality 26557); height 74 mm.

PLATE 7.

[Mollusks common in the St. Marys Formation]

FIGURE

1. *Conus deluvianus* Green, 1830.

Apertural view of neotype (USNM 405343) from above Windmill Point, St. Marys River, St. Marys County, Md. (USGS Locality 26554); height 55.3 mm.

2. *Urosalpinx subrusticus* (d'Orbigny, 1852).

Apertural view of specimen (USNM 405326); height 27.7 mm.

3. *Nassarius (Tritiaria) peralta* (Conrad, 1868).

Apertural view of specimen (USNM 405335) from above Windmill Point, St. Marys River, St. Marys County, Md. (USGS Locality 26554); height 14.9 mm.

4, 6. *Mactrodesma subponderosa* (d'Orbigny, 1852).

4. Exterior of right valve (USNM 405256) from above Windmill Point, St. Marys River, St. Marys County, Md. (USGS Locality 26554); length 103.8 mm, height 78.2 mm.

6. Interior view of left valve (USNM 405257) from the same locality; length 104.2 mm, height 80.9 mm.

5. *Buccinofusus parilis* (Conrad, 1832).

Apertural view of specimen (USNM 405339) from above Windmill Point, St. Marys River, St. Marys County, Md. (USGS Locality 26554); height 101.5 mm.

PLATE 8.

[Mollusks common in the Claremont Manor Member of the Eastover Formation. Figures 1, 4, and 6 are from Cobham Wharf, Va. (USGS Locality 26052). Figures 2, 3, 5, 10, and 12 are from just above Sunken Meadow Creek, Surry County, Va. (USGS Locality 26041). Figures 7–9 and 11 are from just below the mouth of Upper Chippokes Creek on the James River, Surry County, Va. (USGS Locality 26042).]

FIGURE

1. *Isognomon* sp.
    Right valve of nearly complete specimen (USNM 258347); length 150.3 mm.
2. *Ecphora gardnerae whiteoakensis* Ward and Gilinsky, 1988.
    Apertural view of specimen (USNM 258348); height 74.4 mm.
3. *Mercenaria* sp.
    Left valve of specimen (USNM 258349); length 93.5 mm, height 75.9 mm.
4. *Glycymeris virginiae* Dall, 1898.
    Left valve of specimen (USNM 258350); length 60.5 mm, height 65.1 mm.
5. *"Arca" virginiae* Dall, 1898.
    Right valve of specimen (USNM 258351); length 82.2 mm, height 57.3 mm.
6. *Lirophora dalli* Olsson, 1914.
    Right valve of specimen (USNM 258352); length 19.3 mm, height 17.2 mm.
7. *Dallarca carolinensis clisea* (Dall, 1898).
    Left valve of specimen (USNM 258353); length 42.7 mm, height 44.1 mm.
8. *Glossus fraterna* (Say, 1824).
    Left valve of incomplete specimen (USNM 258354); length 82.3 mm, height 80.2 mm.
9. *Euloxa latisulcata* (Conrad, 1839).
    Left valve of an incomplete specimen (USNM 258355); approximate length 15 mm, height 13.1 mm.
10. *Ostrea compressirostra brucei* Ward, 1992.
    Left valve of specimen (USNM 258356); length 97.7 mm, height 111.9 mm.
11. *Turritella plebeia* ssp.
    Apertural view of incomplete specimen (USNM 258357); height 98.8 mm.
12. *Chesapecten middlesexensis* (Mansfield, 1936).
    Right valve of specimen (USNM 258358); length 98.8 mm, height 91.4 mm.
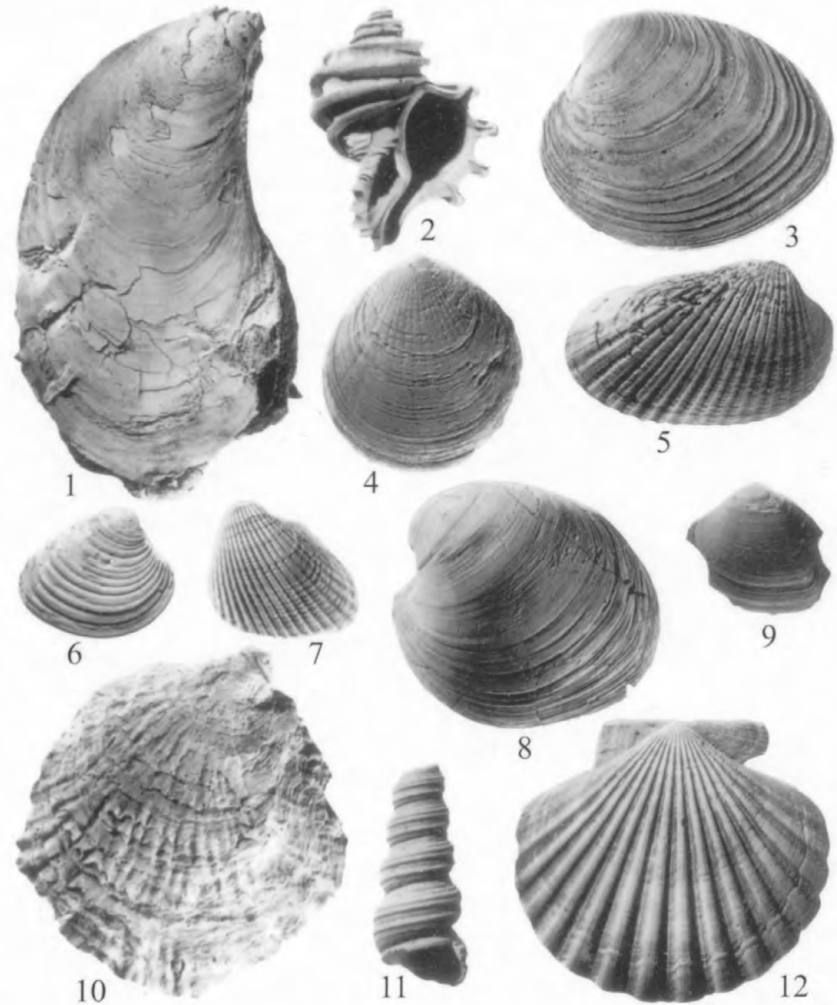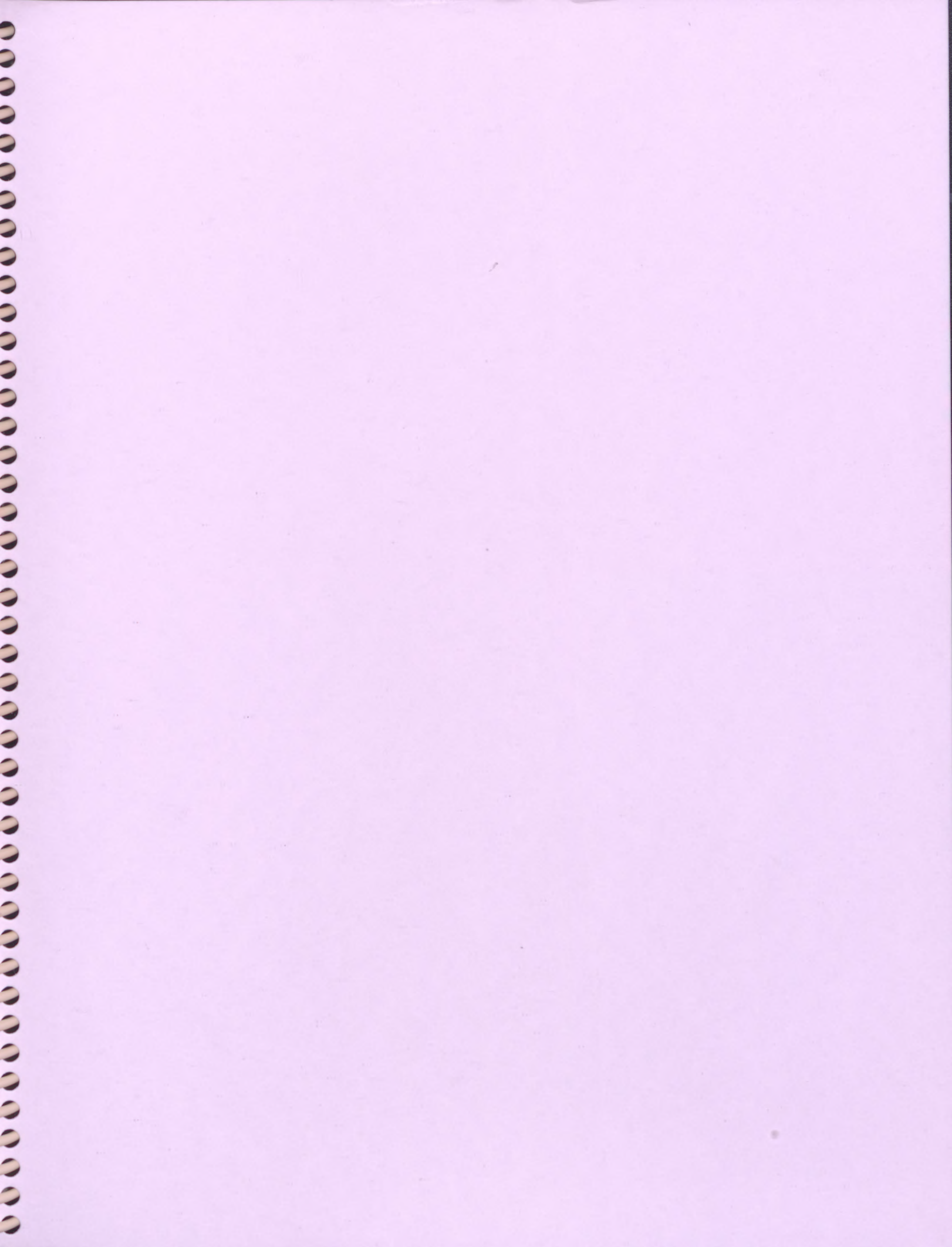
Edited by Scott Southworth and William Burton—**Geology of the National Capital Region**—Circular 1264

Printed on recycled paper